

A PRECAMBRIAN HISTORY OF CRATONIC
NORTH AMERICAN CRUST BENEATH THE SNAKE RIVER PLAIN, IDAHO

by

Emerald Kirke Shirley

A thesis

submitted in partial fulfillment

of the requirements for the degree of

Master of Sciences in Geology

Boise State University

December 2013

© 2013

Emerald Kirke Shirley

ALL RIGHTS RESERVED

BOISE STATE UNIVERSITY GRADUATE COLLEGE

DEFENSE COMMITTEE AND FINAL READING APPROVALS

of the thesis submitted by

Emerald Kirke Shirley

Thesis Title: A Precambrian history of cratonic North American crust beneath the Snake River Plain, Idaho

Date of Final Oral Examination: 09 October 2013

The following individuals read and discussed the thesis submitted by student Emerald Kirke Shirley, and they evaluated her presentation and response to questions during the final oral examination. They found that the student passed the final oral examination.

Mark Schmitz, Ph.D. Chair, Supervisory Committee

Karen Viskupik, Ph.D. Member, Supervisory Committee

Craig White, Ph.D. Member, Supervisory Committee

The final reading approval of the thesis was granted by Mark Schmitz, Ph.D., Chair of the Supervisory Committee. The thesis was approved for the Graduate College by John R. Pelton, Ph.D., Dean of the Graduate College.

ACKNOWLEDGEMENTS

I would like to thank my advisor Dr. Mark Schmitz for providing me with the opportunity to develop this thesis. His guidance and support greatly added to the quality of this thesis. I would also like to thank my committee members, Dr. Karen Viskupic and Dr. Craig White for their valuable suggestions, assistance, and encouragement throughout my master's program.

Dr. James Crowley, Debra Pierce, and Dr. Paul Olin were instrumental in the collection of data. Without their instruction and patience, this thesis would not have been completed. I would also like to thank the Washington State University Radiogenic Isotope and Geochronology Laboratory for assistance in data collection.

The Department of Geosciences at Boise State is an incredibly friendly environment. A thank-you is owed to the students, staff, and professors who make it a space that encourages learning and exploration, as well as a place to find good conversation and fun people. I thank the members of the Geosciences department for making it easy and enjoyable for me to come to work each day. The National Science Foundation GK-12 program and the Department of Geosciences at Boise State University provided funding for this research.

And finally, I thank my parents, siblings, and fiancé, for their unwavering support throughout my master's program.

ABSTRACT

Granulite xenoliths erupted in Neogene basalts, and a rare outcrop of Precambrian basement along the northern margin of the Snake River Plain (SRP), can be used as windows into the origin and stabilization of the lower crust of southern Idaho. Previous work to determine the nature of the lower crust beneath the Snake River Plain was conducted on a suite of xenoliths exposed in Southern Idaho at Square Mountain (SM), Craters of the Moon National Monument and Preserve (CRMO), and the Spencer-Kilgore (SK) area (Leeman, 1979; Leeman et al., 1985; Matty, 1984; Wolf et al., 2005), as well as on a basement outcrop at House Mountain, near Mountain Home, ID (Alexander, 2006). This study uses U/Pb geochronology and Hf isotope geochemistry to determine the history of formation and stabilization of the lower crust of the SRP within the context of other surrounding Precambrian basement terranes of North America.

Results of this investigation reveal that two distinct terranes comprise the lower crust of Southern Idaho. The Kilgore-Craters terrane formed and stabilized >2.7 Ga and the Square Mountain terrane at >2.5 Ga. Hf isotope ratios and U-Pb geochronology of inherited cores of zircons reveal that the Snake River Plain formed in part from older, reworked crust. Archean geologic events and Hf signatures of the Snake River Plain match those of the Wyoming Province, indicating the Snake River Plain is a westward extension of the Wyoming Province. The Kilgore-Craters terrane is equivalent to the

northern Beartooth-Bighorn magmatic zone and the Montana Metasedimentary province area, and the Square-Mountain/Grouse Creek terrane is a westward extension of the Southern Accreted Terranes of the Wyoming Province.

TABLE OF CONTENTS

ACKNOWLEDGEMENTS	iv
ABSTRACT	v
LIST OF TABLES	x
LIST OF FIGURES	xi
LIST OF EQUATIONS	xv
CHAPTER ONE: FORMATION AND STABILIZATION OF THE SNAKE RIVER PLAIN, IDAHO	1
Introduction	1
Geologic Background	7
Sample Materials	8
Spencer-Kilgore	9
Craters of the Moon National Monument and Preserve	11
Square Mountain	13
House Mountain	14
Analytical Methods	15
U/Pb Geochronology	15
Laser Ablation Inductively Coupled Mass Spectrometry	18
Identifying Age Populations and Calculating Ages	19
Results	22
Spencer-Kilgore	22

Craters of the Moon National Monument and Preserve	31
Square Mountain	42
House Mountain	48
Discussion	52
The Use of Trace Element Geochemistry	52
Use of Ti-in-Zircon	56
Formation of the Kilgore-Craters Terrane	57
Neoarchean Metamorphism of the Kilgore-Craters Terrane	64
Boundaries of the Kilgore-Craters Terrane	67
Formation of the Square Mountain Terrane	68
Boundaries of the Square Mountain Terrane	71
Paleogene Reactivation	72
Conclusion	74
CHAPTER TWO: THE SNAKE RIVER PLAIN AND THE WYOMING CRATON	76
Introduction	76
Geologic Background	78
Wyoming Province	78
Sample Materials	82
Analytical Methods	82
Zircon $^{176}\text{Hf}/^{177}\text{Hf}$ Ratio Analysis	82
Zircon U/Pb Geochronology	86
Results	88

Hf Isotope Analysis	88
Discussion	97
Recycled Crust in the Lower Crust of the Snake River Plain	97
The Eastern Snake River Plain and the Wyoming Craton	98
Open System Zircon Growth During the Paleogene	100
REFERENCES	103
APPENDIX	114

LIST OF TABLES

Table 1:	Rock types and mineralogy of samples collected in all field areas	10
Table 2:	Lower crust of the Snake River Plain zircon growth events	59
Table 2:	(cont.) Lower crust of the Snake River Plain zircon growth events ..	60
Table 3:	Epsilon Hf results for samples from Spencer Kilgore, Craters of the Moon, and Square Mountain. If an analysis from WSU did not record a U/Pb age, an age from the same crystal and growth domain from BSU analysis was used, and is in italics	93

LIST OF FIGURES

Figure 1:	Location map of the sample areas for this study, and the surrounding Archean terranes and provinces. Sample locations for this study are marked with red stars. HM = House Mountain; SM = Square Mountain; CRMO = Craters of the Moon National Monument and Preserve; SK = Spencer Kilgore; Grey areas are outcroppings of Archean rock. Modified from Foster et al. (2006), Chamberlain et al. (2003), Frost and Mueller (2006) and Gaschnig et al. (2013)	6
Figure 2:	Photomicrograph of sample SK11-02. Samples collected from Spencer-Kilgore are mostly charnokites, composed of qtz + fsp + pyx + op. Sample SK11-07 also contains garnet	11
Figure 3:	Photomicrographs of CRMO11-05. Xenoliths collected from Craters of the Moon are either charnokites (qtz + fsp + pyx + op) or are granites (qtz + fsp + am).....	12
Figure 4:	Photomicrograph of SM10-C3. Three of the five samples collected at SM are charnokites (qtz + fsp + pyx + op). One sample is a granite (SM10-C4) and one sample is a metagabbro (SM10-C1)	14
Figure 5:	Linearized probability plot. To determine the age of a zircon growth event within a sample, spots with a discordance of greater than 30% (SK, CRMO and HM) or 40% (SM) are discarded. A linearized probability plot is then used to discard outliers due to ancient Pb loss and inheritance. A linearized probability plot is similar to a gaussian curve (a) but uses cumulative probability (b) to display a regression through data that represents a single Gaussian distribution (c). Outliers, shown in hollow circles, are discarded. The dates of filled circles are averaged with errors weighted to determine the age of the event (d).	21
Figure 6:	Examples of CL images from Spencer-Kilgore samples. Paleoarchean dates, indicated with a 1, are recorded in cores of grains. Mesoarchean dates, indicated with a 2, are recorded in domains with oscillatory and blurred oscillatory zoning, as well as domains with no zoning. All samples contain grains recording Mesoarchean dates. Neoarchean dates, indicated with a 3, are overgrowths and grains that do not exhibit zoning	23

Figure 7:	Ages of zircon crystallization in samples from Spencer Kilgore and Craters of the Moon. Grey boxes indicate episodes of igneous activity, perhaps related to orogenic cycles during the growth of the North American continent. Error bars are 2σ	24
Figure 8:	A normal REE pattern for zircon crystalized in a continental crust environment. REE patterns for both igneous and metamorphic zircons record enrichment in HREE (Eu, Gd, Tb, Dy, Ho, Er, Tm, Yb, Lu) and depletion in LREE (La, Ce, Pr, Nd, Pm, Sm) (a). The slope of enrichment of HREE can be displayed by dividing the concentration of Gd by the concentration of Yb (b). In continental crust environments, zircon records a positive Ce anomaly (a) due to the presence of oxygen. If zircon grows in the presence of plagioclase, a negative Eu anomaly is recorded (a). The intensity of the Eu anomaly can be displayed by dividing Eu by radiogenic Eu (Eu*) (b)	27
Figure 9:	Trace element and trace element ratio plots for SK11-01 and SK11-08	28
Figure 10:	Trace element and trace element ratio plots for SK11-07, SK11-01 and SK11-02	29
Figure 11:	Ti-in-Zr temperatures recorded in zircons from Spencer-Kilgore and Craters of the Moon. Samples are listed in order of decreasing means. Dots are the median temperatures for each sample. Samples without dots recorded only two temperatures	30
Figure 12:	Examples of CL images and age growth domains from CRMO samples. Paleoproterozoic dates (1) are recorded in cores of grains. Mesoproterozoic dates (2) are recorded in grains with no zoning or with blurred oscillatory zoning. Neoproterozoic dates (3) are recorded in grains and overgrowths with no zoning, as well as in the cores of the grains that also record a younger Neoproterozoic growth (4). Paleogene dates (5) were recorded in three granitoid samples, all in domains with oscillatory zoning, as well as an overgrowth and an individual grain with no zoning in one Archean sample	32
Figure 13:	Trace element and trace element ratio plots for CRMO11-03, CRMO11-04, and CRMO11-19	37
Figure 14:	Trace element and trace element ratio plots for CRMO11-01, CRMO11-07, and CRMO11-13	38
Figure 15:	Trace element and trace element ratio plots for CRMO11-05, CRMO11-12, and CRMO11-14	39

Figure 16:	Trace element and trace element ratio plots CRMO11-16 and CRMO11-17	40
Figure 17:	Trace element and trace element ratio plots for CRMO11-15 and CRMO11-18	41
Figure 18:	Examples of CL images from SM. Paleoproterozoic and Mesoproterozoic dates (1) were recorded in the cores of samples and in samples with low uranium and no zoning. Neoproterozoic dates (2) are recorded in zircon growth domains with oscillatory zoning and with a mottled pattern. Mottling often cuts across oscillatory zoning, which is preserved in the tips of many grains. Paleogene dates (4) are recorded in oscillatory overgrowths of grains in sample SM10-C4	43
Figure 19:	Trace element and trace element ratio plots of SM10-A3 and SM10-C3	46
Figure 20:	Trace element and trace element ratio plots of SM10-C2 and SM10-C4	47
Figure 21:	Examples of CL images from HM. Paleoproterozoic and Mesoproterozoic dates (1) are recorded in cores of grains. Neoproterozoic dates (2) are recorded in oscillatory zoned domains and in domains with no zoning pattern. Paleoproterozoic dates (3) are recorded in unzoned domains. Paleogene dates (4) are recorded in domains with oscillatory zoning	48
Figure 22:	Trace element and trace element ratio plots of HM11-01 and HM11-06	50
Figure 23:	Terranes of the lower crust of southern Idaho. The lower crust of Southern Idaho is composed of two terranes; the Kilgore-Craters terrane in the west and the Square Mountain terrane in the east. The Kilgore-Craters terrane stabilized by 2.8 Ga and Square Mountain terrane by 2.5 Ga. The boundary between the two terranes is likely the contact between Paleozoic sediments and Tertiary volcanics and Cretaceous and Tertiary intrusives. This contact also aligns with magnetic anomalies from Sims et al. (2005)	68
Figure 24:	Precambrian crust of Idaho, Wyoming and Montana. The Kilgore-Craters terrane is a westward extension of the northern cratonic core of the Wyoming Province. The Grouse Creek Block and the Square Mountain terrane are extensions of the Southern Accreted Terranes of the Wyoming Province. Gray areas are Archean outcrops. Figure modified	

	from Foster et al. (2006) and Gaschnig et al. (2012), and uses elements of Sims et al. (2005)	77
Figure 25:	A general $^{176}\text{Hf}/^{177}\text{Hf}$ vs Age chart (a) and a general epsilon Hf chart where $^{176}\text{Hf}/^{177}\text{Hf}$ of a sample is normalized to CHUR (b). Lu and Hf are incompatible elements, however Hf is more incompatible than Lu and during mantle melting more Hf enters the melt than Lu. ^{176}Lu decays to ^{176}Hf , resulting in a depleted $^{176}\text{Hf}/^{177}\text{Hf}$ crust and an enriched $^{176}\text{Hf}/^{177}\text{Hf}$ mantle (a). Zircon easily incorporates Hf into its structure, due to charge and size, compared to Lu. This results in negligible ingrowth of ^{176}Hf in zircon. Because $^{176}\text{Hf}/^{177}\text{Hf}$ ratios vary only in their 4 th and 5 th decimal places, epsilon Hf notation is used to magnify differences between ratios (b). T_{DM} is the time the source melted from the depleted mantle (b)	84
Figure 26:	Stacked probability chart of Precambrian $^{207}\text{Pb}/^{206}\text{Pb}$ ages from Washington State University (WSU) and Boise State University (BSU) for zircons from Spencer-Kilgore (SK), Craters of the Moon (CRMO) and Square Mountain (SM). The same zircons were used in data collection at both institutions. All data collected at WSU are used. Due to the large amount of data collected at BSU, only dates that were not found as outliers were used (see Chapter 1: Methods for details on outliers)	87
Figure 27:	Initial epsilon Hf values for Precambrian aged zircon domains from SK, CRMO and SM, as well as for inherited zircons from the S. Atlanta lobe of the Idaho Batholith (Gaschnig et al. (2012)). Black outlined fields are results from σ zircons from Snake River Plain xenoliths analyzed by Dufrane et al. (2007). Open shapes are interpreted to be ages of inherited zircon growth domains, dark filled shapes to be ages of igneous growth zones, and dark outlined and light filled shapes to be ages of metamorphic growth	89
Figure 28:	Regression of $\epsilon_{(\text{Hf})}$ values for igneous growth zones to the timing of when source melt separated from the mantle (T_{DM}). Shaded polygons indicate the epsilon Hf values of the melt from which the zircons crystallized, based on average mid-crustal concentrations. A younging of depleted mantle ages is seen from the west (SK) to the east (SM). SK and CRMO share very similar epsilon Hf values, as well as DM ages. Depleted mantle curve assumes a $^{176}\text{Lu}/^{177}\text{Hf}$ ratio of 0.038130, and a $^{176}\text{Hf}/^{177}\text{Hf}$ ratio of 0.2832	92
Figure 29:	A new configuration of the Wyoming Province. The Wyoming Province can be split into two zones, one that is older than 2.8 Ga and one that is older than 2.5 Ga	101

LIST OF EQUATIONS

Equations 1-3: U/Pb decay schemes	15
Equation 4: $^{207}\text{Pb}/^{206}\text{Pb}$ age	17
Equation 5: ε_{Hf} notation	83

CHAPTER ONE: FORMATION AND STABILIZATION OF THE SNAKE RIVER PLAIN, IDAHO

Introduction

There has long been a question mark as to the basement structure of southern Idaho and its context in the formation of the North American continent (e.g. Leeman, 1979; Armstrong, 1977; Chamberlain et al., 2003; Wolf et al., 2005; Frost and Mueller, 2006; Foster et al., 2006; Sims et al., 2005; Gaschnig et al., 2012). This is in large part due to a thick covering of lava erupted during Miocene hotspot propagation and associated Neogene Basin and Range subsidence and sedimentation (Suppe et al., 1975; Rogers, 1990; Brott et al., 1981; Blackwell et al., 1992; McQuarrie and Rodgers, 1998), making it difficult to study the crystalline basement of the region. However, granulite xenoliths erupted in Neogene basalts of the Eastern Snake River Plain (ESRP) and occasional Precambrian outcrops at the uplifted southern margin of the Idaho Batholith can be used as windows into the origin and stabilization of the crystalline basement of southern Idaho.

Previous work to determine the nature of the deep crust beneath the Snake River Plain (SRP) was conducted on a suite of xenoliths erupted in Neogene basalts at Square

Mountain (SM), Craters of the Moon National Monument and Preserve (CRMO), and the Spencer-Kilgore (SK) area (fig 1). The xenoliths of the ESRP are dominantly intermediate to felsic granulite gneisses (Leeman, 1979; Matty, 1984; Leeman et al., 1985; this study), and range in size from a few centimeters to over a meter in diameter. Many are banded and exhibit a granoblastic texture. Leeman et al. (1985) presented neodymium and lead isotopic data on ESRP xenoliths that indicated metamorphic ages of 2.8 Ga, supporting preliminary Pb isotopic data from Leeman (1979) that reported Archean ages. A Sm-Nd isochron also suggested an older date of 3.1-3.4 Ga for the protoliths of the xenoliths (Leeman et al., 1985). Wolf et al. (2005) confirmed a range of Archean ages (3.5 Ga to 2.5 Ga) using LA-ICPMS zircon analyses.

Jacob (1985) and Alexander (2007) identified Precambrian outcrops on the uplifted southern margin of the Atlanta lobe of the Idaho Batholith, north of Mountain Home, Idaho. This is the westernmost Precambrian exposure that has been identified in southern Idaho. Three dominant gneissic lithologies were identified in outcrop: a bimodal suite of banded tonalite and amphibolite orthogneisses and a muscovite bearing paragneiss, which together were mapped as Orthogneiss B (Jacob, 1985; Alexander 2007).

Although it has been known for decades that the deep crust of the ESRP is likely Archean (Leeman, 1979; Leeman, 1985; Wolf et al., 2005), there has been no comprehensive geochronological study of the xenoliths and the Precambrian history they record. The first aim of this study is to use *in situ* geochronology, trace element geochemistry, and CL maps of zircons to interpret the protolith formation, metamorphism and inheritance patterns of a large suite of granulite xenoliths, and establish whether and

how their ages vary throughout the SRP. This information will clarify how the ESRP xenoliths compare to the basement beneath the western extent of the SRP via the study of the westernmost outcrops of Precambrian gneisses at House Mountain.

The second focus of this study is to interpret how the crystalline basement of southern Idaho correlates to surrounding provinces, in particular the Precambrian terranes mapped in the adjacent Wyoming Province. The western margin of the Wyoming Province has been poorly constrained due to lack of outcrop, and it has been suggested that the western margin may extend into the ESRP (Wolf et al., 2005). Alternatively, to the south of the SRP lies the Archean Grouse Creek Block and to the north of the ESRP lies the Selway Terrane, composed of juvenile arcs that helped to suture Archean provinces during the Trans-Hudson orogen (Foster et al., 2006). It is possible that the basement beneath southern Idaho to be composed of one or more distinct microcontinents, is an integral part of the nearby Wyoming province, or is a combination of distinct microcontinents and sections of surrounding provinces.

Uranium-lead geochronology of zircon crystals is the ideal tool to use when investigating Precambrian-aged rocks due to the long half-life of uranium, the incorporation of uranium into zircon to the exclusion of lead, the slow diffusion rates of both uranium and lead in the zircon lattice, the ubiquity of zircon in intermediate to felsic granitoids, and the participation of zircon in metamorphic reactions. Internal domains of zircons can be identified by cathodoluminescence imaging, and dated *in situ* using laser ablation inductively coupled plasma mass spectrometry (LA-ICPMS). Dating numerous zones in a zircon creates a timeline of the zircon's growth, which can be used as a proxy for the geologic history of the rock it is sourced from. Rare earth element and other

incompatible trace element concentrations are collected at the same time as U/Pb data, and can be used in identifying populations within samples, which sometimes correlate to geologic events. Trace element chemistry is also useful in recognizing the petrologic setting of zircon crystallization. In this study, zircons were extracted from approximately 30 ESRP xenoliths and from outcrops at House Mountain.

To determine how the geologic history of the Snake River Plain compares to surrounding Archean provinces, hafnium (Hf) isotope data were collected. The unstable radionuclide ^{176}Lu decays to stable ^{176}Hf by β - decay, creating an isotope tracer that can be used in several applications. Isotopes can trace crust formation and differentiation because Lu-Hf fractionation occurs during magma generation (Patchett et al., 1981, Kinny and Maas, 2003). Both Lu and Hf are incompatible elements, however, Hf is more incompatible than Lu. During melting, more Hf enters the melt than Lu creating a crust with lower time integrated Lu/Hf and $^{176}\text{Hf}/^{177}\text{Hf}$, and a complementary high Lu/Hf, high $^{176}\text{Hf}/^{177}\text{Hf}$ residual mantle (Patchett et al., 1981). In zircon, Hf readily substitutes for zirconium (Zr) because of their similar size and charge, while Lu does not easily enter into the crystal lattice, producing an even more severe fractionation of Lu and Hf in zircon. This results in a very low Lu/Hf ratio in zircons, so low that the amount of ^{176}Lu that decays to ^{176}Hf is negligible. Thus, the initial $^{176}\text{Hf}/^{177}\text{Hf}$ ratio of the source environment is preserved in the zircon. This initial ratio can be used to calculate a model age, and if a crystallization age of the zircon is known, the epsilon(Hf) value can be calculated and compared in a crustal evolution diagram. Hf data for this study were collected at Washington State University by in-situ laser ablation of the same zircons used for U/Pb analysis.

The results of this study reveal that two distinct terranes comprise the lower crust beneath the SRP. The eastern Kilgore-Craters terrane stabilized by 2.7 Ga and the western Square Mountain terrane stabilized by 2.5 Ga. Negative epsilon(Hf) values were calculated for both of these terranes, indicating the lower crust of the SRP formed from recycled crust. The Southern Accreted Terranes of the Wyoming Province share stabilization ages with the Square Mountain terrane, as well as a signature of recycled crust, with the Square Mountain terrane and the Grouse Creek Block. We propose the Square Mountain terrane is a northward extension of the Grouse Creek Block, and both comprise a westward extension of the Southern Accreted Terranes.

The Kilgore-Craters terrane shares a crustal evolution and stabilization history with the Montana Metasedimentary province and the Beartooth-Bighorn magmatic zone of the Wyoming Province. We interpret the Kilgore-Craters terrane to be a western extension of the northern Wyoming Province.

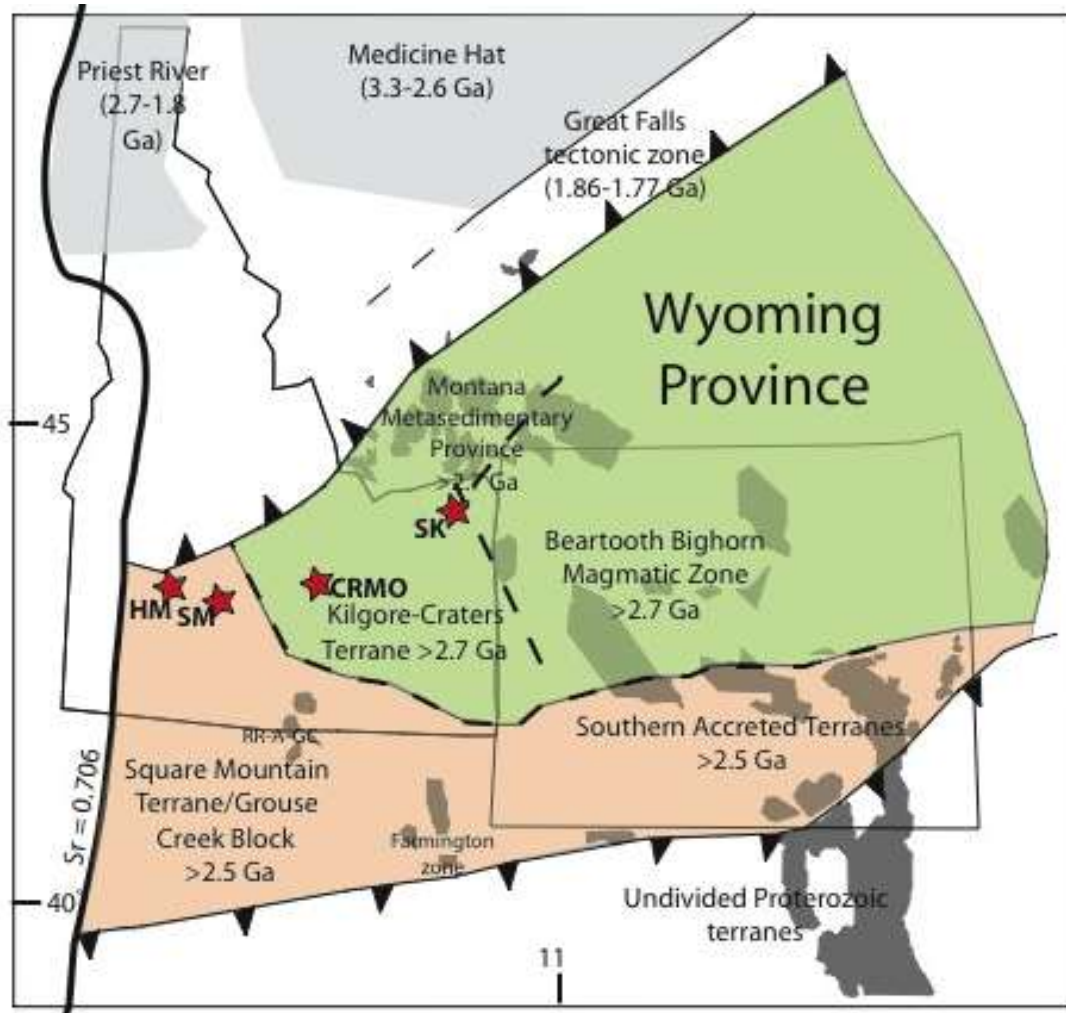


Figure 1: Location map of the sample areas for this study, and the surrounding Archean terranes and provinces. Sample locations for this study are marked with red stars. HM = House Mountain; SM = Square Mountain; CRMO = Craters of the Moon National Monument and Preserve; SK = Spencer Kilgore; Grey areas are outcroppings of Archean rock. Modified from Foster et al. (2006), Chamberlain et al. (2003), Frost and Mueller (2006) and Gaschnig et al. (2013).

Geologic Background

The Snake River Plain is a broad arcuate topographic depression stretching from the Columbia River Plateau in Oregon to the Yellowstone Plateau at the Montana/Wyoming/Idaho border (fig. 1). The Snake River Plain can be split into western and eastern segments with distinct geologic histories. The Western Snake River Plain (WSRP) is graben bounded by normal faults (Malde, 1991; Wood and Clemens, 2002) related to Basin and Range extension (Suppe et al., 1975). The Eastern Snake River Plain (ESRP) is a down-warped basin characterized by bimodal volcanism related to the passage of the northeast trending Yellowstone Hotspot and Basin and Range extension (Pierce and Morgan, 1992; Leeman, 1982; Malde, 1991). Explanations of subsidence of the ESRP include extension (Rogers, 1990; Brott et al., 1981; Blackwell et al., 1992) and subsequent mid-crustal mafic intrusions (McQuarrie and Rodgers, 1998).

Exposures on the ESRP include Quaternary rhyolite and basalt. The bimodal volcanism has been attributed by many to be the result of the passage of a mantle plume (ex. Minster et al., 1974; Suppe et al., 1975; Richards et al., 1989; Wilson, 1990; Malde, 1991). The current day manifestation of this plume is theorized to be the Yellowstone Hotspot, beneath Yellowstone National Park (Pierce and Morgan, 2006). The flat expanse of the Eastern Snake River Plain formed as the North American plate moved southwest over the Yellowstone Hotspot, from McDermitt Field in Nevada (17 Ma) to the Yellowstone Plateau volcanic field (2.05 Ma) (Pierce and Morgan, 1992). The line of volcanic centers is termed the Yellowstone Hotspot track. There are also many hypotheses that do not attribute the Miocene volcanism of the ESRP to a mantle plume.

These hypotheses include the idea that volcanism is a result of complex multi-source magma chambers across the SRP (Bonnichsen et al., 2009), that volcanism is a result of an axis of granite batholiths across southern Idaho caused from decompression melting during extension (Christiansen, 2001), and that the source of hotspot volcanism is upwelling around a deep and fragmented down-going oceanic plate (James et al., 2011).

The Yellowstone Hotspot track cuts Basin and Range extensional structures surrounding the Eastern Snake River Plain. Extension in the ESRP has taken the form of ongoing normal faulting (Rodgers, 1990) and fissure eruptions of basalt throughout the ESRP. The only active fissure, the Great Rift, is protected by the National Park Service and the Bureau of Land Management as a National Monument and Preserve. This fissure trends northwest-southeast, parallel to Basin and Range faulting in the mountains to its north. Basalt has erupted along the plain for millions of years (Champion, 2012) and has produced over a mile thick package of lava in some areas. Together, Yellowstone Hotspot volcanism and Neogene basalt eruptions have formed a thick covering over the basement rock of Snake River Plain.

Sample Materials

For this study, thirty-two crustal orthogneiss and granite xenoliths were collected from the northern margin of the Eastern Snake River Plain, Idaho, at Square Mountain (SM), Craters of the Moon National Monument and Preserve (CRMO), and Spencer-Kilgore (SK) (fig. 1; table 1). The protoliths of the gneisses are igneous, as indicated by a mineralogy of quartz, feldspar, and pyroxene, and the lack of an aluminosilicate. Samples

were collected from outcroppings of both orthogneiss and paragneiss at House Mountain, north of Mountain Home, Idaho. The House Mountain site was chosen because it is the only known outcrop of Precambrian rock on the northern margin of the SRP, and extended the study laterally into the Western SRP. These sample sites were chosen to create an east-west transect across the northern margin of the Snake River Plain (fig. 1). The northern margin is the most accessible margin of the plain, making these sites ideal. The xenolith sites have been used in past studies and results from this study were related and compared to existing data.

Spencer-Kilgore

The eastern-most sample location is a quarried cinder cone between the villages of Spencer and Kilgore. The cone is found on the west side of A2 county road, north of the intersection with Red Road. The basalt cinder cone is named Crystal Butte after the ubiquitous, large feldspar crystals found in the deposit. Xenoliths make up less than 1% of the outcrop, and are found as small (≤ 7 cm) loose fragments where quarrying has exposed them.

The xenoliths found in this locality are charnokites, with one exception of a garnet rich gneiss (fig. 2). In this study, all rocks with a $qtz + fsp + opx \pm cpx$ composition were classified as charnokites, after Le Maitre (1989). The garnet gneiss is composed of $qtz + pl + opx + grt$. All rocks in this area are compositionally banded. Leeman (1975) and Matty (1985) also collected and described xenoliths from Crystal Butte, as well as from Swan Butte, another small cinder cone in the Spencer-Kilgore (SK) area. Leeman (1975)

Table 1: Rock types and mineralogy of samples collected in all field areas

Field area	Sample name	Type of rock	Modal mineralogy	Diameter (cm)
Spencer-Kilgore	SK11-01	two-pyx charnokite	qtz + pl + opx + cpx + op	9
	SK11-02	two-pyx charnokite	qtz + pl + kfs + opx + cpx	6
	SK11-03	charnokite	qtz + pl + opx + op	5
	SK11-07	garnet granulite	qtz + pl + op + grt	5
	SK11-08	granulite	qtz + fsp + op	4
Craters of the Moon	CRMO11-01	charnokite	qtz + pl + opx + melt	8
	CRMO11-03	granite	qtz + pl + melt	7
	CRMO11-04	granite	qtz + pl + kfs + am	7
	CRMO11-05	charnokite	qtz + pl + kfs + opx + op + bt	3
	CRMO11-10	granulite	qtz + fsp + px	4
	CRMO11-11	granulite	qtz + kfs + pl + px	7
	CRMO11-12	granulite	qtz + fsp + px	7
	CRMO11-13	granulite	qtz + pl + px	4
	CRMO11-14	granulite	qtz + pl + px	6
	CRMO11-15	charnokite	qtz + pl + opx	15
Square Mountain	CRMO11-16	charnokite	qtz + pl + op + opx	9
	CRMO11-17	charnokite	pl + qtz + op opx	12
	CRMO11-18	granulite	qtz + pl + op	10
	CRMO11-19	granite	pl + qtz + op + am	20
	SM10-A3	charnokite	qtz + fsp + px + melt	8
Square Mountain	SM10-C1	gabbro	pl + or + ol + opx + op + lithics	20
	SM10-C2	charnokite	qtz + fsp + melt + opx	10
	SM10-C3	charnokite	qtz + pl + mc + melt + opx	10
	SM10-C4	granite	qtz + pl + mc + melt	8
House Mountain	HM11-01	orthogneiss	qtz + fsp + opx + amp	N/A
	HM11-06	paragneiss	qts + fsp + mus + amp	N/A

described these xenoliths as charnokites, and Matty (1984) used the I.U.G.S system (Steckeisen, 1976) to classify charnokitic rocks as norite, enderbite, opdalite, or charnokite depending upon quartz content. Gabbroic cumulate xenoliths were also described by Matty (1984), but were not found at SK in this study. As this site is an active quarry, the abundance and type of xenoliths found depends on what has been recently exposed.

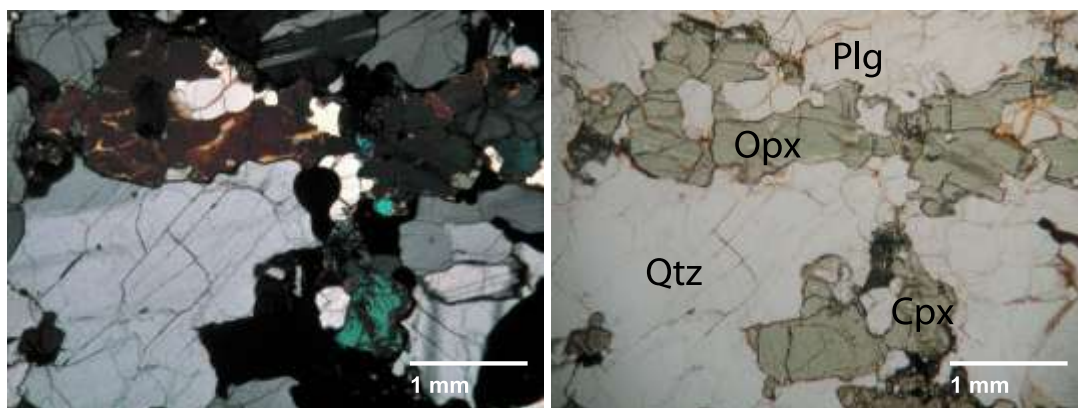


Figure 2: Photomicrograph of sample SK11-02. Samples collected from Spencer-Kilgore are mostly charnokites, composed of $qtz + fsp + pyx + op$. Sample SK11-07 also contains garnet

Craters of the Moon National Monument and Preserve

The second sample locality is Craters of the Moon National Monument and Preserve (CRMO). The CRMO visitor's center is located 18 miles southwest of Arco, Idaho on highway 20/26/93, but the Monument itself is much larger. CRMO encompasses three late Pleistocene-Holocene lava fields erupted along the Great Rift, a volcanic fissure. All xenoliths in this location were collected from the Craters of the Moon lava field, composed of about 60 ferrobasalt and ferrolatite lava flows and 25 volcanic cinder cones, all erupted from the Great Rift (Leeman et al., 1976; Kuntz et al., 2007). Xenoliths were sampled from Grassy Flow ($7,360 \pm 60$ Ka), Big Cinder Flow

($2,400 \pm 300$ Ka), North Crater Cinder Cone ($\sim 2,500$ Ka) and Big Cinder Butte (~ 6000 Ka). Xenoliths make up much less than 1% of flows. Grassy Flow has the most abundant and largest xenoliths.

The crustal xenoliths of CRMO collected in this study are in the majority gneisses and almost all are charnokites (qtz + fsp + px). Most samples exhibit modal layering, and all exhibit grain boundary migration and/or grain boundary bulging indicating high grade metamorphism. Several igneous textured granitoid xenoliths were also collected from North Crater Cinder Cone and Grassy Flow, and have a composition of qtz + fsp \pm hbl \pm op.

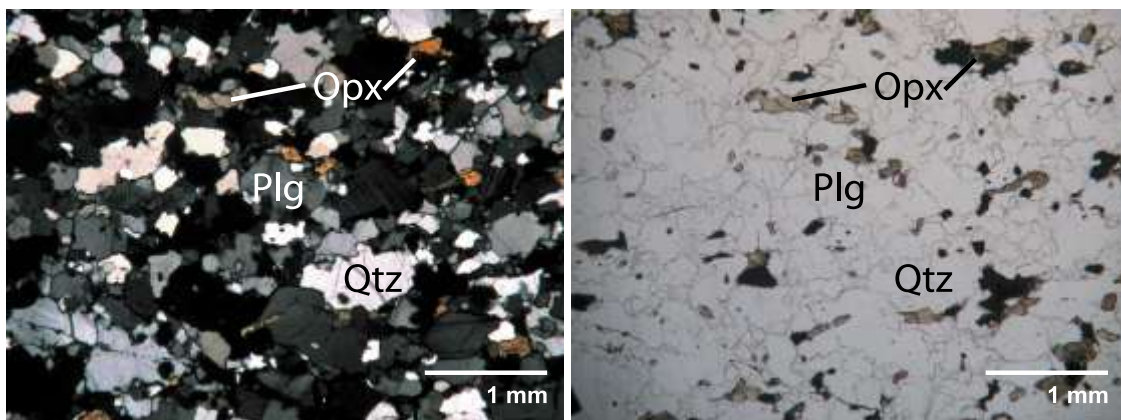


Figure 3: Photomicrographs of CRMO11-05. Xenoliths collected from Craters of the Moon are either charnokites (qtz + fsp + pyx + op) or are granites (qtz + fsp \pm am).

Previous studies also identified charnokites as the main xenolith composition in this area (Leeman, 1975; Matty, 1984). Samples collected by Matty (1984) were from the Serrate-Devils Orchard flow, a flow not investigated in this study. He described these xenoliths as charnokites, with the exception of one biotite garnet gneiss. Surprisingly, the xenoliths found in the Serrate-Devils Orchard flow were described by Matty as small and

friable. In this study, the samples from CRMO are the largest, freshest, and least friable of samples collected, regardless of the flow they were found in.

Square Mountain

Square Mountain (SM) is located northeast of Fairfield, Idaho on the east side of Croy Creek Road and Camp Creek drainage. The host rock of SM xenoliths is a hybrid lava containing both quartz and olivine. It is named the Square Mountain basalt (Schmidt, 1961) and erupted from the Magic Reservoir Caldera 6-3 Ma (Leeman et al., 2004). Numerous small, thin xenoliths averaging 3 cm in length can be found in the talus slopes of the west side of the mountain. More spectacular xenoliths with long axes over a meter in length are found locally composing 10% of the outcrop on the southeast facing slope. Xenoliths sampled for this study are charnokites and one metagabbro (sample SM10-C1). The Matty (1984) study described the xenoliths in this area as locally composing up to 50% of the outcrop, including both whitish and pinkish xenoliths. Only whitish xenoliths (with the exception of the dark cumulate) were seen during collection for this study. It is likely that many of the pinkish xenoliths have been collected during past field trips, also explaining the decrease in outcrop coverage.

Samples SM10-A3, SM10-C2, SM10-C3 have a major mineral assemblage of qtz + fsp + pyx + ox and are modally layered. SM10-C4 is a granite, and SM10-C1 is a cumulate metagabbro. Grain boundary migration is evident in thin sections of all gneissic samples. The host magma infiltrated the samples to varying degrees, and partial melting of the samples is seen at the boundary between basalt and xenolith.

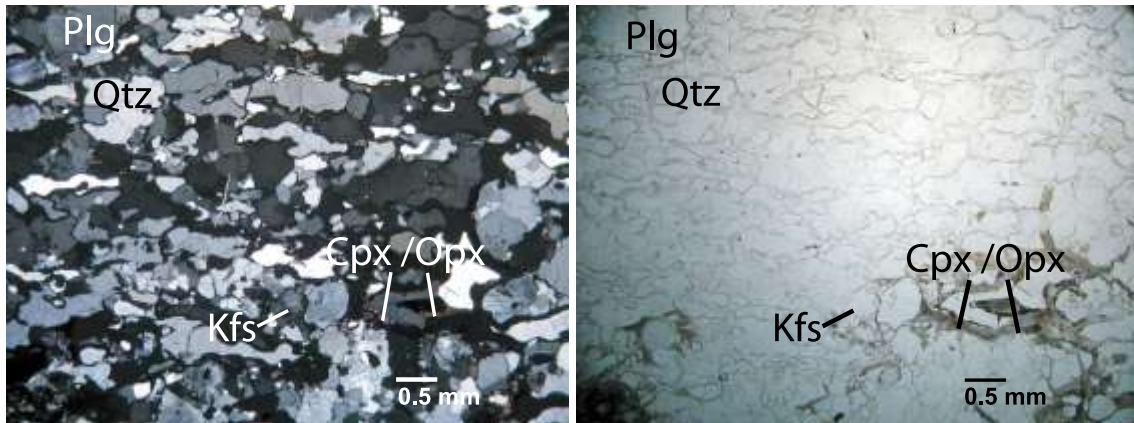


Figure 4: Photomicrograph of SM10-C3. Three of the five samples collected at SM are charnockites (qtz + fsp + pyx + op). One sample is a granite (SM10-C4) and one sample is a metagabbro (SM10-C1).

House Mountain

Outcrops of Precambrian amphibolite-facies gneisses have been reported at House Mountain (HM) near Mountain Home, Idaho (Jacob, 1985; Alexander, 2006). An outcrop section of this unit, informally named Orthogneiss B by Jacob (1985), was sampled along the Cow Creek drainage south of the South Fork Boise River. Within the studied section of House Mountain Orthogneiss B, three dominant gneissic lithologies were identified: a bimodal suite of layered tonalite orthogneiss and amphibolite orthogneiss structurally overlain by a muscovite bearing paragneiss. The section exposed is 33 meters thick, with 31.5 meters of the outcrop bimodal orthogneisses.

The tonalite gneiss is composed mostly of quartz, feldspar and hornblende, and in places contains boudins of the darker amphibolite gneiss. Both layers of the orthogneiss contain a foliation that strikes 275° and dips $20\text{-}30^\circ$ to the southwest. The amphibolite gneiss has more intense foliation. A fault separates the orthogneisses into a section dominated by tonalite bands below and a section dominated by amphibolite bands above.

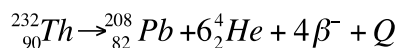
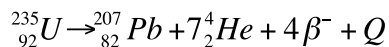
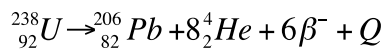
A pegmatite fills in the sub-vertical fault, cuts the gneisses, and extends laterally as sills into both the upper and lower sections. The pegmatite contains layers concordant to foliation, indicating it was emplaced pre- to syn- deformation. The paragneiss is exposed structurally above the orthogneiss, is a finely layered, peraluminous gneiss composed of qtz + fsp + mus + am. Large augens interpreted as relict quartz pebbles are conspicuous. The thickness of this layer is unknown, as outcrop becomes covered in vegetation after a few meters. Of these lithologies, the tonalite orthogneiss and the paragneiss proved to have sufficient zircon crystals to analyze; the amphibolite orthogneiss did not.

Analytical Methods

U/Pb Geochronology

In this study, uranium (U) and lead (Pb) isotopes in zircon were analyzed to date the collected xenoliths. Uranium has three radioactive isotopes, ^{238}U , ^{235}U , and ^{234}U , all of which can be used as geochronometers. ^{234}U is a radiogenic daughter product of ^{238}U , and thus both isotopes decay to stable ^{206}Pb . Thorium (Th) also has an isotope that decays to Pb and can be used as a geochronometer (equation 1.1-1.3).

Equations 1-3: U/Pb decay schemes



Where Q is the sum of the decay energies of the entire series.

In this study, the ^{238}U and ^{235}U decay schemes were used. ^{238}U decays to ^{206}Pb with a half life of 4.468×10^9 years and ^{235}U decays to ^{207}Pb with a half life of 0.7038×10^9 (Steiger and Jäger, 1977). Both of these decay schemes can be solved independently to give dates of zircon formation, which in turn can be interpreted as ages of geologic events. This dual decay scheme provides an internal “check” on closed system behavior. Theoretically, in a closed system, the date found from the decay of ^{238}U to ^{206}Pb should be the same as that found using the $^{235}\text{U}/^{207}\text{Pb}$ scheme. Ahrens (1955) and Wetherill (1956, 1963) developed a graphical procedure to visualize the effect of an open system. Wetherill plotted a curve representing $^{206}\text{Pb}/^{238}\text{U}$ and $^{207}\text{Pb}/^{238}\text{U}$ ratios evolving as a result of time. If U/Pb dates from a sample fall on this curve, they are said to be concordant and can be interpreted as a closed system. If, however, dates fall above or below the line, they are said to be discordant, and are interpreted to be an open system that has been affected by one or more thermal events.

If a series of zircon crystals from one lithology have undergone varying degrees of lead loss (open system), their dates will plot on the concordia diagram to form what is termed a discordia line. If a grain is affected by relatively recent Pb loss, it will plot on a straight line between the timing of crystallization and the origin. Over time, this “lower intercept” will move up the concordia curve, and can be interpreted as the amount of time since Pb-loss. Thus, the upper intercept on a discordia is the timing of crystallization, and the lower intercept is the amount of time that has elapsed since the end of a thermally-induced Pb-loss event. It is important to remember that a zircon can have growth domains that crystallized at different times due to either igneous crystallization or metamorphism. The upper intercept age on a discordia can thus be interpreted as a metamorphic event if a

growth domain or metamorphic zircon is being dated. In this study, almost all the zircons dates were discordant. The potential age of Pb loss is <6 Ma (timing of volcanic activity in the region). This young age will not substantially bias the upper intercept from the calculated $^{207}\text{Pb}/^{206}\text{Pb}$ age, which is insensitive to recent Pb-loss. The equation for the $^{207}\text{Pb}/^{206}\text{Pb}$, or the Pb/Pb age is

Equation 4: $^{207}\text{Pb}/^{206}\text{Pb}$ age

$$\left(\frac{^{207}\text{Pb}}{^{206}\text{Pb}} \right) = \frac{^{235}\text{U} \left(e^{\lambda_{235}t} - 1 \right)}{^{238}\text{U} \left(e^{\lambda_{238}t} - 1 \right)}$$

where λ_{235} is the decay constant for ^{235}U (9.85×10^{-10}) and λ_{238} is the decay constant for ^{238}U (1.55×10^{-10}) and t is the age of the zircon or domain within the zircon. Among the advantages of the Pb/Pb age are that only ratios of isotopes need to be measured, not concentrations, and Uranium ratios do not need to be measured at all because the $^{235}\text{U}/^{238}\text{U}$ is a constant (1/137.8).

Zircon is the ideal mineral for extracting U/Pb geochronology for several reasons. Zircon has a very high closure temperature (+1000°C) for Pb and U diffusion and thus can preserve closed system behavior over billions of years (Cherniak et al., 1997; Cherniak and Watson, 2000). Second, as described previously, it is easily assessed for open or closed system behavior using a concordia diagram (Wetherill, 1956). Third, zircons grow and recrystallize during metamorphic heating events, and record the timing of that event in a new growth or recrystallized domain. The domains of zircons can be used as a record of thermal events that have affected the rock. And fourth, zircon is a

very robust mineral, and will withstand weathering and reheating. Zircon persists through metamorphic and sedimentary processes.

Laser Ablation Inductively Coupled Mass Spectrometry

To prepare for mass spectrometry analysis, zircon crystals were separated from their host rocks using standard density and magnetic methods. Collected samples were crushed using a Bico-Braun “Chipmunk” steel jaw crusher and disk-milled with steel plates. Samples were sieved by size and $< 500 \mu\text{m}$ material was hand washed with water to remove clay-sized particles. After drying and removal of ferromagnetic particles with a hand permanent magnet, a Frantz magnetic separator was used at $1.0 \text{ A}/20^\circ$ to split out the most magnetic material (e.g. oxides, olivine, garnet, altered ferromagnesian minerals) and to reduce the size of the sample. Bromoform heavy liquid separation was used to divide the non-magnetic separates into dense ($>2.8 \text{ g}/\text{cm}^3$) grains, such as zircon and sphene, and lighter ($<2.8 \text{ g}/\text{cm}^3$) grains such as quartz and feldspar. Once dry, dense grains were run through the Frantz magnetic separator at $1.4 \text{ A}/20^\circ$, $1.4 \text{ A}/10^\circ$, and if needed $1.4\text{A}/5^\circ$ to further separate zircon from other minerals and reduce sample size.

The most non-magnetic separates were handpicked for zircons to be analyzed by mass spectrometry. Many of the zircons in this study had magnetic inclusions causing zircon separation at lower magnetic field intensities, and occasionally these separates were also picked for zircon. The largest possible variety in grain morphologies were picked to capture multiple events and styles of growth in the sample’s history. Grains riddled with inclusions were avoided. Most of the picked zircons were annealed at 900°C

for at least 60 hours to enhance cathodoluminescence emission, and with the intention that these zircons could undergo thermal ionization mass spectrometry in a later study.

In order to decide where to place laser analysis spots on grains, black and white cathodoluminescence (CL) images were collected via a scanning electron microscope. To prepare for imaging, picked grains were mounted in epoxy and then polished to reach the centers of the grains. By polishing to the center of grains, a cross section of the grains could be imaged, capturing all domains the zircon may have. CL images were obtained with a JEOL T-300 scanning electron microscope and Gatan MiniCL. Populations of grains based on morphology and growth domains within grains were identified from CL images. Analysis spots were chosen to target as many morphological populations and growth domains as possible.

Laser spots were analyzed for trace elements and U-Th-Pb isotope ratios using the New Wave UP213/X-Series II LA-ICPMS facility at Boise State University. NIST and USGS glasses, and Plesovice and FC-1 zircon standard materials were used for simultaneous acquisition and real-time calibration of trace element concentrations and U-Th-Pb ages on 25-40 micron spot analyses. In-house software was used for data reduction.

Identifying Age Populations and Calculating Ages

Zircon growth ages are interpreted to represent the timing of igneous or metamorphic activity. Populations of growth domains identified first by CL imaging were reassessed following LA-ICPMS by iteratively using CL images, trace element compositions, U/Pb concordia diagrams and $^{207}\text{Pb}/^{206}\text{Pb}$ dates. In some samples, dates

from two populations blend into each other and can be difficult to discern between. However, by comparing trace element compositions and CL images, the boundary between the populations can be determined.

The oldest age population in many zircons is interpreted to be an inherited age. Because it is possible for a sample to have zircons inherited from multiple locations or from sedimentary rocks with multiple protoliths, an average date of the inherited age populations is not appropriate. Mesoarchean and Neoproterozoic ages are interpreted to be zircon growth events from igneous or metamorphic activity. Each sample is treated as having distinct growth events, possibly and likely at different times from other samples. Events that are within a few hundred million years of each other are likely part of the same metamorphic or igneous episode, but occurred at different parts of the episode. The age of a growth event was calculated by taking the error-weighted mean of the $^{207}\text{Pb}/^{206}\text{Pb}$ dates in that population that had less than 40% (SM) or 30% (SK, CRMO and HM) discordance, and that were not outliers on linear cumulative probability plots (fig. 5). Isoplot 3.0 (Ludwig, 2003) was used to create linearized cumulative probability plots, which show a regression through data that represents a single Gaussian distribution. Dates that were interpreted as part of a single distribution were averaged with their errors weighted. Dates that were outliers on cumulative probability plots were interpreted to be biased by ancient Pb loss or inheritance and were not used in determining ages of events. A higher discordance threshold was used for SM because fewer spots were analyzed per sample in this field area, and without a higher threshold not enough dates would have been available to calculate an average date. A population of Cenozoic dates is also recorded in some xenolith samples and interpreted to be igneous crystallization ages, or

growth events during very young metamorphic episodes. The ages of Cenozoic events were calculated as the Precambrian events were, however using $^{238}\text{U}/^{206}\text{Pb}$ dates instead of $^{207}\text{Pb}/^{206}\text{Pb}$ dates, and ignoring discordance. Epoch and age assignments are based on the 2012 GSA timescale (Walker and Geissman et al., 2012).

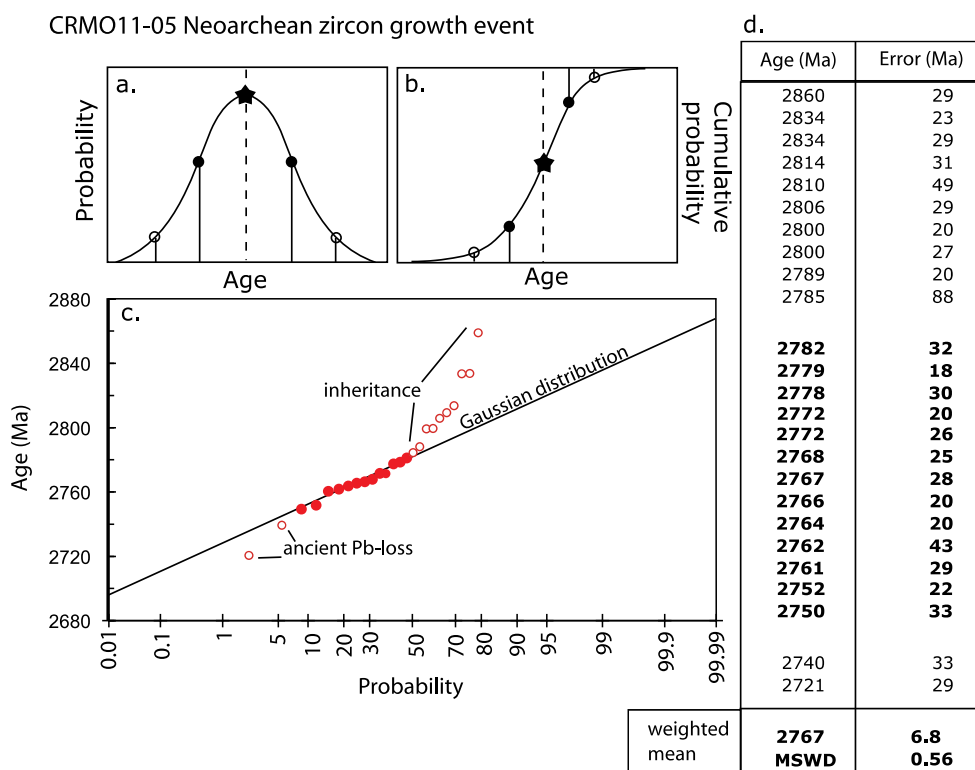


Figure 5: Linearized probability plot. To determine the age of a zircon growth event within a sample, spots with a discordance of greater than 30% (SK, CRMO and HM) or 40% (SM) are discarded. A linearized probability plot is then used to discard outliers due to ancient Pb loss and inheritance. A linearized probability plot is similar to a Gaussian curve (a) but uses cumulative probability (b) to display a regression through data that represents a single Gaussian distribution (c). Outliers, shown in hollow circles, are discarded. The dates of filled circles are averaged with errors weighted to determine the age of the event (d).

Results

Spencer-Kilgore

Petrography

Three samples from this location were petrographically analyzed: SK11-01, SK11-02, and SK11-07. Only a brief description of thin sections is given here. For a more detailed description and mineral percentages for each sample, see appendix A.

SK11-01 and SK11-02 have a major mineralogy of $qtz + fsp + opx + cpx + op$. Both samples are compositionally layered, alternating mafic and felsic bands. These rocks are metamorphic charnockites, or two-pyroxene granulites. SK11-07 has a major mineralogy of $qtz + plg + op + grt$. It is compositionally banded, alternating layers of $qtz + plg$ and $op + grt$. This sample is a garnet granulite.

CL images

Grains from Spencer Kilgore are euhedral but rounded. (fig. 6). CL images differ among samples, however they all have patterns in the images that correlate to comparable age populations. SK11-01, SK11-02 and SK11-03 have similar CL patterns. These samples have two CL populations, cores that are either black or have blurred oscillatory zoning, and overgrowths and discrete grains that are mottled or show no oscillatory zoning. Sector zoning is seen in all samples.

CL images of SK11-07 and SK11-08 exhibit cores and overgrowths, as well as grains with a single domain. The cores in these two samples show blurred oscillatory zoning or no zoning. Overgrowths do not show zoning.

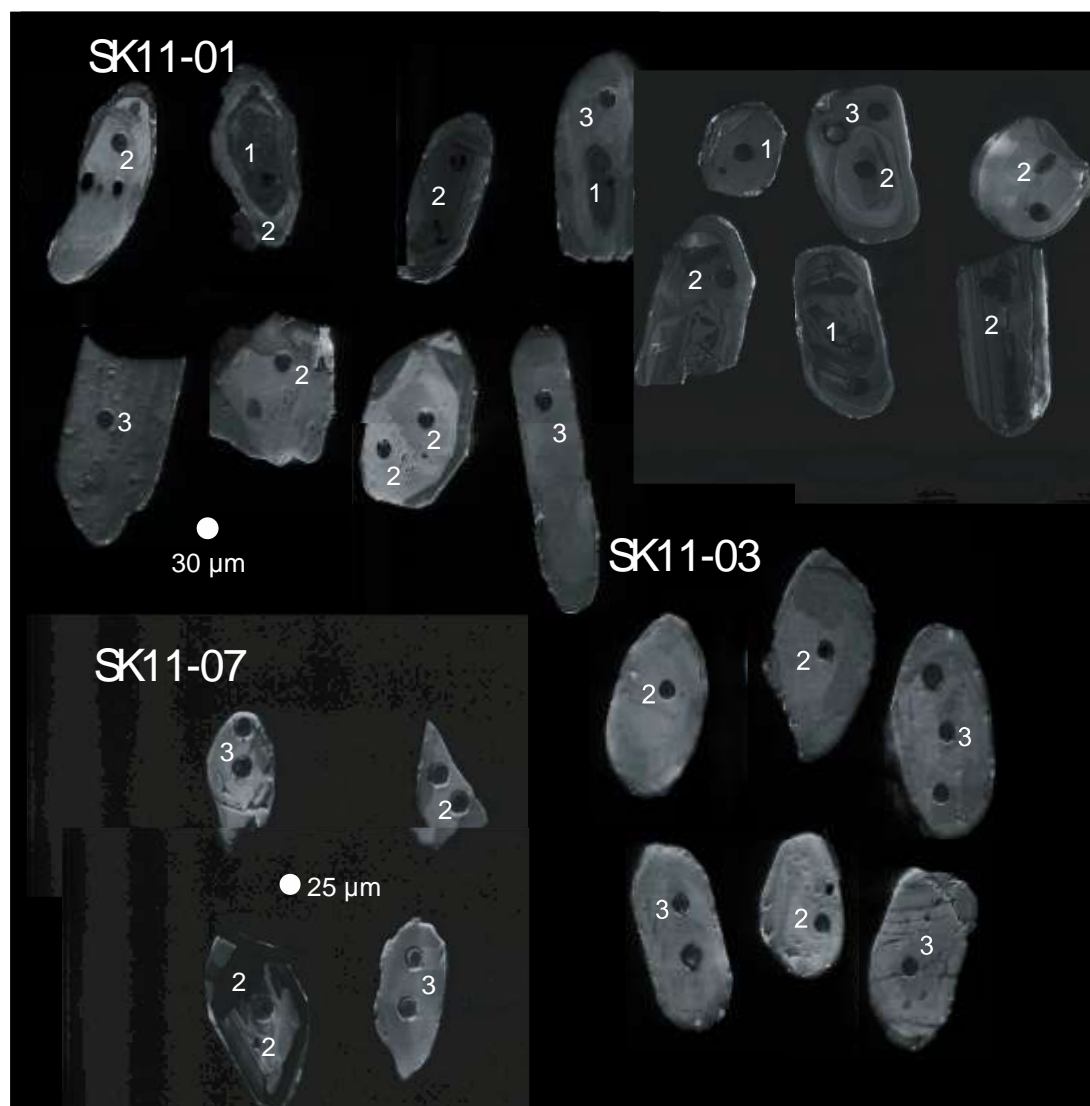


Figure 6: Examples of CL images from Spencer-Kilgore samples. Paleoproterozoic dates, indicated with a 1, are recorded in cores of grains. Mesoproterozoic dates, indicated with a 2, are recorded in domains with oscillatory and blurred oscillatory zoning, as well as domains with no zoning. All samples contain grains recording Mesoproterozoic dates. Neoproterozoic dates, indicated with a 3, are overgrowths and grains that do not exhibit zoning.

U/Pb geochronology

Five samples from Spencer-Kilgore were analyzed by LA-ICPMS for U-Th-Pb dates: SK11-01, SK11-02, SK11-03, SK11-07 and SK11-08. Multiple groupings of dates were recorded in each sample (fig. 6). SK11-01 and SK11-08 recorded a few Paleoproterozoic dates between 3334 ± 33 Ma to 3763 ± 24 Ma. These dates are recorded in cores of grains and in grains with only one growth domain imaged by CL. Mesoarchean and Neoarchean dates were recorded by all SK samples (fig. 6). Mesoarchean and Neoarchean dates are recorded in zircon overgrowths and in grains with only one growth domain. Mesoarchean dates can be split into two groups, with samples recording dates at ~ 3.2 and samples recording younger dates, ~ 3.0 . For full results, see Appendix C.

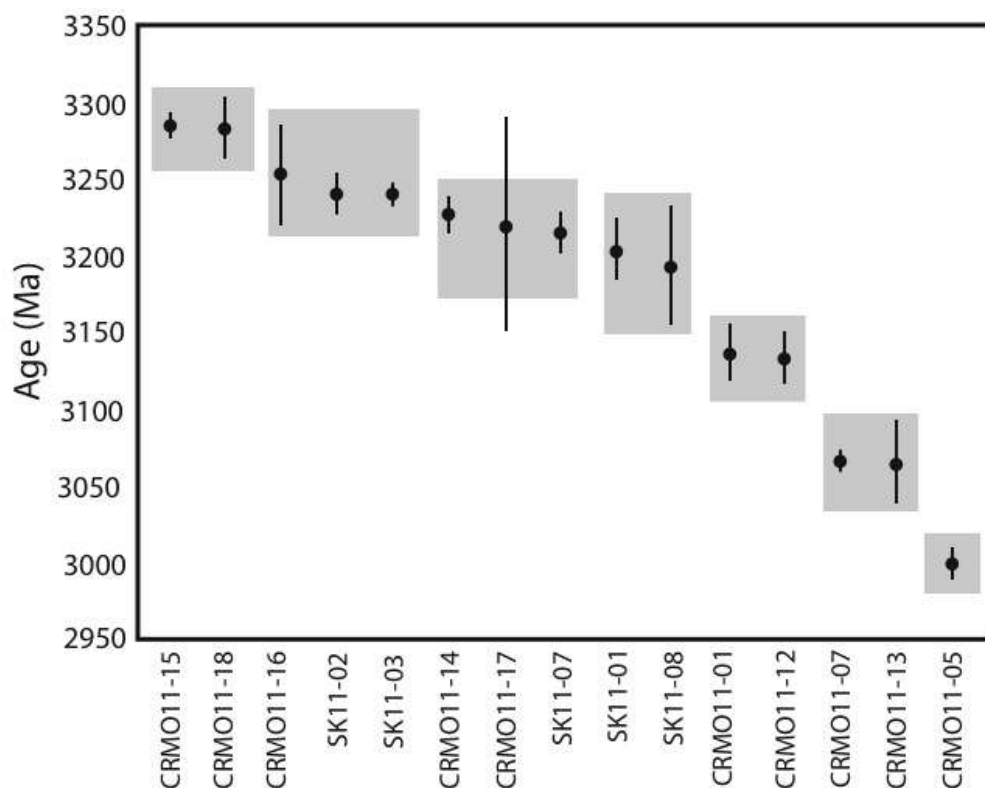


Figure 7: Ages of zircon crystallization in samples from Spencer Kilgore and Craters of the Moon. Grey boxes indicate episodes of igneous activity, perhaps related to orogenic cycles during the growth of the North American continent. Error bars are 2σ .

Trace element geochemistry

Trace element concentrations were collected simultaneously with U/Pb data. REE patterns and other trace element concentrations provide insight into the media that control zircon crystal formation. The partition coefficients for REE in zircon increase with atomic number (Nagasawa, 1970; Hinton and Upton, 1991; Watson, 1980; Thomas et al., 2002; Sano et al., 2002), resulting in a REE pattern of enrichment in HREE (Eu, Gd, Tb, Dy, Ho, Er, Tm, Yb, Lu) and depletion in LREE (La, Ce, Pr, Nd, Pm, Sm) (fig 8a). The slope of HREE enrichment can change during metamorphism. The change in slope can be displayed by dividing the concentration of Gd by the concentration of Yb (fig. 8b). A high Gd/Yb ratio indicates a shallow slope, and a low Gd/Yb ratio indicates a steep slope. In continental crust environments, a positive Ce anomaly will be recorded in the REE pattern. If a zircon is crystalizing after or at the same time as plagioclase, a negative Eu anomaly will be recorded. A change in the magnitude of the Eu anomaly can be displayed by dividing Eu by radiogenic Eu (Eu^*) (fig. 8b). An increase in the Eu/Eu^* ratio indicates a smaller anomaly, and a decrease in the Eu/Eu^* ratio indicates a larger anomaly.

Rare earth element (REE) concentration increases from light REE to heavy REE for all SK samples. All samples also have a positive Ce anomaly and a negative Eu anomaly. The Eu anomaly is slightly larger for Neoproterozoic (metamorphic) zircons in samples SK11-01 and SK11-08, as evident by the lower Eu/Eu^* ratio (fig. 9). There is no change in magnitude of the Eu anomaly between growth domains in samples SK11-02, SK11-03 or SK11-07 (fig. 10). HREE concentrations are lower for Neoproterozoic zircons than they are for Mesoproterozoic zircons, and the slope of the HREE is less steep for

Neoproterozoic zircons than for Mesoproterozoic zircons in samples SK11-01, SK11-07 and SK11-08 (figs. 9,10). This is evident in the Gd/Yb ratio.

For samples SK11-01 and SK11-08, Th/U ratios are higher for metamorphic, Neoproterozoic zircons than for igneous, Mesoproterozoic zircons. Neoproterozoic zircon Th/U ratios range to 5.01 and 1.6 in samples SK11-01 and SK11-08, respectively, whereas Paleoproterozoic and Mesoproterozoic Th/U ratios range to only 1.5 and 1.16, respectively. SK11-07 and SK11-02 also followed a trend of higher Th/U ratios for metamorphic zircons. SK11-03 records an opposite trend, with lower Th/U ratios for metamorphic zircons. In all Spencer-Kilgore samples, U concentration was lower in metamorphic zircons than in igneous zircons (figs. 9,10)

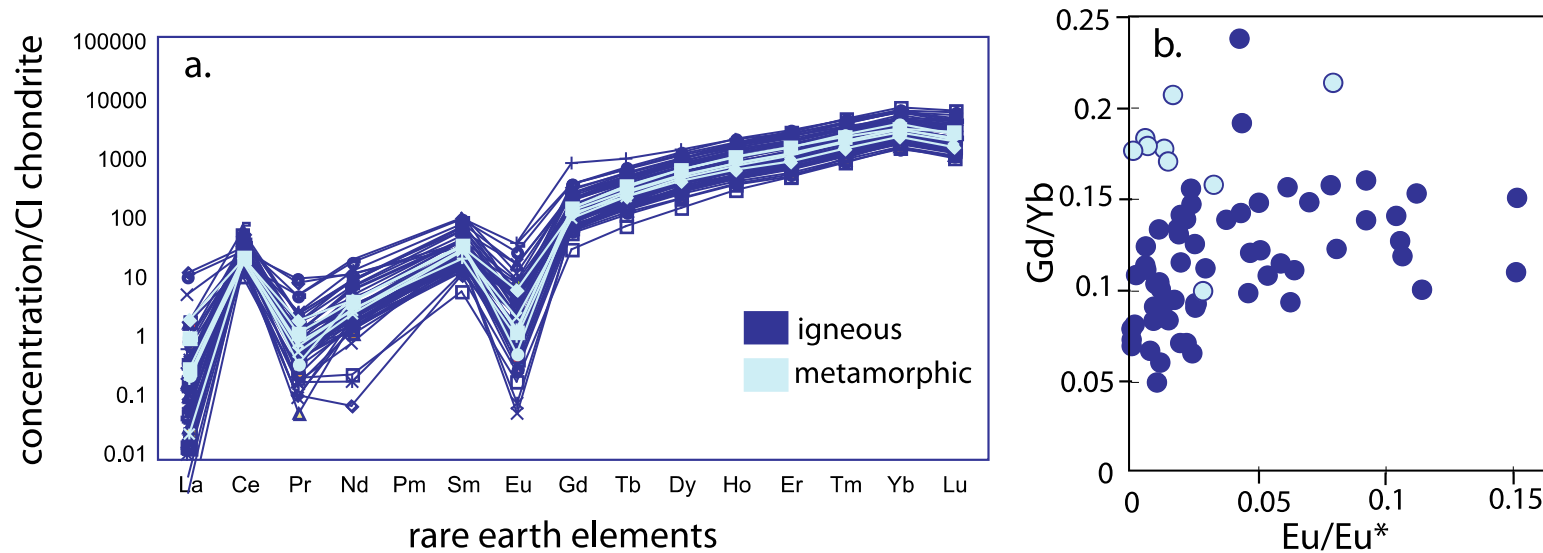


Figure 8: A normal REE pattern for zircon crystalized in a continental crust environment. REE patterns for both igneous and metamorphic zircons record enrichment in HREE (Eu, Gd, Tb, Dy, Ho, Er, Tm, Yb, Lu) and depletion in LREE (La, Ce, Pr, Nd, Pm, Sm) (a). The slope of enrichment of HREE can be displayed by dividing the concentration of Gd by the concentration of Yb (b). In continental crust environments, zircon records a positive Ce anomaly (a) due to the presence of oxygen. If zircon grows in the presence of plagioclase, a negative Eu anomaly is recorded (a). The intensity of the Eu anomaly can be displayed by dividing Eu by radiogenic Eu (Eu^*) (b)

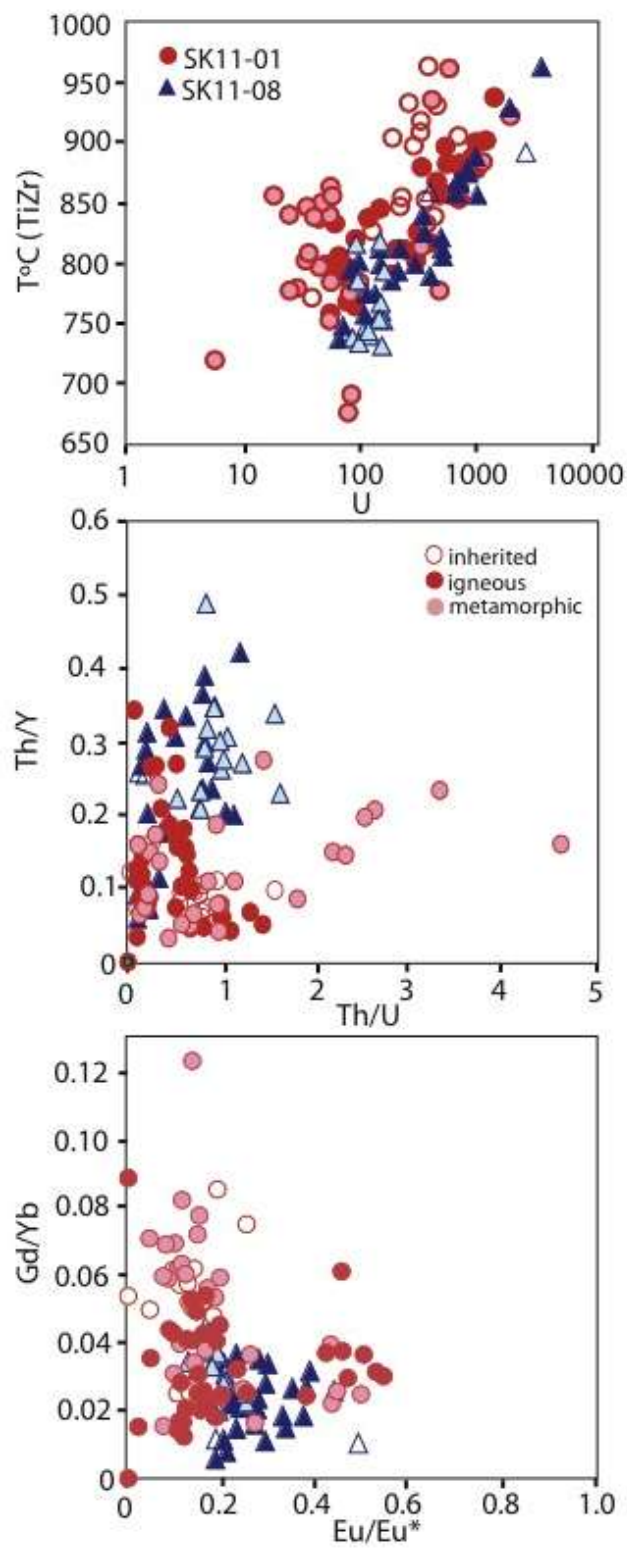


Figure 9: Trace element and trace element ratio plots for SK11-01 and SK11-08.

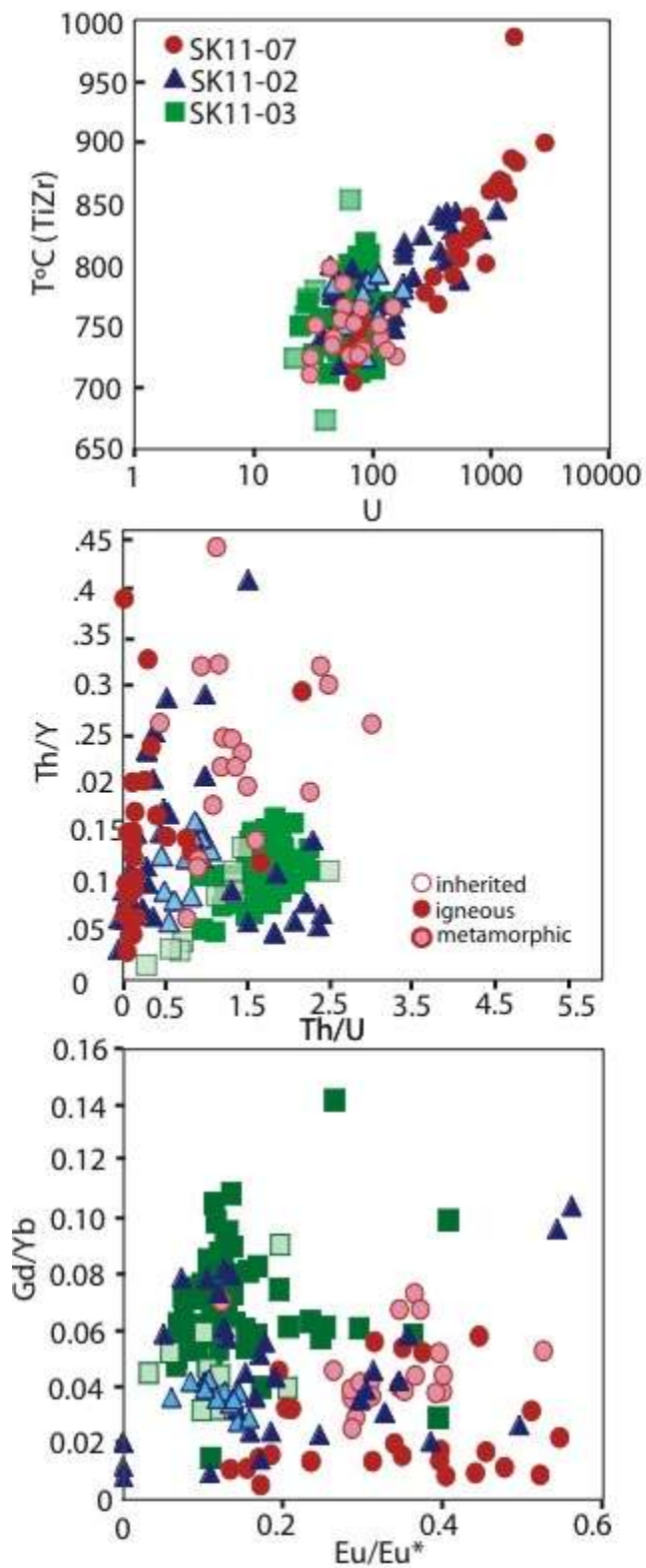


Figure 10: Trace element and trace element ratio plots for SK11-07, SK11-01 and SK11-02.

Ti-in-Zircon (TiZr) temperatures were recorded for each analysis. Temperatures ranged between 600 and 1050°C (fig. 11). Neoproterozoic zircons overall record lower temperatures than Mesoproterozoic zircons. Neoproterozoic zircons record temperatures between 625 and 875°C. Mesoproterozoic zircons record temperatures ranging up to 1000°C.

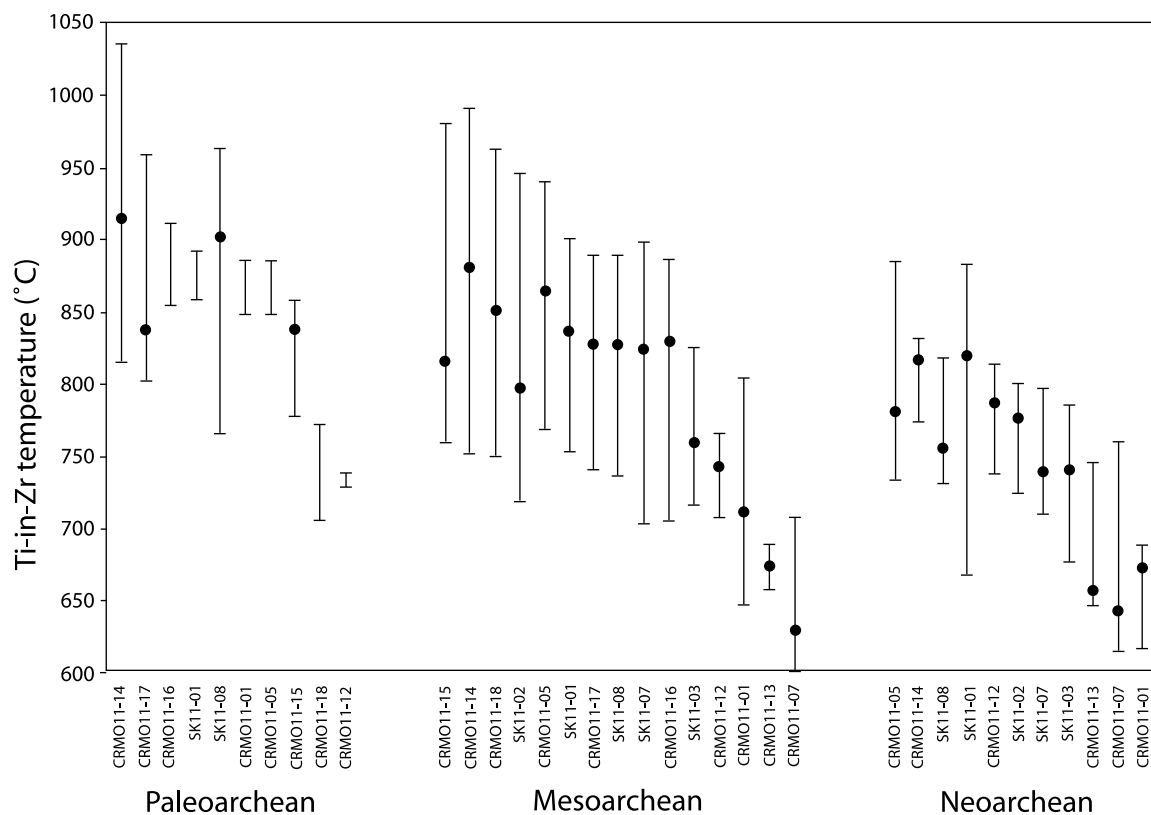


Figure 11: Ti-in-Zr temperatures recorded in zircons from Spencer-Kilgore and Craters of the Moon. Samples are listed in order of decreasing means. Dots are the median temperatures for each sample. Samples without dots recorded only two temperatures.

Craters of the Moon National Monument and Preserve

Petrography

Eleven samples were petrographically analyzed from Craters of the Moon National Monument and Preserve (CRMO): CRMO11-01, CRMO11-03, CRMO11-04, CRMO11-05, CRMO11-06, CRMO11-09, CRMO11-15, CRMO11-16, CRMO11-17, CRMO11-18, CRMO11-19. The major mineralogy of samples from CRMO is dominantly $qtz + fsp + opx$ and are banded gneisses, exhibiting grain boundary migration and/or grain boundary bulging. Exceptions are CRMO11-03, CRMO11-04, and CRMO11-19, which are coarser grained than other samples, have no mineral sorting, and major mineralogies of $qtz + fsp \pm amp$ indicative of intrusive granitoids. They are highly infiltrated by their basalt host, but in areas where basalt is absent, grains are interlocking, also indicative of intrusive granitoids. Samples CRMO11-03, CRMO11-04 and CRMO11-19 are the freshest, least friable of samples collected at CRMO.

CL images

CRMO zircons have the most regular oscillatory zoning of all samples (fig. 12). Domains of zircons seen in CL images can be separated into cores and overgrowths. Cores can be dark or oscillatory, and can be surrounded by one large overgrowth, or by oscillatory band overgrowths. In cases where the oscillatory core is surrounded by oscillatory bands, the difference between domains is identified by a change in orientation of the banding. The core bands are truncated by the overgrowth bands. Cores can also be patchy, or blurred. Cores record either Paleoproterozoic or Mesoproterozoic dates. Grains with

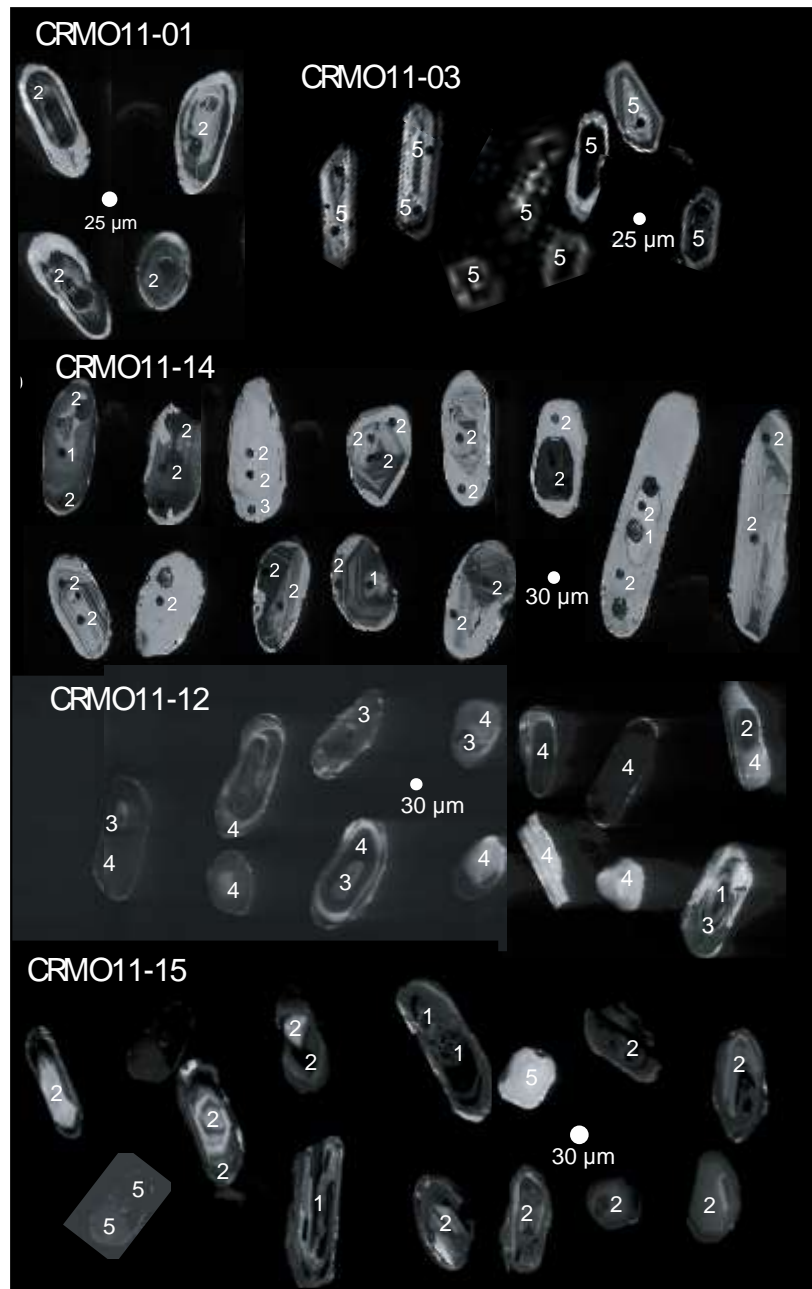


Figure 12: Examples of CL images and age growth domains from CRMO samples. Paleoproterozoic dates (1) are recorded in cores of grains. Mesoproterozoic dates (2) are recorded in grains with no zoning or with blurred oscillatory zoning. Neoproterozoic dates (3) are recorded in grains and overgrowths with no zoning, as well as in the cores of the grains that also record a younger Neoproterozoic growth (4). Paleogene dates (5) were recorded in three granitoid samples, all in domains with oscillatory zoning, as well as an overgrowth and an individual grain with no zoning in one Archean sample.

Only one growth zone of blurred oscillatory zoning and overgrowths of blurred oscillatory zoning record Mesoarchean dates. Grains and overgrowths that are brighter, indicating lower uranium, and have no zonation, record Neoproterozoic dates. Paleoproterozoic growth domains exhibit oscillatory zoning. Many grains exhibit uranium damage.

U/Pb geochronology

Of the 19 samples collected at Craters of the Moon, 14 samples were analyzed for U/Pb geochronology (Appendix C). The other samples collected were deemed too small to crush, contained no zircons, or were determined not to be lower crustal xenoliths and thus were not of interest in this study. Of the samples analyzed, four age groupings were identified. The first grouping is recorded in cores, and range from 3312 ± 50 Ma to 3609 ± 21 Ma. This population is found in only 7 of the samples.

The second and third age groupings comprise both cores and grains that exhibit a blurred oscillatory pattern. These areas record dates in the Mesoarchean. Two groupings in the Mesoarchean are found in CRMO samples, one group at ~ 3.2 Ga and the other at ~ 3.0 Ga. The fourth grouping of Neoproterozoic dates are recorded in 7 CRMO samples. These dates are recorded in overgrowths and unzoned grains. Dates range from 2.68 to 2.92 Ga. Sample CRMO11-12 records dates between 2.4 and 2.6 Ga. No other sample records similar dates. The average of CRMO11-12 Paleoproterozoic dates is 2498 ± 21 and has a MSWD of 1.2.

Four CRMO samples, CRMO11-03, CRMO11-04, CRMO11-15 and CRMO11-19, recorded Paleoproterozoic dates. CRMO11-03, CRMO11-04 and CRMO11-19 dates are from single growth domain zircons with oscillatory zoning, although CRMO11-19

oscillatory zones are blurred. Grains from CRMO11-03, CRMO11-04 and CRMO11-19 are euhedral. These textures are indicative of igneous formation, not surprising as the three samples are granitoids. CRMO11-03 and CRMO11-04 record similar dates, with averages of $36 \pm .60$ Ma and $37 \pm .49$ Ma, respectively. CRMO11-19 records dates a little older, with an average of 45 ± 1.9 Ma. CRMO11-03 records 2 Mesoarchean dates at 2974 ± 67 Ma (discordance 8%) and 2613 ± 79 Ma (discordance 26%). CRMO11-04 and CRMO11-19 only record Paleogene dates.

The two domains from CRMO11-15 that record Paleogene dates do not exhibit zoning patterns, indicating metamorphism. One domain is a single grain that is bright in CL (low U concentration) and the other domain is a dark (high U concentration) overgrowth (fig. 12). CRMO11-15 records fewer than 5 Paleogene dates, and records many Mesoarchean dates.

Trace element geochemistry

Rare earth element concentration increases from light REE to heavy REE for all CRMO samples. All samples also have a positive Ce anomaly and a negative Eu anomaly.

Sample CRMO11-03 and CRMO11-04 record Paleogene dates between 36 and 38 Ma. Both have identical modal mineralogy, very similar CL images and age patterns, and REE patterns that are very similar, as indicated by Gd/Yb ratios (fig. 13). Their REE pattern is a normal HREE-enriched zircon pattern. The Eu anomaly in both samples is very pronounced. Both CRMO11-03 and CRMO11-04 have low Th/U ratios, rarely recording ratios above 1.5. Ti/Zr temperatures for Paleogene zircons from CRMO11-03

range from 518°C -785°C. TiZr temperatures for CRMO11-04 zircons range between 534°C - 903°C. The temperatures recorded in these samples, as well as their similar geochemistry and identical ages indicates these two xenoliths are from the same granitic pluton. CRMO11-19 also records only Paleogene dates, however, the geochemistry and zircon growth ages differ from CRMO11-03 and CRMO11-04. CRMO11-19 records only a slight Eu anomaly (fig. 13) and records much older ages of 45 Ma. CRMO11-19 is also from a granitic pluton, but a different one than the one CRMO11-03 and CRMO11-04 were sourced from.

CRMO11-01, CRMO11-07 and CRMO11-13 record Late Mesoarchean and Neoproterozoic ages. CRMO11-07 and CRMO11-13 record no change in the slope of HREE concentrations (shown by Gd/Yb ratios, fig 14), U concentration, or Ti-in-Zr temperatures between the two age groups. However, CRMO11-01 records changes in lower U concentrations in metamorphic Neoproterozoic ages (fig. 14) as well as lower Th/Y ratios in Neoproterozoic zircons. No change is seen in the Th/U ratio indicating Th and U are both expelled at during metamorphism, with neither being preferentially expelled over the other.

CRMO11-05, CRMO11-12 and CRMO11-14 all record Paleoproterozoic, Mesoarchean, and Neoproterozoic zircon growth domains (fig. 15). CRMO11-12 also records Paleoproterozoic growth domains. For these three samples, the slope of HREE from Gd to Yb does not change between samples, however there is a lowering in concentration of HREE. A steeper Eu anomaly (lower Eu/Eu*) is recorded in metamorphic zircons from CRMO11-12 and CRMO11-05. CRMO11-14 does not record a change in Eu anomaly. U concentrations decrease in metamorphic domains in samples

CRMO11-05 and CRMO11-14. This is also recorded in higher Th/U ratios for these two samples. CRMO11-12 also records a higher Th/U ratio for metamorphic zircons, but only for Paleoproterozoic metamorphic zircon domains, not for Mesoarchean metamorphic zircon domains. Ti-in-Zr temperatures range from 650 to 1000 °C for CRMO11-14 and CRMO11-05. Metamorphic zircons from these samples have a smaller range of temperatures, between 650°C to 875°C, than igneous zircons. CRMO11-12 does not record a change in temperatures, however all four zircon growth domains record temperatures below 860°C.

Samples CRMO11-15, CRMO11-16, and CRMO11-18 all record Paleoproterozoic inherited ages, Mesoarchean igneous ages, but do not record Neoproterozoic metamorphic ages. CRMO11-17 also records Paleoproterozoic ages and Mesoarchean ages, but does record two Neoproterozoic ages. CRMO11-15 and CRMO11-18 record very similar Mesoarchean ages (3.285 and 3.287 Ga, respectively). Their Eu anomalies, Th/U ratios and Ti-in-Zr temperatures are also very similar (fig. 17). It is possible these two xenoliths were part of the same pluton. CRMO11-15 also records three Neoproterozoic dates. The negative Eu anomaly is more pronounced in zircon domains with metamorphic Neoproterozoic ages from CRMO11-15 and metamorphic Paleoproterozoic ages from CRMO11-17 than in domains recording older ages from these samples (figs. 16,17). A decrease in U concentration and an increase in the Th/U ratio is also recorded in Neoproterozoic ages from CRMO11-17. The Neoproterozoic metamorphic zircons from CRMO11-15 record the opposite, an increase in U and a decrease in Th/U. Ti-in-Zr temperatures for the metamorphic domains from CRMO11-17 and CRMO11-15 are lower than for their associated igneous domains.

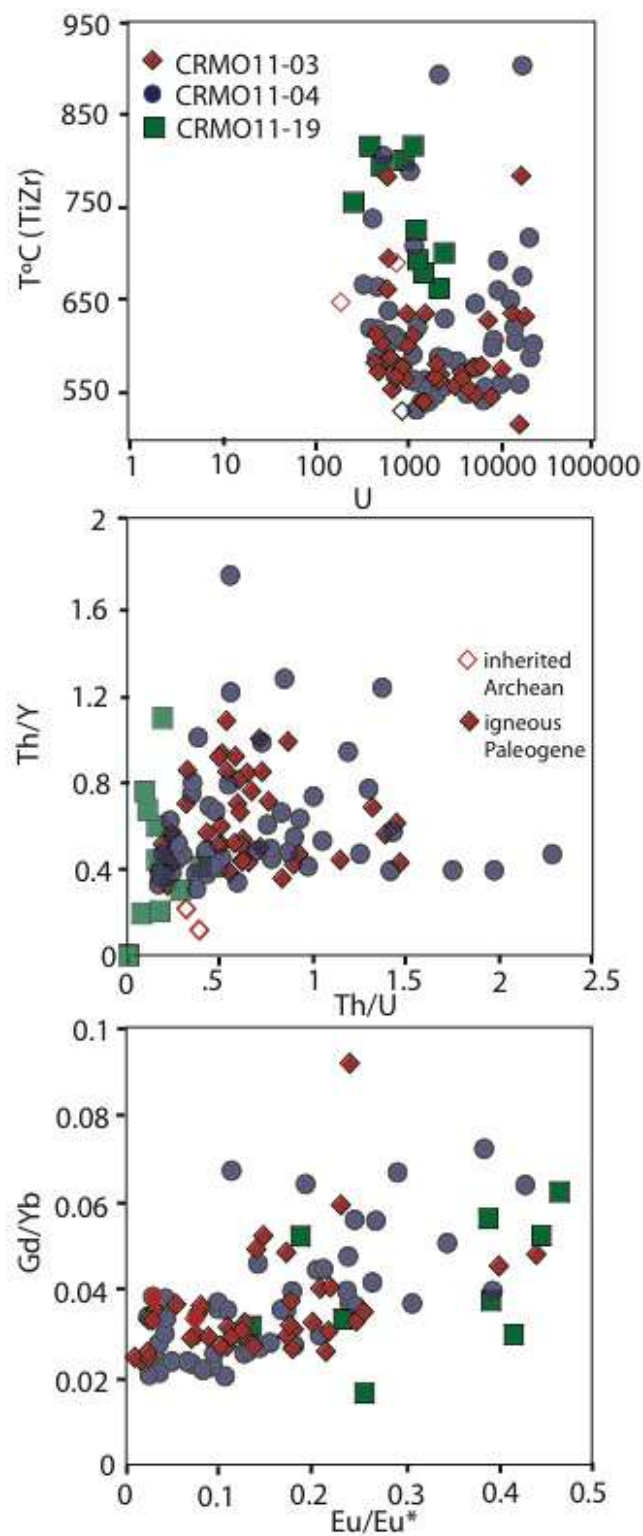


Figure 13: Trace element and trace element ratio plots for CRMO11-03, CRMO11-04 and CRMO11-19.

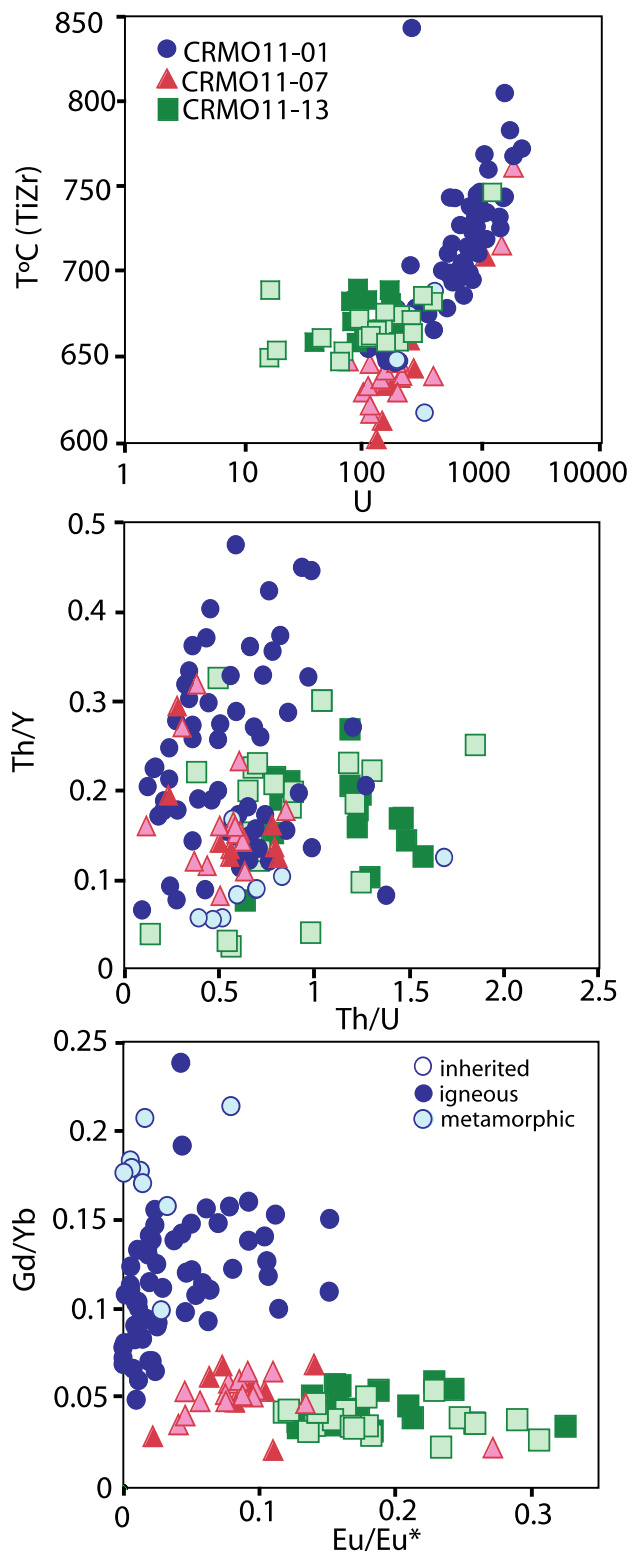


Figure 14: Trace element and trace element ratio plots for CRMO11-01, CRMO11-07 and CRMO11-13.

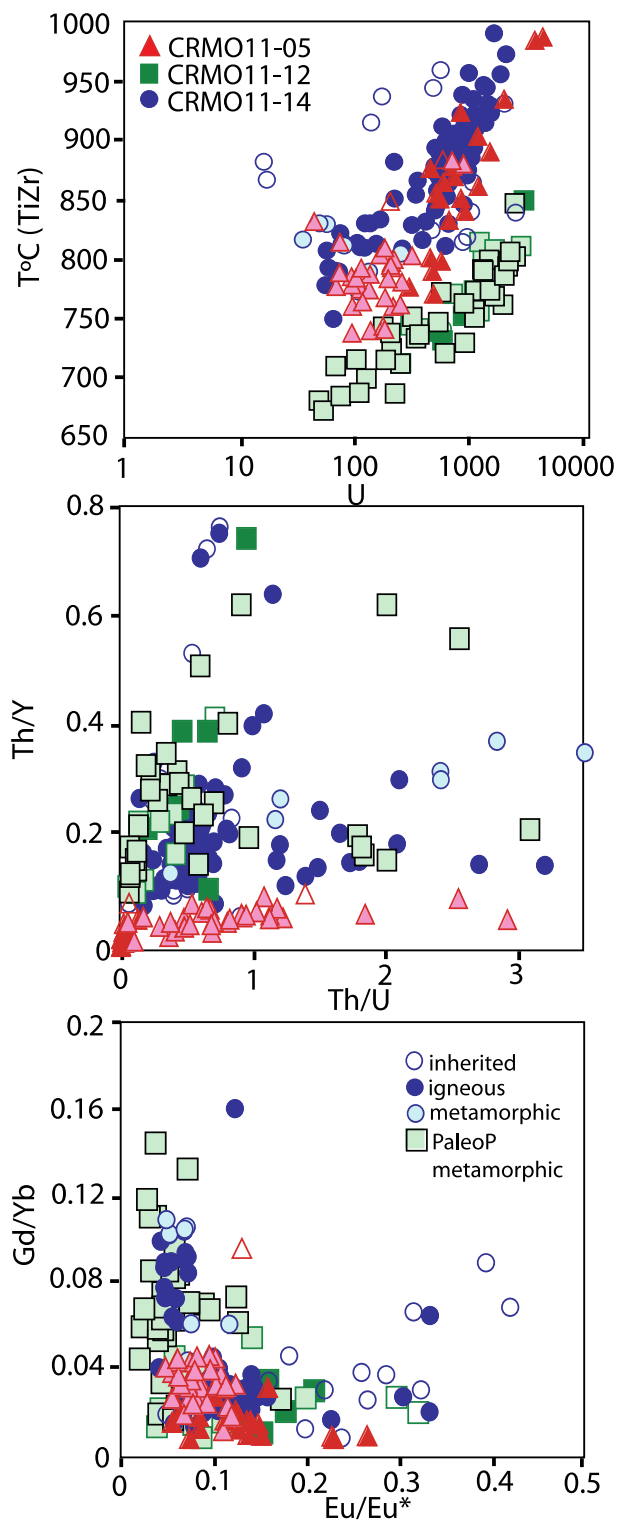


Figure 15: Trace element and trace element ratio plots for CRMO11-05, CRMO11-12 and CRMO11-14.

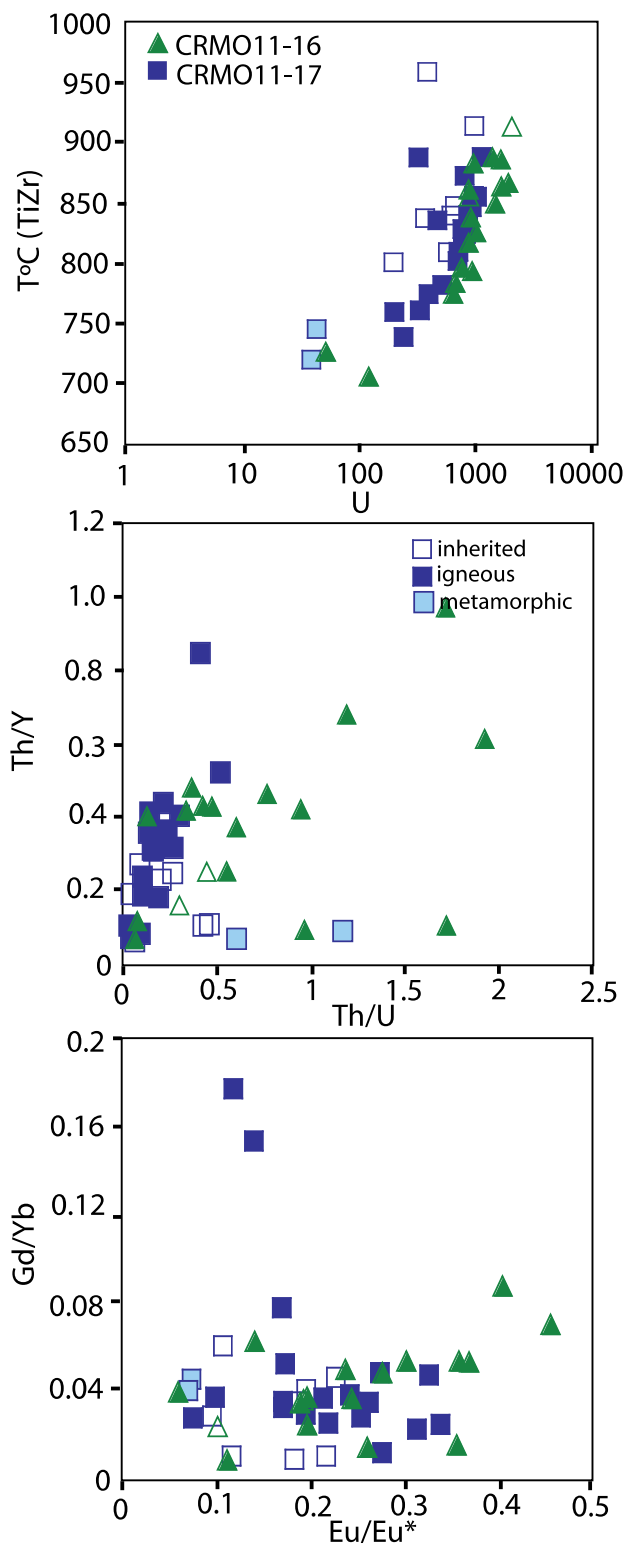


Figure 16: Trace element and trace element ratio plots CRMO11-16 and CRMO11-17.

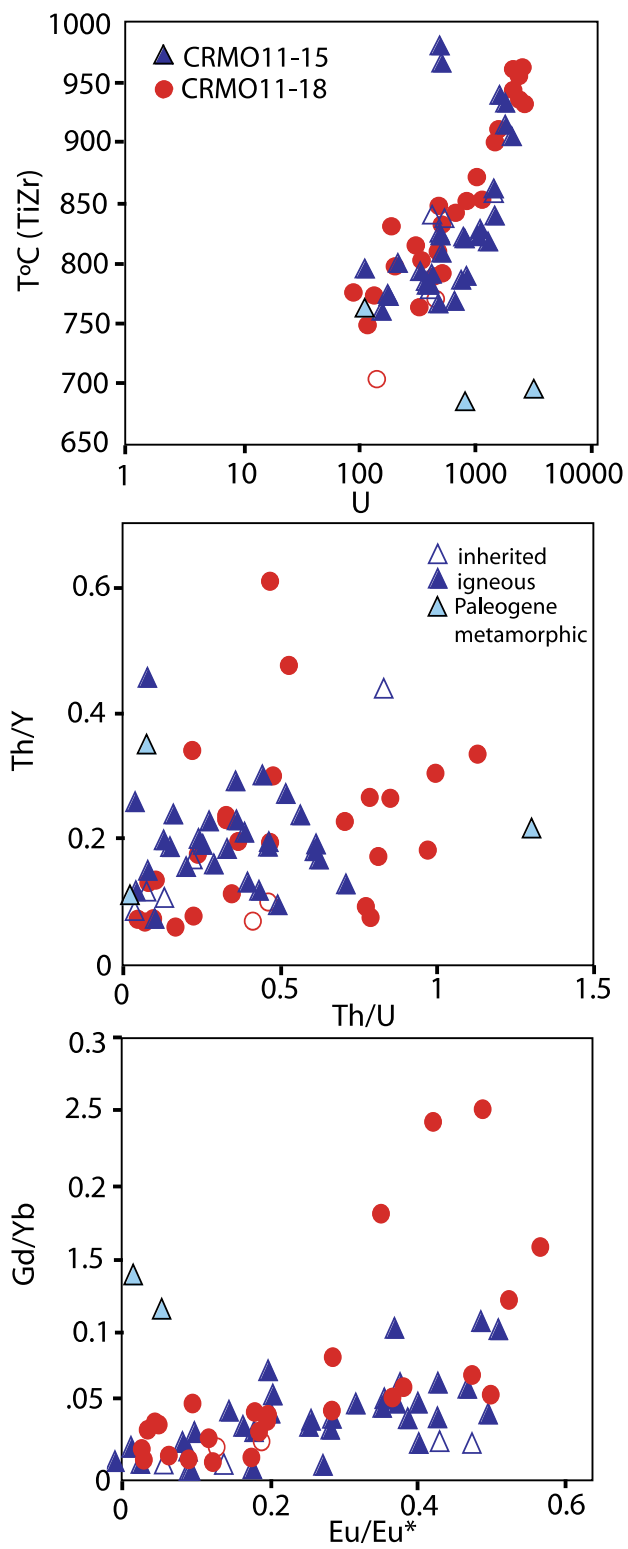


Figure 17: Trace element and trace element ratio plots for CRMO11-15 and CRMO11-18.

Square Mountain

Petrography

Five samples from the Square Mountain (SM) location were petrographically analyzed: SM10-A3, SM10-C1, SM10-C2, SM10-C3 and SM10-C4. Only a brief description of thin sections is given here. For a more detailed description and mineral percentages for each sample, see appendix A.

All samples except SM10-C1 had a major mineral assemblage of $qtz + fsp + pyx + ox$ and are compositionally banded. They are granulites, specifically charnokites. SM10-C1 is a metagabbro, with a major mineral assemblage of $fsp + ol + opx + ox$. Grain boundary migration is evident in all samples. Basalt from the host rock had infiltrated the samples to varying degrees, and partial melting of the sample is seen at the boundaries of basalt and xenolith.

CL images

Grains from SM retain the idiomorphic prismatic crystal form of zircon, with slightly rounded edges. Samples from SM10-A3, SM10-C2, and SM10-C3 show bright cores with mottled, recrystallized overgrowths. Oscillatory zoning can be seen on many of the tips of grains. The mottled overgrowths cut into the oscillatory zoning. Cores are bright white, with no zoning. Not all grains have a core; some are mottled throughout the grain. CL images of SM10-C4 reveal cores of mottled grains, and overgrowths of igneous oscillatory zoning (fig. 18). Grains from SM10-C4 are euhedral.

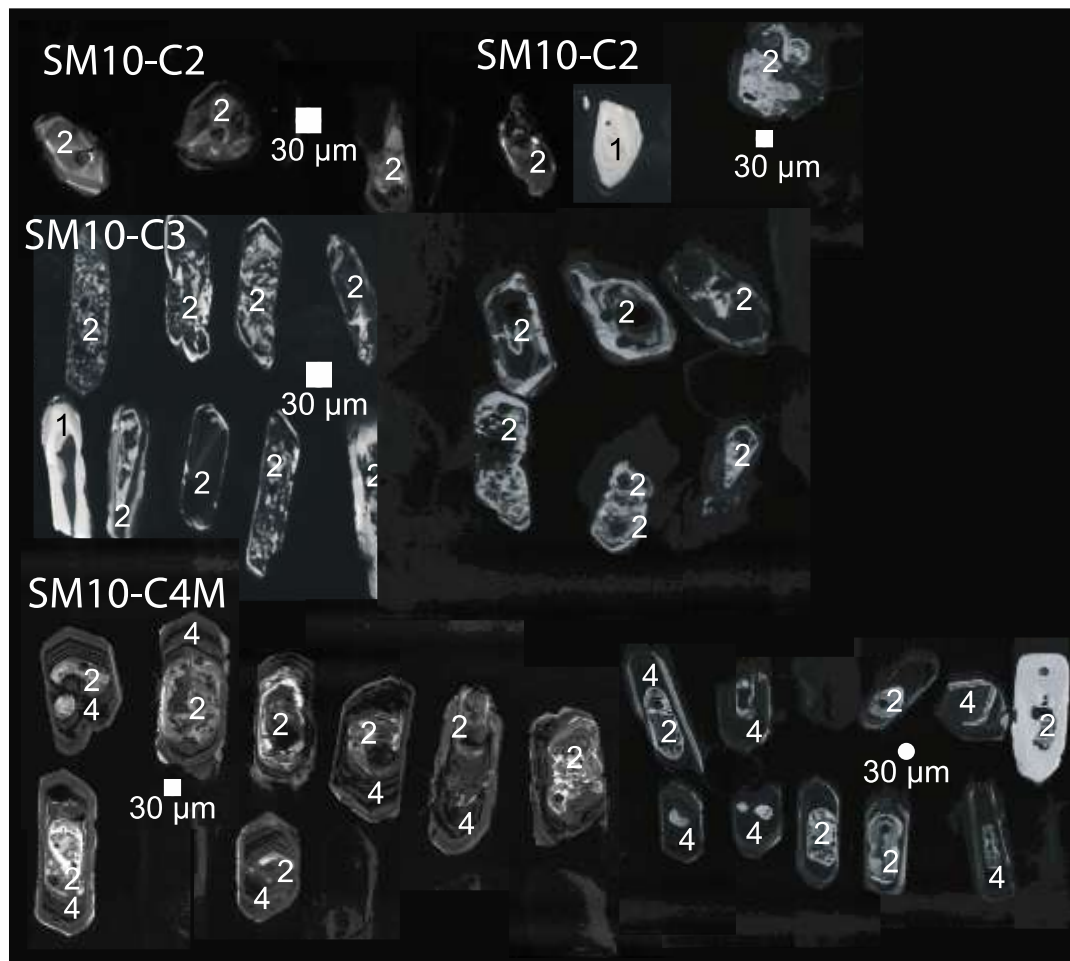


Figure 18: Examples of CL images from SM. Paleoarchean and Mesoarchean dates (1) were recorded in the cores of samples and in samples with low uranium and no zoning. Neoproterozoic dates (2) are recorded in zircon growth domains with oscillatory zoning and with a mottled pattern. Mottling often cuts across oscillatory zoning, which is preserved in the tips of many grains. Paleogene dates (4) are recorded in oscillatory overgrowths of grains in sample SM10-C4.

U/Pb geochronology

Four samples from Square Mountain were analyzed for U-Th-Pb using LA-ICPMS: SM10-A3, SM10-C2, SM10-C3 and SM10-C4. SM10-C1 did not have sufficient zircons to date. Three age populations were identified using (table 2); these populations correlate to the three CL image patterns described above. The oldest dates are from the

Mesoarchean, and are composed of spots taken from cores in the center of grains.

Mesoarchean dates are recorded in all samples except SM10-C4.

All four samples record dates in the Neoproterozoic. These dates are always recorded in mottled CL imaged areas. Thus, in SM10-A3, SM10-C2 and SM10-C3, Neoproterozoic dates are recorded in mottled overgrowths, and in SM10-C4 Neoproterozoic dates are recorded in mottled cores. SM10-C4 also records Paleogene dates. These dates are recorded in oscillatory zoned overgrowths. Paleogene $^{206}\text{U}/^{238}\text{Pb}$ dates range from 53 to 44 Ma, with a weighted mean of $47 \pm .55$ Ma.

Trace element geochemistry

All Square Mountain samples record a normal REE zircon pattern, with element concentrations increasing with atomic number. All samples record negative Eu anomalies, but due to high, flat LREE concentrations, a positive Ce anomaly is often not recorded, especially in samples SM10-C1, SM10-C2 and SM10-C3. However, LREE can be difficult to accurately detect due to their low concentration. In samples where LREE concentrations are flat, only HREE are interpreted as reliable.

As only a few other dates besides those from igneous Neoproterozoic domains were recorded (with the exception of Paleogene dates in SM10-C4), only the U, Th, and Y concentrations for Neoproterozoic dates will be examined. SM10-A3, SM10-C2 and SM10-C3 recorded Th/U ratios between .03 and .8 (figs. 19, 20). A larger range of Th/U ratios are recorded in SM10-C4 (fig. 20). All SM samples recorded Th/Y ratios between .02 and 2.18. However, SM10-C2 had a much tighter range, between .05 and .30. Th/U ratios

are lower for igneous Paleogene domains than for Neoproterozoic domains (fig. 20), a result of U concentrations being higher Paleogene domains than in Archean domains.

A range of high Ti-in-Zr temperatures (800-1000°C) and low temperatures (650-550°C) are recorded in SM samples, indicating the zircons were crystallizing early in the cooling process as well as at the end. TiZr temperatures for Mesoproterozoic dates range from 663°C to 952°C, but range less for individual samples. Neoproterozoic temperatures for SM10-A3 are between 788°C and 986°C, for SM10-C2 are between 716°C and 880°C, for SM10-C3 are between 750°C and 986°C, and for SM10C4 are between 646°C and 941°C. Paleogene domains record temperatures between 494°C and 809°C (fig. 19), lower than temperatures for Neoproterozoic domains.

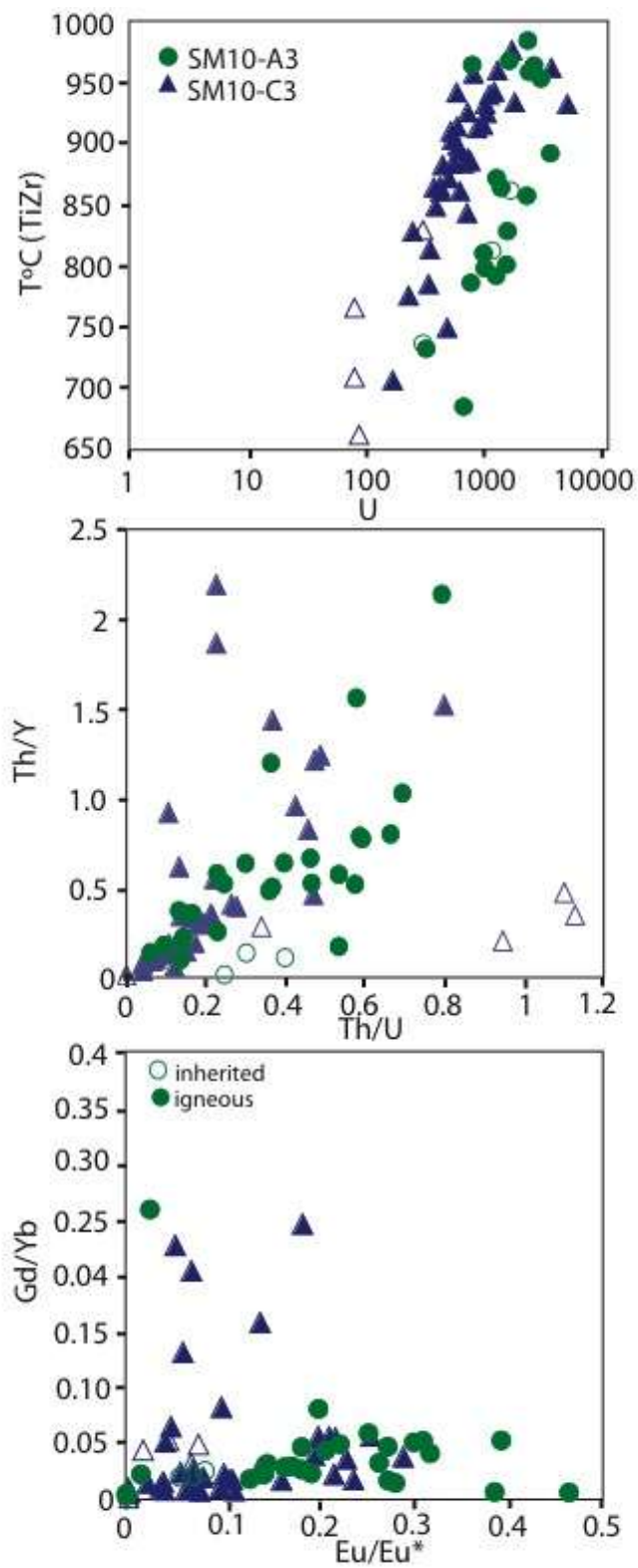


Figure 19: Trace element and trace element ratio plots of SM10-A3 and SM10-C3.

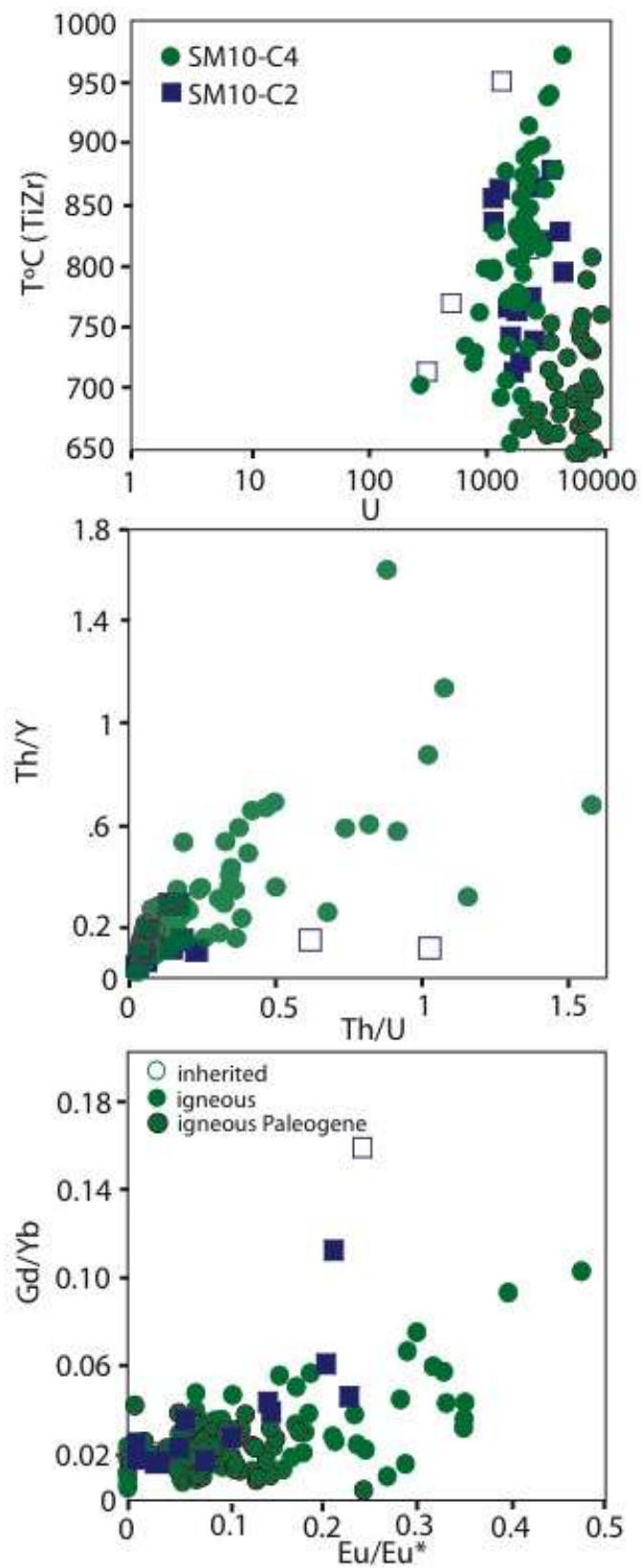


Figure 20: Trace element and trace element ratio plots of SM10-C2 and SM10-C4.

U/Pb geochronology

Both samples from HM containing zircons produced small zircon sets, in size and number. The tonalite orthogneiss, HM11-01, recorded two age populations (table 2). The older age grouping records dates between 2.0 and 2.5 Ga. Unfortunately, only one spot has a discordance of less than 30%, recording a date of 2541 ± 55 Ma. HM11-01 and HM11-06 record two dates each between 1.82 and 1.97 Ga. These dates are recorded on an overgrowth and on discrete grains (fig. 21). Dates of 3.3 Ga, 3.6 Ga, and 1.4 Ga were also recorded, however, little can be said of these data with confidence as they are not reproducible and have high discordance.

HM11-06, a muscovite bearing paragneiss, produced three distinct age groupings (table 2). The oldest population records a weighted mean of 2556 ± 12 Ma (MSWD = .56). The next youngest age grouping has only two spots, with dates of 1917 ± 64 and 1893 ± 57 Ma. A Paleogene grouping is recorded in two spots, with $^{238}\text{U}/^{206}\text{Pb}$ dates of 46 ± 4 Ma and 36 ± 2 Ma.

Trace element geochemistry

Both HM11-01 and HM11-06 record normal zircon REE patterns, with positive Ce anomalies and negative Eu anomalies. Eu anomalies are not as great in Paleogene and Paleoproterozoic domains (fig. 22). The zircon domains recording 1.8 Ga and 1.9 Ga dates in HM11-06 also record very shallow Ce and Eu anomalies.

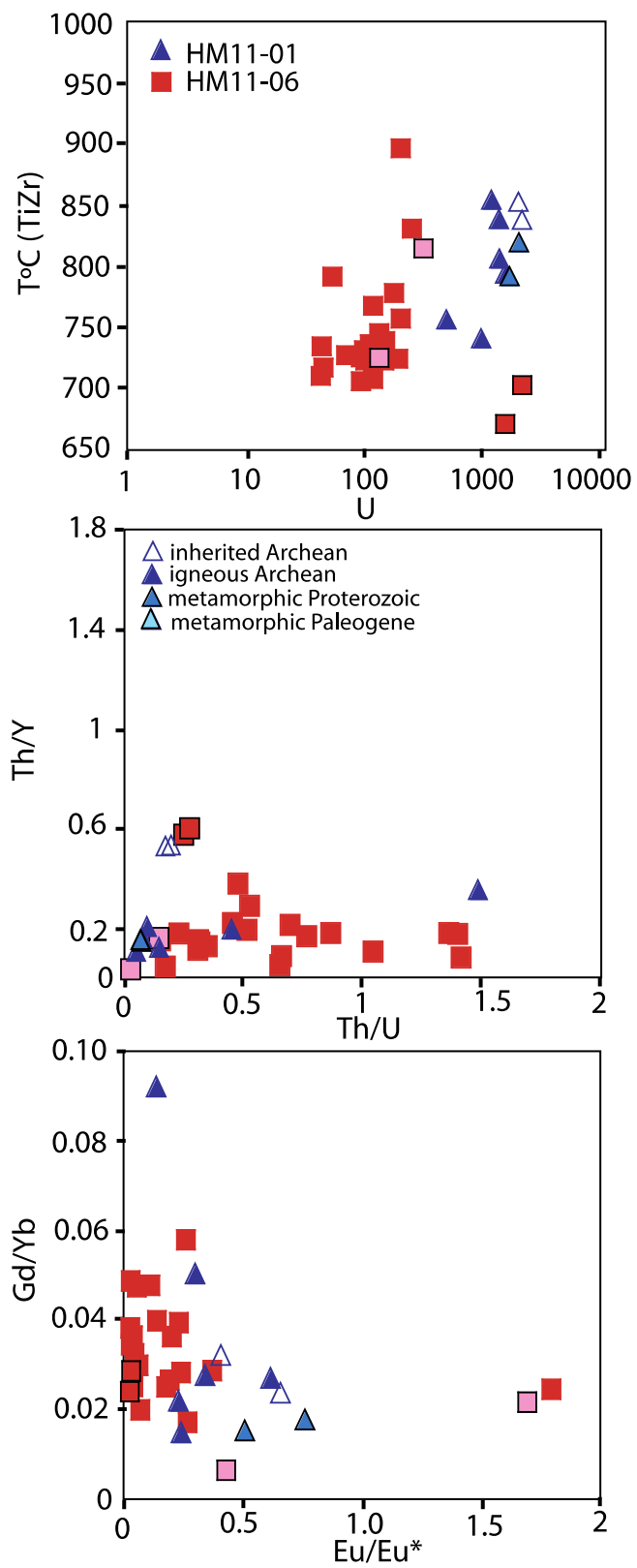


Figure 22: Trace element and trace element ratio plots of HM11-01 and HM11-06.

Mesoarchean zircon domains from HM11-01 record Th/U ratios of .2 and .22. Neoproterozoic domains from this sample record .08 to 1.5. Th/Y ratios for Mesoarchean domains are .54 and .53 and for Neoproterozoic domains are between .11 and .36. Paleoproterozoic domains from HM11-01 record the lowest Th/U ratios, at .09 and .10. Th/Y ratios are also low for this growth population, at .09 and .11. Ti/Zr temperatures for Mesoarchean domains are 852°C and 838°C and for Neoproterozoic domains are between 741°C and 854°C. Paleoproterozoic domains recorded temperatures in the same range of Archean domains, at 819°C and 792°C.

Unlike HM11-01, HM11-06 does not record any Mesoarchean dates, but does record Neoproterozoic dates and two Paleogene dates. Th/U ratios for domains recording Neoproterozoic dates are between .16 and 1.42. The Paleogene domains record Th/U ratios of .26 and .28. Th/Y ratios for Neoproterozoic domains are between .05 and .38, and for Paleogene domains are .58 and .60. Paleoproterozoic domains for this sample also recorded low Th/U ratios of .15 and .03 and low Th/Y ratios of .04 and .16. Ti/Zr temperatures for Neoproterozoic domains range from 580°C to 851°C. The Paleogene domains record temperatures of 530°C and 576°C. Paleoproterozoic domains record temperatures of 735°C and 607°C.

Th/U ratios from metamorphic domains, from both the Paleoproterozoic (HM11-01) and the Paleogene (HM11-06) are lower than those for igneous domains (fig. 21). This must be caused by an intake in Th, as U concentrations do not increase in metamorphic domains (fig. 22).

Discussion

The Use of Trace Element Geochemistry

Investigation of trace element concentrations and patterns in zircons, and interpretation of the source and mineralogical control of the trace elements provide evidence for the conditions under which the zircon formed. This in turn allows for more sophisticated interpretation of what an U/Pb date for a zircon is recording (timing of crystallization, metamorphism, level of metamorphism etc.). The trace element content in zircon is controlled by the medium from which the crystal forms. In the case of igneous zircon growth, the medium is a melt and the associated minerals co-crystallizing with zircon (Watson, 1979; Watson and Harrison, 1983). During metamorphic growth, the medium includes trace elements liberated during breakdown reactions, which communicate with the zircon crystals via grain boundary diffusion or via intracrystalline diffusion if a zircon crystal is occluded within another phase (e.g. Varva et al., 1996; Fraser et al.;1997, Bingen et al., 2001). If earlier formed zircon is dissolving or recrystallizing during metamorphism, then the trace element reservoir can include not only other minerals surrounding the zircon, but also the zircon crystal itself onto which the domain is growing (Watson and Harrison, 1983). At upper amphibolite- to granulite-facies, zircon-bearing protoliths undergo both solid state and melt-forming reactions, therefore, trace element partitioning between melt, other modal and accessory minerals, and pre-existing zircons must be considered (e.g. Fraser et al., 1997; Roberts and Finger, 1997; Davidson and van Breeman, 1988; Schaltegger et al., 1991; Rubatto et al., 2001).

Insight into the media that control a zircon crystal's formation can be gained by observing the REE pattern and other trace element concentrations in the zircon. Igneous

and metamorphic zircons alike follow a REE pattern of enrichment in HREE (Eu, Gd, Tb, Dy, Ho, Er, Tm, Yb, Lu) and depletion in LREE (La, Ce, Pr, Nd, Pm, Sm), and may display a positive Ce anomalies and a negative Eu anomalies. The partition coefficients for REE in zircon increase with atomic number (e.g. Nagasawa, 1970; Watson, 1980; Hinton and Upton, 1991; Sano et al., 2002; Thomas et al., 2002). This is because as atomic number increases, ionic radius decreases. The heavier REE becomes more similar in size to Zr^{4+} and therefore becomes more compatible in zircon (Hinton and Upton, 1991; Guo et al., 1996). Hinton and Upton (1991) observed that the Ce anomaly observed in some zircons is related to oxygen fugacity. In oxidized states, Ce^{3+} becomes Ce^{4+} . Ce^{4+} is similar in size and equal in charge to Zr^{4+} , allowing for substitution of Ce for Zr and compatibility in zircon. Oxidized states can indicate zircon formation in continental crustal environments. The negative Eu anomaly is due to the fugacity of oxygen and plagioclase fractionation during zircon crystallization (Snyder et al.; 1993, Hoskin, 1998; Hoskin et al.; 2000). Because Eu^{2+} is compatible with plagioclase, during plagioclase growth Eu^{2+} will fractionate out of the melt and into plagioclase resulting in an apparent depletion of Eu compared to its neighboring REE. If plagioclase is crystalizing at the same time or is present before the zircon grows, a similarly lower concentration of Eu will be available for zircon resulting in a negative Eu anomaly. All zircons in this study record a positive Ce anomaly, indicating the zircons grew in an oxidized state, in the continental crust. All samples from this study have at least a slight Eu anomaly, although many have a significant one. This is not unexpected, as plagioclase is a modal mineral in almost all samples.

Other trace elements that substitute into zircon include P, U, Th, Hf, Y, Nb and Ta (Es'kova, 1959; Speer, 1982; Caruba and Iaconi, 1983; Halden et al., 1993; Hoskin et al., 2000). Y^{3+} and Nb^{5+} and Ta^{5+} are all compatible in zircon, and substitute into the Zr^{4+} site (Thomas et al., 2002). Hf^{4+} , U^{4+} , and Th^{4+} also substitute into the Zr^{4+} site in zircon (Hoskin and Schaltegger, 2003). P substitutes into the Si^{4+} site, as part of a xenotime-type substitution where $REE^{3+} + P^{5+} = Zr^{4+} + Si^{4+}$ (Speer, 1982). Y behaves much like a REE due its size and charge (Es'kova, 1959).

Minerals in the protolith exert control over the composition of crystallizing zircon during metamorphism. First, for metamorphic zircon to grow, there must be a modally abundant mineral containing tens of ppm of Zr in the reacting protolith in order for a necessary amount of Zr to be release during metamorphism (Bingen et al., 2001). Garnet and ilmenite are two minerals that have been proven to release enough Zr during metamorphism to lead to metamorphic zircon formation (Fraser et al., 1997; Bingen et al., 2001). Mineral breakdowns will not only release Zr, but other trace elements that affect the composition of metamorphic zircon. If a mineral releases a high concentration of REEs when it breaks down, growing metamorphic zircon can incorporate a high concentration of REE into its structure. For example, during dehydration reactions associated with the amphibolite-granulite transition, amphibole breaks down and orthopyroxene forms (Greenwood, 1963; Vernon and Clarke, 2008). High concentrations of trace elements are released from the amphibole structure, but are not easily incorporated into the pyroxene structure. These trace elements are available for incorporation into growing metamorphic zircon. If a high concentration of REE are identified in a granulite facies zircon, it may be inferred that amphibolite breakdown to

pyroxene is a possible reason for the high concentration. During continued metamorphism, a smaller reservoir of trace elements will be available to grow metamorphic zircon, as no minerals are present that will break down and release a large amount of REE.

Metamorphic minerals growing contemporaneously with or prior to metamorphic zircon also exert control over the trace element composition of metamorphic zircon. For example, if garnet is growing contemporaneously with zircon HREE concentrations in the metamorphic zircon will plateau or decrease. This is because HREE are highly compatible in garnet (Harrison and Wood, 1980), leaving a smaller budget of HREE for zircon. Garnet was identified in only one sample in this project (SK11-07), and in that sample a plateau of HREE is recorded, as expected. The lack of garnet, or evidence of garnet, in trace element compositions of all other samples indicates the pressure and or composition of the granulites sampled in this study was not appropriate for garnet production.

If a zircon is recrystallized during metamorphism, trace element concentration is controlled by the concentration in the original zircon. The trace element concentration in recrystallized zircon is likely to be lower than the concentration in the original zircon. During recrystallization, incompatible elements will be ejected as the crystal attempts to become pure ZrSiO_4 , leaving behind a smaller trace element reservoir for the recrystallizing zircon. (Hoskin and Black, 2000; Rubatto, 2002).

Use of Ti-in-Zircon

Because the concentration of the trace element titanium in a zircon crystal is strongly temperature dependent, titanium concentration in zircon can be used as a thermometer (Watson and Harrison, 2005). The titanium-in-zircon (Ti-in-zircon or TiZR) thermometer was calibrated by Watson and Harrison (2005) and Watson et al. (2006). In general, the lower the crystallization temperature, the lower the concentration of titanium in a zircon crystal. Although temperature controls Ti concentration greatly, Ti concentration is not solely dependent on temperature. It is also dependent on pressure, activity of TiO_2 and activity of SiO_2 (Ferry and Watson, 2006). The Ti-in-zircon thermometer takes into account the activity of TiO_2 and SiO_2 , but not pressure.

Uncertainties in this thermometer are both random and systematic. Random uncertainty can occur during the measurement of titanium due to counting statistic errors and analytical instrument fluctuation. Through repeated analysis of the Orapa (Botswana) kimberlite standard, the analytical error in Ti concentration at Boise State University has been determined to be $\pm 10\%$, or $\pm 10^\circ\text{C}$ error. Systematic errors in temperature reported from Ti-in-zircon thermometry include assumptions about the activity (α) of Ti in the rock. If a phase that contains Ti is present, such as rutile, then the activity is fixed at 1. However, if a Ti phase is not present, the α_{Ti} will be less than one. If the assumed α_{Ti} is assumed lower than the actual α_{Ti} , the calculated temperature will be an overestimate. Some rocks in this study do have rutile present, and their α_{Ti} can be assumed to be 1. Watson and Harrison (2005) suggested most melts that crystallize zircon will have an α_{Ti} of .5, and that felsic rocks will have α_{Ti} greater than mafic rocks. An α_{Ti} of .7 was

assumed for all samples during in this study. If α is varied by 10%, then a $\pm 10^{\circ}\text{C} - 15^{\circ}\text{C}$ difference is calculated.

A possible second systematic error in the Ti-in-zircon thermometer is if a spot analysis accidentally intersects an inclusion. During data reduction, evidence of inclusions is looked for in the time-resolved analysis, and affected data thrown out. However, if missed, the temperature reported will be anomalously higher. To account for this, unusually high temperatures ($>1050^{\circ}\text{C}$) were discarded. Because of the systematic uncertainties in the Ti-in-zircon thermometer, we recognize it is more useful to compare the differences in temperatures recorded within and among samples, than to compare absolute temperatures.

Formation of the Kilgore-Craters Terrane

The xenoliths collected from the Snake River Plain (SRP) and exposed lithologies in House Mountain reveal an Archean geologic history of Southern Idaho. The eastern section of the SRP, from the Montana border into Craters of the Moon, records a distinct geologic history from the SRP area to the west, and thus is interpreted to be a distinct terrane. We name this eastern area the Kilgore-Craters terrane. The dominant modal mineralogy of granulite xenoliths from Spencer-Kilgore (SK) and Craters of the Moon (CRMO) is $\text{qtz} + \text{fsp} + \text{pyx}$. Usually orthopyroxene is present, but clinopyroxene may also be present, and one sample also contains garnet. All of these lithologies record Archean crystallization histories. These Archean xenoliths are charnockites, and their mineralogy and texture indicate they have undergone granulite facies metamorphism, buried to the mid to lower crust. Three Paleogene granitoid xenoliths are igneous granodiorites. Zircon from these samples exhibit igneous, oscillatory zoning. It is easiest

to discuss the Archean xenoliths separately from the Paleogene xenoliths due to their differing formations.

Zircons in xenoliths with Archean histories record multiple events. In this discussion, for both terranes, the word “event” refers to a phase of zircon growth due to either metamorphism or igneous processes. For each sample, an average age of a growth event is calculated. Each growth event recorded is part of an igneous or metamorphic episode within a longer orogenic cycle. Because samples are from different lithologies, and formed at different times, their growth events can be different parts of that cycle. It is likely that similar ages in different samples are part of the same episode of metamorphism or igneous activity, but are recording different parts of the cycle. For example, growth events could be during prograde, peak or retrograde metamorphism.

Three dominant age groupings of zircon growth events are recorded in the Archean xenoliths (table 2) from SK and CRMO. The first and oldest group is composed of zircons crystallized in the late Paleoproterozoic and the Eoproterozoic, the second is zircons crystallized in the Mesoproterozoic, and the third is zircons crystallized in the Neoproterozoic. The late Paleoproterozoic and the Eoproterozoic ages recorded in zircons are interpreted to be inherited xenocrysts in the protolith granitoids. These oldest dates range from 3334 ± 33 Ma to 3763 ± 24 Ma. Samples often only record two or three Paleo to Eoproterozoic ages or do not record this age population at all. All dates are discordant. Laser spots that reported these dates are from both cores of crystals and from individual crystals. The CL images of the Eoproterozoic and Paleoproterozoic domains exhibit either oscillatory zoning or no zoning. The trace element chemistry of these spots does not follow any pattern within or between samples, indicating the domains have multiple sources.

Table 2: Lower crust of the Snake River Plain zircon growth events

Multiple zircon growth events were identified in samples from the Snake River Plain. Paleoproterozoic to Paleoarchean ages are weighted mean averages of ICPMS laser spot dates that had a discordance of less than 30% (SK, CRMO, HM) or 40% (HM) and where not considered outliers on linearized probability plots. Paleogene dates did not take into account discordance. Ages are $^{207}\text{Pb}/^{206}\text{Pb}$ ages, except Paleogene dates, which are $^{206}\text{Pb}/^{238}\text{U}$ ages. If a date is *italicized*, there are fewer than 5 dates in that sample that are not outliers. A -- sign indicates the sample did not record dates in that era. A + sign indicates a sample recorded dates in that era, but all dates had high discordance. Inherited dates in a sample are listed as a range of dates. For CRMO and SK, Mesoarchean dates are interpreted to be the timing of igneous xenolith formation and Neoarchean ages are the timing of zircon growth during metamorphism. Neoarchean ages are also interpreted to be the timing of stabilization of the Kilgore-Craters terrane. For SM and HM, Neoarchean dates are the timing of igneous formation.

Sample Name	Paleoarchean	Mesoarchean 1	Mesoarchean 2	Neoarchean	Paleoproterozoic	Paleogene
Sample						
Kilgore-Craters	Date(Ma), n	Date(Ma), MSWD, n	Date(Ma), MSWD, n	Date(Ma), MSWD, n	Date(Ma), MSWD, n	Date(Ma), MSWD, n
Spencer Kilgore						
SK11-01	3334 – 3763, 15	--	3144 ± 25, 11, 27	2829 ± 11, .77, 8	--	--
SK11-08	3393 – 3434, 2	--	3194 ± 39, .16, 5	2762 ± 16, .51, 8	--	--
SK11-02	--	3241 ± 14, 1.4, 12	--	2763 ± 17, .024, 4	--	--
SK11-03	--	3242 ± 6.0, 1.7, 35	--	2826 ± 63, 14, 7	--	--
SK11-07	--	3215 ± 14, .26 10	--	2751 ± 16, .28, 9	--	--
Craters of the Moon						
CRMO11-03	--	--	3059 ± 50, 2	2902 ± 65	--	36 ± .60, 3.4, 41
CRMO11-04	--	--	--	--	--	37 ± .49, 2.5, 53
CRMO11-19	--	--	--	--	--	45 ± 1.9, 5.1, 10
CRMO11-01	--	--	3137 ± 12, .33, 15	2776 ± 33, 2.5, 7	--	--
CRMO11-07	--	--	3067 ± 33, 1.6	2928 ± 21, .17, 4	--	--
CRMO11-13	--	--	3066 ± 21, .40, 6	2706 ± 42, 1.2, 5	--	--
CRMO11-05	3496 – 3609, 2	--	3001 ± 8.0, .04, 5	2766 ± 9.0, 1.0	--	--
CRMO11-12	3411 – 3430, 2	3276 ± 46, 4	--	2703 ± 52, 8, 10	2498 ± 21, 1.2, 8	--
CRMO11-14	3420 – 3776, 17	3227 ± 18, .4, 32	--	2842 ± 150, 5.0, 3	--	--

Table 2: Lower crust of the Snake River Plain zircon growth events con't

Sample Name	Paleoarchean	Mesoarchean 1	Mesoarchean 2	Neoarchean	Paleoproterozoic	Paleogene
CRMO11-15	3356 – 3444, 5	3285 ± 11, .24, 18	--	--	--	34 + 8.7, 3
CRMO11-18	3472 – 3482, 2	3287 ± 14, .20, 12	--	--	--	--
CRMO11-16	3392 – 3482, 2	3254 ± 5.8, .3, 8	--	--	--	--
CRMO11-17	3321 -3595, 8	3222 ± 17, 1.0, 10	--	+	--	--
Square Mt. terrane						
Square Mountain						
SM10-A3		3292 – 3363, 3	--	2679 + 120, 6.0, 3	--	--
SM10-C2	--	--	2778 – 2910, 4	2546 + 27, 1.9, 7	--	--
SM10-C3	2863- 3683, 3			2549 + 6.0, 1.4, 18	--	--
SM10-C4	--	--		2577 + 3.9, .42, 17	--	47 ± .55, 8.8, 62
House Mountain						
HM11-01	3337-3624, 2	--	--	2541 ± 55, 1	+	--
HM11-06	--	--	--	2511 ± 11, .94, 11	1893 ± 57, 2	37 ± 15.0, 2

Typical elevated REE patterns and negative Eu anomalies indicate the zircons formed in the continental crust in the presence of feldspar. Because there is no pattern to the chemistry or dates and the Paleoproterozoic and older domains are never from overgrowths on crystals, this population of cores and crystals are interpreted to be inherited. One explanation of inheritance is the Paleoproterozoic and older cores and crystals crystallized in a crustal melt that inherited zircons from the source rock. These inherited very old ages in zircons indicate the magma was sourced from an older, crustal rock, and that these xenoliths were formed from recycled crust.

Thin sections of the xenoliths record textures of late stage recrystallization. Relic textures that would hold clues to sedimentary or igneous protoliths of the gneisses are not evident. However, the modal mineralogy of qtz + fsp + pyx indicates igneous felsic to intermediate plutonic protoliths. In particular, the presence of pyroxene and lack of aluminosilicates provide evidence of an igneous protolith. Pyroxene indicates amphiboles were present in the protolith. The lack of aluminosilicates indicates sheet silicates were not abundantly present in the protoliths, common minerals in sedimentary rocks. Sheet silicates break down to form aluminosilicates during metamorphism (Spear, 1994, 338-391). Kyanite and sillimanite remain stable under high temperatures and pressures (Holdaway, 1971; Spear, 1994, 338-391) including 8-10 Kb, the pressure these rocks are interpreted to have undergone, indicated by their charnockitic mineralogy. If micas were a major mineral component of the protolith, aluminosilicates would still be present in these xenoliths. Thus, the protoliths of the gneisses are interpreted to be igneous, specifically granodioritic to granitic. Mesoproterozoic grains and domains from SK and

CRMO record TiZR temperatures from 600°C to over 900°C (fig. 11). These temperatures are within the range of typical granodioritic to granitic magmatic conditions.

The crystallization of the plutonic protoliths is recorded in zircon domains from the Mesoarchean. Mesoarchean domains include both volumetrically dominant mantles on older cores and individual crystals. Two groupings of ages are recorded in Mesoarchean domains from SK and CRMO. The older is at ~3200 Ma and the second at ~3050 Ma. However, as each sample is interpreted to be a different lithology, it is best to look at the individual age of crystallization for each sample (table 2).

Two samples, CRMO11-01 and CRMO11-04, have a very large spread of dates that are less than 30% discordant. This results in very long “tails” on their linearized probability plots (see appendix D). Upon first look, it is easy to assume there is more than one event being recorded in these samples, perhaps where there are groupings of dates. The trace element plots of these samples also indicate two distinct chemical groups. However, the different chemistry groupings do not correlate to date groupings, but instead to sector zoning of high uranium and low uranium areas, imaged by cathodoluminescence, and there is no pattern between chemistry and dates. There is also no pattern between dates and discordance, which would indicate the “tails” were due to lead loss. Instead these two sample likely show evidence of ancient Pb loss, which expresses itself as dispersion in the $^{207}\text{Pb}/^{206}\text{Pb}$ age.

Because the Mesoarchean growth events are the oldest recorded events in each sample that are not inherited, it is likely that these events record the crystallization of the protolith. Mesoarchean events are recorded in domains that exhibit oscillatory zoning and

sector zoning, both common internal structures of igneous zircon (Varva, 1990; Hanchar and Miller, 1993; Benisek and Finger, 1993; Hoskin and Schaltegger, 2003). However, the oscillatory zoning is always blurred, and sector zoning is also an internal structure associated with metamorphic zircons (Hoskin and Schaltegger, 2003; Watson & Liang, 1995). Mesoarchean domains are also imaged as unzoned mantles on inherited cores, for example in sample CRMO11-14 (fig. 11). An unzoned internal structure indicates a zircon has completely recrystallized during metamorphism (Hoskin and Schaltegger, 2003). In amphibolite facies and granulite facies metamorphism, it is possible for large amounts of new zircon to form at subsolidus conditions and during anatexis (Watson and Harrison, 1983; Watson, 1996a; Schaltegger et al., 1999; Rubatto et al., 2001; Hoskin and Schaltegger, 2003), and that may be what happened during the Mesoarchean zircon growth events recorded in zircons from SK and CRMO. However, there is a definite metamorphic episode in the Neoproterozoic that affected these xenoliths (described below). It is most likely that the blurring of the oscillatory zoning is an effect of the younger metamorphism. For the Mesoarchean grains that have no zoning, it is possible that transgressive recrystallization during younger metamorphism left “ghosts” of U/Pb ratios from the protolith zircon, as described by Hoskin and Black (2000). The most potent evidence that the Mesoarchean dates are igneous and not metamorphic is that they are the oldest common dates recorded in all the zircons in a sample. One of the characteristics of zircon that makes it a robust tool for complicated geochronological studies is its ability to retain U/Pb ratios under extreme pressure and temperature. If the crystallization of the grains occurred previously, it is likely there would be a record of a grouping of common dates within zircons of a sample. We interpret the Mesoarchean

ages to be the crystallization ages for the igneous protoliths of the xenoliths. Thus, the rocks now beneath Southern Idaho began forming by at least 3.2 Ga. Two periods of igneous activity are recorded at ~3200 Ma and ~3050 Ma, indicating formation continued for hundreds of millions of years. Because the xenolith samples in this study are small fragments lacking geologic context, it is difficult to put their formation and stabilization into a precise tectonic context. However, as the samples' protoliths were part of the growth of the continental crust, it is likely these rocks formed and metamorphosed during an orogenic cycle.

Neoproterozoic Metamorphism of the Kilgore-Craters Terrane

The third growth event recorded in Archean xenoliths is recorded in overgrowth domains and individual crystals of zircons. Distinction between Mesoarchean and Neoproterozoic populations can be made by comparing $^{207}\text{Pb}/^{206}\text{Pb}$ dates, U/Pb concordia diagrams, trace element chemistry, and CL images of grains. The dates of the Neoproterozoic event range from 2.9 Ga to 2.6 Ga. Within samples, these dates form well-defined, linear, discordia lines below the older events. They are obvious, distinct growth events.

Zircon growth during the Neoproterozoic is interpreted to be due to metamorphism. Evidence for this is found in CL images and trace element chemistry. CL images indicate that Neoproterozoic dates are recorded in overgrowths and individual grains. Both domain types exhibit unzoned internal textures. Overgrowths cut across primary oscillatory zoning from the Mesoarchean. An unzoned zircon texture in metamorphic zircon has been described at length in the literature (e.g. Black et al., 1986; Schaltegger et al., 1999; Hoskin and Black, 2000). This texture can be formed through transgressive recrystallization, where recrystallizing begins on the outer edges of the crystal and

recrystallizes in the center last. Complete recrystallization results in a completely featureless zircon (Hoskin and Schaltegger, 2003). Unzoned zircon can also result from subsolidus neoblastic growth (Schaltegger et al., 1999).

Trace element chemistry often cannot indicate igneous activity or metamorphism if only one domain is recorded in a zircon. However, if more than one age domain is recorded, chemistry patterns can be compared and patterns may help to interpret growth processes. In samples from SK and CRMO, comparison of trace elements between Mesoarchean and Neoproterozoic domains indicate the Neoproterozoic domains are metamorphic. All REE plots from SK and CRMO samples record Neoproterozoic domain HREE concentrations peaking lower than Mesoarchean concentrations, sometimes by two orders of magnitude. Hoskin and Black (2000) noted that HREE are expelled from zircon during sub-solidus recrystallization, which promotes one mechanism to explain this depletion. Alternatively, the reservoir of REE in the protolith may be depleted by progressive metamorphic reactions, particularly dehydration and partial melt reactions. This mechanism is possible for the samples in this study, given the granulite facies conditions recorded by the xenolith mineralogy. REE can also be sequestered by other minerals. Sample SK11-07 contains garnet, which can easily incorporate HREE into its structure, depleting the availability of HREE for other minerals, such as zircon (Schaltegger et al., 1999). If garnet and zircon grow in equilibrium, a decrease in HREE in the metamorphic zircon domains would be expected. Sample SK11-07 does display a flattening of HREE in metamorphic zones, making it likely the metamorphic zircon grew in the presence of garnet (fig. 10).

Previous workers have observed a decrease in Th/U ratio in metamorphic zircon, under the explanation that Th^{4+} is preferentially expelled over U^{4+} because Th has a larger radius (Hoskin and Black, 2000; Rubatto et al, 2002). However, we observed in this study that most zircon domains associated with metamorphism during the Neoproterozoic have a higher Th/U ratio than older zircon. This is explained by the understanding that metamorphism ~2.8 Ga was high pressure/high temperature, and therefore dehydrating. During dehydration metamorphism, U^{4+} complexes in water form the uranyl oxyanion $(\text{UO}_2)^{2-}$, which is very mobile in water. During Neoproterozoic metamorphism, uranium was preferentially lost from the protolith, resulting in higher Th/U ratios in the subsequently crystallized zircon. In the same samples, Th/Y ratios increase in Neoproterozoic domains as well, again because of the sequestering of U in other metamorphic phases.

Neoproterozoic domains record temperatures between 650°C and 900°C. This temperature range overlaps with Mesoproterozoic domains, however, the mean temperatures are lower for Neoproterozoic domains than Mesoproterozoic domains (fig. 11). Within samples, temperatures of Neoproterozoic metamorphic domains are always below that of the Mesoproterozoic domains. Granulite facies metamorphism can occur at temperatures starting at 600°C for pressures of 6-8 Kbar, the pressure in the mid to lower crust (Spear, 1994, 9). The temperatures recorded in Neoproterozoic domains compound evidence of granulite facies metamorphism. Due to the uncertainties of the Ti-in-Zr method, the mean temperatures of growth events in a sample are not interpreted to be the exact temperatures during metamorphism. Fraser et al. (1997) investigated the control of metamorphic net-transfer reactions on zircons growing at granulite facies conditions and found it difficult

to say with certainty during which phase of metamorphism zircons grow. We do not attempt to assign prograde, peak or retrograde growth to samples or zircons within samples. However, in samples with a large range in temperatures ($>50^{\circ}\text{C}$), and especially for SK11-01 and CRMO11-05, it is likely zircons were growing during more than one part of a metamorphic event.

One sample, CRMO11-12, records a Neoproterozoic age at 2.5 Ga. As will be discussed below, ~ 2.5 Ga is the formation age of the SM terrane. This indicates that certain lithologies of the Kilgore-Craters terrane may have been reworked and metamorphosed as late as 2.5 Ga. However, as this is the only sample of 14 collected recording activity after 2.7 Ga, the stabilization and cratonization of the Kilgore-Craters terrane is interpreted to be completed by 2.7 Ga.

Boundaries of the Kilgore-Craters Terrane

Because the only available data on the lower crust of the ESRP are from the three xenolith field sites discussed in this study, and they are non-continuous along the northern margin of the ESRP, the western boundary of the Kilgore-Craters terrane is difficult to discern with certainty. What is known is the border must be between CRMO and SM, as SM preserves a different geologic story than SK and CRMO. Although no Precambrian outcrops are exposed between SM and CRMO, there is a contact of Paleozoic sediments and Tertiary volcanics in the east and Cretaceous and Tertiary intrusives in the west, which lies between CRMO and SM. This contact may have been shaped by underlying, lower crustal, basement anisotropy. It is possible the western boundary of the Kilgore-Craters terrane is near the contact of Paleozoic sediments and

Cretaceous intrusive rocks and tertiary volcanics (fig. 23). Magnetic anomalies of southern Idaho (Sims et al., 2005) also indicate there is a lower crustal transition at this contact. A possible northern boundary for Archean crust can also be hypothesized using magnetic anomalies.

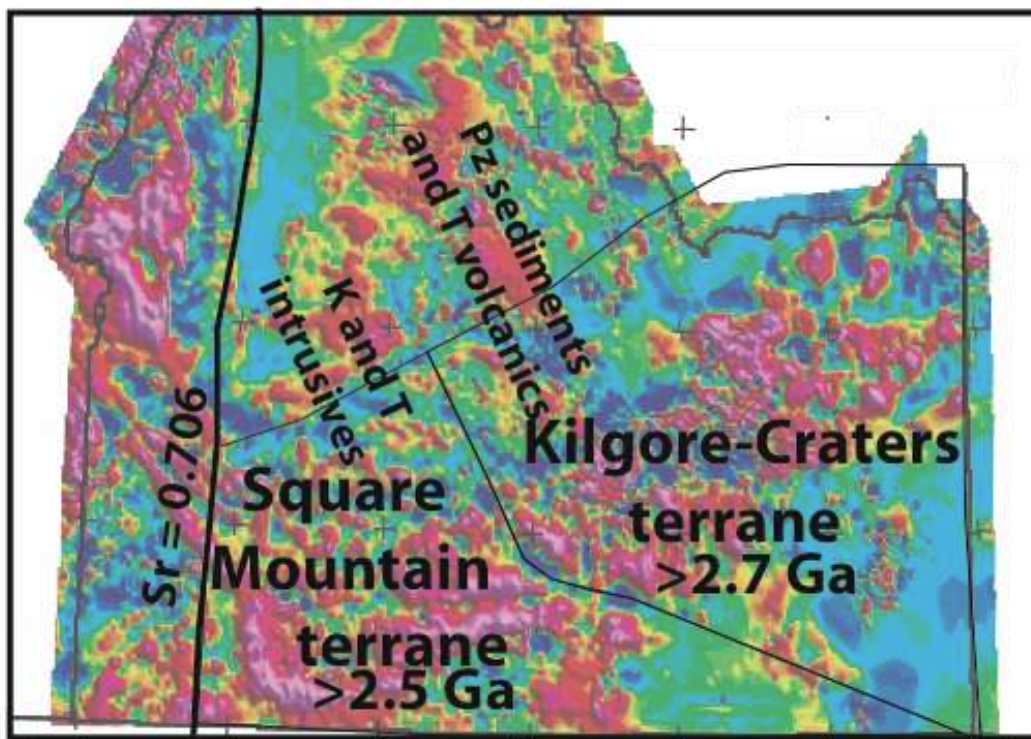


Figure 23: Terranes of the lower crust of southern Idaho. The lower crust of Southern Idaho is composed of two terranes; the Kilgore-Craters terrane in the west and the Square Mountain terrane in the east. The Kilgore-Craters terrane stabilized by 2.8 Ga and Square Mountain terrane by 2.5 Ga. The boundary between the two terranes is likely the contact between Paleozoic sediments and Tertiary volcanics and Cretaceous and Tertiary intrusives. This contact also aligns with magnetic anomalies from Sims et al. (2005).

Formation of the Square Mountain Terrane

The basement underlying Square Mountain (SM) and House Mountain (HM) is interpreted to be distinct from the Kilgore-Craters terrane because samples from Square Mountain and House Mountain record different growth events than those recorded in

Spencer-Kilgore and Craters of the Moon samples (table 2). The events recorded in SM and HM are similar, indicating SM and HM share a geologic history. The region comprising SM and HM will be referred to as the Square Mountain terrane. With the exception of the muscovite-rich paragneiss of HM, the samples from SM and samples HM11-01 are composed primarily of $qtz + fsp + pyx$ and are identified as charnokites. Again, as in SK and CRMO samples, this mineralogy and the lack of aluminosilicates is indicative of metamorphic igneous protoliths of a granodioritic composition. By contrast, the major mineralogy of $qtz + fsp + msc + bt$ for HM11-06 demands a pelitic sedimentary protolith.

Most HM and SM samples record two zircon growth events. All samples record a growth event in the Neoproterozoic, circa 2.5 Ga. The CL images of grains and domains of grains that record this event record oscillatory zoning, blurred or faded oscillatory zoning, and in SM samples, very mottled domains crosscutting oscillatory zoning or from domains with oscillatory zoning. SM10-C3 records mostly mottled grains, although there are grains with mottled cores, clear growth rings, followed by mottled growth rings on the edges. SM10-A3 records the clearest relic oscillatory zoning. In all samples, areas that are more highly mottled are more discordant. Relic oscillatory zoning domains are less discordant. Square Mountain zircons have a high uranium concentration, and in particular the mottled areas have the highest uranium concentrations, making it likely they contain radiation damage. If the zircons were reheated, these areas were easily recrystallized due to radiation damage. We interpret the mottling to be an effect of recent entrainment or underplating, both of which would cause reheating and generate the zero-intercept discordias exhibited by SM zircons. Thus, the relic oscillatory zoning is

indicative of the zircon texture produced during the Neoproterozoic. Oscillatory zoning is associated with igneous zircons. Thus SM terrane zircons crystallized from magmas during the Neoproterozoic.

When zircons record metamorphism, comparing element data between domains provides insight into the changes in chemistry of the rock over time. In rocks that do not record metamorphism, like most of the SM terrane (one sample that is the exception will be discussed below), trace element chemistry is restricted to trying to understand the chemistry of the melt from which the zircons crystallized. As described in the Kilgore-Craters section, thorium and uranium and their concentrations in zircons have been studied greatly. SM10-A3 and SM10-C3 have Th/U ratios ranging from .05 to .6, SM10-C4 and HM11-01 Th/U concentrations range from .02 to over 1, and SM10-C2 ratios range from .04 to .23. All of these are not unusual concentrations for igneous zircons, however, SM10-C2 has low enough concentrations to, if trace element chemistry were the only tool used, consider these zircons as metamorphic. Rubatto (2002) observed that metamorphic zircon produces low Th/U ratios, often below .05. The relic igneous texture and anhedral to sub-anhedral morphology of SM10-C2 grains contradict a metamorphic origin for SM10-C2 samples. The low Th/U ratio comes from a high concentration of U in this rock, and from a high concentration of U in the parent material of the melt.

All except two samples from HM and SM also record zircon growth in the Meso and/or Paleoproterozoic. Zircon domains that record Paleo to Mesoarchean dates are obvious cores or are laser spots from the middle of crystal. These dates are interpreted to be inherited ages. It is likely the inherited ages were sourced from the Kilgore-Craters terrane, as this region is close in proximity and the inherited dates match growth events

recorded in the Kilgore-Craters terrane. Despite the very low Th/U ratio of SM terrane rocks, the Neoproterozoic zircons from SM and HM11-01 are interpreted to have formed from igneous processes. The mineral assemblage of the xenoliths and one of the HM samples (opx ± cpx + fsp + qtz), the gneissic banding, and the granoblastic texture of the grains indicate that at some point these samples, and the lithologies they are sourced from, reached granulite facies conditions. No other events are recorded after 2.5 Ga in SM zircons and in the zircons from the HM orthogneiss sample, making it impossible to determine the timing of metamorphism in the samples using zircons. The lack of metamorphic overgrowths on zircons indicates metamorphism did not lead to anatexis. There was no reservoir for zircon growth. The ~2.5 Ga growth events could be interpreted as the timing of metamorphism, but as there is no evidence of complete recrystallization (which would be evident in CL images). One hypothesis to explain the data is that these melts intruded and crystallized in the lower crust under granulite facies conditions. Regardless of the exact history of magmatism and metamorphism, we interpret the lower crust of the Square Mountain terrane to be stable since the end of the Neoproterozoic, approximately 2.5 Ga.

Boundaries of the Square Mountain Terrane

The eastern limit of the SM region is hypothesized to be at the contact of the Paleozoic sediments and Cretaceous intrusive rocks and tertiary volcanics in southern Idaho, for reasons described in the border of the Kilgore-Craters terrane section. No other Precambrian outcrops are exposed west of HM, making it difficult to discern the western margin of the Square Mountain terrane. As with the eastern boundary, other geochemical

and geological boundaries that are exposed on the surface can be used to hypothesize lower crustal boundaries. The $^{87}\text{Sr}/^{86}\text{Sr} = .706$ line (Armstrong et al., 1977) and associated Salmon River suture zone along the Idaho-Oregon border is likely the western boundary of the Square Mountain Terrane.

Paleogene Reactivation

Four samples (CRMO11-03, CRMO11-04, CRMO11-15 and CRMO11-19) collected from the Kilgore-Craters terrain and two samples (SM10-C4 and HM11-06) collected from the SM terrane record zircon growth during the Paleogene between 33 and 50 Ma. CRMO11-03, CRMO 11-04, CRMO11-19 and SM10-C4 record Paleogene ages in oscillatory zoned, euhedral, igneous zircons. SM10-C4 also records large Archean cores, however the interlocking texture and mineralogy of SM10-C4 leave no doubt of the xenoliths igneous plutonic origins. CRMO11-03 and CRMO11-04 share near identical geochemistry and ages, and thus are likely xenoliths of the same pluton. CRMO11-15 and HM11-06 record Paleogene dates in overgrowths and metamorphic crystals. These growth domains were most likely driven by contact heat from surrounding plutons or possibly by melt infiltration from the plutons.

Eocene volcanic fields are found throughout the Pacific Northwest US, and the Challis Volcanic region is the field closest to the Snake River Plain (Gest and McBirney, 1979; Moye and others, 1988; Carlson et al., 1991; Suayah and Rodgers, 1991; O'Brien et al., 1991; Armstrong and Ward, 1991). The Challis Volcanics, a region of intermediate to felsic caldera complexes volcanic and metamorphic rock to the north of the Snake River Plain, initiated at 51 Ma (Lipman et al., 1971; Fox, 1983; Armstrong and Ward,

1991). The Challis volcanics are part of the Kamloops-Challis-Absaroka igneous episode (Armstrong and Ward, 1991). The xenoliths from the SRP recording Paleogene ages are interpreted to have formed in connection to Paleogene volcanism of the western US, perhaps directly to the Kamloops-Challis-Absaroka igneous episode.

Conclusion

Lower crustal Precambrian xenoliths collected from the northern margin of the Eastern Snake River Plain, and a Precambrian outcrop in the Western Snake River Plain have provided insight into formation of Archean continental crust in what is now southern Idaho. This study has discovered that two distinct terranes comprise the lower crust of the Snake River Plain. Each terrane had a separate formation and stabilization history.

The Kilgore-Craters terrane stretches from the Wyoming Province into Craters of the Moon National Monument and Preserve. It is impossible to tell the exact location of the western boundary of the terrane, however it is possible the boundary is near the surface contact between Paleozoic sediments and Tertiary volcanics, and Cretaceous and Tertiary intrusives and a negative aeromagnetic anomaly identified in this same area by Sims et al. (2005).

Igneous plutonic rocks of the The Kilgore-Craters terrane began forming at ~3.2 Ga, continued until ~3.0 Ga. The Kilgore-Craters terrane then underwent a cycle of granulite facies metamorphism that lasted between 2.8 and 2.7 Ga, which is interpreted to be the timing of cratonization of the Kilgore-Craters terrane given the lack of subsequent zircon growth events.

The Square Mountain terrane stretches from the western border of the Kilgore-Craters terrain to the $^{87}\text{Sr}/^{86}\text{Sr} = .706$ line. Much of this terrane also has igneous plutonic origins, although one sedimentary layer with similar formation age was identified in the Western Snake River Plain. The crust-forming episode that led to the formation of this

terrane lasted from 2.6 to 2.5 Ga. Mineralogy and petrography indicate the Square Mountain terrane also underwent granulite facies metamorphism. However, zircons from SM and HM samples do not record a metamorphic growth event. There is no indication of metamorphism in the CL images of zircons or U/Pb geochronology patterns. Thus, it is likely the metamorphic event did not produce melt from which zircon overgrowths could form or that metamorphism was immediately following igneous activity, within a time frame too fine for techniques used in this study. The stabilization of the Square Mountain terrane is interpreted to have happened by 2.5 Ga. A 1.9 Ga event was recorded at HM, indicating the collision associated with the formation of Laurentia was recorded in parts of the lower crust of southern Idaho.

CHAPTER VY Q: THE SNAKE RIVER PLAIN AND THE WYOMING CRATON

Introduction

Granulite xenoliths erupted in Neogene basalts of the Eastern Snake River Plain (ESRP) and a Precambrian outcrop on the southern margin of the Idaho Batholith have constrained the nature and timing of formation and stabilization of the lower crust of southern Idaho. Based upon these samples, the lower crust of southern Idaho formed as two distinct terranes. The Kilgore-Craters terrane in the east began forming 3.2 Ga and cratonized at 2.7 Ga. The Square Mountain terrane in the west formed and stabilized between 2.68 Ga and 2.54 Ga (fig. 23).

Now that the Precambrian history of the underlying crust of the Snake River Plain has been constrained, it is possible and important to place it within the context of surrounding Precambrian crustal formation. This chapter aims to compare the crystalline basement of southern Idaho to the Precambrian terranes mapped in the adjacent Wyoming Province and Grouse Creek Block (Compton et al.; 1977; Todd et al.; 1973; Hoffman et al.; 1988; Foster et al.; 2006). The western margin of the Wyoming Province has been poorly constrained due to lack of outcrop, and it has been suggested that the western margin may extend into the ESRP (Sims et al., 2005; Wolf et al., 2005). To the south of the SRP lies the Archean Grouse Creek Block (Foster et al. 2006). To the north of the SRP lies the Selway Terrane, composed of juvenile arcs that helped to suture Archean provinces during the Trans-Hudson orogen (Compton et al., 1977; Foster et al.,

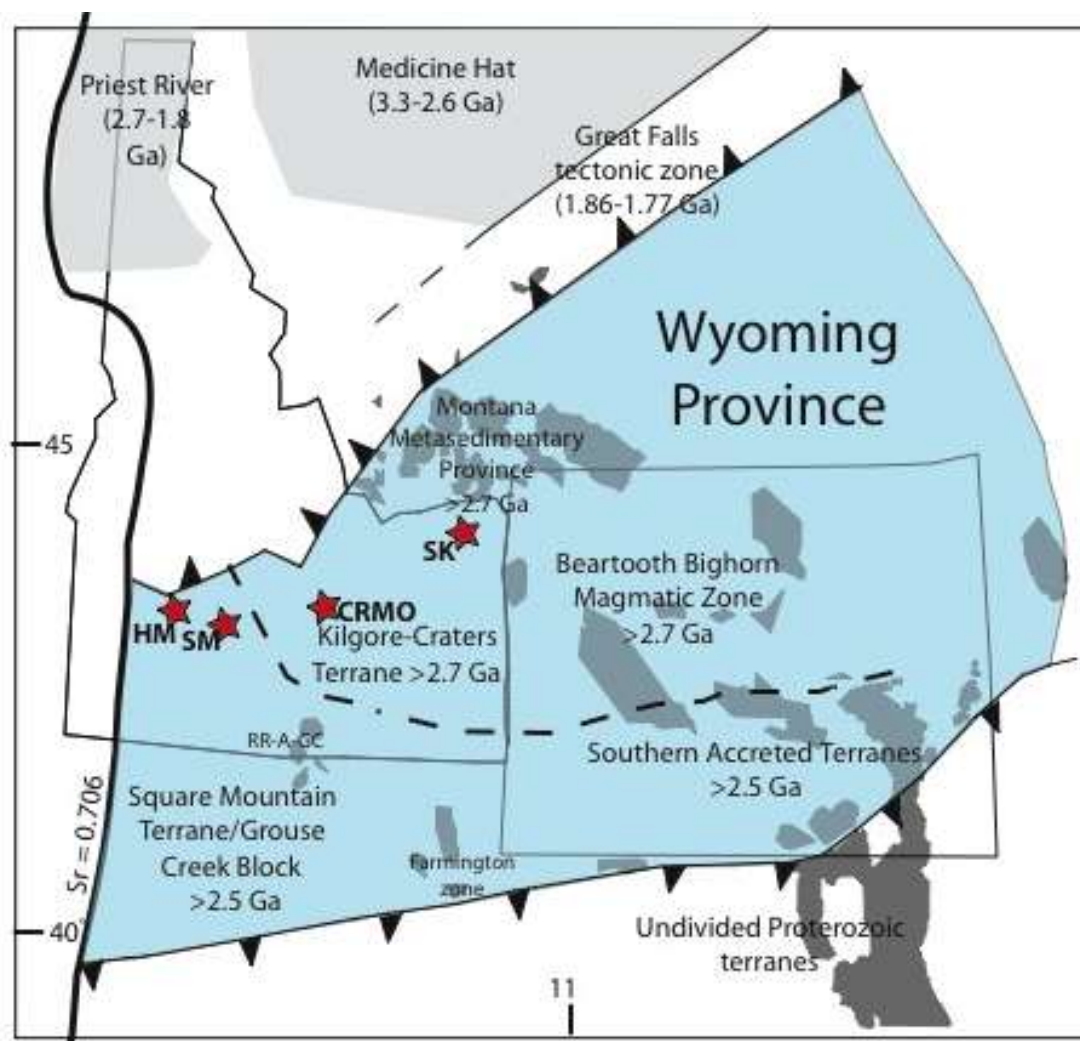


Figure 24: Precambrian crust of Idaho, Wyoming and Montana. The Kilgore-Craters terrane is a westward extension of the northern cratonic core of the Wyoming Province. The Grouse Creek Block and the Square Mountain terrane are extensions of the Southern Accreted Terranes of the Wyoming Province. Gray areas are Archean outcrops. Figure modified from Foster et al. (2006) and Gaschnig et al. (2012), and uses elements of Sims et al. (2005).

2006). This study correlates the Southern Idaho lower crust with these surrounding provinces using U/Pb geochronology and Hf isotope ratios in zircon. Archean geologic events and Hf signatures of samples across the Snake River Plain match those of the Wyoming Province. The Kilgore-Craters terrane is interpreted as a westward extension of the northern cratonic cores of the Wyoming Province. The Square Mountain terrane is

correlated to the Grouse Creek Block, both are westward extensions of the Southern Accreted Terranes of the Wyoming Province (fig. 24).

Geologic Background

Wyoming Province

The basement rock of the Eastern Snake River Plain is unknown except for xenoliths, as it has been extensively covered by rhyolite and then basalt from the Miocene to present. Because the basement rock of the Eastern Snake River Plain is covered, investigations of surrounding regions provide insight into possible early geologic context of the ESRP. To the east of the ESRP lies the Wyoming Province, one of several Archean microcontinents that collided to form Laurentia, the core of the North American Plate, at 1.8 Ga (Hoffman, 1988; Ross and Villeneuve, 2003). Within the Wyoming Province is the Wyoming Craton. Cratons represent the oldest and coldest, often thickest, continental crust, and have survived generations of rifting and collisions. The Wyoming Province has been delineated based on outcropping Archean rocks. To the north of the province is the Great Falls tectonic zone (GFTZ), to the east the Trans-Hudson Orogen, and to the south the Cheyenne belt. These three zones are Proterozoic collisional origins. The western margin of the Wyoming Province is poorly constrained, as any basement rock that may have been exposed is now covered by Miocene volcanics. It has been suggested that the western margin may extend into the ESRP (Wolf et al., 2005). Sims et al. (2005) has also suggested the Wyoming craton extends across the ESRP, and that the western Snake River Plain (WSRP) is also composed of Archean crust. Sims et al. (2005) does not attach the WSRP Archean crust to the Wyoming

Province, but instead calls it extended crust. This study in part investigates the western margin of the Wyoming Craton.

The Wyoming Province has been split into three provinces: the Montana Metasedimentary province (MMP), the Beartooth-Bighorn magmatic zone (BBMZ) and the Southern Accreted Terranes (SAT) (fig. 24). The MMP and BBMZ have been linked to a common Archean crustal history by a distinctive elevated $^{207}\text{Pb}/^{204}\text{Pb}$ isotopic signature (Wooden and Mueller, 1988; Mueller et al., 1993; Frost et al., 1998) as well as detrital zircon grains and domains from 2.80 to 3.00 Ga gneisses that yield U/Pb and Nd model ages up to 4.0 Ga (Mueller et al., 1992, 1998; Frost and Fanning, 2006; Grace et al., 2006). These commonalities mark the two terranes as a single block sharing similar formation processes (Mognk et al., 1992).

Two Archean lithologies characterize the Montana Metasedimentary province: quartzofeldspathic gneisses and low to high grade metamorphosed supracrustal assemblages (Mueller et al., 1993). Supracrustal assemblages include quartzites, pelites and carbonates (Mueller et al., 1993; Mueller and Frost, 2006). The gneisses are the oldest lithologies of the province, with ages between 3.0 and 3.5 Ga (Mueller et al., 1993; Mueller and Frost, 2006).

The Early Archean rocks of the Beartooth Mountains are mostly supracrustal in origin and are interpreted to have been deposited on a continental shelf environment, sourced from ultramafic and quartz-rich igneous rocks (Mueller et al., 1982; Muller et al., 1985). They are exposed as both kilometer-sized terranes and as xenoliths in and plutonic and meta-plutonic rocks (Meuller et al., 1985). Mineral assemblage geothermometers (Wells, 1977; Ferry and Spear, 1978; Dahl, 1980) and geobarometers (Newton and

Perkins, 1982) indicate granulite facies metamorphism of the rocks occurred at 800°C and 6 kb (Henry et al., 1982). Rb-Sr whole rock geochronology indicates granulite-facies metamorphism at 3.35 Ga (Mueller et al., 1985). These data supports pre-3.4 Ga crust in the Beartooth Mountains (Mueller et al., 1985), first suggested by zircon U-Pb ages of 3.3 Ga (Mueller et al., 1982). Mueller et al (1985) interpret the event to be a continental collision along the margin of an Early Archean continent, a model that allows for rapid burial from crustal thickening and an orogenic geotherm of 40-45°C/km.

Dioritic to granitic rocks are the most common composition of Late Archean exposures in the Beartooth Mountains (Muller et al., 1985). A 2.8 Ga amphibolite facies tectonic event has been interpreted from a Rb-Sr whole-rock isochron age of 2.8 Ga from granite, granodiorite and amphibolite in the Long Lake region of the Beartooth Mountains (Wooden et al., 1982; Mueller et al., 1985). The three lithologies of plutonic rocks give a similar age (2.8 Ga), however the granodiorite and amphibolite are found as inclusions in the granite and must be older (Mueller et al., 1985). Mueller et al. (1985) interpreted this event to be the result of calc-alkaline magmatism associated with subduction beneath the Archean plate boundary followed by continued contraction and collision and associated amphibolite facies metamorphism and granitoid magmatism. These contractional events and associated magmatism lasted until 2.6 Ga (Mueller, 1979; Wooden et al., 1982).

The Southern Accreted Terranes (SAT) are characterized by late Archean magmatism and mid-neo Archean supracrustal sequences. Late Archean magmatism originated during pulses of orogenesis along the southern Margin of the Wyoming Craton at 2.71-2.67, 2.65-2.62, and 2.55-2.50 Ga (Chamberlain et al., 2003) as a result of active

margin tectonics (Frost et al., 1998). Past hypotheses for orogenesis include a western block colliding with the Wyoming Province, forming an east-northeast striking subduction zone that transitioned to a north verging zone at ~2.65 Ga (Frost et al., 1998; Chamberlain et al., 2003; Grace et al., 2006; Keane et al., 2006).

The supracrustal sequences of the SAT block consist of metavolcanics and metasediments. Metasediments have been linked to older continental detritus, perhaps from the BBMZ and MMP, as well as juvenile sources by Nd isotopic data (Frost et al. 2006b; Grace et al., 2006; Souders and Frost, 2006). Juvenile sources are inferred to be from accreted terranes and indicate collisional tectonics. Collisional tectonics and associated magmatism of the Late Archean contributed to crustal growth of the Wyoming craton (Mueller and Frost, 2006). Cratonization of the Wyoming Province occurred during this time of accretion (Mueller et al., 2004; Mueller and Frost, 2006).

Tectonic and magmatic quiescence followed the addition of the SAT until the Wyoming Province was incorporated into Laurentia ca. 1.8-1.9 Ga. A series of collisional events welded the Wyoming Province to the Hearne-Medicine Hat terrane in the north and the Superior terrane to the east, by way of the Great Falls tectonic zone and Dakota segment of the TransHudson Orogen, respectively. The accretion of arcs and microcontinents to the margins of the Wyoming craton commenced at about 1.90 Ga and extended to about 1.6 Ga (Mueller et al., 2004a). There is no significant associated arc magmatism or tectonic activity within the Wyoming Province during this time (Mueller et al., 2005).

Sample Materials

Thirty-two crustal xenoliths were collected from the northern margin of the Eastern Snake River Plain at Square Mountain (SM) in Fairfield, Idaho, at Craters of the Moon National Monument and Preserve (CRMO), Idaho, and at Spencer-Kilgore (SK), Idaho. Two samples were also collected from a known Precambrian outcrop at House Mountain, near Mountain Home, ID. The xenolith sample sites were chosen because they create an east west transect across the northern margin of the Snake River Plain. The sites have been used in past studies, also making them ideal field locations. The House Mountain site was chosen because it is the only known outcrop of Precambrian rock on the northern flank of the Snake River Plain, and extends the study further westward toward the inferred rifted margin of Laurentia (Armstrong, 2001). For specifics on the samples collected, see Chapter 1: Sample Materials.

Analytical Methods

Zircon $^{176}\text{Lu}/^{177}\text{Hf}$ Ratio Analysis

The unstable radionuclide ^{176}Lu decays to stable ^{176}Hf by β - decay, creating an isotopic tracer that can be used in several geological applications. In this study, $^{176}\text{Lu}/^{177}\text{Hf}$ ratios in zircons were used as isotope tracers of crustal growth, since fractionation of Lu-Hf occurs during magma generation and crustal differentiation (Patchett et al., 1981; Kinny and Maas, 2003). Both Lu and Hf are incompatible elements, however Hf is more incompatible than Lu. During mantle melting more Hf enters the melt than Lu, ultimately creating a crust that has a lower $^{176}\text{Lu}/^{177}\text{Hf}$, which in

time evolves to lower $^{176}\text{Hf}/^{177}\text{Hf}$. This differentiation leads to a mantle with higher time evolves to higher $^{176}\text{Hf}/^{177}\text{Hf}$ (Patchett et al., 1981) (fig 25a). The $^{176}\text{Hf}/^{177}\text{Hf}$ can continue to be lowered in the crust if melt is further extracted from early crust, or can become re-enriched (higher $^{176}\text{Hf}/^{177}\text{Hf}$) and move toward chondritic levels through mantle derived additions (Patchett et al., 1981).

$^{176}\text{Hf}/^{177}\text{Hf}$ ratios vary only in their fourth or fifth decimal place, making it difficult to compare ratios between samples. Thus, an epsilon (ϵ) notation is used for an easier comparison. The ϵ notation is defined as

Equation 5: ϵ_{Hf} notation

$$\epsilon^t(\text{Hf}) = \left[\frac{\left(^{176}\text{Hf}/^{177}\text{Hf} \right)_{\text{sample}}^t}{\left(^{176}\text{Hf}/^{177}\text{Hf} \right)_{\text{CHUR}}^t} - 1 \right] * 10^4$$

where the ratio of Hf in the sample at time t is compared to the ratio of CHUR (chondritic uniform reservoir) at time t. Samples derived from an enriched $^{176}\text{Lu}/^{177}\text{Hf}$ source (mantle) will produce positive ϵ values. Samples derived from a depleted $^{176}\text{Lu}/^{177}\text{Hf}$ source (crust) will produce negative ϵ values (fig 25b). In this study ϵ values of the Snake River Plain were compared to surrounding Archean terranes to determine if they share an early history.

$^{147}\text{Sm}/^{144}\text{Nd}$ isotope analysis has traditionally been used as a geochemical tracer and indicator of crustal evolution and its systematics are similar to the Lu/Hf system (DePaolo and Wasserburg, 1976). However, the fractionation of Lu/Hf during mantle melting is double that of Sm/Nd, and the half-life of ^{176}Lu is shorter than that of ^{147}Sm

(Patchett and Tatsumoto, 1980; Patchett, 1983), providing a greater resolution of mantle evolution and melt source. It is also possible to analyze Hf in-situ on the same zircons

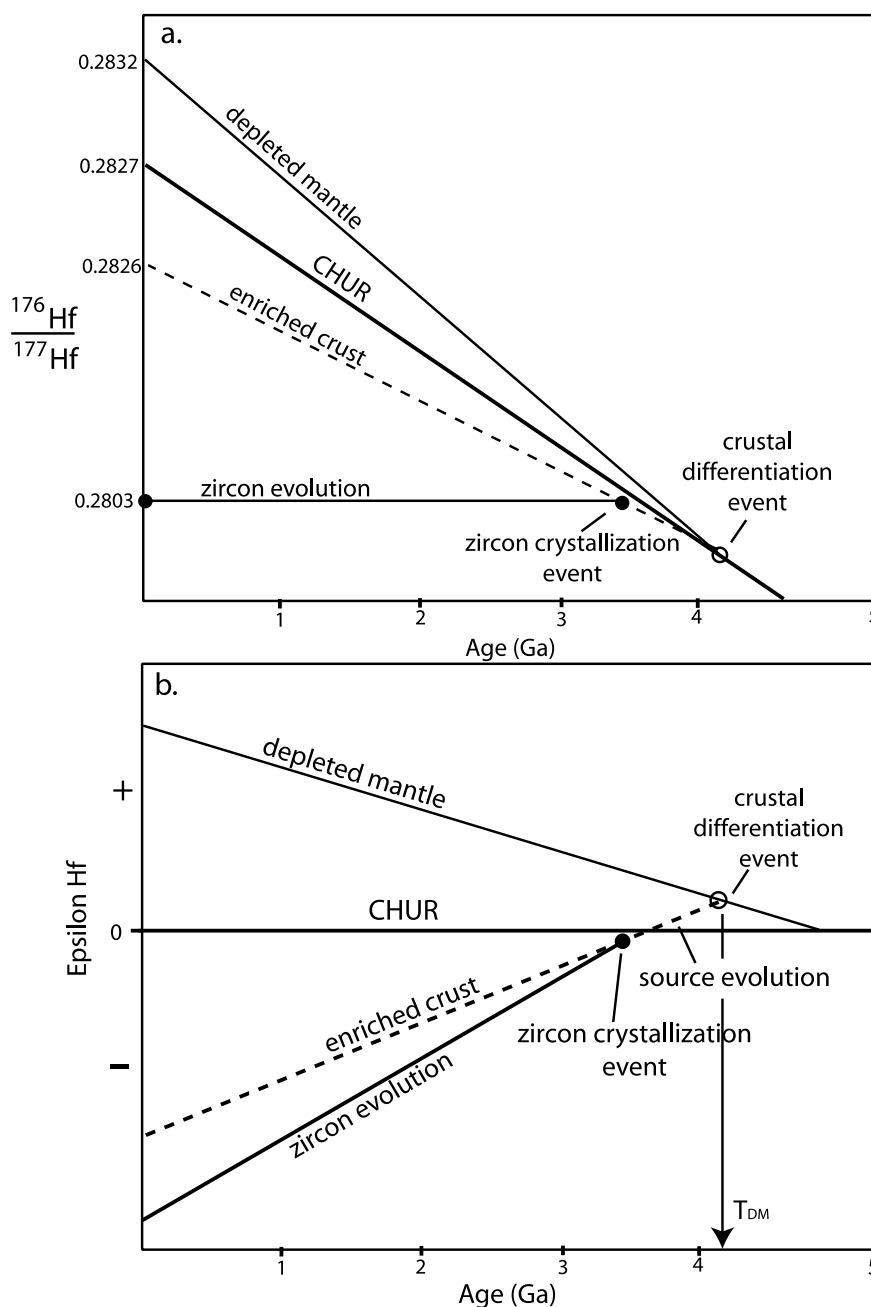


Figure 25: A general $^{176}\text{Hf}/^{177}\text{Hf}$ vs Age chart (a) and a general epsilon Hf chart where $^{176}\text{Hf}/^{177}\text{Hf}$ of a sample is normalized to CHUR (b). Lu and Hf are incompatible elements, however Hf is more incompatible than Lu and during mantle melting more Hf enters the melt than Lu. ^{176}Lu decays to ^{176}Hf , resulting in a depleted $^{176}\text{Hf}/^{177}\text{Hf}$ crust and an enriched $^{176}\text{Hf}/^{177}\text{Hf}$ mantle (a). Zircon easily incorporates Hf into its structure, due to charge and size, compared to Lu. This

results in negligible ingrowth of ^{176}Hf in zircon. Because $^{176}\text{Hf}/^{177}\text{Hf}$ ratios vary only in their 4th and 5th decimal places, epsilon Hf notation is used to magnify differences between ratios (b). T_{DM} is the time the source melted from the depleted mantle (b).

used for U/Pb analysis. For these reasons, Lu/Hf analysis was used in this study, instead of Sm/Nd.

Zircon is a practical mineral for Hf isotope ratio analysis, and convenient in this study as zircons were already being used for U/Pb geochronology. The ionic radii of hafnium (Hf) and zirconium (Zr) are practically the same, and they have the same charge (+4). Thus, Hf readily substitutes for Zr in zircon. Lutetium, the radioactive parent of isotope ^{176}Hf , does not substitute as readily into Zr, and so the ratio of Hf isotopes today in a zircon is nearly what it was when the crystal formed. A correction is made to subtract any radiogenic Hf formed from the small amount of Lu in the zircon, based on the measurement of Lu in the crystal, to yield the initial Hf ratios when the zircon formed.

Hf isotope data were collected at Washington State University by in-situ laser ablation on a New Wave Nd:YAG UC 213 nm laser at a 40 μm spot. In order to ensure the Hf data could be correlated to the samples analyzed in the first part of this study (U/Pb ages), the same zircon grains polished, imaged and LA-ICPMS dated at Boise State University were used for Hf analysis. U/Pb data were also collected at Washington State University simultaneously with Hf isotope data using a split stream. U/Pb geochronology results from Boise State University and Washington State University were comparable (fig 26).

Laser spots were analyzed from samples SK11-01, SK11-03, SK11-07, SK11-08, CRMO11-05, CRMO11-14, CRMO11-15, CRMO11-16, CRMO11-17, SM10-A3, SM10-C3, SM10-C4 (table 3). B144, Piexe, FC1, 91500 and Mud Tank were analyzed as secondary standards. Using a 40 μm spot size made it difficult to target individual growth

domains on most zircons, and impossible to analyze small zircons, thus limiting samples that could be analyzed. Raw data were reduced using Iolite.

Zircon U/Pb Geochronology

As mentioned above, the same zircon crystals subject to U/Pb age analysis at Boise State were used in the Hf isotope study. U/Pb data were also collected contemporaneously with Lu/Hf and Hf isotope data at Washington State University (WSU) by in-situ LA-ICPMS. Fewer data were collected at WSU due to time constraints. The high U content of the zircons also caused the pulse-counting detector of the Element 2 at WSU to ‘trip’ during many analyses; most spots that caused the collector to trip were discarded, resulting in even less data. Thus, the dates recorded at WSU were not used in age analysis, but were used to compare and confirm that analyses at both institutions are from the same material. Analysis and probability density functions demonstrate that the U/Pb data collected at WSU concur with U/Pb data collected at BSU (fig. 26).

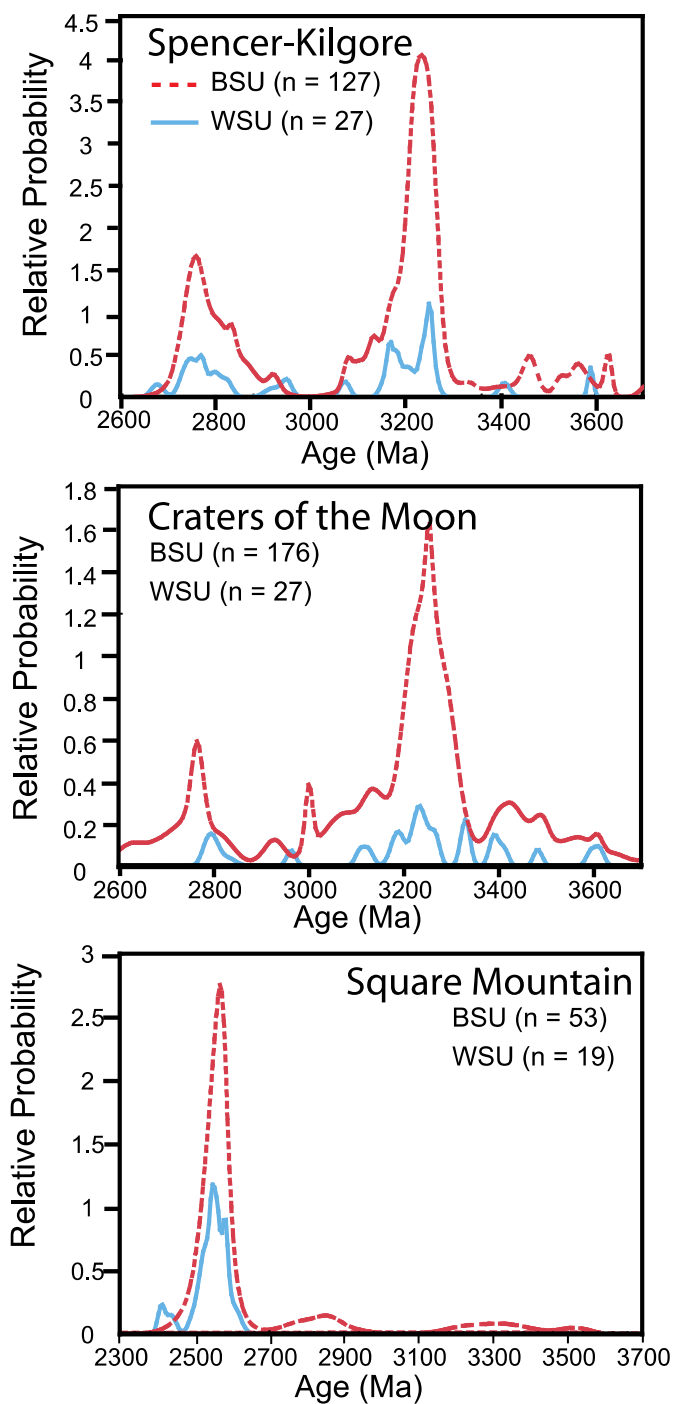


Figure 26: Stacked probability chart of Precambrian $^{207}\text{Pb}/^{206}\text{Pb}$ ages from Washington State University (WSU) and Boise State University (BSU) for zircons from Spencer-Kilgore (SK), Craters of the Moon (CRMO) and Square Mountain (SM). The same zircons were used in data collection at both institutions. All data collected at WSU are used. Due to the large amount of data collected at BSU, only dates that were not found as outliers were used (see Chapter 1: Methods for details on outliers).

Results

Hf Isotope Analysis

Samples from Spencer Kilgore (SK), Craters of the Moon (CRMO) and Square Mountain (SM) were analyzed for Hf isotope concentrations (table 3, fig. 27). Results from all three field areas align with results from Snake River Plain xenoliths analyzed by Dufrane et al. (2007). Analyses from Spencer-Kilgore samples targeted grains with U/Pb crystallization ages of 3.76 Ga – 2.4 Ga. These crystallization ages encompass the formation and stabilization of Spencer-Kilgore crust as estimated from the magmatic and metamorphic zircon components, as well as inherited ages. Calculated $\epsilon_{\text{(Hf)}}$ values for inherited domains (>3.3 Ga) fell between -11.8 and -2.4. Domains associated with igneous formation (3.0 – 3.3 Ga) and with metamorphism (2.4 – 3.0 Ga) produced similar calculated $\epsilon_{\text{(Hf)}}$ values between -13.7 to -0.7, and one positive value of +2.60 (igneous domain). The average $\epsilon_{\text{(Hf)}}$ value for igneous domains was -5.7 and for metamorphic domains was -7.6.

Analysis of samples from Craters of the Moon (CRMO) targeted domains of grains with U/Pb crystallization ages of >3.3 Ga, 3.2 – 3.0 Ga, and ~2.8 Ga. Just as in SK samples, these age groups cover the formation and stabilization of the CRMO area, as well as inherited ages. $\epsilon_{\text{(Hf)}}$ values between -12.9 and 4.9 were calculated for domains with U/Pb crystallization ages of >3.3 Ga, although some spots drilled into surrounding domains. These domains are inherited. Laser spots that drilled in 3.2-3.0 Ga growth domains produced mainly negative $\epsilon_{\text{(Hf)}}$ values from -7.9 to -0.40, as well as two positive values at +0.36 and +0.88. Only five metamorphic domains (2.5 -3.0 Ga) were analyzed

and produced ϵ_{Hf} values between -13.9 and -3.69. The average ϵ_{Hf} value for igneous domains is -2.6 and for metamorphic domains is -9.0.

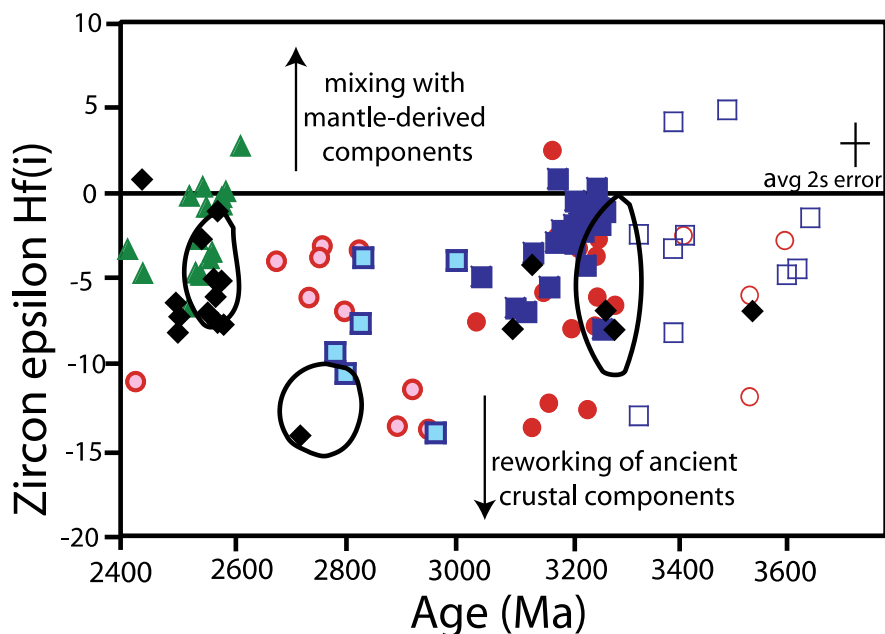


Figure 27: Initial epsilon Hf values for Precambrian aged zircon domains from SK, CRMO and SM, as well as for inherited zircons from the S. Atlanta lobe of the Idaho Batholith (Gaschnig et al. (2012)). Black outlined fields are results from σ zircons from Snake River Plain xenoliths analyzed by Dufrane et al. (2007). Open shapes are interpreted to be ages of inherited zircon growth domains, dark filled shapes to be ages of igneous growth zones, and dark outlined and light filled shapes to be ages of metamorphic growth.

Analysis from Square Mountain samples targeted grains with U/Pb crystallization ages of 2.4 to 2.6 Ga (igneous formation of samples) and 44 Ma, 48 Ma, 53 Ma, 53 Ma and 67 Ma (Paleogene igneous and metamorphic activity of the area). ϵ_{Hf} values ranged from -25.4 to +2.8. The most negative values (-13.7 to -25.4) were produced from Paleogene domains. Values for Precambrian domains range between -6.6 and 2.8. The average ϵ_{Hf} for Precambrian igneous formation domains is -2.0. The average ϵ_{Hf} value of values for Paleogene domains is -21.9.

For the three field areas analyzed, the highest ϵ_{Hf} values were produced from inherited cores. Positive values were also recorded in igneous growth domains (fig 27). The lowest values produced were from Square Mountain Paleogene metamorphic overgrowths. Paleogene domains also produced the most elevated $^{176}\text{Hf}/^{177}\text{Hf}$, both today and during the Paleogene.

Hf model ages were calculated for all samples where Hf isotope data were collected. Model ages indicated when the Hf in the grain was first extracted from the depleted mantle, or a depleted mantle age (DM). DM ages for SK grains are between 3.07 and 4.08 Ga, for CRMO grains are between 3.21 and 3.97 Ga, and for SM are between 1.20 and 3.05 Ga. SM Precambrian domains all produced DM ages between 2.77 and 3.05. Paleogene ages were between 1.20 and 1.67 Ga. SK and CRMO reported similar DM ages, and ages older than SM.

Laser spots that produced DM ages of >3.75 were produced from domains that are interpreted to be inherited, as well as from igneous and metamorphic domains, indicating recycling in both inherited as well as igneous zircon growth. In almost analysis from SK and CRMO the DM was at least 100 Ma older than the U/Pb crystallization age. Inherited domains from CRMO often produced similar DM ages to crystallization ages. CRMO did record the same DM and U/Pb crystallization age in one analysis. DM ages from SM Precambrian domains were at least 100 Ma older than crystallization ages. The oldest DM ages calculated for each field area are underestimates, as the ages were calculated using zircon Lu and Hf measurements. The melt the zircons formed from contain higher Lu and Hf concentrations than found in the zircon, and a different DM age can be found if a melt concentration is used instead of the zircon concentrations. We also calculated

DM ages using a two-step process, accounting for melt concentrations being different than that of the zircons for the igneous growth domains (fig. 28). We assumed a $^{176}\text{Lu}/^{177}\text{Hf}$ ratio of 0.038130 and a $^{176}\text{Hf}/^{177}\text{Hf}$ ratio of 0.2832 for the depleted mantle, an average $^{176}\text{Lu}/^{177}\text{Hf}$ ratio of 0.012659 for the middle crust, and a 5.0 Ga extraction age from CHUR. DM ages for igneous zircon growth domains using a two-step process are between 3300 and 4150 Ma for the SK area, between 3400 and 3950 Ma for the CRMO area, and between 2875 and 3300 Ma for the SM area.

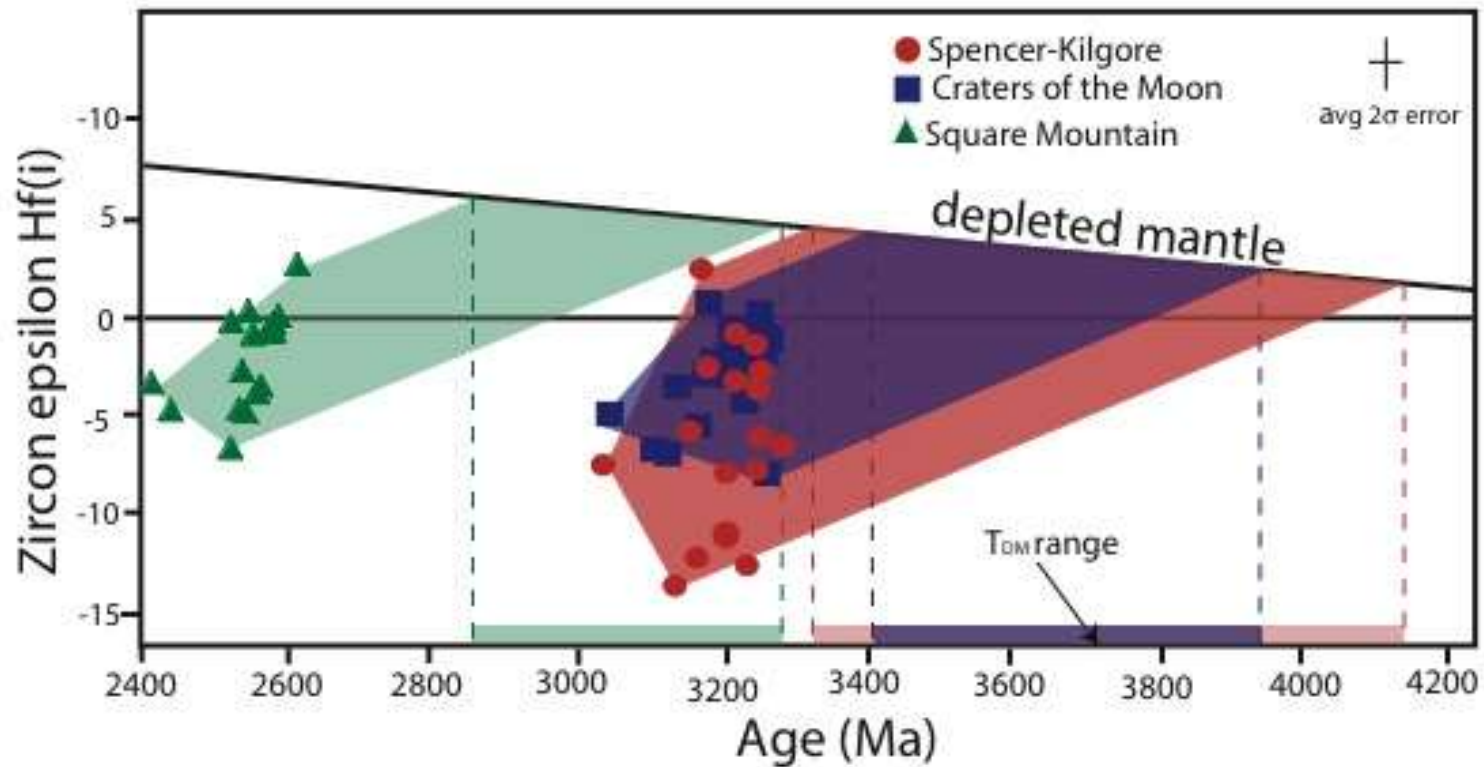


Figure 28: Regression of ϵ_{Hf} values for igneous growth zones to the timing of when source melt separated from the mantle (T_{DM}). Shaded polygons indicate the epsilon Hf values of the melt from which the zircons crystallized, based on average mid-crustal concentrations. A younging of depleted mantle ages is seen from the west (SK) to the east (SM). SK and CRMO share very similar epsilon Hf values, as well as DM ages. Depleted mantle curve assumes a $^{176}\text{Lu}/^{177}\text{Hf}$ ratio of 0.038130, and a $^{176}\text{Hf}/^{177}\text{Hf}$ ratio of 0.2832.

Table 3: Epsilon Hf results for samples from Spencer Kilgore, Craters of the Moon, and Square Mountain. If an analysis from WSU did not record a U/Pb age, an age from the same crystal and growth domain from BSU analysis was used, and is in italics.

Spot	t-xstal (Ga) WSU	± 1sm	$\frac{176\text{Lu}}{177\text{Hf}}$	± 2sm	$\frac{176\text{Hf}}{177\text{Hf}}$	± 2sm	<i>f</i> Lu/Hf	Epsilon Hf (o)	Epsilon Hf (t)	t (DM)
Spencer-Kilgore										
SK11-01S-15	<i>3.76</i>	<i>12</i>	0.000624	0.0000590	0.280207	0.0000410	-0.981	-90.7	-4.0	4.01
SK11-01S-16	<i>3.59</i>	<i>6</i>	0.001798	0.0000900	0.280420	0.0000520	-0.946	-83.2	-2.7	3.85
SK11-01S-17	<i>3.53</i>	<i>12</i>	0.000509	0.0000170	0.280138	0.0000420	-0.985	-93.1	-11.8	4.08
SK11-01S-18	<i>3.53</i>	<i>12</i>	0.000604	0.0000800	0.280311	0.0000610	-0.982	-87.0	-5.9	3.87
SK11-01L-4	<i>3.18</i>	<i>7</i>	0.000920	0.0000140	0.280631	0.0000500	-0.972	-75.7	-2.4	3.49
SK11-01L-3	<i>3.17</i>	<i>6</i>	0.000549	0.0000370	0.280527	0.0000420	-0.983	-79.4	-12.2	3.59
SK11-01M-8	<i>3.04</i>	<i>11</i>	0.000718	0.0000180	0.280401	0.0000310	-0.978	-83.8	-7.4	3.77
SK11-01S_19	<i>2.95</i>	<i>11</i>	0.002170	0.0002600	0.280590	0.0000480	-0.935	-77.2	-13.7	3.66
SK11-01M-9	<i>2.92</i>	<i>18</i>	0.000429	0.0000046	0.280368	0.0000350	-0.987	-85.0	-11.4	3.78
SK11-03M-7	<i>3.25</i>	<i>10</i>	0.000575	0.0000360	0.280565	0.0000420	-0.983	-78.0	-6.0	3.54
SK11-03L-9	<i>3.25</i>	<i>6</i>	0.000611	0.0000150	0.280568	0.0000350	-0.982	-77.9	-3.6	3.54
SK11-03L-10	<i>3.25</i>	<i>6</i>	0.000549	0.0000080	0.280538	0.0000380	-0.983	-79.0	-7.7	3.58
SK11-03L-8	<i>3.24</i>	<i>6</i>	0.000668	0.0000180	0.280579	0.0000420	-0.980	-77.6	-12.6	3.53
SK11-03M-6	<i>3.17</i>	<i>10</i>	0.000528	0.0000060	0.280677	0.0000390	-0.984	-74.1	2.6	3.40
SK11-03S-20	<i>3.16</i>	<i>11</i>	0.000544	0.0000470	0.280526	0.0000570	-0.984	-79.4	-5.7	3.59
SK11-03M-4	<i>2.83</i>	<i>11</i>	0.000584	0.0000620	0.280568	0.0000600	-0.982	-77.9	-3.3	3.54
SK11-03L-11	<i>2.74</i>	<i>13</i>	0.001079	0.0000400	0.280850	0.0000560	-0.968	-68.0	-6.0	3.22
SK11-07M-4	<i>3.29</i>	<i>19</i>	0.000963	0.0000180	0.280480	0.0001000	-0.971	-81.1	-6.5	3.69
SK11-07S-4	<i>3.25</i>	<i>12</i>	0.000582	0.0000660	0.280650	0.0001800	-0.982	-75.0	-1.3	3.44
SK11-07M-5	<i>3.22</i>	<i>16</i>	0.002620	0.0001200	0.280723	0.0000350	-0.921	-72.5	-3.1	3.53
SK11-07M-6	<i>3.14</i>	<i>29</i>	0.001001	0.0000750	0.280381	0.0000530	-0.970	-84.6	-13.6	3.82
SK11-07L-5	<i>2.89</i>	<i>37</i>	0.000256	0.0000021	0.280500	0.0000290	-0.992	-80.3	-13.5	3.60
SK11-07L-6	<i>2.80</i>	<i>12</i>	0.001335	0.0000160	0.280845	0.0000490	-0.960	-68.1	-6.8	3.25

t-xstal Spot	± (Ga)	¹⁷⁶ Lu WSU 1sm	± 177Hf	¹⁷⁶ Hf 2sm	± 177Hf	<i>f</i> 2sm	Epsilon Lu/Hf	Epsilon Hf (o)	t Hf (t)	t (DM)
SK11-07L-4	2.68	13	0.000413	0.0000160	0.280879	0.0000420	-0.988	-66.9	-3.9	3.13
SK11-08S-9	3.41	12	0.000686	0.0000180	0.280505	0.0000620	-0.979	-80.2	-2.4	3.63
SK11-08S-7	3.26	14	0.001960	0.0003400	0.280720	0.0001700	-0.941	-72.6	-2.6	3.47
SK11-08S-8	3.22	12	0.000528	0.0000180	0.280630	0.0001100	-0.984	-75.8	-0.7	3.46
SK11-08S-10	3.21	12	0.001656	0.0000720	0.280557	0.0000540	-0.950	-78.3	-7.8	3.66
SK11-08M-8	2.76	13	0.000306	0.0000021	0.280894	0.0000390	-0.991	-66.4	-3.0	3.10
SK11-08M-7	2.76	13	0.000353	0.0000060	0.280916	0.0000290	-0.989	-65.6	-3.7	3.07
SK11-08L-7	2.42	43	0.000639	0.0000460	0.280905	0.0000270	-0.981	-66.0	-10.9	3.11
Craters of the Moon										
CRM011-05M-14	3.39	10	0.001030	0.0000920	0.280370	0.0000490	-0.969	-84.9	-8.1	3.84
CRM011-05L-2	3.19	13	0.004930	0.0001000	0.280917	0.0000400	-0.852	-65.6	-2.1	3.48
CRM011-05L-1	3.14	9	0.003302	0.0000680	0.280808	0.0000320	-0.901	-69.5	-3.4	3.48
CRM011-05S-4	3.05	9	0.001750	0.0002400	0.280732	0.0000430	-0.947	-72.1	-4.8	3.43
CRM011-05S-6	3.00	8	0.001820	0.0001400	0.280792	0.0000510	-0.945	-70.0	-3.9	3.36
CRM011-05S-5	2.83	11	0.001784	0.0000260	0.280902	0.0000540	-0.946	-66.1	-3.7	3.21
CRM011-05M-13	2.83	18	0.002366	0.0000910	0.280830	0.0001200	-0.929	-68.7	-7.5	3.36
CRM011-05S-7	2.80	11	0.001258	0.0000180	0.280703	0.0000440	-0.962	-73.2	-10.5	3.43
CRM011-05M-12	2.78	11	0.001603	0.0000180	0.280769	0.0000650	-0.952	-70.8	-9.2	3.37
CRM011-14S-7	3.72	25	0.000712	0.0000450	0.280385	0.0000700	-0.979	-84.4	1.0	3.79
CRM011-14M-4	3.64	26	0.000527	0.0000240	0.280358	0.0000430	-0.984	-85.4	-1.4	3.81
CRM011-14S-5	3.61	9	0.000530	0.0000190	0.280290	0.0000370	-0.984	-87.8	-4.3	3.89
CRM011-14L-4	3.60	10	0.000905	0.0000430	0.280320	0.0000410	-0.973	-86.7	-4.7	3.89
CRM011-14M-5	3.39	11	0.000572	0.0000260	0.280477	0.0000420	-0.983	-81.2	-3.2	3.66
CRM011-14S-6	3.33	10	0.000368	0.0000081	0.280528	0.0000600	-0.989	-79.4	-2.3	3.57
CRM011-14S-8	3.33	10	0.001440	0.0001700	0.280302	0.0000640	-0.957	-87.3	-12.92	3.97
CRM011-14L-6	3.26	10	0.000550	0.0000024	0.280428	0.0000310	-0.983	-82.9	-7.9	3.72
CRM011-14S-9	3.18	10	0.001710	0.0003000	0.280801	0.0000440	-0.948	-69.7	0.9	3.34
CRM011-14L-5	3.13	10	0.000289	0.0000078	0.280532	0.0000350	-0.991	-79.2	-6.9	3.56
CRM011-14L-7	3.11	10	0.000536	0.0000049	0.280566	0.0000340	-0.984	-78.0	-6.7	3.54
CRM011-14L-8	2.96	10	0.000527	0.0000440	0.280458	0.0000370	-0.984	-81.8	-13.9	3.68

Spot	t-xstal (Ga) WSU	± 1sm	<u>176Lu</u> 177Hf	± 2sm	<u>176Hf</u> 177Hf	± 2sm	f Lu/Hf	Epsilon Hf (o)	Epsilon Hf (t)	t (DM)
CRM011-15S-10	3.41	9	0.000806	0.0000700	0.280500	0.0000460	-0.976	-80.3	-2.4	3.65
CRM011-15S-11	3.27	9	0.000323	0.0000590	0.280602	0.0000420	-0.990	-76.7	-1.0	3.47
CRM011-15S-13	3.24	25	0.001295	0.0000880	0.280674	0.0000400	-0.961	-74.2	-1.3	3.47
CRM011-15S-14	3.24	10	0.000782	0.0000036	0.280636	0.0000640	-0.976	-75.5	-1.5	3.47
CRM011-15S-16	3.24	9	0.000820	0.0000430	0.280637	0.0000720	-0.975	-75.5	-1.7	3.47
CRM011-15S-15	3.21	26	0.003180	0.0001800	0.280770	0.0000360	-0.904	-70.8	-2.9	3.52
CRM011-16S-9	3.39	15	0.000800	0.0000110	0.280699	0.0000820	-0.976	-73.3	4.2	3.39
CRM011-16S-10	3.26	11	0.001375	0.0000560	0.280655	0.0000530	-0.959	-74.9	-1.8	3.50
CRM011-16S-12	3.26	9	0.001059	0.0000760	0.280662	0.0000400	-0.968	-74.6	-0.8	3.46
CRM011-16S-11	3.25	5	0.000888	0.0000390	0.280688	0.0000810	-0.973	-73.7	0.4	3.41
CRM011-16M-11	3.23	17	0.000760	0.0001800	0.280566	0.0000570	-0.977	-78.0	-4.2	3.56
CRM011-16S-13	3.22	7	0.001026	0.0000570	0.280690	0.0000610	-0.969	-73.6	-0.6	3.42
CRM011-16S-14	3.22	14	0.000542	0.0000770	0.280629	0.0000570	-0.984	-75.8	-1.7	3.46
CRM011-16S-8	3.18	13	0.000990	0.0001100	0.280654	0.0000520	-0.970	-74.9	-2.8	3.47
CRM011-16M-10	3.17	9	0.001041	0.0000530	0.280592	0.0000360	-0.969	-77.1	-5.4	3.55
CRM011-17S-17	3.49	32	0.000433	0.0000190	0.280629	0.0000300	-0.987	-75.8	4.9	3.45
CRM011-17S-19	3.23	10	0.001170	0.0002400	0.280651	0.0000630	-0.965	-75.0	-2.2	3.49
CRM011-17S-18	3.23	9	0.000705	0.0000170	0.280660	0.0000440	-0.979	-74.7	-0.8	3.43
CRM011-17S-20	3.22	9	0.000780	0.0000260	0.280685	0.0000440	-0.977	-73.8	-0.4	3.41
CRM011-17S-21	3.21	26	0.001134	0.0000510	0.280671	0.0000800	-0.966	-74.3	-1.8	3.46
Square Mountain										
SM10A3-7	2.59	16	0.000680	0.0001300	0.281110	0.0001100	-0.980	-58.8	0.1	2.85
SM10A3-4	2.56	20	0.001350	0.0001800	0.281053	0.0000790	-0.959	-60.8	-3.8	2.97
SM10A3-5	2.44	14	0.001800	0.0001600	0.281128	0.0000540	-0.946	-58.1	-4.6	2.91
SM10C3M-13	2.56	6	0.001600	0.0001100	0.281074	0.0000350	-0.952	-60.0	-3.4	2.96
SM10C3M-14	2.55	7	0.000960	0.0001200	0.281159	0.0000350	-0.971	-57.0	0.4	2.80
SM10C3S-10	2.54	19	0.002428	0.0000410	0.281091	0.0000560	-0.927	-59.4	-4.7	3.01
	t-xstal	±	<u>176Lu</u>	±	<u>176Hf</u>	±	f	Epsilon	Epsilon	t

Spot	(Ga) WSU	1sm	177Hf	2sm	177Hf	2sm	Lu/Hf	Hf (o)	Hf (t)	(DM)
SM10C3S-8	2.54	15	0.001861	0.0000270	0.281124	0.0000570	-0.944	-58.3	-2.7	2.92
SM10C3S-9	2.53	11	0.001710	0.0001200	0.281064	0.0000990	-0.948	-60.4	-4.6	2.99
SM10C3M-11	2.52	17	0.001868	0.0000310	0.281205	0.0000630	-0.944	-55.4	-0.1	2.81
SM10C3M-12	2.52	11	0.001822	0.0000860	0.281022	0.0000640	-0.945	-61.9	-6.6	3.05
SM10C3S-11	2.41	9	0.001980	0.0001300	0.281193	0.0000770	-0.940	-55.8	-3.2	2.83
SM10C4M-9	2.615	16	0.001060	0.0001100	0.281187	0.0000490	-0.968	-56.1	2.8	2.77
SM10C4L-4	2.582	10	0.002250	0.0001000	0.281172	0.0000560	-0.932	-56.6	-0.7	2.88
SM10C4L-6	2.581	23	0.000954	0.0000820	0.281119	0.0000410	-0.971	-58.5	-0.2	2.85
SM10C4M-10	2.575	13	0.001200	0.0001600	0.281123	0.0000390	-0.964	-58.3	-0.7	2.87
SM10C4M-6	2.575	11	0.001100	0.0001300	0.281119	0.0000340	-0.967	-58.5	-0.6	2.86
SM10C4M-5	2.553	6	0.000940	0.0000100	0.281121	0.0000530	-0.972	-58.4	-0.8	2.85
SM10C4M-8	0.067	23	0.001369	0.0000970	0.282017	0.0000340	-0.959	-26.7	-25.2	1.67
SM10C4L-7	0.053	1	0.001209	0.0000650	0.282020	0.0001900	-0.964	-26.6	-25.4	1.66
SM10C4L-8	0.053	1	0.001500	0.0001500	0.282040	0.0000730	-0.955	-25.9	-24.7	1.65
SM10C4M-7	0.048	1	0.001510	0.0001200	0.282172	0.0000280	-0.955	-21.2	-20.2	1.47
SM10C4L-10	0.044	1	0.001311	0.0000600	0.282358	0.0000510	-0.961	-14.6	-13.7	1.20

Discussion

Recycled Crust in the Lower Crust of the Snake River Plain

The initial $\epsilon_{(\text{Hf})}$ values recorded in samples from the three field areas analyzed (SK, CRMO and SM) were dominantly negative, with most values falling between 0 and -10. The age domains these results were recorded in were dominantly from Archean magmatic and metamorphic events, although an effort was made to analyze the Paleogene zircon growth event recorded in SM and to analyze cores of grains that have been interpreted as inherited.

The oldest growth domains targeted by Hf isotope analysis are inherited cores and grains. These domains were only analyzed in samples from SK and CRMO. The $\epsilon_{(\text{Hf})}$ values recorded in this population range from -13 to +5. Results from inherited zircon yielded both positive and negative values. This indicates that these inherited zircon domains were sourced from a region that was formed from both enriched crust (e.g. granites and diorites) recently separated from the depleted mantle and from older crustal components with a longer crustal residence. The most obvious source for inheritance is the nearby Montana Metasedimentary province (MMP) and the Beartooth-Bighorn magmatic zone (BBMZ). The lithologies of this area are mostly quartzofeldspathic, tonalitic to granitic gneisses and metasupracrustal rocks, including quartzite, amphibolite, marble, and iron formation (Chamberlain et al., 2003). These lithologies easily explain zircon cores with negative to slightly positive $\epsilon_{(\text{Hf})}$ values. There could be another source for these domains other than the zones to the east. It is possible there was early Paleoproterozoic crust formed in the Kilgore-Craters terrane, and it was recycled during

orogenesis. Wherever the Paleoproterozoic zircons were recycled from, they were dominantly sourced from an early, sialic crust.

The results from SM samples, which will have to represent all of the SM terrain, as House Mountain (HM) samples were not analyzed, also produced overwhelmingly negative $\epsilon_{\text{(Hf)}}$ values. However, in Archean igneous growth domains, these values did not range as negative as SK and CRMO. SM values only range down to -6.6. The negative and positive values indicate the SM terrain was also formed from mantle derived and recycled crustal components, however, the depleted mantle model ages for SM are significantly younger than SK and CRMO (fig. 28), in the range of ages during which SK and CRMO underwent magmatic growth (2.9 to 3.3 Ga). The discrepancy in model ages indicates the source for lithologies from SM is not the same as that from SK and CRMO. The inherited core ages in zircons from SM and HM also match the igneous formation ages of the Kilgore-Craters terrane (3.3 to 2.9 Ga). This is a good indication that crustal magmas in the SM terrane were sourced in part from the lithologies similar to those of the Kilgore-Craters terrane.

The Eastern Snake River Plain and the Wyoming Craton

There are two possible ways to configure the Snake River Plain terranes to the Wyoming Province. The first is the SRP terranes are two individual microcontinents and are not related to each other or to the Wyoming Province. In this scenario, the two microcontinents were sutured to the craton during their stabilization events. The second possible scenario is the Kilgore-Craters and Square Mountain terranes are extensions of the Wyoming Province and thus extend the western boundary of the Wyoming Province

to the $^{87}\text{Sr}/^{87}\text{Sr} = .706$ line. The Kilgore-Craters terrane would be an extension of the Montana Metasedimentary Province and Beartooth Bighorn Magmatic Zone, and the Square Mountain terrane would be an extension of the Southern Accreted Terranes (fig. 29).

Results of this study support the second scenario. We interpret a 2.8 Ga stabilization event in the CRMO and SK area. Similarly, the timing of cratonization for the Beartooth Mountains and the Montana Metasedimentary zone has been identified at 2.8 (Mueller and Frost, 2006). The stabilization event of the Kilgore-Craters area that produced metamorphic zircons and overgrowths is likely related to the same 2.8 Ga event that has been recorded in the Long Lake region of the Beartooth Mountains (Wooden et al., 1982; Mueller et al., 1985). Evidence for a larger Wyoming craton that includes the Kilgore-Craters terrane is compounded by Hf analysis. The negative ϵ_{Hf} values recorded in zircons from across the SRP indicate the lower crust of southern Idaho is composed of crust that had been recycled and enriched. Nd and Pb model ages and U/Pb detrital zircon ages of >4.0 Ga from the BBM and MMP of the Wyoming Province also indicate the existence of Paleoproterozoic components (Frost, 1993; Wooden and Mueller, 1998; Mueller and Frost, 2006).

The last collisional events and cratonization of the Southern Accreted Terranes (SAT) to the Wyoming Province occurred at 2.55-2.50 Ga (Mueller and Frost, 2006). This matches the timing of formation and cratonization found for the Square Mountain terrane (2.5 Ga). This is also the timing of stabilization in the earlier defined Grouse Creek Block (Gashnig et al., 2013). Later tectonism was recorded in the SAT at 1.8-1.6

Ga, associated with the formation of Laurentia. This tectonism was also recorded in the House Mountain area of the Square Mountain terrane.

Both negative and positive $\varepsilon_{(\text{Hf})}$ values recorded in zircons from SM indicate the SM terrane formed from mantle derived and recycled crustal components, and Hf model ages indicate the recycled components were similar in age to the Kilgore-Craters terrane, the MMP and the BBMZ. Negative $\varepsilon_{(\text{Nd})}$ values recorded in the SAT also indicate both mantle derived and recycled components, with those components possibly sourced from the MMP and BBMZ (Frost et al., 2006). These timing and isotopic patterns tie together the SAT, the Grouse Creek Block, and the Square Mountain terrane as one zone in the Wyoming Province (Foster et al., 2006; Gaschnig et al., 2013).

Open System Zircon Growth During the Paleogene

Hf isotope analysis on zircons from SM also targeted Paleogene growth domains. These domains are magmatic overgrowths on Archean zircons. $^{176}\text{Hf}/^{177}\text{Hf}$ concentrations of Paleogene domains are elevated compared to the Archean growth domains both today and at the timing of growth ca. 50 Ma. The elevated concentration could be modeled as an injection of mantle derived melt or fluid external to the granulite host, resulting in a mixture of low $^{176}\text{Hf}/^{177}\text{Hf}$ Archean crustal Hf and higher $^{176}\text{Hf}/^{177}\text{Hf}$ younger, mantle-derived Hf. This outside source would have to be mantle-derived, or at least more recently separated from the mantle, as it must be enriched in $^{176}\text{Hf}/^{177}\text{Hf}$. Injection of melt or fluid could be added to the rock during open system metamorphism, suggesting that the Challis-aged zircon growth event was not just a thermal re-equilibration, but was promoted by mass flux of mantle-derived melts through the crust.

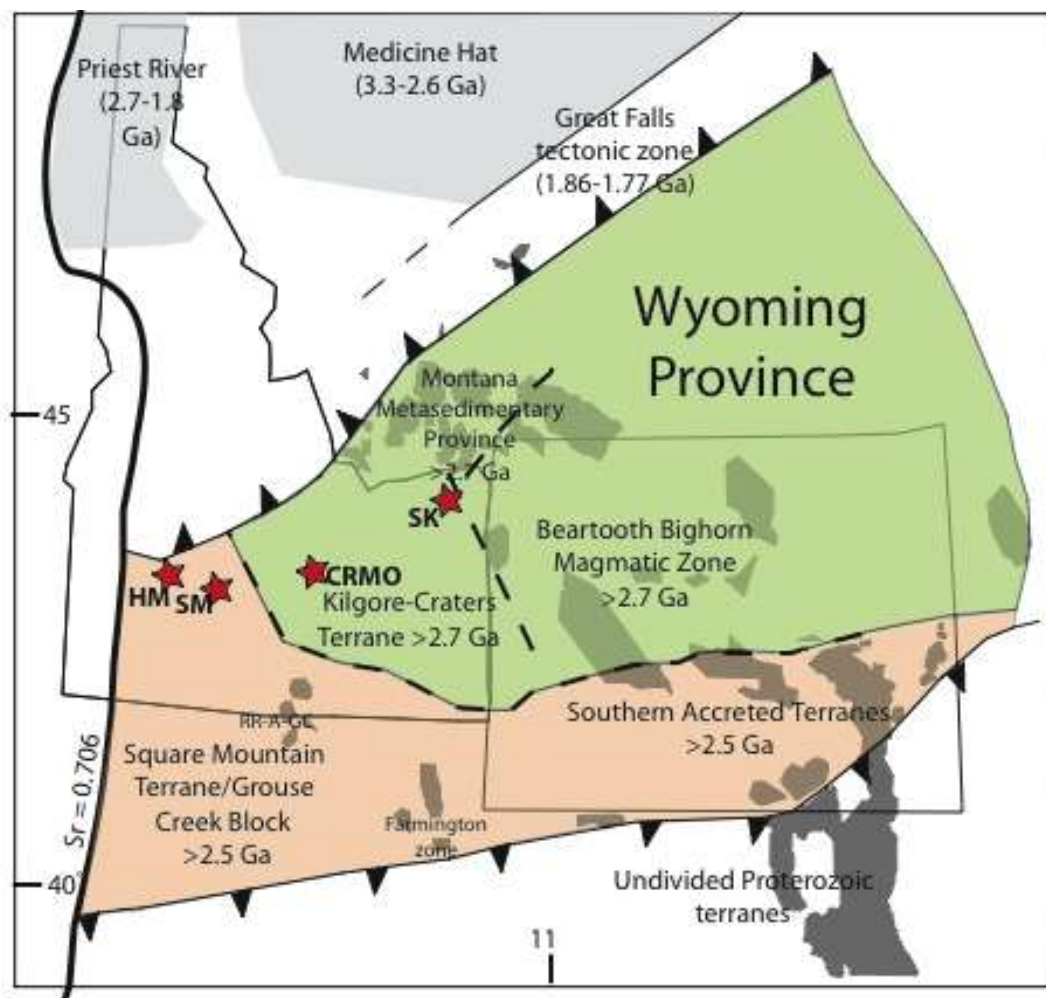


Figure 29: A new configuration of the Wyoming Province. The Wyoming Province can be split into two zones, one that is older than 2.8 Ga and one that is older than 2.5 Ga.

Conclusions

Evidence from this study supports the hypothesis that the lower crust of Southern Idaho is an extension of the Wyoming Province. The lower crust underlying the SRP of Southern Idaho is composed of two distinct terranes. The Kilgore Craters terrane stretches from the Montana/Wyoming/Idaho border west into Craters of the Moon National Monument and Preserve. The Kilgore-Craters terrane formed during an igneous episode that lasted from 3.0 to 3.3 Ga, with major pulses at 3.2 and 3.1 Ga. Granulite facies metamorphism occurred between 2.8 and 2.7 Ga, and resulted in stabilization of the region.

To the west of the Kilgore-Craters terrane is the Square Mountain terrane. This region stretches west to the $^{87}\text{Sr}/^{87}\text{Sr} = .706$ line. Igneous activity circa 2.5 Ga formed this region. Granulite facies metamorphism stabilized the region, contemporaneously at the timing of formation. The igneous activity and metamorphism of both Southern Idaho terranes is due to collisional orogenesis as the early North American continent was growing.

Sources of melts for the formation of both terranes included contributions from older continental crust. The Hf chemical signatures and timings of formation and stabilization tie the two Southern Idaho terranes to the Wyoming Province. The Kilgore-Craters terrane is correlative with the northern Montana Metasedimentary province and the Beartooth-Bighorn magmatic zone. The Square Mountain terrane is a northward correlative of the Grouse Creek Block, and together are westward extensions of the Southern Accreted Terranes of the Wyoming Province.

REFERENCES

- Anders, M. H., Geissman, J. W., Piety, L. A. and Sullivan, J. T., 1989, Parabolic distribution of circum-eastern Snake River Plain seismicity and latest Quaternary faulting: Migratory pattern and association with the Yellowstone hot spot. *Journal of Geophysical Research*, 94, 1589–1621.
- Armstrong, R.L., Taubeneck, W.H., and Hales, P.O., 1977. Rb-Sr and K-Ar geochronometry of Mesozoic granitic rocks and the Sr isotopic composition, Oregon, Washington, and Idaho. *Geological Society of America Bulletin*, 88 (3), 397–411.
- Armstrong, R.L., and Ward, P., 1991, Evolving geographic patterns of Cenozoic magmatism in the North American Cordillera—The temporal and spatial association of magmatism and metamorphic core complexes. *Journal of Geophysical Research*, 96 (B8), 13201–13224.
- Bingen B., Austrheim H., Whitehouse M., 2001, Ilmenite as a source for zirconium during high-grade metamorphism? Textural evidence from the Caledonides of Western Norway and implications for zircon geochronology. *Journal of Petrology*, 42, 355–375.
- Bonnichsen, B., Leeman, W.P., Honjo, N., McIntosh, W.C. and Godchaux, M.M., 2007. Miocene silicic volcanism in southwestern Idaho: geochronology, geochemistry, and evolution of the central Snake River Plain. *Bulletin of Volcanology*, 70, 315–342.
- Brott, C.A., Blackwell, D.D., and Ziagos, J.P., 1981, Thermal and tectonic implications of heat flow in the eastern SRP, Idaho. *Journal of Geophysical Research*, 86, 11.
- Camp, V.E., 1995, Mid-Miocene propagation of the Yellowstone mantle plume head beneath the Columbia River Basalt source region. *Geology*, 23, 435–438.
- Camp, V.E. and Ross, M.E., 2004, Mantle dynamics and genesis of mafic magmatism in the intermontane Pacific Northwest. *Journal of Geophysical Research*, 109 B08204, 14 pp.
- Carlson, D.H., Fleck, R., Moye, F.J., and Fox, K.F., 1991, Geology, geochemistry, and isotopic character of the Colville igneous complex, northeastern Washington. *Journal of Geophysical Research*, 96 (B8), 13313–13333.

- Caruba, R., and Iacconi, P., 1983, Les zircons des pegmatites de Narssârssuk (Groëland)—l'eau et les groupements OH dans les zircons meamictes. *Chemical Geology*, 38, 75-92.
- Chamberlain, K.R., Frost, C.D. and Frost, B.R., 2003, Early Archean to Mesoproterozoic evolution of the Wyoming Province: Archean origins to modern lithospheric architecture. *Canadian Journal of Earth Sciences*, 40 (10): 1357–1374.
- Cherniak, D.J., Hanchar, J.M., and Watson, E.B., 1997, Diffusion of tetravalent cations in zircon. *Contributions to Mineralogy and Petrology* 127, 383-390.
- Cherniak, D.J. and Watson, E.B, 2000, Pb diffusion in zircon. *Chemical Geology*, 172, 5-24.
- Christiansen, R.L., 2001, The Quaternary and Pliocene Yellowstone Plateau volcanic field of Wyoming, Idaho, and Montana. U.S. Geological Survey Professional Paper, 729 G, 145 pp.
- DePaolo, D. J. and Wasserburg, G. J., 1976, Nd isotopic variations and petrogenetic models. *Geophysical Research Letters*, 3, 249–252.
- Dickinson, W.R., 1991, Tectonic setting of faulted Tertiary strata associated with the Catalina core complex in southern Arizona. *Geological Society of America Special Paper* 264. 106.
- Dickinson, W.R., 2002, The Basin and Range Province as a composite extensional domain. *International Geology Review*, 44 1-38.
- Draper, D.S. ,1991, Late Cenozoic bimodal magmatism in the northern Basin and Range Province of Southeastern Oregon. *Journal of Volcanology and Geothermal Research*, 47, 299–328.
- Dufrane, S.A., Vervoort, J.D., Leeman, W.P., and Wolf, D.E., 2007, Hafnium isotope composition of Archean zircons from xenoliths of the Snake River Plain, Idaho. *Eos Transactions, American Geophysical Union*, 88, 52, Fall meeting supplement, abstract V43B-1375.
- Es'kova, E.M., 1959, Geochemistry of Nb and Ta in the nepheline syenite massifs of the Vishnevyye Mountains. *Geokhimiya* 2, 130-139 (in Russian).
- Fraser, G., Ellis, D., and Eggins, S., 1997, Zirconium abundance in granulite-facies minerals, with implications for zircon geochronology in high-grade rocks. *Geology* 25 (7), 607–610.
- Foster, D.A., and Fanning, C.M., 1997, Geochronology of the northern Idaho batholith and the Bitterroot metamorphic core complex: Magmatism preceding and contemporaneous with extension: *Geological Society of America Bulletin*, 109 (4), 379–394.

Foster, D.A., Mueller, P.A., Mogk, D.W., Wooden, J.L., and Vogl, J.J., 2006, Proterozoic evolution of the western margin of the Wyoming craton: Implications for the tectonic and magmatic evolution of the northern Rocky Mountains: *Canadian Journal of Earth Sciences*, 43, 1601–1619.

Frost, C.D., 1993, Nd isotopic evidence for the antiquity of the Wyoming Province: *Geology*, 21, 4, 351–354.

Frost, C.D., Frost, B.R., Chamberlain, K.R. and Hulsebosch, T.P., 1998, The Late Archean history of the Wyoming province as recorded by granitic magmatism in the Wind River Range, Wyoming. *Precambrian Research*, 89, 145–173.

Frost, C.D., and Fanning, C.M., 2006, Archean geochronological framework of the Bighorn Mountains, Wyoming. *Canadian Journal of Earth Sciences*, 43, 1399– 1418.

Frost, C.D., Fruchey, B.L., Chamberlain, K.R. and Frost, B.R., 2006, Archean crustal growth by lateral accretion of juvenile supracrustal belts in the southern Wyoming Province. *Canadian Journal of Earth Sciences*, 43, 1533-1526.

Gaschnig, R.M, Vervoort, J.D., Lewis, R.S, and Tikoff, B., 2012 Probing for Proterozoic and Archean crust in northern U.S. Cordillera with inherited zircon from the Idaho batholith. *Geological Society of America Bulletin*, 125, (1-2), 73-88.

Gest, D.E., and McBirney, A.R., 1979, Genetic relations of shoshonite and absarokite magmas, Absaroka Mountains, Wyoming. *Journal of Volcanology and Geothermal Research*, 6, 85–104.

Geist D. and Richards M., 1993, Origin of the Columbia Plateau and Snake River Plain: deflection of the Yellowstone plume. *Geology*, 21, 789–792.

Glen J.M.G. and Ponce D.A., 2002, Large-scale fractures related to inception of the Yellowstone hotspot. *Geology*, 30, 647–650.

Grace, R.L.B., Chamberlain, K.R., Frost, B.R. and Frost, C.D., 2006, Tectonic histories of the Paleoproterozoic to Mesoproterozoic Sacawee Block and Neoproterozoic Oregon Trail structural belt of the south-central Wyoming Province. *Canadian Journal of Earth Sciences*, 43, 1445-3313.

Guo, J., O'Reilly, S.Y., and Griffin, W.L., 1996, Zircon inclusions in corundum megacrysts: I. Trace element geochemistry and clues to the origin of corundum megacrysts in alkali basalts. *Geochimica et Cosmochimica Acta*, 60, 2347-2363.

Halden, N.M., and Hawthorne, F.C., 1993, The fractal geometry of oscillatory zoning in crystals: application to zircon. *Am Mineral*, 78, 1113-1116.

Harrison, W.J. and Wood, B.J., 1980, An experimental investigation of the partitioning of REE between garnet and liquid with reference to the role of defect equilibria, *Contributions to mineralogy and petrology*, 72 (2), 145-155.

Harry, D.L., Sawyer, D.S. and Leeman W.P., 1993, The mechanics of continental extension in western North America: Implications for the magmatic and structural evolution of the Great Basin. *Earth and Planetary Science Letters*, 117, 59-71.

Henry, D.J., Mueller, P.A., Wooden, J.L., Warner, J.L. and Lee-Berman R., 1982, Granulite grade supracrustal assemblages of the Quad Creek area, eastern Beartooth Mountains, Montana. *Montana Bureau of Mines and Geology Special Publication*, 84, 147-159.

Hildreth, W., 1981, Gradients in silicic magma chambers: Implications for lithospheric magmatism. *Journal of Geophysical Research*, 86, 10153-10192.

Hinton, R.W., and Upton, B.G.J., 1991, The chemistry of zircon: variations within and between large crystals from syenite and alkali basalt xenoliths. *Geochimica et Cosmochimica Acta*, 55, 3287– 3302.

Hoffman, P.F., 1988, United plates of America, the birth of a craton; early Proterozoic assembly and growth of Laurentia. *Annual Review of Earth and Planetary Sciences*, 16, 543–603.

Holdaway, M.J., 1971, Stability of andalusite and the aluminum silicates phase diagram. *American Journal of Science*, 271, 97-131.

Hooper, P.R., Camp, V., Reidel, S. and Ross, M., 2007, The origin of the Columbia River flood basalt province: plume versus nonplume models. In: Foulger, G.R., Jurdy, D.M. (Eds.), *Plates, Plumes, and Planetary Processes: Geological Society of America Special Paper*, 430, 635–668.

Hoskin, P.W.O., 1998, Minor and trace element analysis of natural zircon (ZrSiO₄) by SIMS and laser ablation ICPMS: a consideration and comparison of two broadly competitive techniques. *Journal of Trace and Microprobe Techniques*, 16 (3), 301–326.

Hoskin, P.W.O., and Black, L.P., 2000, Metamorphic zircon formation by solid-state recrystallization of protolith igneous zircon. *Journal of Metamorphic Geology*, 18, 423–439.

Hoskin, P.W.O., and Ireland, T.R., 2000, Rare earth element chemistry of zircon and its use as a provenance indicator. *Geology*, 28 (7), 627 – 630.

Hoskin, P.W.O. and Schaltegger, 2003, The composition of zircon and igneous and metamorphic petrogenesis. In *Zircon*

Hughes, S.S., McCurry, M., 2002, Bulk major and trace element evidence for a time–space evolution of Snake River Plain rhyolites, Idaho. In: Bonnicksen, Bill, White, C.M., McCurry, Micheal (Eds.), *Tectonic and Magmatic Evolution of the Snake River Plain Volcanic Province*. Idaho Geological Survey Bulletin, 30, 161–171.

Huppert, H. E. and Sparks, S. I., 1988, The generation of granitic magmas by intrusion of basalt into continental crusts. *Journal of Petrology*, 29, 599–624.

Jacob, T.M., 1985, Reconnaissance geology of House Mountain, Elmore County, Idaho. Thesis (M.S.) University of Idaho.

James, D. E., Fouch, M. J., Carlson, R. W., and Roth, J. B., 2011, Slab fragmentation, edge flow and the origin of the Yellowstone hotspot track. *Earth and Planetary Science Letters*, 311, 1, 124–135

John, D.A., Wallace, A.R., Ponce, D.A, Fleck ,R.B., Conrad, J.E., 2000, New perspectives on the geology and origin of the northern Nevada rift, J.K. In: Cluer, J.G. Price, E.M. Struhsacker, R.F. Hardyman, D.L. Morris, (Eds.) *Geology and Ore deposits 2000: The Great Basin and Beyond*. Geological Society of Nevada Symposium Proceedings, May 15–18, 127–154.

Jordan, T. 1975, The continental tectosphere. *Reviews of Geophysics and Space Physics*, 13, 1–12.

Jordan, B.J., Grunder, A.L., Duncan, R. and Deino, A., 2004, Geochronology of age-progressive volcanism of the Oregon High Lava Plains: implications for the plume interpretation of Yellowstone. *Journal of Geophysical Research*, 109, B10202

Keane, S.D., DeWolf, C.P., Essene, E.J., Halliday, A.N., Hall, C.M. and Cosca, M.A., 2006, Isotopic constraints on the thermal history of the Wind River Range, Wyoming: implications for Archean metamorphism. *Canadian Journal of Earth Sciences*, 43 (10), 1511–1532.

Kinny P.D. and Maas, R., 2003, Lu-Hf and Sm-Nd Isotope Systems in Zircon, in Zircon. eds. J.M Hanchar and P.W.O. Hoskin. 327–341.

Le Maitre, R.W., ed., 1989, *A Classification of Igneous Rocks and Glossary of Terms*. Blackwell, Oxford, 193 pp.

Leeman, W.P., 1982, Development of the Snake River Plain– Yellowstone Plateau province, Idaho and Wyoming: An overview and petrologic model, in Bonnicksen, B., and Breckenridge, R.M., eds., *Cenozoic geology of Idaho*. Idaho Bureau of Mines and Geology Bulletin 26, 155–177.

Lipman, P.W., Prostka, H.J. and Christiansen, R.L., 1971, Evolving subduction zones in the western United States, as interpreted from igneous rocks. *Science*, 174, 821–825.

Malde, H.E., 1991, Quaternary geology and structural history of the Snake River Plain, Idaho and Oregon, in Morrison, R.B., ed., Quaternary non-glacial geology, Conterminous U.S.: Boulder, Geological Society of America, The Geology of North America, v.K-2, 251–280.

McQuarrie N. and Rodgers D.W., 1998, Subsidence of a volcanic basin by flexure and lower crustal flow: The eastern Snake River Plain, Idaho. *Tectonics*, 17, 203-220.

Minster, J. B., Jordan, T. H., Molnar, P. and Haines, E., 1974, Numerical Modeling of instantaneous plate tectonics. *Royal Astronomical Society Geophysical Journal*, 36, 541-576.

Mogk, D.W., Mueller, P.A. and Wooden, J.L. 1992, The significance of Archean terrane boundaries: evidence from the northern Wyoming Province. *Precambrian Research*, 55, 155–168.

Moye, F.J., Hackett, W.R., Blakley, J.D., and Snider, L.G., 1988, Regional geologic setting and volcanic stratigraphy of the Challis volcanic field, central Idaho, *in* Link, P.K., and Hackett, W.R., eds., Guidebook to the geology of central and Southern Idaho. Idaho Geological Survey Bulletin 27, 87–97.

Mueller P.A, Wooden J.L, Henry D.J and Bowes D.R, 1985, Archean Crustal Evolution of the Eastern Beartooth Mountains, Montana and Wyoming. In: Czamanske, G. K. and Zientek, M. L., (eds.), The Stillwater Complex. Montana Bureau of Mines and Geology Special Publication, 92, 9-20.

Mueller, P.A., Mogk, D.W. Wooden, J.L. and Henry D.J., 1982, Granitoids, granulites and continental collision: The Late Archean of southwestern Montana. *Geological Society of America Abstracts*, 14 (7), 572

Mueller, P.A., Wooden, J. and Nutman, A., 1992, 3.96 Ga zircons from an Archean quartzite, Beartooth Mountains. *Montana Geology*, 20, 327–330.

Mueller, P.A., Shuster, R., Wooden, J., Erslev, E. and Bowes, D., 1993, Age and composition of Archean crystalline rocks from the southern Madison Range: implications for crustal evolution in the Wyoming craton. *Geological Society of America Bulletin*, 105, 437–446.

Mueller, P.A., Wooden, J.L., Nutman, A.P. and Mogk, D.W., 1998, Early Archean crust in the northern Wyoming province: evidence from U–Pb ages of detrital zircons. *Precambrian Research*, 91, 295–307.

Mueller, P.A., Foster, D.A., Mogk, D.W. and Wooden, J.L., 2004a, New insights into the Proterozoic evolution of the western margin of Laurentia and their tectonic implications. *Geological Society of America, Abstracts with Programs*, 36(5),404.

Mueller, P.A., Burger, H.R., Heatherington, A., Wooden, J., Mogk, D.W. and D'Arcy, K., 2004b, Age and evolution of the Precambrian crust, Tobacco Root Mountains, Montana. In: J.B. Brady, H.R. Burger, J.T. Cheney, and T.A. Harms, (eds.) Precambrian geology of the Tobacco Root Mountains, Montana. Geological Society of America, Special Paper 377, 179–201.

Mueller, P.A., Burger, R.H., Wooden, J.L., Brady J.B., Cheney, J.T., Harms, T.A., Heatherington, A.L. and Mogk, D.W. 2005. Paleoproterozoic metamorphism in the northern Wyoming province: implications for the assembly of Laurentia. *Journal of Geology*, 113, 169–179.

Mueller, P.A. and Frost C.D, 2006, The Wyoming Province: a distinctive Archean craton in Laurentian North America. *Can. J. Earth Sci.*, 43 (10), 1391-1397

Nagasawa, H., 1970, Rare earth concentrations in zircons and apatites and their host dacites and granites. *Earth and Planetary Science Letters* 9, 359–364.

Nir-El, Y. and Lavi, N., 1998, Measurement of the half-life of ^{176}Lu . *Applied Radioactive Isotopes*, 49, 1653-1655.

O'Brien, H.E., Irving, A.J., and McCallum, I.S., 1991, Eocene potassic magmatism in the Highwood Mountains, Montana— Petrology, geochemistry, and tectonic implications. *Journal of Geophysical Research*, 96, (B8), 13237–13260.

Ono, A., 1976, Chemistry and zoning of zircon from some Japanese granitic rocks. *J Japan Assoc Mineral Petrol Econ Geol*, 71, 6-17.

Patchett, P.J., Kouvo, O., Hedge, C.E. and Tatsumoto, M., 1981, Evolution of continental crust and mantle heterogeneity: evidence from Hf isotopes. *Contributions to Mineralogy and Petrology*, 78, 279-297.

Parsons T., 1995, The Basin and Range Province, Developments in Geotectonics, In: K.H. Olsen, (ed.), *Continental Rifts: Evolution, Structure, Tectonics*. Elsevier, Amsterdam, 25, 277–324.

Parsons, T., Thompson, G.A. and Sleep, N.H., 1994, Mantle plume influence on the Neogene uplift and extension of the U.S. western Cordillera. *Geology*, 22, 83–86.

Perkins, M.E. and Nash, B.P., 2002. Explosive silicic volcanism of the Yellowstone hotspot: the ash fall tuff record. *Geologic Society of America Bulletin*, 114, 367–381.

Perkins, M.E., Brown, F.H., Nash, W.P., McIntosh, W. and Williams, S.K., 1998. Sequence, age, and source of silicic fallout tuffs in middle to late Miocene basins of the Basin and Range province. *Geological Society of America Bulletin*, 110, 344–360.

- Pierce K.L. and Morgan, 1990, The track of the Yellowstone hot spot: volcanism, faulting, and uplift. U.S. Geological Survey Open-File Report, 90-415, 49 pp.
- Pierce, K.L., and Morgan, L.A., 1992, The track of the Yellowstone hot spot: Volcanism, faulting, and uplift. In: Link, P.K., Kuntz, M.A., and Platt, L.B., (eds.), Regional geology of eastern Idaho and western Wyoming. Geological Society of America Memoir, 179, 1–53.
- Pierce, K.L. and Morgan, L.A., 2009, Is the track of the Yellowstone hotspot driven by a deep mantle plume? — Review of volcanism, faulting, and uplift in light of new data. *Journal of Volcanology and Geothermal Research*. 188, 1-25.
- Pierce, K.L., Morgan, L.A. and Saltus, R.W., 2002, Yellowstone plume head: postulated tectonic relations to the Vancouver slab, continental boundaries, and climate. In: Bill Bonnichsen, C.M. White, Micheal McCurry, (eds.) , Tectonic and Magmatic Evolution of the Snake River Plain Volcanic Province. Idaho Geological Survey Bulletin, 30, 5–33.
- Pollack, H.N., 1986, Cratonization and thermal evolution of the mantle. *Earth and Planetary Science Letters*, 80, 175–182.
- Richards, M.A., Duncan, R.A. and Courtillot, V.E., 1989, Flood basalts and hot spot tracks: Plume heads and tails. *Science*, 246, 103-107.
- Roberts, M.P., and Finger, F., 1997. Do U – Pb zircon ages from granulites reflect peak metamorphic conditions? *Geology*, 25 (4), 319 – 322.
- Rodger D.W., Hackett W.R. and Ore H.T., 1990, Extension of the Yellowstone plateau, eastern Snake River Plain and Owyhee plateau. *Geology*, 18, 1138-1141.
- Ross, G.M. and Villeneuve, M.E., 2003, Provenance of the Mesoproterozoic (1.45 Ga) Belt basin (western North America): Another piece in the pre-Rodinia paleogeographic puzzle. *Geological Society of America Bulletin*, 115, 1191–1217.
- Rubatto, D., 2002, Zircon trace element geochemistry: partitioning with garnet and the link between U-Pb ages and metamorphism. *Chemical Geology*, 184, 123-138.
- Rubatto, D., Williams, I.S., and Buick, I.S, 2001 Zircon and monazite response to prograde metamorphism in the Reynolds Range, central Australia. *Contributions to Mineralogy and Petrology*, 140, 458-468.
- Rowley, P.W., 2001, The Cenozoic evolution of the Great Basin area, U.S.A.—new interpretations based on regional geologic mapping. In: M.C. Erskine, (ed.), *The Geologic Transition, High Plateaus to Great Basin — A Symposium and Field Guide (The Mackin Volume)*. Utah Geological Association Publication. 30, 169–188.

- Sano, Y., Terada, K., and Fukuoka, T. 2002, High mass resolution ion microprobe analysis of rare earth elements in silicate glass, apatite and zircon: lack of matrix dependency. *Chemical Geology*, 184, 217-230
- Shore, M., Fowler, A.D., 1996, Oscillatory zoning in minerals: a common phenomenon. *Can Mineral*, 34, 1111-1126.
- Smith, R.B. and Braile, L.W., 1993. Topographic signature, space-time evolution, and physical properties of the Yellowstone-Snake River Plain volcanic system: the Yellowstone hotspot. In: Snoke, A.W., Steidtmann, J.R., Roberts, S.M. (eds.), *Geology of Wyoming: Geological Survey of Wyoming Memoir*. 5, 694-754.
- Snyder, G.A., Taylor, L.A., and Crozaz, G., 1993, Rare earth element selenochemistry of immiscible liquids and zircon at Apollo 14: an ion probe study of evolved rocks on the Moon. *Geochimica et Cosmochimica Acta*, 57, 1143-1149.
- Speer, F. S., 1991, *Metamorphic Phase Equilibria and Pressure-Temperature-Time Paths* 2nd edition. Washington, D.C.: Mineralogical Society of America.
- Speer, J.A., 1982, Zircon. *Rev Mineral* 5, 67-112.
- Spencer, J.E. and Pearthree, P.A., 2001, Headward erosion versus closed-basin spillover as alternative causes of Neogene capture of the ancestral Colorado River by the Gulf of California. In: Young, R.A., and Spamer, E.E., (eds.), *The Colorado River: Origin and evolution: Grand Canyon, Arizona*, Grand Canyon Association Monograph. 12, 215-219.
- Souders, A.K. and Frost, C.D., 2006, In suspect terrane? Provenance of the late Archean Phantom Lake Metamorphic Suite, Sierra Madre, Wyoming. *Canadian Journal of Earth Sciences*, 43, 1557-1577.
- Steiger, R.H., and Jäger, E., 1977, Subcommittee on Geochronology: Convention on the use of decay constants in geo- and cosmochronology. *Earth and Planetary Science Letters*, 13, 359-362.
- Suayah, I.B., and Rodgers, J.J.W., 1991, Petrology of the lower Tertiary Clarno Formation in north central Oregon— The importance of magma mixing: *Journal of Geophysical Research*, 96 (B8), 13,357-13,371.
- Suppe, J., Powell, C. and Barry, R., 1975, Regional topography, seismicity, Quaternary volcanism, and the present day tectonics of the western United States. *American Journal of Science*, 275-A, 397-436.
- Takahashi, E., Katsuji, N. and Wright T.L., 1998, Origin of the Columbia River basalts: melting model of a heterogeneous plume head. *Earth and Planetary Science Letters*, 162 1-4, 63-80.

- Thomas J.B., Bodnar, R.J., Shimizu, N., and Sinha, A.K., 2002, Determination of zircon/melt trace element partition coefficients from SIMS analysis of melt inclusions in zircon. *Geochimica et Cosmochimica Acta*, 66, 2887-2901.
- Thompson, G.A., 1998, Deep mantle plumes and geoscience vision. *GSA Today*, 84, 7–25.
- Vavra, G., 1990, On the kinematics of zircon growth and its petrogenetic significance: a cathodoluminescence study. *Contributions to Mineralogy and Petrology*, 106, 90-99.
- Vavra, G., Gebauer, D., Schmid, R., and Compston, W., 1996, Multiple zircon growth and recrystallisation during polyphase Late Carboniferous to Triassic metamorphism in granulites of the Ivrea zone (Southern Alps): An ion microprobe (SHRIMP) study. *Contributions to Mineralogy and Petrology*, 122, 337–358.
- Waite, G.P., Smith, R.L. and Allen, R.L., 2006, VP and VS structure of the Yellowstone Hotspot from teleseismic tomography: evidence for an upper mantle plume. *Journal of Geophysical Research*, 111, B04303.
- Walker, J.D., Geissman, Bowring, S.A. and Babcock, L.E., 2012, *Geologic Time Scale (v.4.0)*. GSA.
- Watson, B.E., 1980, Zircon saturation in felsic liquids: Experimental results and applications to trace element geochemistry. *Contributions to Mineralogy and Petrology*, 70 (4), 407-419
- Watson, B.E., 1980, Some experimentally determined zircon/liquid partition coefficients for the rare earth elements. *Geochimica et Cosmochimica Acta*, 44, 895–897.
- Watson, E. B., and Harrison, T. M., 1983, Zircon saturation revisited: Temperature and composition effects in a variety of crustal magma types. *Earth and Planetary Science Letters*, 64, 295–304.
- Watson, E.B., Harrison, T.M., 2005, Zircon thermometer reveals minimum melting conditions on earliest Earth. *Science*, 308, 841–844.
- Wetherill, G.W., 1956, Discordant uranium-lead ages, I. *Transactions of the American Geophysical Union*, 37, 320-326.
- Whitmeyer, S.J. and Karlstrom, K.E., 2007, Tectonic model for the Proterozoic growth of North America. *Geosphere*. 3 (4), 220-259.
- Wolf D.E., Vervoort J.D. and Leeman W.P., 2005, U-Pb Zircon geochronology of crustal xenoliths confirms presence of Archean basement beneath the central and eastern snake river plain. *Geological Society of America Abstracts with Programs*, 37, 60

Wood, S.H. and Clemens, D.M., 2002, Geologic and tectonic history of the western Snake River Plain, Idaho, and Oregon, in Bonnichsen, B., White, C.M., and McCurry, M., eds., Tectonic and magmatic evolution of the Snake River Plain Volcanic Province. Idaho Geological Survey Bulletin, 30, 69–103

Wooden, J.L. and Mueller, P.A. 1988. Pb, Sr, and Nd isotopic compositions of a suite of Late Archean, igneous rocks, eastern Beartooth Mountains: implications for crust–mantle evolution. Earth and Planetary Science Letters, 87, 59–72.

APPENDIX A

Thin Section Petrography

A1: Thin section descriptions for Spencer-Kilgore samples. All SK GPS points are in NAD 27 CON US

SK11-01 : Two Pyroxene Charnokite

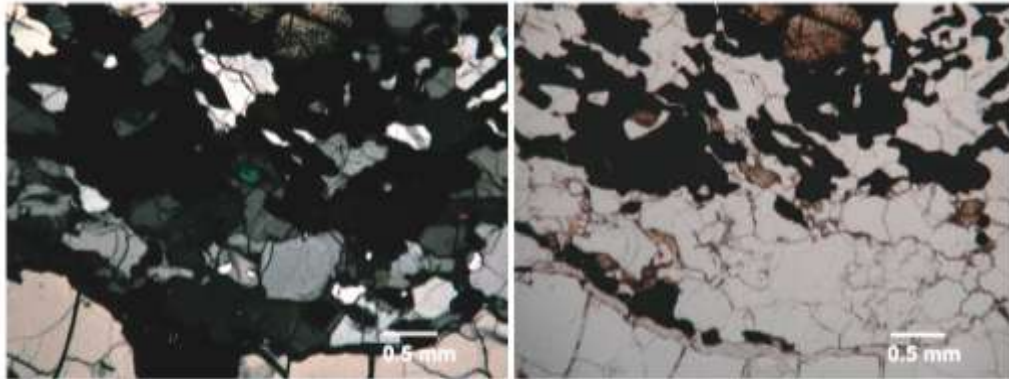


Figure A2 Crossed polar (left) and plain polarized light (right) images of SK11-01

Geologic Setting:

SK11-01 is a crustal xenolith found on Crystal Butte between the hamlets of Spencer and Kilgore, ID. Its exact location was 0426764 E 4906613 N.

Hand sample description:

This sample is white with red/black cm size bands. Bands clumped with three or four centimeters of white between them. In clumps, bands are spaced a cm or two apart. This sample is very friable. Dark bands are also boudinaged.

Mineralogy:

Quartz (30%): Grains are sub rounded in felsic layers and slightly more rounded in mafic layers. Grains are 2-3 mm in felsic layers and .5mm and smaller in mafic layers.

Plagioclase (40%): Grains are sub angular. Patchy lenticular deformation twinning visible in crossed polars. Grains range from 1-3 mm in bands of felsic, large crystals and .5 mm in mafic bands.

Orthopyroxene(15%): In some mafic layers, large clusters of grains occur. Clusters are split into rounded to subrounded pieces .5-1mm in length. A cluster is on average 5-8mm. Smaller (.5mm and less) individual grains also are present in the mafic layers. Grains are fractured parallel to layering

Clinopyroxene (5%): Grains are subrounded and avg .4 mm in size. Second order birefringence is evident with crossed polars.

Opagues (10%): Grains are subrounded to rounded, and form puzzle-piece recrystallization fabric with quartz and feldspar. Grains and clusters of grains are elongated with layering. In hand sample they appear red, and are most likely hematite.

Accessory Mineralogy:

Zircons are present as rounded grains.

Texture:

Sample SK11-01 is compositionally layered, coarse-grained rock. Felsic layers are composed of coarse grains of quartz and plagioclase feldspar. More mafic layers are composed of finer grains of quartz, plagioclase feldspar, orthopyroxene, clinopyroxene and opaques. Within the mafic layers, large clusters of orthopyroxene are also present. Fractures in orthopyroxene are parallel to layering and opaque grains are elongated to layering. Ostwald ripening is seen in both layers.

SK11-02 : Two Pyroxene Charnokite

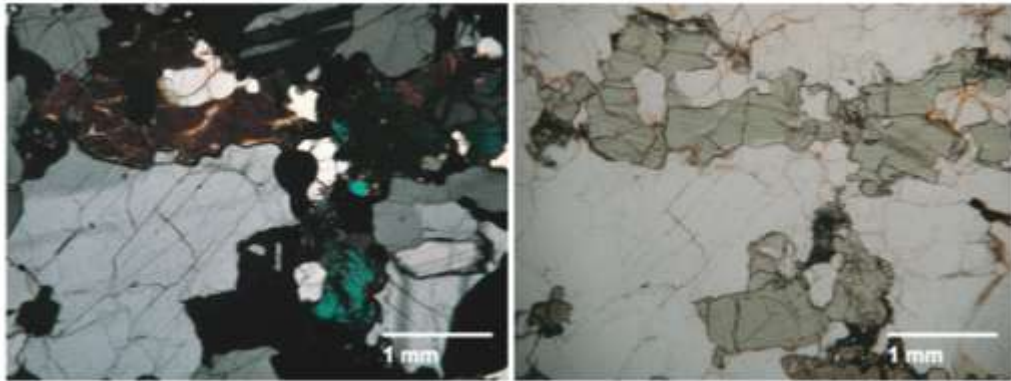


Figure A3 Crossed polar (left) and plain polarized light (right) images of SK11-02

Geologic Setting: SK11-02 is a crustal xenolith found on Crystal Butte between the hamlets of Spencer and Kilgore, ID. Its exact location is 0426770 E 4906562 N.

Hand Sample Description:

Sample SK11-02 is grey and pink with no banding. It is granular, but not friable.

Mineralogy:

Quartz (30%): Grains are subangular to subrounded and many boundaries exhibit boundary bulging. Grains textures are subgranular, have deformation lamellae or show no deformation or metamorphism within the grain (recrystallized?). Small (~.2mm), rounded recrystallized grains formed due to grain boundary migration are common in felsic layers. Size in felsic layers ranges up to 6 mm. Size in mafic layers is ~.5-1.5 mm.

Plagioclase (35%): Grains are subrounded with multiple lenticular deformation twins. Average grain size is 1 mm in felsic bands and ranging down to .2 mm in mafic bands.

Potassium Feldspar (5%): Twinning is perpendicular to each other, but not as well developed as in microcline.

Orthopyroxene (15%): Grains are subrounded. In plain light crystals are light pink. Grains have been partially melted? (One large grain became many smaller grains)

Clinopyroxene (15%): Grains are subrounded. In plain light crystals are green.

Melt (5%) : Quenched melt pocket is parallel to layering. Pocket has partially melted surrounding pyroxene. Felsic needle grains float randomly oriented in glass matrix.

Accessory Mineralogy:

None.

Texture:

Sample SK11-02 is a coarse grained, compositionally layered rock. Felsic layers are composed of large grains of quartz and plagioclase feldspar. More mafic layers are composed of smaller grains of quartz, plagioclase feldspar, orthopyroxene, and clinopyroxene. Pyroxene grains are composed of subgrains. A melt pocket is surrounded by partially melted pyroxenes, and melt occurs between many grains. Serrated boundaries and subgrains formed from serrated boundary bulging are evident, indicating dynamic recrystallization.

SK11-03 : Charnokite

Geologic Setting:

SK11-03 is a crustal xenolith found on Crystal Butte between the hamlets of Spencer and Kilgore, ID. Its exact location is 0426745 E 4906530 N.

Hand sample description:

This xenolith was found broken in two pieces and few chips. The pieces are 5cm x 3cm x 4cm. This sample is banded light grey and dark grey on a mm scale. The light white, felsic bands are 1-2 cm scale. Felsic bands are composed of quartz and feldspar, the darker bands are composed of quartz and pyroxene.

SK11-07 : Garnet Granulite

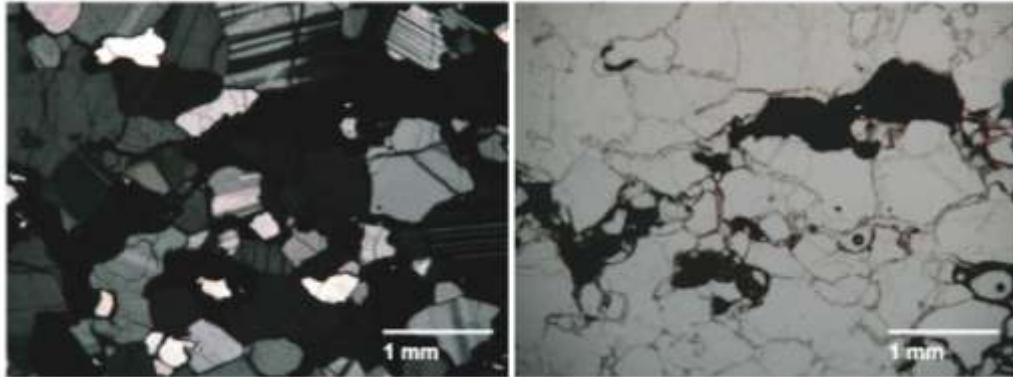


Figure A4 Crossed polar (left) and plain polarized light (right) images of SK11-07

Geologic Setting:

SK11-07 is a crustal xenolith found on Crystal Butte between the hamlets of Spencer and Kilgore, ID. Its exact location is 0426684 E 4906593 N.

Hand sample description:

SK11-07 is white with dark red bands. Bands are not continuous, and very iron rich. Bands are 1mm to 1 cm wide. This rock breaks easily when hit, but is not friable enough to break with hands alone.

Mineralogy:

Quartz (20%) – Grains are subangular, some exhibiting subgrains and deformation lamellae. Grains are white to grey to first order yellow in crossed polars. Average grain size is 1 mm. Smaller (~.2mm) recrystallized grains from grain boundary migration and larger, ribbons parallel to banding grains are also present.

Plagioclase (58%) – Grains are subangular with multiple lenticular deformation twins. Average grains size is 1mm. Some grains form aggregates that range to 4 mm.

Opaques (15%)- Grains are subrounded and elongated parallel to banding. Grains are red in hand sample and may be hematite.

Garnet (7%) – Grains are rounded. Average grain size is .4mm. Grains occur most commonly in opaque bands

Accessory Mineralogy

Rutile grains are present on the edges of major mineral grains, particularly opaques.

Texture:

Sample SK11-07 is coarse grained and granoblastic. It is compositionally layered parallel to foliation. Felsic layers are composed of plagioclase feldspar and quartz. Mafic layers

are .5mm thick bands of opaques and garnet. Mafic bands occur on the cm scale and are sub-parallel to foliation. They are discontinuous. The largest quartz grains are elongated parallel to foliation, and groupings of quartz grains form ribbons parallel to foliation. Grain boundaries bulge to form serrated edges. Melt occurs between many grain boundaries.

SK11-08 : Granulite

Geologic Setting:

SK11-08 is a crustal xenolith found on Crystal Butte between the hamlets of Spencer and Kilgore, ID. Its exact location is 0426667 E 4906548 N.

Hand sample description:

This sample is 4 cm x 3 cm wide. It is light white and composed of quartz and feldspar. Strands of basalt infiltrate the xenolith, many with red iron weathering.

A2: Thin section descriptions for Craters of the Moon samples. All CRMO GPS points are in NAD 27 CON US

CRMO11-01 : Charnokite

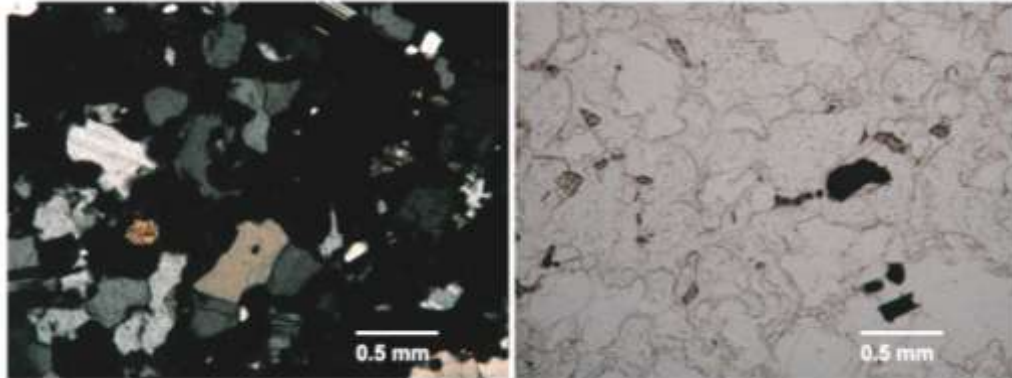


Figure A5 Crossed polar (left) and plain polarized light (right) images of CRMO11-01

Geologic Background:

CRMO11-01 is a crustal xenolith collected by Doug Owen on Big Cinder Butte at Craters of the Moon NM and P. Its exact location was 294114 E 4810643N.

Hand Sample Description:

Sample is generally whitish grey in color, with mm-sized bands alternating white and black. Grains are sugary in texture

Mineralogy:

Quartz (30%) – Grains are white, grey and pale yellow and exhibit deformation subgrains. Boundaries are puzzle piece shaped. Average grain size is .3mm

Plagioclase (25%) – Grains exhibit lenticular deformation twinning of ranging thicknesses. Average grain size is .6mm.

Orthopyroxene (5%) – Grains are rounded and medium brown to pale green in plain light. Some grain boundaries are wavy, perhaps from partial melting? Average grain size is .2 mm.

Melt (40%)

Accessory Minerals

Zircon- rounded grains are found as an inclusion in plagioclase

Texture:

Sample CRMO11-01 is a medium-sized grained rock. Melt has infiltrated much of the rock, causing irregular grain boundaries. Grains are grouped in loose aggregates of 1 to 2 mm with <.5mm of melt between aggregates. Aggregates and elongated quartz grains form a weak fabric. Rounded orthopyroxene grains are also found scattered throughout aggregates, and show no elongation or orientation.

CRMO11-03 : Granite

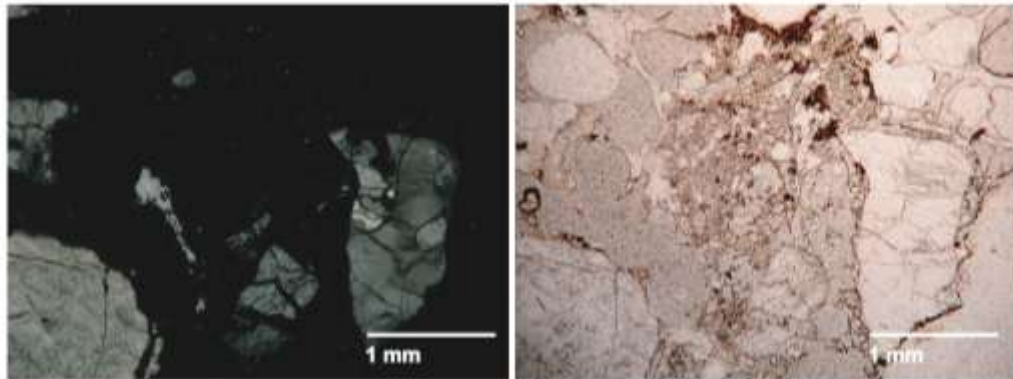


Figure A6 Crossed polar (left) and plain polarized light (right) images of CRMO11-03

Geologic Background: CRMO11-03 is a xenolith found by Doug Owen in a SW striking fissure off of North Crater at Craters of the Moon NM and P.

Hand Sample Description:

This sample generally has a whitish-brown color, with splotches of black. The black is infiltrated basalt. Iron staining has added a brown tint to the white quartz and plagioclase. The sample is friable due to its popcorn texture. Crystals are large, over a cm in size.

Mineralogy:

Quartz (40%) – Grains are grey to first order yellow. Large (4-7mm) grain aggregates show differing types of deformation. Some aggregates are composed of only a few grains and show subgrain recrystallization, others are composed of many mm sized grains and exhibit grain boundary bulging.

Plagioclase (20%) – Grains are grouped in large aggregates of polygonal grains. Some exhibit multiple and patchy lenticular deformation twinning. 50% of grains are blue in polarized light, indicating they are Labradorite. These grains record growth zoning.

Melt (40%) – Fine grains of plagioclase are held in a matrix of glass. Plagioclase grains do not have an orientation, indicating growth was not under pressure.

Accessory Mineralogy:

Zircon- One .3mm polygonal zircon is found as an inclusion in plagioclase, and empty zircon shaped casts are found in quartz grains.

Texture:

Sample CRMO11-03 is composed of very coarse grains and large aggregates held in basalt melt matrix. Quartz grains exhibit subgrain extinction and boundary migration. Plagioclase aggregates exhibit deformation twinning and zoning. There is no preferred orientation of grains.

CRMO11-04 : Granite

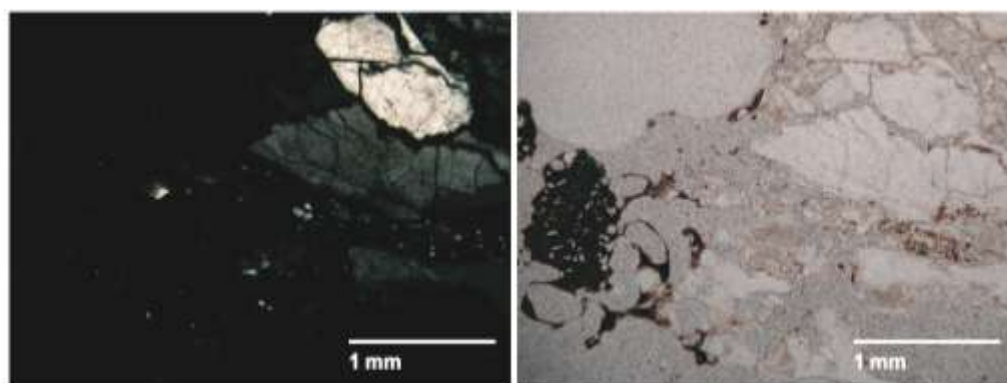


Figure A7 Crossed polar (left) and plain polarized light (right) images of CRMO11-04

Geologic Background: CRMO11-04 is a xenolith found by Doug Owen in a W striking fissure off of North Crater at Craters of the Moon NM and P.

Hand Sample Description:

This sample is very fresh, does not break easily. It has easily seen crystals of quartz, feldspar, and amphibole. A very light lamination is evident, with layers of felsic minerals alternating with mafic minerals.

Mineralogy:

Quartz (48%) – Grains are grey to first order yellow. Large (4-7mm) grain aggregates show differing types of deformation. Some aggregates are composed of only a few grains

and show subgrain recrystallization, others are composed of many mm sized grains and exhibit grain boundary bulging.

Plagioclase (20%) – Grains are grouped in large, fractured aggregates. Some exhibit multiple and patchy lenticular deformation twinning. Some grains are blue in polarized light.

Potassium Feldspar (20%) – Grains are angular with patchy, poorly developed tartan twinning.

Amphibole (7%) – Amphibole grains have been weathered and melted, forming irregular grain boundaries and grains that have many holes, some in filled by other minerals.

Orthopyroxene (2%) – Small, rounded grains of orthopyroxene have grown in weathered amphibole grains.

Accessory Mineralogy:

Zircon- zircon is found as an inclusion in quartz.

Texture:

Sample CRMO11-04 is composed of aggregates and coarse grains. All grains are fractured. Quartz has puzzle piece texture of interlocking grains, indicating grain boundary migration. There is no preferred orientation of grains.

CRMO11-05 : Charnokite

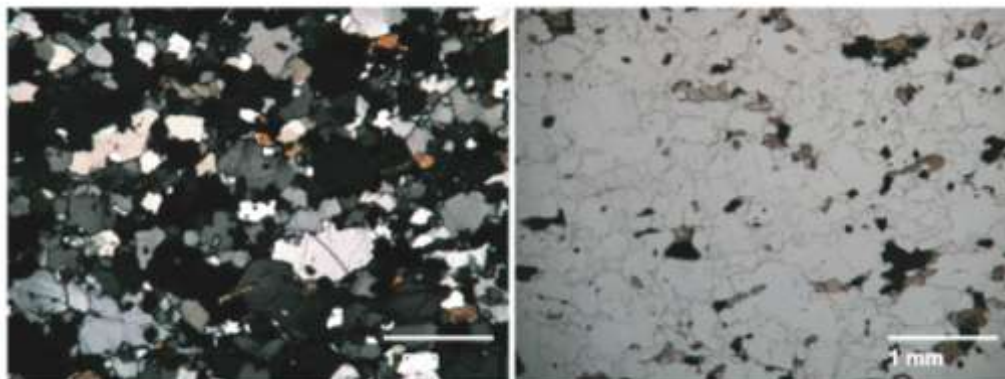


Figure A8 Crossed polar (left) and plain polarized light (right) images of CRMO11-05

Geologic Background: CRMO11-05 is a crustal xenolith found in the Sunset Lava Flow at Craters of the Moon NM and P. Its exact location was 0293930 E 4815578 N.

Hand Sample Description:

Sample is generally medium grey in color, with distinctive mm-sized pink bands of plagioclase, as well as white bands less than 1mm. A large augen of quartz is present.

Mineralogy:

Quartz (45%) – Grains are subrounded with irregular boundaries, indicating grain boundary migration. Quartz ribbons and individual grains are oriented and elongated to form a fabric. Most grains exhibit subgrain deformation. Grain size varies from .1mm to ribbons longer than 5mm.

Plagioclase (25%) – Grains are subrounded with irregular boundaries. Quartz inclusions are prolific. Multiple lenticular deformation twinning is present. Grains are randomly oriented and some large grains are elongated parallel to quartz ribbon fabric. Average grain size is .8mm.

Potassium Feldspar (15%) – Grains are subrounded. Tartan twinning is patchy.

Orthopyroxene (8%) – Grains are subangular with irregular boundaries. Grains are randomly oriented, but multiple grains are usually found in the same plane or connected, parallel to quartz ribbon fabric. Green to pink pleochroism is seen in plain light. Average grain size is .3mm.

Opaques (5%) – Irregular, subangular boundaries are most common, however some grains are rectangular. Grains have a slight orientation parallel to quartz ribbon fabric. Average grain size is .2mm.

Biotite (2%) – Average grain size is .6mm.

Accessory mineralogy:

Zircon – Rounded and polygonal zircon are found as inclusions.

Texture:

Sample CRMO11-05 is a medium grained rock composed mainly of quartz, feldspar and orthopyroxene. Grains have irregular boundaries and quartz grains exhibit puzzle piece boundaries. A fabric is evident from elongated grains and quartz ribbons, although it is easier to see it in hand sample than in thin section. Compositional banding is formed from pyroxene-rich layers.

CRMO11-06 : Rhyolite

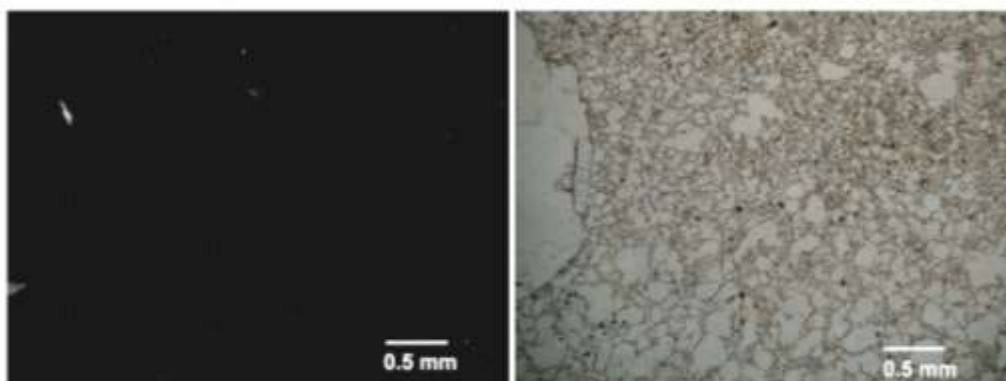


Figure A9 Crossed polar (left) and plain polarized light (right) images of **CRMO11-06**

Geologic Background: CRMO11-06 is a xenolith found on North Crater at Craters of the Moon NM and P. Its exact location was 0292463 E 4813915 N.

Mineralogy:

Glassy matrix (95%) – Fine grained glassy matrix. In plain light perlitic cracks are seen.

Phenocrysts (5%) – Both quartz and feldspar phenocrysts are present. Simple and lamellar twinning is present, indicating both sanidine and plagioclase. Inclusions of glass and zircon are present. Average grain size is 1mm.

Accessory Mineralogy:

Zircon - .1mm zircons are present as inclusions in quartz.

Texture: Sample CRMO11-06 is composed of a fine grained, glassy matrix with phenocrysts of feldspar and quartz.

CRMO11-10 : Granulite

Geologic Background:

Sample CRMO11-10 is a small (4 x 4 x 3 cm) xenolith in vesiculated, oxidized basalt of the grassy flow at Craters of the Moon NM and P. Its exact location was 0287570E 4809833N.

Hand Sample Description: This sample is very felsic, consisting of quartz and feldspar. In it are 3 mafic bands in 4 cm surface, varying 1-2 cm apart. Mafic bands are .4 cm

thick, thicker than many other xenoliths and composed of pyroxenes and perhaps other mafic minerals. This sample is too small to analyze.

CRMO11-11 : Granulite

Geologic Background:

Sample CRMO11-101 is a 4 x 7 cm wide xenolith in found in the Grassy flow at Craters of the Moon NM and P. Its exact location was 0287554E 4809861N.

Hand Sample Description: This sample is a thinly banded granulite xenolith. Quartz and feldspar are .5 cm or greater, mafics smaller. Mafic bands are .2 cm thick and include pyroxene. Iron weathering from basalt around edges. Orange weathering of feldspar is noticed throughout. Crystals are elongated parallel to banding. This sample is too small to analyze.

CRMO11-12 : Granulite

Geologic Background: CRMO11-12 is a small (2.5 x 4 cm) banded crustal xenolith found loose on the basalt in the Grassy Flow at Craters of the Moon NM and P. The exact sampling location is 0287499 E 4809884 N.

Hand Sample Description: In general, this sample is whitish. It is granular, so granular it feels similar to pumice. Iron weathering is evident on surface. It is very felsic, to the point where banding is weak only because there are not many mafic minerals (pyroxene). Mafic bands are only 1 or two crystals wide. This sample is too small for a thin section, but large enough for analysis.

CRMO11-13 : Granulite

Geologic Background: CRMO11-13 is composed of two small (3 x 4 cm) banded crustal xenolith found in the Grassy Flow at Craters of the Moon NM and P. They were found embedded in basalt. These samples were found right next to CRMO11-12.

Hand Sample Description: This xenolith has weak to no banding. It is dominantly composed of quartz and plagioclase feldspar. Mafic minerals are also present, and are probably pyroxene. It is a granulite with granoblastic texture. Crystals are less than .5 cm in length. This sample is too small for a thin section, but large enough for analysis.

CRMO11-14 : Granulite

Geologic background:

CRMO11-14 is a small (6 x3 cm) banded crustal xenolith found in a loose piece of vesiculated basalt in the Grassy Flow at Craters of the Moon NM and P. It was found embedded in basalt. The exact sampling location is 0287480 E 4809908 N.

Hand Sample Description:

CRMO11-14 is a felsic granulite xenolith with mm bands of mafic minerals every 1-1.5cm. It is fresh, not friable. Major mineralogy includes quartz, plagioclase and a mafic that is most likely a pyroxene. Crystal size is very small, <1mm. Sample is too small for a thin section.

CRMO11-15 : Charnokite

Geologic background: CRMO11-15 is a very large (15x10cm) banded crustal xenolith found in the Grassy Flow at Craters of the Moon NM and P. It was found embedded in basalt. The exact sampling location is 0287691 E 4809800 N.

Hand Sample Description:

Xenolith with alternating mafic and felsic bands. Felsic bands 1-3 cm thick. Mafic bands are <1 to 1 cm thick. Iron weathering around edge of xenolith is present. It is easy to break crystal off with a fingernail. Fractures across bands are present. Airspace where crystals have fallen out are easily seen with the naked eye.

Mineralogy:

Quartz (65%) – Grains are subrounded with irregular boundaries. Interference colors are gray to white to first order yellow. Ribbons are present, orientated parallel to each other. Individual grains are less elongated, and randomly oriented. Average grain size is .5mm.

Plagioclase (24%) – Grains are subangular. Multiple lenticular deformation twinning is present. Grains are randomly oriented. Average grain size is .5mm.

Glass pockets with plagioclase (9%) – Elongated pockets and strings oriented to fabric. Glass and plagioclase are dominant. Minerals with second order interference colors are identified in crossed polars, but are too small to identify. They are possibly olivine.

Orthopyroxene (2%) – Grains are subrounded, fractured, and partially dissolved. In plain light, grain changes from pale green to light pink with stage rotation.

Accessory Mineralogy:

Zircon- Polygonal zircon is found as inclusion in quartz. A larger grain (.1mm) is identified between quartz and feldspar grains, and is rounded.

Texture:

Sample CRMO11-015 is a medium grained rock with a granoblastic texture. Finer grained bands of mafic material occur in <1mm layers. Mafic bands and quartz ribbons are parallel to each other forming a fabric. Ribbons of quartz indicate high-grade metamorphism. Quartz grains have serrated boundaries, and many small, rounded subgrains most likely formed from boundary migration are present, indicating dynamic recrystallization.

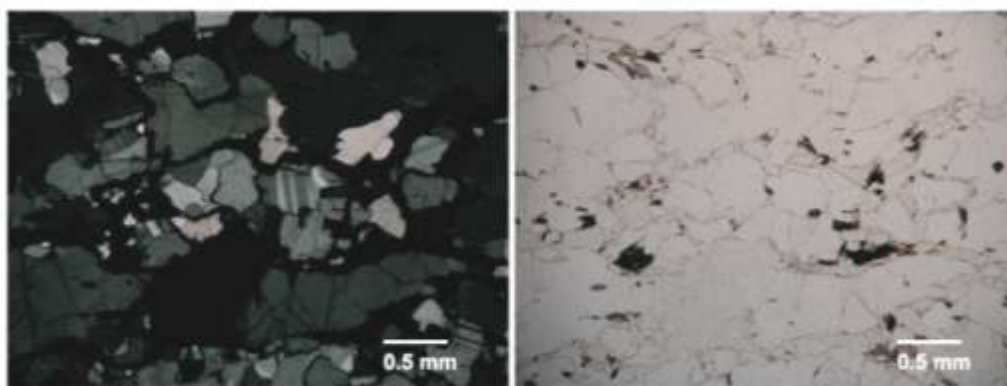
CRMO11-16 : Charnokite

Figure A10 Crossed polar (left) and plain polarized light (right) images of CRMO11-16

Geologic background: CRMO11-16 is a gneiss crustal xenolith found in the Grassy Flow at Craters of the Moon NM and P. It was found south of CRMO11-15, loose in Aa.

Hand Sample Description:

This sample is a weakly banded granulite alternating white and black bands. Feldspar is weathered brown throughout. Orange iron weathering is present in patches. Rock can be broken in hands with a hammer easily, but does not crumble in hands.

Mineralogy:

Quartz (57%) – Grains are subrounded with irregular boundaries. Interference colors are gray to white to first order yellow. Ribbons are present, orientated parallel to each other. Individual grains are less elongated, and randomly oriented. Average grain size is .5mm to 1mm.

Plagioclase (25%) – Grains are subangular. Multiple lenticular deformation twinning is present. Grains are randomly oriented. Average grain size is .5mm.

Opagues (10%) – Weak layers of elongated pockets of crystals and individual crystals oriented parallel to layering.

Orthopyroxene (8%) – Grains are subrounded and fractured. In plain light, grain changes from pale green to light pink with stage rotation. Grains are partially dissolved to be elongated parallel to layering

Accessory Mineralogy:

Zircon- Polygonal zircon is found as inclusion in quartz and plagioclase.

Texture: Sample CRMO11-016 is a coarse grained rock of mainly quartz and plagioclase with <1mm bands of fine grained mafic material. Grains are granoblastic. Mafic bands and quartz ribbons are parallel to each other forming a gneissosity. Ribbons of quartz indicate high grade metamorphism.

CRMO11-17 : Charnokite

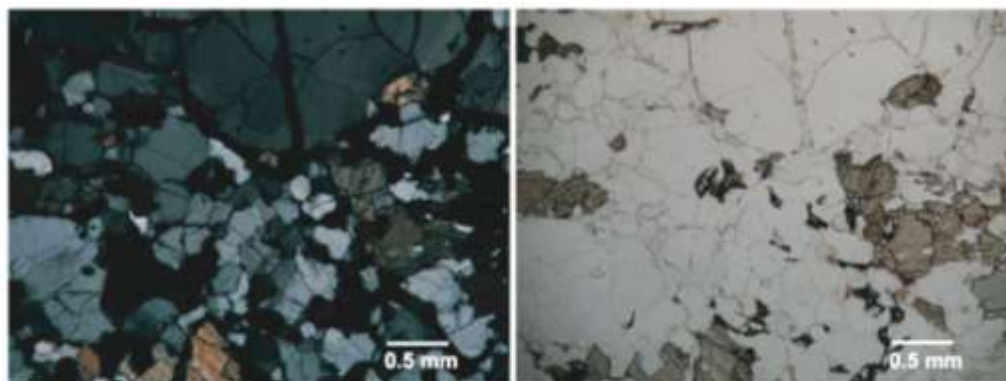


Figure A11 Crossed polar (left) and plain polarized light (right) images of CRMO11-17

Geologic background: CRMO11-17 is a gneissic crustal xenolith found in the Grassy Flow at Craters of the Moon NM and P. The exact sampling location was 0287550 E 4809904 N.

Hand Sample Description:

This sample is a weakly banded granulite. Generally, the sample has blotches of black, orange/brown, and white. Feldspar is weathered brown in patches. Rock can be broken in hands with a hammer easily, but does not crumble in hands. Individual crystals fall out easily. Airspace from weathered out crystals is seen with naked eye.

Mineralogy:

Plagioclase (40%) – Grains are subangular. Multiple lenticular deformation twinning is present. Grains are randomly oriented. Average grain size is .75mm, although larger grains up to 4mm are present as well.

Quartz (35%) – Grains are subrounded with irregular boundaries. Interference colors are gray to white to first order yellow. Ribbons are present, orientated parallel to each other. Individual grains are randomly oriented, but packed together parallel to ribbons. Average grain size is .5mm to 1mm.

Opaques (10%) – Interspersed grains are grouped to create a weak layering. Some grains are elongated pockets.

Orthopyroxene (15%) – Grains are subrounded and fractured. In plain light, grain changes from pale green to light pink with stage rotation. Grains are partially dissolved to be elongated parallel to layering. Average grain size is 1mm.

Accessory Mineralogy:

Zircon- Rounded zircon is found as inclusion in quartz.

Texture:

Sample CRM011-017 is medium grained and granoblastic. Grains are equigranular, but form aggregates that are elongated and parallel to compositional banding. Felsic bands are composed of quartz and plagioclase and mafic bands are composed of orthopyroxene and opaques. Mafic minerals and quartz ribbons are elongated and/or oriented parallel to compositional banding as well. This forms a weak fabric.

CRM011-18 : Granulite

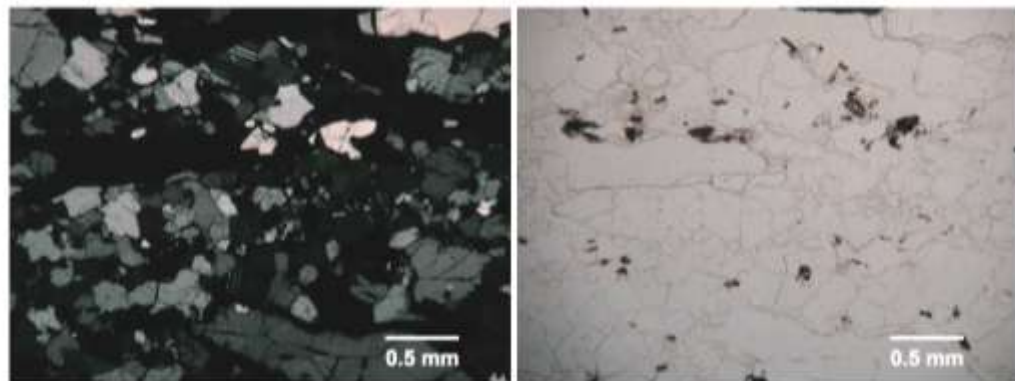


Figure A12 Crossed polar (left) and plain polarized light (right) images of CRM011-18

Geologic Background: CRMO11-18 is a crustal xenolith found in the Grassy Flow at Craters of the Moon NM and P.

Hand Sample Description:

In general, the sample is a brownish white color. It is almost banded, and looks like a granite that has undergone metamorphism. Streaks of black and white are layered on each other, but not continuous to be defined as banded. Alteration in the form staining is present.

Mineralogy:

Quartz (47%) - Grains are subrounded with irregular boundaries. Interference colors are gray to white to first order yellow. Ribbons are present, orientated parallel to each other. Individual grains are randomly oriented, but packed together parallel to ribbons. Average grain size is .5mm to 1mm.

Plagioclase (40%) – Grains are subrounded with irregular boundaries. Grains exhibit multiple lenticular deformation lamellae. Average grain size is .5mm.

Opaques (8%) – Grains are both rounded and angular, and are oriented parallel to quartz ribbons. They are grouped to form weak compositional layering, with ~2mm separating each layer.

Texture: Sample CRMO11-18 is medium grained. Opaque grains are grouped together to form compositional layering. Ribbons of quartz and aggregates of quartz and feldspar are elongated parallel to this layering. Grains have been weathered, creating space between many of the grains.

Accessory Minerals:

Zircon- Grains are found as inclusions in quartz as well as independent grains.

CRMO11-19 : Granite

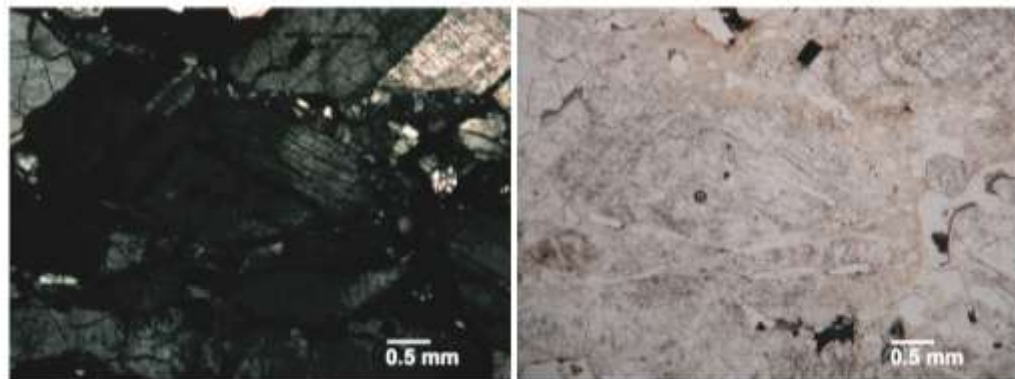


Figure A13 Crossed polar (left) and plain polarized light (right) images of CRMO11-19

Geologic Background: CRMO11-19 is a crustal xenolith sampled from the Grass Flow at Craters of the Moon NM and P. The exact sampling location is 0287513 E 4809946 N.

Hand Sample Description:

Sample is overall white, with black blotches of amphibole throughout. Crystals are large and angular, up to a cm in size. Iron staining is present, especially near the edges of the xenolith.

Mineralogy:

Plagioclase (53%) Crystals are subangular, cloudy and highly fractured. Subgrains are common, as well as intergrowths. Multiple lenticular deformation lamellae are present; some lamellae are kinked. Average crystal size is 3mm, but can be as large as a cm.

Quartz (40%) – Crystals are subangular and fractured. Quartz veins composed of rounded grains are .1mm in size and randomly oriented throughout rock. Average grain size is 2mm, but can be up to a cm in size.

Opaques (5%)

Amphibole (2%) Crystals are angular and green. Crystals range up to a cm in size.

Accessory Minerals: none

Texture: Sample CRMO11-19 is composed of very coarse grains. Course grains can be interlocking or can be separated by fine grained aggregates. Grains are randomly oriented. Many of the large grains are highly fractured. Grain boundaries are irregular.

A3: Thin section descriptions for Square Mountain samples. All GPS coordinates for Square Mountain samples are in 11T.

SM10-A3 : Charnokite

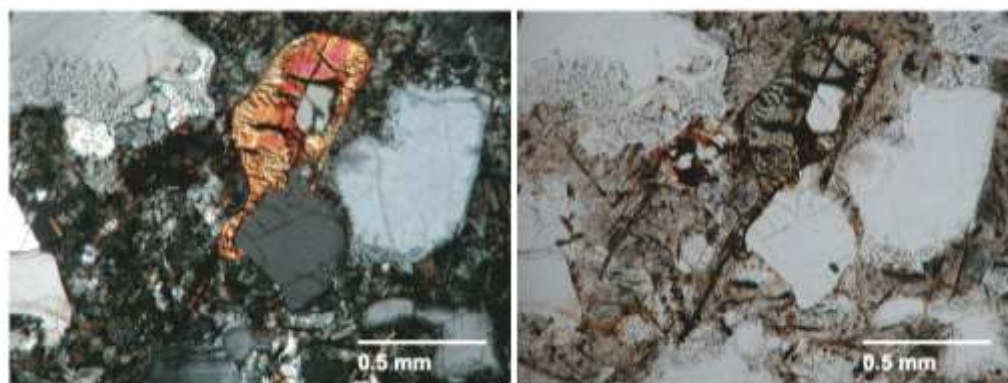


Figure A14: Crossed polar (left) and plain polarized light (right) images of SM10-A3

Geologic Setting

SM10-A3 is from a xenolith within Square Mountain Basalt at Square Mountain, Fairfield, ID. The exact sampling location is 4806446 E 0702003N in 11T

Hand Sample Description:

Overall, this sample is a yellow-whitish color with streaks of dark grey every few centimeters. The whitish area is composed of quartz and plagioclase, and the dark grey streaks are composed of quartz aggregates and scarce pyroxene.

Mineralogy

Quartz (35%) - Grains are subrounded to rounded with subgrains. Grain color is gray to white to first order yellow birefringence in crossed polars. Grain boundaries are partially melted and boundaries between grains exhibit bulging grain boundary migration. Average size .7mm.

Feldspar (31%) - Grains are subrounded with glass infiltrated grain boundaries, clear in plain light. Lenticular deformation twinning and tartan twinning is visible in crossed polars, indicating both plagioclase and K-feldspar are present.

Pyroxene (4%) – Grains are yellow to brown in plain polarized light and been dissolved to a great extent.

Basalt melt (30%) – Between xenolith grains is a fine grained mass of glass, feldspar, and mafic minerals

Accessory mineralogy

Zircon- Grains are found as inclusions in quartz and feldspar grains and free floating in the melt. Zircons are both euhedral and anhedral.

Rutile- Grains are found as inclusions in quartz and free floating in the melt.

Texture:

Sample SM10-A3 is bimodal in grain size: grains are fine grained and medium grained. Fine grains are in a glassy matrix. In hand sample and outcrop, it is evident the fine grains and glass are part of the Square Mountain Basalt, the host rock. Medium size grains (those part of the xenolith) are not oriented, and are equigranular. Boundaries are irregular and smooth, but not rounded.

SM10-C1: Gabbro

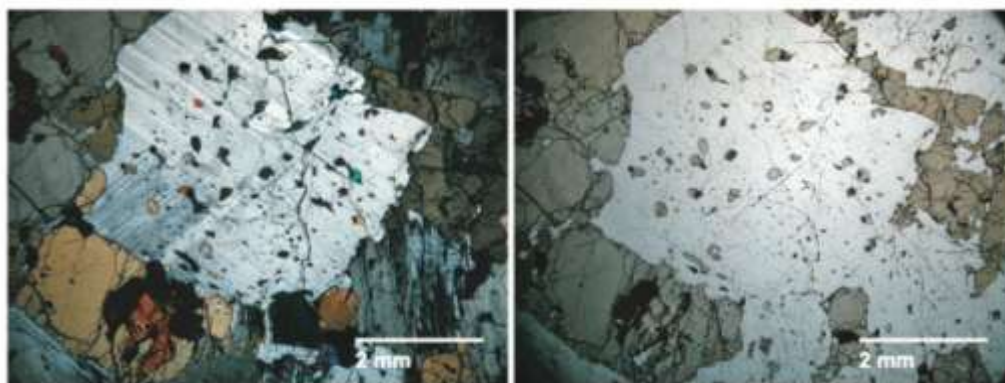


Figure A15: Crossed polar (left) and plain polarized light (right) images of SM10-C1

Geologic Setting

SM10-C1 is a xenolith within the Square Mountain Basalt at Square Mountain, Fairfield, ID. Its exact location is 0702276 N 4806066 E.

Hand Sample Description

This sample is dark greyish-blue and very friable. Plagioclase and olivine grains are obvious, and can range up to a cm in size.

Mineralogy

Plagioclase (65%) – Grains are anhedral. Lenticular deformation twinning and step growth twinning are visible in crossed polars.

Orthoclase (20%) – Grains are pleichroic and anhedral. They are also found as inclusions in feldspar.

Olivine (9%) – Found as centers of orthoclase growth. Has weathered to itingsite at grain edges.

Opaque minerals (3%) – Inclusions in feldspar oriented along cleavage and larger anhedral grains in orthoclase.

Lithic Fragments (3%)- quartz, feldspar, biotite, amphiboles, pyroxene and oxides

Accessory Mineralogy:

none

Texture:

Sample SM10-C1 is coarse grained. Grains are euhedral with irregular boundaries. Olivine is always surrounded by orthopyroxene, suggesting olivine mineralization started at a high temperature and was taken over by pyroxene as the magma cooled. All grains are fractured, and some fractures are in-filled with melt.

SM10-C2 : Charnokite

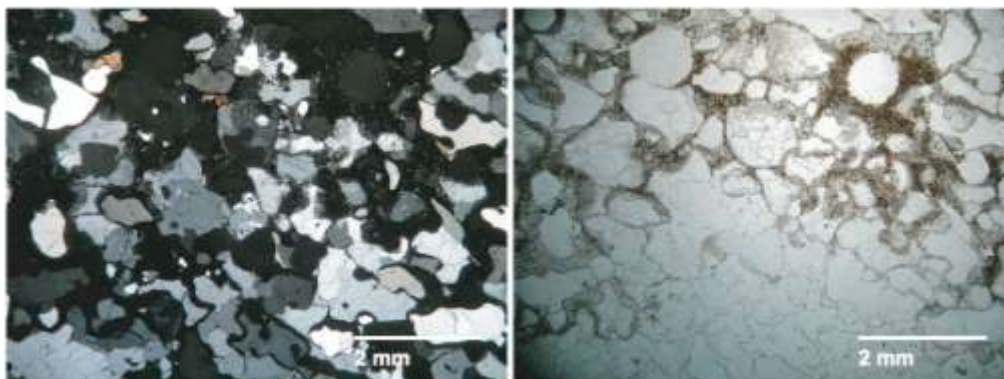


Figure A16 Crossed polar (left) and plain polarized light (right) images of SM10-C2

Geologic Setting:

SM10-C2 is a crustal xenolith found in the Square Mountain Basalt in Fairfield Idaho. It was found about 50 feet east of SM10-C1.

Hand Sample Description:

This sample is very bright white, with streaks of reddish-brown where basalt has infiltrated the xenolith. Speckled throughout are dark mm size pyroxenes.

Mineralogy:

Quartz (80%) - Grains are in-equigranular, interlobate and subgranular. Grain color in crossed polars range from gray to first order yellow. Grains exhibit undulose extinction.

Feldspar (8%) – Both plagioclase (80%) and microcline (20%) are present. Plagioclase exhibit lenticular deformation twinning.

Melt (10%) – Composed of glass and needle shaped minerals. Almost all grain boundaries are partially melted. Alternating bands of high melt concentration are on a 1-3 cm scale.

Orthopyroxene (2%) – Small grains (.5mm) have been greatly dissolved by melt.

Accessory Mineralogy:

Zircon

Texture:

This sample is medium to coarse grained. It has a weak fabric composed of elongated grains and quartz ribbons. Bands of basalt melt have infiltrated the rock parallel to this fabric. Bands of melt are 1-3 cm thick. Quartz grains have very irregular boundaries. Many boundaries have been melted, however those that have not exhibit grain boundary migration. Grains are anhedral.

SM10-C3: Charnokite

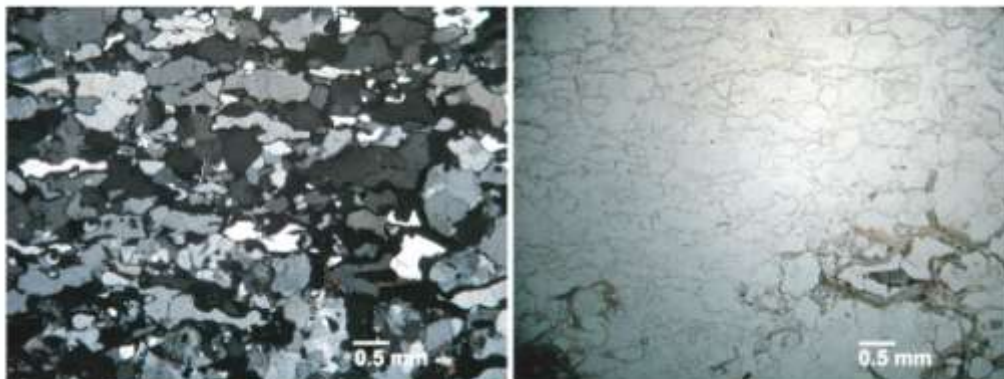


Figure A17 Crossed polar (left) and plain polarized light (right) images of SM10-C3

Geologic Setting:

SM10-C3 is a crustal xenolith found in the Square Mountain Basalt in Fairfield Idaho. It was found about 50 feet east of SM10-C1.

Hand Sample Description:

This samples is lightly banded on a cm scale. Bands alternate between white and medium grey. Millimeter size holes are common throughout where minerals have weathered out.

Mineralogy:

Quartz (55%) - Grains are inequigranular and interlobate. Grains exhibit subgranular and deformation lamelle. Grain color in crossed polars range from grey to first order yellow

and exhibit undulose extinction. Average grain size ranges from .25 to 1.5m. Smaller grains exist between the boundaries of larger grains.

Plagioclase (10%) - Grains exhibit lenticular deformation twinning.

Microcline (20%)

Melt (4%) – Composed of glass and needle shaped minerals. Zones of melted grain boundaries are elongated in the orientation of deformation.

Orthopyroxene (1%)

Accessory Mineralogy:

None

Texture:

This sample is mainly quartz and feldspar grains that are elongated in the same orientation. Boundaries of grains are irregular because they re-melted and/or recrystallized. Zones of melting occur on a centimeter scale, and are elongated in the same orientation as the grains. Grain boundaries are irregular and bulging.

SM10-C4 : Granite

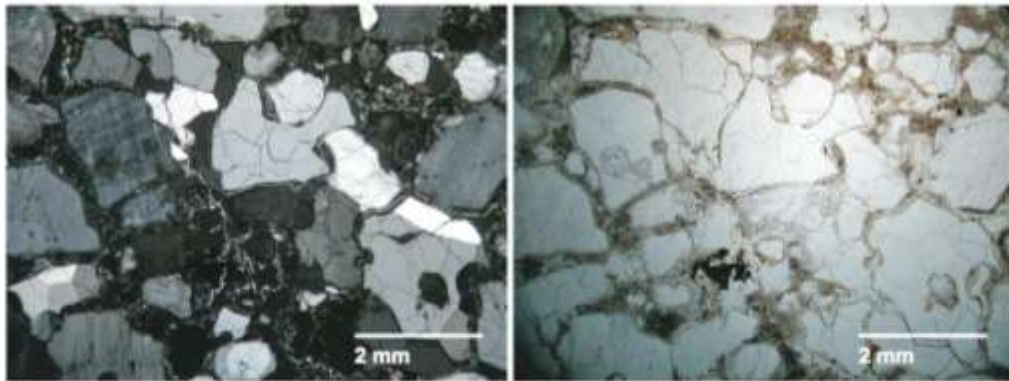


Figure A18 Crossed polar (left) and plain polarized light (right) images of SM10-C4

Geologic Setting:

SM10-C4 is a crustal xenolith found in the Square Mountain Basalt in Fairfield Idaho. It was found about 50 feet from SM10-C1.

Hand Sample Description:

Overall, this sample is medium grey. The xenolith is lighter grey, but basalt has infiltrated the rock. This xenoliths is very solid and fresh looking.

Mineralogy:

Quartz (25%) - Grains are subangular and fractured. Grain color in crossed polars range from gray to first order yellow and exhibit planar extinction. Grain boundaries have not been partially melted. Average grain size ranges from 1 - 3mm.

Plagioclase (30%) - Grains exhibit lenticular deformation twinning. Grain boundaries are partially melted.

Microcline (35%) – Grains exhibit well developed tartan twinning. Grain boundaries are partially melted. Avg grain size is 1 – 3mm.

Melt (10%) – Composed of glass and needle shaped minerals, with strands of quartz formation.

Accessory Mineralogy:

Large zircons (.2mm) are found as inclusions in feldspar.

Texture:

SM10-C4 is composed very coarse grains held in melt. Grain boundaries are irregular from partial melting. Quartz grains are composed of subgrains indicating metamorphism.

A4: Descriptions of House Mountain samples.**HM11-01 : Tonalite Orthogneiss/Charnokite****Hand Sample Description:**

Generally, the sample is whitish grey. Quartz, feldspar, and orthopyroxene are present. Banding of alternating mafic and felsic concentrations occur on a mm scale. This sample is from a section of alternating tonalite orthogneiss and amphibolite gneiss. The amphibolite gneiss was also sampled, but proved not to have sufficient zircons to analyze.

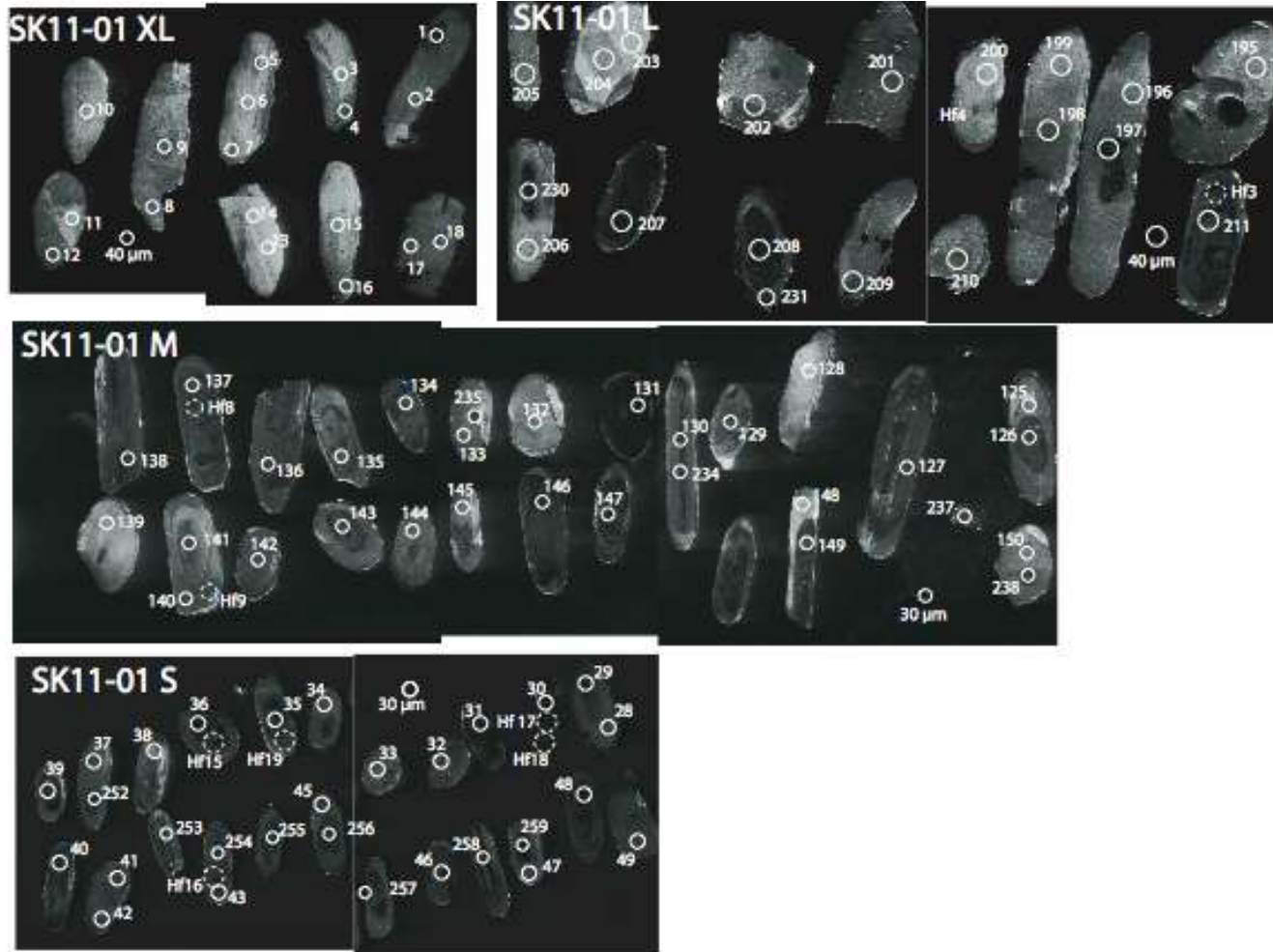
HM11-06 : Amphibolite Paragneiss**Hand Sample Description:**

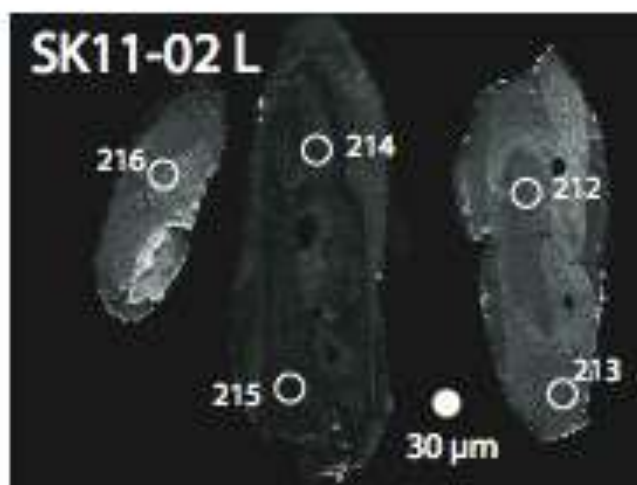
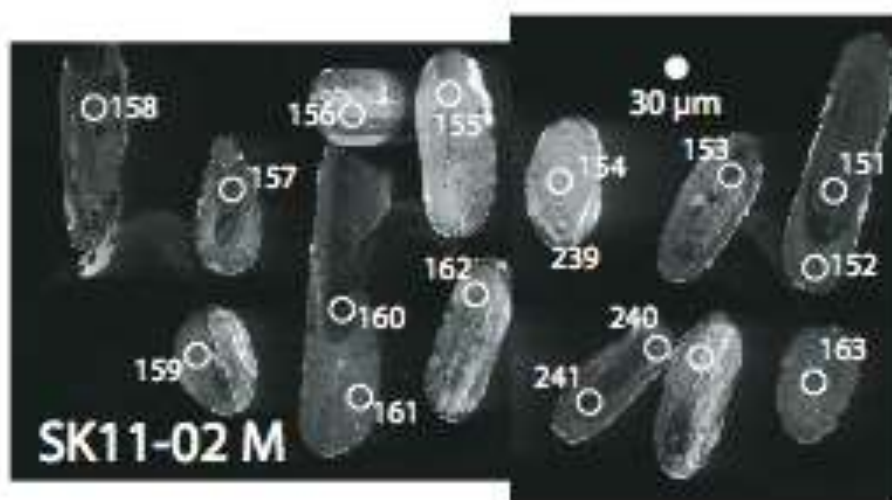
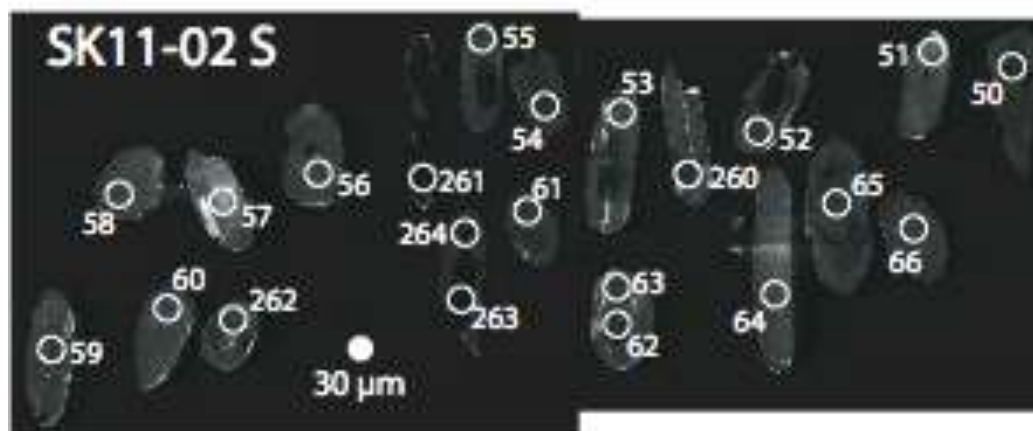
Generally, the rock is brownish orange, and is peraluminous as made evident by abundant muscovite. Elongate quartz crystals, feldspar, muscovite, and amphibole create a visible lamination. Feldspar has weathered orange, and iron staining is obvious. Fresh breaks in the rock reveal a greenish hue. This lithology is found sitting structurally above the granite orthogneiss and tonalite gneiss.

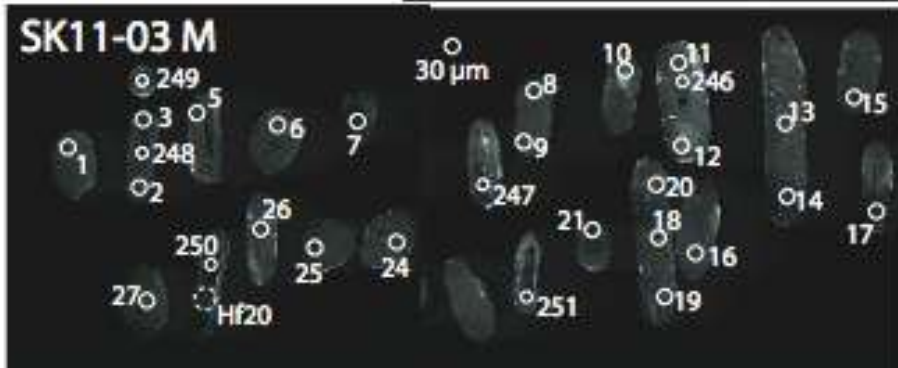
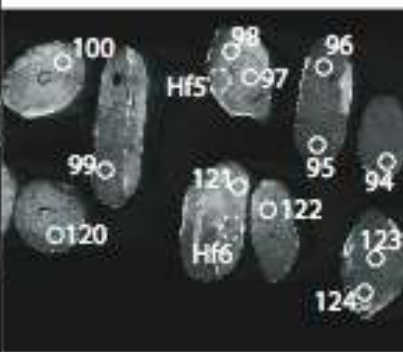
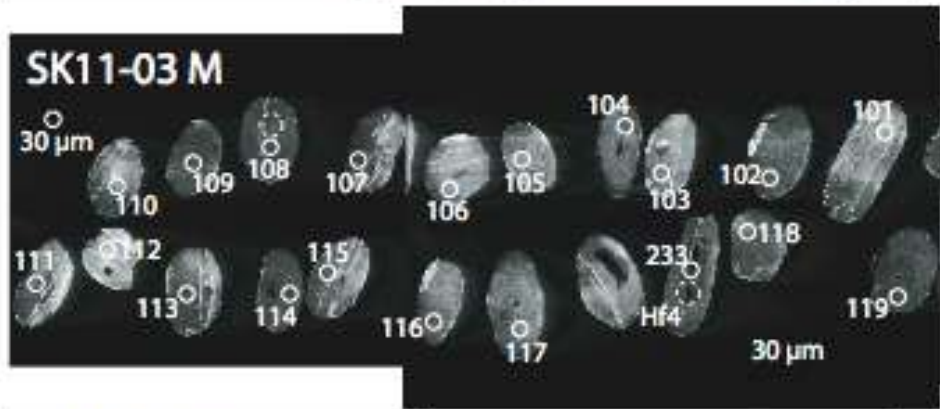
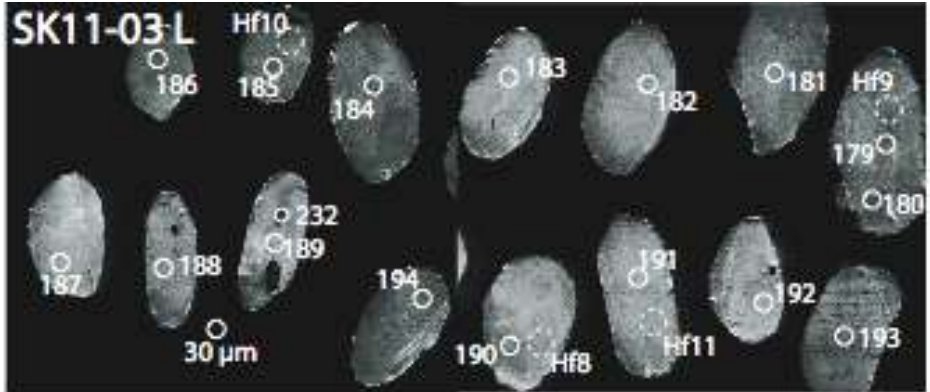
APPENDIX B

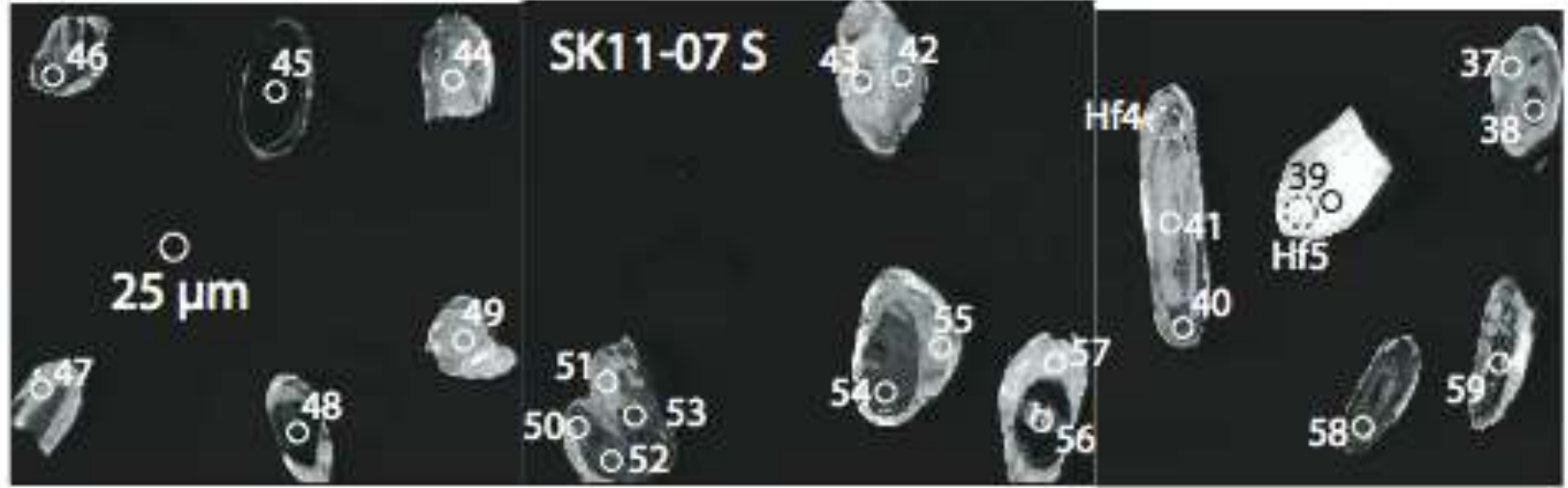
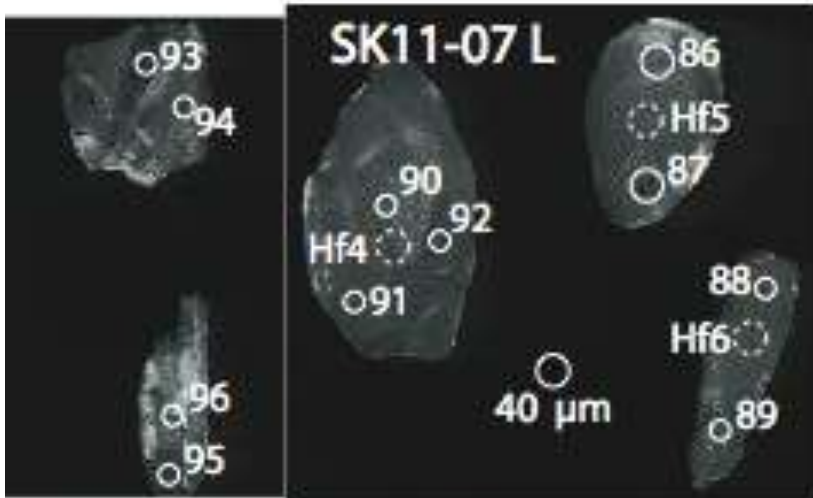
Cathodoluminescence Images with Laser Spots

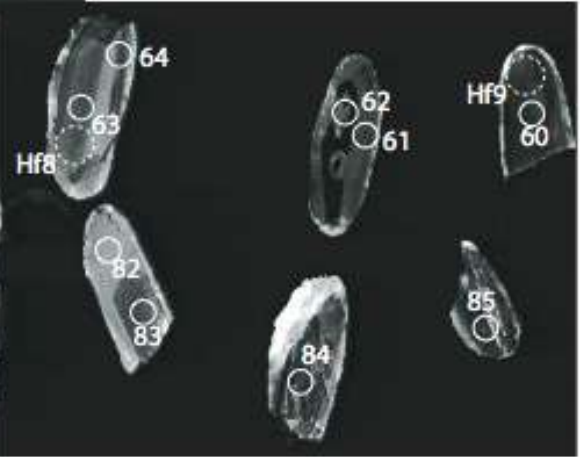
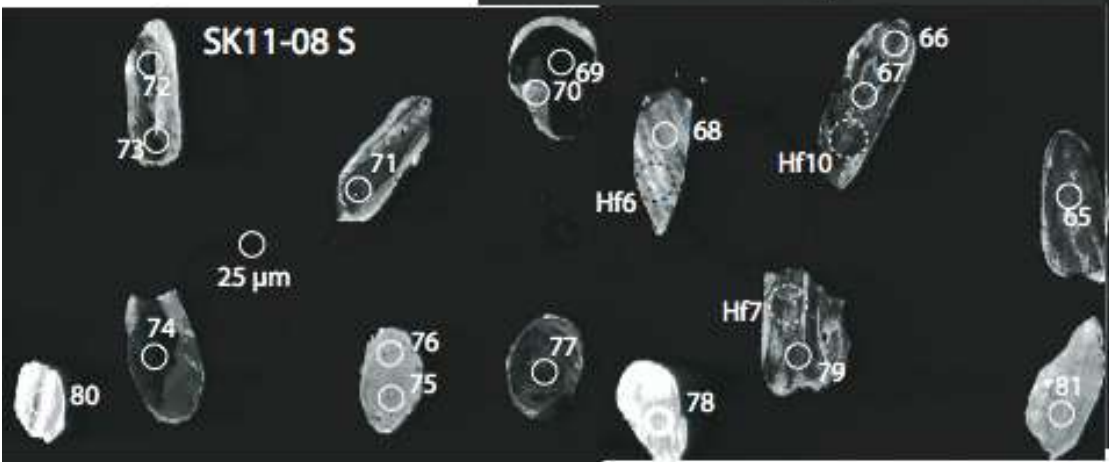
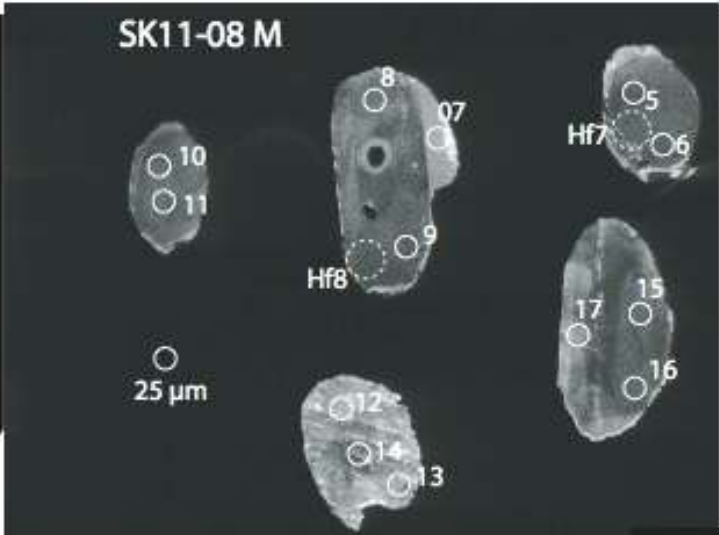
B1: Cathodoluminescence Images of Zircons from Spencer-Kilgore Samples



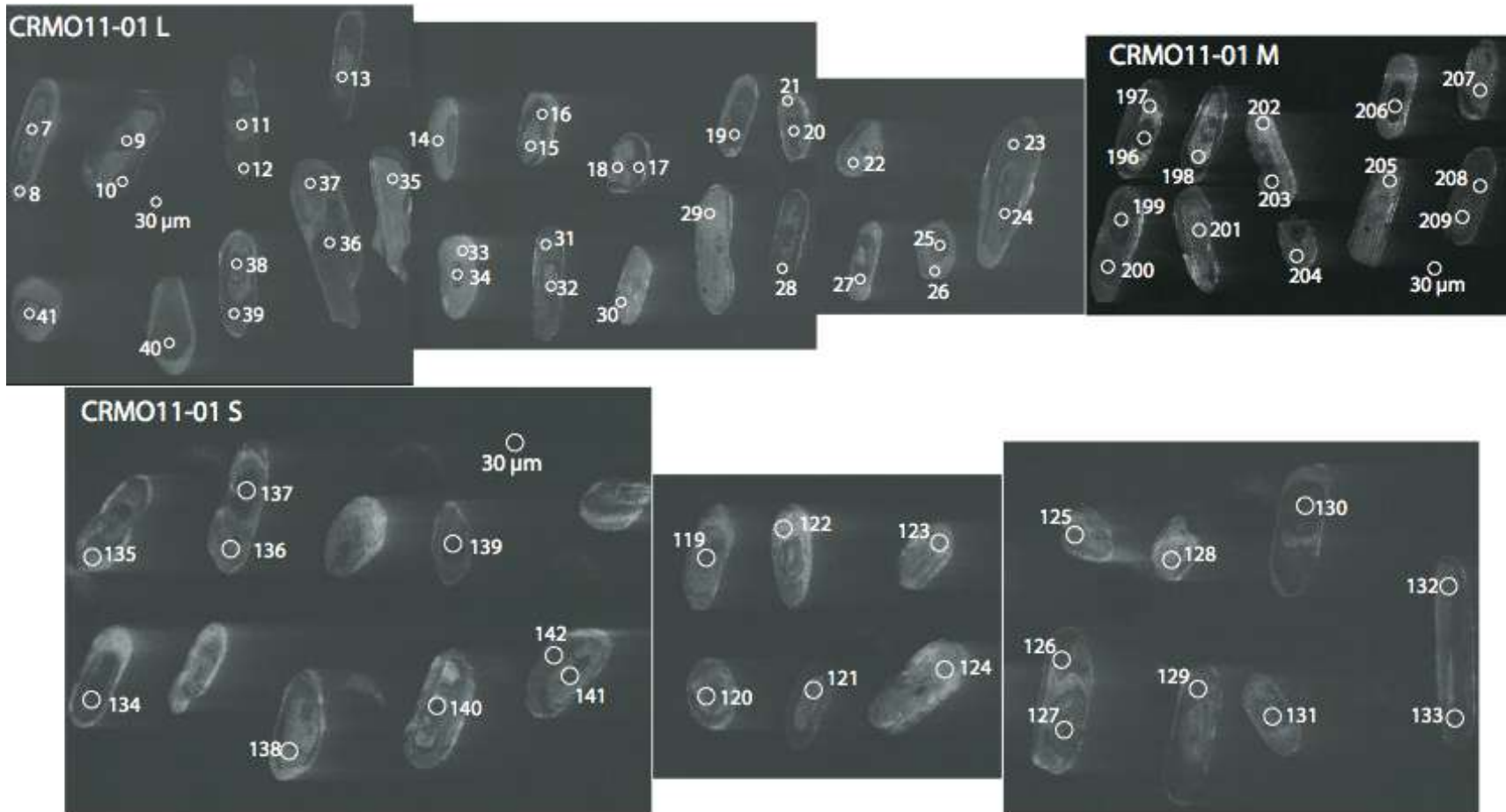


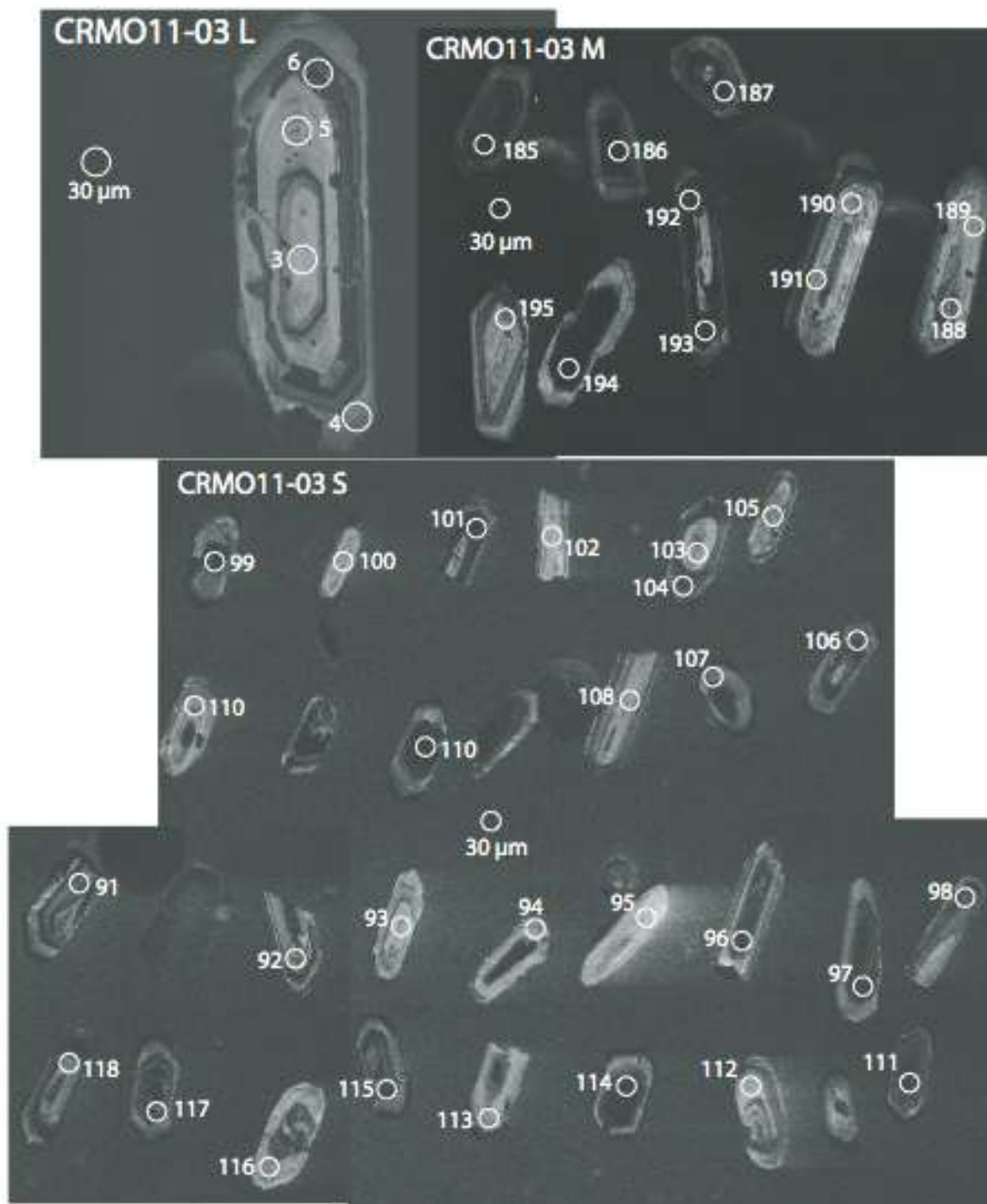


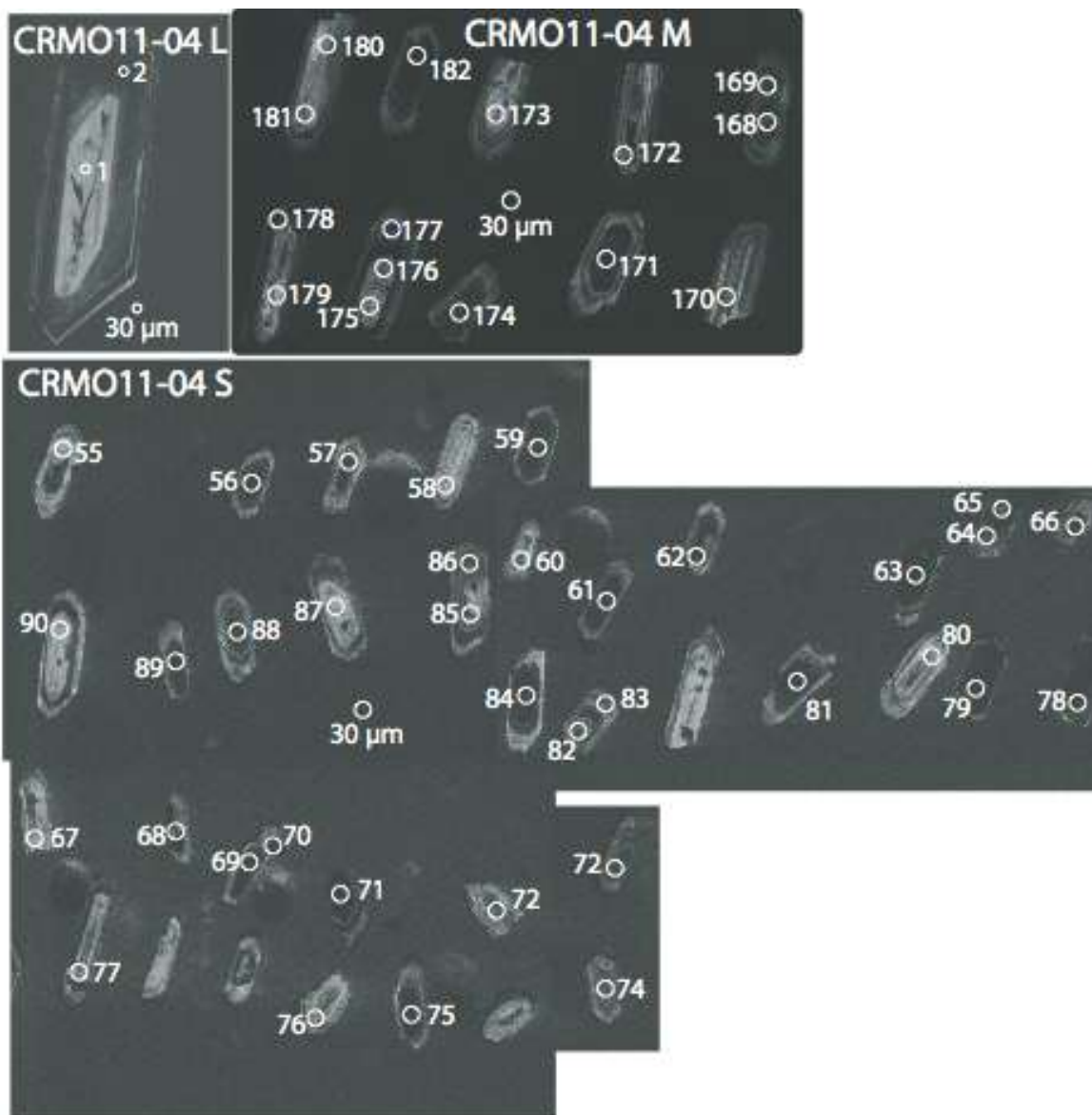


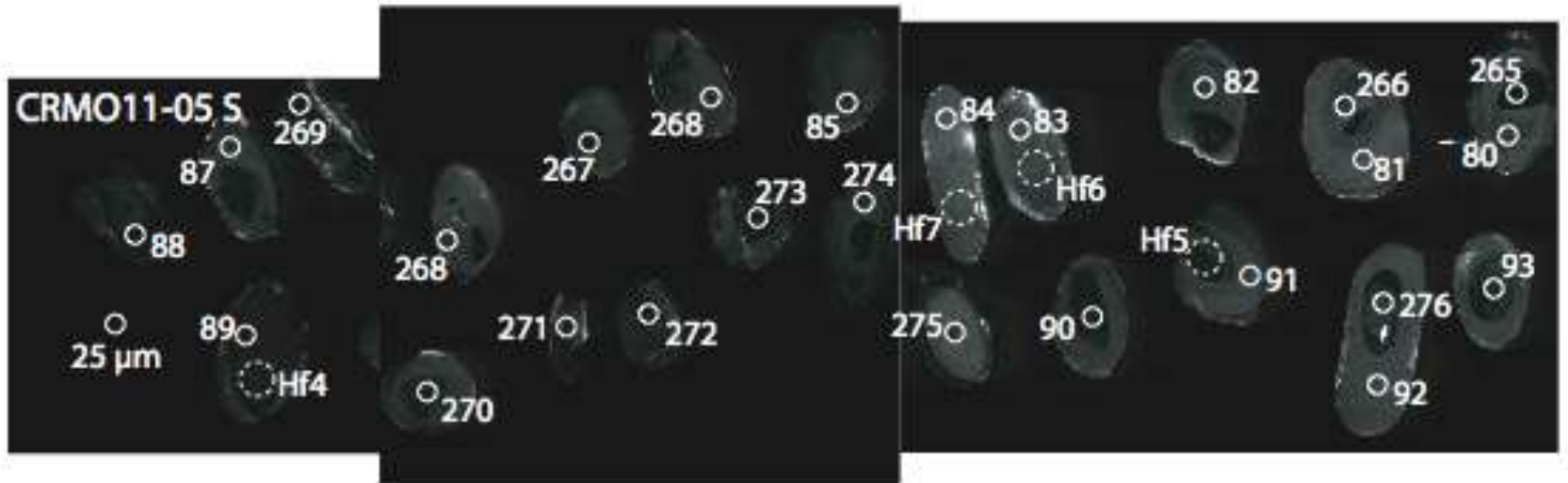
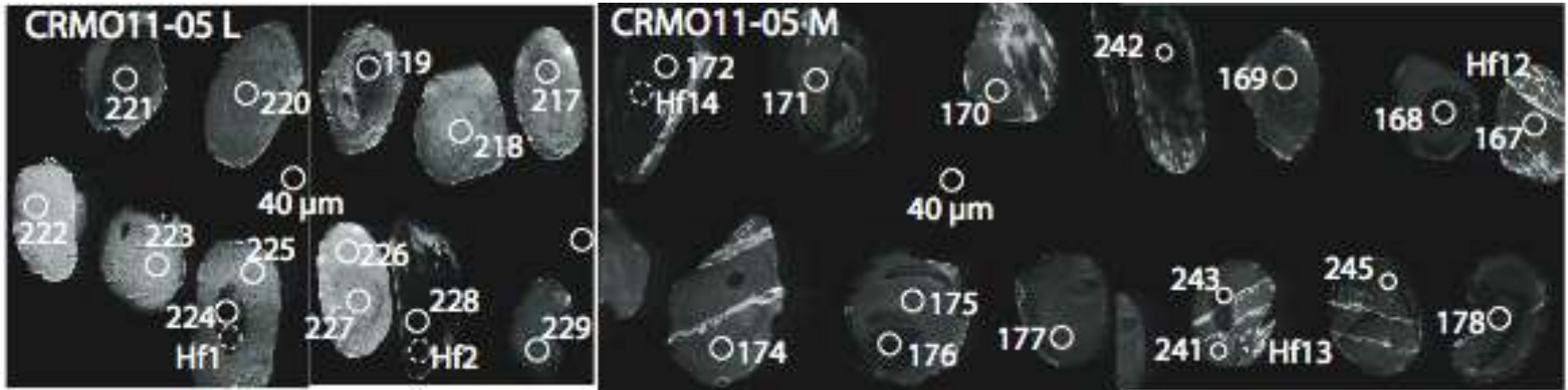


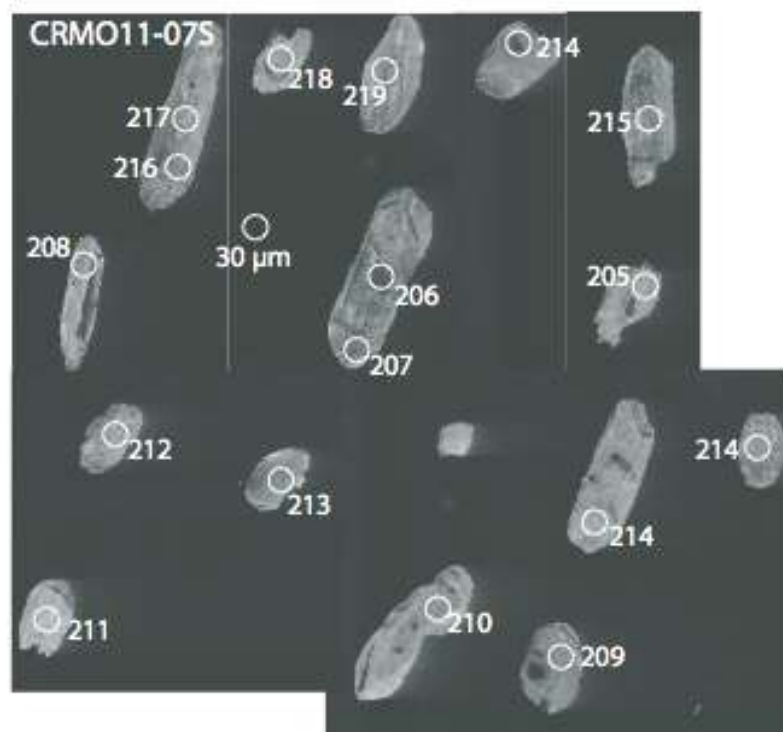
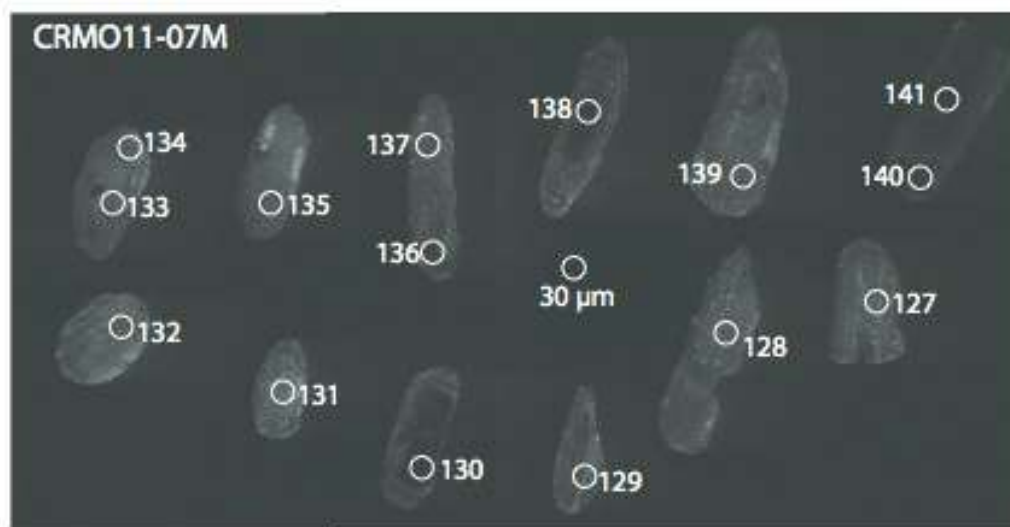
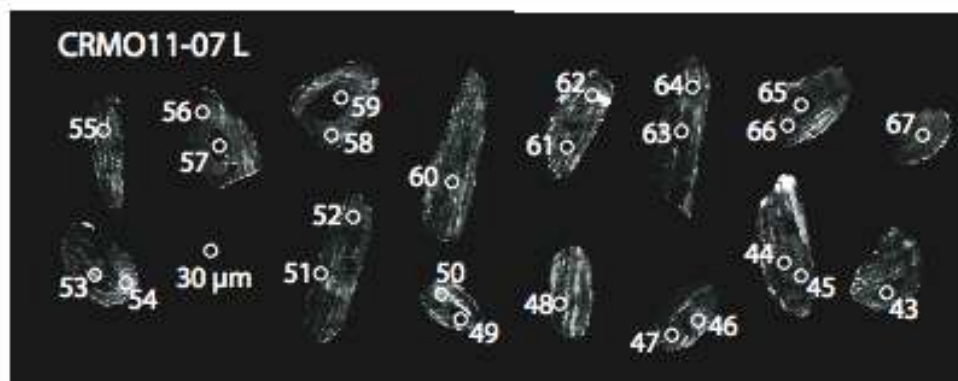
B2: Cathodoluminescence images of zircons from Craters of the Moon samples

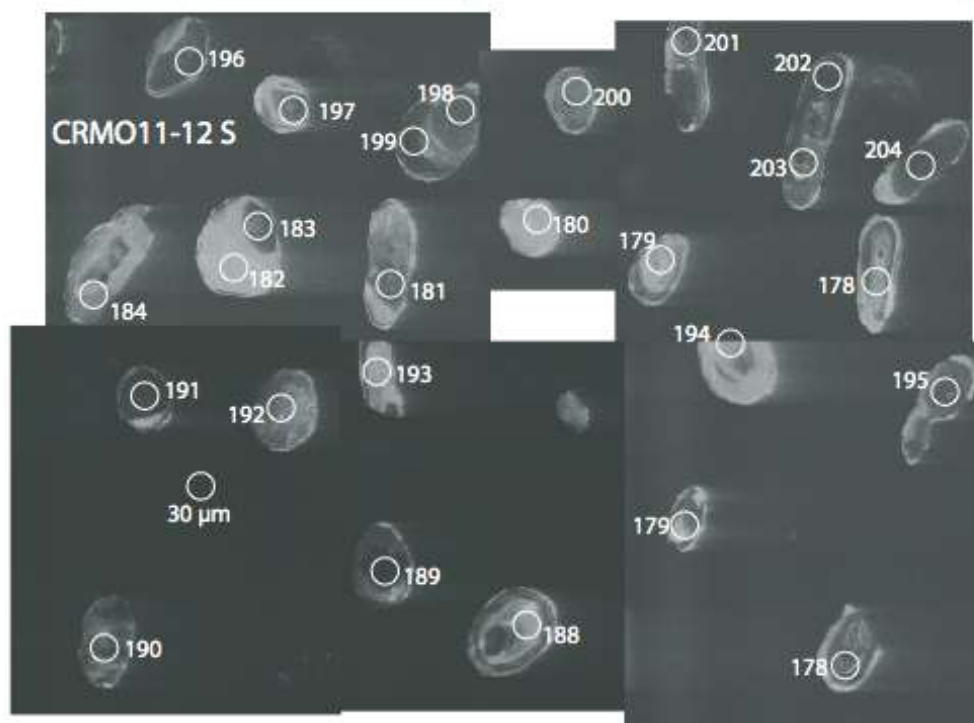
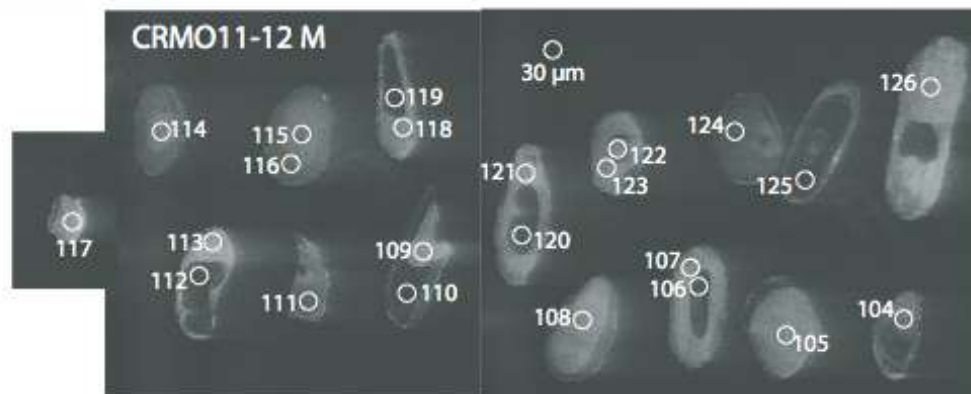
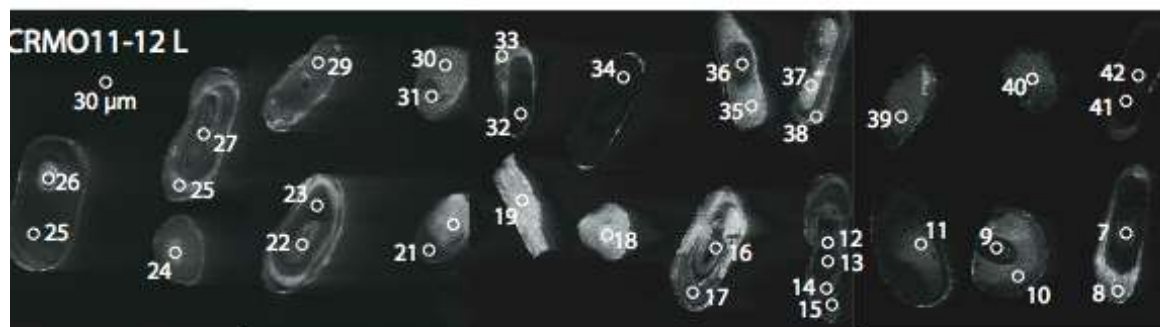


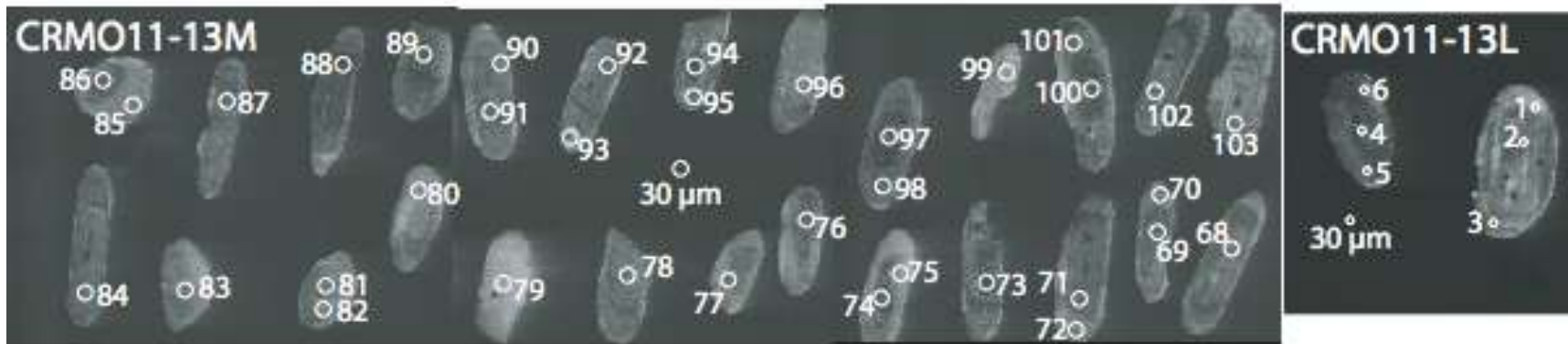


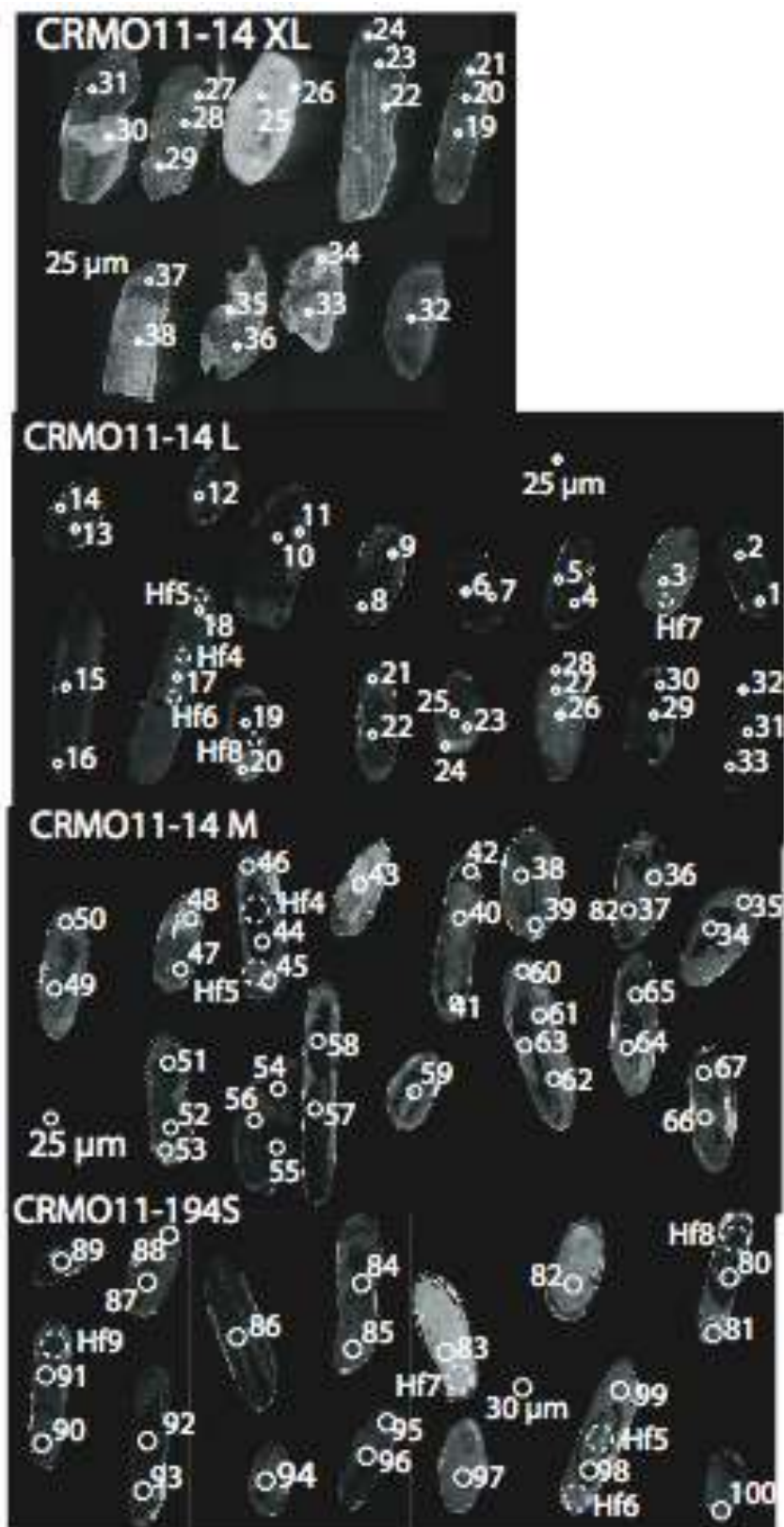


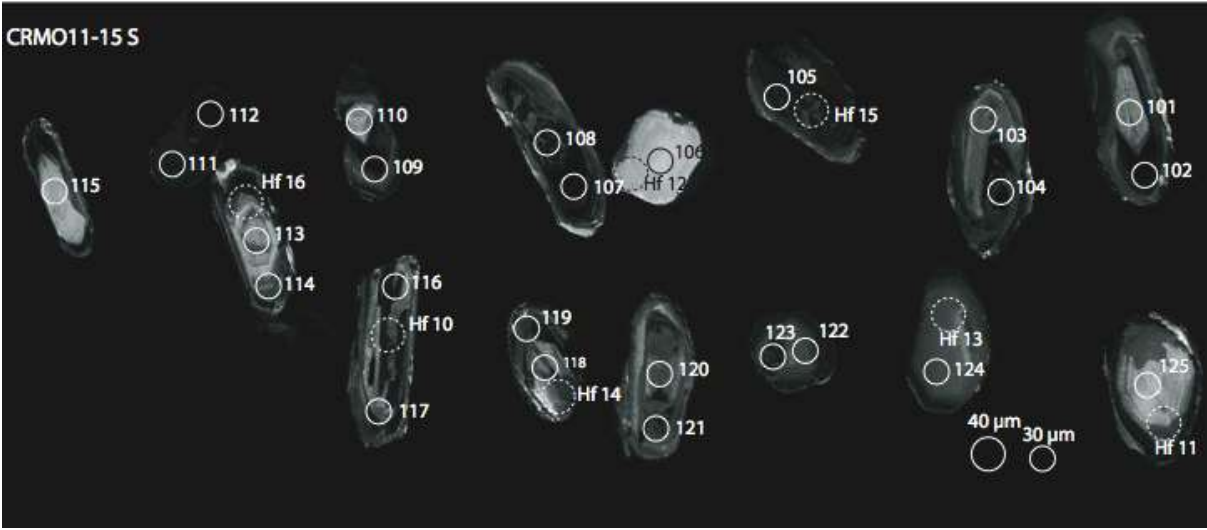
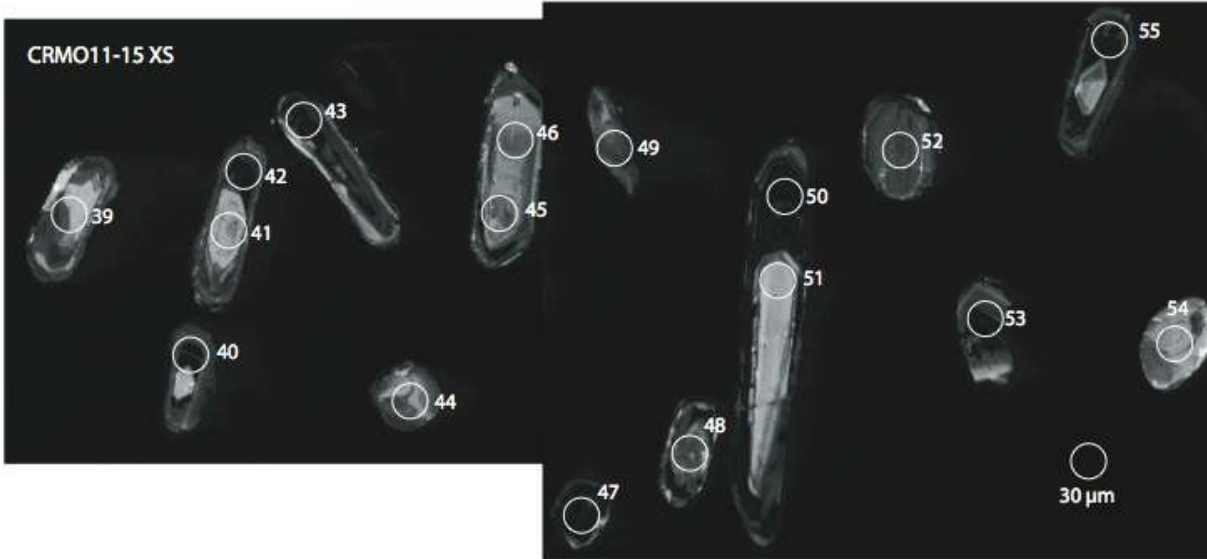


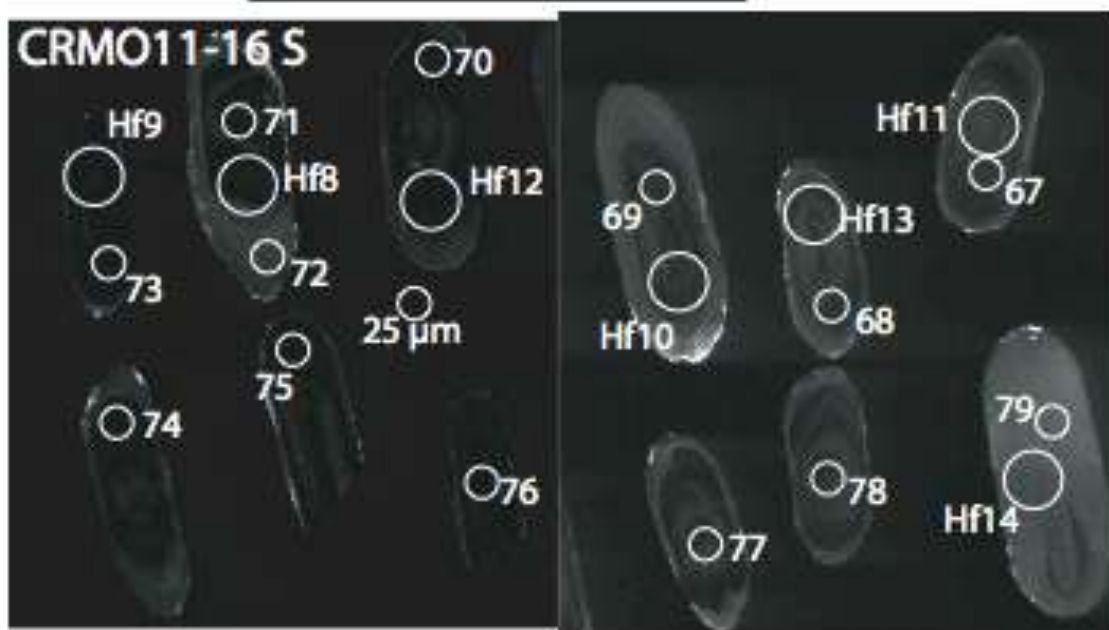
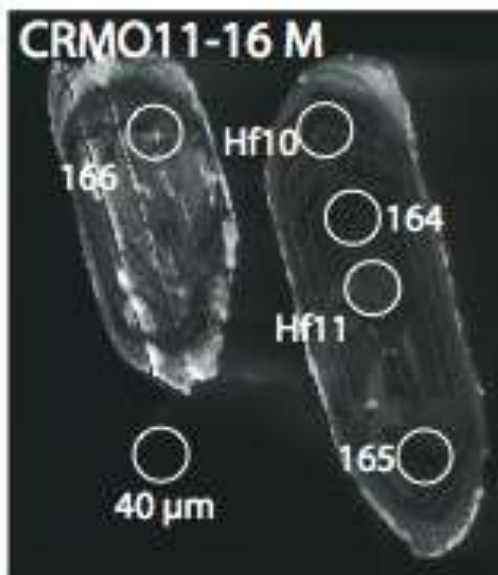




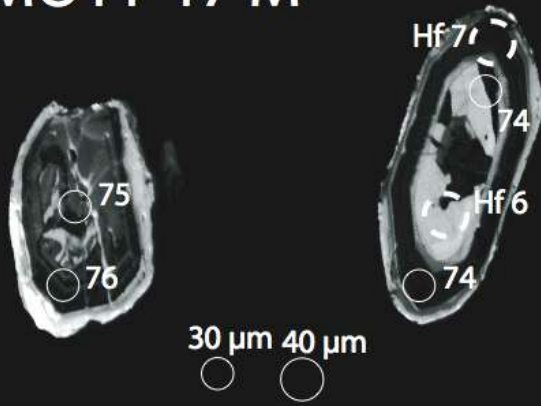




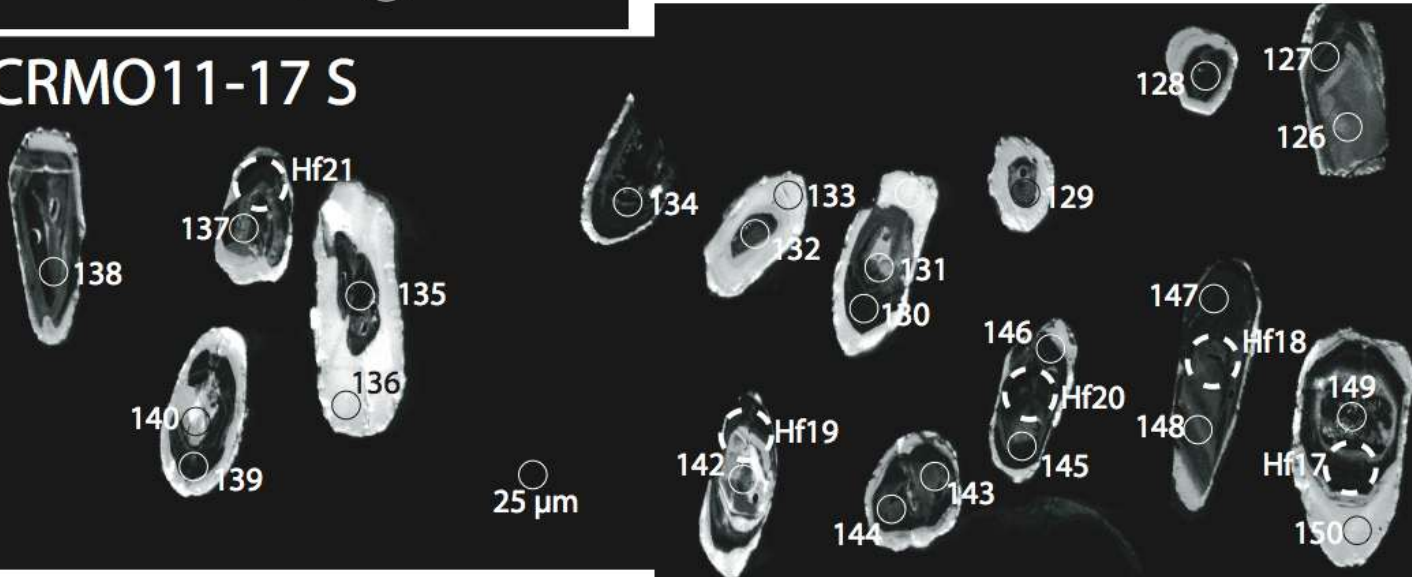


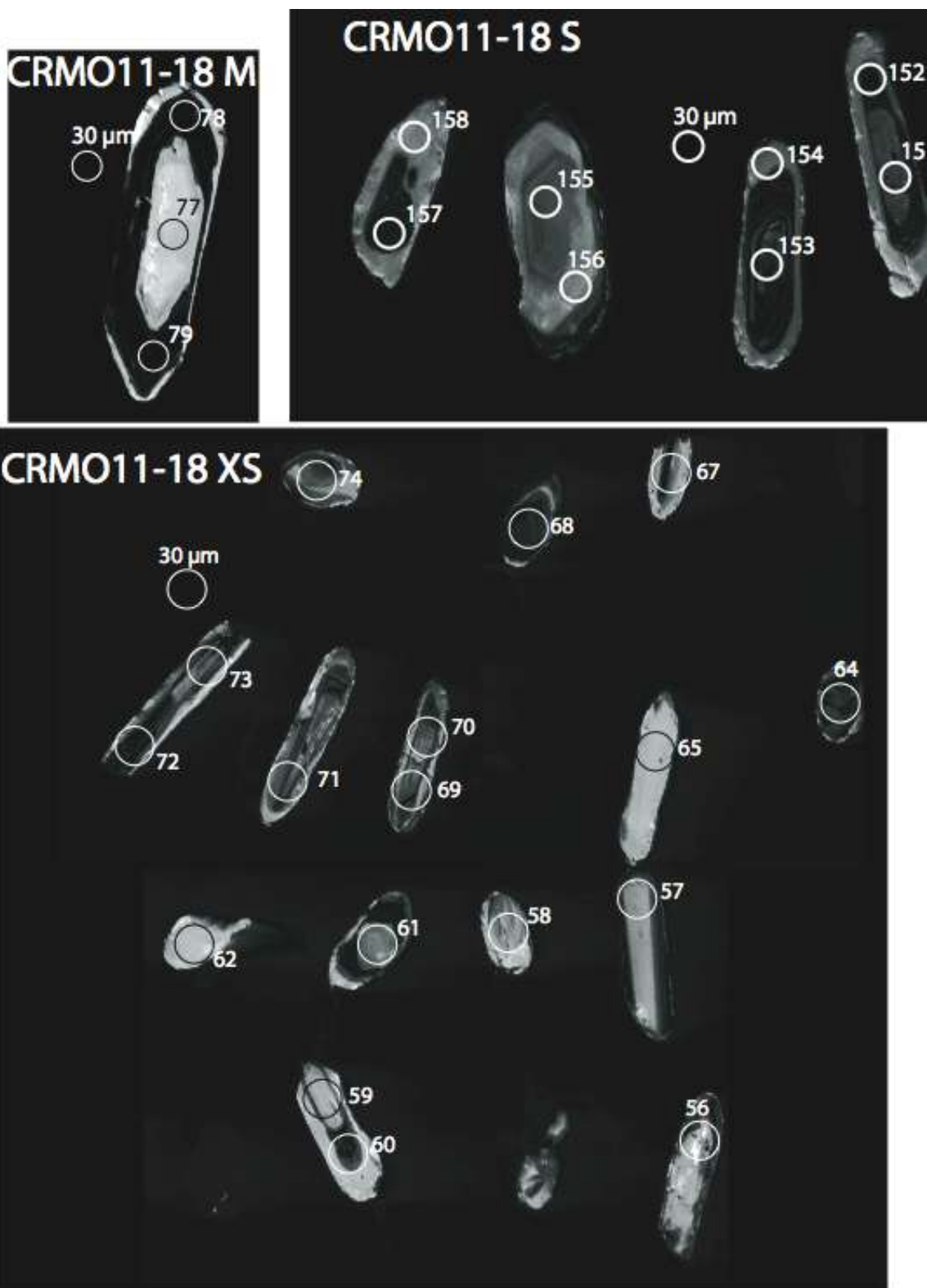


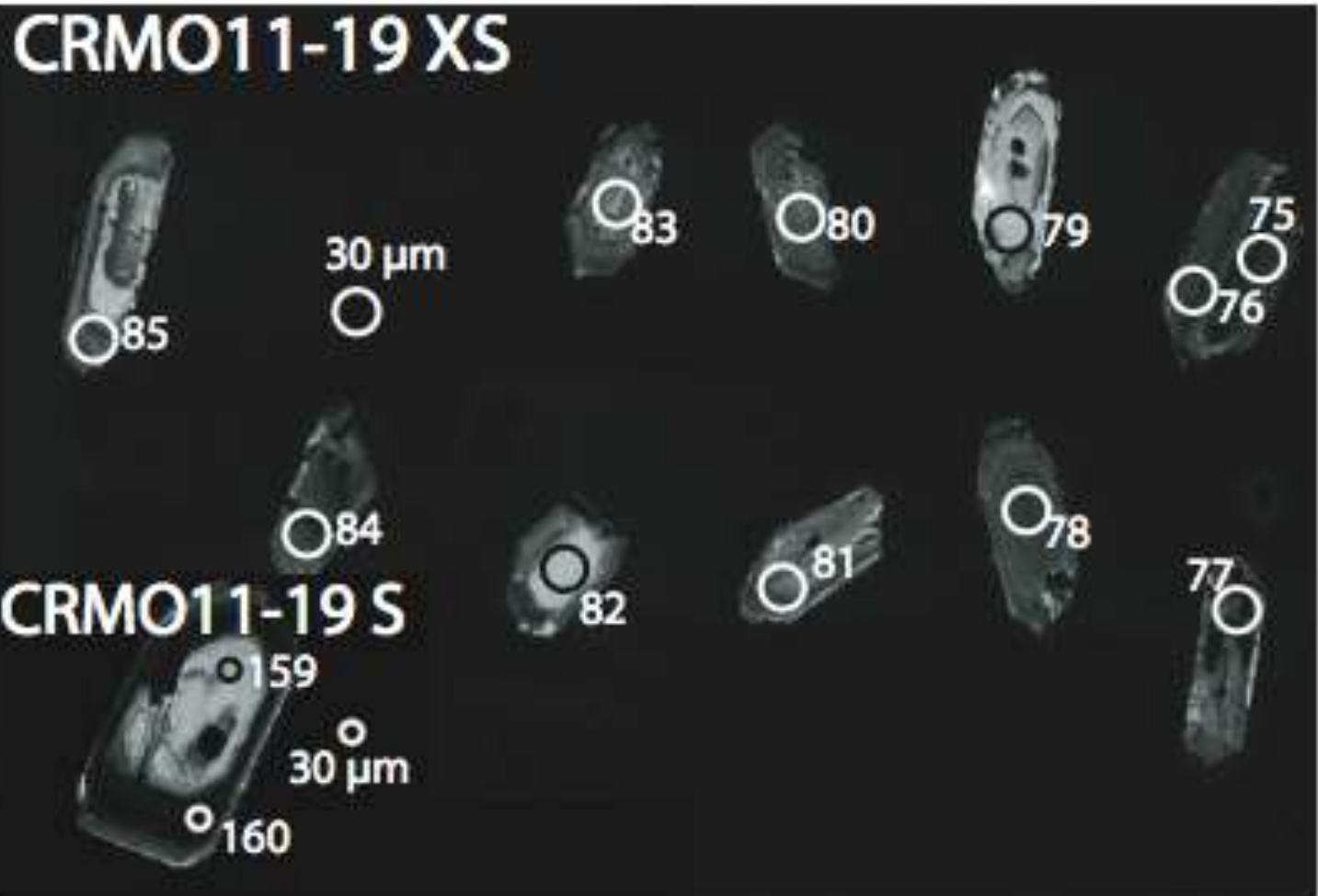
CRMO11-17 M



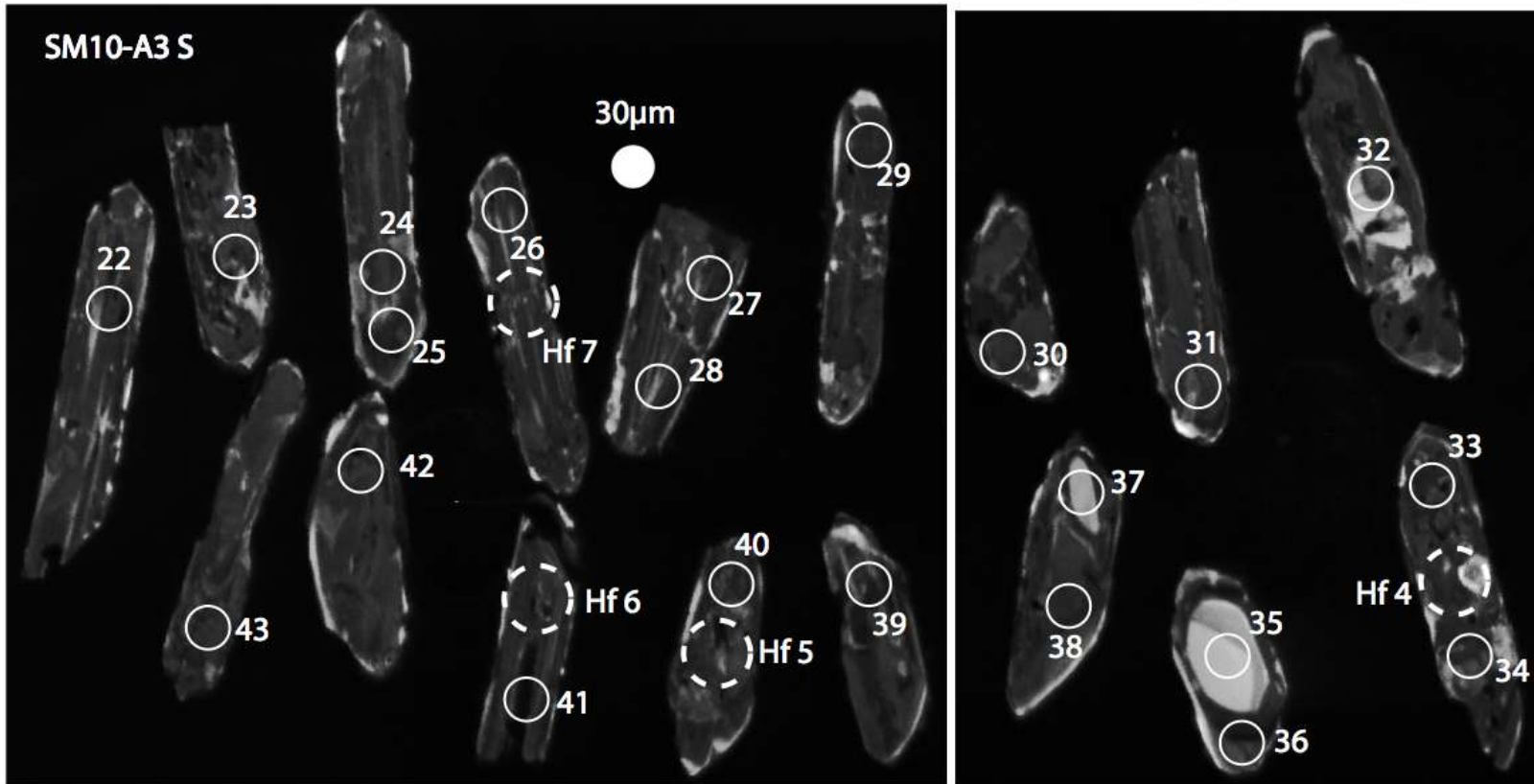
CRMO11-17 S

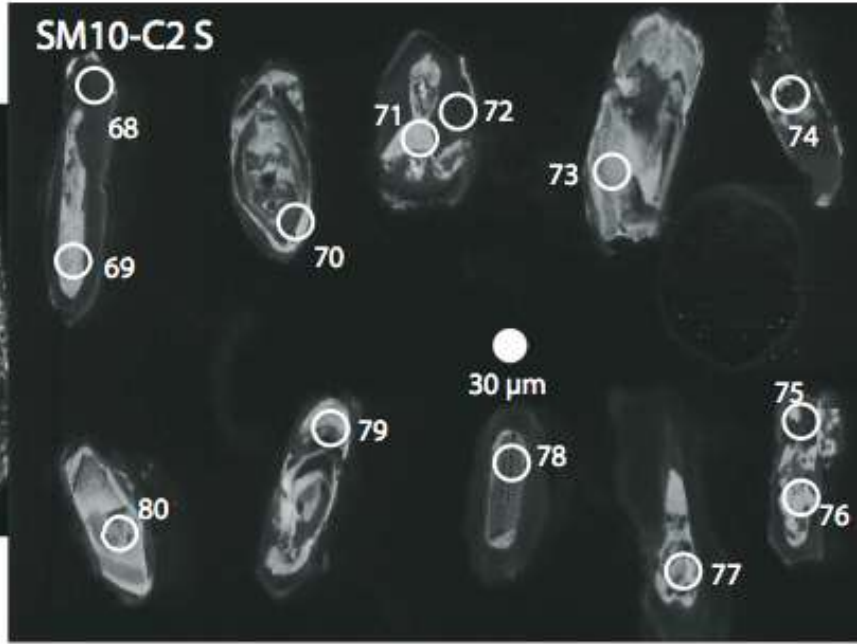
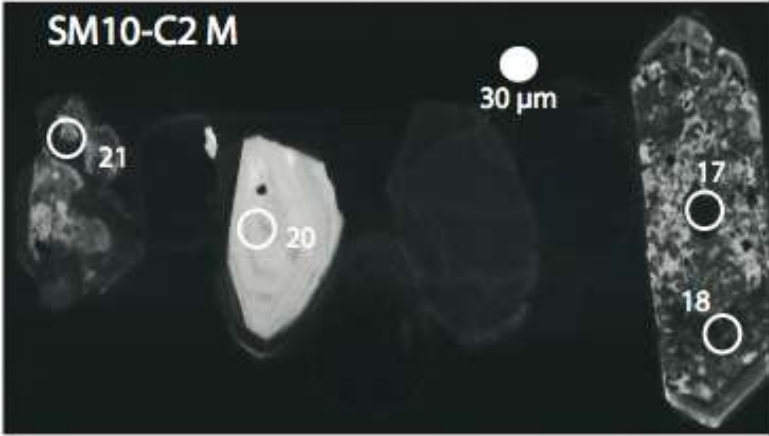


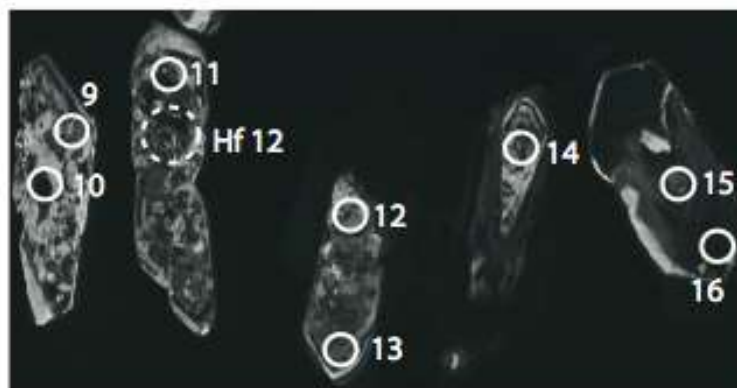
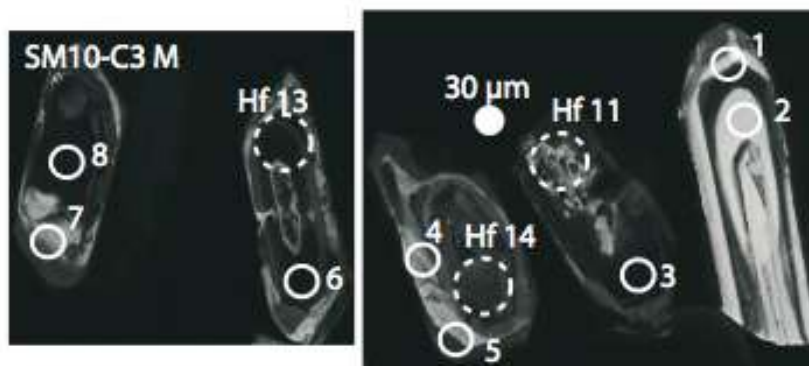
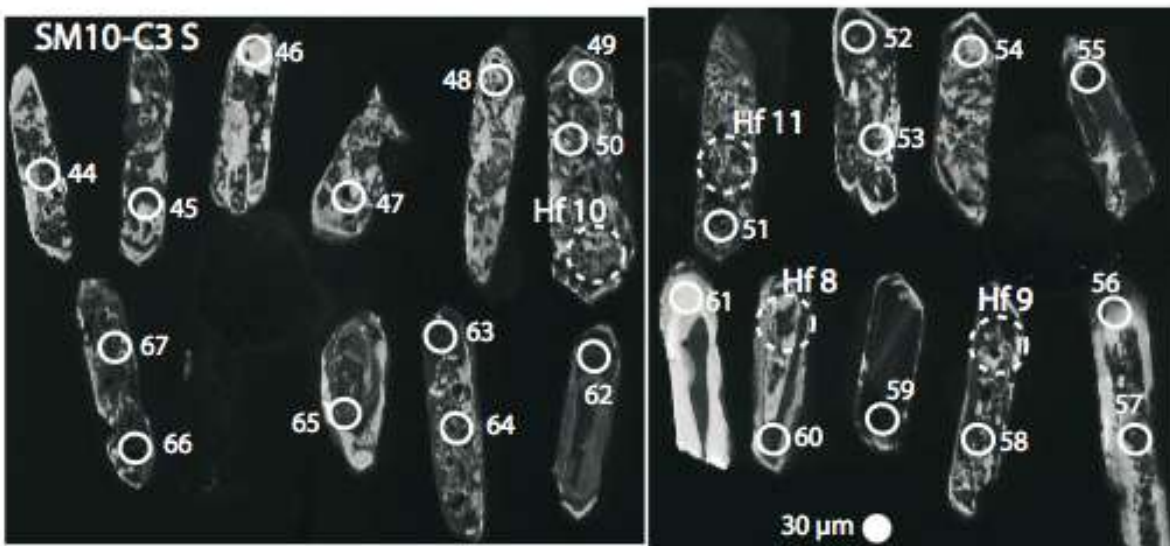


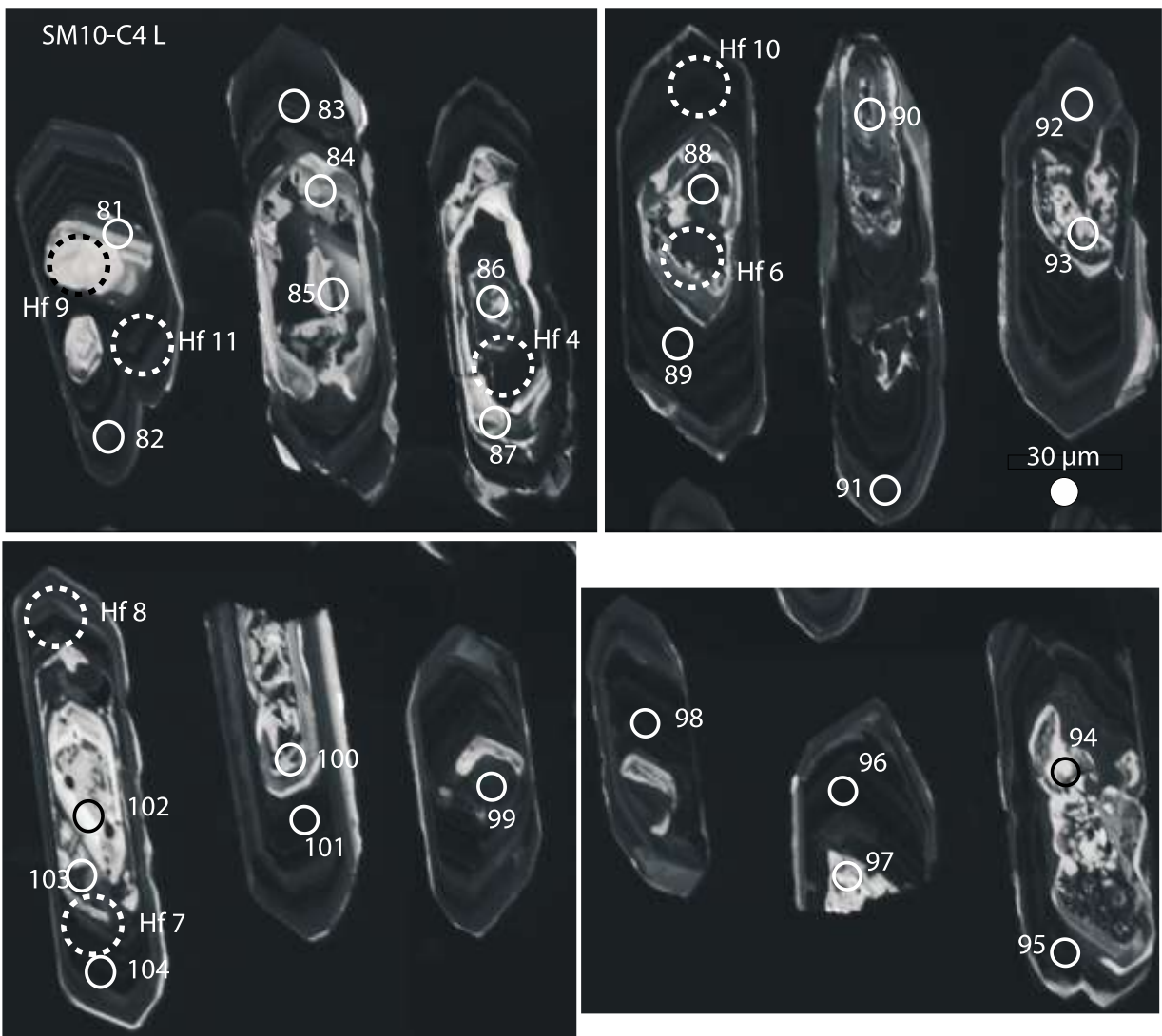


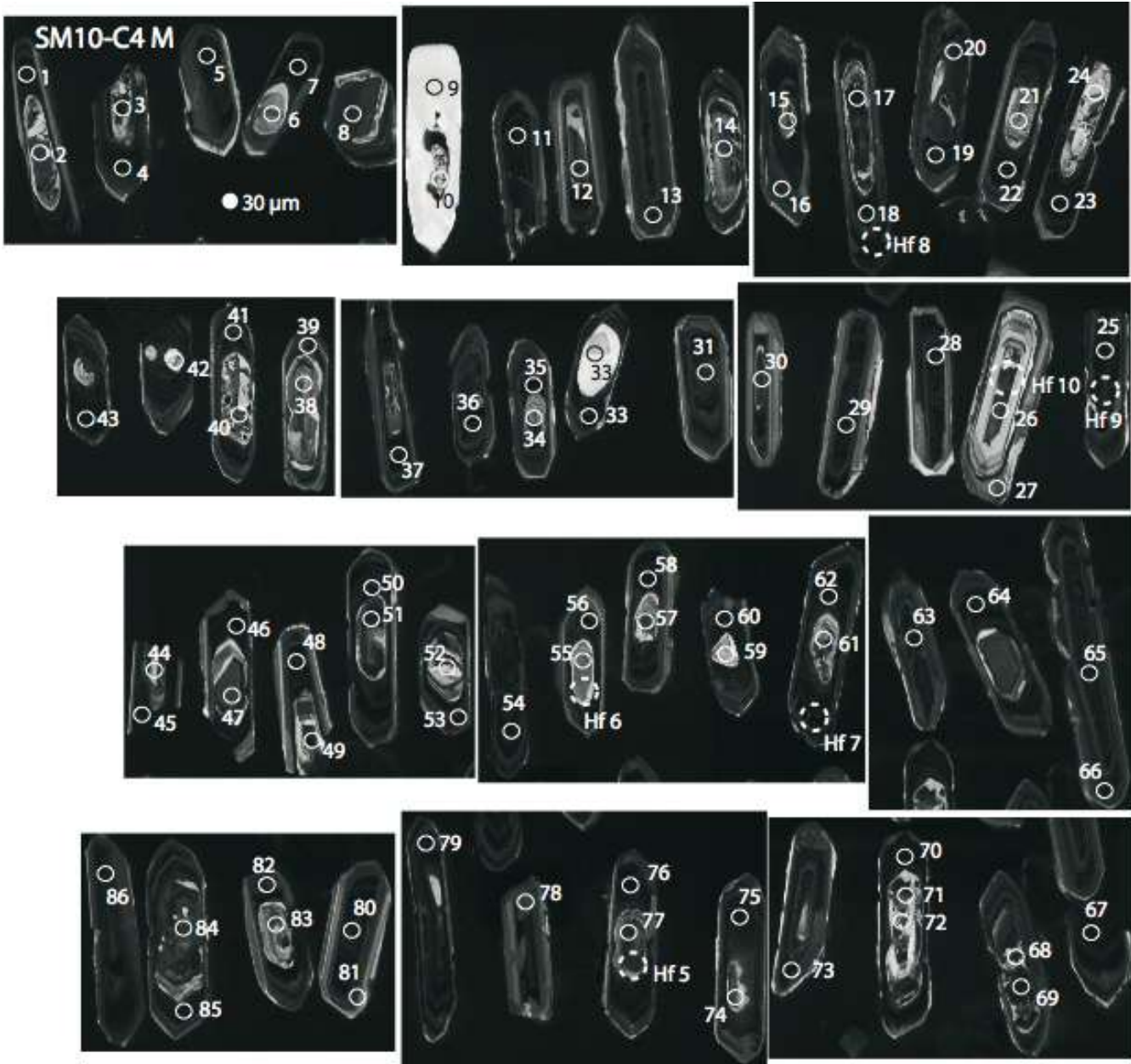
B3: Cathodoluminescence images of zircons from Square Mountain samples

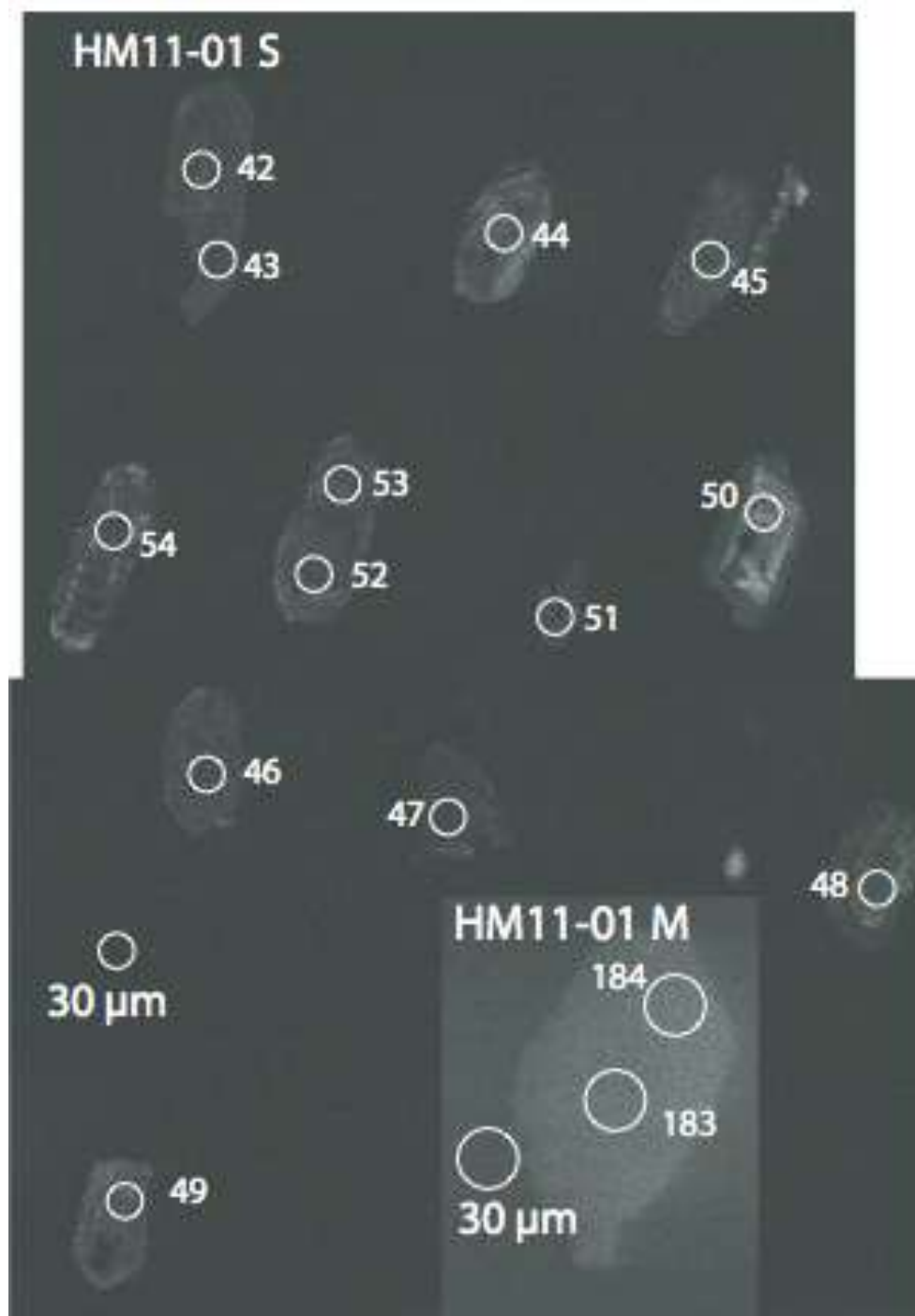


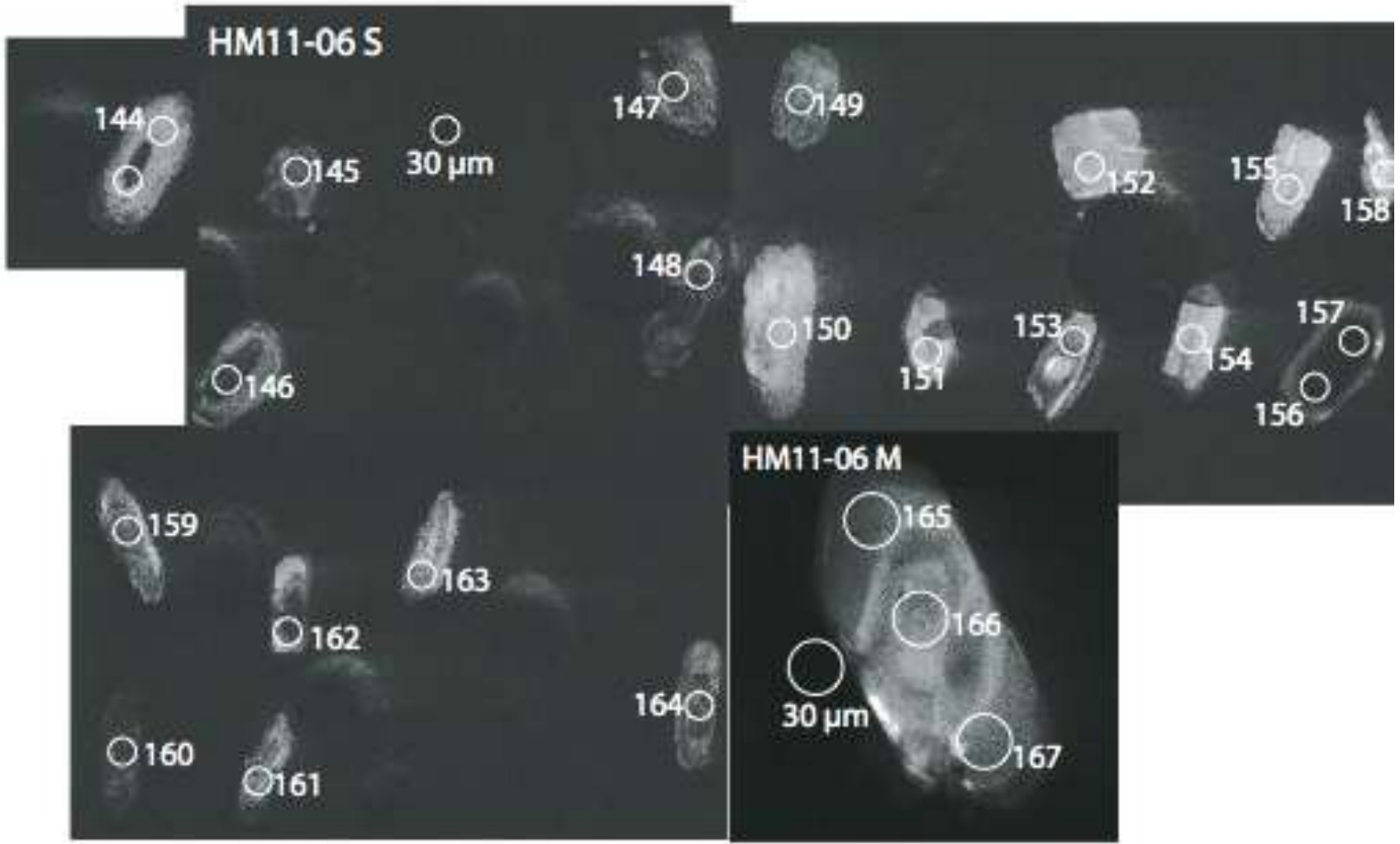








B4: Cathodoluminescence images of zircons from House Mountain samples



APPENDIX C

U/Pb Geochronology

Table C1: Corrected Isotope Ratios and Apparent Ages for Spencer Kilgore

Spots in **bold** were used in the calculation of zircon growth event averages. Spots in **bold and italics** were less than 30% discordant, but were not used to calculate averages because the sample did not have more than 5 spots with discordance less than 30%.

Discordance was not used as a filter on Paleogene dates.

Spot	Corrected Isotope Ratios								Apparent Ages (Ma)						
	U ppm	Th/U ppm	<u>206Pb</u> 204Pb	<u>207Pb*</u> 235U*	$\pm 2s$ (%)	<u>206Pb*</u> 238U	$\pm 2s$ (%)	error corr.	<u>207Pb*</u> 206Pb*	$\pm 2s$ (Ma)	<u>207Pb*</u> 235U	$\pm 2s$ (Ma)	<u>206Pb*</u> 238U*	$\pm 2s$ (Ma)	% disc.
SK11-01															
Paleoarchean															
SK11S-01_36	701	0.02	222369	29.024	2.74	0.5798	2.24	0.82	3763	24	3454	27	2948	53	27
SK11S-01_38	123	1.57	940	34.525	3.57	0.7144	3.00	0.84	3709	30	3625	35	3475	81	8
SK11S-01_46	325	0.95	60470	31.688	2.36	0.6912	2.20	0.93	3629	13	3541	23	3387	58	9
SK11S-01_41	258	0.84	14455	30.873	2.99	0.6748	2.73	0.91	3625	19	3515	29	3324	71	11
SK11-01M_129	384	0.76	40214	30.204	3.66	0.6749	3.10	0.85	3592	30	3493	36	3325	81	9
SK11-01M_143	216	0.56	10533	29.081	4.34	0.6598	3.78	0.87	3568	33	3456	43	3266	97	11
SK11-01L_231	362	0.10	3958	23.723	3.19	0.5403	2.77	0.87	3562	24	3257	31	2785	63	27
SK11-01M_142	185	0.68	3648	29.485	3.80	0.6760	2.66	0.70	3552	42	3470	37	3329	69	8
SK11S-01_30	2754	0.71	910117	23.294	3.54	0.5426	3.20	0.90	3528	23	3239	34	2794	73	26
SK11-01L_230	328	0.71	4339	23.885	4.34	0.5774	4.11	0.95	3470	22	3264	42	2938	97	19
SK11-01M_237	285	0.56	4497	23.430	9.68	0.5710	7.14	0.74	3458	101	3245	94	2912	167	20
SK11S-01_39	453	0.80	16961	22.729	3.75	0.5542	3.48	0.93	3457	21	3215	36	2843	80	22
SK11S-01_32	224	0.79	3274	23.265	3.75	0.5675	2.85	0.76	3456	38	3238	37	2897	67	20
SK11-01L_196	36	0.79	27	0.064	40.80	0.0016	16.31	0.40	3372	584	63	25	11	2	100
SK11-01M_137	435	0.26	19643	15.432	3.18	0.4073	2.37	0.74	3334	33	2842	30	2202	44	40
Mesoarchean 2															
SK11-01M_136	346	0.45	7438	19.152	3.32	0.5198	2.33	0.70	3290	37	3049	32	2698	51	22
SK11-01M_148	398	0.09	279	19.013	24.13	0.5236	18.96	0.79	3267	235	3042	233	2714	420	21
SK11S-01_31	1511	0.14	56460	15.940	2.46	0.4413	2.14	0.87	3259	19	2873	24	2356	42	33
SK11-01M_126A	484	0.53	13121	17.400	5.67	0.4832	5.10	0.90	3254	39	2957	54	2541	107	26
SK11-01L_207	1006	0.61	607985	20.019	5.30	0.5618	4.79	0.90	3237	36	3092	51	2874	111	14
SK11S-01_48	308	0.10	7855	19.243	2.41	0.5416	2.12	0.88	3233	18	3054	23	2790	48	17
SK11-01L_200	58	1.31	2429	22.483	2.70	0.6365	2.32	0.86	3223	22	3205	26	3175	58	2
SK11-01M_145	144	0.57	3938	18.030	5.61	0.5173	4.22	0.75	3202	58	2991	54	2688	93	20
SK11-01M_135	200	0.65	25176	19.553	4.10	0.5627	3.35	0.82	3197	38	3069	40	2878	78	12
SK11-01M_126B	543	0.60	61735	17.471	4.77	0.5038	3.93	0.82	3194	43	2961	46	2630	85	21

Spot	Corrected Isotope Ratios								Apparent Ages (Ma)						
	U ppm	Th/U ppm	<u>206Pb</u> <u>204Pb</u>	<u>207Pb*</u> <u>235U*</u>	$\pm 2s$ (%)	<u>206Pb*</u> <u>238U</u>	$\pm 2s$ (%)	error corr.	<u>207Pb*</u> <u>206Pb*</u>	$\pm 2s$ (Ma)	<u>207Pb*</u> <u>235U</u>	$\pm 2s$ (Ma)	<u>206Pb*</u> <u>238U*</u>	$\pm 2s$ (Ma)	% disc.
SK11-01M_141	581	0.30	6308	16.060	5.73	0.4638	4.63	0.81	3192	53	2880	55	2456	95	28
SK11-01L_203	88	0.67	2937	22.002	3.16	0.6413	2.84	0.90	3177	22	3184	31	3194	71	1
SK11-01L_204	53	0.81	2564	20.967	3.96	0.6140	3.53	0.89	3170	29	3137	38	3086	87	3
SK11-01L_209	64	1.01	1064	20.162	3.01	0.5915	2.61	0.87	3167	24	3099	29	2996	63	7
SK11-01M_139	48	1.44	2201	20.881	4.34	0.6162	3.24	0.75	3158	46	3133	42	3095	80	2
SK11-01M_131	3806	0.07	994828	15.757	4.09	0.4654	3.31	0.81	3156	38	2862	39	2464	68	26
SK11-01S_259	925	0.15	58289	15.617	3.51	0.4680	3.30	0.94	3133	19	2854	34	2475	68	25
SK11-01S_258	453	0.51	6168	15.953	3.36	0.4791	3.00	0.89	3130	24	2874	32	2524	63	23
SK11-01L_208	801	0.45	18682	12.351	3.37	0.3719	2.90	0.86	3126	27	2631	32	2038	51	40
SK11-01M_132	63	1.10	860	19.728	6.42	0.6001	5.31	0.83	3109	57	3078	62	3030	128	3
SK11-01M_235	1003	0.25	8508	14.628	3.89	0.4466	3.37	0.87	3104	31	2791	37	2380	67	28
SK11-01M_128	74	0.67	2914	20.128	2.98	0.6180	2.30	0.77	3095	30	3098	29	3102	57	0
SK11-01M_238	238	0.15	3451	17.179	7.28	0.5311	5.44	0.75	3084	77	2945	70	2746	122	13
SK11-01L_195	113	0.99	6103	18.790	2.20	0.5832	1.94	0.88	3077	17	3031	21	2962	46	5
SK11-01S_252	556	0.35	27367	12.902	5.41	0.4045	4.96	0.92	3061	35	2672	51	2190	92	33
SK11-01M_138	1450	0.13	138837	16.325	3.69	0.5146	3.18	0.86	3053	30	2896	35	2676	70	15
SK11-01L_202B	75	0.70	6677	17.953	4.30	0.5697	3.38	0.79	3042	43	2987	41	2907	79	6
SK11-01L_202A	65	0.70	4070	15.829	4.73	0.5089	3.46	0.73	3021	52	2867	45	2652	75	15
SK11-01M_147	722	0.12	18145	14.123	3.75	0.4596	3.32	0.89	3001	28	2758	36	2438	67	22
SK11-01M_127	708	0.15	10051	14.115	4.55	0.4633	3.62	0.80	2988	44	2757	43	2454	74	21
SK11-01M_149	334	0.09	93	14.482	42.33	0.4828	34.93	0.83	2963	385	2782	402	2539	733	17
SK11-01S_257	1071	0.52	5927	12.727	2.13	0.4297	1.82	0.86	2942	18	2660	20	2304	35	26
SK11-01L_211	298	0.23	13883	14.305	1.31	0.4839	1.00	0.76	2939	14	2770	12	2544	21	16
SK11-01M_146	1226	0.15	17413	13.734	3.42	0.4658	2.80	0.82	2935	32	2732	32	2465	57	19
SK11S-01_44	88	0.51	1909	11.065	3.63	0.3757	3.04	0.84	2933	32	2529	34	2056	54	35
SK11-01L_210	186	0.21	1763	13.947	2.13	0.4754	1.15	0.54	2927	29	2746	20	2507	24	17
SK11S-01_35	708	0.63	4803	11.246	2.09	0.3850	1.34	0.64	2920	26	2544	20	2100	24	33
SK11-01M_125	154	0.77	13487	13.561	4.50	0.4693	4.17	0.93	2902	27	2720	43	2481	86	17
Neoproterozoic															
SK11S-01_29	1150	0.33	25284	13.696	2.49	0.4770	2.02	0.81	2892	24	2729	24	2514	42	16
SK11-01S_254	583	0.23	9481	11.211	3.46	0.3927	3.15	0.91	2882	23	2541	32	2136	57	30
SK11-01M_140	5	1.81	395	2.398	26.88	0.0841	15.18	0.56	2881	360	1242	193	520	76	85
SK11-01M_144	42	2.64	1854	13.129	5.59	0.4698	4.23	0.76	2848	60	2689	53	2483	87	15
SK11-01M_150	23	4.63	2131	14.060	5.07	0.5031	4.24	0.84	2848	45	2754	48	2627	91	9

Spot	Corrected Isotope Ratios								Apparent Ages (Ma)						
	U ppm	Th/U ppm	²⁰⁶ Pb ²⁰⁴ Pb	²⁰⁷ Pb* ²³⁵ U*	±2s (%)	²⁰⁶ Pb* ²³⁸ U	±2s (%)	error corr.	²⁰⁷ Pb* ²⁰⁶ Pb*	±2s (Ma)	²⁰⁷ Pb* ²³⁵ U	±2s (Ma)	²⁰⁶ Pb* ²³⁸ U*	±2s (Ma)	% disc.
SK11S-01_28	331	0.33	4113	12.063	4.22	0.4347	4.11	0.97	2836	16	2609	40	2327	80	21
SK11S-01_49	42	0.66	1899	11.606	4.98	0.4186	3.94	0.79	2835	50	2573	47	2254	75	24
SK11-01L_197	477	0.13	118	0.364	5.73	0.0132	3.81	0.67	2829	70	315	16	84	3	98
SK11S-01_42	52	1.00	1850	7.338	3.91	0.2660	2.45	0.63	2827	50	2153	35	1520	33	52
SK11S-01_33	44	0.43	1232	16.866	3.54	0.6131	2.86	0.81	2822	34	2927	34	3082	70	12
SK11S-01_34	33	0.97	308	14.469	4.03	0.5268	2.55	0.63	2820	51	2781	38	2728	57	4
SK11-01L_206	38	0.70	7210	7.527	5.39	0.2752	4.25	0.79	2813	54	2176	48	1567	59	50
SK11-01M_130	1773	0.11	38776	10.503	4.86	0.3844	4.52	0.93	2811	29	2480	45	2097	81	30
SK11S-01_37	53	0.98	966	12.890	3.32	0.4725	2.66	0.80	2809	33	2672	31	2494	55	13
SK11-01M_236A	32	2.19	237	10.729	7.99	0.3964	4.50	0.56	2796	108	2500	74	2152	82	27
SK11-01L_201	53	0.96	18129	8.631	4.03	0.3218	3.44	0.86	2781	34	2300	37	1799	54	40
SK11S-01_40	370	0.29	12350	9.888	3.51	0.3691	3.17	0.90	2779	24	2424	32	2025	55	32
SK11-01S_255	753	0.18	35150	10.830	2.93	0.4081	2.55	0.87	2763	24	2509	27	2206	48	24
SK11-01S_256	410	0.94	29948	9.602	3.10	0.3622	2.75	0.89	2762	23	2397	28	1993	47	32
SK11-01M_236B	27	2.33	5152	12.474	9.00	0.4707	5.24	0.58	2761	120	2641	85	2486	108	12
SK11S-01_47	55	1.14	1142	11.814	3.99	0.4535	3.11	0.78	2733	41	2590	37	2411	63	14
SK11-01L_205	52	0.57	1267	7.671	4.12	0.2948	3.15	0.76	2731	44	2193	37	1665	46	44
SK11-01M_133	17	5.01	2198	15.380	5.04	0.5912	3.65	0.72	2731	57	2839	48	2994	87	12
SK11-01L_198	23	3.33	942	7.888	5.13	0.3033	3.72	0.73	2730	58	2218	46	1708	56	42
SK11-01M_234	1998	0.11	17387	9.229	5.43	0.3678	4.78	0.88	2671	43	2361	50	2019	83	28
SK11S-01_45	78	0.86	4778	6.660	3.26	0.2684	2.39	0.73	2653	37	2067	29	1532	33	47
SK11-01S_253	95	1.45	453	8.586	5.69	0.3500	3.81	0.67	2634	70	2295	52	1935	64	31
SK11S-01_43A	80	0.22	50	0.295	23.83	0.0123	9.66	0.41	2600	363	262	55	79	8	98
SK11S-01_43B	76	0.21	28	0.347	15.23	0.0147	6.92	0.45	2568	227	303	40	94	6	97
SK11-01L_199	34	2.53	729	6.443	3.60	0.2732	2.12	0.59	2568	49	2038	32	1557	29	44

Spot number	Corrected Isotope Ratios								Apparent Ages (Ma)						
	U ppm	Th/U	²⁰⁶ Pb ²⁰⁴ Pb	²⁰⁷ Pb* ²³⁵ U*	±2s (%)	²⁰⁶ Pb* ²³⁸ U	±2s (%)	error corr.	²⁰⁷ Pb* ²⁰⁶ Pb*	±2s (Ma)	²⁰⁷ Pb* ²³⁵ U	±2s (Ma)	²⁰⁶ Pb* ²³⁸ U*	±2s (Ma)	% disc.
SK11-02 Mesoarchean 1															
SK11-02M_240	45	0.94	366	20.801	8.64	0.5482	7.26	0.84	3336	73	3129	84	2818	166	19
SK11S-02_57	76	2.22	2053	21.607	4.57	0.5883	3.66	0.80	3285	43	3166	44	2982	87	11

Spot	Corrected Isotope Ratios								Apparent Ages (Ma)						
	U ppm	Th/U ppm	<u>206Pb</u> <u>204Pb</u>	<u>207Pb*</u> <u>235U*</u>	$\pm 2s$ (%)	<u>206Pb*</u> <u>238U</u>	$\pm 2s$ (%)	error corr.	<u>207Pb*</u> <u>206Pb*</u>	$\pm 2s$ (Ma)	<u>207Pb*</u> <u>235U</u>	$\pm 2s$ (Ma)	<u>206Pb*</u> <u>238U*</u>	$\pm 2s$ (Ma)	% disc.
SK11S-02_50	415	0.31	129248	22.505	1.97	0.6161	1.71	0.87	3276	15	3206	19	3094	42	7
SK11-02M_163	68	0.99	3832	22.607	4.24	0.6246	3.58	0.84	3262	36	3210	41	3128	89	5
SK11S-02_58	87	0.87	1085	21.873	2.06	0.6047	1.49	0.72	3261	22	3178	20	3049	36	8
SK11-02M_151	809	0.36	40943	22.003	4.29	0.6088	3.67	0.86	3260	35	3184	42	3065	89	7
SK11-02S_264	218	0.13	2905	20.889	3.95	0.5803	3.24	0.82	3253	36	3133	38	2950	77	12
SK11-02M_153	531	0.45	30585	22.230	3.90	0.6212	3.21	0.82	3244	35	3194	38	3115	79	5
SK11-02M_152	123	1.04	1280	22.243	2.70	0.6257	2.01	0.74	3233	29	3194	26	3133	50	4
SK11-02M_154	47	1.86	5054	22.993	3.58	0.6477	2.73	0.76	3231	37	3227	35	3219	69	0
SK11-02S_260	181	0.11	5649	20.305	5.33	0.5725	4.69	0.88	3230	40	3106	52	2918	110	12
SK11-02M_157	696	0.36	57934	20.265	5.92	0.5750	4.92	0.83	3220	52	3104	57	2928	116	11
SK11S-02_64	83	2.37	2048	20.961	3.27	0.5963	2.94	0.90	3216	23	3137	32	3015	71	8
SK11S-02_62	260	1.04	8416	18.868	2.92	0.5383	2.25	0.77	3211	29	3035	28	2776	51	17
SK11-02M_241	494	0.09	31214	15.367	7.35	0.4413	5.76	0.78	3201	72	2838	70	2357	114	31
SK11S-02_65	491	0.37	344422	18.868	2.72	0.5455	2.31	0.85	3190	23	3035	26	2806	53	15
SK11S-02_56	355	0.24	4570	16.802	3.23	0.4905	2.62	0.81	3175	30	2924	31	2573	56	23
SK11S-02_52	184	1.54	7435	18.725	4.19	0.5504	3.07	0.73	3164	45	3028	40	2827	70	13
SK11-02L_213	56	1.35	3462	18.704	2.51	0.5527	1.83	0.73	3156	27	3027	24	2836	42	12
SK11-02L_212A	181	2.30	113605	18.175	2.44	0.5386	2.18	0.89	3151	17	2999	23	2778	49	15
SK11S-02_54	364	0.62	4832	18.308	1.95	0.5426	1.50	0.77	3151	20	3006	19	2794	34	14
SK11S-02_56	399	0.43	231177	18.025	4.89	0.5344	4.12	0.84	3150	42	2991	47	2760	92	15
SK11-02M_155	38	1.54	58010	19.484	3.51	0.5816	2.88	0.82	3140	32	3066	34	2955	68	7
SK11-02M_162	155	1.88	10307	19.798	6.50	0.6000	6.03	0.93	3115	38	3082	63	3030	146	3
SK11-02L_212B	64	2.41	18649	21.759	2.49	0.6622	1.94	0.78	3109	25	3173	24	3276	50	7
SK11-02M_156A	154	0.43	6632	18.438	10.65	0.5622	9.56	0.90	3106	75	3013	103	2876	222	9
SK11-02M_158	460	0.20	43881	15.971	5.34	0.4890	5.02	0.94	3099	29	2875	51	2566	106	21
SK11-02L_215	171	0.53	5749	15.724	5.44	0.4846	5.19	0.95	3089	26	2860	52	2547	109	21
SK11S-02_53	396	0.59	5755	16.743	2.24	0.5160	1.66	0.74	3089	24	2920	21	2682	37	16
SK11-02L_214	181	0.56	16144	15.515	1.66	0.4915	1.32	0.80	3045	16	2847	16	2577	28	19
SK11-02M_160	1088	0.16	25635	15.796	3.73	0.5029	3.26	0.87	3037	29	2865	36	2626	70	16
SK11-02S_261	4592	0.04	206519	15.397	2.82	0.4947	2.64	0.94	3022	16	2840	27	2591	56	17
SK11-02S_263	1320	0.03	43716	13.387	2.75	0.4347	2.57	0.94	3005	15	2707	26	2327	50	27
SK11-02M_156B	54	2.09	106820	18.016	5.48	0.5860	3.36	0.61	3002	70	2991	53	2973	80	1
Neoproterozoic															
SK11S-02_61	47	0.88	942	14.016	2.79	0.4999	1.86	0.67	2853	34	2751	26	2613	40	10

Spot	Corrected Isotope Ratios								Apparent Ages (Ma)						
	U ppm	Th/U ppm	<u>206Pb</u> <u>204Pb</u>	<u>207Pb*</u> <u>235U*</u>	$\pm 2s$ (%)	<u>206Pb*</u> <u>238U</u>	$\pm 2s$ (%)	error corr.	<u>207Pb*</u> <u>206Pb*</u>	$\pm 2s$ (Ma)	<u>207Pb*</u> <u>235U</u>	$\pm 2s$ (Ma)	<u>206Pb*</u> <u>238U*</u>	$\pm 2s$ (Ma)	% disc.
SK11S-02_66	92	1.11	1908	14.112	2.16	0.5147	1.57	0.73	2817	24	2757	21	2677	34	6
SK11-02M_239	89	0.82	1357	12.556	5.42	0.4607	4.18	0.77	2807	56	2647	51	2443	85	16
SK11S-02_55	111	1.00	6212	13.386	2.03	0.4925	1.45	0.72	2803	23	2707	19	2581	31	10
SK11S-02_63	113	0.57	2237	13.121	2.35	0.4849	1.79	0.76	2795	25	2688	22	2548	38	11
<i>SK11S-02_51</i>	<i>47</i>	<i>0.69</i>	<i>821</i>	<i>11.098</i>	<i>3.04</i>	<i>0.4176</i>	<i>2.33</i>	<i>0.77</i>	<i>2765</i>	<i>32</i>	<i>2531</i>	<i>28</i>	<i>2250</i>	<i>44</i>	<i>22</i>
<i>SK11-02M_161</i>	<i>83</i>	<i>1.01</i>	<i>3688</i>	<i>12.647</i>	<i>4.33</i>	<i>0.4762</i>	<i>3.52</i>	<i>0.81</i>	<i>2764</i>	<i>41</i>	<i>2654</i>	<i>41</i>	<i>2511</i>	<i>73</i>	<i>11</i>
<i>SK11-02L_216</i>	<i>60</i>	<i>0.90</i>	<i>5390</i>	<i>13.386</i>	<i>2.50</i>	<i>0.5047</i>	<i>1.93</i>	<i>0.77</i>	<i>2763</i>	<i>26</i>	<i>2707</i>	<i>24</i>	<i>2634</i>	<i>42</i>	<i>6</i>
<i>SK11S-02_60</i>	<i>45</i>	<i>0.62</i>	<i>552</i>	<i>13.228</i>	<i>3.49</i>	<i>0.5000</i>	<i>2.11</i>	<i>0.60</i>	<i>2758</i>	<i>46</i>	<i>2696</i>	<i>33</i>	<i>2614</i>	<i>45</i>	<i>6</i>
SK11-02M_159	179	0.92	148266	13.765	6.31	0.5258	5.54	0.88	2741	50	2734	60	2724	123	1
SK11S-02_59	122	0.53	5748	8.474	3.50	0.3435	1.75	0.50	2643	50	2283	32	1903	29	32

Spot number	Corrected Isotope Ratios								Apparent Ages (Ma)						
	U ppm	Th/U	<u>206Pb</u> <u>204Pb</u>	<u>207Pb*</u> <u>235U*</u>	$\pm 2s$ (%)	<u>206Pb*</u> <u>238U</u>	$\pm 2s$ (%)	error corr.	<u>207Pb*</u> <u>206Pb*</u>	$\pm 2s$ (Ma)	<u>207Pb*</u> <u>235U</u>	$\pm 2s$ (Ma)	<u>206Pb*</u> <u>238U*</u>	$\pm 2s$ (Ma)	% disc.
SK11-03															
Mesoarchean 1															
SK11-03M_121	57	1.58	3157	18.516	3.77	0.4912	3.19	0.84	3326	32	3017	36	2576	68	27
SK11S-03_02	59	1.59	1968	24.401	2.97	0.6519	2.61	0.88	3315	22	3285	29	3236	66	3
SK11-03S_246	37	1.62	403	24.310	4.54	0.6599	3.59	0.79	3289	44	3281	44	3267	92	1
SK11-03M_104	58	1.53	3395	24.990	4.22	0.6801	3.18	0.75	3286	43	3308	41	3345	83	2
SK11S-03_19	71	1.83	1324	22.235	2.84	0.6059	2.28	0.80	3283	27	3194	28	3054	55	9
SK11-03M_102	77	1.73	6465	22.515	4.07	0.6174	2.97	0.73	3274	44	3206	40	3100	73	7
SK11S-03_24	95	2.13	3664	20.354	2.80	0.5602	2.59	0.92	3268	17	3108	27	2867	60	15
SK11-03M_115B	53	1.86	439	20.251	5.39	0.5580	4.15	0.77	3266	54	3103	52	2859	96	15
SK11S-03_06	82	1.96	2178	22.086	2.07	0.6093	1.62	0.78	3264	20	3188	20	3067	40	8
SK11S-03_10	86	1.89	1870	22.214	2.51	0.6154	2.14	0.85	3257	21	3193	24	3092	52	6
SK11S-03_23	76	1.90	4528	23.004	2.32	0.6378	1.90	0.82	3256	21	3227	23	3180	48	3
SK11S-03_17	91	2.31	2764	23.227	2.40	0.6449	1.91	0.80	3254	23	3237	23	3208	48	2
SK11-03M_100	97	1.69	1997	22.677	5.47	0.6307	4.39	0.80	3251	51	3213	53	3152	109	4
SK11S-03_15	85	2.00	14239	22.315	1.89	0.6209	1.43	0.76	3251	19	3198	18	3114	35	5
SK11S-03_20	82	2.26	2132	18.436	2.38	0.5130	2.08	0.87	3251	18	3013	23	2669	46	22
SK11S-03_25	100	2.26	5073	21.736	2.02	0.6054	1.69	0.84	3249	17	3172	20	3052	41	8

Spot	Corrected Isotope Ratios								Apparent Ages (Ma)						
	U ppm	Th/U ppm	<u>206Pb</u> 204Pb	<u>207Pb*</u> 235U*	±2s (%)	<u>206Pb*</u> 238U	±2s (%)	error corr.	<u>207Pb*</u> 206Pb*	±2s (Ma)	<u>207Pb*</u> 235U	±2s (Ma)	<u>206Pb*</u> 238U*	±2s (Ma)	% disc.
SK11-03M_103	98	1.81	2815	22.239	3.61	0.6197	2.76	0.76	3248	37	3194	35	3109	68	5
SK11-03M_95A	91	1.61	1382	20.202	4.58	0.5634	4.07	0.89	3247	33	3101	44	2880	95	14
SK11-03M_233	153	0.11	10872	21.063	7.04	0.5883	6.18	0.88	3245	53	3141	68	2983	147	10
SK11-03M_95B	87	1.78	1374	21.700	4.57	0.6075	3.58	0.78	3241	45	3170	44	3060	87	7
SK11-03M_122	91	1.90	17370	19.376	5.06	0.5426	4.53	0.90	3241	35	3061	49	2794	103	17
SK11-03L_180	65	1.73	3754	21.151	2.66	0.5923	2.29	0.86	3241	21	3146	26	2999	55	9
SK11-03L_181	103	2.45	15442	17.419	1.88	0.4878	1.55	0.82	3240	17	2958	18	2561	33	25
SK11-03M_96	96	1.76	1157	16.983	3.64	0.4759	3.08	0.85	3240	30	2934	35	2509	64	27
SK11-03L_194	79	1.71	1662077	21.487	1.86	0.6043	1.54	0.83	3234	16	3161	18	3047	37	7
SK11-03M_99	84	1.57	2026	16.650	4.50	0.4684	3.87	0.86	3233	36	2915	43	2477	80	28
SK11-03M_106	84	1.82	2778	22.836	3.06	0.6447	2.52	0.82	3228	28	3220	30	3207	64	1
SK11-03M_105	90	1.86	1955	23.222	4.38	0.6562	3.54	0.81	3226	41	3236	43	3253	90	1
SK11S-03_01	72	1.97	3815	21.987	2.50	0.6214	1.85	0.74	3226	27	3183	24	3116	46	4
SK11-03M_124	73	2.04	7880	22.379	3.73	0.6332	3.02	0.81	3224	35	3200	36	3162	75	2
SK11-03M_94	97	1.84	3966	20.904	2.97	0.5925	2.51	0.85	3222	25	3134	29	2999	60	9
SK11-03M_113	106	2.36	2165	21.916	3.22	0.6212	2.79	0.86	3221	26	3180	31	3115	69	4
SK11-03L_188	85	2.00	97610	18.822	2.61	0.5348	1.96	0.75	3218	27	3033	25	2762	44	17
SK11-03L_192	25	0.99	329	20.580	2.82	0.5852	2.35	0.83	3216	25	3119	27	2970	56	10
SK11-03M_120	85	1.58	48097	20.290	3.36	0.5770	2.28	0.68	3216	39	3105	33	2936	54	11
SK11S-03_27	80	1.94	784	20.591	3.79	0.5863	3.26	0.86	3214	30	3120	37	2974	78	9
SK11S-03_21	56	2.14	188383	21.976	3.41	0.6261	2.87	0.84	3213	29	3183	33	3134	71	3
SK11-03S_250	247	0.07	2621	25.198	3.98	0.7208	2.76	0.69	3207	45	3316	39	3499	74	12
SK11S-03_03	62	1.24	1160	20.385	4.28	0.5840	3.62	0.85	3205	36	3110	41	2965	86	9
SK11-03M_118	80	1.69	16165	19.720	4.37	0.5689	3.76	0.86	3194	35	3078	42	2903	88	11
SK11-03M_97	62	1.84	2107	22.293	4.29	0.6446	3.40	0.79	3190	41	3197	42	3207	86	1
SK11S-03_16	75	1.55	10774	21.092	2.09	0.6101	1.73	0.83	3189	18	3143	20	3070	42	5
SK11-03L_189	57	1.30	995	14.384	3.22	0.4168	2.49	0.77	3187	32	2775	31	2246	47	35
SK11-03M_115A	52	1.59	658	16.122	5.63	0.4684	4.67	0.83	3183	50	2884	54	2476	96	27
SK11-03M_107	87	1.97	6007	16.018	2.98	0.4670	2.54	0.85	3177	25	2878	28	2470	52	27
SK11S-03_13	44	1.57	2605	11.647	3.22	0.3416	2.23	0.69	3168	37	2576	30	1894	37	46
SK11-03L_186	108	1.61	30351	20.665	2.92	0.6084	2.39	0.82	3161	27	3123	28	3064	58	4
SK11-03M_109	104	2.38	2233	21.061	2.81	0.6225	2.33	0.83	3155	25	3141	27	3120	58	1
SK11-03M_116	108	2.17	13321	20.428	4.28	0.6053	3.13	0.73	3151	46	3112	41	3051	76	4
SK11-03M_119B	42	1.82	991	17.929	6.17	0.5316	4.07	0.66	3150	74	2986	59	2748	91	16

Spot	Corrected Isotope Ratios								Apparent Ages (Ma)						% disc.
	U ppm	Th/U ppm	$\frac{206\text{Pb}}{204\text{Pb}}$	$\frac{207\text{Pb}^*}{235\text{U}^*}$	$\pm 2s$ (%)	$\frac{206\text{Pb}^*}{238\text{U}}$	$\pm 2s$ (%)	error corr.	$\frac{207\text{Pb}^*}{206\text{Pb}^*}$	$\pm 2s$ (Ma)	$\frac{207\text{Pb}^*}{235\text{U}}$	$\pm 2s$ (Ma)	$\frac{206\text{Pb}^*}{238\text{U}^*}$	$\pm 2s$ (Ma)	
SK11S-03_18	85	2.32	3590	14.570	2.59	0.4326	2.15	0.83	3148	23	2788	25	2318	42	31
SK11-03M_110A	73	1.61	142463	18.204	4.38	0.5406	2.09	0.48	3148	61	3001	42	2786	47	14
SK11S-03_07	261	0.43	4759	19.910	3.42	0.5926	3.27	0.95	3144	16	3087	33	3000	78	6
SK11-03M_108	86	1.82	1639	20.211	4.51	0.6021	3.61	0.80	3143	43	3102	44	3038	87	4
SK11S-03_04	90	1.23	268219	15.192	5.73	0.4527	3.32	0.58	3142	74	2827	55	2407	67	28
SK11-03M_119A	55	1.99	13749	16.950	5.47	0.5059	4.22	0.77	3140	55	2932	52	2639	91	19
SK11-03L_187	97	1.93	5048	19.801	2.51	0.5933	2.13	0.85	3133	21	3082	24	3003	51	5
SK11-03M_114	71	1.41	706	20.365	3.27	0.6144	2.45	0.75	3123	35	3109	32	3088	60	1
SK11-03S_249	52	0.97	454	18.678	6.71	0.5659	5.79	0.86	3116	54	3025	65	2891	135	9
SK11-03L_185	59	1.27	4295	15.490	3.20	0.4709	2.34	0.73	3110	35	2846	31	2487	48	24
SK11S-03_05	33	1.56	1442	20.128	5.10	0.6122	4.09	0.80	3110	48	3098	49	3079	100	1
SK11-03L_183	98	2.09	2957	19.787	2.77	0.6020	2.41	0.87	3109	22	3081	27	3038	58	3
SK11-03M_123	65	1.38	960	18.480	5.03	0.5642	3.68	0.73	3104	55	3015	48	2884	86	9
SK11S-03_14	57	1.40	469	15.866	5.54	0.4887	5.08	0.92	3090	35	2869	53	2565	108	21
SK11-03L_182	104	2.43	3144	18.909	1.91	0.5827	1.65	0.86	3089	15	3037	18	2960	39	5
SK11-03M_117	62	1.47	14467	19.163	5.02	0.5917	4.19	0.83	3086	44	3050	48	2996	100	4
SK11S-03_09	55	1.53	1030	18.829	2.65	0.5820	2.08	0.79	3084	26	3033	26	2957	49	5
SK11S-03_22	140	0.71	13366	18.041	2.71	0.5680	2.03	0.75	3055	29	2992	26	2900	47	6
SK11-03M_111	80	2.04	1920	17.342	2.30	0.5486	1.71	0.74	3047	25	2954	22	2819	39	9
SK11S-03_08	29	1.15	611	18.867	3.65	0.6076	2.87	0.79	3018	36	3035	35	3060	70	2
SK11-03M_112	87	2.01	1296	15.168	4.43	0.4942	2.75	0.62	3000	56	2826	42	2589	59	17
Neoproterozoic															
SK11S-03_26	83	2.57	1367	16.038	2.37	0.5478	1.90	0.80	2923	23	2879	23	2816	43	5
SK11-03M_101A	58	1.40	2452	13.499	5.39	0.4615	4.11	0.76	2922	56	2715	51	2446	84	20
SK11-03L_193	47	1.38	841	11.190	3.42	0.3928	2.41	0.70	2879	39	2539	32	2136	44	30
SK11S-03_11	28	0.75	603	14.140	3.38	0.5021	2.09	0.62	2861	43	2759	32	2623	45	10
SK11-03L_190	67	1.50	3080	9.449	2.58	0.3358	1.83	0.71	2859	30	2383	24	1867	30	40
SK11-03L_179	80	1.38	6113	8.380	4.18	0.2984	3.07	0.73	2856	46	2273	38	1683	45	46
SK11-03M_101B	41	1.17	436	14.682	11.62	0.5277	9.27	0.80	2841	114	2795	110	2732	206	5
SK11S-03_12	34	0.72	602	14.591	2.94	0.5387	2.31	0.79	2797	30	2789	28	2778	52	1
SK11-03L_191	29	0.60	661	13.453	3.27	0.5103	2.20	0.67	2753	40	2712	31	2658	48	4
SK11-03M_98	22	0.30	1239	7.993	6.36	0.3501	3.99	0.63	2513	83	2230	57	1935	67	27

Spot number	U ppm	Corrected Isotope Ratios							Apparent Ages (Ma)						
		Th/U	206Pb 204Pb	207Pb* 235U*	±2s (%)	206Pb* 238U	±2s (%)	error corr.	207Pb* 206Pb*	±2s (Ma)	207Pb* 235U	±2s (Ma)	206Pb* 238U*	±2s (Ma)	% disc.
SK11-07															
Mesoarchean 1															
SK11-07M_27	1508	0.12	74913	20.339	6.71	0.5534	6.26	0.93	3286	38	3108	65	2839	144	17
SK11-07S_53	972	0.12	30377	18.162	10.55	0.4970	8.58	0.81	3277	97	2998	102	2601	184	25
SK11-07M_36	2604	0.13	38338	21.837	3.25	0.6045	3.11	0.96	3259	15	3176	32	3048	76	8
SK11-07S_54	693	0.15	11962	18.580	8.83	0.5146	6.74	0.76	3258	90	3020	85	2676	148	22
SK11-07S_41	261	0.54	5670	23.236	11.42	0.6551	7.95	0.70	3230	129	3237	111	3248	203	1
SK11-07S_58	608	0.07	25468	19.598	12.67	0.5529	9.97	0.79	3229	123	3072	122	2837	229	15
SK11-07M_35	512	0.06	62716	21.561	4.64	0.6084	4.26	0.92	3229	29	3164	45	3063	104	6
SK11-07S_49	76	0.78	8829	20.294	9.47	0.5744	7.41	0.78	3224	93	3105	92	2926	174	11
SK11-07M_30	1435	0.15	11197	21.619	4.85	0.6132	4.38	0.90	3220	33	3167	47	3083	107	5
SK11-07S_51	620	0.13	20776	16.059	9.15	0.4559	6.82	0.75	3219	96	2880	87	2421	138	30
SK11-07L_87	73	2.17	5718	22.423	6.19	0.6382	5.28	0.85	3215	51	3202	60	3182	133	1
SK11-07S_40	302	0.35	4933	19.980	11.47	0.5696	8.43	0.73	3213	123	3090	111	2906	197	12
SK11-07M_25	1160	0.07	22847	17.397	4.64	0.4988	4.30	0.93	3203	27	2957	45	2609	92	23
SK11-07M_21	65	1.67	1569	20.917	3.72	0.5998	3.06	0.82	3203	34	3135	36	3029	74	7
SK11-07S_45	1362	0.02	12165	16.167	7.18	0.4680	6.00	0.84	3188	62	2887	69	2475	123	27
SK11-07S_48	1270	0.03	23181	18.536	7.95	0.5383	5.73	0.72	3183	87	3018	77	2776	129	16
SK11-07M_20	66	1.68	4061	19.462	4.01	0.5694	3.33	0.83	3171	35	3065	39	2905	78	10
SK11-07S_50	722	0.11	8387	15.796	7.94	0.4650	5.43	0.68	3161	92	2865	76	2462	111	27
SK11-07L_94	62	0.83	3675	19.560	7.56	0.5806	6.04	0.80	3148	72	3070	73	2951	143	8
SK11-07M_24	664	0.16	34257	15.712	6.75	0.4700	5.72	0.85	3136	57	2859	64	2483	118	25
SK11-07S_56	897	0.10	30882	22.156	8.47	0.6692	6.46	0.76	3121	87	3191	82	3303	167	7
SK11-07S_47	1087	0.31	11703	17.008	9.11	0.5169	7.45	0.82	3111	84	2935	87	2686	164	17
SK11-07S_46	836	0.08	56473	17.813	10.94	0.5416	8.67	0.79	3110	106	2980	105	2790	196	13
SK11-07S_38	460	0.41	18194	16.826	6.71	0.5122	5.67	0.84	3108	57	2925	64	2666	124	17
SK11-07M_31	459	0.27	5805	16.638	6.80	0.5116	6.13	0.90	3092	47	2914	65	2663	134	17
SK11-07M_28	330	0.17	19678	18.033	6.68	0.5686	6.12	0.92	3052	43	2991	64	2902	143	6
SK11-07S_52	447	0.13	8538	12.964	7.62	0.4124	4.91	0.64	3038	93	2677	72	2226	92	32
SK11-07M_26	1028	0.04	49332	13.509	5.36	0.4316	4.66	0.87	3031	42	2716	51	2313	91	28
SK11-07M_29	575	0.13	7157	16.929	8.85	0.5587	7.54	0.85	2979	75	2931	85	2861	174	5
Neoarchean															
SK11-07L_93	45	1.10	2780	16.739	6.16	0.5728	4.55	0.74	2921	67	2920	59	2919	107	0
SK11-07L_86	44	3.01	410	11.089	5.89	0.3856	3.65	0.62	2895	75	2531	55	2102	66	32

Spot	Corrected Isotope Ratios								Apparent Ages (Ma)						
	U ppm	Th/U ppm	²⁰⁶ Pb ²⁰⁴ Pb	²⁰⁷ Pb* ²³⁵ U*	±2s (%)	²⁰⁶ Pb* ²³⁸ U	±2s (%)	error corr.	²⁰⁷ Pb* ²⁰⁶ Pb*	±2s (Ma)	²⁰⁷ Pb* ²³⁵ U	±2s (Ma)	²⁰⁶ Pb* ²³⁸ U*	±2s (Ma)	% disc.
SK11-07S_57	32	0.78	1893	16.226	21.58	0.5864	20.49	0.95	2832	111	2890	206	2975	488	6
SK11-07M_33	55	1.22	5320	15.458	5.23	0.5654	4.61	0.88	2812	40	2844	50	2889	107	3
SK11-07S_44	42	0.93	768	14.876	7.44	0.5552	6.02	0.81	2779	72	2807	71	2847	139	3
SK11-07L_92	79	1.33	10992	13.099	5.71	0.4917	3.71	0.65	2770	71	2687	54	2578	79	8
SK11-07M_34	52	1.20	1155	13.634	3.85	0.5140	3.14	0.82	2763	37	2725	36	2674	69	4
SK11-07L_95	61	1.45	2162	11.658	5.36	0.4410	4.14	0.77	2757	56	2577	50	2355	82	17
SK11-07L_88	148	2.49	2388	13.265	4.52	0.5040	3.51	0.78	2750	47	2699	43	2631	76	5
SK11-07L_96	76	2.27	2865	13.789	3.67	0.5248	3.04	0.83	2747	34	2735	35	2720	67	1
SK11-07L_90	54	1.51	1568	13.229	7.67	0.5044	5.46	0.71	2744	89	2696	72	2633	118	5
SK11-07M_18B	28	0.92	440	10.894	5.49	0.4156	3.58	0.65	2743	68	2514	51	2240	68	22
SK11-07M_19	47	1.61	1116	12.720	3.73	0.4876	3.00	0.80	2735	36	2659	35	2560	63	8
SK11-07L_89	141	2.39	1573	7.320	5.66	0.2866	4.28	0.76	2701	61	2151	51	1624	61	45
SK11-07L_91	67	1.37	12494	13.232	6.94	0.5198	5.24	0.76	2695	75	2696	65	2698	116	0
SK11-07S_37	111	1.09	8130	9.128	8.70	0.3630	6.23	0.72	2675	100	2351	80	1996	107	29
SK11-07S_43	125	0.46	3251	9.309	12.10	0.3726	9.08	0.75	2664	132	2369	111	2042	159	27
SK11-07M_18A	29	0.91	158	7.624	6.73	0.3084	3.82	0.57	2646	92	2188	60	1733	58	39
SK11-07M_32	108	1.14	2457	9.974	4.57	0.4038	3.49	0.76	2645	49	2432	42	2187	65	20
SK11-07S_55	80	0.95	754	8.100	8.08	0.3491	5.78	0.71	2541	95	2242	73	1930	96	28
SK11-07S_42	71	1.17	425	7.422	11.36	0.3339	8.66	0.76	2468	124	2164	102	1857	140	28

Spot number	Corrected Isotope Ratios								Apparent Ages (Ma)						
	U ppm	Th/U	²⁰⁶ Pb ²⁰⁴ Pb	²⁰⁷ Pb* ²³⁵ U*	±2s (%)	²⁰⁶ Pb* ²³⁸ U	±2s (%)	error corr.	²⁰⁷ Pb* ²⁰⁶ Pb*	±2s (Ma)	²⁰⁷ Pb* ²³⁵ U	±2s (Ma)	²⁰⁶ Pb* ²³⁸ U*	±2s (Ma)	% disc.
SK11-08															
Paleoarchean															
SK11-08S_69	2696	0.06	1659251	22.658	10.66	0.5606	8.91	0.84	3434	91	3212	104	2869	206	20
SK11-08S-60	408	0.13	16124	19.573	5.90	0.4974	4.52	0.76	3393	59	3070	57	2603	97	28
Mesoarchean 2															
SK11-08S_77	700	0.15	34474	18.969	9.63	0.4999	6.65	0.69	3336	109	3040	93	2613	143	26
SK11-08S_65	354	0.04	8167	19.865	9.03	0.5310	6.24	0.69	3314	102	3085	87	2746	140	21
SK11-08M_15A	101	0.85	5031	21.554	7.65	0.5839	6.73	0.88	3293	57	3164	74	2965	160	12

Spot	Corrected Isotope Ratios								Apparent Ages (Ma)						
	U ppm	Th/U ppm	<u>206Pb</u> <u>204Pb</u>	<u>207Pb*</u> <u>235U*</u>	±2s (%)	<u>206Pb*</u> <u>238U</u>	±2s (%)	error corr.	<u>207Pb*</u> <u>206Pb*</u>	±2s (Ma)	<u>207Pb*</u> <u>235U</u>	±2s (Ma)	<u>206Pb*</u> <u>238U*</u>	±2s (Ma)	% disc.
SK11-08S_64	218	0.17	3883	23.737	10.12	0.6506	8.04	0.79	3274	97	3258	99	3231	204	2
SK11-08M_16	154	0.77	2224	20.885	5.64	0.5759	5.08	0.90	3265	38	3133	55	2932	120	13
SK11-08S_63	508	0.14	15614	18.493	9.50	0.5117	6.65	0.70	3259	107	3016	91	2664	145	22
SK11-08S_66	1003	0.05	13296	17.529	10.78	0.4855	7.55	0.70	3258	121	2964	104	2551	159	26
SK11-08S_61_B	304	0.17	13418	26.912	7.11	0.7496	4.70	0.66	3249	84	3380	70	3606	130	14
SK11-08S_84	855	0.75	171267	19.008	9.23	0.5324	6.59	0.71	3240	102	3042	89	2752	148	18
SK11-08S_62	1955	0.13	230321	18.935	12.57	0.5347	10.88	0.87	3228	99	3039	121	2761	244	18
SK11-08M_15B	152	0.89	4502	19.514	6.23	0.5618	4.39	0.70	3197	70	3068	60	2874	102	12
SK11-08S_68	227	1.16	26249	18.905	8.86	0.5466	6.24	0.71	3190	99	3037	85	2811	142	15
SK11-08S_79	869	0.10	15044	14.072	11.65	0.4076	9.17	0.79	3187	114	2755	110	2204	171	36
SK11-08S_80	191	0.28	2794	24.562	12.33	0.7133	9.27	0.75	3183	129	3291	120	3471	249	12
SK11-08S_67	677	0.57	23355	17.342	8.81	0.5049	7.40	0.84	3179	76	2954	85	2635	160	21
SK11-08S_85	738	0.78	8957	20.171	6.36	0.5875	4.36	0.69	3178	73	3100	62	2979	104	8
SK11-08M_7A	68	1.01	1755	12.385	5.49	0.3671	4.59	0.83	3151	48	2634	52	2016	79	42
SK11-08S_70	410	0.33	86103	17.592	12.15	0.5254	9.63	0.79	3139	118	2968	117	2722	214	16
SK11-08M_13	117	0.46	887	11.949	7.19	0.3624	6.67	0.93	3114	43	2600	67	1994	114	42
SK11-08S_61_a	524	0.15	7869	22.232	23.18	0.6930	18.68	0.81	3070	219	3194	225	3394	493	14
SK11-08S_73	519	0.15	23154	17.058	8.75	0.5360	6.80	0.78	3058	88	2938	84	2767	153	12
SK11-08M_7B	74	1.10	3903	8.335	12.13	0.2647	9.30	0.77	3041	125	2268	110	1514	125	56
SK11-08S_72	139	0.30	25726	18.953	16.45	0.6305	11.45	0.70	2966	190	3039	159	3152	285	8
SK11-08S_83	364	1.40	6824	13.849	8.97	0.4730	6.59	0.74	2924	98	2739	85	2497	136	18
SK11-08S_71	1032	0.39	379017	12.546	10.13	0.4343	7.47	0.74	2902	111	2646	95	2325	146	24
Neoproterozoic															
SK11-08S_78	113	0.81	1365	12.055	20.36	0.4205	17.74	0.87	2889	162	2609	191	2263	338	26
SK11-08S_74	3637	0.09	71434	11.698	7.21	0.4106	5.60	0.78	2879	74	2581	67	2218	105	27
SK11-08S_82	86	0.75	10090	10.597	9.70	0.3881	7.16	0.74	2810	107	2488	90	2114	129	29
SK11-08L_99	96	0.96	2111	10.782	8.18	0.3994	5.79	0.71	2792	95	2505	76	2166	107	26
SK11-08M_17	167	1.03	9006	12.584	4.35	0.4694	3.91	0.90	2780	31	2649	41	2481	81	13
SK11-08M_8	98	0.88	1065	12.900	5.06	0.4840	4.21	0.83	2770	46	2672	48	2545	89	10
SK11-08M_12	99	0.72	3758	13.386	5.32	0.5064	4.76	0.89	2757	39	2707	50	2641	103	5
SK11-08L_98	154	1.60	8303	13.966	6.91	0.5287	4.91	0.71	2756	80	2747	66	2736	109	1
SK11-08M_9	156	0.79	5449	11.312	4.49	0.4293	3.86	0.86	2752	38	2549	42	2303	75	19
SK11-08M_10	111	0.73	6270	12.276	5.31	0.4688	4.71	0.89	2741	40	2626	50	2478	97	12
SK11-08S_81	155	1.19	17125	14.106	8.94	0.5392	6.90	0.77	2740	93	2757	85	2780	156	2

Spot	Corrected Isotope Ratios								Apparent Ages (Ma)						% disc.
	U ppm	Th/U ppm	$\frac{206\text{Pb}}{204\text{Pb}}$	$\frac{207\text{Pb}^*}{235\text{U}^*}$	$\pm 2s$ (%)	$\frac{206\text{Pb}^*}{238\text{U}}$	$\pm 2s$ (%)	error corr.	$\frac{207\text{Pb}^*}{206\text{Pb}^*}$	$\pm 2s$ (Ma)	$\frac{207\text{Pb}^*}{235\text{U}}$	$\pm 2s$ (Ma)	$\frac{206\text{Pb}^*}{238\text{U}^*}$	$\pm 2s$ (Ma)	
SK11-08S_75	124	0.99	1015	8.616	8.88	0.3307	6.46	0.73	2733	100	2298	81	1842	103	37
SK11-08M_14	164	1.54	1967	18.489	4.62	0.7125	3.90	0.84	2726	41	3016	45	3468	105	35
SK11-08M_11	89	0.73	2860	9.373	8.47	0.3620	7.80	0.92	2723	55	2375	78	1992	134	31
SK11-08M_6	151	0.95	1316	8.504	4.46	0.3342	3.74	0.84	2694	40	2286	41	1859	60	36
SK11-08M_5	102	0.81	1095	4.690	6.15	0.1888	5.26	0.86	2654	53	1765	51	1115	54	63
SK11-08S_76	121	0.78	2475	7.041	9.94	0.3064	7.64	0.77	2524	107	2117	88	1723	116	36
SK11-08L_97	159	0.48	1015	9.000	6.80	0.4155	4.49	0.66	2425	87	2338	62	2240	85	9

Table C2: Corrected Isotope Ratios and Apparent Ages of Craters of the Moon National Monument and Preserve
 Spots in **bold** were used in the calculation of zircon growth event averages. Spots in ***bold and italics*** were less than 30% discordant, but were not used to calculate averages because the sample did not have more than 5 spots with discordance less than 30%.
 Discordance was not used as a filter on Paleogene dates.

Spot	Corrected Isotope Ratios								Apparent ages (Ma)						
	U ppm	Th/U ppm	<u>206Pb</u> 204Pb	<u>207Pb*</u> 235U*	±2s (%)	<u>206Pb*</u> 238U	±2s (%)	error corr.	<u>207Pb*</u> 206Pb*	±2s (Ma)	<u>207Pb*</u> 235U	±2s (Ma)	<u>206Pb*</u> 238U*	±2s (Ma)	% disc.
CRMO11-01															
Mesoarchean 2															
CRMO11-01_L_37	541	0.76	17173	18.863	7.26	0.5555	6.16	0.85	3161	61	3035	70	2848	142	12
CRMO11-01_L_7	582	0.39	89878	18.863	7.85	0.5558	7.08	0.90	3160	54	3035	76	2849	163	12
CRMO11-01_L_40	881	0.84	53756	19.524	6.63	0.5774	5.59	0.84	3154	56	3068	64	2938	132	9
CRMO11-01_S_198	486	0.46	24676	19.185	4.84	0.5676	4.32	0.89	3154	35	3051	47	2898	101	10
CRMO11-01_L_29	144	0.66	96586	19.580	6.18	0.5828	5.29	0.86	3144	51	3071	60	2960	126	7
CRMO11-01_L_15	192	0.77	2782	18.955	6.40	0.5658	5.59	0.87	3140	49	3040	62	2890	130	10
CRMO11-01_L_39	670	0.45	11236	19.152	8.11	0.5720	7.22	0.89	3139	59	3050	78	2916	169	9
CRMO11-01_L_31	503	0.67	15122	18.667	6.11	0.5576	5.17	0.85	3138	52	3025	59	2857	119	11
CRMO11-01_L_41	657	0.59	24919	19.533	7.49	0.5836	6.65	0.89	3138	55	3069	72	2963	158	7
CRMO11-01_L_12	791	0.59	10891	18.784	6.82	0.5647	5.95	0.87	3128	53	3031	66	2886	139	10
CRMO11-01_M_128	195	0.54	36416	18.659	5.69	0.5613	5.10	0.90	3127	40	3024	55	2872	118	10
CRMO11-01_M_123	170	0.71	19131	19.466	5.40	0.5857	5.04	0.93	3127	31	3065	52	2972	120	6
CRMO11-01_L_23	494	0.94	269903	17.414	5.77	0.5246	4.97	0.86	3125	47	2958	55	2719	110	16
CRMO11-01_M_124	117	0.61	3092	19.535	6.26	0.5885	5.88	0.94	3125	34	3069	60	2984	140	6
CRMO11-01_L_28	855	0.43	349823	18.937	6.26	0.5721	5.32	0.85	3120	52	3039	60	2916	125	8
CRMO11-01_L_24	266	0.99	146385	18.221	6.01	0.5523	5.18	0.86	3115	49	3001	58	2835	119	11
CRMO11-01_L_25	914	0.27	108390	16.990	6.00	0.5179	5.17	0.86	3106	49	2934	58	2690	114	16
CRMO11-01_S_209	578	1.21	34842	18.872	6.05	0.5769	5.55	0.92	3102	38	3035	58	2936	131	7
CRMO11-01_M_129	745	0.78	27921	18.826	6.44	0.5758	6.02	0.93	3101	36	3033	62	2931	142	7
CRMO11-01_L_35	106	0.43	53850	16.323	7.89	0.5013	6.53	0.83	3094	71	2896	76	2619	140	19
CRMO11-01_S_200	531	0.99	19837	17.214	5.18	0.5293	4.76	0.92	3092	33	2947	50	2738	106	14
CRMO11-01_L_32	512	0.65	16381	17.469	6.09	0.5373	5.10	0.84	3092	53	2961	58	2772	115	13
CRMO11-01_L_10	1351	0.24	727802	18.189	6.54	0.5608	5.56	0.85	3088	55	3000	63	2870	129	9
CRMO11-01_M_132	563	0.92	18664	19.033	5.50	0.5879	5.05	0.92	3085	35	3043	53	2981	120	4
CRMO11-01_M_120	474	1.28	9680	17.221	5.24	0.5337	4.74	0.90	3080	36	2947	50	2757	106	13

Spot	Corrected Isotope Ratios								Apparent ages (Ma)						
	U ppm	Th/U ppm	<u>206Pb</u> <u>204Pb</u>	<u>207Pb*</u> <u>235U*</u>	$\pm 2s$ (%)	<u>206Pb*</u> <u>238U</u>	$\pm 2s$ (%)	error corr.	<u>207Pb*</u> <u>206Pb*</u>	$\pm 2s$ (Ma)	<u>207Pb*</u> <u>235U</u>	$\pm 2s$ (Ma)	<u>206Pb*</u> <u>238U*</u>	$\pm 2s$ (Ma)	% disc.
CRMO11-01_S_207	158	1.38	11782	17.841	5.83	0.5532	5.38	0.92	3079	36	2981	56	2839	124	10
CRMO11-01_M_134	714	0.44	93858	19.328	6.07	0.5993	5.68	0.94	3079	34	3058	59	3027	137	2
CRMO11-01_S_205	190	0.86	32445	16.396	5.22	0.5086	4.78	0.91	3078	34	2900	50	2651	104	17
CRMO11-01_M_133	832	0.12	360005	16.484	6.97	0.5141	6.40	0.92	3070	44	2905	67	2674	140	16
CRMO11-01_L_20	993	0.73	16426	17.005	5.86	0.5312	4.94	0.84	3067	51	2935	56	2746	110	13
CRMO11-01_L_16	442	0.36	17853	15.778	6.01	0.4935	5.16	0.86	3065	49	2863	57	2586	110	19
CRMO11-01_L_17	1027	0.21	41895	16.584	6.19	0.5192	5.37	0.87	3064	49	2911	59	2696	118	15
CRMO11-01_L_11	245	0.72	13153	17.868	7.55	0.5594	6.78	0.90	3064	53	2983	73	2864	157	8
CRMO11-01_M_125	205	0.69	29038	15.935	6.35	0.4990	5.95	0.94	3063	36	2873	61	2609	128	18
CRMO11-01_M_136	239	0.60	34605	16.216	5.75	0.5095	5.31	0.92	3058	35	2890	55	2654	115	16
CRMO11-01_L_38	1736	0.34	53731	18.204	7.50	0.5726	6.52	0.87	3056	59	3001	72	2919	153	6
CRMO11-01_M_138	202	0.66	6106	17.377	5.12	0.5473	4.63	0.90	3054	35	2956	49	2814	106	10
CRMO11-01_L_18	148	0.63	3086	14.191	8.64	0.4476	7.91	0.92	3052	56	2763	82	2385	158	26
CRMO11-01_M_135	991	0.21	112233	16.340	5.53	0.5156	5.10	0.92	3051	34	2897	53	2680	112	15
CRMO11-01_M_121	179	0.74	2773	16.426	5.94	0.5198	5.50	0.93	3046	36	2902	57	2698	121	14
CRMO11-01_M_126	862	0.36	34274	15.396	6.43	0.4922	6.11	0.95	3030	32	2840	61	2580	130	18
CRMO11-01_S_201	1074	0.97	34140	15.810	5.42	0.5058	5.02	0.93	3029	33	2865	52	2639	109	16
CRMO11-01_M_130	751	0.32	29526	12.585	5.75	0.4037	5.33	0.93	3025	34	2649	54	2186	99	33
CRMO11-01_L_19	1477	0.18	3218440	14.615	6.65	0.4700	5.80	0.87	3021	52	2790	63	2484	120	21
CRMO11-01_M_142	633	0.09	7002	15.450	5.44	0.4977	4.99	0.92	3018	35	2843	52	2604	107	17
CRMO11-01_S_197	337	0.63	15372	16.930	5.58	0.5466	5.00	0.90	3014	40	2931	54	2811	114	8
CRMO11-01_M_131	778	0.87	25776	16.431	7.37	0.5306	6.61	0.90	3014	52	2902	71	2744	148	11
CRMO11-01_M_139	1330	0.36	69269	16.597	5.77	0.5365	5.37	0.93	3012	34	2912	55	2769	121	10
CRMO11-01_S_203	802	0.49	64070	14.638	4.63	0.4742	4.17	0.90	3009	32	2792	44	2502	87	20
CRMO11-01_S_208	627	0.82	20545	15.971	6.19	0.5180	5.78	0.93	3007	35	2875	59	2691	127	13
CRMO11-01_M_141	681	0.50	20696	15.387	5.72	0.5046	5.31	0.93	2989	34	2839	55	2634	115	14
CRMO11-01_L_36	1467	0.16	18501	12.777	6.86	0.4236	5.71	0.83	2972	61	2663	65	2277	109	28
CRMO11-01_M_119	1438	0.56	12673	14.327	7.47	0.4764	7.19	0.96	2967	33	2772	71	2511	149	18
CRMO11-01_L_22	152	0.59	3917	11.896	7.46	0.3987	6.68	0.90	2954	53	2596	70	2163	123	31
CRMO11-01_L_8	374	0.28	6354	9.849	6.89	0.3313	6.04	0.88	2948	53	2421	64	1845	97	43
CRMO11-01_L_27	793	0.34	12507	11.473	6.06	0.3873	5.09	0.84	2943	53	2562	57	2110	92	33
CRMO11-01_S_199	892	0.68	132155	12.153	4.83	0.4108	4.39	0.91	2940	33	2616	45	2218	82	29
CRMO11-01_S_196	2448	0.21	70575	14.068	6.21	0.4774	5.92	0.95	2934	30	2754	59	2516	123	17
CRMO11-01_L_9	1723	0.16	24291	11.231	7.44	0.3812	6.58	0.88	2934	56	2543	69	2082	117	34

Spot	Corrected Isotope Ratios								Apparent ages (Ma)						
	U ppm	Th/U ppm	<u>206Pb</u> 204Pb	<u>207Pb*</u> 235U*	±2s (%)	<u>206Pb*</u> 238U	±2s (%)	error corr.	<u>207Pb*</u> 206Pb*	±2s (Ma)	<u>207Pb*</u> 235U	±2s (Ma)	<u>206Pb*</u> 238U*	±2s (Ma)	% disc.
CRMO11-01_M_137	1626	0.24	1400221	13.409	4.80	0.4581	4.28	0.89	2923	35	2709	45	2431	87	20
CRMO11-01_M_140	745	0.28	11654	11.167	4.78	0.3824	4.35	0.91	2919	32	2537	45	2087	78	33
CRMO11-01_M_127	1043	0.51	35413	13.583	5.26	0.4681	4.82	0.92	2909	34	2721	50	2475	99	18
CRMO11-01_L_34	511	0.24	17983	12.624	6.35	0.4383	5.12	0.81	2897	61	2652	60	2343	101	23
Neoproterozoic															
CRMO11-01_S_206	2043	0.36	144038	11.963	5.55	0.4182	5.19	0.94	2886	32	2601	52	2252	99	26
CRMO11-01_L_14	160	133.51	118	11.800	6.78	0.4277	5.93	0.87	2827	54	2589	63	2295	115	22
CRMO11-01_L_21	184	128.84	110	12.636	6.10	0.4598	5.21	0.85	2821	52	2653	57	2439	106	16
CRMO11-01_L_13	315	179.70	72	3.997	5.93	0.1462	4.98	0.84	2812	53	1634	48	880	41	73
CRMO11-01_L_30	199	103.30	113	13.400	5.73	0.4943	4.80	0.84	2798	51	2708	54	2589	102	9
CRMO11-01_L_26	107	180.30	57	12.092	6.27	0.4477	5.19	0.83	2792	57	2612	59	2385	104	17
CRMO11-01_L_33	162	75.83	74	11.271	6.58	0.4212	5.59	0.85	2777	57	2546	61	2266	107	22
CRMO11-01_S_204	382	150.35	209	10.706	6.16	0.4039	5.84	0.95	2762	32	2498	57	2187	108	24
CRMO11-01_S_202	233	162.41	80	5.806	6.42	0.2210	5.96	0.93	2747	39	1947	56	1287	70	58
CRMO11-01_M_122	184	109.20	26	10.062	6.24	0.3875	5.80	0.93	2728	38	2441	58	2111	104	26

Spot	Corrected Isotope Ratios								Apparent ages (Ma)						
	U ppm	Th/U ppm	<u>206Pb</u> 204Pb	<u>207Pb*</u> 235U*	±2s (%)	<u>206Pb*</u> 238U	±2s (%)	error corr.	<u>207Pb*</u> 206Pb*	±2s (Ma)	<u>207Pb*</u> 235U	±2s (Ma)	<u>206Pb*</u> 238U*	±2s (Ma)	% disc.
CRMO11-03															
Mesoarchean 2															
CRMO11-03_M_112	747	0.33	64306	17.716	6.93	0.5562	6.19	0.89	3059	50	2974	67	2851	143	8
CRMO11-03_M_95	190	0.40	13685	12.116	8.44	0.4192	7.41	0.88	2902	65	2613	79	2257	141	26
Paleogene															
CRMO11-03_S_188A	595	1.46	80	0.202	16.27	0.0078	7.24	0.45	2729	240	187	28	50	4	99
CRMO11-03_M_92	942	0.68	197	0.044	8.38	0.0062	5.24	0.63	273	150	44	4	40	2	86
CRMO11-03_M_103	614	1.33	129	0.095	15.61	0.0062	6.68	0.43	1818	256	92	14	40	3	98
CRMO11-03_M_108	454	0.84	97	0.045	13.07	0.0062	7.41	0.57	314	245	44	6	40	3	88
CRMO11-03_M_106	2100	0.55	265	0.041	8.39	0.0061	6.68	0.80	167	119	41	3	39	3	77
CRMO11-03_M_91	3128	0.52	1828	0.037	8.97	0.0060	6.71	0.75	-73	146	37	3	39	3	153
CRMO11-03_M_118	2005	0.72	1751	0.039	8.06	0.0060	5.50	0.68	58	140	39	3	38	2	34
CRMO11-03_M_96	9766	0.23	1408	0.039	6.14	0.0059	5.10	0.83	107	81	39	2	38	2	65

Spot	Corrected Isotope Ratios								Apparent ages (Ma)						% disc.
	U ppm	Th/U ppm	$\frac{206\text{Pb}}{204\text{Pb}}$	$\frac{207\text{Pb}^*}{235\text{U}^*}$	$\pm 2s$ (%)	$\frac{206\text{Pb}^*}{238\text{U}}$	$\pm 2s$ (%)	error corr.	$\frac{207\text{Pb}^*}{206\text{Pb}^*}$	$\pm 2s$ (Ma)	$\frac{207\text{Pb}^*}{235\text{U}}$	$\pm 2s$ (Ma)	$\frac{206\text{Pb}^*}{238\text{U}^*}$	$\pm 2s$ (Ma)	
CRMO11-03_M_97	3671	0.52	1130	0.037	7.23	0.0059	5.72	0.79	4	106	37	3	38	2	884
CRMO11-03_S_185	3724	0.74	2429	0.038	6.53	0.0058	5.55	0.85	76	82	38	2	37	2	51
CRMO11-03_M_111	4911	0.23	699	0.040	6.86	0.0058	5.67	0.83	193	90	40	3	37	2	81
CRMO11-03_M_109	17604	0.34	9906	0.038	8.06	0.0058	7.16	0.89	76	88	38	3	37	3	52
CRMO11-03_M_115	4319	0.51	418	0.038	6.43	0.0058	4.75	0.74	84	103	38	2	37	2	56
CRMO11-03_S_194	12859	0.25	2324	0.038	5.76	0.0057	5.24	0.91	122	57	38	2	37	2	70
CRMO11-03_M_102	666	0.56	123	0.035	11.27	0.0057	7.36	0.65	-117	211	35	4	37	3	132
CRMO11-03_M_114	7668	0.25	10893	0.037	6.63	0.0057	5.34	0.81	25	94	37	2	37	2	50
CRMO11-03_M_98	1514	0.63	1657	0.096	9.19	0.0057	7.55	0.82	1985	93	93	8	37	3	98
CRMO11-03_M_99	23731	0.33	10695	0.037	5.95	0.0057	5.03	0.85	28	76	36	2	37	2	29
CRMO11-03_M_104	1894	0.66	360	0.038	7.59	0.0057	5.49	0.72	116	124	38	3	36	2	69
CRMO11-03_L_4	1923	0.61	1435	0.037	7.28	0.0057	5.38	0.74	93	116	37	3	36	2	61
CRMO11-03_M_101	15308	0.20	2861	0.036	7.16	0.0057	6.11	0.85	12	90	36	3	36	2	199
CRMO11-03_M_116	478	0.59	528	0.037	11.61	0.0056	4.93	0.42	51	251	37	4	36	2	30
CRMO11-03_M_113	585	0.63	272	0.069	15.54	0.0056	6.30	0.41	1397	272	68	10	36	2	98
CRMO11-03_S_193	6013	0.88	684	0.038	5.03	0.0056	4.03	0.80	117	71	38	2	36	1	69
CRMO11-03_M_93	637	0.90	83	0.040	14.66	0.0056	5.13	0.35	268	315	40	6	36	2	87
CRMO11-03_M_117	2174	0.59	493	0.036	8.41	0.0056	5.99	0.71	5	142	36	3	36	2	692
CRMO11-03_S_187	1442	0.77	241	0.037	7.12	0.0056	5.32	0.75	63	113	37	3	36	2	43
CRMO11-03_S_192	7035	0.50	111572	0.039	5.81	0.0056	4.98	0.86	233	69	39	2	36	2	85
CRMO11-03_L_3	591	0.66	84	0.108	16.24	0.0056	9.12	0.56	2227	233	104	16	36	3	99
CRMO11-03_L_6	5209	0.55	1456	0.036	6.81	0.0056	5.59	0.82	3	94	35	2	36	2	1221
CRMO11-03_M_107	1447	0.52	257	0.035	9.43	0.0056	7.24	0.77	-8	146	35	3	36	3	551
CRMO11-03_S_191	737	1.15	448	0.037	9.08	0.0055	6.01	0.66	156	159	37	3	36	2	78
CRMO11-03_S_189	854	1.48	878	0.038	9.20	0.0055	5.58	0.61	205	170	38	3	35	2	83
CRMO11-03_S_186	15994	0.44	2811	0.038	5.82	0.0055	4.98	0.86	221	70	38	2	35	2	84
CRMO11-03_M_94	966	0.61	621	0.041	9.77	0.0055	5.25	0.54	375	186	41	4	35	2	91
CRMO11-03_M_110	737	0.62	172	0.035	11.10	0.0054	5.90	0.53	54	224	35	4	35	2	36
CRMO11-03_S_195	851	0.63	195	0.034	9.74	0.0054	5.19	0.53	-4	199	34	3	35	2	942
CRMO11-03_S_190	442	0.94	175	0.036	12.34	0.0054	5.87	0.48	104	256	36	4	35	2	67
CRMO11-03_L_5	520	0.73	187	0.039	10.29	0.0053	5.37	0.52	303	200	38	4	34	2	89
CRMO11-03_M_100	980	0.63	548	0.038	11.72	0.0053	7.45	0.64	280	207	38	4	34	3	88
CRMO11-03_S_188B	1117	1.40	449	0.036	9.59	0.0051	5.38	0.56	280	182	36	3	33	2	89

Spot	Corrected Isotope Ratios								Apparent ages (Ma)						% disc.
	U ppm	Th/U ppm	$\frac{206\text{Pb}}{204\text{Pb}}$	$\frac{207\text{Pb}^*}{235\text{U}^*}$	$\pm 2s$ (%)	$\frac{206\text{Pb}^*}{238\text{U}}$	$\pm 2s$ (%)	error corr.	$\frac{207\text{Pb}^*}{206\text{Pb}^*}$	$\pm 2s$ (Ma)	$\frac{207\text{Pb}^*}{235\text{U}}$	$\pm 2s$ (Ma)	$\frac{206\text{Pb}^*}{238\text{U}^*}$	$\pm 2s$ (Ma)	
CRMO11-04															
Paleogene															
CRMO11-04_S_68	1440	0.50	325	0.047	13.50	0.0071	11.80	0.87	89	156	46	6	45	5	49
CRMO11-04_S_65	2384	1.37	11747	0.046	10.06	0.0065	6.38	0.63	265	179	46	4	42	3	85
CRMO11-04_S_66	1626	0.44	8702	0.041	8.33	0.0065	5.84	0.70	29	143	41	3	41	2	45
CRMO11-04_S_82	1116	0.43	167	0.052	9.57	0.0064	6.44	0.67	572	154	52	5	41	3	93
CRMO11-04_S_85	512	1.05	411	0.170	11.06	0.0064	6.73	0.61	2770	144	159	16	41	3	99
CRMO11-04_S_56	8870	0.27	1285	0.043	7.02	0.0063	6.19	0.88	163	78	42	3	40	2	75
CRMO11-04_S_59	9621	0.18	1755	0.041	7.52	0.0063	6.48	0.86	46	91	40	3	40	3	13
CRMO11-04_S_69	6197	0.26	1827	0.041	7.66	0.0063	6.53	0.85	63	95	41	3	40	3	37
CRMO11-04_S_57	1341	0.38	183	0.043	9.27	0.0062	6.90	0.74	180	144	42	4	40	3	78
CRMO11-04_S_87	396	1.25	45	0.103	22.31	0.0062	7.41	0.33	1979	375	100	21	40	3	98
CRMO11-04_S_77	1096	0.52	2067	0.041	11.59	0.0061	8.89	0.77	137	175	41	5	39	3	71
CRMO11-04_S_88	8038	0.28	5112	0.040	7.03	0.0061	5.77	0.82	87	95	40	3	39	2	55
CRMO11-04_S_84	7732	0.25	2660	0.040	7.12	0.0061	5.97	0.84	111	91	40	3	39	2	65
CRMO11-04_S_75	13822	0.18	36713	0.038	7.15	0.0060	6.16	0.86	18	87	38	3	39	2	118
CRMO11-04_S_81	19471	1.00	7211	0.040	7.23	0.0060	6.16	0.85	113	89	40	3	38	2	66
CRMO11-04_S_70	3203	0.31	3276	0.039	7.92	0.0059	6.80	0.86	98	96	39	3	38	3	61
CRMO11-04_M_171	5059	0.43	76102	0.051	8.79	0.0059	4.78	0.54	674	158	50	4	38	2	95
CRMO11-04_S_62	5025	0.28	9772	0.039	8.17	0.0059	6.95	0.85	64	102	38	3	38	3	41
CRMO11-04_S_78	16420	0.39	1626	0.039	8.09	0.0059	7.09	0.88	94	92	39	3	38	3	60
CRMO11-04_S_67	1079	0.78	478	0.041	13.07	0.0059	10.41	0.80	220	183	41	5	38	4	83
CRMO11-04_M_181	589	1.43	61	0.038	10.48	0.0059	5.14	0.49	77	217	38	4	38	2	51
CRMO11-04_S_71	15190	0.20	8569	0.038	6.89	0.0058	5.70	0.83	52	93	38	3	38	2	28
CRMO11-04_L_1	6445	0.28	8743	0.040	6.83	0.0058	5.75	0.84	153	86	39	3	38	2	76
CRMO11-04_M_172	2043	0.38	940	0.042	6.85	0.0058	4.82	0.70	312	111	42	3	38	2	88
CRMO11-04_S_61	12150	0.56	2057	0.039	7.64	0.0058	6.75	0.88	164	84	39	3	37	3	77
CRMO11-04_S_80	839	0.78	124	0.051	9.69	0.0058	6.56	0.68	725	151	50	5	37	2	95
CRMO11-04_S_73	8897	0.56	9847	0.040	8.08	0.0058	6.99	0.87	234	93	40	3	37	3	84
CRMO11-04_M_174	1747	0.44	683	0.036	6.34	0.0058	4.78	0.75	-13	101	36	2	37	2	394
CRMO11-04_S_60	1214	0.93	1626	0.039	11.55	0.0058	9.61	0.83	179	150	39	4	37	4	80
CRMO11-04_S_79	19918	0.36	17853	0.038	8.22	0.0057	7.25	0.88	90	92	38	3	37	3	59
CRMO11-04_S_55	449	0.76	161	0.050	10.23	0.0057	5.61	0.55	707	182	49	5	37	2	95
CRMO11-04_S_86	2342	0.73	308	0.037	7.33	0.0057	5.47	0.75	24	117	36	3	37	2	51

Spot	Corrected Isotope Ratios								Apparent ages (Ma)						
	U ppm	Th/U ppm	<u>206Pb</u> <u>204Pb</u>	<u>207Pb*</u> <u>235U*</u>	$\pm 2s$ (%)	<u>206Pb*</u> <u>238U</u>	$\pm 2s$ (%)	error corr.	<u>207Pb*</u> <u>206Pb*</u>	$\pm 2s$ (Ma)	<u>207Pb*</u> <u>235U</u>	$\pm 2s$ (Ma)	<u>206Pb*</u> <u>238U*</u>	$\pm 2s$ (Ma)	% disc.
CRMO11-04_S_64	1930	0.45	735	0.037	8.81	0.0057	6.98	0.79	66	128	37	3	37	3	45
CRMO11-04_S_83	1423	0.55	15768	0.038	8.18	0.0057	5.86	0.72	118	134	38	3	37	2	69
CRMO11-04_S_63	21338	0.36	6560	0.037	6.29	0.0057	5.36	0.85	91	78	37	2	37	2	60
CRMO11-04_M_180	440	1.41	254	0.041	10.35	0.0057	4.52	0.44	329	211	41	4	36	2	89
CRMO11-04_S_89	2297	0.48	601	0.036	7.68	0.0056	4.93	0.64	25	141	36	3	36	2	45
CRMO11-04_M_170	589	2.28	105	0.063	10.37	0.0056	6.01	0.58	1227	166	62	6	36	2	97
CRMO11-04_S_76	635	1.00	135	0.039	9.49	0.0056	5.77	0.61	198	175	39	4	36	2	82
CRMO11-04_S_90	700	0.90	1084	0.047	11.22	0.0056	6.15	0.55	613	203	46	5	36	2	94
CRMO11-04_M_177	2082	0.84	462	0.056	8.55	0.0056	4.72	0.55	976	145	55	5	36	2	97
CRMO11-04_M_178	4076	0.85	4120	0.039	5.75	0.0056	4.94	0.86	195	68	39	2	36	2	82
CRMO11-04_M_179	374	1.97	101	0.037	15.94	0.0056	5.15	0.32	72	359	37	6	36	2	50
CRMO11-04_S_72	1123	0.70	1518	0.038	8.13	0.0056	6.35	0.78	165	119	38	3	36	2	78
CRMO11-04_S_74	1176	0.47	183	0.033	9.92	0.0056	7.13	0.72	-133	170	33	3	36	3	127
CRMO11-04_L_2	316	0.60	117	0.079	15.88	0.0056	8.50	0.54	1690	247	78	12	36	3	98
CRMO11-04_M_182	13310	0.22	1103	0.036	7.22	0.0056	6.85	0.95	80	54	36	3	36	2	56
CRMO11-04_M_176	607	1.30	242	0.037	9.38	0.0055	5.83	0.62	133	173	37	3	35	2	74
CRMO11-04_M_173	843	0.97	299	0.041	11.33	0.0055	5.16	0.46	356	228	40	4	35	2	90
CRMO11-04_S_58	1004	0.87	86	0.051	11.03	0.0055	6.71	0.61	836	182	50	5	35	2	96
CRMO11-04_M_175	455	1.75	71	0.040	10.65	0.0055	4.67	0.44	325	217	40	4	35	2	89
CRMO11-04_M_169	1516	1.19	468	0.035	7.89	0.0054	5.15	0.65	14	144	34	3	35	2	149
CRMO11-04_M_168	16301	0.24	6242	0.043	13.33	0.0053	12.53	0.94	584	99	43	6	34	4	94

Spot	Corrected Isotope Ratios								Apparent ages (Ma)						
	U ppm	Th/U ppm	<u>206Pb</u> <u>204Pb</u>	<u>207Pb*</u> <u>235U*</u>	$\pm 2s$ (%)	<u>206Pb*</u> <u>238U</u>	$\pm 2s$ (%)	error corr.	<u>207Pb*</u> <u>206Pb*</u>	$\pm 2s$ (Ma)	<u>207Pb*</u> <u>235U</u>	$\pm 2s$ (Ma)	<u>206Pb*</u> <u>238U*</u>	$\pm 2s$ (Ma)	% disc.
CRMO11-05															
Paleoarchean															
CRMO11-05M_172	621	0.08	7822	27.533	2.86	0.6083	2.51	0.88	3609	21	3403	28	3063	61	19
CRMO11-05S_276	211	1.39	8309	27.558	2.74	0.6553	2.26	0.83	3496	24	3403	27	3249	58	9
Mesoarchean 1															
<i>CRMO11S-05_90</i>	1280	0.02	39942	18.755	2.47	0.5304	2.13	0.86	3225	20	3029	24	2743	47	18
<i>CRMO11-05S_267</i>	481	0.04	3297	19.378	2.17	0.5481	1.86	0.86	3225	18	3061	21	2817	43	16
CRMO11-05S_270	543	0.08	7666	19.286	3.04	0.5528	2.90	0.95	3204	14	3056	29	2837	66	14

Spot	Corrected Isotope Ratios								Apparent ages (Ma)						
	U ppm	Th/U ppm	<u>206Pb</u> <u>204Pb</u>	<u>207Pb*</u> <u>235U*</u>	$\pm 2s$ (%)	<u>206Pb*</u> <u>238U</u>	$\pm 2s$ (%)	error corr.	<u>207Pb*</u> <u>206Pb*</u>	$\pm 2s$ (Ma)	<u>207Pb*</u> <u>235U</u>	$\pm 2s$ (Ma)	<u>206Pb*</u> <u>238U*</u>	$\pm 2s$ (Ma)	% disc.
CRMO11-05L_228	4177	0.01	56051	19.518	2.76	0.5641	2.17	0.79	3191	27	3068	27	2884	51	12
CRMO11-05M_176	584	0.04	147077	17.609	2.66	0.5121	2.06	0.78	3181	27	2969	26	2665	45	20
CRMO11-05S_265	909	0.02	11239	19.332	2.55	0.5671	2.31	0.91	3167	17	3059	25	2896	54	11
CRMO11-05S_269	895	0.05	9191	14.297	4.16	0.4224	3.55	0.85	3156	35	2770	39	2271	68	33
CRMO11-05L_224A	2203	0.04	71460	15.343	2.36	0.4580	2.09	0.88	3140	18	2837	23	2431	42	27
CRMO11S-05_80	504	0.02	23429	19.407	1.92	0.5817	1.75	0.91	3133	12	3062	19	2956	42	7
CRMO11-05S_271	629	0.14	6067	15.064	12.47	0.4524	11.57	0.93	3130	74	2819	119	2406	232	28
CRMO11-05L_224B	1640	0.04	25155	15.507	3.35	0.4787	3.25	0.97	3086	12	2847	32	2522	68	22
CRMO11-05L_221	513	0.04	94089	18.624	4.01	0.5762	3.46	0.86	3082	32	3023	39	2933	82	6
CRMO11S-05_82	790	0.06	10889	16.621	2.55	0.5161	2.27	0.89	3077	19	2913	24	2683	50	16
CRMO11-05M_178	483	0.02	7507	16.811	3.63	0.5237	3.24	0.89	3072	26	2924	35	2715	72	14
CRMO11-05S_266	313	0.02	19034	17.916	3.08	0.5631	2.59	0.84	3057	26	2985	30	2879	60	7
CRMO11S-05_89	1290	0.04	28541	15.052	1.93	0.4764	1.58	0.82	3046	18	2819	18	2511	33	21
CRMO11-05M_243	768	0.07	4532	15.484	4.29	0.5028	3.53	0.82	3005	39	2845	41	2626	76	15
CRMO11S-05_83	708	0.08	8289	14.029	1.87	0.4565	1.59	0.85	3002	16	2752	18	2424	32	23
CRMO11-05L_219	976	0.05	17473	16.960	2.17	0.5521	1.97	0.91	3001	15	2933	21	2834	45	7
CRMO11S-05_88	603	0.04	4377	15.110	1.75	0.4920	1.46	0.83	3001	16	2822	17	2579	31	17
Neoproterozoic															
CRMO11-05M_242	4907	0.04	51864	16.629	4.97	0.5435	4.52	0.91	2995	33	2914	48	2798	103	8
CRMO11-05S_273	270	0.12	4571	17.396	5.87	0.5780	5.20	0.89	2968	44	2957	56	2941	123	1
CRMO11-05M_168	952	0.07	15074	12.099	4.07	0.4082	3.19	0.78	2943	41	2612	38	2207	60	29
CRMO11-05M_173	96	0.38	3793	16.449	4.06	0.5583	3.59	0.88	2934	31	2903	39	2860	83	3
CRMO11-05S_274	141	0.42	10344	14.610	3.81	0.5010	3.51	0.92	2917	24	2790	36	2618	75	12
CRMO11S-05_93	753	0.19	8901	14.633	1.87	0.5035	1.73	0.93	2912	11	2792	18	2629	37	12
CRMO11-05S_275	223	0.49	82212	13.507	4.47	0.4694	4.00	0.89	2895	33	2716	42	2481	82	17
CRMO11-05S_268	217	0.55	1550	12.745	2.86	0.4528	2.23	0.78	2860	29	2661	27	2408	45	19
CRMO11S-05_91	227	0.49	29235	13.920	2.39	0.5024	1.91	0.80	2834	23	2744	23	2624	41	9
CRMO11-05M_167	217	0.31	14993	13.084	4.53	0.4722	4.17	0.92	2834	29	2686	43	2493	86	14
CRMO11-05L_217	171	0.62	7462	13.421	2.76	0.4903	1.98	0.72	2814	31	2710	26	2572	42	10
CRMO11-05M_245B	182	0.68	4282	11.706	6.23	0.4288	5.47	0.88	2810	49	2581	58	2300	106	21
CRMO11-05M_177	104	0.81	22895	12.324	3.86	0.4524	3.44	0.89	2806	29	2629	36	2406	69	17
CRMO11-05M_244	114	0.93	9043	9.323	5.16	0.3430	4.08	0.79	2803	52	2370	47	1901	67	37
CRMO11S-05_81	137	0.70	8405	13.591	2.20	0.5008	1.83	0.83	2800	20	2722	21	2617	39	8
CRMO11S-05_92	96	1.23	2522	12.615	3.14	0.4649	2.65	0.85	2800	27	2651	30	2461	54	15

Spot	Corrected Isotope Ratios								Apparent ages (Ma)						
	U ppm	Th/U ppm	<u>206Pb</u> 204Pb	<u>207Pb*</u> 235U*	±2s (%)	<u>206Pb*</u> 238U	±2s (%)	error corr.	<u>207Pb*</u> 206Pb*	±2s (Ma)	<u>207Pb*</u> 235U	±2s (Ma)	<u>206Pb*</u> 238U*	±2s (Ma)	% disc.
CRMO11-05L_226	95	1.13	7540	11.488	2.57	0.4263	2.28	0.89	2789	20	2564	24	2289	44	21
CRMO11-05M_245A	188	0.66	2341	11.471	7.93	0.4266	5.86	0.74	2785	88	2562	74	2291	113	21
CRMO11S-05_84	75	1.84	4387	13.980	2.99	0.5210	2.29	0.76	2782	32	2748	28	2703	50	3
CRMO11-05M_171	212	0.49	7798	13.420	2.79	0.5010	2.57	0.92	2779	18	2710	26	2618	55	7
CRMO11-05M_174	139	0.71	1934	12.365	2.91	0.4618	2.26	0.77	2778	30	2633	27	2448	46	14
CRMO11-05L_220	202	1.09	12571	13.894	2.93	0.5208	2.67	0.91	2772	20	2742	28	2703	59	3
CRMO11S-05_86	189	0.69	5656	12.886	3.38	0.4831	2.98	0.88	2772	26	2671	32	2541	63	10
CRMO11S-05_85	188	0.92	3758	12.963	3.44	0.4870	3.08	0.90	2768	25	2677	32	2558	65	9
CRMO11-05L_218	105	1.03	820	13.053	2.91	0.4909	2.37	0.81	2767	28	2683	27	2574	50	8
CRMO11-05L_229	259	0.39	12045	10.885	2.27	0.4095	1.90	0.84	2766	20	2513	21	2213	36	24
CRMO11S-05_87	69	2.54	1445	11.712	2.35	0.4411	2.02	0.86	2764	20	2582	22	2356	40	18
CRMO11-05L_223	96	1.18	2301	10.542	5.79	0.3975	5.17	0.89	2762	43	2484	54	2158	95	26
CRMO11-05M_169	330	0.53	113037	13.930	3.13	0.5257	2.58	0.82	2761	29	2745	30	2723	57	2
CRMO11-05L_227	119	0.95	11741	11.902	2.54	0.4516	2.16	0.85	2752	22	2597	24	2402	43	15
CRMO11-05L_222	74	1.13	830	11.270	2.97	0.4282	2.17	0.73	2750	33	2546	28	2298	42	20
CRMO11-05M_170	44	2.90	2962	14.100	4.30	0.5391	3.79	0.88	2740	33	2756	41	2780	86	2
CRMO11-05M_175	116	0.83	1300	11.200	3.32	0.4330	2.80	0.85	2721	29	2540	31	2319	55	18

Spot	Corrected Isotope Ratios								Apparent ages (Ma)						
	U ppm	Th/U ppm	<u>206Pb</u> 204Pb	<u>207Pb*</u> 235U*	±2s (%)	<u>206Pb*</u> 238U	±2s (%)	error corr.	<u>207Pb*</u> 206Pb*	±2s (Ma)	<u>207Pb*</u> 235U	±2s (Ma)	<u>206Pb*</u> 238U*	±2s (Ma)	% disc.
CRMO11-07															
Mesoarchean 1															
CRMO11-07_M_127	2033	0.71	4190	16.932	8.36	0.5198	7.94	0.95	3095	42	2931	80	2699	175	16
CRMO11-07_S_211	2455	0.49	26398	17.681	9.57	0.5448	9.17	0.96	3089	44	2973	92	2803	208	11
CRMO11-07_S_206	3210	0.69	11470	16.923	8.61	0.5265	8.28	0.96	3074	37	2931	83	2727	184	14
CRMO11-07_M_131	1543	0.43	517	2.794	11.82	0.0871	10.09	0.85	3071	98	1354	88	538	52	86
CRMO11-07_S_207	1770	0.48	5933	17.280	8.39	0.5477	7.95	0.95	3044	43	2951	81	2816	181	9
CRMO11-07_M_140	2963	0.18	54345	15.946	9.00	0.5085	8.61	0.96	3034	42	2874	86	2650	187	15
CRMO11-07_M_133	1733	0.72	50942	10.094	9.55	0.3285	9.01	0.94	3001	51	2443	88	1831	144	45
CRMO11-07_M_130	12942	0.23	155025	15.261	10.05	0.5119	9.69	0.96	2953	43	2832	96	2665	211	12
Neoarchean															
CRMO11-07_M_128	2424	0.50	2189	11.837	9.41	0.4012	9.00	0.96	2936	44	2592	88	2175	166	30

Spot	Corrected Isotope Ratios								Apparent ages (Ma)						
	U ppm	Th/U ppm	<u>206Pb</u> <u>204Pb</u>	<u>207Pb*</u> <u>235U*</u>	$\pm 2s$ (%)	<u>206Pb*</u> <u>238U</u>	$\pm 2s$ (%)	error corr.	<u>207Pb*</u> <u>206Pb*</u>	$\pm 2s$ (Ma)	<u>207Pb*</u> <u>235U</u>	$\pm 2s$ (Ma)	<u>206Pb*</u> <u>238U*</u>	$\pm 2s$ (Ma)	% disc.
<i>CRMO11-07_M_129</i>	2538	0.54	4186	15.223	9.04	0.5165	8.61	0.95	2934	45	2829	86	2684	189	10
<i>CRMO11-07_M_141</i>	22589	0.32	178909	14.360	9.57	0.4898	9.26	0.97	2926	39	2774	91	2570	196	15
CRMO11-07_M_134	1191	0.52	1150	10.089	8.78	0.3460	8.14	0.93	2917	53	2443	81	1916	135	40
<i>CRMO11-07_S_218</i>	1319	0.56	1948	14.349	8.93	0.4926	8.42	0.94	2915	48	2773	85	2582	179	14
CRMO11-07_S_216	1682	0.44	1654	9.994	8.52	0.3457	8.00	0.94	2903	48	2434	79	1914	132	39
CRMO11-07_S_212	1836	0.55	3791	10.831	12.35	0.3804	12.08	0.98	2878	42	2509	115	2078	215	32
CRMO11-07_M_138	17923	0.25	20674	12.627	14.47	0.4556	13.88	0.96	2834	67	2652	136	2420	280	17
CRMO11-07_M_139	1371	0.51	3237	7.690	9.11	0.2788	8.58	0.94	2827	50	2195	82	1585	121	49
CRMO11-07_M_135	893	0.44	4948	11.419	8.91	0.4193	8.54	0.96	2806	42	2558	83	2257	163	23
CRMO11-07_S_217	2334	0.53	2285	6.942	9.17	0.2552	8.83	0.96	2804	41	2104	81	1465	116	53
CRMO11-07_S_220	1367	0.37	3234	9.255	8.78	0.3420	8.26	0.94	2795	49	2364	80	1897	136	37
CRMO11-07_S_209	1365	0.76	2877	12.843	9.08	0.4839	8.67	0.96	2764	44	2668	86	2544	182	10
CRMO11-07_S_213	2281	0.31	4650	12.528	8.70	0.4886	8.34	0.96	2707	41	2645	82	2565	177	6
CRMO11-07_M_136	4716	0.07	1219	2.932	12.28	0.1155	10.60	0.86	2690	103	1390	93	705	71	78

Spot	Corrected Isotope Ratios								Apparent ages (Ma)						
	U ppm	Th/U ppm	<u>206Pb</u> <u>204Pb</u>	<u>207Pb*</u> <u>235U*</u>	$\pm 2s$ (%)	<u>206Pb*</u> <u>238U</u>	$\pm 2s$ (%)	error corr.	<u>207Pb*</u> <u>206Pb*</u>	$\pm 2s$ (Ma)	<u>207Pb*</u> <u>235U</u>	$\pm 2s$ (Ma)	<u>206Pb*</u> <u>238U*</u>	$\pm 2s$ (Ma)	% disc.
CRMO11-12															
Paleoarchean															
CRMO11-12_S_184	6802	0.40	66337	24.549	8.51	0.6089	8.18	0.96	3430	37	3290	83	3066	200	13
CRMO11-12_L_17	551	0.71	18842	19.961	9.34	0.5013	8.32	0.89	3411	66	3089	90	2620	179	28
Mesoarchean I															
<i>CRMO11-12_L_14</i>	588	0.66	16607	18.595	6.89	0.5091	6.25	0.91	3276	46	3021	66	2653	136	23
CRMO11-12_S_179	2875	0.60	3681	14.077	8.90	0.4107	8.54	0.96	3176	40	2755	84	2218	160	35
CRMO11-12_L_13	3148	0.95	1042914	14.303	6.34	0.4189	5.56	0.88	3170	48	2770	60	2256	106	34
CRMO11-12_L_7	529	0.45	15021	13.886	8.11	0.4110	7.43	0.92	3153	52	2742	77	2220	139	35
CRMO11-12_S_190	10278	0.19	12948	10.442	10.75	0.3237	10.15	0.94	3079	57	2475	100	1808	160	47
CRMO11-12_L_36	1481	0.47	39941	8.718	10.18	0.2756	9.62	0.95	3048	53	2309	93	1569	134	54
Neoarchean															
CRMO11-12_L_31	1349	0.10	11664	10.208	7.92	0.3704	6.60	0.83	2825	71	2454	73	2031	115	33
CRMO11-12_L_16	2972	0.19	32900	9.930	8.77	0.3638	7.97	0.91	2809	60	2428	81	2000	137	33
CRMO11-12_S_181	20648	0.36	234933	9.415	8.08	0.3556	7.73	0.96	2760	39	2379	74	1961	131	33

Spot	Corrected Isotope Ratios								Apparent ages (Ma)						
	U ppm	Th/U ppm	<u>206Pb</u> <u>204Pb</u>	<u>207Pb*</u> <u>235U*</u>	$\pm 2s$ (%)	<u>206Pb*</u> <u>238U</u>	$\pm 2s$ (%)	error corr.	<u>207Pb*</u> <u>206Pb*</u>	$\pm 2s$ (Ma)	<u>207Pb*</u> <u>235U</u>	$\pm 2s$ (Ma)	<u>206Pb*</u> <u>238U*</u>	$\pm 2s$ (Ma)	% disc.
CRMO11-12_S_201	8286	0.13	7433	8.000	8.91	0.3038	7.96	0.89	2751	66	2231	80	1710	120	43
CRMO11-12_L_26	362	0.42	19200	10.412	8.16	0.4002	7.63	0.94	2731	48	2472	76	2170	141	24
CRMO11-12_L_22	1261	0.11	22962	4.708	6.61	0.1846	5.95	0.90	2698	47	1769	55	1092	60	64
CRMO11-12_S_178	3498	0.27	8569	12.867	10.04	0.5157	9.30	0.93	2662	63	2670	95	2681	204	1
CRMO11-12_L_29	1128	0.12	20890	6.399	8.42	0.2601	7.93	0.94	2639	47	2032	74	1490	106	49
CRMO11-12_L_12B	1265	0.49	3207	3.340	7.61	0.1378	7.02	0.92	2614	49	1490	59	832	55	72
CRMO11-12_S_185	19679	0.06	131509	8.266	8.42	0.3413	7.85	0.93	2612	51	2261	76	1893	129	32
Paleoproterozoic															
CRMO11-12_L_12A	937	0.43	6361	2.411	7.63	0.1010	6.84	0.90	2589	57	1246	55	620	40	80
CRMO11-12_S_189	29844	0.07	458571	9.861	8.79	0.4137	8.34	0.95	2586	46	2422	81	2232	157	16
CRMO11-12_S_196	17590	0.07	54162	5.932	9.02	0.2524	8.63	0.96	2562	44	1966	78	1451	112	48
CRMO11-12_L_25	2249	0.26	41274	8.492	6.31	0.3622	5.78	0.92	2558	42	2285	57	1993	99	26
CRMO11-12_S_203	13230	0.13	51433	4.712	8.45	0.2010	8.00	0.95	2558	46	1769	71	1181	86	59
CRMO11-12_S_200	7127	0.32	21137	9.253	8.26	0.3948	7.92	0.96	2557	39	2363	76	2145	145	19
CRMO11-12_S_197	15375	0.12	17170	8.101	9.00	0.3461	8.68	0.96	2555	40	2242	81	1916	144	29
CRMO11-12_L_18	66	1.83	11471	12.054	10.06	0.5171	9.48	0.94	2548	56	2609	94	2687	208	7
CRMO11-12_L_34	2045	0.23	59551	6.855	6.23	0.2944	5.45	0.87	2546	51	2093	55	1664	80	39
CRMO11-12_L_32	1140	0.29	45691	8.607	6.17	0.3700	5.64	0.91	2545	42	2297	56	2029	98	24
CRMO11-12_L_8	47	1.77	945	10.039	17.77	0.4326	17.45	0.98	2541	56	2438	164	2318	340	10
CRMO11-12_L_21	1719	0.23	169476	8.947	6.52	0.3864	5.99	0.92	2537	43	2333	60	2106	108	20
CRMO11-12_L_9	1134	0.35	16584	6.795	8.90	0.2936	8.50	0.96	2537	44	2085	79	1659	124	39
CRMO11-12_L_19	52	2.00	813	10.717	7.09	0.4649	6.14	0.87	2530	60	2499	66	2461	126	3
CRMO11-12_S_191	17954	0.18	134380	7.812	10.73	0.3401	10.38	0.97	2524	46	2210	97	1887	170	29
CRMO11-12_S_199	23883	0.15	16782	9.038	8.56	0.3946	8.19	0.96	2519	41	2342	78	2144	149	17
CRMO11-12_L_37A	915	0.45	10293	10.333	7.00	0.4515	6.25	0.89	2518	53	2465	65	2402	125	5
CRMO11-12_S_202	30276	0.07	20528	7.550	9.47	0.3299	9.19	0.97	2518	39	2179	85	1838	147	31
CRMO11-12_S_187	2557	0.49	911	6.769	16.95	0.2976	16.73	0.99	2507	46	2082	150	1679	247	37
CRMO11-12_L_23	2285	0.12	17518	6.640	5.84	0.2931	5.26	0.90	2500	43	2065	52	1657	77	38
CRMO11-12_L_20	124	3.06	4620	5.708	7.14	0.2526	6.37	0.89	2496	54	1933	62	1452	83	47
CRMO11-12_S_188	3927	0.44	3055	8.683	9.12	0.3845	8.67	0.95	2495	48	2305	83	2097	155	19
CRMO11-12_S_204	15582	0.12	396079	7.537	9.76	0.3357	9.48	0.97	2485	39	2177	87	1866	154	29
CRMO11-12_L_35	73	1.81	803	6.558	10.21	0.2932	9.48	0.93	2479	64	2054	90	1657	139	37
CRMO11-12_S_182	2003	0.73	11579	9.996	8.66	0.4486	8.30	0.96	2473	42	2434	80	2389	166	4
CRMO11-12_S_194	1224	0.87	19870	6.465	12.55	0.2903	12.25	0.98	2472	46	2041	110	1643	178	38

Spot	Corrected Isotope Ratios								Apparent ages (Ma)						
	U ppm	Th/U ppm	<u>206Pb</u> 204Pb	<u>207Pb*</u> 235U*	±2s (%)	<u>206Pb*</u> 238U	±2s (%)	error corr.	<u>207Pb*</u> 206Pb*	±2s (Ma)	<u>207Pb*</u> 235U	±2s (Ma)	<u>206Pb*</u> 238U*	±2s (Ma)	% disc.
CRMO11-12_L_10	319	1.91	7918	7.970	7.70	0.3612	7.05	0.92	2456	52	2228	69	1988	121	22
CRMO11-12_S_180	1154	0.53	2295	7.478	8.57	0.3400	8.07	0.94	2450	49	2170	77	1887	132	26
CRMO11-12_L_24	576	0.91	7253	7.936	6.42	0.3615	5.63	0.88	2447	52	2224	58	1989	96	22
CRMO11-12_S_192	2377	1.80	1545	8.797	9.43	0.4018	9.02	0.96	2443	46	2317	86	2177	167	13
CRMO11-12_L_33	249	0.71	4737	5.793	6.77	0.2651	6.09	0.90	2440	50	1945	59	1516	82	42
CRMO11-12_L_30	185	0.63	1566	6.723	7.46	0.3081	6.95	0.93	2437	46	2076	66	1731	105	33
CRMO11-12_L_11	202	2.53	10017	7.310	6.73	0.3354	6.10	0.91	2435	48	2150	60	1864	99	27
CRMO11-12_S_183	26998	0.07	45258	5.524	8.56	0.2535	8.21	0.96	2435	41	1904	74	1456	107	45
CRMO11-12_L_15	542	0.60	52191	7.264	7.15	0.3340	6.59	0.92	2432	47	2144	64	1858	106	27
CRMO11-12_L_28	367	1.60	11189	8.839	7.30	0.4083	6.76	0.93	2424	47	2322	67	2207	126	11

Spot	Corrected Isotope Ratios								Apparent ages (Ma)						
	U ppm	Th/U ppm	<u>206Pb</u> 204Pb	<u>207Pb*</u> 235U*	±2s (%)	<u>206Pb*</u> 238U	±2s (%)	error corr.	<u>207Pb*</u> 206Pb*	±2s (Ma)	<u>207Pb*</u> 235U	±2s (Ma)	<u>206Pb*</u> 238U*	±2s (Ma)	% disc.
CRMO11-13 Mesoarchean 2															
CRMO11-13_S_177	1008	1.17	1995	22.397	8.74	0.6187	8.41	0.96	3262	37	3201	85	3105	207	6
CRMO11-13_S_175	1867	1.33	48490	20.077	8.92	0.5621	8.50	0.95	3241	43	3095	86	2875	197	14
CRMO11-13_L_5	86	1.23	967	14.938	7.91	0.4240	7.37	0.93	3219	45	2811	75	2278	142	35
CRMO11-13_S_164	1209	1.11	4855	20.872	9.19	0.6010	8.69	0.95	3197	47	3133	89	3034	210	6
CRMO11-13_S_166	5375	1.07	116555	21.535	11.45	0.6234	11.16	0.98	3188	40	3163	111	3123	276	3
CRMO11-13_S_160	1408	0.79	226326	18.822	8.99	0.5553	8.52	0.95	3158	45	3033	87	2847	196	12
CRMO11-13_S_144	1133	0.72	5662	19.475	8.80	0.5747	8.37	0.95	3158	43	3066	85	2927	197	9
CRMO11-13_S_157	1988	1.13	7471	15.842	10.08	0.4797	9.42	0.93	3117	57	2867	96	2526	197	23
CRMO11-13_L_3B	86	1.49	30659	19.198	7.71	0.5925	6.96	0.90	3086	53	3052	74	3000	167	4
CRMO11-13_S_152	1862	1.31	2959	15.602	8.59	0.4825	8.04	0.94	3083	48	2853	82	2538	169	21
CRMO11-13_S_161	436	0.58	731	19.457	10.45	0.6092	9.46	0.91	3063	71	3065	101	3067	231	0
CRMO11-13_S_150	905	1.42	1595	13.892	10.74	0.4364	10.22	0.95	3058	53	2742	102	2335	200	28
CRMO11-13_S_172	2041	1.07	3345	14.956	9.86	0.4700	9.44	0.96	3057	46	2812	94	2484	195	23
CRMO11-13_S_176	1902	0.74	1750	16.999	9.04	0.5389	8.29	0.92	3044	58	2935	87	2779	187	11
CRMO11-13_S_151	882	0.71	2771	18.944	8.86	0.6092	8.44	0.95	3020	43	3039	85	3067	206	2

Spot	Corrected Isotope Ratios								Apparent ages (Ma)						
	U ppm	Th/U ppm	<u>206Pb</u> 204Pb	<u>207Pb*</u> 235U*	±2s (%)	<u>206Pb*</u> 238U	±2s (%)	error corr.	<u>207Pb*</u> 206Pb*	±2s (Ma)	<u>207Pb*</u> 235U	±2s (Ma)	<u>206Pb*</u> 238U*	±2s (Ma)	% disc.
Neoproterozoic															
CRMO11-13_S_159	1428	0.79	1107	8.859	9.37	0.2915	8.63	0.92	2984	59	2324	85	1649	126	50
CRMO11-13_L_6	150	1.31	14202	16.094	6.36	0.5304	5.76	0.91	2981	44	2882	61	2743	129	10
CRMO11-13_S_142	2270	1.67	3507	7.234	8.91	0.2382	8.54	0.96	2983	41	2141	80	1377	106	60
CRMO11-13_S_165	1032	0.80	9299	18.764	8.90	0.6370	8.52	0.96	2933	42	3030	86	3177	214	11
CRMO11-13_S_147	4296	0.61	25569	14.051	9.48	0.4822	9.15	0.96	2916	41	2753	90	2537	192	16
CRMO11-13_L_3A	44	1.25	6445	17.712	9.52	0.6185	8.52	0.90	2888	69	2974	91	3104	210	9
CRMO11-13_S_154	1643	1.07	963	11.195	9.34	0.4098	8.93	0.96	2811	45	2539	87	2214	167	25
CRMO11-13_S_146	2852	0.63	69901	11.328	9.14	0.4184	8.51	0.93	2796	55	2550	85	2253	162	23
CRMO11-13_S_168	1202	0.71	956	8.764	8.97	0.3339	8.35	0.93	2745	54	2314	82	1857	135	37
CRMO11-13_S_162	13525	0.45	78335	11.004	9.17	0.4196	8.65	0.94	2744	50	2524	85	2259	165	21
CRMO11-13_S_173	767	0.64	9329	6.833	10.73	0.2659	10.19	0.95	2711	56	2090	95	1520	138	49
CRMO11-13_L_2	128	0.72	2092	12.070	7.99	0.4729	6.31	0.79	2699	81	2610	75	2496	131	9
CRMO11-13_S_174	2220	0.59	2245	5.829	9.56	0.2300	8.68	0.91	2688	66	1951	83	1334	105	56
CRMO11-13_S_156	1288	0.61	1890	10.406	9.02	0.4120	8.31	0.92	2682	58	2472	84	2224	156	20
CRMO11-13_S_148	2917	0.94	1839	6.322	8.59	0.2548	8.22	0.96	2652	41	2021	75	1463	108	50
CRMO11-13_L_1	16	0.98	502	12.259	10.66	0.4970	6.54	0.61	2642	140	2624	100	2601	140	2
CRMO11-13_S_143	714	0.12	457	10.379	13.03	0.4230	11.06	0.85	2634	115	2469	121	2274	212	16
CRMO11-13_S_153	3549	0.34	3543	9.450	12.10	0.4050	11.76	0.97	2550	48	2383	111	2192	219	17
CRMO11-13_S_169	1733	1.10	831	3.396	9.99	0.1463	9.52	0.95	2541	51	1503	78	880	78	70
CRMO11-13_S_149	186	0.51	403	13.833	15.56	0.6072	15.07	0.97	2510	65	2738	147	3059	367	28
CRMO11-13_S_171	212	0.49	857	8.547	10.22	0.3960	8.44	0.83	2419	98	2291	93	2151	154	13

Spot	Corrected Isotope Ratios								Apparent ages (Ma)						
	U ppm	Th/U ppm	<u>206Pb</u> 204Pb	<u>207Pb*</u> 235U*	±2s (%)	<u>206Pb*</u> 238U	±2s (%)	error corr.	<u>207Pb*</u> 206Pb*	±2s (Ma)	<u>207Pb*</u> 235U	±2s (Ma)	<u>206Pb*</u> 238U*	±2s (Ma)	% disc.
CRMO11-14 Paleoproterozoic															
CRMO11-14S_98	297	0.59	8848	31.202	7.26	0.6177	6.42	0.88	3776	51	3525	71	3101	158	22
CRMO11-14S_83	42	0.91	3700	35.136	6.39	0.7242	5.50	0.86	3715	49	3642	63	3512	149	7
CRMO11-14S_86	1062	0.55	105382	32.428	6.85	0.6966	6.00	0.88	3652	50	3563	67	3408	159	9
CRMO11-14M_44	964	0.31	47716	26.892	8.55	0.5835	7.86	0.92	3637	52	3380	84	2963	187	23

Spot	Corrected Isotope Ratios								Apparent ages (Ma)						% disc.
	U ppm	Th/U ppm	<u>206Pb</u> / <u>204Pb</u>	<u>207Pb*</u> / <u>235U*</u>	±2s (%)	<u>206Pb*</u> / <u>238U</u>	±2s (%)	error corr.	<u>207Pb*</u> / <u>206Pb*</u>	±2s (Ma)	<u>207Pb*</u> / <u>235U</u>	±2s (Ma)	<u>206Pb*</u> / <u>238U*</u>	±2s (Ma)	
CRMO11-14S_89	817	0.13	267647	27.711	10.02	0.6229	9.45	0.94	3582	51	3409	98	3121	234	16
CRMO11-14S_92	1856	0.66	815410	27.705	7.58	0.6271	6.83	0.90	3572	51	3409	74	3138	170	15
CRMO11-14M_41	582	0.07	25645	25.341	7.51	0.5763	6.69	0.89	3565	52	3321	73	2934	158	22
CRMO11-14M_40	456	0.21	21224	24.409	6.86	0.5608	5.90	0.86	3549	54	3285	67	2870	137	24
CRMO11-14L_17B	256	0.84	4997	20.918	8.69	0.4867	7.06	0.81	3529	78	3135	84	2556	149	33
CRMO11-14M_46	133	0.54	7984	27.966	7.65	0.6699	6.87	0.90	3485	52	3418	75	3305	178	7
CRMO11-14M_45B	997	0.11	374186	22.983	7.74	0.5591	6.69	0.86	3461	60	3226	75	2863	155	21
CRMO11-14M_42	2327	0.24	250386	22.173	7.89	0.5532	7.02	0.89	3421	56	3191	77	2839	161	21
CRMO11-14L_31B	889	0.75	664032	24.385	13.99	0.6086	10.88	0.78	3421	137	3284	136	3064	265	13
CRMO11-14M_45A	165	0.40	10085	22.061	9.94	0.5509	9.25	0.93	3420	57	3186	97	2829	212	21
Mesoarchean 2															
CRMO11-14M_34	1411	0.35	167300	19.585	8.18	0.5356	7.31	0.89	3278	58	3071	79	2765	164	19
CRMO11-14XL_25	511	0.30	13836	18.164	6.98	0.4969	6.20	0.89	3278	51	2998	67	2600	133	25
CRMO11-14L_13	769	0.56	15688	18.431	6.80	0.5091	6.04	0.89	3262	49	3013	66	2653	131	23
CRMO11-14XL_33	580	0.43	58557	19.988	6.45	0.5538	5.54	0.86	3257	52	3091	62	2841	127	16
CRMO11-14M_65	892	0.49	790652	22.478	6.71	0.6231	5.76	0.86	3257	54	3205	65	3122	143	5
CRMO11-14L_17A	118	0.72	3993	16.392	7.92	0.4557	7.11	0.90	3252	55	2900	76	2421	144	31
CRMO11-14M_56	828	0.47	31954	19.323	6.86	0.5373	5.84	0.85	3252	57	3058	66	2772	132	18
CRMO11-14L_24	460	0.70	17793	19.626	5.93	0.5480	5.04	0.85	3245	49	3073	57	2817	115	16
CRMO11-14XL_31	803	0.57	3420801	21.484	6.95	0.6001	6.20	0.89	3245	50	3161	67	3030	150	8
CRMO11-14XL_36	904	0.61	28439	21.165	6.73	0.5912	5.90	0.88	3245	51	3146	65	2994	141	10
CRMO11-14L_1	863	0.67	47870	20.628	6.86	0.5765	5.96	0.87	3244	54	3121	66	2935	140	12
CRMO11-14XL_27	159	0.27	367487	20.216	7.88	0.5655	7.06	0.90	3242	55	3102	76	2889	164	13
CRMO11-14M_39	606	0.40	14380	16.892	7.03	0.4732	6.04	0.86	3240	57	2929	67	2498	125	28
CRMO11-14L_22	658	0.58	25435	20.183	7.13	0.5656	6.35	0.89	3239	51	3100	69	2890	148	13
CRMO11-14L_6	1001	0.67	886973	19.927	7.19	0.5603	6.46	0.90	3234	50	3088	70	2868	149	14
CRMO11-14M_38	861	0.46	552990	18.851	7.45	0.5300	6.58	0.88	3234	55	3034	72	2742	147	19
CRMO11-14S_97	592	0.50	76248	21.645	6.97	0.6088	6.06	0.87	3234	54	3168	68	3065	148	7
CRMO11-14XL_20	846	0.58	36058	21.672	6.24	0.6101	5.45	0.87	3232	48	3169	61	3070	133	6
CRMO11-14M_67	589	0.49	72192	20.848	7.64	0.5873	6.66	0.87	3231	59	3132	74	2979	159	10
CRMO11-14XL_24	615	0.47	27183	20.893	6.60	0.5893	5.84	0.88	3229	49	3134	64	2987	140	9
CRMO11-14S_91	851	0.52	48932	21.540	6.86	0.6080	6.08	0.89	3228	50	3163	67	3062	148	6
CRMO11-14L_23	573	0.52	10040	19.269	6.44	0.5446	5.58	0.87	3226	51	3055	62	2803	127	16
CRMO11-14M_51	1016	0.59	250405	21.941	8.78	0.6202	7.99	0.91	3226	57	3181	85	3111	197	4

Spot	Corrected Isotope Ratios								Apparent ages (Ma)						
	U ppm	Th/U ppm	<u>206Pb</u> <u>204Pb</u>	<u>207Pb*</u> <u>235U*</u>	$\pm 2s$ (%)	<u>206Pb*</u> <u>238U</u>	$\pm 2s$ (%)	error corr.	<u>207Pb*</u> <u>206Pb*</u>	$\pm 2s$ (Ma)	<u>207Pb*</u> <u>235U</u>	$\pm 2s$ (Ma)	<u>206Pb*</u> <u>238U*</u>	$\pm 2s$ (Ma)	% disc.
CRMO11-14L_29	1327	0.92	29116	20.878	6.59	0.5905	5.74	0.87	3225	51	3133	64	2992	137	9
CRMO11-14XL_21	366	0.38	51734	21.370	6.84	0.6045	6.11	0.89	3225	48	3156	66	3048	148	7
CRMO11-14XL_37	522	0.55	348313	21.502	6.67	0.6084	5.96	0.89	3224	47	3161	65	3064	145	6
CRMO11-14XL_19	978	0.58	41478	20.389	6.21	0.5771	5.41	0.87	3224	48	3110	60	2937	128	11
CRMO11-14L_14	467	0.52	23327	20.467	8.07	0.5796	7.43	0.92	3223	49	3114	78	2947	176	11
CRMO11-14L_7	494	0.57	166908	20.021	7.11	0.5671	6.37	0.90	3223	50	3092	69	2896	149	13
CRMO11-14L_16	632	0.64	22953	20.871	7.12	0.5912	6.40	0.90	3223	49	3133	69	2994	153	9
CRMO11-14XL_23	862	0.51	82342	22.023	7.34	0.6248	6.56	0.89	3220	52	3185	71	3129	163	4
CRMO11-14M_64	578	0.42	15717	20.371	7.65	0.5781	6.85	0.89	3220	54	3109	74	2941	162	11
CRMO11-14S_90	881	0.56	27926	21.142	7.89	0.6003	7.16	0.91	3219	52	3145	77	3031	173	7
CRMO11-14L_12	745	0.71	28540	19.361	6.80	0.5514	5.96	0.88	3214	52	3060	66	2831	137	15
CRMO11-14M_35	248	0.35	40437	19.285	7.02	0.5506	6.01	0.85	3210	58	3056	68	2828	137	15
CRMO11-14L_4	1515	0.80	50064	20.558	6.93	0.5871	6.19	0.89	3210	50	3118	67	2978	147	9
CRMO11-14M_61	526	0.39	18054	19.835	7.13	0.5666	6.12	0.86	3209	58	3083	69	2894	143	12
CRMO11-14L_8	1027	0.79	53363	20.414	6.60	0.5832	5.79	0.88	3209	50	3111	64	2962	138	10
CRMO11-14L_11	148	0.42	39528	20.731	6.68	0.5926	5.87	0.88	3208	51	3126	65	3000	141	8
CRMO11-14M_55	1168	0.60	30831	21.255	6.95	0.6081	6.04	0.87	3207	54	3150	67	3062	147	6
CRMO11-14M_47	546	0.40	128251	21.123	8.19	0.6053	7.43	0.91	3204	55	3144	79	3051	181	6
CRMO11-14S_100	511	0.44	31188	20.705	7.20	0.5946	6.28	0.87	3201	56	3125	70	3008	151	8
CRMO11-14L_10	1430	0.83	132712	21.073	6.53	0.6058	5.68	0.87	3199	51	3142	63	3053	138	6
CRMO11-14M_66	333	0.27	16439	19.578	7.32	0.5629	6.39	0.87	3199	56	3071	71	2879	148	12
CRMO11-14S_95	1231	0.58	18158	20.037	6.40	0.5769	5.55	0.87	3197	50	3093	62	2936	131	10
CRMO11-14M_62	323	0.32	17649	18.965	6.78	0.5460	5.96	0.88	3197	51	3040	65	2809	136	15
CRMO11-14L_30	1924	1.09	79615	19.497	6.83	0.5646	5.94	0.87	3188	54	3067	66	2886	138	12
CRMO11-14L_31A	210	1.00	59398	18.010	8.16	0.5219	6.88	0.84	3186	69	2990	78	2707	152	18
CRMO11-14XL_29	298	0.40	15342	15.759	6.35	0.4577	5.45	0.86	3183	52	2862	61	2430	110	28
CRMO11-14S_96	1303	0.61	144614	20.275	6.41	0.5894	5.51	0.86	3181	52	3105	62	2987	132	8
CRMO11-14XL_32	785	0.46	950113	18.069	6.01	0.5258	5.19	0.86	3180	48	2993	58	2724	115	18
CRMO11-14M_54	983	0.63	61906	20.816	6.97	0.6068	6.06	0.87	3177	54	3130	68	3057	148	5
CRMO11-14S_82B	476	0.25	13484	17.709	7.87	0.5166	7.14	0.91	3176	53	2974	76	2685	157	19
CRMO11-14L_5	766	0.59	14835	17.825	6.40	0.5212	5.60	0.88	3172	49	2980	62	2704	124	18
CRMO11-14M_58	2270	0.14	50588	18.721	7.30	0.5483	6.39	0.88	3170	56	3028	70	2818	146	14
CRMO11-14XL_22	934	0.56	207291	19.200	5.79	0.5690	4.97	0.86	3151	47	3052	56	2904	116	10
CRMO11-14XL_35	212	0.19	26061	15.999	6.77	0.4747	5.94	0.88	3149	52	2877	65	2504	123	25

Spot	Corrected Isotope Ratios								Apparent ages (Ma)						
	U ppm	Th/U ppm	<u>206Pb</u> 204Pb	<u>207Pb*</u> 235U*	$\pm 2s$ (%)	<u>206Pb*</u> 238U	$\pm 2s$ (%)	error corr.	<u>207Pb*</u> 206Pb*	$\pm 2s$ (Ma)	<u>207Pb*</u> 235U	$\pm 2s$ (Ma)	<u>206Pb*</u> 238U*	$\pm 2s$ (Ma)	% disc.
CRMO11-14S_94	508	0.41	54621	17.967	6.76	0.5347	5.88	0.87	3144	53	2988	65	2761	132	15
CRMO11-14XL_30	58	1.18	1485	18.497	5.97	0.5523	5.06	0.85	3139	50	3016	58	2835	116	12
CRMO11-14L_3	118	1.49	4858	18.511	6.73	0.5558	5.81	0.86	3130	54	3017	65	2849	134	11
CRMO11-14L_21	131	1.25	3001	19.592	6.68	0.5884	5.82	0.87	3130	52	3071	64	2983	139	6
CRMO11-14L_25	1052	0.80	28178	19.291	6.86	0.5801	6.09	0.89	3128	50	3056	66	2949	144	7
CRMO11-14L_32	809	0.75	18865	17.418	6.26	0.5247	5.39	0.86	3125	51	2958	60	2719	119	16
CRMO11-14S_88	392	0.38	80398	18.463	6.75	0.5573	5.96	0.88	3122	51	3014	65	2856	137	11
CRMO11-14L_33	921	1.15	46384	18.805	6.76	0.5686	5.94	0.88	3119	51	3032	65	2902	139	9
CRMO11-14L_18A	70	1.73	2798	12.011	7.18	0.3638	6.23	0.87	3116	57	2605	67	2000	107	41
CRMO11-14L_27	55	2.70	2281	17.657	6.88	0.5351	6.06	0.88	3115	52	2971	66	2763	136	14
CRMO11-14M_52	1276	0.72	35179	20.602	8.83	0.6261	7.60	0.86	3111	72	3120	86	3134	189	1
CRMO11-14M_59	471	0.40	31143	19.539	6.65	0.5939	5.71	0.86	3111	55	3069	64	3005	137	4
CRMO11-14M_48	73	2.10	12936	17.113	7.09	0.5214	6.03	0.85	3107	60	2941	68	2705	133	16
CRMO11-14L_18B	76	1.80	10587	12.759	7.00	0.3897	6.12	0.87	3103	54	2662	66	2121	111	37
CRMO11-14M_37	969	0.25	29096	16.362	7.94	0.4999	7.00	0.88	3102	60	2898	76	2614	150	19
CRMO11-14L_26	54	3.20	1039	17.162	6.30	0.5247	5.29	0.84	3101	54	2944	60	2719	117	15
CRMO11-14M_49	825	0.54	15253	16.528	7.82	0.5115	7.02	0.90	3082	55	2908	75	2663	153	17
CRMO11-14S_82A	108	1.40	5112	16.634	8.06	0.5149	7.21	0.89	3082	58	2914	77	2677	158	16
CRMO11-14M_57	1723	0.18	99891	16.919	7.50	0.5239	6.74	0.90	3081	53	2930	72	2716	149	15
CRMO11-14M_53	74	1.21	5024	24.939	11.01	0.7742	10.24	0.93	3077	65	3306	108	3696	288	27
CRMO11-14XL_28	987	0.51	19804	14.349	5.96	0.4464	4.95	0.83	3074	53	2773	57	2379	98	27
CRMO11-14M_63	482	0.43	24842	17.798	6.70	0.5560	5.74	0.86	3067	55	2979	64	2850	132	9
CRMO11-14L_19	757	0.15	8239	11.558	6.46	0.3613	5.57	0.86	3066	52	2569	60	1988	95	41
CRMO11-14M_36	891	0.18	18235	14.353	6.55	0.4503	5.52	0.84	3060	56	2773	62	2397	111	26
CRMO11-14L_15A	686	0.53	28425	13.849	6.75	0.4359	5.84	0.87	3055	54	2739	64	2332	114	28
CRMO11-14L_2	492	0.53	60505	13.511	9.01	0.4258	8.44	0.94	3053	51	2716	85	2287	163	30
CRMO11-14S_81	65	1.66	1435	17.019	6.91	0.5393	5.89	0.85	3044	58	2936	66	2781	133	11
CRMO11-14L_15B	638	0.54	100324	13.912	6.84	0.4411	6.03	0.88	3043	52	2744	65	2356	119	27
CRMO11-14S_93	616	0.61	115183	14.334	6.53	0.4576	5.25	0.81	3032	62	2772	62	2429	106	24
CRMO11-14S_99	102	1.51	15593	16.534	6.53	0.5306	5.53	0.85	3024	56	2908	62	2744	124	11
CRMO11-14S_87	533	0.33	11665	12.287	6.57	0.4030	5.51	0.84	2989	58	2627	62	2183	102	32
CRMO11-14L_20	63	2.09	2451	7.581	6.81	0.2501	5.88	0.86	2979	55	2183	61	1439	76	57
CRMO11-14S_84	700	0.46	365996	12.291	6.18	0.4062	5.20	0.84	2976	54	2627	58	2198	97	31

Spot	Corrected Isotope Ratios								Apparent ages (Ma)						
	U ppm	Th/U ppm	<u>206Pb</u> 204Pb	<u>207Pb*</u> 235U*	±2s (%)	<u>206Pb*</u> 238U	±2s (%)	error corr.	<u>207Pb*</u> 206Pb*	±2s (Ma)	<u>207Pb*</u> 235U	±2s (Ma)	<u>206Pb*</u> 238U*	±2s (Ma)	% disc.
Neoproterozoic															
<i>CRMO11-14S_85</i>	238	0.38	9569	12.313	6.62	0.4245	5.74	0.87	2908	53	2629	62	2281	110	26
CRMO11-14M_43B	104	1.17	4069	9.395	7.72	0.3244	6.49	0.84	2906	68	2377	71	1811	102	43
CRMO11-14M_43A	128	1.21	10827	9.275	7.84	0.3279	6.81	0.87	2867	63	2366	72	1828	108	41
CRMO11-14XL_34	35	3.50	458	9.013	6.95	0.3263	6.09	0.88	2829	55	2339	63	1820	97	41
<i>CRMO11-14L_28</i>	78	2.84	1449	12.790	5.98	0.4661	5.08	0.85	2818	51	2664	56	2466	104	15
<i>CRMO11-14M_60</i>	55	2.41	14495	10.221	7.13	0.3792	6.05	0.85	2789	62	2455	66	2073	107	30
CRMO11-14M_50	48	2.42	879	8.751	6.84	0.3286	5.80	0.85	2769	59	2312	62	1832	93	39

Spot	Corrected Isotope Ratios								Apparent ages (Ma)						
	U ppm	Th/U ppm	<u>206Pb</u> 204Pb	<u>207Pb*</u> 235U*	±2s (%)	<u>206Pb*</u> 238U	±2s (%)	error corr.	<u>207Pb*</u> 206Pb*	±2s (Ma)	<u>207Pb*</u> 235U	±2s (Ma)	<u>206Pb*</u> 238U*	±2s (Ma)	% disc.
CRMO11-15															
Paleoproterozoic															
CRMO11-15S_116	445	0.83	156010	27.253	8.19	0.6702	6.83	0.83	3444	70	3393	80	3307	177	5
CRMO11-15S_117	428	0.14	41192	21.093	7.18	0.5220	6.41	0.89	3434	50	3143	70	2708	142	26
CRMO11-15S_108	2543	0.08	601404	17.543	7.05	0.4376	6.28	0.89	3421	50	2965	68	2340	123	37
CRMO11-15XL_41	566	0.23	13190	17.977	5.68	0.4558	4.85	0.85	3396	46	2989	55	2421	98	34
CRMO11-15S_107	1498	0.04	52960	20.232	6.72	0.5264	5.92	0.88	3356	50	3103	65	2726	132	23
Mesoproterozoic 1															
CRMO11-15XL_42	1875	0.31	45754	20.553	7.43	0.5491	6.86	0.92	3315	45	3118	72	2821	157	18
CRMO11-15XL_50	1877	0.33	598954	21.767	9.47	0.5853	9.00	0.95	3304	46	3173	92	2970	214	13
CRMO11-15XL_51	118	0.86	1450	22.034	5.71	0.5948	4.83	0.85	3298	48	3185	55	3009	116	11
CRMO11-15XL_46	536	0.31	13228	20.653	6.21	0.5575	5.45	0.88	3298	47	3122	60	2856	126	17
CRMO11-15S_110	228	0.50	8915	21.030	6.16	0.5679	5.17	0.84	3298	53	3140	60	2899	121	15
CRMO11-15XL_48	515	0.45	28686	19.138	6.24	0.5178	5.46	0.87	3295	48	3049	60	2690	120	22
CRMO11-15XL_55	1666	0.36	25333	24.302	8.16	0.6578	7.62	0.93	3294	46	3281	80	3259	195	1
CRMO11-15S_103	505	0.29	62554	21.980	6.34	0.5963	5.52	0.87	3291	49	3183	62	3015	133	10
CRMO11-15S_109	424	0.47	19782	26.815	5.99	0.7301	5.01	0.84	3285	52	3377	59	3534	136	10
CRMO11-15XL_54	189	0.61	7411	20.998	6.11	0.5718	5.29	0.87	3285	48	3139	59	2915	124	14
CRMO11-15S_101	187	0.57	8032	21.055	6.68	0.5734	5.88	0.88	3284	50	3141	65	2922	138	14
CRMO11-15XL_39	536	0.37	18065	20.403	5.85	0.5557	5.06	0.86	3284	46	3111	57	2849	116	16

Spot	Corrected Isotope Ratios								Apparent ages (Ma)						
	U ppm	Th/U ppm	<u>206Pb</u> <u>204Pb</u>	<u>207Pb*</u> <u>235U*</u>	$\pm 2s$ (%)	<u>206Pb*</u> <u>238U</u>	$\pm 2s$ (%)	error corr.	<u>207Pb*</u> <u>206Pb*</u>	$\pm 2s$ (Ma)	<u>207Pb*</u> <u>235U</u>	$\pm 2s$ (Ma)	<u>206Pb*</u> <u>238U*</u>	$\pm 2s$ (Ma)	% disc.
CRMO11-15XL_45	526	0.71	17722	22.061	5.79	0.6011	4.99	0.86	3284	46	3186	56	3034	121	10
CRMO11-15S_115	402	0.28	3743	20.736	6.68	0.5667	5.75	0.86	3279	54	3126	65	2894	134	15
CRMO11-15S_118	518	0.47	32821	21.019	6.60	0.5765	5.78	0.88	3273	50	3139	64	2935	136	13
CRMO11-15S_104	1491	0.21	393092	21.238	6.37	0.5835	5.54	0.87	3270	50	3150	62	2963	132	12
CRMO11-15S_102	443	0.63	12964	24.732	6.14	0.6799	5.26	0.86	3270	50	3298	60	3344	137	3
CRMO11-15XL_40	594	0.52	42461	24.797	9.79	0.6828	9.34	0.95	3267	46	3300	96	3355	244	3
CRMO11-15S_120	845	0.44	38859	20.687	6.76	0.5702	5.95	0.88	3266	50	3124	65	2909	139	14
CRMO11-15S_125	165	0.62	21296	19.847	7.02	0.5495	6.28	0.89	3259	50	3084	68	2823	144	16
CRMO11-15S_122	695	0.17	17846	13.558	6.91	0.3754	6.15	0.89	3259	50	2719	65	2055	108	43
CRMO11-15XL_44	820	0.25	14830	16.036	6.33	0.4445	5.52	0.87	3257	49	2879	61	2371	109	32
CRMO11-15XL_39A	786	0.08	39439	14.395	6.55	0.3997	5.87	0.90	3254	45	2776	62	2168	108	39
CRMO11-15S_114	353	0.39	4866	20.366	6.39	0.5683	5.45	0.85	3246	53	3109	62	2901	127	13
CRMO11-15S_124	1148	0.15	23568	16.472	7.71	0.4601	7.05	0.91	3245	49	2905	74	2440	143	30
CRMO11-15S_113	395	0.50	8067	21.081	6.97	0.5900	6.06	0.87	3242	54	3142	68	2989	145	10
CRMO11-15XL_49	497	0.26	27309	19.967	6.48	0.5595	5.79	0.89	3240	46	3090	63	2864	134	14
CRMO11-15S_121	1083	0.11	29909	18.191	6.93	0.5138	6.13	0.88	3227	51	3000	67	2673	134	21
CRMO11-15S_119	1336	0.13	88571	13.624	7.03	0.3874	6.25	0.89	3217	51	2724	67	2111	112	40
CRMO11-15S_105	1519	0.05	14971	14.326	8.32	0.4080	7.66	0.92	3214	52	2772	79	2206	143	37
CRMO11-15S_123	2137	0.04	11300	13.088	7.32	0.3735	6.53	0.89	3211	52	2686	69	2046	114	42
CRMO11-15XL_52	877	0.08	41890	13.040	5.36	0.3766	4.43	0.83	3192	48	2683	51	2060	78	41
CRMO11-15XL_43	4080	0.40	91128	17.791	5.83	0.5472	5.05	0.87	3092	46	2978	56	2814	115	11
CRMO11-15XL_53	6000	0.34	190763	17.554	6.35	0.5454	5.66	0.89	3076	46	2966	61	2806	129	11
Paleogene															
CRMO11-15S_111	849	0.08	1318	0.035	12.38	0.0053	7.77	0.63	100	228	35	4	34	3	66
CRMO11-15S_112	3273	0.03	1346	0.038	7.24	0.0059	5.50	0.76	57	112	38	3	38	2	34
CRMO11-15S_106	119	1.30	41	0.029	37.33	0.0049	7.46	0.20	-151	908	29	11	31	2	121

Spot	Corrected Isotope Ratios								Apparent ages (Ma)						
	U ppm	Th/U ppm	<u>206Pb</u> <u>204Pb</u>	<u>207Pb*</u> <u>235U*</u>	$\pm 2s$ (%)	<u>206Pb*</u> <u>238U</u>	$\pm 2s$ (%)	error corr.	<u>207Pb*</u> <u>206Pb*</u>	$\pm 2s$ (Ma)	<u>207Pb*</u> <u>235U</u>	$\pm 2s$ (Ma)	<u>206Pb*</u> <u>238U*</u>	$\pm 2s$ (Ma)	% disc.
CRMO11-16 Neoarchean CRMO11S-16_71	2028	0.31	154586	26.469	4.30	0.6352	3.93	0.91	3482	27	3364	42	3170	98	11

CRMO11S-16_73	873	0.46	60253	23.577	2.50	0.5996	1.62	0.65	3392	30	3251	24	3028	39	13
Mesoarchean I															
CRMO11S-16_69	865	1.96	134387	20.896	2.64	0.5778	2.29	0.87	3261	21	3134	26	2940	54	12
CRMO11S-16_70	906	1.22	128495	20.560	2.04	0.5690	1.70	0.83	3259	18	3118	20	2904	40	14
CRMO11S-16_72	123	0.99	3888	19.570	2.31	0.5419	1.71	0.74	3258	24	3070	22	2791	39	18
CRMO11S-16_77	1002	0.62	512257	21.017	1.46	0.5826	1.10	0.75	3257	15	3139	14	2959	26	11
CRMO11S-16_67	756	0.97	94674	20.939	1.98	0.5816	1.87	0.94	3254	10	3136	19	2955	44	11
CRMO11S-16_76	865	0.57	61846	19.185	3.72	0.5344	3.40	0.92	3249	24	3051	36	2760	76	18
CRMO11S-16_78	1385	1.75	43743	20.554	1.87	0.5729	1.64	0.88	3248	14	3118	18	2920	39	13
CRMO11S-16_74a	1887	0.38	39492	18.457	4.23	0.5149	3.50	0.83	3246	37	3014	41	2678	77	21
CRMO11-16M_164	1627	0.49	162280	23.493	4.84	0.6605	4.37	0.90	3234	33	3248	47	3269	112	1
CRMO11S-16_74b	1650	0.35	25976	19.535	3.43	0.5504	2.83	0.83	3231	30	3069	33	2827	65	15
CRMO11S-16_68	666	0.78	18697	20.280	2.05	0.5739	1.86	0.91	3224	14	3105	20	2924	44	12
CRMO11S-16_75	1463	0.43	140820	18.572	2.45	0.5256	2.23	0.91	3224	16	3020	24	2723	49	19
CRMO11S-16_79	53	1.76	1876	22.787	3.07	0.6458	2.52	0.82	3222	28	3218	30	3212	64	0
CRMO11-16M_166	641	0.08	8914	17.724	3.65	0.5087	2.82	0.77	3202	37	2975	35	2651	61	21
CRMO11-16M_165	931	0.13	22037	16.783	2.78	0.4918	2.53	0.91	3169	19	2923	27	2579	54	23

Spot	Corrected Isotope Ratios								Apparent ages (Ma)						% disc.
	U ppm	Th/U ppm	$\frac{206\text{Pb}}{204\text{Pb}}$	$\frac{207\text{Pb}^*}{235\text{U}^*}$	$\pm 2s$ (%)	$\frac{206\text{Pb}^*}{238\text{U}}$	$\pm 2s$ (%)	error corr.	$\frac{207\text{Pb}^*}{206\text{Pb}^*}$	$\pm 2s$ (Ma)	$\frac{207\text{Pb}^*}{235\text{U}}$	$\pm 2s$ (Ma)	$\frac{206\text{Pb}^*}{238\text{U}^*}$	$\pm 2s$ (Ma)	
CRMO11-17															
Paleoarchean															
CRMO11-17M_75	405	0.14	15786	28.600	7.44	0.6378	6.57	0.88	3595	54	3440	73	3180	165	15
CRMO11-17M_73	216	0.70	6985	27.663	7.04	0.6469	6.18	0.88	3522	52	3407	69	3216	156	11
CRMO11-17S_149	1511	0.34	115575	21.777	5.89	0.5206	4.17	0.71	3488	64	3174	57	2702	92	27
CRMO11-17S_142	423	0.65	10263	26.806	5.80	0.6573	4.05	0.70	3448	64	3376	57	3257	104	7
CRMO11-17S_130	728	0.42	158721	23.493	6.12	0.5892	5.25	0.86	3413	49	3248	60	2986	125	16
CRMO11-17M_72	633	0.11	20860	22.913	6.63	0.5756	5.73	0.86	3411	52	3223	64	2931	135	17
CRMO11-17M_76	683	0.32	16369	20.233	7.11	0.5274	6.22	0.87	3353	54	3103	69	2731	138	23
CRMO11-17S_134	1071	0.18	61871	20.967	6.18	0.5577	5.27	0.85	3321	50	3137	60	2857	122	17
Mesoarchean I															
CRMO11-17S_138	1124	0.47	47886	19.378	9.62	0.5300	8.72	0.91	3278	64	3061	93	2741	195	20
CRMO11-17S_148	778	0.20	266408	19.544	6.43	0.5396	4.97	0.77	3263	64	3069	62	2782	112	18
CRMO11-17S_147	848	0.33	21834	19.426	6.24	0.5383	4.70	0.75	3257	65	3063	60	2776	106	18
CRMO11-17S_145	355	0.78	11847	16.509	5.67	0.4598	3.94	0.69	3249	64	2907	54	2439	80	30

Spot	Corrected Isotope Ratios								Apparent ages (Ma)						
	U ppm	Th/U ppm	<u>206Pb</u> 204Pb	<u>207Pb*</u> 235U*	$\pm 2s$ (%)	<u>206Pb*</u> 238U	$\pm 2s$ (%)	error corr.	<u>207Pb*</u> 206Pb*	$\pm 2s$ (Ma)	<u>207Pb*</u> 235U	$\pm 2s$ (Ma)	<u>206Pb*</u> 238U*	$\pm 2s$ (Ma)	% disc.
CRMO11-17S_132	1060	0.28	50516	18.618	8.60	0.5234	7.78	0.91	3234	58	3022	83	2714	172	20
CRMO11-17S_126	220	0.11	7897	20.967	6.60	0.5897	5.82	0.88	3234	49	3137	64	2988	139	9
CRMO11-17S_144	432	0.27	15508	18.292	5.56	0.5158	3.85	0.69	3230	63	3005	54	2681	84	21
CRMO11-17S_131	517	0.32	7330	19.782	7.85	0.5584	7.13	0.91	3228	52	3081	76	2860	165	14
CRMO11-17S_143	365	0.20	356053	20.637	6.85	0.5827	5.44	0.80	3227	66	3122	66	2960	129	10
CRMO11-17S_146	769	0.24	15597	17.868	6.08	0.5072	4.49	0.74	3219	65	2983	58	2645	98	22
CRMO11-17S_135	2732	0.25	37559	15.219	6.00	0.4322	5.08	0.85	3219	50	2829	57	2315	99	33
CRMO11-17S_128	848	0.34	44584	20.216	6.32	0.5752	5.50	0.87	3216	49	3102	61	2929	129	11
CRMO11-17M_74	883	0.35	27486	18.501	6.81	0.5269	6.02	0.88	3214	50	3016	66	2728	134	18
CRMO11-17S_139	906	0.63	61604	19.301	6.42	0.5499	5.56	0.87	3213	51	3057	62	2825	127	15
CRMO11-17S_137	1239	0.43	17083	18.428	6.44	0.5254	5.49	0.85	3212	53	3012	62	2722	122	19
CRMO11-17S_140	1016	0.28	15253	18.755	7.86	0.5398	7.16	0.91	3197	51	3029	76	2783	162	16
CRMO11-17S_133	265	0.18	5739	16.451	6.67	0.4747	5.83	0.88	3193	51	2903	64	2504	121	26
CRMO11-17S_129	944	0.38	44593	18.114	7.30	0.5282	6.49	0.89	3177	53	2996	70	2734	145	17
CRMO11-17S_127	568	0.09	42673	17.202	6.09	0.5052	5.12	0.84	3165	52	2946	58	2636	111	20
Neoarchean															
<i>CRMO11-17S_136</i>	<i>48</i>	<i>1.69</i>	<i>9</i>	<i>0.166</i>	<i>172.91</i>	<i>0.0060</i>	<i>15.62</i>	<i>0.09</i>	<i>2817</i>	<i>2813</i>	<i>156</i>	<i>250</i>	<i>39</i>	<i>6</i>	<i>99</i>
<i>CRMO11-17S_150</i>	<i>43</i>	<i>0.90</i>	<i>33</i>	<i>0.369</i>	<i>20.20</i>	<i>0.0139</i>	<i>15.93</i>	<i>0.79</i>	<i>2759</i>	<i>204</i>	<i>319</i>	<i>55</i>	<i>89</i>	<i>14</i>	<i>97</i>

Spot	Corrected Isotope Ratios								Apparent ages (Ma)						
	U ppm	Th/U ppm	<u>206Pb</u> 204Pb	<u>207Pb*</u> 235U*	$\pm 2s$ (%)	<u>206Pb*</u> 238U	$\pm 2s$ (%)	error corr.	<u>207Pb*</u> 206Pb*	$\pm 2s$ (Ma)	<u>207Pb*</u> 235U	$\pm 2s$ (Ma)	<u>206Pb*</u> 238U*	$\pm 2s$ (Ma)	% disc.
CRMO11-18															
Paleoarchean															
CRMO11-18S_156	137	0.41	5764	24.320	5.72	0.5833	4.03	0.70	3482	63	3281	56	2962	96	19
CRMO11-18S_155	434	0.46	5977	24.487	5.94	0.5914	4.34	0.73	3472	63	3288	58	2995	104	17
Mesoarchean I															
CRMO11-18S_153	640	0.48	72786	21.487	5.66	0.5740	3.95	0.70	3315	64	3161	55	2924	93	15
CRMO11-18S_152	2217	0.10	160292	18.791	5.74	0.5059	4.00	0.70	3303	65	3031	55	2639	87	24
CRMO11-18M_77	182	0.97	3795	23.667	8.66	0.6375	7.92	0.91	3302	55	3255	84	3179	199	5
CRMO11-18XS_61	86	0.81	3072	18.020	8.98	0.4859	8.38	0.93	3300	50	2991	86	2553	177	27
CRMO11-18XS_56	454	0.70	44637	24.453	6.32	0.6597	5.61	0.89	3299	46	3287	62	3266	144	1

Spot	Corrected Isotope Ratios								Apparent ages (Ma)						
	U ppm	Th/U ppm	<u>206Pb</u> <u>204Pb</u>	<u>207Pb*</u> <u>235U*</u>	$\pm 2s$ (%)	<u>206Pb*</u> <u>238U</u>	$\pm 2s$ (%)	error corr.	<u>207Pb*</u> <u>206Pb*</u>	$\pm 2s$ (Ma)	<u>207Pb*</u> <u>235U</u>	$\pm 2s$ (Ma)	<u>206Pb*</u> <u>238U*</u>	$\pm 2s$ (Ma)	% disc.
CRMO11-18XS_72	2378	0.53	62575	19.822	6.71	0.5353	6.09	0.91	3298	44	3083	65	2764	137	20
CRMO11-18XS_69	329	0.99	14461	23.297	5.81	0.6300	5.06	0.87	3296	45	3239	57	3149	126	6
CRMO11-18XS_73	459	0.78	25598	21.383	5.56	0.5788	4.72	0.85	3294	46	3156	54	2944	112	13
CRMO11-18S_151	195	0.85	24068	13.416	6.46	0.3641	4.87	0.75	3290	67	2709	61	2002	84	45
CRMO11-18XS_70	292	1.13	4073	19.816	6.40	0.5379	5.72	0.89	3290	45	3082	62	2775	129	19
CRMO11-18M_79	1981	0.33	76475	21.508	8.23	0.5847	7.56	0.92	3287	51	3162	80	2968	180	12
CRMO11-18XS_71	1380	0.32	104721	19.313	6.36	0.5281	5.65	0.89	3278	46	3058	61	2734	126	20
CRMO11-18XS_62	129	0.79	1794	21.272	5.97	0.5818	5.16	0.87	3278	47	3151	58	2956	122	12
CRMO11-18XS_60	1969	0.22	43658	17.279	6.58	0.4735	5.89	0.89	3275	46	2950	63	2499	122	28
CRMO11-18XS_64	1480	0.46	21707	16.649	6.41	0.4564	5.73	0.89	3274	45	2915	61	2424	116	31
CRMO11-18XS_68	2482	0.08	167524	18.070	6.51	0.4961	5.83	0.90	3272	46	2993	63	2597	125	25
CRMO11-18S_154	1075	0.07	2902874	17.658	5.61	0.4852	3.87	0.69	3270	64	2971	54	2550	81	27
CRMO11-18S_157	2081	0.04	37549	17.751	5.68	0.4878	3.99	0.70	3270	64	2976	55	2561	84	26
CRMO11-18XS_59	490	0.47	117961	19.547	6.11	0.5378	5.38	0.88	3268	46	3069	59	2774	121	19
CRMO11-18XS_65	313	0.22	6083	12.429	6.54	0.3426	5.66	0.87	3266	51	2637	61	1899	93	48
CRMO11-18S_158	114	0.77	2699	18.445	6.46	0.5090	5.00	0.77	3264	64	3013	62	2652	109	23
CRMO11-18XS_58	421	0.34	31835	19.094	6.21	0.5295	5.45	0.88	3256	47	3047	60	2739	122	19
CRMO11-18M_78	2236	0.23	211766	21.795	7.38	0.6050	6.38	0.86	3254	58	3175	72	3050	155	8
CRMO11-18XS_57	492	0.16	34919	18.679	5.47	0.5195	4.55	0.83	3251	48	3025	53	2697	100	21
CRMO11-18XS_67	796	0.36	168544	19.846	6.35	0.5530	5.63	0.89	3248	46	3084	61	2838	129	16
CRMO11-18XS_74	967	0.09	48875	14.783	6.62	0.4128	5.97	0.90	3245	45	2801	63	2228	112	37

Spot	Corrected Isotope Ratios								Apparent ages (Ma)						
	U ppm	Th/U ppm	<u>206Pb</u> <u>204Pb</u>	<u>207Pb*</u> <u>235U*</u>	$\pm 2s$ (%)	<u>206Pb*</u> <u>238U</u>	$\pm 2s$ (%)	error corr.	<u>207Pb*</u> <u>206Pb*</u>	$\pm 2s$ (Ma)	<u>207Pb*</u> <u>235U</u>	$\pm 2s$ (Ma)	<u>206Pb*</u> <u>238U*</u>	$\pm 2s$ (Ma)	% disc.
CRMO11-19 Paleogene															
CRMO11-19XS_79	256	0.44	77	0.054	19.29	0.0074	7.39	0.38	320	405	53	10	48	4	85
CRMO11-19XS_83	505	1.24	4347	0.059	10.55	0.0074	4.57	0.43	529	208	58	6	48	2	91
CRMO11-19XS_82	381	0.73	410	0.051	14.01	0.0073	6.21	0.44	247	289	51	7	47	3	81
CRMO11-19XS_78	1421	0.47	1601	0.050	6.28	0.0072	4.91	0.78	181	91	49	3	46	2	75
CRMO11-19XS_75	1233	0.51	1624	0.047	7.71	0.0072	5.46	0.71	45	130	46	3	46	3	3

Spot	Corrected Isotope Ratios								Apparent ages (Ma)						% disc.
	U ppm	Th/U ppm	$\frac{206\text{Pb}}{204\text{Pb}}$	$\frac{207\text{Pb}^*}{235\text{U}^*}$	$\pm 2s$ (%)	$\frac{206\text{Pb}^*}{238\text{U}}$	$\pm 2s$ (%)	error corr.	$\frac{207\text{Pb}^*}{206\text{Pb}^*}$	$\pm 2s$ (Ma)	$\frac{207\text{Pb}^*}{235\text{U}}$	$\pm 2s$ (Ma)	$\frac{206\text{Pb}^*}{238\text{U}^*}$	$\pm 2s$ (Ma)	
CRMO11-19XS_81	1102	1.28	230	0.053	8.99	0.0070	5.20	0.58	381	165	52	5	45	2	88
CRMO11-19XS_80	1180	0.61	467	0.049	7.84	0.0069	4.87	0.62	249	141	48	4	44	2	83
CRMO11-19XS_85	868	1.95	9145	0.044	8.51	0.0069	5.13	0.60	31	163	44	4	44	2	41
CRMO11-19XS_76	2345	0.41	3042	0.042	6.58	0.0065	5.03	0.76	43	102	42	3	42	2	4
CRMO11-19XS_84	2076	0.37	9173	0.041	6.23	0.0063	4.69	0.75	35	98	40	2	40	2	14

Table C3: Corrected Isotope Ratios and Apparent Ages for Square Mountain

Spots in **bold** were used in the calculation of zircon growth event averages. Spots in **bold and italics** were less than 40% discordant, but were not used to calculate averages because the sample did not have more than 5 spots with discordance less than 40%.

Discordance was not used as a filter on Paleogene dates.

Spot	Corrected Isotope Ratios								Apparent Ages (Ma)						
	U ppm	Th/U ppm	<u>206Pb</u> 204Pb	<u>207Pb*</u> 235U*	±2s (%)	<u>206Pb*</u> 238U	±2s (%)	error corr.	<u>207Pb*</u> 206Pb*	±2s (Ma)	<u>207Pb*</u> 235U	±2s (Ma)	<u>206Pb*</u> 238U*	±2s (Ma)	% disc.
SM10-A3															
Mesoarchean															
SM10A3S_35B	1485	0.30	6263	7.582	6.49	0.1964	5.00	0.77	3363	65	2183	58	1156	53	71
SM10A3S_36B	1041	0.40	3979	6.507	12.66	0.1734	11.99	0.95	3318	64	2047	111	1031	114	74
SM10A3S_35A	277	0.25	18459	19.725	8.02	0.5344	5.91	0.74	3292	85	3078	78	2760	133	20
Neoarchean															
<i>SM10A3S_37</i>	<i>294</i>	<i>0.53</i>	<i>5948</i>	<i>11.722</i>	<i>3.49</i>	<i>0.4590</i>	<i>3.10</i>	<i>0.89</i>	<i>2700</i>	<i>27</i>	<i>2582</i>	<i>33</i>	<i>2435</i>	<i>63</i>	<i>12</i>
SM10A3S_36A	2023	0.36	2622	1.684	13.19	0.0660	10.31	0.78	2699	136	1002	84	412	41	87
SM10A3S_32A	1363	0.17	2466	3.057	8.82	0.1227	7.62	0.86	2660	74	1422	67	746	54	76
<i>SM10A3S_38A</i>	<i>711</i>	<i>0.10</i>	<i>31913</i>	<i>8.497</i>	<i>7.20</i>	<i>0.3437</i>	<i>5.62</i>	<i>0.78</i>	<i>2647</i>	<i>75</i>	<i>2286</i>	<i>65</i>	<i>1904</i>	<i>93</i>	<i>32</i>
SM10A3S_31	690	0.23	1908	6.972	5.48	0.2829	4.29	0.78	2641	57	2108	49	1606	61	44
SM10A3S_22A	1422	0.53	27625	3.136	10.03	0.1301	9.39	0.94	2605	59	1442	77	788	70	74
SM10A3S_26A	1126	0.57	4775	3.666	6.64	0.1534	6.33	0.95	2590	33	1564	53	920	54	69
SM10A3S_33B	877	0.16	1462	4.661	13.05	0.1955	12.42	0.95	2586	67	1760	109	1151	131	60
<i>SM10A3S_43</i>	<i>603</i>	<i>0.06</i>	<i>9733</i>	<i>9.159</i>	<i>8.19</i>	<i>0.3844</i>	<i>7.24</i>	<i>0.88</i>	<i>2585</i>	<i>64</i>	<i>2354</i>	<i>75</i>	<i>2097</i>	<i>130</i>	<i>22</i>
SM10A3S_39	1439	0.14	1249	1.028	10.17	0.0432	9.44	0.93	2584	63	718	52	273	25	91
SM10A3S_32B	1135	0.14	1442	3.808	8.44	0.1622	7.42	0.88	2560	67	1594	68	969	67	67
SM10A3S_34	1541	0.58	15535	1.551	13.12	0.0661	12.90	0.98	2559	39	951	81	413	52	86
SM10A3S_23A	1257	0.25	1706	1.877	17.40	0.0803	16.88	0.97	2554	70	1073	115	498	81	83
SM10A3S_23B	903	0.13	3409	2.463	13.56	0.1072	13.39	0.99	2525	37	1261	98	656	84	78
SM10A3S_25	1468	0.37	6948	1.561	7.06	0.0682	6.52	0.92	2519	45	955	44	425	27	86
SM10A3S_42A	1584	0.36	1337	1.158	6.05	0.0507	5.46	0.90	2515	44	781	33	319	17	89
SM10A3S_41A	1237	0.47	2094	2.377	6.71	0.1049	6.49	0.97	2501	28	1236	48	643	40	78
SM10A3S_33A	1626	0.30	1631	1.814	18.41	0.0802	17.70	0.96	2499	85	1051	120	497	85	83
SM10A3S_42B	1395	0.23	4637	1.806	8.88	0.0799	6.96	0.78	2497	93	1048	58	495	33	83
SM10A3S_40	1895	0.14	1274	1.294	8.47	0.0592	8.32	0.98	2439	27	843	49	371	30	87
SM10A3S_27A	1848	0.40	2256	1.254	14.50	0.0574	14.29	0.99	2439	42	825	82	360	50	88
SM10A3S_24	2062	0.69	1203	0.996	4.75	0.0463	4.27	0.90	2411	35	702	24	292	12	90

Spot	Corrected Isotope Ratios								Apparent Ages (Ma)						
	U ppm	Th/U ppm	<u>206Pb</u> <u>204Pb</u>	<u>207Pb*</u> <u>235U*</u>	$\pm 2s$ (%)	<u>206Pb*</u> <u>238U</u>	$\pm 2s$ (%)	error corr.	<u>207Pb*</u> <u>206Pb*</u>	$\pm 2s$ (Ma)	<u>207Pb*</u> <u>235U</u>	$\pm 2s$ (Ma)	<u>206Pb*</u> <u>238U*</u>	$\pm 2s$ (Ma)	% disc.
SM10A3S_28A	2274	0.66	4240	0.819	10.74	0.0404	9.61	0.89	2311	82	607	49	255	24	91
SM10A3S_29B	2101	0.59	4475	0.808	9.02	0.0407	8.26	0.92	2277	62	601	41	257	21	90
SM10A3S_30	3175	0.79	1372	0.389	14.60	0.0197	13.31	0.91	2262	104	333	41	126	17	95
SM10A3S_41B	2650	0.46	2354	0.830	7.76	0.0438	6.27	0.81	2196	79	614	36	276	17	89
SM10A3S_29A	2312	0.59	1143	0.641	8.89	0.0343	7.53	0.85	2172	82	503	35	217	16	91

Spot	Corrected Isotope Ratios								Apparent Ages (Ma)						
	U ppm	Th/U ppm	<u>206Pb</u> <u>204Pb</u>	<u>207Pb*</u> <u>235U*</u>	$\pm 2s$ (%)	<u>206Pb*</u> <u>238U</u>	$\pm 2s$ (%)	error corr.	<u>207Pb*</u> <u>206Pb*</u>	$\pm 2s$ (Ma)	<u>207Pb*</u> <u>235U</u>	$\pm 2s$ (Ma)	<u>206Pb*</u> <u>238U*</u>	$\pm 2s$ (Ma)	% disc.
SM10-C2															
Mesoarchean															
SM10C2M_17	1342	0.04	358	7.806	6.07	0.2689	4.89	0.81	2910	58	2209	55	1535	67	53
SM10C2M_20A	511	0.62	11007	6.642	14.63	0.2409	14.24	0.97	2826	54	2065	129	1392	178	56
SM10C2M_20B	321	1.03	2171	12.376	7.63	0.4578	6.62	0.87	2794	62	2633	72	2430	134	16
SM10C2S_70A	2251	0.05	263605	12.349	7.29	0.4613	6.65	0.91	2778	49	2631	69	2445	135	14
Neoarchean															
SM10C2S_80	1144	0.23	47663	9.227	3.70	0.3919	2.79	0.75	2565	41	2361	34	2132	51	20
SM10C2S_73	1518	0.18	22561	9.876	3.52	0.4202	3.19	0.91	2562	25	2423	32	2261	61	14
SM10C2S_78	1800	0.14	16157	9.701	7.92	0.4138	6.90	0.87	2558	65	2407	73	2232	130	15
SM10C2S_69	2367	0.05	57619	7.164	6.28	0.3075	5.14	0.82	2548	60	2132	56	1728	78	37
SM10C2S_74	2938	0.17	11177	6.736	7.98	0.2922	7.34	0.92	2530	53	2077	71	1653	107	39
SM10C2S_79	4133	0.14	1738167	6.352	3.65	0.2775	2.89	0.79	2518	38	2026	32	1579	40	42
SM10C2S_71	1156	0.05	7065	9.568	7.83	0.4225	7.21	0.92	2500	51	2394	72	2272	138	11
SM10c2M_18	3515	0.06	15673	6.276	6.08	0.2779	5.44	0.89	2495	46	2015	53	1581	76	41
SM10C2S_72B	1926	0.03	8359	3.048	11.63	0.1360	10.25	0.88	2482	93	1420	89	822	79	71
SM10C2S_76	1293	0.06	5978	6.742	6.41	0.3010	5.40	0.84	2481	58	2078	57	1696	80	36
SM10C2S_68	2520	0.04	66031	4.901	8.99	0.2210	8.65	0.96	2464	42	1802	76	1287	101	53
SM10c2M_21B	2435	0.04	15386	6.082	7.15	0.2745	6.58	0.92	2463	47	1988	62	1564	91	41
SM10c2M_21A	1595	0.04	127767	3.243	14.44	0.1465	14.30	0.99	2462	34	1467	112	881	118	69
SM10C2S_77	4414	0.06	9391	1.904	11.89	0.0877	11.77	0.99	2428	29	1082	79	542	61	81
SM10C2S_75	1693	0.04	3679	2.407	11.69	0.1122	10.81	0.92	2408	76	1245	84	686	70	75

Spot	Corrected Isotope Ratios								Apparent Ages (Ma)						
	U ppm	Th/U ppm	$\frac{206\text{Pb}}{204\text{Pb}}$	$\frac{207\text{Pb}^*}{235\text{U}^*}$	$\pm 2s$ (%)	$\frac{206\text{Pb}^*}{238\text{U}}$	$\pm 2s$ (%)	error corr.	$\frac{207\text{Pb}^*}{206\text{Pb}^*}$	$\pm 2s$ (Ma)	$\frac{207\text{Pb}^*}{235\text{U}}$	$\pm 2s$ (Ma)	$\frac{206\text{Pb}^*}{238\text{U}^*}$	$\pm 2s$ (Ma)	% disc.
SM10-C3															
Paleo/Mesoarchean															
SM10C3S_61	1199	0.34	31738	27.778	7.89	0.5847	7.66	0.97	3683	29	3411	77	2968	182	24
SM10C3M_2B	233	0.95	148383	22.842	4.69	0.5343	3.90	0.83	3521	40	3220	46	2760	87	26
SM10C3M_2A	232	1.13	13762	15.146	8.04	0.4306	7.29	0.91	3217	54	2824	77	2308	141	33
SM10C3M_1B	261	1.10	7777	17.563	3.83	0.6228	3.31	0.87	2863	31	2966	37	3121	82	11
Neoarchean															
SM10C3M_1A	1639	0.47	39028	10.672	4.28	0.4233	4.18	0.98	2679	15	2495	40	2275	80	18
SM10C3S_62	2478	0.22	26110	9.437	3.29	0.3953	2.85	0.86	2588	28	2381	30	2148	52	20
SM10C3M_16	3721	0.12	68488	10.849	2.48	0.4595	2.38	0.96	2570	12	2510	23	2437	48	6
SM10C3S_64	5080	0.47	1100523	4.295	8.58	0.1826	8.45	0.98	2564	25	1692	71	1081	84	63
SM10C3M_6	5507	0.18	4886087	11.185	2.54	0.4756	2.44	0.96	2563	12	2539	24	2508	51	3
SM10C3M_5	1568	0.28	35954	9.253	3.30	0.3938	3.23	0.98	2562	11	2363	30	2140	59	19
SM10C3S_67	2923	0.11	10896	8.249	10.75	0.3515	10.36	0.96	2560	49	2259	97	1942	174	28
SM10C3S_45	2866	0.04	55679	7.578	3.96	0.3231	3.62	0.91	2559	27	2182	36	1805	57	34
SM10C3S_57	4054	0.21	72587	7.494	5.93	0.3201	5.71	0.96	2555	26	2172	53	1790	89	34
SM10C3S_65	1377	0.46	22371	11.030	7.77	0.4721	6.77	0.87	2552	64	2526	72	2493	140	3
SM10C3M_7	4408	0.14	407861	9.727	2.64	0.4174	2.36	0.89	2548	20	2409	24	2249	45	14
SM10C3M_15	2739	0.17	41205	9.682	2.80	0.4156	2.66	0.95	2547	14	2405	26	2240	50	14
SM10C3M_4	850	0.20	9475	9.810	2.88	0.4212	2.77	0.96	2547	14	2417	27	2266	53	13
SM10C3S_63	3195	0.16	102544	7.937	4.51	0.3410	4.05	0.90	2546	33	2224	41	1892	66	30
SM10C3S_49	1426	0.07	9871	8.969	4.80	0.3861	4.22	0.88	2543	38	2335	44	2105	76	20
SM10C3S_60A	1556	0.07	7137	6.246	12.44	0.2696	12.31	0.99	2538	30	2011	109	1539	168	44
SM10C3M_13A	2687	0.08	16044	6.987	2.71	0.3017	2.32	0.86	2537	23	2110	24	1700	35	37
SM10C3M_14A	1816	0.07	55567	8.355	4.10	0.3609	3.63	0.89	2537	32	2270	37	1986	62	25
SM10C3S_58	2755	0.18	25040	7.039	4.26	0.3046	4.06	0.95	2534	22	2116	38	1714	61	37
SM10C3S_53	1933	0.06	14996	7.744	4.77	0.3354	4.21	0.88	2532	38	2202	43	1865	68	30
SM10C3M_12A	2333	0.04	10387	7.352	4.03	0.3187	3.75	0.93	2531	25	2155	36	1783	58	34
SM10C3S_52	3501	0.15	81818	6.978	3.73	0.3028	3.52	0.94	2529	21	2109	33	1705	53	37
SM10C3S_48	2416	0.11	12992	8.129	5.89	0.3533	5.30	0.90	2527	43	2245	53	1950	89	26
SM10C3M_3	2156	0.06	2437	2.526	20.25	0.1100	20.15	1.00	2523	34	1280	147	673	129	77
SM10C3S_66A	6691	0.49	20335	5.273	10.37	0.2298	9.97	0.96	2522	48	1865	88	1333	120	52
SM10C3M_11	3448	0.43	23332	7.415	4.81	0.3232	4.64	0.96	2522	22	2163	43	1805	73	32
SM10C3S_47B	26174	0.23	40812	0.937	17.20	0.0411	16.21	0.94	2512	97	671	84	259	41	91

Spot	Corrected Isotope Ratios								Apparent Ages (Ma)						
	U ppm	Th/U ppm	<u>206Pb</u> <u>204Pb</u>	<u>207Pb*</u> <u>235U*</u>	$\pm 2s$ (%)	<u>206Pb*</u> <u>238U</u>	$\pm 2s$ (%)	error corr.	<u>207Pb*</u> <u>206Pb*</u>	$\pm 2s$ (Ma)	<u>207Pb*</u> <u>235U</u>	$\pm 2s$ (Ma)	<u>206Pb*</u> <u>238U*</u>	$\pm 2s$ (Ma)	% disc.
SM10C3S_55	5331	0.26	32774	7.476	5.63	0.3283	5.07	0.90	2509	41	2170	50	1830	81	31
SM10C3S_56	7186	0.22	55087	5.118	12.06	0.2260	11.92	0.99	2500	31	1839	102	1314	142	52
SM10C3S_66B	3548	0.13	13886	7.249	6.65	0.3209	5.46	0.82	2496	64	2143	59	1794	85	32
SM10C3M_8A	10844	0.13	17690	2.880	11.39	0.1279	11.35	1.00	2490	17	1377	86	776	83	73
SM10C3S_44	1802	0.80	431876	5.824	12.43	0.2587	12.29	0.99	2490	31	1950	108	1483	163	45
SM10C3S_46	580	0.04	7026	9.403	4.18	0.4178	3.38	0.81	2489	41	2378	38	2250	64	11
SM10C3S_59	5885	0.18	70159	7.284	3.63	0.3239	3.34	0.92	2488	24	2147	32	1809	53	31
SM10C3M_8B	38224	0.23	12351	0.493	5.29	0.0222	5.05	0.95	2465	27	407	18	142	7	95
SM10C3M_10	935	0.12	2429	8.007	4.35	0.3614	3.98	0.91	2463	30	2232	39	1989	68	22
SM10C3S_50	2222	0.07	184285	7.204	8.78	0.3323	7.51	0.86	2426	77	2137	78	1849	121	27
SM10C3S_51	10171	0.37	15328	2.670	11.34	0.1242	11.28	1.00	2412	19	1320	84	754	80	73
SM10C3S_54	64535	0.11	6257	0.240	15.90	0.0117	15.66	0.98	2335	48	218	31	75	12	97

Spot	Corrected Isotope Ratios								Apparent Ages (Ma)						
	U ppm	Th/U ppm	<u>206Pb</u> <u>204Pb</u>	<u>207Pb*</u> <u>235U*</u>	$\pm 2s$ (%)	<u>206Pb*</u> <u>238U</u>	$\pm 2s$ (%)	error corr.	<u>207Pb*</u> <u>206Pb*</u>	$\pm 2s$ (Ma)	<u>207Pb*</u> <u>235U</u>	$\pm 2s$ (Ma)	<u>206Pb*</u> <u>238U*</u>	$\pm 2s$ (Ma)	% disc.
SM10-C4															
Neoarchean															
SM10C4M_32	264	1.29	2037	13.493	2.68	0.5308	2.04	0.76	2693	29	2715	25	2745	46	2
SM10C4M_14B	1154	1.02	7464	9.994	2.20	0.4095	1.38	0.63	2625	28	2434	20	2213	26	19
SM10C4M_40	669	0.34	45302	10.981	3.13	0.4526	2.50	0.80	2615	31	2521	29	2407	50	10
SM10C4M_5B	974	0.41	21367	10.612	3.94	0.4410	3.81	0.97	2602	17	2490	37	2355	75	11
SM10C4M_69	2168	0.76	22382	11.637	2.20	0.4848	2.09	0.95	2597	12	2576	21	2548	44	2
SM10C4M_15B	2123	1.20	90017	9.908	3.00	0.4135	2.12	0.71	2595	35	2426	28	2231	40	17
SM10C4M_3	2920	0.34	15611	9.491	2.15	0.3962	2.04	0.95	2594	12	2387	20	2152	37	20
SM10C4M_30A	2641	0.45	15945	10.573	4.92	0.4424	4.78	0.97	2590	20	2486	46	2361	94	11
SM10C4L_87	1835	0.29	18938	10.495	2.70	0.4403	2.38	0.88	2586	21	2479	25	2352	47	11
SM10C4M_26A	2304	1.77	15580	10.382	2.67	0.4358	2.56	0.96	2585	13	2469	25	2332	50	12
SM10C4L_90	2069	0.56	9099	8.182	5.69	0.3437	5.17	0.91	2583	40	2251	51	1905	85	30
SM10C4M_49	4436	0.98	36082	4.974	13.59	0.2090	13.51	0.99	2583	25	1815	115	1223	151	58
SM10C4M_44	783	0.14	39828	9.910	2.42	0.4164	1.89	0.78	2583	25	2426	22	2244	36	15
SM10C4L_86	2153	0.21	1423521	9.073	2.83	0.3814	2.59	0.91	2582	19	2345	26	2083	46	23
SM10C4M_65	1998	0.38	18929	7.890	6.37	0.3318	5.95	0.93	2582	38	2219	57	1847	96	33

Spot	Corrected Isotope Ratios								Apparent Ages (Ma)						
	U ppm	Th/U ppm	<u>206Pb</u> <u>204Pb</u>	<u>207Pb*</u> <u>235U*</u>	$\pm 2s$ (%)	<u>206Pb*</u> <u>238U</u>	$\pm 2s$ (%)	error corr.	<u>207Pb*</u> <u>206Pb*</u>	$\pm 2s$ (Ma)	<u>207Pb*</u> <u>235U</u>	$\pm 2s$ (Ma)	<u>206Pb*</u> <u>238U*</u>	$\pm 2s$ (Ma)	% disc.
SM10C4L_81A	1976	0.11	29719	6.440	12.94	0.2710	12.65	0.98	2581	46	2038	114	1546	174	45
SM10C4M_68	1462	0.43	21829	10.386	2.62	0.4373	2.53	0.97	2580	11	2470	24	2339	50	11
SM10C4M_17	3471	0.91	31740	8.131	2.55	0.3426	2.42	0.95	2578	14	2246	23	1899	40	30
SM10C4L_84A	1160	0.18	5782	6.861	5.03	0.2891	3.87	0.77	2578	53	2094	45	1637	56	41
SM10C4M_57	1735	0.13	17542	9.369	2.46	0.3952	2.41	0.98	2577	9	2375	23	2147	44	20
SM10C4M_55	879	0.22	3750	8.878	4.05	0.3749	3.84	0.95	2575	21	2326	37	2053	68	24
SM10C4L_103	3300	1.14	22246	8.025	3.37	0.3392	3.15	0.93	2573	20	2234	30	1883	51	31
SM10C4M_21B	2057	0.47	99041	9.144	5.55	0.3866	5.47	0.99	2573	16	2353	51	2107	98	21
SM10C4M_51	2351	0.18	13649	10.099	2.72	0.4275	2.04	0.75	2571	30	2444	25	2294	39	13
SM10C4M_6	1326	0.38	14879	10.314	1.50	0.4368	1.28	0.85	2570	13	2463	14	2336	25	11
SM10C4M_38B	1744	0.26	85986	8.428	1.34	0.3570	1.14	0.85	2570	12	2278	12	1968	19	27
SM10C4M_14A	1830	0.12	9183	9.178	3.42	0.3888	3.04	0.89	2569	26	2356	31	2117	55	21
SM10C4L_90B	1554	0.36	44058	10.284	5.02	0.4357	3.63	0.72	2569	58	2461	46	2331	71	11
SM10C4L_85	276	0.02	24353	10.636	4.94	0.4513	4.14	0.84	2567	45	2492	46	2401	83	8
SM10C4M_61	2107	0.09	25797	6.453	2.36	0.2744	2.07	0.88	2563	19	2040	21	1563	29	44
SM10C4M_59	888	0.11	6391	8.977	3.03	0.3821	2.93	0.97	2561	13	2336	28	2086	52	22
SM10C4M_12	2704	0.20	30930	9.013	2.96	0.3842	2.61	0.88	2559	23	2339	27	2096	47	21
SM10C4M_83	2213	0.36	32244	7.765	1.84	0.3317	1.61	0.88	2555	15	2204	17	1847	26	32
SM10C4L_88A	2426	0.82	11122	4.709	5.65	0.2012	5.50	0.97	2555	21	1769	47	1182	59	59
SM10C4M_77	1847	0.42	68594	7.625	1.94	0.3262	1.78	0.92	2553	13	2188	17	1820	28	33
SM10C4M_24A	807	0.15	7725	9.062	3.15	0.3877	2.45	0.78	2553	33	2344	29	2112	44	20
SM10C4M_72	2337	0.39	371509	6.346	2.14	0.2715	1.91	0.89	2553	16	2025	19	1549	26	44
SM10C4L_94	2015	0.10	193268	6.626	3.51	0.2841	2.95	0.84	2549	32	2063	31	1612	42	41
SM10C4M_15A	1593	0.06	7560	5.577	14.78	0.2392	14.55	0.98	2549	43	1913	127	1382	181	51
SM10C4L_100	3153	0.40	28388	7.417	2.68	0.3183	2.40	0.90	2548	20	2163	24	1781	37	34
SM10C4M_38A	1210	0.21	5575	8.863	3.58	0.3805	2.05	0.57	2547	49	2324	33	2078	36	21
SM10C4M_29	2238	0.06	8642542	3.162	11.28	0.1368	11.00	0.98	2534	41	1448	87	827	85	72
SM10C4M_84	2366	0.08	19513	5.901	2.06	0.2569	1.88	0.91	2524	14	1961	18	1474	25	46
SM10C4M_27	1595	0.16	13758	3.375	21.63	0.1474	21.58	1.00	2519	25	1499	169	886	179	69
SM10C4M_2B	2706	0.14	23112	8.673	2.32	0.3794	1.79	0.77	2515	25	2304	21	2074	32	21
SM10C4M_71	1949	0.52	33960	4.423	3.07	0.1936	2.79	0.91	2514	22	1717	25	1141	29	59
SM10C4M_31	1475	0.05	77557	3.439	6.47	0.1508	6.33	0.98	2511	22	1513	51	906	53	68
SM10C4M_47	3810	0.27	71000	7.186	2.96	0.3154	2.58	0.87	2510	24	2135	26	1767	40	34
SM10C4L_84B	1529	0.12	1896	3.111	4.77	0.1371	4.22	0.88	2503	38	1435	37	828	33	71

Spot	Corrected Isotope Ratios								Apparent Ages (Ma)						
	U ppm	Th/U ppm	<u>206Pb</u> <u>204Pb</u>	<u>207Pb*</u> <u>235U*</u>	$\pm 2s$ (%)	<u>206Pb*</u> <u>238U</u>	$\pm 2s$ (%)	error corr.	<u>207Pb*</u> <u>206Pb*</u>	$\pm 2s$ (Ma)	<u>207Pb*</u> <u>235U</u>	$\pm 2s$ (Ma)	<u>206Pb*</u> <u>238U*</u>	$\pm 2s$ (Ma)	% disc.
SM10C4L_102	1979	0.55	11808	3.628	5.19	0.1620	4.94	0.95	2481	27	1556	41	968	44	65
SM10C4M_53	1857	0.10	129007	2.995	9.40	0.1343	9.12	0.97	2474	39	1406	72	812	70	71
SM10C4M_52	2092	0.20	32178	1.201	7.52	0.0540	7.07	0.94	2469	43	801	42	339	23	88
SM10C4M_2A	1530	0.11	8112	7.786	3.16	0.3550	2.87	0.91	2446	22	2207	28	1958	48	23
SM10C4M_21A	1989	0.11	4877	0.851	9.87	0.0393	9.60	0.97	2425	39	625	46	248	23	91
SM10C4M_33	2259	0.05	3221	1.331	13.13	0.0615	12.79	0.97	2424	51	860	76	385	48	87
SM10C4M_10	1829	0.05	19372	2.530	8.34	0.1190	8.01	0.96	2394	40	1281	61	725	55	74
SM10C4L_93	2431	0.12	79114	4.627	3.18	0.2185	2.62	0.83	2386	31	1754	27	1274	30	51
SM10C4L_97A	3046	0.06	13950	1.175	9.63	0.0575	9.31	0.97	2325	43	789	53	361	33	87
Paleogene															
SM10C4M_19	3282	0.04	1233	0.093	15.73	0.0101	9.44	0.60	814	263	90	14	65	6	92
SM10C4M_18A	7772	0.04	4356	0.073	14.67	0.0089	9.00	0.61	600	251	72	10	57	5	91
SM10C4L_104	5159	0.07	4765	0.054	3.12	0.0083	1.82	0.58	51	60	53	2	53	1	4
SM10C4M_54	4863	0.05	11330	0.057	7.81	0.0081	2.69	0.34	225	169	56	4	52	1	77
SM10C4M_63B	5397	0.06	5384	0.053	6.79	0.0081	4.68	0.69	97	116	53	4	52	2	46
SM10C4M_82	3477	0.08	1354	0.058	5.68	0.0080	4.00	0.70	286	92	57	3	52	2	82
SM10C4M_46	6069	0.04	2025	0.052	4.23	0.0080	2.67	0.63	53	78	51	2	51	1	3
SM10C4L_82A	4142	0.08	1182	0.048	11.48	0.0079	7.17	0.62	-97	220	48	5	51	4	153
SM10C4M_13B	5666	0.05	418	0.050	5.34	0.0079	3.06	0.57	13	105	50	3	51	2	286
SM10C4L_96	7316	0.07	4317	0.051	3.49	0.0078	2.34	0.67	71	61	51	2	50	1	29
SM10C4M_23	7802	0.05	1272	0.049	3.58	0.0078	2.81	0.78	-14	54	49	2	50	1	453
SM10C4L_101	8304	0.06	2689	0.051	3.39	0.0078	2.64	0.78	57	51	50	2	50	1	12
SM10C4M_11	7895	0.05	1808	0.052	5.14	0.0078	3.49	0.68	112	89	51	3	50	2	56
SM10C4M_37	7071	0.05	2714	0.050	4.65	0.0078	2.87	0.62	43	88	50	2	50	1	15
SM10C4M_76	8408	0.06	704	0.051	5.18	0.0078	3.29	0.64	64	95	50	3	50	2	22
SM10C4M_48B	6420	0.04	408	0.052	6.78	0.0077	2.01	0.30	151	152	52	3	50	1	68
SM10C4M_70	6760	0.04	794	0.050	4.16	0.0077	3.31	0.80	39	60	49	2	50	2	27
SM10C4M_79	6177	0.06	5340	0.050	3.16	0.0077	2.46	0.78	72	47	50	2	49	1	31
SM10C4M_16	5508	0.05	560	0.051	3.24	0.0077	2.27	0.70	107	55	51	2	49	1	54
SM10C4M_22	4220	0.04	593	0.050	4.49	0.0077	3.53	0.79	80	66	50	2	49	2	38
SM10C4M_28B	5775	0.05	1540	0.050	4.71	0.0076	2.77	0.59	88	90	50	2	49	1	44
SM10C4M_75	6459	0.05	2004	0.050	3.25	0.0076	2.04	0.63	63	60	49	2	49	1	22
SM10C4M_7A	6671	0.04	2555	0.051	5.74	0.0076	1.62	0.28	108	130	50	3	49	1	55
SM10C4M_60	3887	0.04	32229	0.049	4.23	0.0075	2.57	0.61	48	80	48	2	48	1	1

Spot	Corrected Isotope Ratios								Apparent Ages (Ma)						
	U ppm	Th/U ppm	<u>206Pb</u> <u>204Pb</u>	<u>207Pb*</u> <u>235U*</u>	$\pm 2s$ (%)	<u>206Pb*</u> <u>238U</u>	$\pm 2s$ (%)	error corr.	<u>207Pb*</u> <u>206Pb*</u>	$\pm 2s$ (Ma)	<u>207Pb*</u> <u>235U</u>	$\pm 2s$ (Ma)	<u>206Pb*</u> <u>238U*</u>	$\pm 2s$ (Ma)	% disc.
SM10C4M_45	6442	0.06	1138	0.051	5.15	0.0075	3.97	0.77	166	77	51	3	48	2	71
SM10C4M_62	6709	0.04	12183	0.049	3.72	0.0074	2.66	0.72	85	62	49	2	48	1	44
SM10C4M_4A	6348	0.10	591	0.052	10.22	0.0074	5.67	0.55	205	197	51	5	48	3	77
SM10C4L_83	3999	0.16	435	0.050	4.36	0.0074	2.59	0.59	140	82	50	2	48	1	66
SM10C4M_35	8769	0.05	1428	0.049	4.15	0.0074	3.16	0.76	102	64	49	2	48	2	53
SM10C4M_4B	3546	0.09	433	0.047	9.75	0.0074	6.30	0.65	5	179	47	4	48	3	921
SM10C4M_67	6823	0.05	1841	0.049	3.04	0.0074	2.28	0.75	76	48	48	1	48	1	37
SM10C4L_91	7812	0.07	973	0.046	3.50	0.0074	2.46	0.70	-40	61	46	2	48	1	220
SM10C4M_86	3388	0.08	897	0.047	3.90	0.0074	1.98	0.51	12	81	47	2	47	1	313
SM10C4M_50	5605	0.05	9535	0.049	3.82	0.0074	2.42	0.64	85	70	48	2	47	1	44
SM10C4M_58	7395	0.05	1398	0.048	3.31	0.0074	2.61	0.79	46	49	47	2	47	1	3
SM10C4M_42	6452	0.04	2323	0.047	3.61	0.0074	2.41	0.67	18	64	47	2	47	1	160
SM10C4M_43	7178	0.04	1858	0.049	3.18	0.0074	2.05	0.65	101	58	48	2	47	1	54
SM10C4M_1	6272	0.04	2332	0.047	3.01	0.0073	1.61	0.54	43	61	47	1	47	1	9
SM10C4M_64	7024	0.04	863	0.048	3.72	0.0073	3.11	0.84	88	48	48	2	47	1	47
SM10C4M_66	3501	0.09	860	0.047	8.50	0.0073	4.36	0.51	47	174	47	4	47	2	1
SM10C4M_28A	3088	0.10	13793	0.047	8.03	0.0072	3.77	0.47	57	169	47	4	46	2	18
SM10C4L_82B	7954	0.08	1770	0.047	8.04	0.0072	5.09	0.63	71	148	47	4	46	2	35
SM10C4M_81	7073	0.05	1005	0.048	3.62	0.0072	2.67	0.74	95	58	47	2	46	1	51
SM10C4M_74	2758	0.03	1523	0.049	10.32	0.0072	4.08	0.40	180	221	49	5	46	2	75
SM10C4M_7B	8138	0.05	2197	0.046	6.49	0.0072	2.72	0.42	15	142	46	3	46	1	201
SM10C4M_36	6224	0.04	3695	0.046	5.33	0.0072	2.96	0.56	4	107	45	2	46	1	1141
SM10C4M_20A	7431	0.05	909	0.047	6.80	0.0071	4.74	0.70	91	116	47	3	46	2	50
SM10C4L_95	4851	0.05	61090	0.046	3.98	0.0071	2.87	0.72	65	66	46	2	45	1	30
SM10C4M_73	7117	0.12	4045	0.047	7.13	0.0070	3.47	0.49	122	147	47	3	45	2	63
SM10C4M_41	6002	0.05	1789	0.048	3.29	0.0070	2.16	0.66	163	58	47	2	45	1	73
SM10C4M_5	10173	0.05	887	0.045	3.25	0.0070	2.63	0.81	15	46	44	1	45	1	205
SM10C4L_98	6519	0.06	2205	0.047	4.37	0.0070	3.07	0.70	133	73	47	2	45	1	67
SM10C4M_13A	6292	0.05	1004	0.045	5.20	0.0069	3.49	0.67	80	92	45	2	45	2	45
SM10C4L_89	6773	0.06	1669	0.048	3.81	0.0069	2.39	0.63	194	69	47	2	44	1	77
SM10C4M_56	3206	0.08	855	0.046	4.13	0.0068	2.68	0.65	140	74	46	2	44	1	69
SM10C4M_48A	9405	0.04	470	0.045	7.16	0.0068	2.22	0.31	128	160	45	3	44	1	66
SM10C4L_92	2055	0.10	441	0.042	5.33	0.0066	3.25	0.61	12	102	42	2	42	1	259
SM10C4L_99	2521	0.04	579	0.042	6.09	0.0065	3.11	0.51	42	125	42	3	42	1	1

Spot	Corrected Isotope Ratios								Apparent Ages (Ma)						
	U ppm	Th/U ppm	$\frac{206\text{Pb}}{204\text{Pb}}$	$\frac{207\text{Pb}^*}{235\text{U}^*}$	$\pm 2s$ (%)	$\frac{206\text{Pb}^*}{238\text{U}}$	$\pm 2s$ (%)	error corr.	$\frac{207\text{Pb}^*}{206\text{Pb}^*}$	$\pm 2s$ (Ma)	$\frac{207\text{Pb}^*}{235\text{U}}$	$\pm 2s$ (Ma)	$\frac{206\text{Pb}^*}{238\text{U}^*}$	$\pm 2s$ (Ma)	% disc.
SM10C4M_78A	3786	0.05	5218	0.046	13.00	0.0065	10.46	0.81	232	178	45	6	42	4	82
SM10C4M_63A	6131	0.05	1015	0.041	8.07	0.0062	4.84	0.60	76	153	41	3	40	2	47
SM10C4M_8	2211	0.03	1369	0.041	5.28	0.0062	2.13	0.40	83	115	41	2	40	1	52
SM10C4M_80A	7858	0.06	615	0.043	7.64	0.0060	4.08	0.53	287	148	43	3	39	2	87

Table C4: Corrected Isotope Ratios and Apparent Ages for House Mountain

Spots in **bold** were used in the calculation of zircon growth event averages. Spots in ***bold and italics*** were less than 30% discordant, but were not used to calculate averages because the sample did not have more than 4 spots with discordance less than 30%.

Discordance was not used as a filter for Paleogene dates.

Spot	Corrected Isotope Ratios								Apparent ages (Ma)						
	U ppm	Th/U ppm	<i>206Pb</i> <i>204Pb</i>	<i>207Pb*</i> <i>235U*</i>	$\pm 2s$ (%)	<i>206Pb*</i> <i>238U</i>	$\pm 2s$ (%)	error corr.	<i>207Pb*</i> <i>206Pb*</i>	$\pm 2s$ (Ma)	<i>207Pb*</i> <i>235U</i>	$\pm 2s$ (Ma)	<i>206Pb*</i> <i>238U*</i>	$\pm 2s$ (Ma)	% disc.
HM11-01															
Paleoarchean															
HM11-01_M_43	2041	0.22	62	4.425	10.08	0.0968	9.49	0.94	3624	52	1717	83	596	54	87
HM11-01_M_42	2189	0.20	76	2.798	11.83	0.0737	10.75	0.91	3337	77	1355	88	458	48	89
Neoarchean															
<i>HM11-01_M_50</i>	<i>501</i>	<i>1.50</i>	<i>15688</i>	<i>8.396</i>	<i>6.15</i>	<i>0.3617</i>	<i>5.19</i>	<i>0.84</i>	<i>2541</i>	<i>55</i>	<i>2275</i>	<i>56</i>	<i>1990</i>	<i>89</i>	<i>25</i>
HM11-01_M_48	989	0.17	9670	3.691	10.55	0.1647	8.78	0.83	2482	99	1569	84	983	80	65
HM11-01_M_44	1206	0.47	22437	3.353	7.28	0.1595	6.30	0.87	2374	62	1493	57	954	56	64
HM11-01_M_45	1411	0.08	16525	2.361	12.96	0.1172	11.58	0.89	2301	100	1231	92	714	78	73
HM11-01_M_52	1398	0.10	4117	2.032	6.87	0.1098	5.63	0.82	2154	69	1126	47	672	36	72
HM11-01_M_49	1574	0.12	2532	1.041	8.78	0.0586	7.80	0.89	2083	71	725	45	367	28	85
Paleogene															
HM11-01_M_53	2052	0.10	1689	1.327	6.55	0.0808	5.39	0.82	1943	67	858	38	501	26	77
HM11-01_M_46	1724	0.09	3052	0.683	9.29	0.0444	5.99	0.64	1824	129	529	38	280	16	86
HM11-01_M_54	1635	0.10	1472	0.665	11.43	0.0525	10.15	0.89	1465	100	518	46	330	33	79

Spot	Corrected Isotope Ratios								Apparent ages (Ma)						
	U ppm	Th/U ppm	<i>206Pb</i> <i>204Pb</i>	<i>207Pb*</i> <i>235U*</i>	$\pm 2s$ (%)	<i>206Pb*</i> <i>238U</i>	$\pm 2s$ (%)	error corr.	<i>207Pb*</i> <i>206Pb*</i>	$\pm 2s$ (Ma)	<i>207Pb*</i> <i>235U</i>	$\pm 2s$ (Ma)	<i>206Pb*</i> <i>238U*</i>	$\pm 2s$ (Ma)	% disc.
HM11-06															
Neoarchean															
HM11-06_S_149	530	0.70	92954	10.792	5.98	0.4555	5.52	0.92	2575	38	2505	56	2420	111	7
HM11-06_S_150	296	1.37	4352	10.843	5.30	0.4592	4.91	0.93	2570	33	2510	49	2436	100	6
HM11-06_S_155	119	1.42	10998	9.870	5.83	0.4185	5.23	0.90	2568	43	2423	54	2253	99	14
HM11-06_S_152	113	1.05	3494	10.473	5.84	0.4461	5.43	0.93	2560	36	2478	54	2378	108	8
HM11-06_M_165	369	0.77	25023	9.905	4.86	0.4234	4.41	0.91	2554	34	2426	45	2276	84	13
HM11-06_S_147	476	0.46	14406	10.443	5.66	0.4465	5.23	0.92	2554	36	2475	52	2380	104	8
HM11-06_M_167	321	0.87	2818	9.170	4.96	0.3934	4.51	0.91	2548	35	2355	45	2139	82	19

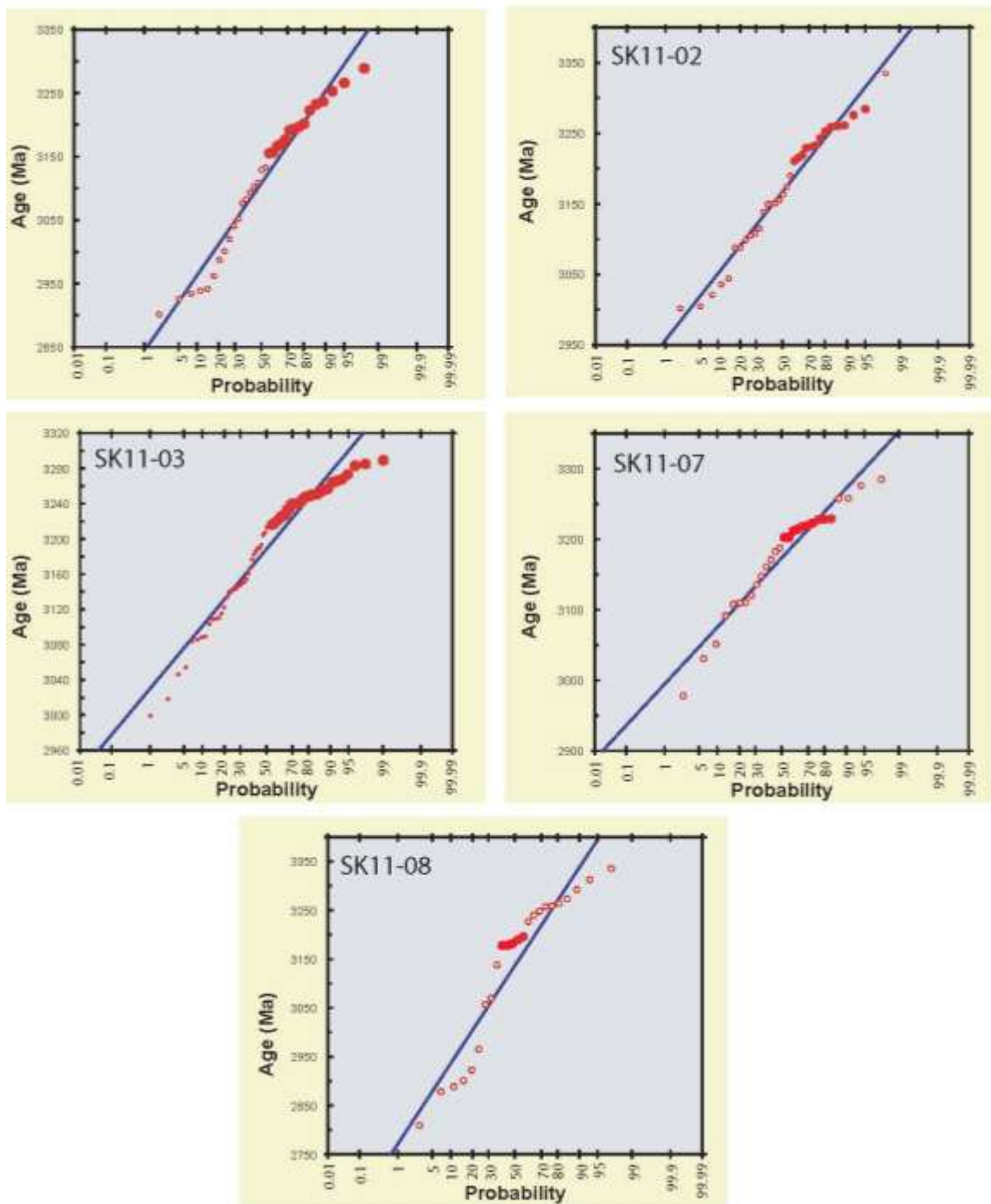
Spot	Corrected Isotope Ratios								Apparent Ages (Ma)						
	U ppm	Th/U ppm	$\frac{206\text{Pb}}{204\text{Pb}}$	$\frac{207\text{Pb}^*}{235\text{U}^*}$	$\pm 2s$ (%)	$\frac{206\text{Pb}^*}{238\text{U}}$	$\pm 2s$ (%)	error corr.	$\frac{207\text{Pb}^*}{206\text{Pb}^*}$	$\pm 2s$ (Ma)	$\frac{207\text{Pb}^*}{235\text{U}}$	$\pm 2s$ (Ma)	$\frac{206\text{Pb}^*}{238\text{U}^*}$	$\pm 2s$ (Ma)	% disc.
HM11-06_M_166	206	1.40	11635	9.916	4.79	0.4257	4.36	0.91	2547	33	2427	44	2286	84	12
HM11-06_S_151	111	0.66	1510	9.994	5.82	0.4343	5.24	0.90	2527	43	2434	54	2325	102	10
HM11-06_S_146A	397	0.32	12782	9.340	6.43	0.4065	5.95	0.92	2524	41	2372	59	2199	111	15
HM11-06_S_145	781	0.24	7764	9.313	6.50	0.4061	6.09	0.94	2521	38	2369	60	2197	113	15
HM11-06_S_161B	728	0.32	4027	4.182	8.96	0.1840	8.22	0.92	2506	60	1670	73	1089	82	61
HM11-06_S_154	148	0.66	2522	9.957	6.05	0.4410	5.55	0.92	2495	41	2431	56	2355	109	7
HM11-06_S_159	296	0.52	20133	8.371	5.85	0.3775	4.85	0.83	2465	55	2272	53	2064	86	19
HM11-06_S_146B	1028	0.16	6459	2.953	9.37	0.1337	8.61	0.92	2458	62	1396	71	809	65	71
HM11-06_S_143	666	0.53	5423	5.088	12.49	0.2312	12.32	0.99	2451	35	1834	106	1341	149	50
HM11-06_S_163	461	0.35	2312	6.294	14.89	0.2876	14.31	0.96	2442	70	2018	130	1629	206	38
HM11-06_S_158	332	0.31	13034	4.678	14.60	0.2240	14.31	0.98	2363	50	1763	122	1303	169	49
HM11-06_S_161A	524	0.18	1251	3.266	30.39	0.1575	28.86	0.95	2351	163	1473	236	943	253	64
HM11-06_S_162	782	0.16	17487	3.981	13.10	0.1927	12.38	0.95	2344	73	1630	106	1136	129	56
HM11-06_S_144	395	0.48	5108	7.511	5.96	0.3670	4.19	0.70	2328	73	2174	53	2015	73	16
Paleoproterozoic															
HM11-06_S_160	1354	0.15	2497	1.111	7.90	0.0666	7.03	0.89	1971	64	759	42	416	28	81
HM11-06_S_153	460	0.03	2349	3.784	8.16	0.2370	7.52	0.92	1893	57	1589	66	1371	93	31
Paleogene															
HM11-06_S_156	9941	0.26	1645	0.046	9.57	0.0058	4.35	0.45	509	187	46	4	38	2	93
HM11-06_S_157	15106	0.28	4734	0.036	6.43	0.0055	5.48	0.85	64	80	36	2	35	2	45

APPENDIX D

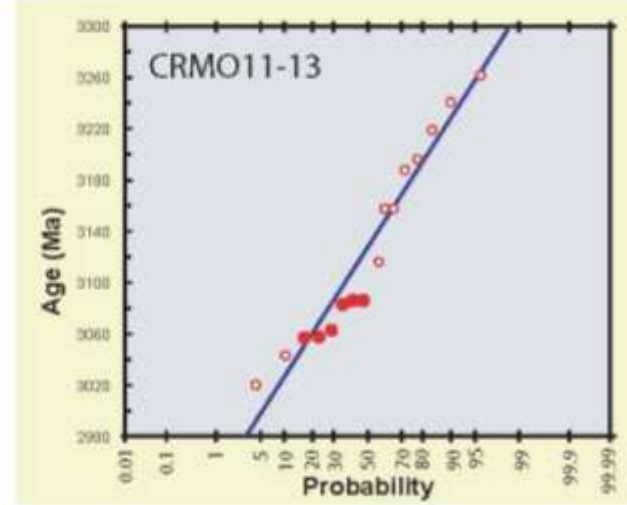
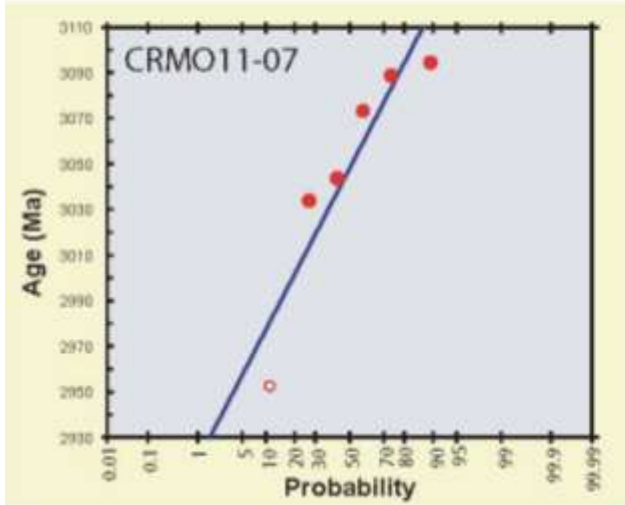
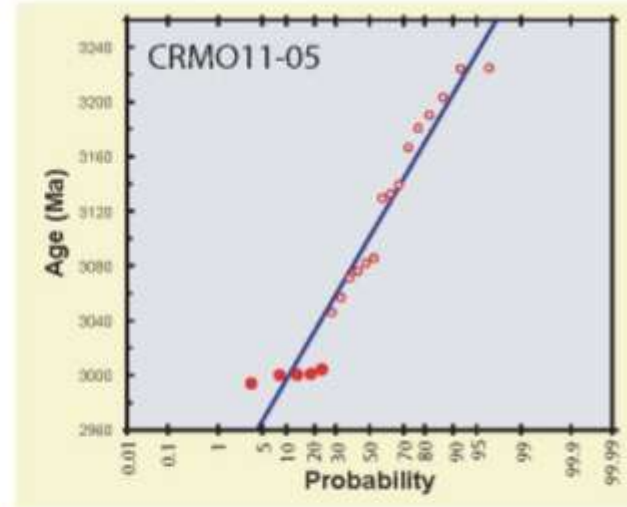
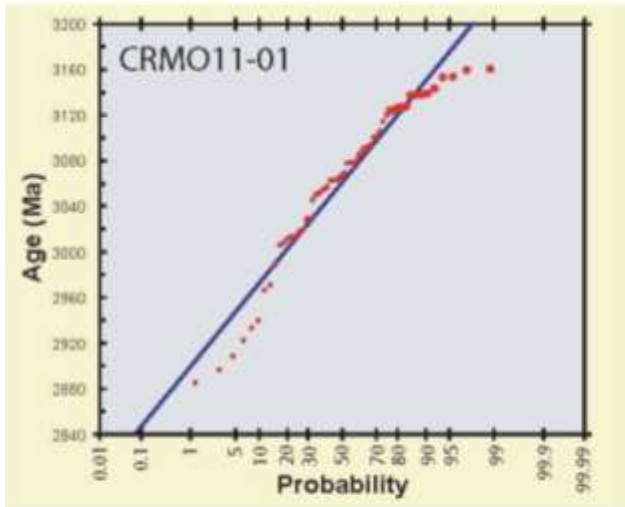
Linearized probability plots

D1: Linearized probability plots for Kilgore-Craters terrane Mesozoic ages.
 Unfilled circles are considered outliers and were not used in the calculation of population averages.

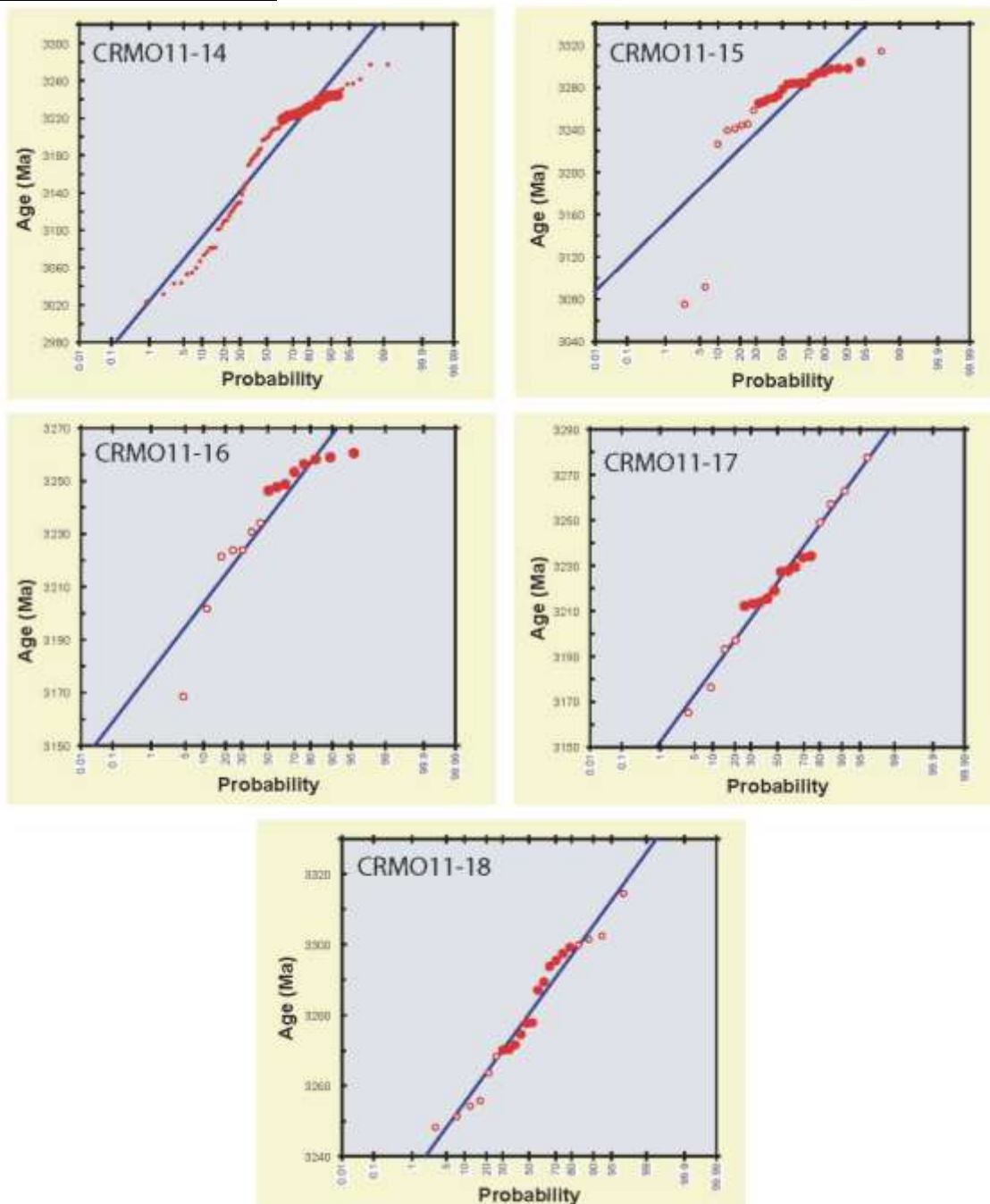
Spencer Kilgore



Craters of the Moon

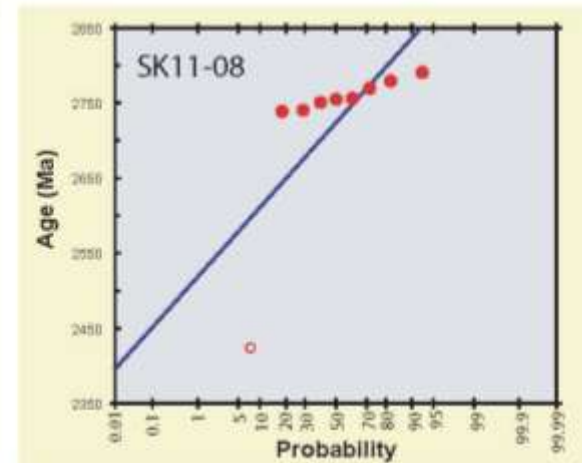
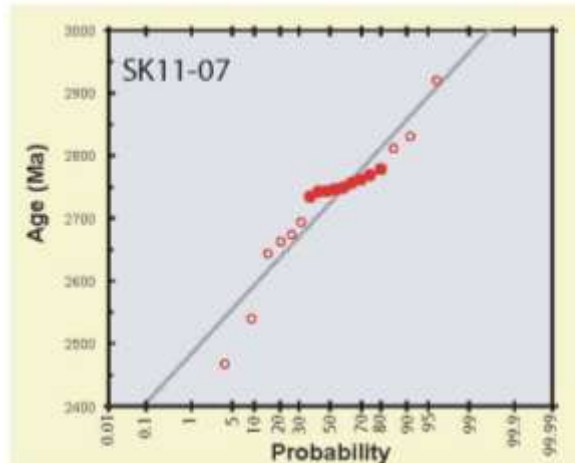
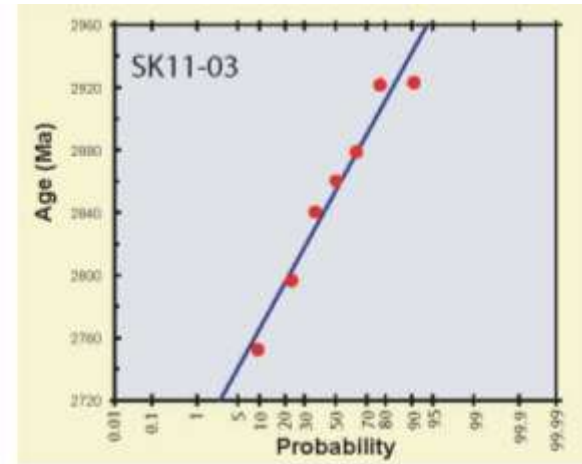
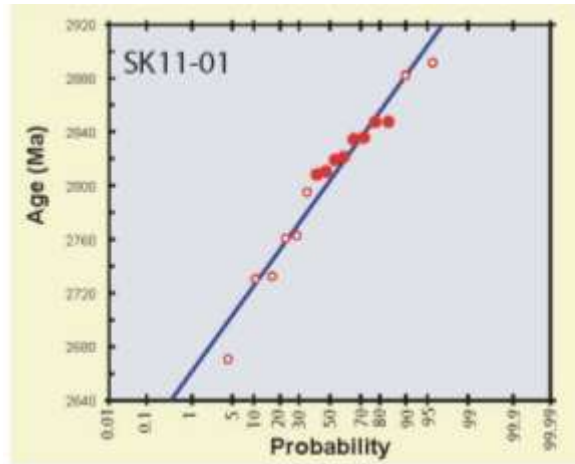


Craters of the Moon con't

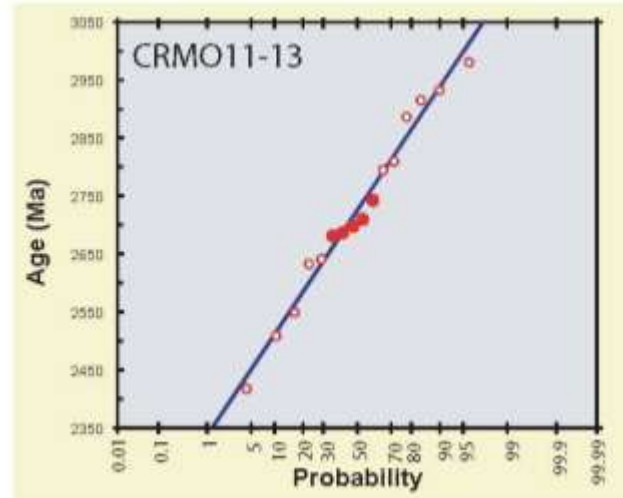
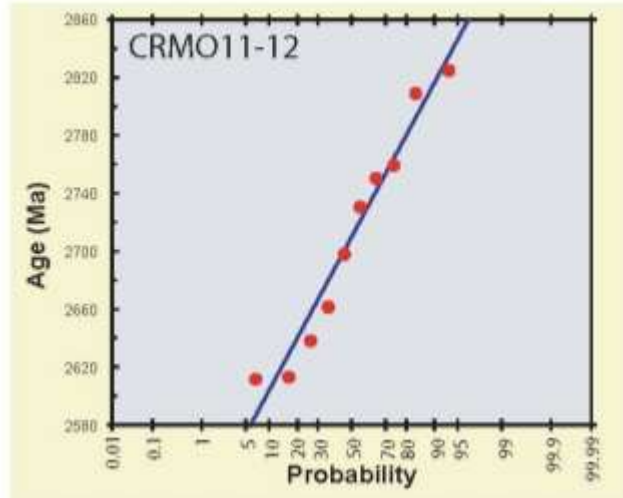
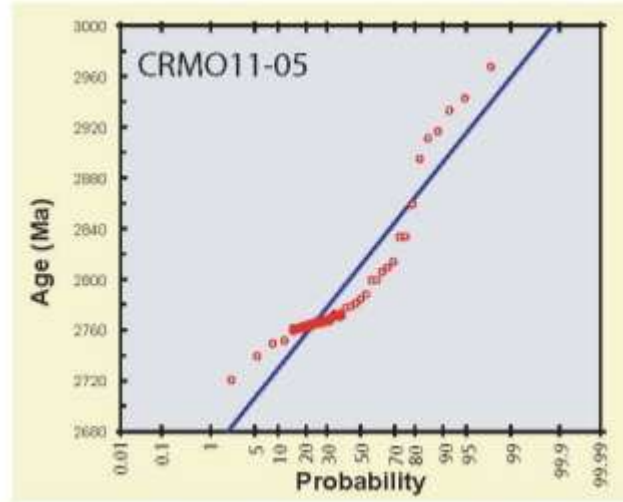
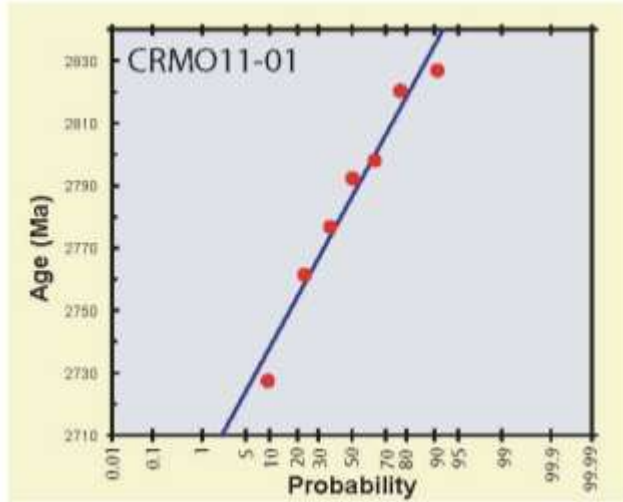


D2: Linearized probability plots for Kilgore-Craters terrane Neoproterozoic ages. Unfilled circles are considered outliers and were not used in the calculation of population averages.

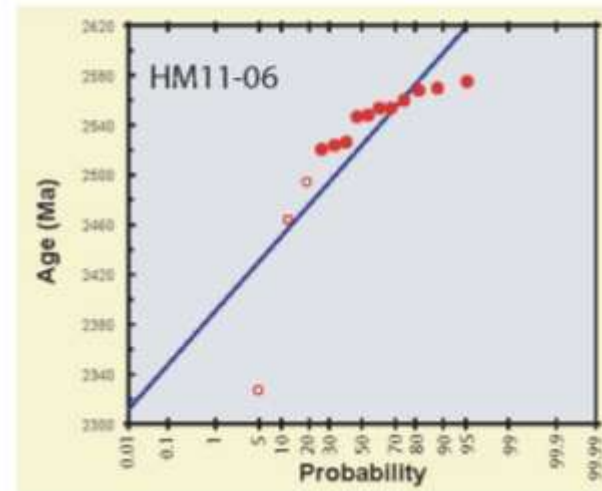
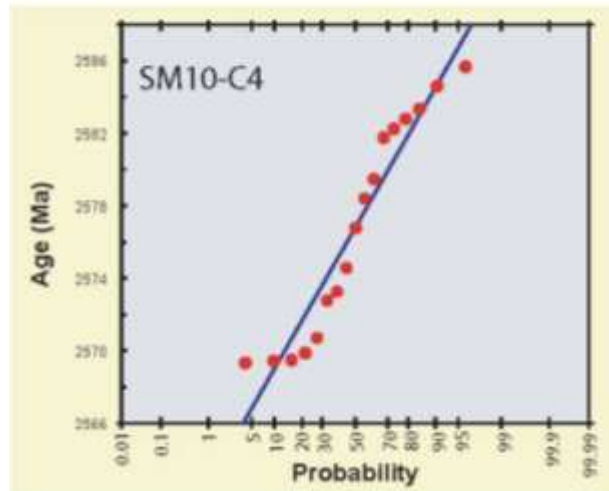
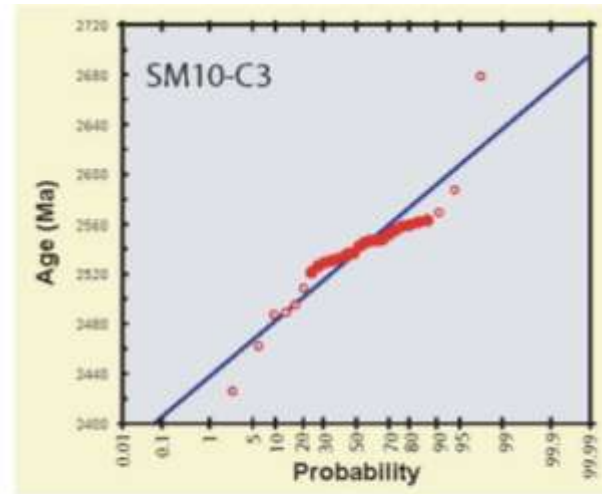
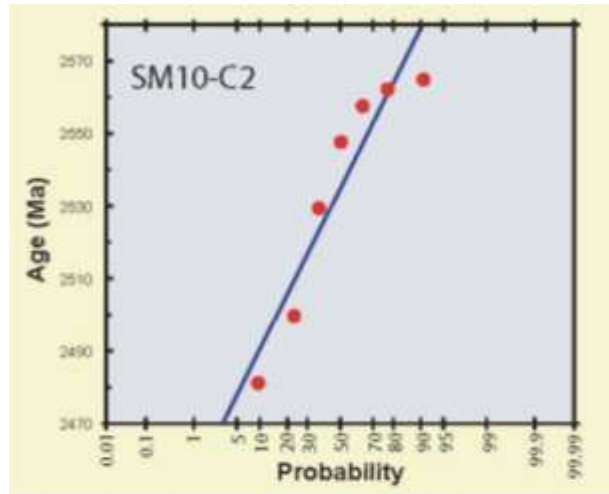
Spencer-Kilgore



Craters of the Moon



D3: Linearized probability plots for Square Mountain terrane Neoproterozoic ages. Unfilled circles are considered outliers and were not used in the calculation of population averages.



APPENDIX E

Geochemistry

Spencer-Kilore trace element concentrations

Table E1.1 Spencer-Kilgore Trace Element Concentrations
Concentrations (ppm)

Spot	P	Ti	Y	Zr	Nb	La	Ce	Pr	Nd	Sm	Eu	Gd	Tb	Dy	Ho	Er	Tm	Yb	Lu	Hf	Ta	Th	U
SK11-01																							
Paleoarchean																							
SK11S-01_36	82.68	34.51	133.56	927693.32	1.08	0.03	0.86		0.03	0.03		3.08	1.03	11.88	3.31	15.14	4.08	47.20	8.56	16458.43	4.39	16.32	701.04
SK11S-01_38	567.11	17.27	1974.04	914242.18	6.12		29.91	0.06	1.56	4.80	0.28	36.93	13.16	168.02	65.48	289.81	66.14	612.66	90.21	15459.84	2.58	193.07	123.02
SK11S-01_46	284.53	35.45	2790.57	901617.91	5.71	0.05	9.52	0.13	2.54	7.61	1.17	57.87	19.34	250.59	92.53	410.46	89.53	805.31	108.84	11116.58	2.67	309.20	324.93
SK11S-01_41	174.68	43.02	2981.07	921848.11	3.80	0.18	7.60	0.16	3.62	8.77	1.43	60.45	20.73	258.45	97.74	429.67	94.39	807.70	118.65	11246.07	1.93	217.99	258.43
SK11-01M_129	305.95	54.18	3203.34	738226.37	5.51	0.11	9.04	0.19	4.11	9.59	1.23	66.75	23.24	311.28	108.96	463.21	106.32	965.50	115.11	9426.02	2.86	293.47	383.75
SK11-01M_143	192.38	20.82	1291.42	758477.60	5.17	0.04	6.21	0.05	1.08	4.07	0.83	26.83	8.78	124.75	42.31	192.28	47.41	461.70	56.08	8867.63	5.31	121.81	216.26
SK11-01L_231	302.40	21.84	494.14	617975.19	0.81	0.00	5.96	0.06	0.02	1.65	0.13	6.51	2.99	37.61	14.53	67.60	19.66	213.87	26.80	10306.32	1.42	36.06	361.82
SK11-01M_142	489.74	34.09	1272.11	702791.80	3.57	3.70	14.33	1.17	7.34	4.68	0.62	26.14	8.64	119.20	41.82	184.69	45.76	428.90	50.30	8326.23	1.76	126.52	185.11
SK11S-01_30	852.44	82.88	3030.21	823945.62	7.37	0.78	55.80	0.37	3.28	9.73	2.26	71.48	23.99	293.39	96.16	383.16	79.77	692.41	80.48	16163.66	2.39	1949.60	2754.38
SK11-01L_230	1725.92	38.20	2413.68	576397.92	3.84	9.86	36.53	3.44	21.38	9.05	1.18	53.57	17.00	223.81	80.82	350.59	78.60	768.55	82.45	7591.90	2.05	232.59	327.83
SK11-01M_237	346.27	32.29	1952.47	634112.99	5.11	0.04	8.30	0.13	1.47	5.32	1.06	41.09	13.00	167.63	59.74	256.91	63.24	653.69	65.42	7361.18	3.74	158.69	285.39
SK11S-01_39	512.37	42.24	3453.76	913443.80	8.28	0.14	11.09	0.20	3.16	8.43	1.09	69.84	23.22	305.80	112.30	498.47	109.98	938.54	133.99	12157.72	7.48	362.61	452.55
SK11S-01_32	384.70	22.28	2564.98	927912.35	3.64	0.06	8.32	0.06	2.92	8.75	1.06	47.10	17.46	244.78	87.08	367.96	83.60	746.79	99.71	11568.07	3.73	175.94	223.60
SK11-01L_196	217.35	9.90	468.83	715814.60	0.90		24.52	0.15	2.55	2.92	0.61	13.21	3.83	45.01	14.59	60.53	15.09	145.50	16.33	10422.72	0.52	28.63	36.41
Mesoarchean 2																							
SK11-01M_137	254.41	19.30	685.69	733355.64	2.82	0.06	5.68		0.16	0.82	0.20	9.73	3.75	55.20	21.14	107.36	29.07	314.95	42.80	11788.54	1.49	112.17	434.91
SK11-01M_136	313.32	16.18	831.27	696554.71	3.55	0.01	6.38	0.00	0.14	1.15	0.28	10.24	4.70	70.92	27.32	132.49	35.18	378.95	49.51	11440.40	1.38	154.79	345.90
SK11-01M_148	472.86	15.64	295.32	141916.34	1.53		7.07					15.77	2.02	24.80	8.15	44.97	7.47	147.04	10.29	2453.50		37.48	397.94
SK11S-01_31	1222.94	71.85	3024.19	769771.87	22.51	6.39	22.46	1.23	6.39	3.08	0.46	24.11	12.96	215.96	90.39	453.64	118.48	1195.47	175.92	16062.29	65.45	207.05	1510.80

Table E1.1 SK11-01 Trace Element Concentrations con't
Concentrations (ppm)

Spot	P	Ti	Y	Zr	Nb	La	Ce	Pr	Nd	Sm	Eu	Gd	Tb	Dy	Ho	Er	Tm	Yb	Lu	Hf	Ta	Th	U
SK11-01M_126A	547.27	22.69	1632.83	703384.38	8.24	0.17	18.18	0.06	1.30	3.56	0.44	27.34	9.35	138.38	51.05	228.25	57.01	528.82	59.46	8860.66	6.17	255.24	483.73
SK11-01L_207	1614.51	27.32	3959.20	647627.50	8.70	0.25	20.82	0.17	1.93	6.60	1.43	54.42	23.27	324.90	125.07	606.58	159.79	1741.36	199.87	8649.48	2.74	617.81	1006.50
SK11S-01_48	308.70	17.07	866.82	872460.71	5.28		2.55	0.03	0.18	1.56	0.35	13.61	5.91	79.41	27.46	122.03	28.51	263.87	33.31	15378.08	4.86	29.74	307.94
SK11-01L_200	425.04	18.29	1123.77	691887.64	4.73		33.00	0.09	1.93	5.42	0.80	27.09	8.14	110.93	37.41	166.72	41.49	415.30	48.91	9830.57	1.59	75.99	58.10
SK11-01M_145	263.66	20.50	802.21	742945.98	3.74		11.16	0.10	1.25	2.70	0.51	14.84	5.32	74.28	25.89	112.47	27.42	271.03	31.18	10870.58	3.80	82.89	144.44
SK11-01M_135	239.41	14.90	1059.75	689404.69	4.13		7.45	0.03	0.67	2.85	0.39	18.46	6.82	93.96	33.61	147.45	37.97	371.03	44.09	7638.96	2.14	130.60	200.32
SK11-01M_126B	637.90	32.10	1802.00	695508.86	10.60	0.67	20.97	0.25	1.39	3.79	0.46	32.00	11.71	155.24	57.01	259.20	65.00	601.33	71.06	8851.00	6.40	325.98	542.79
SK11-01M_141	276.19	22.75	650.65	734406.24	12.76	0.03	7.29	0.02	0.51	0.80	0.20	7.93	2.72	44.69	17.07	96.50	27.83	325.66	44.02	12547.80	30.51	173.67	581.33
SK11-01L_203	404.68	16.12	1277.55	669936.16	2.44	0.01	24.52	0.11	2.15	5.17	2.29	23.82	7.64	109.52	39.78	198.06	56.93	625.12	78.99	7463.45	0.70	58.87	88.25
SK11-01L_204	586.27	8.63	911.37	635162.80	0.92		15.48	0.09	1.58	3.91	1.59	19.44	6.63	82.77	29.98	138.76	38.45	426.92	49.69	7094.47	0.21	42.87	52.95
SK11-01L_209	436.81	13.13	1066.50	684490.32	5.69		28.85	0.04	1.07	4.12	0.50	20.85	7.40	98.91	35.96	161.77	41.53	423.46	48.90	9876.96	1.89	64.89	64.07
SK11-01M_139	396.41	13.13	1360.63	757820.48	4.82		30.76	0.07	2.28	6.04	0.74	30.37	9.58	128.49	45.61	200.44	49.07	477.13	58.78	10477.04	1.64	68.98	47.89
SK11-01M_131	186.90	67.01	758.88	727314.29	1.69	0.11	8.88		0.33	1.30	0.73	11.85	3.66	54.01	21.87	115.30	33.64	403.71	69.06	14922.67	2.61	260.01	3805.72
SK11-01S_259	294.17	29.74	966.36	769978.71	2.83	0.25	8.27	0.08	0.92	1.25	0.31	12.88	5.54	78.39	29.63	142.57	33.76	345.29	50.35	13153.69	2.62	135.01	924.81
SK11-01S_258	1629.37	25.01	1374.90	771042.87	2.09	16.07	45.61	3.93	25.29	9.89	3.05	34.35	10.55	121.05	41.52	199.89	46.67	464.52	68.88	10094.39	0.81	230.59	453.08
SK11-01L_208	482.82	27.31	1116.93	685450.42	11.96	0.17	11.34	0.09	0.65	1.46	0.21	11.68	4.90	80.10	33.16	170.28	51.66	569.99	61.85	10762.75	23.32	356.72	801.17
SK11-01M_132	686.82	14.07	1623.15	731149.60	4.10		28.14	0.10	3.08	6.33	0.90	35.53	12.11	157.40	52.63	236.17	61.14	595.88	73.13	9983.14	1.35	68.84	62.70
SK11-01M_235	439.84	33.03	933.57	619130.24	1.51	0.61	11.49	0.17	1.09	2.04	0.12	15.42	5.61	74.62	28.79	139.22	33.87	358.76	42.21	10776.65	2.23	248.37	1003.36
SK11-01M_128	159.51	12.86	505.90	758114.72	0.53	0.07	14.95	0.03	0.54	0.98	0.65	8.54	2.73	40.82	15.80	76.56	21.97	237.77	33.32	10812.06	0.24	49.70	73.80
SK11-01M_238	171.62	14.83	298.25	615275.71	0.70	0.10	4.71			1.08	0.22	4.59	1.54	23.47	9.38	45.45	12.03	150.25	19.40	8208.87	0.79	35.52	238.04
SK11-01L_195	543.03	19.02	1828.72	724136.65	3.85		37.93	0.12	2.75	6.01	2.55	34.85	11.11	157.54	59.22	287.76	74.73	777.33	101.20	8440.06	0.96	112.08	113.21
SK11-01S_252	319.64	28.45	940.25	760453.58	25.43	0.05	14.23		0.28	0.56	0.13	7.06	3.70	54.98	23.84	143.27	41.28	473.44	82.62	16144.08	50.64	196.06	556.01
SK11-01M_138	801.66	44.61	2249.25	744068.55	6.55	0.05	6.94	0.03	0.50	1.95	0.46	23.99	11.08	173.90	69.69	340.11	92.55	966.41	125.64	11527.84	5.41	193.77	1450.19
SK11-01L_202B	358.68	9.58	898.52	619003.51	2.13		23.40		0.68	2.97	1.60	16.95	5.63	76.61	30.35	142.73	40.72	464.21	55.33	7225.32	0.70	52.10	74.67
SK11-01L_202A	329.31	11.87	807.70	686245.59	2.09		19.89	0.02	1.29	2.92	1.51	17.52	5.12	66.60	25.27	123.44	34.89	395.82	49.49	7825.57	0.55	45.33	64.61

Table E1.1 SK11-01 Trace Element Concentrations con't
Concentrations (ppm)

Spot	P	Ti	Y	Zr	Nb	La	Ce	Pr	Nd	Sm	Eu	Gd	Tb	Dy	Ho	Er	Tm	Yb	Lu	Hf	Ta	Th	U
SK11-01M_147	279.36	28.52	752.54	747406.60	2.30	0.09	4.80	0.01	0.40	0.56	0.24	8.30	3.29	54.54	22.41	117.12	34.70	379.58	53.84	13141.10	1.66	87.57	721.79
SK11-01M_127	512.43	23.82	1212.36	739941.49	1.82	0.01	5.73	0.03	0.52	1.66	0.51	16.11	6.75	97.38	37.59	188.64	50.08	540.02	73.66	9555.34	1.25	104.50	708.33
SK11-01M_149		27.77	273.19	106807.68										14.05	3.79	26.64	5.31	126.71	13.20	1878.82	1.39	30.46	334.22
SK11-01S_257	635.10	90.34	2065.78	728270.36	81.77	0.24	21.65	0.02	0.98	1.51	0.05	15.02	6.91	115.56	48.84	274.78	77.62	817.60	121.15	17577.38	186.85	556.61	1070.59
SK11-01L_211	266.06	13.59	795.08	773877.90	1.81		7.52	0.02	0.62	2.05	0.51	12.88	4.68	64.98	24.67	120.21	31.68	329.60	45.50	9738.46	0.91	69.95	297.98
SK11-01M_146	439.31	33.42	1774.31	724794.18	6.23	0.04	11.37	0.03	0.43	2.94	0.60	24.23	9.54	141.86	57.47	276.70	74.17	801.88	105.77	9309.34	4.23	188.26	1226.43
SK11S-01_44	274.68	9.17	608.41	890408.13	2.15	0.04	11.62	0.05	0.99	2.86	0.37	9.94	3.82	49.76	19.33	88.84	21.53	202.54	31.28	14398.24	1.90	44.90	87.78
SK11-01L_210	301.74	12.10	525.34	661942.62	6.32	0.04	9.90		0.00	1.42	0.12	6.25	2.31	36.94	16.15	92.41	28.53	361.58	52.03	8876.02	2.53	38.17	185.78
SK11S-01_35	989.79	21.99	3059.97	918672.31	6.43	0.40	14.99	0.14	1.32	3.47	0.66	37.43	15.58	241.70	97.15	470.50	115.42	1091.80	172.48	15461.63	3.03	446.56	708.16
SK11-01M_125	361.95	10.35	812.41	743331.46	3.87		19.41	0.02	0.79	2.45	0.29	15.61	5.41	70.83	25.91	119.61	30.91	323.83	40.87	11599.00	1.77	117.77	153.65
Neoproterozoic																							
SK11S-01_29	498.58	28.85	1554.07	855130.02	2.81	0.16	9.31	0.03	0.35	2.66	1.01	24.04	9.01	134.36	49.09	225.87	57.13	543.05	77.51	13588.83	2.40	375.92	1149.97
SK11-01S_254	489.51	53.45	912.13	644927.53	2.14	4.32	12.14	0.86	2.78	0.84	0.42	9.88	3.10	54.89	26.99	159.89	45.36	499.75	93.48	12341.22	3.41	136.64	582.68
SK11-01M_140	154.10	5.58	108.65	760304.54	0.23	0.01	6.67	0.04	0.20	0.40	0.16	1.80	0.65	8.31	3.24	16.75	4.53	60.18	9.55	8992.74	0.06	9.28	5.12
SK11-01M_144	261.91	12.87	542.81	734943.77	1.83		33.91	0.12	2.60	3.72	0.29	15.54	4.46	52.98	17.17	75.82	18.90	185.11	21.80	10940.46	0.61	112.16	42.48
SK11-01M_150	327.67	19.53	667.57	724801.31	2.19	0.03	14.35	0.08	1.59	4.16	0.15	17.22	5.72	67.13	21.28	92.33	21.99	200.96	22.80	12104.32	0.82	107.07	23.11
SK11S-01_28	337.47	15.16	811.55	847566.90	1.59	0.10	13.19	0.07	0.85	2.30	0.37	12.92	5.02	68.40	26.11	117.69	29.74	282.15	39.50	13620.06	0.86	110.93	331.30
SK11S-01_49	253.00	18.96	552.47	888638.78	1.91		12.43	0.05	0.75	2.06	0.22	11.90	4.34	49.84	16.73	74.57	17.49	159.82	19.54	13828.39	0.79	27.78	41.97
SK11-01L_197	403.03	10.51	925.09	700040.44	2.87	0.06	22.75	0.17	2.38	3.02	0.63	14.29	4.81	76.21	28.76	142.20	41.23	447.90	56.88	11318.41	25.38	59.94	477.29
SK11S-01_42	265.96	19.48	664.85	930931.66	1.47		12.78	0.06	1.49	3.32	0.30	14.30	5.00	59.53	20.61	90.36	20.10	186.69	26.56	15236.68	0.92	52.03	52.17
SK11S-01_33	210.51	21.39	597.11	869713.19	0.87	0.00	7.03	0.07	1.09	2.95	0.41	15.55	4.45	54.54	19.46	80.72	18.88	178.28	25.30	13067.36	0.24	19.26	44.33
SK11S-01_34	246.30	20.72	772.13	922477.43	2.02	0.03	13.23	0.10	1.40	3.01	0.33	13.59	6.00	70.14	24.00	103.95	24.05	212.41	27.87	14154.58	0.94	32.24	33.11
SK11-01L_206	259.46	19.21	413.10	633604.66	1.23		10.76	0.06	1.13	2.21	0.35	9.71	3.24	39.73	12.10	55.20	13.75	135.32	13.91	9013.59	0.54	26.86	38.19
SK11-01M_130	488.43	131.35	1206.67	710421.48	3.54	2.52	10.15	0.27	1.39	2.09	0.51	15.51	5.57	88.01	35.50	180.87	49.47	533.82	71.76	11582.71	5.43	192.56	1773.10
SK11S-01_37	273.23	24.09	671.42	916210.15	2.04	0.04	12.04	0.07	1.69	2.63	0.21	15.38	5.01	58.08	20.72	91.76	20.91	184.09	25.77	14624.97	0.83	52.04	53.19

Table E1.1 SK11-01 Trace Element Concentrations con't
Concentrations (ppm)

Spot	P	Ti	Y	Zr	Nb	La	Ce	Pr	Nd	Sm	Eu	Gd	Tb	Dy	Ho	Er	Tm	Yb	Lu	Hf	Ta	Th	U
SK11-01M_236A	278.34	13.57	472.89	624265.61	1.81		33.17	0.16	1.30	2.45	0.19	12.54	4.08	46.33	15.72	68.91	16.56	175.42	19.18	9870.48	0.30	70.75	32.24
SK11-01L_201	338.32	11.35	653.36	670860.72	1.43	0.02	19.44	0.01	1.22	2.49	1.03	13.62	4.73	58.62	21.27	99.32	26.51	285.07	35.28	8096.08	0.32	51.27	53.41
SK11S-01_40	207.90	18.19	625.76	928819.83	2.61		13.78	0.01	0.55	1.13	0.15	9.70	3.21	46.93	18.82	92.64	24.23	259.68	42.12	15489.82	2.20	108.40	369.60
SK11-01S_255	619.81	27.37	1816.64	757322.41	13.54	0.02	10.97	0.04	0.32	0.72	0.19	17.03	7.30	127.70	55.50	304.90	84.14	909.25	145.19	17632.51	71.09	134.37	752.96
SK11-01S_256	612.49	43.92	2068.91	752170.91	7.26	1.58	15.57	0.37	1.61	1.79	0.47	20.30	8.97	139.13	61.90	314.37	72.64	663.54	100.82	10953.51	3.18	386.59	409.78
SK11-01M_236B	293.65	10.77	433.26	617180.42	1.69		29.18	0.17	1.71	2.29	0.15	11.49	3.82	38.55	13.35	68.99	14.88	159.11	17.79	10021.24	0.41	63.10	27.08
SK11S-01_47	261.32	22.55	569.94	879546.85	1.27		16.61	0.01	1.34	2.52	0.35	11.27	4.04	51.07	18.12	77.76	18.08	165.93	22.22	14322.58	0.53	62.66	54.87
SK11-01L_205	254.00	8.09	575.08	668351.27	1.71		11.73	0.03	1.17	2.39	0.29	13.54	4.29	59.67	18.65	78.61	19.02	185.66	19.46	9466.37	1.02	29.69	52.00
SK11-01M_133	256.58	22.63	374.93	713344.47	1.29	0.03	30.86	0.18	2.56	3.98	0.28	12.00	3.56	38.23	12.42	52.37	12.14	120.76	14.17	9924.13	0.29	84.22	16.82
SK11-01L_198	193.74	10.53	333.83	720436.62	0.40		13.77	0.09	2.10	4.16	0.40	15.23	3.57	38.52	11.65	44.08	10.34	102.15	12.17	10081.53	0.11	77.96	23.38
SK11-01M_234	549.86	39.43	1354.15	639970.30	3.55	0.24	11.51	0.09	1.27	2.72	0.47	18.32	6.41	94.55	39.67	207.85	56.75	635.14	83.29	10816.14	8.08	215.47	1998.18
SK11S-01_45	238.13	10.29	614.18	970167.68	1.85		13.12	0.07	1.45	3.18	0.41	11.58	4.65	55.94	17.91	84.01	19.29	179.03	24.66	14786.22	0.74	67.22	78.36
SK11-01S_253	260.84	11.30	502.69	716778.93	1.10	0.10	16.16	0.04	2.01	2.04	0.20	7.56	3.47	41.93	15.20	76.21	18.15	182.88	29.88	13383.86	0.75	138.02	95.18
SK11S-01_43A	129.70	3.95	194.73	972572.36	0.54		3.58	0.01	0.22	0.42	0.18	2.43	0.95	13.99	4.97	30.18	8.00	91.11	16.72	13933.64	0.68	17.71	80.44
SK11S-01_43B	135.14	3.28	175.58	909886.26	0.53	0.06	3.62	0.00	0.27	0.57	0.21	2.58	0.95	12.52	5.12	26.58	7.53	83.11	14.91	13069.89	0.61	16.17	75.73
SK11-01L_199	287.35	14.42	439.13	721828.39	1.05	0.15	24.32	0.22	3.14	4.08	0.41	13.77	3.90	44.27	14.69	59.39	15.05	146.49	16.90	10528.27	0.34	86.49	34.17

Table E1.2 SK11-02 Trace Element Concentrations
Concentrations (ppm)

Spot	P	Ti	Y	Zr	Nb	La	Ce	Pr	Nd	Sm	Eu	Gd	Tb	Dy	Ho	Er	Tm	Yb	Lu	Hf	Ta	Th	U
Mesoarchean 1																							
SK11-02M_240	245.66	7.77	311.27	576262.32	0.50		14.02	0.10	0.67	1.40	0.13	6.93	2.23	26.88	9.81	43.82	11.47	137.27	14.24	8025.99	0.28	42.24	45.03
SK11S-02_57	493.16	7.68	2138.92	904839.79	1.73	0.08	21.97	0.18	2.79	10.11	1.14	53.78	16.34	200.53	70.24	312.35	68.78	604.74	87.31	13308.26	0.60	168.63	75.79

Table E1.2 SK11-02 Trace Element Concentrations con't
Concentrations (ppm)

Spot	P	Ti	Y	Zr	Nb	La	Ce	Pr	Nd	Sm	Eu	Gd	Tb	Dy	Ho	Er	Tm	Yb	Lu	Hf	Ta	Th	U
SK11S-02_50	254.43	20.87	1784.08	884583.36	3.04		8.30	0.03	0.35	2.22	1.28	27.52	9.93	147.24	55.86	270.79	66.29	642.24	91.50	13109.76	0.77	129.15	414.55
SK11-02M_163	192.24	13.63	438.02	762864.00	0.73		10.03	0.03	0.94	1.66	0.23	7.52	2.86	38.15	13.72	64.96	17.74	171.41	22.69	10207.17	0.25	66.83	67.82
SK11S-02_58	188.85	12.48	600.22	934582.63	0.64	0.04	10.99	0.05	0.75	2.06	0.38	11.54	3.63	48.89	18.36	88.48	22.50	219.40	33.34	13404.27	0.38	76.19	87.24
SK11-02M_151	243.35	18.34	1253.27	772058.81	3.93	0.01	8.96	0.01	0.43	2.03	0.98	18.38	6.84	105.57	39.86	192.80	49.54	493.34	64.54	12214.55	1.51	291.95	809.18
SK11-02S_264	193.94	12.71	344.85	746342.05	0.97		1.93				0.09	3.59	1.63	24.89	10.32	57.27	14.18	146.91	25.43	15003.02	0.61	28.39	217.62
SK11-02M_153	215.60	12.44	946.77	743579.05	3.03	0.06	9.73	0.04	0.44	2.62	1.07	18.41	6.17	87.68	30.68	140.64	35.88	360.99	45.05	11245.31	0.73	238.74	530.83
SK11-02M_152	252.79	10.15	615.73	784545.33	1.25	0.01	17.67	0.04	1.19	1.65	0.23	9.26	3.34	48.56	18.16	90.72	23.45	239.89	34.49	10646.48	0.76	127.78	122.80
SK11-02M_154	764.39	11.03	1816.93	712279.86	1.95	0.08	17.85	0.18	3.12	7.62	1.00	45.99	14.38	185.42	60.57	265.07	65.78	620.31	78.07	8803.72	0.57	86.49	46.58
SK11-02S_260	141.73	15.19	338.48	810985.46	0.92		2.35	0.05		0.34	0.24	3.89	1.60	22.49	10.53	53.58	14.76	157.12	25.90	15157.64	0.98	20.69	180.90
SK11-02M_157	453.76	19.39	2160.23	760059.40	2.51	0.06	13.00		0.80	3.63	2.26	27.42	12.05	183.92	69.19	338.98	85.06	858.74	113.22	10339.49	0.70	249.45	695.83
SK11S-02_64	825.23	10.23	3605.00	943228.74	1.44	0.07	23.91	0.66	12.90	20.41	2.44	100.82	29.65	351.42	123.15	530.28	117.20	1038.17	153.96	12509.67	0.75	197.06	83.14
SK11S-02_62	269.17	17.59	932.87	968964.03	1.46	0.06	18.53	0.10	1.68	3.49	0.46	20.15	6.15	78.29	30.58	133.47	31.62	289.36	45.63	15580.55	0.71	271.26	260.46
SK11-02M_241	242.88	21.06	465.88	620724.42	1.56	0.01	3.11				0.07	3.99	1.96	31.03	15.58	78.57	22.58	284.08	35.91	8508.33	0.94	42.31	494.07
SK11S-02_65	373.97	15.02	1845.88	991112.06	2.64	0.01	9.91	0.03	0.36	3.93	1.53	30.50	11.52	151.29	60.29	276.75	67.62	644.92	95.55	14828.71	0.67	181.11	490.96
SK11S-02_56	169.16	20.40	574.11	1003088.76	1.00		8.75	0.01	0.54	0.81	0.24	7.95	2.80	41.58	17.08	95.43	24.39	271.91	49.58	15521.49	6.10	85.56	355.13
SK11S-02_52	247.97	16.67	699.36	908102.43	0.91	0.01	18.69	0.07	1.00	1.44	0.27	11.63	4.49	56.25	20.88	102.19	25.26	244.49	38.19	14092.27	0.69	284.64	184.28
SK11-02L_213	322.45	10.12	829.52	740678.31	1.83		19.33	0.09	2.21	4.30	0.67	20.92	6.80	82.51	28.63	126.26	30.64	308.51	36.90	8552.56	0.57	75.21	55.69
SK11-02L_212A	781.40	12.11	2938.72	808212.59	3.36	0.03	35.16	0.31	5.08	16.35	1.08	82.63	24.80	309.58	99.15	412.01	95.10	865.83	101.61	11544.08	1.50	417.50	181.14
SK11S-02_54	284.84	15.65	1328.92	893418.30	1.84		15.23	0.08	1.55	4.67	1.86	30.75	9.11	120.93	43.31	195.96	46.61	434.53	65.34	13209.90	0.63	224.83	363.68
SK11S-02_56	213.33	19.66	845.77	922460.13	1.00		9.18	0.03	1.15	2.72	0.91	16.95	5.66	70.17	25.74	127.56	31.07	304.62	51.08	13649.14	1.83	173.14	398.74
SK11-02M_155	448.87	7.83	999.31	701057.32	1.92		16.81	0.04	1.32	3.94	0.56	20.85	7.12	96.44	33.57	150.24	36.94	381.76	45.73	9183.77	0.44	58.88	38.14
SK11-02M_162	1020.35	9.19	2678.03	779222.05	3.26	0.03	28.20	0.19	4.48	10.04	0.51	57.64	19.75	263.42	86.54	369.68	88.63	808.40	98.15	10953.33	1.25	290.23	154.66
SK11-02L_212B	618.24	6.87	2296.12	708616.42	1.78	0.04	23.71	0.18	4.42	11.70	1.20	65.25	18.67	245.32	81.11	331.42	75.77	684.54	84.88	9312.84	0.32	154.10	63.95
SK11-02M_156A	374.89	8.25	1036.65	735269.77	0.79	0.00	10.34	0.06	1.20	5.53	0.81	26.17	7.38	104.07	35.26	156.98	42.63	419.39	53.09	10337.76	0.51	66.57	153.75
SK11-02M_158	350.13	18.38	1180.99	670022.07	4.49	0.66	11.49	0.14	1.27	1.79	0.61	15.24	5.98	89.11	37.96	188.81	52.37	550.58	73.21	10180.61	1.04	91.09	459.95

Table E1.2 SK11-02 Trace Element Concentrations con't
Concentrations (ppm)

Spot	P	Ti	Y	Zr	Nb	La	Ce	Pr	Nd	Sm	Eu	Gd	Tb	Dy	Ho	Er	Tm	Yb	Lu	Hf	Ta	Th	U
SK11-02L_215	871.00	10.74	599.41	651983.98	0.62	5.56	28.22	1.42	7.06	6.95	2.46	22.82	6.05	62.47	17.59	76.81	19.48	195.30	21.96	6407.72	0.24	89.70	170.64
SK11S-02_53	265.52	14.45	818.61	873065.32	1.45	0.08	11.67	0.04	1.14	1.15	0.25	9.60	4.52	61.97	23.96	122.07	32.76	332.43	53.54	13308.80	2.51	234.96	396.44
SK11-02L_214	576.41	15.99	582.19	691527.37	0.90	4.73	27.72	1.18	7.77	4.96	2.34	22.93	5.48	61.62	18.23	74.57	18.07	181.21	20.47	8000.55	0.44	101.48	181.35
SK11-02M_160	481.24	21.20	1556.52	767402.12	5.19	0.18	7.87	0.01	0.35	0.75	0.32	12.21	6.50	109.86	47.35	249.35	69.85	710.85	103.72	15582.09	4.30	174.97	1087.84
SK11-02S_261	573.80	47.42	2672.00	733728.33	7.53	0.21	6.06	0.04	0.31	1.20	0.27	16.11	8.79	158.56	73.91	447.48	123.64	1424.79	264.32	19880.11	11.69	165.58	4591.62
SK11-02S_263	451.62	28.87	1279.53	727706.37	13.46	0.20	1.89	0.06	0.30	0.25		4.81	3.19	67.60	32.97	188.92	50.18	505.53	85.46	34077.77	73.20	39.44	1320.39
SK11-02M_156B	634.35	5.98	1889.82	682966.79	1.51	0.06	19.97	0.18	4.79	13.72	1.39	59.27	16.41	203.63	66.22	275.32	62.77	596.20	73.95	8744.69	0.53	112.59	53.92
Neoproterozoic																							
SK11S-02_61	206.61	11.74	484.33	954418.76	0.85		10.68		0.54	1.56	0.21	8.07	2.82	38.13	14.88	74.74	18.05	175.17	28.07	13901.97	0.36	41.33	46.82
SK11S-02_66	237.72	12.33	776.61	918687.52	1.08	0.04	13.04	0.04	0.99	2.26	0.29	13.08	4.21	61.39	22.68	113.92	28.86	281.49	41.12	13673.09	0.54	102.32	92.41
SK11-02M_239	233.17	6.41	594.61	636908.02	1.33		12.26	0.06	0.95	1.93	0.23	8.64	3.22	49.13	19.40	90.45	24.40	259.55	30.13	9266.53	0.33	73.49	89.17
SK11S-02_55	291.20	9.18	771.11	928558.67	1.26		15.60	0.00	0.71	1.97	0.27	11.84	4.26	59.38	22.97	115.01	29.48	287.55	44.28	14268.36	0.87	111.26	111.17
SK11S-02_63	268.94	13.03	713.73	944209.68	1.73	0.04	15.07	0.06	0.81	1.64	0.22	10.88	4.22	56.33	22.06	101.43	26.34	251.22	39.23	15477.82	1.19	64.10	112.96
SK11S-02_51	181.13	11.94	402.48	885252.15	0.75		10.54	0.02	0.67	1.28	0.15	8.23	2.32	32.37	12.77	60.19	15.64	158.86	22.27	12581.68	0.36	32.47	47.37
SK11-02M_161	283.04	11.17	676.92	769725.53	1.30		13.90	0.03	0.79	1.98	0.12	11.55	3.93	55.79	20.83	100.25	25.83	264.21	36.81	10763.25	0.78	83.89	83.40
SK11-02L_216	224.36	8.50	369.42	697765.78	0.77		9.67	0.03	0.76	0.93	0.15	5.67	2.23	31.11	11.72	55.50	15.00	162.76	20.07	9317.48	0.47	53.99	60.18
SK11S-02_60	176.42	13.99	474.24	936556.49	0.80	0.01	10.27	0.03	0.38	1.64	0.13	8.85	2.73	36.77	14.99	70.21	16.95	175.12	27.05	13609.09	0.44	27.91	44.74
SK11-02M_159	281.70	11.52	1029.07	754558.47	1.18		14.23	0.08	1.02	2.33	0.32	18.73	6.07	91.06	34.45	164.77	40.58	393.66	55.24	11993.01	0.63	165.92	179.48
SK11S-02_59	187.56	8.36	515.28	963545.48	0.89	0.04	12.89	0.09	0.67	1.86	0.23	9.18	2.38	41.16	16.42	78.19	21.35	212.62	35.43	14725.07	0.44	65.00	121.70

Table E1.3 SK11-03 Trace Element Concentrations

Concentrations (ppm)

Spot	P	Ti	Y	Zr	Nb	La	Ce	Pr	Nd	Sm	Eu	Gd	Tb	Dy	Ho	Er	Tm	Yb	Lu	Hf	Ta	Th	U
Mesoarchean 1																							
SK11-03M_121	346.58	10.54	814.12	804586.23	1.72	0.01	12.23	0.02	1.59	3.78	0.82	18.37	6.02	73.66	26.00	109.90	27.74	264.28	34.18	10388.78	0.53	89.39	56.55
SK11S-03_02	351.20	11.64	912.98	881026.03	1.49	0.03	12.67	0.05	1.47	3.22	0.25	20.84	6.32	83.82	29.79	130.92	30.64	275.46	41.71	12927.46	0.67	94.71	59.49
SK11-03S_246	399.62	9.46	900.72	708547.48	1.01		8.67	0.01	0.24	1.69	0.48	19.80	5.91	83.76	28.53	126.75	28.48	270.25	38.52	10165.22	0.32	59.89	37.03
SK11-03M_104	26431.49	10.02	1382.59	626217.57	1.31	260.45	521.21	60.11	298.05	62.99	6.14	79.65	14.47	147.31	47.29	190.95	45.26	464.32	53.69	8178.83	0.36	89.07	58.13
SK11S-03_19	372.73	10.63	1061.74	845159.38	2.36		18.50	0.09	2.27	4.86	0.66	27.34	8.01	98.66	34.31	148.46	33.48	309.48	42.88	11506.05	0.73	130.63	71.49
SK11-03M_102	488.47	10.71	1216.79	789321.90	1.98		16.05	0.15	2.49	6.10	0.51	30.18	9.82	116.74	40.59	171.48	41.25	402.94	46.79	10417.28	0.73	132.82	76.97
SK11S-03_24	421.48	12.40	1281.40	873294.43	2.33	0.01	20.24	0.13	2.24	6.97	0.86	34.91	10.65	122.18	42.83	176.96	39.11	360.26	51.57	12432.56	0.77	202.17	95.04
SK11-03M_115B	423.70	8.76	1111.49	743801.57	1.44	0.01	13.79	0.25	3.17	6.72	1.52	27.30	9.82	106.97	36.57	157.03	38.64	370.05	43.93	8945.36	0.58	98.11	52.66
SK11S-03_06	393.87	11.08	1212.97	883016.29	2.09	0.04	17.28	0.07	1.75	5.48	0.48	30.67	9.22	112.75	39.39	172.08	38.42	354.80	51.29	12677.45	0.76	160.72	81.96
SK11S-03_10	420.83	12.42	1098.35	839101.41	2.43		18.15	0.07	2.08	5.63	0.56	27.44	8.53	105.47	35.82	153.33	35.91	332.68	43.55	11653.13	0.74	163.28	86.39
SK11S-03_23	373.75	13.18	1115.31	878911.07	2.07		17.39	0.09	1.52	4.67	0.37	27.97	8.39	103.73	36.43	161.69	35.98	333.63	46.23	12517.53	0.78	144.81	76.26
SK11S-03_17	480.66	11.92	1929.66	852725.83	1.48	0.04	17.86	0.18	5.14	11.43	1.07	55.00	16.95	196.88	65.54	268.66	59.37	533.57	68.01	12035.95	0.60	211.65	91.49
SK11-03M_100	417.74	14.82	1044.22	769105.66	2.70		19.00	0.10	2.16	5.12	0.66	26.12	9.00	106.17	35.29	146.41	35.49	343.42	40.33	10389.86	0.74	163.05	96.54
SK11S-03_15	429.74	15.02	1260.81	850516.88	2.55		18.18	0.10	2.72	4.49	0.57	34.45	10.18	119.96	42.04	174.72	40.63	371.50	49.61	11672.24	0.93	168.95	84.56
SK11S-03_20	447.32	7.91	1542.36	853925.65	2.05		18.20	0.20	4.10	8.72	0.97	44.91	12.92	151.26	51.12	211.18	47.91	424.15	57.46	11652.69	0.76	186.42	82.49
SK11S-03_25	452.33	10.94	1380.55	886648.48	2.54	0.01	21.57	0.16	2.80	7.52	0.75	37.72	11.30	135.51	45.20	195.03	42.26	381.41	53.21	12731.31	0.81	225.76	100.04
SK11-03M_103	458.40	15.91	1129.03	750972.95	2.32	0.03	19.68	0.12	2.29	6.12	0.59	32.08	9.39	115.83	36.68	156.64	36.31	358.15	41.65	9720.59	0.74	177.37	97.98
SK11-03M_95A	378.09	15.60	988.30	803291.16	2.11		19.14	0.08	1.58	5.00	0.50	24.69	8.60	99.06	32.82	139.44	32.31	324.70	36.87	10074.23	0.82	147.01	91.44
SK11-03M_233	192.27	10.83	294.37	620688.05	1.02	0.14	1.63	0.04	0.27	0.37	0.33	5.46	1.71	27.00	8.86	45.18	13.18	154.00	21.14	10869.00	1.65	17.13	152.87
SK11-03M_95B	419.62	14.39	1018.73	765220.39	2.39	0.04	18.29	0.06	2.10	6.00	0.62	27.87	8.73	99.69	33.20	137.59	32.48	320.86	38.77	10418.23	0.76	154.94	87.23
SK11-03M_122	398.44	17.41	1053.19	743516.56	2.48	0.06	18.97	0.13	2.55	5.53	0.66	29.07	8.79	108.08	35.16	149.26	35.51	338.42	41.12	10151.85	0.71	171.82	90.64
SK11-03L_180	334.95	14.67	916.01	792794.87	1.66		14.11	0.06	1.85	3.61	0.42	21.94	6.88	88.79	31.16	130.82	30.40	291.34	39.18	11104.86	0.68	112.83	65.25
SK11-03L_181	458.43	10.44	1865.75	755065.79	1.70	0.20	19.70	0.45	8.52	15.64	1.73	68.70	18.53	208.77	62.93	254.74	56.51	522.33	61.95	9804.61	0.69	253.34	103.32
SK11-03M_96	442.04	11.57	1097.81	775589.69	2.42		19.46	0.16	2.48	5.95	0.68	30.12	8.88	109.23	35.68	152.91	36.31	356.79	40.68	10116.53	0.83	169.53	96.42

Table E1.3 SK11-03 Trace Element Concentrations con't
Concentrations (ppm)

Spot	P	Ti	Y	Zr	Nb	La	Ce	Pr	Nd	Sm	Eu	Gd	Tb	Dy	Ho	Er	Tm	Yb	Lu	Hf	Ta	Th	U
SK11-03L_194	392.72	15.65	929.32	701133.05	2.07		15.97	0.08	1.98	4.67	0.49	24.89	7.77	93.25	30.66	127.79	31.28	307.62	35.43	9025.75	0.73	134.35	78.79
SK11-03M_99	405.30	9.74	1030.87	809649.45	2.25		14.73	0.12	1.76	4.06	0.72	25.17	8.03	101.83	34.62	149.34	36.33	354.17	44.35	11686.66	0.73	132.58	84.48
SK11-03M_106	428.65	8.24	1240.64	753325.53	2.04	0.14	16.94	0.09	2.52	6.46	0.82	35.48	10.51	127.11	41.33	173.97	40.30	391.91	45.97	9908.34	0.80	153.79	84.28
SK11-03M_105	462.40	9.29	1421.51	756864.94	1.86	0.05	16.94	0.10	4.30	8.30	0.98	42.37	12.13	143.10	47.02	190.76	45.40	446.60	50.70	10265.72	0.70	168.37	90.29
SK11S-03_01	594.38	14.63	1607.33	877697.26	1.60	0.02	16.32	0.11	3.16	7.46	0.62	41.01	12.03	150.44	51.71	223.93	50.26	450.96	66.92	12350.64	0.67	142.61	72.48
SK11-03M_124	418.59	14.26	1229.14	774410.13	2.13		17.14	0.13	2.28	7.07	0.81	34.12	10.49	123.50	39.87	167.89	38.57	374.14	46.29	9914.33	0.58	147.67	72.56
SK11-03M_94	473.43	13.11	1199.45	771021.51	2.71	0.03	20.60	0.12	3.00	7.52	0.71	34.21	10.11	119.87	39.10	161.81	37.93	368.19	42.99	9976.23	0.87	178.80	97.15
SK11-03M_113	445.48	6.09	1972.10	759197.16	1.57		20.89	0.29	7.76	16.94	1.51	70.79	19.26	214.29	67.27	263.36	58.82	555.92	63.69	9972.52	0.56	250.63	106.28
SK11-03L_188	453.16	7.63	1295.74	651078.67	1.76	0.02	17.03	0.29	4.93	10.91	1.09	45.43	13.09	140.63	43.07	176.46	43.20	404.53	43.80	8191.59	0.55	170.59	85.29
SK11-03L_192	259.62	8.86	485.57	694815.89	0.75		8.69	0.02	0.93	1.57	0.30	10.04	3.41	44.54	16.86	73.74	19.77	207.42	25.66	8616.96	0.22	24.69	24.97
SK11-03M_120	394.64	14.08	953.68	768204.03	1.99	0.03	16.46	0.13	2.34	4.97	0.52	25.26	8.14	97.20	32.70	140.99	33.78	334.36	39.86	10772.39	0.86	133.71	84.58
SK11S-03_27	381.65	14.23	1162.36	891413.55	1.85	0.06	16.68	0.04	1.64	4.52	0.57	28.36	9.07	107.77	37.18	162.49	36.90	331.67	48.24	12931.43	0.70	154.63	79.81
SK11S-03_21	338.58	11.96	1246.10	905942.23	1.17	0.06	14.66	0.10	3.90	7.46	1.08	35.36	9.79	122.56	41.17	173.03	38.78	352.55	50.27	11789.16	0.56	120.57	56.46
SK11-03S_250	256.07	8.60	700.30	712739.29	1.05	0.14	2.15			0.34	0.11	6.90	2.73	44.62	19.29	104.22	30.53	380.34	70.85	15156.93	0.50	18.25	246.68
SK11S-03_03	357.17	7.58	1040.19	929245.05	1.00		11.23	0.07	1.83	3.52	0.24	22.28	7.65	89.75	33.47	151.76	35.34	325.72	49.07	13311.89	0.39	76.86	62.13
SK11-03M_118	424.78	10.76	1259.59	771534.29	1.96	0.01	14.62	0.09	2.87	6.44	0.76	32.63	10.74	120.94	41.54	178.42	41.48	408.78	46.73	10532.35	0.73	135.12	80.10
SK11-03M_97	476.86	7.29	1487.62	809937.96	1.25		12.51	0.12	2.70	7.02	0.54	41.34	12.17	148.56	49.72	208.25	49.81	473.54	56.08	11299.94	0.40	114.00	61.89
SK11S-03_16	389.29	8.46	1024.18	846301.36	1.80	0.03	15.16	0.03	1.68	3.65	0.37	22.80	7.13	94.06	32.53	150.57	34.63	326.69	45.23	11986.51	0.75	115.95	75.00
SK11-03L_189	354.39	7.44	708.90	692730.32	1.25	0.02	11.73	0.02	1.18	2.97	0.28	16.76	5.43	71.79	23.67	99.35	25.95	260.64	31.26	9096.27	0.48	74.74	57.37
SK11-03M_115A	456.73	7.02	1096.08	805347.50	1.44	0.09	12.93	0.11	2.74	6.01	1.28	27.54	8.26	108.20	35.88	158.58	37.31	371.66	45.87	9518.59	0.63	83.14	52.36
SK11-03M_107	448.26	7.12	1234.12	760499.99	1.80	0.35	17.82	0.22	3.16	7.28	1.06	37.72	10.93	128.82	41.75	171.40	40.31	384.14	45.20	10135.92	0.67	171.69	87.22
SK11S-03_13	289.17	5.74	824.44	905554.58	1.18		11.31	0.03	1.62	2.99	0.48	17.82	5.76	75.37	27.01	118.90	28.50	270.15	36.87	12577.17	0.46	69.58	44.21
SK11-03L_186	518.83	9.16	1071.40	633838.13	2.25	0.01	14.95	0.12	2.38	7.15	0.41	27.48	9.20	113.02	36.05	150.82	38.44	365.48	41.45	8856.31	0.78	173.13	107.61
SK11-03M_109	465.13	6.64	1939.87	778146.11	1.50	0.05	20.10	0.16	4.82	13.09	1.40	66.84	18.68	213.34	67.56	274.64	60.75	559.45	65.29	10560.62	0.55	247.43	103.97
SK11-03M_116	456.13	6.03	1836.11	745899.62	1.50	0.04	19.76	0.18	4.09	12.16	1.49	60.35	17.88	196.79	63.49	255.60	58.39	555.36	61.59	10314.31	0.62	234.11	107.97

Table E1.3 SK11-03 Trace Element Concentrations con't
Concentrations (ppm)

Spot	P	Ti	Y	Zr	Nb	La	Ce	Pr	Nd	Sm	Eu	Gd	Tb	Dy	Ho	Er	Tm	Yb	Lu	Hf	Ta	Th	U
SK11-03M_119B	392.86	7.42	918.59	729458.32	1.68	0.09	13.18	0.13	2.26	4.75	0.98	23.29	7.17	87.95	31.44	124.19	30.89	303.91	36.75	9006.16	0.43	77.37	42.42
SK11S-03_18	440.61	5.98	1486.61	861795.53	1.99		18.01	0.09	3.31	8.27	0.97	43.54	12.66	147.31	49.57	205.97	46.53	410.81	55.59	11839.18	0.66	196.51	84.76
SK11-03M_110A	373.86	7.98	996.17	805564.44	1.42	0.05	15.19	0.06	2.95	6.31	0.63	30.43	8.44	99.44	34.89	142.96	33.16	334.33	39.97	11103.14	0.72	118.27	73.34
SK11S-03_07	366.67	9.15	764.18	886584.63	1.50	1.23	14.32	0.30	3.95	3.96	1.78	25.70	7.30	72.97	23.42	95.06	22.03	213.91	33.10	12194.64	0.81	111.94	260.90
SK11-03M_108	466.67	7.56	1415.00	771501.32	1.81	0.01	15.41	0.13	2.86	7.43	0.82	42.04	12.41	142.59	47.63	198.94	46.07	450.88	52.13	10789.72	0.66	156.19	85.67
SK11S-03_04	374.64	10.83	1057.17	867792.30	2.39	0.30	12.91	0.09	1.58	3.37	0.84	23.99	7.55	103.61	34.50	154.01	34.98	322.71	48.32	13045.78	0.75	110.48	90.14
SK11-03M_119A	379.21	9.87	1123.49	785656.90	1.28	0.31	16.29	0.28	4.49	7.78	1.28	35.70	10.00	120.65	39.54	165.90	39.67	395.36	45.02	9894.57	0.61	109.36	54.96
SK11-03L_187	529.36	6.49	1577.42	635442.46	1.95		16.47	0.15	3.58	10.80	0.98	50.15	14.82	174.28	54.56	211.99	50.24	495.00	51.68	8185.57	0.53	187.82	97.39
SK11-03M_114	498.67	13.25	1152.00	755068.40	1.87		14.02	0.12	2.34	6.32	0.78	28.53	9.06	111.71	37.75	162.41	39.79	399.33	46.60	10294.50	0.72	99.68	70.57
SK11-03S_249	259.58	7.20	477.20	749205.41	0.37	0.18	2.06	0.04	0.50	1.30	0.11	9.92	3.13	38.05	14.32	67.27	17.11	161.66	27.05	12833.13	0.46	50.21	52.01
SK11-03L_185	455.91	8.70	872.73	666950.09	1.30	0.00	11.59	0.09	1.47	4.31	0.57	20.46	6.84	86.65	28.10	121.84	31.15	312.39	36.85	9165.24	0.55	74.53	58.54
SK11S-03_05	266.76	6.88	755.83	900008.43	0.72	0.03	9.38	0.11	1.21	2.34	0.99	16.27	5.26	68.36	24.15	110.90	25.73	229.68	36.51	12763.89	0.33	50.71	32.60
SK11-03L_183	499.34	6.31	1768.98	745638.89	1.61	0.05	16.38	0.12	2.42	7.89	0.92	45.80	14.60	182.12	58.39	246.04	57.10	526.45	62.44	10215.87	0.53	203.99	97.80
SK11-03M_123	503.75	9.04	1086.51	786361.99	1.73	0.01	12.81	0.05	2.42	5.72	0.48	25.16	7.92	101.56	34.56	149.58	37.07	359.30	45.43	10533.33	0.62	89.86	65.15
SK11S-03_14	358.01	11.60	870.37	869405.11	1.33	0.36	12.31	0.09	1.48	3.19	0.39	18.39	5.84	78.16	27.66	124.80	29.78	284.77	40.85	12599.48	0.61	80.15	57.09
SK11-03L_182	463.01	5.97	1895.09	743896.29	1.64		19.15	0.16	5.33	13.13	1.47	61.17	18.50	207.50	64.49	256.65	57.00	530.74	61.46	9849.21	0.45	252.49	103.74
SK11-03M_117	526.04	7.50	1191.74	767912.86	2.12		21.57	0.05	2.30	5.93	0.53	27.93	9.27	117.18	42.39	179.92	45.56	481.68	56.82	10056.27	0.66	91.61	62.22
SK11S-03_09	423.88	10.35	1062.94	864474.73	1.04		12.12	0.05	1.82	3.75	0.25	20.72	7.08	95.34	34.43	156.47	37.37	359.22	50.48	12395.95	0.54	83.67	54.85
SK11S-03_22	415.26	8.58	989.85	845179.43	1.93	0.01	11.73	0.02	2.08	3.32	0.33	22.41	6.65	89.24	31.89	141.31	33.83	315.03	45.60	12827.13	0.89	98.95	140.26
SK11-03M_111	573.50	5.76	1590.21	773954.22	1.17	0.08	15.10	0.06	2.54	6.81	0.78	40.32	12.39	153.03	52.42	222.99	51.69	496.24	61.09	10326.78	0.50	163.18	80.03
SK11S-03_08	333.81	10.81	685.86	842888.08	0.92		9.89	0.05	1.16	2.43	0.27	13.77	4.62	58.00	21.63	101.32	24.08	247.40	35.07	12360.29	0.36	33.17	28.82
SK11-03M_112	448.04	7.26	1412.32	824200.09	2.34	0.01	19.61	0.20	2.99	8.40	0.88	42.89	13.02	146.76	45.48	192.94	41.84	420.81	50.28	10683.05	0.73	174.66	86.88
Neorarchean																							
SK11S-03_26	482.54	7.40	1954.01	904504.55	1.66		20.45	0.27	5.74	13.39	2.11	57.75	15.81	189.39	65.16	275.12	60.48	527.45	78.78	11425.34	0.69	214.12	83.47
SK11-03M_101A	398.23	6.45	924.08	810185.51	1.07	0.00	11.59	0.09	1.52	3.68	0.11	19.19	6.81	82.76	30.24	130.39	33.95	352.28	43.57	10875.05	0.47	81.25	57.83

Table E1.3 SK11-03 Trace Element Concentrations con't

Concentrations (ppm)																							
Spot	P	Ti	Y	Zr	Nb	La	Ce	Pr	Nd	Sm	Eu	Gd	Tb	Dy	Ho	Er	Tm	Yb	Lu	Hf	Ta	Th	U
SK11-03L_193	323.98	8.42	656.17	738700.48	1.19	0.06	10.40	0.09	1.04	3.24	0.38	15.97	4.58	60.07	20.98	93.86	23.27	228.09	30.20	10321.51	0.41	64.32	46.52
SK11S-03_11	274.21	9.57	550.16	839558.61	0.74		8.87		0.75	1.83	0.35	9.60	3.67	49.05	17.81	81.86	19.87	199.06	28.22	12346.46	0.32	21.04	27.91
SK11-03L_190	352.23	23.97	749.72	705025.81	1.67	0.35	13.54	0.07	1.56	3.44	0.34	18.86	5.36	71.60	24.07	109.05	26.75	261.42	31.45	9325.58	0.67	99.74	66.69
SK11-03L_179	377.78	6.72	1000.45	730846.87	1.39		11.34	0.03	0.98	3.66	0.22	20.85	7.69	92.41	32.68	144.83	35.88	328.48	43.20	10618.13	0.74	109.77	79.80
SK11-03M_101B	302.90	3.64	573.77	741572.79	0.91	0.01	8.20	0.05	1.04	1.83	0.20	9.81	3.61	50.27	18.17	79.82	21.67	251.01	33.65	10742.34	0.44	48.36	41.28
SK11S-03_12	329.97	11.92	820.28	855122.89	1.02	0.01	10.96	0.07	0.73	2.45	0.31	16.98	5.25	71.50	26.11	118.53	30.63	301.50	43.31	12647.25	0.46	24.26	33.87
SK11-03L_191	297.55	11.13	561.26	709879.24	0.88		8.75	0.03	0.98	1.66	0.24	11.94	4.03	51.31	18.52	84.27	21.86	223.38	28.89	10191.45	0.31	17.48	29.2
SK11-03M_98	245.69	6.63	445.97	797558.96	0.41		4.61	0.03	0.61	1.56	0.13	7.37	2.93	38.31	14.12	66.38	17.62	191.48	25.81	11593.68	0.17	6.63	22.47

Table D1.4 SK11-07 Trace Element Concentrations

Concentrations (ppm)																							
Spot	P	Ti	Y	Zr	Nb	La	Ce	Pr	Nd	Sm	Eu	Gd	Tb	Dy	Ho	Er	Tm	Yb	Lu	Hf	Ta	Th	U
Mesoarchean 1																							
SK11-07M_27	246.65	28.78	918.07	555024.72	5.64		3.20		0.15	0.50	0.15	7.19	4.35	69.49	30.54	153.11	46.86	576.34	70.95	13077.93	9.45	184.21	1507.67
SK11-07S_53	347.08	23.88	877.13	612942.86	4.14	0.16	4.69	0.02	0.43	0.50	0.19	7.95	4.20	64.86	29.33	146.29	47.07	615.10	79.37	12787.44	10.98	120.57	971.77
SK11-07M_36	387.99	32.75	2833.53	591705.02	30.96	0.06	10.55	0.00	0.32	2.74	2.03	32.47	16.36	250.92	101.66	487.29	132.94	1569.11	194.55	11559.77	11.56	350.96	2603.60
SK11-07S_54	227.63	18.11	624.45	567657.92	1.46	0.18	6.09	0.03	0.51	1.03	0.22	7.08	3.64	50.53	21.51	106.65	30.55	375.62	44.24	10988.68	2.10	106.25	692.63
SK11-07S_41	1057.76	10.96	978.41	554219.14	0.70	6.65	32.42	1.63	14.63	9.73	4.43	37.37	10.65	118.88	37.93	160.82	38.81	422.13	49.25	7160.90	0.24	141.55	261.43
SK11-07S_58	132.81	17.32	275.81	536729.34	1.74		1.42		0.20	0.23	0.13	2.04	1.37	24.34	10.25	51.00	15.71	211.97	25.88	10667.35	2.43	41.04	608.24
SK11-07M_35	435.68	14.50	1128.77	586858.01	1.34		2.07		0.19	0.70	0.61	8.80	5.06	88.94	40.91	210.16	62.34	802.58	104.76	11304.00	1.62	29.68	511.54
SK11-07S_49	159.90	8.52	411.70	560466.23	0.91		11.30	0.03	0.48	1.38	0.28	7.92	2.90	35.12	13.69	63.48	17.56	202.98	24.04	8201.56	0.32	58.80	75.67

Table E1.4 SK11-07 Trace Element Concentrations con't
Concentrations (ppm)

Spot	P	Ti	Y	Zr	Nb	La	Ce	Pr	Nd	Sm	Eu	Gd	Tb	Dy	Ho	Er	Tm	Yb	Lu	Hf	Ta	Th	U
SK11-07M_30	366.77	62.41	2315.91	553001.88	23.22	0.06	10.71	0.01	0.32	2.18	2.03	28.85	13.32	201.71	82.06	409.33	117.53	1438.60	174.17	9239.18	6.93	209.55	1435.15
SK11-07S_51	204.68	19.77	539.81	606254.08	1.51		3.15	0.01	0.05	0.61	0.15	5.27	2.69	41.66	17.42	85.32	25.00	304.00	39.39	12223.31	2.57	80.99	619.65
SK11-07L_87	194.26	7.94	540.40	675720.41	0.80		11.43	0.05	0.93	2.16	0.43	12.76	4.46	58.19	21.07	92.35	22.29	232.94	31.03	11947.32	0.29	158.95	73.12
SK11-07S_40	159.23	12.45	445.47	569045.91	0.95	0.04	8.22	0.03	0.92	2.84	1.07	13.21	4.00	46.46	16.20	67.94	17.30	189.42	20.53	8739.04	0.47	105.68	302.41
SK11-07M_25	376.32	25.17	962.12	553972.63	4.75	0.03	2.58	0.00		0.41	0.13	4.70	3.42	66.80	31.24	173.36	58.83	814.43	96.49	12636.48	17.30	80.06	1160.36
SK11-07M_21	187.04	5.00	911.85	578694.85	0.50		14.27	0.04	1.89	3.97	1.48	24.65	8.84	103.69	35.04	146.82	36.83	381.27	42.97	7413.45	0.23	108.39	64.98
SK11-07S_45	65.96	29.54	72.58	608296.05	1.37	0.05	1.23		0.14	0.36	0.22	2.59	0.83	8.08	2.20	6.45	1.31	11.07	0.99	13798.72	3.10	28.29	1362.47
SK11-07S_48	122.76	23.24	521.01	567487.88	3.43	0.01	1.29			0.27	0.33	4.16	2.11	36.45	17.67	96.40	29.92	409.99	51.81	11826.55	4.82	33.61	1270.34
SK11-07M_20	205.68	6.11	930.68	566109.15	0.66		14.15	0.05	1.08	3.99	1.33	24.56	8.33	98.50	34.72	139.06	34.01	365.35	41.89	7042.65	0.22	110.33	65.65
SK11-07S_50	237.91	255.73	565.28	584059.54	2.28	0.02	6.96	0.03	0.43	1.02	0.26	6.58	2.69	43.44	18.45	99.29	33.39	412.96	60.58	12903.22	7.98	77.94	722.18
SK11-07L_94	130.51	6.74	399.13	705042.04	0.49		9.53		0.30	1.18	0.73	8.53	3.06	36.90	15.11	69.67	19.24	227.26	32.20	7159.63	0.24	51.50	62.03
SK11-07M_24	270.89	17.38	1001.78	558308.70	1.16	0.05	4.11	0.05	0.52	0.66	0.30	8.02	3.76	67.93	33.70	170.93	46.98	498.34	85.78	12381.72	1.83	102.91	663.95
SK11-07S_56	453.25	23.60	2095.19	570992.16	7.96	0.01	5.32	0.01	0.30	2.74	1.46	26.02	11.87	178.38	75.00	373.49	112.43	1422.42	173.41	9314.45	3.45	90.91	896.73
SK11-07S_47	338.42	25.51	1020.10	533855.29	2.21	0.17	10.54	0.04	0.86	3.08	0.68	18.82	7.95	98.96	37.32	160.73	43.97	488.43	53.62	8802.64	1.43	333.51	1086.72
SK11-07S_46	476.90	13.86	1602.89	561398.01	3.56		5.10	0.02	0.38	1.62	1.09	17.33	8.50	128.30	54.56	277.51	82.55	1072.91	137.32	11170.75	4.72	69.18	835.57
SK11-07S_38	379.56	15.00	1138.19	607678.47	1.65	0.05	13.45	0.04	1.60	4.80	1.82	28.00	9.88	116.57	41.12	169.58	41.74	447.07	51.00	9903.64	0.68	190.14	459.78
SK11-07M_31	256.06	16.19	611.24	535678.67	1.86	0.05	7.72		0.41	1.77	0.79	13.85	5.25	60.13	21.54	94.04	24.12	289.61	31.34	8862.70	0.80	123.50	458.95
SK11-07M_28	410.17	9.98	916.85	535954.32	2.10		4.43		0.19	1.26	0.73	9.10	4.46	72.36	31.94	167.29	50.00	681.42	85.52	9084.13	1.08	56.14	330.15
SK11-07S_52	210.04	12.60	420.05	562530.42	1.09	0.03	7.16	0.03	0.46	1.10	0.37	6.15	2.74	37.80	14.82	73.21	21.45	261.44	36.18	11811.41	2.78	58.10	446.72
SK11-07M_26	202.58	24.82	465.45	564088.19	3.54	0.04	2.24	0.01	0.23	0.42	0.43	5.03	2.91	41.54	15.84	67.84	17.00	191.35	21.80	14097.44	5.52	44.75	1027.50
SK11-07M_29	449.52	16.67	1647.08	493184.48	1.39	0.17	10.56	0.10	0.77	1.74	0.81	16.02	6.79	116.19	55.33	307.08	86.26	996.93	190.89	11374.61	1.86	73.36	575.01
Neoarchean																							
SK11-07L_93	123.64	7.52	277.56	708916.17	0.41		7.76	0.04	0.86	1.59	0.57	8.02	2.75	31.65	10.45	44.48	11.81	128.27	16.50	11115.85	0.19	49.15	44.81
SK11-07L_86	198.91	7.02	504.00	679489.09	0.64		15.33	0.07	1.75	3.43	0.35	15.67	4.65	57.50	19.23	78.19	19.06	184.61	24.78	12876.14	0.19	131.49	43.66
SK11-07S_57	140.15	8.38	408.21	402435.41	0.32	0.26	10.05	0.13	1.28	1.43	0.90	10.26	3.14	40.58	15.25	68.75	15.44	161.63	26.98	6792.97	0.12	24.92	31.89

Table E1.4 SK11-07 Trace Element Concentrations con't
Concentrations (ppm)

Spot	P	Ti	Y	Zr	Nb	La	Ce	Pr	Nd	Sm	Eu	Gd	Tb	Dy	Ho	Er	Tm	Yb	Lu	Hf	Ta	Th	U
SK11-07M_33	142.09	9.75	270.28	591119.89	0.42		7.50		0.46	1.07	0.46	6.66	2.23	28.49	10.02	45.04	12.62	144.96	17.31	8759.91	0.24	66.64	54.71
SK11-07S_44	154.94	13.40	333.66	575168.38	0.51	0.04	8.69	0.07	0.98	1.93	0.58	8.72	2.92	36.28	13.37	54.03	14.26	165.27	18.82	8958.97	0.25	38.69	41.81
SK11-07L_92	128.02	6.87	425.01	750777.29	0.54		10.02	0.02	0.50	1.45	0.40	7.98	2.90	36.19	14.69	67.67	18.29	185.74	28.41	12160.93	0.30	104.20	78.61
SK11-07M_34	135.11	8.77	284.87	582982.54	0.39		7.51		0.74	1.09	0.39	7.40	2.22	28.33	10.69	46.24	12.35	147.41	17.45	8261.68	0.24	61.75	51.56
SK11-07L_95	149.79	6.39	381.07	714069.32	0.51		8.46		0.42	1.63	0.42	7.96	2.81	35.33	13.52	64.48	16.55	170.95	26.32	11401.92	0.23	87.93	60.73
SK11-07L_88	209.69	6.35	1221.92	725189.84	0.67	0.06	15.86	0.46	6.95	9.35	2.73	40.54	12.26	132.81	45.37	187.71	44.74	460.11	62.74	8935.22	0.32	367.81	147.62
SK11-07L_96	173.26	9.65	902.59	747389.44	0.50		12.71	0.26	4.22	5.97	1.83	26.96	8.70	94.18	33.13	140.41	32.33	332.00	47.65	10798.12	0.33	172.10	75.97
SK11-07L_90	136.77	11.80	413.54	732758.19	0.43		8.26	0.01	0.56	1.52	0.43	9.44	3.03	37.33	14.53	70.84	16.96	172.00	25.33	12149.57	0.14	81.45	53.93
SK11-07M_18B	111.66	5.39	215.29	576911.50	0.40		6.65		0.15	0.51	0.20	4.10	1.30	19.09	7.96	34.15	10.06	117.92	16.12	9209.82	0.23	26.14	28.38
SK11-07M_19	153.41	95.71	541.68	619876.14	1.15	0.16	10.88	0.05	1.09	1.97	0.93	13.78	4.49	57.23	19.68	85.30	23.01	259.61	30.64	7218.17	0.36	76.46	47.43
SK11-07L_89	200.71	9.74	1057.36	747591.20	0.74	0.17	15.65	0.27	3.29	6.06	1.95	31.87	9.53	107.18	40.50	174.81	38.45	392.38	61.90	12110.19	0.44	338.33	141.31
SK11-07L_91	124.10	8.49	420.41	723086.81	0.60		8.94	0.04	0.38	1.20	0.43	9.09	3.10	38.12	13.87	71.25	18.66	194.05	25.91	10927.48	0.29	91.18	66.55
SK11-07S_37	124.93	7.41	215.39	607007.24	0.33	0.06	7.67	0.03	0.54	1.27	0.29	5.15	1.68	21.84	7.98	34.14	9.43	103.37	12.71	10454.26	0.18	120.53	110.85
SK11-07S_43	139.26	6.72	217.26	630082.99	1.61	0.04	14.48	0.02	0.15	2.02	2.90	12.42	3.47	35.12	10.15	41.51	12.34	158.78	18.23	7411.33	0.73	56.89	125.01
SK11-07M_18A	120.07	6.31	232.50	605931.55	0.40		7.28	0.02	0.16	0.46	0.18	3.85	1.74	19.58	8.09	36.82	10.33	127.54	15.11	9366.90	0.29	26.37	29.06
SK11-07M_32	122.72	8.37	278.61	629794.28	0.42	0.05	11.48	0.01	0.64	1.07	0.38	6.14	2.03	26.87	9.79	45.38	11.16	132.42	17.38	10689.15	0.23	123.24	108.42
SK11-07S_55	122.46	6.73	237.66	578333.31	0.23		7.78	0.02	0.48	1.02	0.29	5.22	1.92	24.78	8.95	39.03	10.09	118.79	14.18	8913.65	0.14	76.09	79.68
SK11-07S_42	131.40	6.43	258.45	587285.25	0.34		7.23	0.03	0.51	0.98	0.36	5.30	1.88	23.94	9.48	39.10	10.07	116.38	14.34	9015.22	0.18	83.26	71.38
SK11-07M_22	207.67	7.51	665.66	608182.04	1.03		13.32	0.04	0.62	2.07	0.74	15.15	5.22	65.61	24.12	106.33	27.49	311.89	36.19	8919.42	0.35	67.81	20.91
SK11-07S_39	293.18	7.56	967.27	550422.93	0.90		14.56	0.09	2.44	4.45	1.49	27.42	8.24	95.48	34.29	146.60	35.82	394.40	44.99	8461.38	0.36	62.52	27.04
SK11-07M_23	209.54	7.63	546.37	585888.07	0.98		17.25	0.03	0.94	2.35	0.64	12.70	4.09	53.49	20.62	89.66	23.88	263.12	29.26	9238.49	0.50	168.39	44.05

Table E1.5 SK11-08 Trace Element Concentrations

Concentrations (ppm)																							
Spot	P	Ti	Y	Zr	Nb	La	Ce	Pr	Nd	Sm	Eu	Gd	Tb	Dy	Ho	Er	Tm	Yb	Lu	Hf	Ta	Th	U
Paleoarchean																							
SK11-08S_69	128.49	31.19	597.48	543453.68	1.83	0.04	4.75		0.18	0.47	0.15	5.39	2.51	39.89	18.80	98.51	34.12	483.84	69.57	11782.99	4.59	152.53	2695.77
SK11-08S-60	90.00	23.66	206.00	595018.00	0.64	0.03	2.43	0.02	0.11	0.15	0.13	1.65	0.93	14.10	6.07	35.43	12.02	168.93	24.79	11999.64	1.16	51.90	407.56
Mesoarchean 2																							
SK11-08S_77	116.80	25.61	532.30	602544.53	1.34	0.03	3.56		0.16	0.58	0.21	4.38	2.02	34.09	15.25	86.09	29.36	413.27	56.70	11213.07	1.77	105.65	700.20
SK11-08S_65	56.23	20.01	163.62	615204.98	0.59		1.02			0.13	0.04	1.40	0.65	10.63	4.91	27.01	8.87	127.00	18.56	12417.39	1.02	13.92	353.91
SK11-08M_15A	163.67	14.05	367.70	612742.64	0.63		7.81		0.24	1.04	0.10	5.80	2.14	28.57	11.77	58.91	17.23	201.87	24.27	9424.89	0.57	85.68	100.84
SK11-08S_64	150.53	12.96	562.86	595681.70	0.53		3.01		0.37	1.63	0.63	9.56	4.32	51.97	19.78	91.00	25.55	316.68	35.88	10098.59	0.21	36.45	217.71
SK11-08M_16	160.93	13.69	304.94	584664.68	0.52		7.10	0.04	0.41	0.89	0.10	4.47	1.79	23.70	9.53	46.98	14.24	174.58	20.28	9813.72	0.60	119.08	153.71
SK11-08S_63	254.81	16.94	745.72	544142.52	0.82		3.60	0.01	0.36	1.53	0.94	13.14	5.05	67.38	26.77	124.65	35.97	453.18	51.97	10154.11	0.29	71.62	507.97
SK11-08S_66	398.40	30.32	905.82	541723.22	9.28	0.11	2.41	0.03		0.27	0.11	3.85	2.70	57.64	30.55	185.23	64.97	944.13	114.85	11887.57	16.36	47.12	1003.48
SK11-08S_61_B	134.46	13.74	748.30	423266.28	0.63	0.14	5.83	0.04	0.57	1.10	0.42	9.46	3.52	57.60	24.05	131.57	37.53	425.76	84.88	8737.30	0.95	50.97	303.88
SK11-08S_84	583.08	27.93	1758.42	568021.62	7.84	0.71	29.74	0.16	1.96	4.02	1.22	26.57	10.06	139.08	55.85	280.40	80.85	1013.92	117.89	9510.81	4.56	642.59	854.98
SK11-08S_62	275.08	41.86	907.30	533127.83	1.35	0.11	8.52	0.05	0.89	2.82	0.99	16.43	6.08	81.07	32.64	154.69	43.34	549.91	66.18	12481.63	1.52	260.89	1955.31
SK11-08M_15B	155.24	15.48	386.67	573208.93	0.63		7.78	0.06	0.84	1.22	0.23	5.21	2.18	28.14	12.83	60.08	17.21	209.98	24.91	9628.55	1.17	134.62	151.94
SK11-08S_68	192.13	15.51	623.95	605151.79	1.01		10.07	0.05	1.20	2.60	0.59	11.91	4.22	54.66	19.92	92.08	26.18	293.94	32.31	10170.34	1.15	264.16	227.26
SK11-08S_79	366.15	27.14	782.01	563974.07	5.21	0.18	4.06	0.07	0.34	0.29	0.17	5.52	3.34	58.15	26.94	152.79	53.46	824.85	97.75	12956.69	12.36	86.67	869.00
SK11-08S_80	180.28	12.03	487.26	542474.40	0.67	0.08	4.07	0.05	0.49	1.90	0.65	9.31	4.09	49.29	17.96	77.51	20.59	257.57	27.47	9479.79	0.29	52.84	191.13
SK11-08S_67	470.07	23.51	1163.30	522719.58	7.27	0.87	13.90	0.20	1.16	1.78	0.58	16.94	6.93	102.58	42.17	206.34	57.55	702.06	83.13	10396.32	5.53	388.75	676.70
SK11-08S_85	585.79	25.30	1930.16	590200.44	7.74	0.59	22.06	0.17	2.16	4.44	0.94	28.14	11.97	158.81	64.38	301.31	82.66	923.04	116.22	10568.87	4.04	572.16	737.97
SK11-08M_7A	128.47	7.27	343.47	568522.24	0.54		7.47	0.01	0.53	1.13	0.32	6.45	2.01	27.79	10.95	54.11	15.92	203.94	25.92	8198.38	0.44	68.70	68.35
SK11-08S_70	165.47	12.50	393.41	569663.34	0.49	0.03	7.76	0.02	0.15	0.74	0.22	3.69	2.08	27.56	11.94	63.79	19.47	238.18	31.97	10894.17	0.98	135.43	410.47
SK11-08M_13	127.42	10.79	175.69	573365.01	0.33		6.51	0.04	0.79	0.92	0.14	3.93	1.55	16.39	6.52	30.37	8.12	100.28	11.91	8181.61	0.24	53.62	116.84
SK11-08S_61_a	152.10	14.62	912.15	539827.52	1.01	0.08	4.78	0.08	0.80	0.65	0.67	11.89	4.85	70.62	32.22	182.19	53.15	602.50	120.55	12249.30	1.35	76.59	523.59

Table E1.5 SK11-08 Trace Element Concentrations con't
Concentrations (ppm)

Spot	P	Ti	Y	Zr	Nb	La	Ce	Pr	Nd	Sm	Eu	Gd	Tb	Dy	Ho	Er	Tm	Yb	Lu	Hf	Ta	Th	U
SK11-08S_73	147.02	15.50	248.18	527958.22	0.34	0.08	2.61	0.01	0.19	0.31	0.15	4.15	1.61	19.51	8.07	42.84	13.01	182.19	23.22	9431.63	0.61	77.34	518.52
SK11-08M_7B	140.80	8.18	414.20	617992.13	0.68		8.07	0.04	0.83	1.45	0.47	9.47	2.45	33.87	13.91	63.76	20.42	243.49	31.16	9348.02	0.59	81.28	74.22
SK11-08S_72	118.88	10.75	245.21	566307.13	0.40	0.06	6.44	0.01	0.33	0.68	0.14	2.90	1.36	17.37	8.29	40.96	12.87	173.43	20.67	9531.83	0.40	42.17	139.41
SK11-08S_83	164.37	17.53	573.75	592265.95	0.47		10.57	0.15	1.98	4.33	0.57	12.31	4.20	52.84	19.55	86.87	24.23	290.74	33.26	10335.61	0.58	509.36	364.03
SK11-08S_71	887.04	23.24	2186.52	541556.93	11.89	1.82	14.26	0.41	1.82	3.38	0.82	27.86	13.83	212.19	85.85	403.88	112.28	1299.14	128.59	13080.78	7.83	405.96	1031.91
Neoarchean																							
SK11-08S_78	136.90	9.05	339.69	662059.73	0.51	0.00	8.04	0.03	0.52	0.69	0.21	3.62	1.46	21.43	10.70	53.56	15.47	183.28	27.57	10222.10	0.71	91.51	112.65
SK11-08S_74	368.78	53.83	1219.57	610530.26	1.04	0.16	5.94	0.05	0.59	1.37	0.49	13.64	6.81	100.16	40.70	212.54	68.80	905.83	121.39	15019.18	1.33	324.30	3636.67
SK11-08S_82	159.96	13.17	277.98	596485.59	0.63		7.88	0.01	0.52	0.58	0.15	4.05	1.68	21.92	8.80	40.66	12.36	156.14	18.84	10410.66	0.82	64.75	86.27
Sk11-08L_99	139.37	16.12	354.36	648271.11	0.71	0.06	8.36	0.00	0.51	0.92	0.17	6.10	2.06	28.54	11.78	56.34	15.49	185.25	28.32	13982.82	1.26	92.02	95.90
SK11-08M_17	224.41	12.98	560.79	552975.71	0.70	0.18	11.30	0.05	0.99	2.05	0.30	10.33	3.66	43.99	17.82	84.88	24.22	288.21	32.77	9444.57	1.03	171.35	166.88
SK11-08M_8	140.17	12.14	247.68	584629.61	0.50		6.98	0.02	0.23	0.73	0.14	4.06	1.46	19.89	8.01	38.67	11.40	139.66	16.67	10680.06	0.80	85.74	97.59
SK11-08M_12	164.63	12.00	348.00	573911.14	0.71		8.02	0.03	0.56	0.94	0.20	5.68	2.37	27.67	11.04	56.15	16.16	212.06	24.74	10530.08	1.21	71.59	99.08
Sk11-08L_98	208.83	16.37	1088.33	689781.09	1.02		13.28	0.09	1.82	4.28	0.64	21.52	7.06	94.09	35.57	163.52	40.99	462.80	65.26	14117.05	1.42	245.91	153.64
SK11-08M_9	131.60	9.30	252.11	580205.57	0.47		7.39	0.03	0.08	0.31	0.12	3.10	1.36	18.86	7.71	40.18	12.23	151.13	18.22	10501.11	0.46	123.85	156.12
SK11-08M_10	167.51	7.83	352.40	524510.18	0.86		7.86	0.04	0.49	0.93	0.13	5.60	2.26	26.35	11.03	55.62	15.62	201.46	23.78	9860.40	1.40	80.88	110.63
SK11-08S_81	189.26	10.00	688.14	572962.15	0.83		10.13	0.03	0.89	2.77	0.41	12.10	4.93	58.94	23.05	105.10	29.53	341.67	39.00	10962.84	1.23	184.56	155.32
SK11-08S_75	171.12	7.48	445.73	607713.84	0.85		9.56	0.03	0.84	2.02	0.18	8.19	3.03	36.46	14.07	68.46	20.49	250.51	27.25	10994.40	1.13	122.10	123.76
SK11-08M_14	205.39	8.57	750.62	361514.33	0.19	0.03	10.44		1.12	1.95	0.34	11.90	4.35	56.74	23.97	122.41	30.15	287.05	55.58	7265.62	0.19	253.39	164.18
SK11-08M_11	167.04	7.36	318.40	550482.94	0.56		8.34	0.04	0.33	0.99	0.17	4.94	1.87	25.99	10.30	50.15	15.22	189.17	21.36	9700.89	1.09	65.09	89.07
SK11-08M_6	192.85	8.68	479.14	594314.03	0.94		11.89	0.03	0.57	1.33	0.23	7.82	2.88	38.16	15.06	74.90	21.64	249.69	29.31	10379.37	1.60	143.27	151.30
SK11-08M_5	142.18	7.03	258.62	584616.27	0.43	0.02	7.97	0.02	0.52	0.64	0.10	3.83	1.44	20.18	8.43	42.93	12.36	163.86	20.25	10944.96	0.72	81.82	101.52
SK11-08S_76	164.35	7.81	325.71	559581.14	0.47	0.21	7.53	0.05	0.40	0.91	0.20	4.70	2.05	27.60	11.01	53.47	15.96	202.32	24.58	10780.14	0.97	94.38	121.46
SK11-08L_97	125.45	6.82	346.68	695479.21	0.77		6.85	0.02	0.21	0.85	0.13	3.84	1.65	25.21	11.10	59.02	17.29	213.73	32.84	14491.46	1.09	75.92	158.91

Craters of the Moon trace element concentrations

Table E2.1 CRMO11-01 Trace Element Concentrations
Concentrations (ppm)

Spot	P	Ti	Y	Nb	La	Ce	Pr	Nd	Sm	Eu	Gd	Tb	Dy	Ho	Er	Tm	Yb	Lu	Hf	Ta	Th	U
Mesoarchean 2																						
CRMO11-01_L_37	200.29	3.34	976.61	12.15	0.07	20.62	0.03	1.14	3.02	0.06	17.88	7.25	94.56	34.00	151.23	38.84	433.55	42.61	12069.37	10.09	413.42	540.83
CRMO11-01_L_7	145.95	3.57	1194.67	6.44		9.19	0.07	1.44	3.17	0.12	25.47	9.05	125.83	46.07	194.17	49.37	528.74	54.73	10388.34	4.20	227.47	581.86
CRMO11-01_L_40	254.19	4.05	1446.40	19.40		32.56	0.08	1.87	6.20	0.11	32.56	11.91	155.76	52.25	213.55	55.27	602.63	57.16	11143.70	11.90	737.36	881.09
CRMO11-01_S_198	145.37	2.78	1184.34	5.14		13.64	0.05	1.22	3.75	0.26	24.26	8.62	107.37	41.24	183.73	44.91	449.90	62.34	14347.34	6.84	223.81	485.56
CRMO11-01_L_29	124.49	2.02	780.50	1.84		10.94	0.04	1.59	3.27	0.26	18.68	6.36	81.00	28.54	119.54	31.11	322.03	35.07	9329.45	0.96	95.09	143.95
CRMO11-01_L_15	150.38	1.88	1218.00	2.21		13.48	0.11	2.76	6.28	0.48	35.19	11.32	134.26	45.29	184.56	45.34	466.70	48.72	9189.86	1.42	146.98	192.08
CRMO11-01_L_39	149.85	3.05	755.13	9.59		17.56	0.06	0.80	2.57	0.00	13.56	5.72	75.47	26.52	115.94	32.52	372.95	35.78	11091.22	8.82	304.57	670.44
CRMO11-01_L_31	189.89	3.51	927.09	12.82	0.02	19.20	0.05	0.99	3.00	0.02	16.85	6.96	96.17	33.89	147.29	38.09	415.88	41.44	12802.91	11.48	334.62	503.14
CRMO11-01_L_41	187.94	3.83	1349.99	6.78		20.87	0.08	2.30	6.67	0.12	32.11	11.16	139.38	50.64	209.30	52.41	556.21	54.40	9967.09	5.50	388.94	656.88
CRMO11-01_L_12	182.32	3.40	982.96	14.19		23.05	0.04	1.31	3.64	0.02	18.82	7.55	95.53	35.36	152.88	40.22	446.36	45.97	12021.25	10.58	466.42	790.67
CRMO11-01_M_128	102.95	2.30	687.52	2.11	0.01	10.25	0.03	1.10	2.62	0.15	15.74	5.24	70.14	25.65	110.09	28.15	310.40	32.80	9872.21	1.72	105.80	194.99
CRMO11-01_M_123	142.28	2.34	893.89	2.03	0.01	12.16	0.08	1.41	4.77	0.45	24.16	7.95	97.04	34.11	137.50	34.91	365.85	38.22	8597.64	1.34	120.76	170.30
CRMO11-01_L_23	168.07	4.06	1030.25	11.64		21.76	0.08	0.98	2.72	0.03	17.80	7.47	100.58	37.80	164.13	41.94	433.03	48.53	14560.56	9.73	463.25	494.11
CRMO11-01_M_124	112.42	2.11	627.75	1.48	0.03	8.19	0.07	0.50	2.37	0.29	15.85	5.06	65.52	23.52	95.77	24.97	274.74	28.87	8911.90	0.94	71.34	116.51
CRMO11-01_L_28	177.67	4.83	998.47	16.09		21.99	0.06	1.28	3.63	0.03	18.75	7.39	99.94	35.98	159.16	42.60	453.13	48.49	13085.77	14.61	370.20	855.12
CRMO11-01_L_24	204.95	2.79	1942.00	2.61		15.27	0.24	5.96	12.13	0.93	54.82	18.37	215.70	73.39	289.95	68.80	707.70	77.80	10542.37	1.39	263.38	265.84
CRMO11-01_L_25	169.17	6.03	902.50	9.02	0.21	15.64	0.07	1.17	2.53		15.62	5.64	79.96	29.85	141.84	38.27	411.83	48.29	14442.85	10.07	250.80	913.80
CRMO11-01_S_209	230.75	3.35	2577.80	6.45	0.04	29.77	0.20	3.99	10.65	0.52	64.23	21.41	253.58	94.17	400.52	91.10	825.08	120.26	14944.84	4.43	698.09	577.81
CRMO11-01_M_129	216.29	4.09	1641.18	8.61	0.02	28.21	0.10	3.09	7.46	0.17	40.58	13.90	175.98	62.60	257.38	62.04	657.82	64.07	9629.73	5.09	583.70	745.48
CRMO11-01_L_35	121.62	2.07	511.86	3.80	0.03	7.57		0.62	2.38	0.31	11.10	4.16	52.98	20.45	81.97	21.54	253.26	25.60	7787.28	2.77	45.35	106.43
CRMO11-01_S_200	184.16	4.33	1177.07	12.61		21.94	0.10	1.26	3.91	0.04	22.20	8.20	114.53	42.69	186.35	45.45	467.46	55.20	15796.86	10.62	524.94	530.94
CRMO11-01_L_32	1202.06	5.83	1839.03	4.42	21.07	58.32	5.75	34.96	18.06	0.66	52.36	17.16	199.25	68.75	284.53	70.16	724.89	74.33	9828.93	4.05	334.07	511.73
CRMO11-01_L_10	207.16	4.79	1294.29	19.36	0.04	17.93	0.04	0.77	3.53	0.03	19.82	8.25	121.36	45.76	204.93	57.22	648.14	66.93	13119.42	19.72	320.27	1351.46
CRMO11-01_M_132	306.33	5.82	2630.15	8.76	0.19	21.66	0.45	8.19	14.36	1.49	75.12	24.43	301.63	103.72	415.48	103.89	1139.84	108.22	9213.53	6.39	518.49	562.53
CRMO11-01_M_120	718.24	143.23	2944.69	8.53	739.12	1255.95	166.59	739.17	138.36	2.14	171.60	36.73	357.08	117.66	437.46	103.18	1022.61	104.81	8080.74	2.17	604.07	473.53
CRMO11-01_S_207	217.94	2.19	2649.04	2.57	0.07	10.22	0.46	8.94	14.94	2.05	75.89	24.08	281.32	98.77	400.63	85.92	745.09	108.36	12088.34	1.15	219.09	158.43
CRMO11-01_M_134	201.56	4.25	1065.69	12.20		17.00	0.06	0.97	3.58	0.03	18.17	7.52	102.43	37.57	168.36	45.17	492.27	49.25	12170.92	11.75	317.68	713.93
CRMO11-01_S_205	234.29	2.65	1045.71	2.42	2.78	18.90	0.73	5.18	4.79	0.27	26.30	8.44	101.28	38.88	164.09	37.60	354.57	49.85	14116.28	1.76	162.43	189.52
CRMO11-01_M_133	110.20	5.13	502.09	8.26	0.01	6.17	0.02	0.10	0.85	0.01	5.88	2.64	37.08	16.48	79.93	25.58	320.31	35.98	13847.41	17.54	102.44	832.08

Table D2.1 CRMO11-01 Trace Element Concentrations con't
Concentrations (ppm)

Spot	P	Ti	Y	Nb	La	Ce	Pr	Nd	Sm	Eu	Gd	Tb	Dy	Ho	Er	Tm	Yb	Lu	Hf	Ta	Th	U
CRMO11-01_L_20	307.22	7.59	2214.36	9.65	0.38	36.38	0.23	3.91	10.16	0.34	51.48	18.84	231.55	81.37	332.08	82.16	831.01	92.15	11005.64	6.35	728.20	993.12
CRMO11-01_L_16	247.24	3.62	1113.66	13.97	0.04	15.04	0.06	0.94	2.97	0.03	17.80	7.52	106.17	40.83	178.94	48.02	525.38	55.90	13351.61	16.26	159.62	442.11
CRMO11-01_L_17	179.99	4.47	1205.16	16.95		8.94	0.02	0.08	1.76	0.05	13.79	6.89	100.70	40.16	190.10	55.96	634.58	70.97	14981.54	23.27	214.33	1027.00
CRMO11-01_L_11	159.79	15.31	677.85	2.92		15.34	0.07	0.92	2.77	0.13	14.75	5.50	70.18	25.39	109.02	27.91	295.17	30.60	9309.48	1.97	176.22	245.22
CRMO11-01_M_125	195.46	2.31	907.49	2.70	0.06	15.12	0.11	1.29	4.12	0.22	25.24	8.26	99.52	34.04	139.14	34.76	372.15	37.88	9057.51	1.42	142.32	204.97
CRMO11-01_M_136	996.26	3.75	834.85	2.80	17.59	48.34	5.43	31.43	12.81	0.30	31.75	9.54	98.56	32.71	128.90	32.85	335.97	33.79	9215.59	1.68	144.09	238.84
CRMO11-01_L_38	311.62	7.51	1962.13	18.43	0.09	16.45	0.12	1.39	5.30	0.12	41.39	15.49	206.68	76.41	316.14	77.87	816.39	78.39	10565.42	11.02	593.35	1735.94
CRMO11-01_M_138	172.61	2.31	894.42	2.43	0.40	14.21	0.16	2.05	3.71	0.27	22.19	8.28	97.03	33.32	138.47	34.72	377.45	37.85	8349.96	1.49	133.29	201.55
CRMO11-01_L_18	159.80	1.94	740.28	1.96		10.72	0.05	0.95	2.88	0.33	18.53	6.28	75.89	27.80	112.52	28.23	309.09	33.53	9639.55	1.11	93.98	148.39
CRMO11-01_M_135	244.14	5.28	1155.58	19.38	0.02	14.73	0.04	0.59	2.51	0.06	16.10	7.09	106.23	41.74	195.71	57.34	649.96	67.29	12935.53	24.87	205.20	990.92
CRMO11-01_M_121	141.80	1.86	768.88	2.32		12.50	0.01	0.92	4.12	0.34	20.55	6.84	86.70	29.48	120.33	30.14	326.04	33.49	8745.16	1.47	132.91	178.76
CRMO11-01_M_126	166.62	5.94	857.29	10.78	0.01	17.31	0.05	0.71	2.80	0.04	13.29	5.94	78.45	30.35	135.58	37.47	431.27	42.49	12041.74	12.55	310.08	861.74
CRMO11-01_S_201	354.31	6.92	3192.79	9.05		30.90	0.22	4.07	10.59	0.23	75.08	26.40	324.38	120.03	493.32	114.35	1025.34	136.90	13851.55	6.42	1043.54	1073.94
CRMO11-01_M_130	156.17	5.52	757.29	10.16	0.09	15.72	0.01	0.60	2.25	0.06	13.00	5.20	69.36	26.77	118.80	33.04	374.78	37.85	12180.54	10.85	241.40	750.96
CRMO11-01_L_19	291.86	10.80	1554.22	22.41	0.03	8.27	0.01	0.66	2.03		18.70	9.11	131.70	54.10	256.77	72.49	779.48	88.68	16123.86	36.66	265.77	1477.05
CRMO11-01_M_142	179.80	3.74	911.90	9.18	0.00	11.84	0.01	0.03	1.60	0.01	12.16	5.49	81.73	34.24	158.62	44.73	530.70	55.33	12237.75	8.72	59.95	633.37
CRMO11-01_S_197	226.21	2.66	1471.75	4.45		17.99	0.05	1.09	4.27	0.23	29.71	10.76	141.42	54.30	236.46	56.78	550.86	73.88	13238.63	3.01	210.86	337.20
CRMO11-01_M_131	287.33	5.48	2348.31	8.92	0.04	27.71	0.16	4.06	9.08	0.95	46.92	17.42	217.71	83.48	379.02	96.86	1003.64	117.57	10732.55	9.89	673.80	778.15
CRMO11-01_M_139	248.99	5.16	1762.46	14.13		9.14		0.35	3.99	0.03	32.60	13.42	180.77	68.08	282.07	71.85	733.69	73.35	11896.94	9.83	480.36	1329.80
CRMO11-01_S_203	230.07	4.31	1544.83	9.57		15.79	0.04	0.62	3.92	0.12	28.07	10.68	142.91	55.21	247.05	59.99	583.05	79.83	17115.08	11.00	396.30	801.73
CRMO11-01_S_208	188.24	4.89	1382.24	11.22	0.08	20.22	0.07	1.33	3.80	0.04	25.38	9.20	119.09	46.91	215.67	51.04	468.46	71.71	19451.25	9.94	515.85	626.63
CRMO11-01_M_141	351.61	3.74	1691.74	5.45	0.14	14.86	0.06	1.83	6.07	0.28	38.86	14.77	183.38	65.57	272.79	68.70	708.02	70.30	10088.01	3.89	337.42	681.43
CRMO11-01_L_36	244.55	5.86	1018.55	11.39	0.08	10.27	0.10	0.62	1.82		12.93	6.04	90.97	36.28	172.09	48.65	532.79	55.91	13100.93	14.61	228.22	1467.46
CRMO11-01_M_119	459.27	5.81	2460.64	9.27	0.01	21.59	0.16	3.20	8.98	0.22	51.95	20.00	244.81	92.30	387.99	96.48	1037.85	108.20	11720.96	9.41	807.62	1438.07
CRMO11-01_L_22	128.36	1.88	600.73	1.74	0.16	10.50	0.02	0.80	1.93	0.13	12.30	4.70	54.92	21.53	90.59	23.32	251.71	28.69	11697.01	1.33	89.48	152.02
CRMO11-01_L_8	313.42	2.37	1329.89	11.94	0.10	11.14	0.04	0.98	3.06	0.05	20.66	8.90	128.14	48.62	221.49	60.65	677.98	70.83	10929.46	12.34	102.95	373.93
CRMO11-01_L_27	170.66	4.68	814.47	5.62	0.08	16.15	0.06	0.80	2.55	0.00	14.62	5.27	74.41	27.42	131.99	35.50	378.08	43.85	13796.55	8.13	271.59	793.22
CRMO11-01_S_199	1207.16	5.66	2258.53	7.94	22.04	50.91	6.33	37.66	18.15	0.27	59.15	21.03	250.05	85.57	351.02	80.28	740.49	91.58	15424.14	6.33	610.72	892.07
CRMO11-01_S_196	799.12	73.34	2737.66	26.59	11.59	31.30	3.56	18.39	9.96	0.15	41.53	16.75	237.85	95.20	446.99	116.22	1192.84	159.07	18589.78	32.06	514.87	2448.33
CRMO11-01_L_9	298.54	61.09	1255.16	12.34	0.41	9.70	0.13	1.18	2.11	0.03	13.57	6.63	103.88	42.10	203.76	58.53	688.17	74.04	11419.61	17.45	283.56	1722.84
CRMO11-01_M_137	357.73	8.74	1814.43	25.37	0.04	10.38	0.04	0.90	3.03	0.06	26.38	11.62	166.79	65.81	304.56	80.75	894.16	94.03	12194.40	23.78	385.55	1626.11

Table D2.1 CRMO11-01 Trace Element Concentrations con't
Concentrations (ppm)

Spot	P	Ti	Y	Nb	La	Ce	Pr	Nd	Sm	Eu	Gd	Tb	Dy	Ho	Er	Tm	Yb	Lu	Hf	Ta	Th	U
CRMO11-01_M_140	257.99	3.56	1178.68	5.65		10.52	0.00	0.84	2.86	0.09	20.36	8.18	112.57	43.34	193.94	52.14	562.84	59.69	11031.17	6.91	209.44	745.17
CRMO11-01_M_127	395.96	5.30	1929.37	7.77	1.19	14.56	0.11	2.80	6.39	0.07	40.08	15.71	199.67	73.44	306.24	75.89	781.80	79.81	10973.09	6.39	529.18	1042.63
CRMO11-01_L_34	303.37	3.56	1334.61	11.39	0.06	13.08	0.04	1.50	3.70	0.05	22.34	9.41	126.69	48.41	219.10	59.74	664.17	67.79	12182.45	11.16	124.09	510.85
CRMO11-01_S_206	587.27	7.85	2850.25	14.25	2.34	16.06	0.89	4.98	5.72		41.77	17.37	247.16	101.48	460.65	113.01	1043.59	149.41	18354.14	15.49	735.06	2043.35
Neoarchean																						
CRMO11-01_L_14	319.61	2.59	1285.88	12.12	0.06	11.28		1.20	4.56	0.13	22.18	9.30	130.80	47.39	205.83	54.70	602.33	58.82	10607.75	9.20	133.51	160.22
CRMO11-01_L_21	283.41	2.78	1440.21	8.11	0.01	13.15	0.08	1.36	4.87	0.08	29.62	11.59	147.52	51.25	216.83	52.60	523.65	55.91	13369.00	3.85	128.84	184.14
CRMO11-01_L_13	299.24	1.26	1073.75	2.38	0.48	13.45	0.19	2.05	5.35	0.38	26.51	9.42	116.76	40.44	163.81	41.69	438.27	44.01	9456.12	1.83	179.70	315.40
CRMO11-01_L_30	384.61	2.66	1807.93	11.92	0.06	14.34	0.03	2.03	5.72	0.03	33.06	13.41	182.85	65.71	280.48	71.49	730.45	73.02	12512.53	6.40	103.30	199.27
CRMO11-01_L_26	288.53	2.35	1446.36	9.78	0.05	12.95	0.07	1.45	3.39	0.06	24.71	10.81	140.50	52.77	223.06	56.54	586.94	63.21	13169.55	5.43	180.30	106.66
CRMO11-01_L_33	326.88	2.70	1378.72	8.63		11.65	0.06	0.99	3.81	0.03	25.55	10.45	144.56	52.66	221.09	56.49	592.60	58.28	11295.91	4.79	75.83	161.76
CRMO11-01_S_204	425.99	3.14	2636.28	25.55	0.01	13.22	0.05	0.94	3.82	0.15	33.25	15.58	232.55	96.94	452.69	114.65	1133.83	156.13	16526.15	26.80	150.35	382.33
CRMO11-01_S_202	317.20	2.66	1823.26	9.31	0.07	14.46	0.12	1.93	5.78	0.07	32.83	14.27	183.35	67.69	288.28	65.91	600.48	80.29	16623.15	4.84	162.41	233.05
CRMO11-01_M_122	278.35	1.90	1317.78	8.70	0.01	11.31	0.05	0.90	3.75	0.00	24.48	10.11	135.72	49.90	213.37	55.08	566.46	57.24	11704.34	5.59	109.20	183.50

Table D2.2 CRMO11-03 Trace Element Concentrations
Concentrations (ppm)

Spot	P	Ti	Y	Nb	La	Ce	Pr	Nd	Sm	Eu	Gd	Tb	Dy	Ho	Er	Tm	Yb	Lu	Hf	Ta	Th	U
Mesoarchean 2																						
CRMO11-03_M_112	171.77	3.24	1142.11	6.12		17.62	0.07	1.66	4.39	0.13	25.07	9.28	113.78	42.63	177.79	47.98	551.19	55.34	10905.16	7.89	245.34	747.12
CRMO11-03_M_95	144.81	1.92	647.86	6.24		11.00	0.02	0.75	2.61	0.16	12.06	4.81	62.97	24.04	103.40	26.92	306.59	32.74	8564.46	3.16	75.93	190.42
Paleogene																						
CRMO11-03_S_188A	501.47	8.85	1430.09	8.29	23.68	59.86	4.01	21.57	9.20	0.96	33.49	10.89	123.85	48.19	214.04	53.99	536.72	89.78	11870.88	4.00	865.70	594.58
CRMO11-03_M_92	96.13	0.59	850.88	9.08	0.04	24.35		1.41	3.03	0.62	16.20	6.28	78.95	29.51	136.42	38.13	449.91	49.94	10280.67	5.49	640.77	942.19
CRMO11-03_M_103	619.21	3.45	1200.46	5.20	15.28	67.15	3.32	16.30	12.34	3.19	34.59	10.00	119.22	40.78	182.56	50.54	603.74	69.98	7335.29	2.50	814.15	613.59
CRMO11-03_M_108	130.77	1.21	1084.11	4.32	0.50	27.29	0.29	5.30	7.21	2.15	28.21	9.19	107.48	36.98	157.41	45.60	521.60	56.86	9177.38	2.29	383.26	454.27

Table D2.2 CRMO11-03 Trace Element Concentrations con't
Concentrations (ppm)

Spot	P	Ti	Y	Nb	La	Ce	Pr	Nd	Sm	Eu	Gd	Tb	Dy	Ho	Er	Tm	Yb	Lu	Hf	Ta	Th	U
CRMO11-03_M_106	790.62	0.58	1366.25	22.85	12.43	49.86	3.39	17.57	7.38	0.66	26.81	10.12	125.57	47.31	209.93	60.46	699.28	71.33	10497.90	13.47	1149.17	2100.23
CRMO11-03_M_91	265.24	0.53	3196.40	40.23	0.87	32.11	0.41	4.05	8.99	0.64	52.49	20.56	293.27	109.04	477.18	132.36	1538.50	172.01	12344.54	18.72	1618.95	3127.92
CRMO11-03_M_118	151.94	0.76	1463.91	21.14	3.53	33.58	0.80	2.93	4.97	0.80	26.28	10.53	139.08	51.49	230.23	62.58	755.95	79.63	11185.00	11.42	1450.95	2005.07
CRMO11-03_M_96	348.97	0.70	5117.90	208.51	0.22	24.86	0.25	3.08	8.65	0.29	73.18	35.09	482.10	181.40	812.26	225.97	2550.43	250.49	13189.27	106.19	2260.72	9765.95
CRMO11-03_M_97	139.41	0.67	2073.24	40.39	0.18	27.63	0.08	1.12	5.19	0.58	33.60	14.79	194.42	70.75	320.29	91.31	1054.89	109.51	11580.45	24.06	1917.21	3670.51
CRMO11-03_S_185	125.10	0.60	3258.89	48.96		28.98	0.01	1.26	5.80	0.64	51.73	21.34	284.66	109.17	498.57	127.63	1277.20	184.24	16138.49	27.37	2744.31	3723.67
CRMO11-03_M_111	3662.35	0.72	3504.93	72.23	32.28	106.27	14.86	77.41	30.41	1.67	67.50	24.62	328.48	119.43	532.71	151.03	1815.60	184.34	13651.96	40.13	1122.38	4910.81
CRMO11-03_M_109	361.55	1.58	6983.16	323.18	0.99	43.34	0.71	6.17	16.76	0.50	122.86	54.10	694.25	249.39	1074.72	289.60	3136.20	313.34	13689.39	141.72	5913.67	17603.83
CRMO11-03_M_115	131.80	0.51	2400.06	46.70	0.02	27.48	0.01	1.02	5.63	0.61	41.13	17.40	231.94	84.40	370.82	104.54	1195.26	123.66	11291.62	25.50	2183.47	4318.88
CRMO11-03_S_194	280.66	1.64	7775.86	320.03	0.54	25.15	0.23	2.25	9.11	0.14	91.09	41.73	601.93	236.09	1149.98	306.81	3165.49	469.54	24504.46	253.76	3218.94	12859.34
CRMO11-03_M_102	128.87	0.50	988.43	5.93	1.84	20.62	0.48	3.86	4.19	0.64	19.52	7.45	98.02	35.71	160.11	43.94	535.21	55.68	10475.88	3.91	375.23	665.71
CRMO11-03_M_114	179.97	0.44	3368.98	142.16		20.76	0.02	0.60	7.19	0.20	52.00	22.50	323.13	118.64	529.74	150.70	1723.43	175.58	14748.99	87.58	1887.78	7667.87
CRMO11-03_M_98	97.23	1.64	1797.65	14.24	0.26	25.09	0.12	2.40	7.88	1.35	37.01	14.55	186.01	65.58	280.46	77.77	962.59	93.72	8864.45	6.72	955.53	1513.60
CRMO11-03_M_99	1044.62	3.25	11282.87	324.40	10.89	83.35	5.35	37.72	37.71	1.01	201.38	83.76	1117.02	397.85	1730.13	475.49	5147.85	519.82	12234.45	118.38	7832.18	23730.80
CRMO11-03_M_104	138.92	0.61	1490.00	22.32	0.35	31.61	0.12	2.00	5.32	0.55	26.94	11.32	139.79	50.11	231.55	66.67	781.53	76.43	10036.41	13.21	1243.19	1894.25
CRMO11-03_L_4	99.47	0.62	1460.76	19.99		22.26	0.09	0.96	3.72	0.56	27.04	10.52	144.74	51.93	232.55	63.25	745.15	78.09	10293.66	10.67	1175.01	1922.88
CRMO11-03_M_101	271.29	0.27	6120.03	341.50		30.55	0.04	1.25	11.22	0.24	86.83	42.90	566.79	204.37	926.49	265.01	3119.03	304.29	14854.96	184.73	3111.26	15308.20
CRMO11-03_M_116	74.90	0.67	546.41	4.49	0.01	16.52	0.01	0.36	1.66	0.34	11.60	3.69	48.63	18.95	85.64	24.60	308.39	33.51	10062.67	3.05	280.83	477.52
CRMO11-03_M_113	5521.81	0.82	731.17	5.07	112.10	221.97	28.27	132.92	35.77	2.97	39.57	8.37	83.11	26.18	101.06	28.38	359.25	41.48	9633.46	3.65	367.44	584.74
CRMO11-03_S_193	175.37	0.74	5371.89	150.80	0.01	45.37	0.07	2.86	10.87	0.77	87.03	37.20	473.50	183.48	831.48	207.04	2001.05	281.71	17779.67	64.23	5264.24	6012.53
CRMO11-03_M_93	132.13	0.84	1386.15	5.82	0.18	25.78	0.22	4.39	8.67	1.36	32.09	11.61	136.94	49.98	214.46	58.67	664.94	73.34	9378.51	3.49	575.95	637.29
CRMO11-03_M_117	107.96	0.64	1418.02	20.62	0.08	19.85	0.03	0.80	4.11	0.53	24.83	10.99	140.37	50.44	226.69	62.88	710.89	77.05	11630.88	11.81	1291.06	2174.42
CRMO11-03_S_187	89.37	0.40	1577.51	14.31		17.24	0.02	1.18	3.49	0.37	27.44	9.98	138.89	54.66	248.13	63.10	636.89	97.98	15662.35	9.54	1112.49	1442.20
CRMO11-03_S_192	262.69	1.49	6949.31	204.28	0.14	62.67	0.24	3.55	13.96	1.44	111.28	45.09	604.76	235.98	1069.11	272.34	2675.47	374.59	18199.93	88.16	3517.19	7035.15
CRMO11-03_L_3	77.76	2.30	916.55	4.27	2.76	19.63	0.64	4.12	3.76	0.64	20.58	7.29	88.92	31.09	136.96	40.45	464.26	52.72	9070.90	3.11	391.46	590.65
CRMO11-03_L_6	145.11	0.45	2649.24	61.50		31.05	0.03	1.17	6.51	0.57	44.91	19.51	252.63	90.30	420.48	113.73	1282.52	138.27	11596.35	29.51	2845.82	5208.76
CRMO11-03_M_107	99.39	0.40	1261.72	17.24	0.02	21.97	0.01	0.75	3.33	0.50	21.22	8.59	115.66	44.04	196.91	56.08	666.58	70.46	10344.07	10.19	747.88	1447.05
CRMO11-03_S_191	93.30	0.60	1951.13	5.89	0.01	21.48	0.13	2.54	8.39	1.04	41.43	14.78	180.10	66.85	297.84	71.40	705.14	106.65	14431.92	3.57	851.29	737.43
CRMO11-03_S_189	544.90	0.73	2966.36	6.13	16.44	57.20	2.99	21.33	16.67	3.04	70.86	23.80	269.30	97.97	435.12	104.08	998.66	154.34	13467.12	3.56	1259.05	853.53
CRMO11-03_S_186	1544.92	8.94	12556.47	265.90	14.80	80.92	5.68	37.48	31.76	1.05	197.93	80.95	1064.64	424.99	1921.55	481.89	4718.59	666.23	16521.62	107.47	7043.36	15994.20
CRMO11-03_M_94	87.51	1.63	841.46	8.90	0.11	20.04	0.04	0.96	2.60	0.45	14.14	6.08	76.76	29.43	129.40	37.30	452.99	49.09	9935.95	5.11	584.63	966.02
CRMO11-03_M_1108	2.95	0.62	694.28	6.28	0.05	18.00	0.06	0.91	1.91	0.45	12.26	5.07	65.41	23.87	110.10	32.54	402.68	43.75	9641.99	4.23	455.64	737.15
CRMO11-03_S_195	87.17	0.34	1235.00	14.19	0.04	18.42	0.04	0.46	2.58	0.32	17.80	7.52	104.97	42.70	199.57	53.68	558.12	82.04	14265.29	9.15	534.57	851.43

Table D2.2 CRMO11-03 Trace Element Concentrations con't
Concentrations (ppm)

Spot	P	Ti	Y	Nb	La	Ce	Pr	Nd	Sm	Eu	Gd	Tb	Dy	Ho	Er	Tm	Yb	Lu	Hf	Ta	Th	U
CRMO11-03_S_190	70.88	0.78	892.20	5.03		21.11	0.07	0.98	2.38	0.68	15.59	5.90	76.19	29.74	143.14	36.24	376.52	58.75	13972.39	3.72	413.43	442.07
CRMO11-03_L_5	132.68	1.06	765.51	5.81	1.27	26.83	0.37	2.07	2.45	0.66	15.74	5.39	69.56	25.27	114.05	33.24	405.39	45.27	9190.17	3.51	378.63	520.02
CRMO11-03_M_100	247.97	1.02	1427.26	7.90	0.99	28.39	0.72	7.04	8.62	1.33	33.51	11.41	141.28	49.12	213.49	64.58	701.15	71.84	8609.12	4.80	618.53	979.55
CRMO11-03_S_188B	1253.11	1.18	2806.91	16.00	84.19	164.18	13.42	65.18	20.37	2.16	61.25	20.07	259.41	93.46	423.61	104.04	1060.25	160.33	14701.38	7.22	1559.33	1116.99

Table D2.3 CRMO11-04 Trace Element Concentrations
Concentrations (ppm)

Spot	P	Ti	Y	Nb	La	Ce	Pr	Nd	Sm	Eu	Gd	Tb	Dy	Ho	Er	Tm	Yb	Lu	Hf	Ta	Th	U
Paleogene																						
CRMO11-04_S_68	128.94	0.59	1829.13	14.73	0.24	17.07	0.14	2.21	5.75	1.04	35.31	13.91	177.04	65.84	283.43	74.43	831.48	101.25	10068.25	8.56	725.77	1439.97
CRMO11-04_S_65	462.11	1.54	2672.74	61.66	1.37	152.83	0.79	10.27	17.52	3.41	75.45	24.62	280.86	95.86	390.79	102.75	1113.99	113.02	9211.06	22.56	3270.86	2384.48
CRMO11-04_S_66	161.83	0.41	1699.68	19.66		18.29	0.03	1.19	4.62	0.67	29.19	11.63	155.47	58.84	261.85	73.76	866.47	95.66	11061.39	10.89	720.21	1626.43
CRMO11-04_S_82	95.23	4.05	1030.79	10.56	0.04	12.07	0.06	0.82	2.82	0.39	18.12	7.04	99.60	35.77	161.51	46.29	593.10	61.01	11055.42	5.95	478.82	1116.45
CRMO11-04_S_85	101.46	11.09	1038.09	4.23	2.41	24.77	0.51	4.38	5.65	1.74	23.88	8.22	99.56	35.28	154.87	42.74	497.89	60.47	6548.38	2.44	539.12	511.79
CRMO11-04_S_56	470.09	2.28	5099.97	160.43	2.58	31.14	1.72	11.22	12.43	0.39	72.88	33.42	466.29	170.15	749.85	214.57	2392.34	262.04	13622.37	67.72	2430.85	8869.81
CRMO11-04_S_59	515.23	0.55	4677.74	157.73	0.93	21.76	0.35	3.24	7.91	0.29	62.34	28.44	408.34	157.16	725.04	202.40	2363.02	252.27	14941.52	92.96	1761.88	9621.36
CRMO11-04_S_69	195.86	0.42	2918.72	107.59	0.09	21.85	0.03	1.06	4.98	0.33	40.97	18.36	240.82	94.09	430.58	124.56	1443.61	150.46	12827.40	65.19	1583.91	6197.45
CRMO11-04_S_57	119.07	0.40	1361.57	21.80		14.76	0.02	0.49	2.28	0.31	17.52	8.55	117.30	46.22	217.98	60.09	721.75	88.83	11692.92	13.01	503.31	1341.07
CRMO11-04_S_87	173.71	5.59	1078.80	5.53	2.81	30.42	0.83	7.74	9.02	2.10	31.20	9.93	116.10	39.18	162.58	43.18	509.00	57.90	8128.77	2.22	496.50	396.38
CRMO11-04_S_77	171.80	0.58	1289.81	9.79	0.12	15.31	0.06	1.36	2.87	0.49	20.50	8.31	109.19	42.04	198.33	55.59	635.96	68.44	9761.40	5.05	566.27	1096.27
CRMO11-04_S_88	338.08	1.12	4448.49	136.00	0.62	27.48	0.37	3.76	9.05	0.39	67.42	29.09	409.62	151.63	684.39	189.01	2021.72	213.89	13361.07	55.83	2259.54	8037.71
CRMO11-04_S_84	652.82	1.00	5164.33	136.23	3.14	27.34	0.89	4.58	7.41	0.38	67.63	30.90	465.86	178.65	801.73	236.06	2684.06	269.40	11766.86	59.43	1920.48	7731.55
CRMO11-04_S_75	745.10	1.10	7703.80	224.60	1.05	26.91	0.51	4.29	10.65	0.37	92.67	44.16	648.02	250.00	1149.50	321.48	3761.82	404.34	13389.39	106.87	2454.49	13822.23
CRMO11-04_S_81	600.39	4.46	6615.35	243.15	20.10	80.34	10.00	62.41	45.22	1.20	143.34	49.69	623.16	232.24	1018.53	278.81	3120.42	339.78	13533.82	149.08	19456.80	19470.59
CRMO11-04_S_70	179.86	0.80	2173.86	58.90	0.21	20.26	0.06	1.14	4.19	0.37	31.99	14.17	187.83	74.16	337.05	98.60	1150.83	119.22	12305.07	36.46	988.16	3202.71
CRMO11-04_M_171	1879.02	1.90	4613.22	95.98	65.62	146.46	18.37	93.17	25.19	1.57	79.74	28.84	382.47	157.12	736.24	188.88	1851.15	279.48	19049.25	57.04	2196.34	5058.94
CRMO11-04_S_62	244.79	0.72	3200.35	78.06	0.02	25.15	0.01	1.10	6.39	0.51	46.20	20.54	291.95	104.54	498.22	139.42	1629.55	167.64	11971.40	42.88	1384.52	5024.95
CRMO11-04_S_78	375.77	2.75	6436.13	276.90	11.01	61.59	3.84	25.84	23.73	0.86	116.64	50.63	673.09	235.23	1031.61	281.89	3238.64	321.40	12614.77	105.57	6407.18	16419.79

Table D2.3 CRMO11-04 Trace Element Concentrations con't
Concentrations (ppm)

Spot	P	Ti	Y	Nb	La	Ce	Pr	Nd	Sm	Eu	Gd	Tb	Dy	Ho	Er	Tm	Yb	Lu	Hf	Ta	Th	U
CRMO11-04_S_67	105.73	0.89	1924.27	6.39	0.03	23.55	0.19	3.49	9.56	1.36	41.29	16.56	196.71	71.20	300.93	77.49	861.83	98.36	9567.77	3.89	842.46	1079.27
CRMO11-04_M_181	142.19	1.05	1499.06	8.53	1.07	39.11	0.35	3.70	5.95	1.18	32.98	10.90	133.43	51.06	230.04	59.66	611.97	95.91	13690.80	4.25	841.64	589.25
CRMO11-04_S_71	334.10	0.55	6672.24	369.27	0.05	32.24	0.07	1.58	11.27	0.37	96.26	42.74	602.10	221.01	966.56	287.47	3307.35	338.69	14504.03	191.80	3047.68	15190.41
CRMO11-04_L_1	3374.25	0.52	3553.11	117.62	75.24	185.67	24.61	132.88	38.60	1.77	76.27	26.68	337.26	124.92	560.72	154.88	1701.49	182.28	14349.39	70.71	1801.32	6445.47
CRMO11-04_M_172	125.93	0.86	2615.63	67.86	0.19	20.88	0.07	0.87	3.16	0.45	31.05	13.99	197.73	85.02	413.95	112.39	1157.56	181.96	16844.04	31.43	776.37	2043.45
CRMO11-04_S_61	323.87	2.00	5679.58	205.39	4.04	44.74	2.22	15.06	19.73	0.79	104.82	43.16	559.97	203.55	883.39	239.61	2603.62	277.58	13270.26	91.94	6842.86	12150.04
CRMO11-04_S_80	2289.26	0.73	1348.64	7.27	41.78	103.27	11.51	59.71	17.15	2.11	39.89	11.09	136.38	49.95	210.22	58.77	692.67	76.49	9693.89	4.17	651.75	839.05
CRMO11-04_S_73	366.79	3.36	2860.21	79.64	7.08	35.84	3.06	20.14	12.80	0.84	47.37	16.96	230.02	94.54	476.32	146.16	1746.58	199.78	11532.35	43.06	4984.42	8897.00
CRMO11-04_M_174	223.92	0.54	2066.20	25.50	0.11	14.06	0.02	0.65	2.24	0.32	24.28	11.14	157.45	68.46	333.11	91.16	932.16	140.61	16774.16	15.81	759.76	1746.52
CRMO11-04_S_60	577.91	1.36	1827.34	12.49	3.44	71.08	1.32	10.73	9.75	2.16	45.15	15.75	183.22	64.94	266.09	73.85	896.07	98.34	8102.90	4.77	1132.31	1213.69
CRMO11-04_S_79	1681.29	0.85	9616.50	290.80	18.01	99.71	10.45	67.23	49.03	1.05	198.00	75.42	955.89	332.24	1441.84	391.33	4269.17	423.81	11245.18	110.22	7086.95	19918.41
CRMO11-04_S_55	417.35	2.39	572.66	4.42	3.27	25.64	0.97	5.33	3.19	0.58	12.80	3.98	53.66	19.46	84.62	24.33	286.41	33.84	9727.77	2.91	340.41	448.68
CRMO11-04_S_86	296.13	0.84	1752.72	36.40	4.89	34.24	1.23	8.00	6.09	0.68	36.19	13.65	166.45	60.50	269.66	75.20	848.74	89.54	10550.53	13.07	1706.30	2342.38
CRMO11-04_S_64	104.22	0.46	1278.22	20.70	0.02	19.50	0.04	0.79	3.28	0.34	21.15	8.69	118.34	44.63	200.37	57.72	691.98	72.89	10442.95	13.88	867.00	1929.65
CRMO11-04_S_83	87.70	0.53	1006.23	14.92		22.42	0.01	0.80	2.98	0.48	18.17	7.31	96.90	35.38	160.47	44.54	541.63	57.57	9719.57	8.77	784.34	1422.68
CRMO11-04_S_63	936.33	1.05	9774.40	351.68	5.43	69.42	2.81	18.87	25.95	0.70	175.88	73.70	981.06	338.25	1429.35	384.89	4303.14	424.12	12302.36	131.90	7700.21	21338.30
CRMO11-04_M_180	136.97	0.86	1630.91	3.43	1.12	27.07	0.56	6.28	9.86	2.10	42.60	13.53	146.37	54.22	240.59	60.22	630.52	91.97	12527.52	2.25	622.80	440.38
CRMO11-04_S_89	110.76	0.53	1696.75	26.97	0.10	22.25	0.04	0.82	4.16	0.65	30.95	12.33	161.36	60.86	265.63	74.98	879.47	94.80	11116.27	15.54	1111.96	2296.80
CRMO11-04_M_170	131.82	1.72	2934.72	4.73	0.65	42.23	0.83	13.71	17.49	6.42	83.11	25.52	279.25	99.13	434.11	105.62	1072.33	178.45	11729.84	2.83	1341.59	588.97
CRMO11-04_S_76	106.78	1.22	880.96	7.51	0.01	38.11	0.14	2.35	4.25	1.16	21.21	7.51	91.76	31.99	136.21	37.90	475.94	49.27	8405.61	3.98	637.66	634.55
CRMO11-04_S_90	774.24	1.18	1181.91	7.64	18.29	50.16	4.64	18.69	7.95	1.24	25.19	8.78	112.73	40.89	180.59	50.51	573.29	65.07	10084.44	4.04	632.60	700.16
CRMO11-04_M_177	13764.19	23.66	2674.36	21.99	236.30	619.65	106.17	622.93	174.36	10.79	199.40	36.52	305.70	93.35	372.24	89.21	857.27	125.42	15821.78	14.28	1738.74	2081.97
CRMO11-04_M_178	112.70	0.47	2731.65	36.57	0.20	30.27	0.15	1.97	5.52	1.21	40.50	16.57	221.39	89.36	434.72	119.14	1232.57	183.12	16609.79	19.56	3460.16	4075.61
CRMO11-04_M_179	262.22	1.34	1918.30	3.31	4.19	39.19	1.50	15.19	17.89	4.70	63.07	17.26	195.37	66.09	280.03	68.62	720.24	106.62	11747.83	1.78	736.14	373.67
CRMO11-04_S_72	217.82	0.59	1657.16	9.89	1.60	28.36	0.42	4.55	7.53	1.11	37.20	12.90	170.23	60.94	263.29	73.55	869.01	87.07	9898.06	5.74	785.56	1123.35
CRMO11-04_S_74	167.97	0.35	1362.30	11.66	0.02	13.19	0.02	0.97	3.31	0.51	23.29	8.97	123.55	47.73	216.88	63.42	742.96	80.42	10265.97	6.33	551.78	1176.31
CRMO11-04_L_2	145.14	2.46	578.31	4.57	0.68	14.83	0.27	1.70	1.88	0.40	11.33	4.00	53.37	20.47	95.80	26.99	317.76	37.53	10193.64	2.44	189.53	316.38
CRMO11-04_M_182	396.82	1.36	8210.72	243.75	0.86	31.26	0.49	4.62	10.09	0.32	93.28	45.01	638.35	248.40	1193.88	326.69	3312.45	499.02	20862.08	150.21	2934.93	13309.98
CRMO11-04_M_176	456.75	0.80	1038.17	5.68	10.48	44.90	2.38	13.79	6.41	0.95	23.31	7.22	92.58	35.19	160.77	41.46	431.41	65.48	13946.98	3.88	788.53	607.30
CRMO11-04_M_173	3228.42	1.09	2044.35	14.18	98.17	194.25	29.84	145.20	40.18	3.18	63.58	17.60	188.81	71.69	318.19	79.84	817.87	130.13	13667.86	6.35	821.45	842.80
CRMO11-04_S_58	330.66	9.44	1879.90	7.17	2.96	41.93	1.01	10.36	11.07	1.94	43.38	15.11	179.61	65.12	286.64	81.03	904.72	107.75	9478.33	3.90	877.02	1004.34
CRMO11-04_M_175	177.04	1.31	2069.04	4.86	1.26	39.24	0.82	12.09	15.01	3.25	59.15	18.52	212.43	73.84	307.47	74.56	730.76	107.20	12322.96	2.60	794.82	454.88
CRMO11-04_M_169	135.17	0.40	1939.62	15.24	0.93	33.42	0.30	2.10	5.33	0.92	39.09	13.36	172.23	67.19	294.70	72.17	702.82	117.74	15591.86	9.07	1804.29	1515.98
CRMO11-04_M_168	6108.59	25.65	6359.13	238.95	179.17	434.28	74.94	456.87	147.65	6.43	205.81	55.90	624.39	215.22	985.61	249.45	2524.95	396.27	19283.07	122.58	3891.91	16301.13

Table D2.4 CRMO11-05 Trace Element Concentrations

Concentrations (ppm)

Spot	P	Ti	Y	Nb	La	Ce	Pr	Nd	Sm	Eu	Gd	Tb	Dy	Ho	Er	Tm	Yb	Lu	Hf	Ta	Th	U
Paleoarchean																						
CRMO11-05M_172	247.96	29.61	596.92	7.53		3.62	0.03	0.15	0.46	0.11	5.72	2.48	42.20	17.78	95.66	28.37	321.73	44.09	10781.77	7.88	48.43	621.49
CRMO11-05S_276	371.76	21.76	3039.75	3.83	0.11	16.02	0.29	6.39	13.99	1.75	75.58	23.17	285.32	102.62	442.14	91.59	794.11	109.81	9380.85	1.30	294.68	211.46
Mesoarchean 2																						
CRMO11S-05_90	871.05	34.98	2561.05	9.16	0.05	5.49	0.02	0.22	1.04	0.28	16.43	9.32	180.07	80.39	420.41	110.21	1041.68	155.99	18018.10	21.28	30.22	1279.62
CRMO11-05S_267	674.64	27.83	1360.81	1.80	0.02	2.29			0.62	0.25	11.73	4.99	92.60	41.51	235.62	68.76	762.90	130.51	15118.54	2.53	16.88	481.08
CRMO11-05S_270	944.07	23.17	2382.13	6.95	0.13	5.11		0.39	1.18	0.16	18.31	8.98	163.51	73.57	422.93	114.51	1240.08	217.40	14947.02	7.22	41.25	542.82
CRMO11-05L_228	1891.13	65.13	3695.11	17.12		6.48		0.72	3.65	0.68	30.17	17.85	306.18	119.68	670.01	238.13	3249.79	410.85	13056.60	31.45	61.66	4177.39
CRMO11-05M_176	596.40	22.17	1469.61	3.32	0.03	2.88	0.01	0.38	1.59	0.24	14.93	7.89	122.57	44.33	206.19	54.34	553.93	72.74	12885.44	3.96	21.19	584.12
CRMO11-05S_265	413.88	22.24	1090.09	3.96	0.03	2.54			1.31	0.30	11.73	6.70	96.29	34.05	153.52	38.12	378.68	59.40	14360.08	6.17	19.89	908.76
CRMO11-05S_269	674.97	41.10	1758.86	6.14		5.70			1.68	0.32	14.21	6.36	115.88	51.18	300.01	85.70	919.38	161.22	15391.78	11.26	43.05	895.17
CRMO11-05L_224A	1284.21	44.92	2629.73	5.92	0.08	6.99	0.03	1.04	3.10	0.48	22.82	10.33	185.58	81.01	471.52	156.44	1958.50	259.48	12090.03	13.29	81.81	2202.80
CRMO11S-05_80	1024.31	12.36	2666.36	3.25	0.10	2.52	0.04	0.62	2.47	0.32	26.27	13.72	216.15	85.43	428.15	115.46	1144.09	176.03	16922.36	2.93	10.57	503.51
CRMO11-05S_271	617.64	25.08	1754.39	7.71	0.06	6.73	0.17	1.35	2.41	0.35	16.52	6.84	112.35	50.43	283.21	76.02	821.21	157.08	15442.63	8.18	91.05	628.71
CRMO11-05L_224B	1132.61	31.35	1945.49	4.60	0.13	6.01	0.01	0.33	1.29	0.54	12.58	7.87	133.40	59.44	348.63	115.34	1467.16	193.95	11004.60	10.10	58.20	1639.79
CRMO11-05L_221	843.96	10.13	1695.85	2.49		2.55	0.02	0.49	2.56	0.19	19.68	10.04	148.02	55.39	246.87	69.60	763.02	86.75	9777.19	2.62	19.68	512.88
CRMO11S-05_82	1402.16	26.22	3908.28	6.19	0.07	5.43	0.02	0.64	3.23	0.39	27.95	15.08	267.41	122.93	708.10	209.07	2351.32	385.67	16983.09	6.79	45.76	789.83
CRMO11-05M_178	1140.34	13.85	2145.16	1.45	0.06	2.93		0.47	1.75	0.38	15.37	9.49	169.47	70.98	402.79	135.19	1740.48	244.90	12621.91	1.12	9.05	482.60
CRMO11-05S_266	1070.39	10.76	2286.24	3.30	0.16	2.93	0.04	0.83	1.81	0.46	19.63	10.23	177.24	74.45	417.61	121.56	1398.29	230.10	14349.47	2.82	4.99	312.78
CRMO11S-05_89	683.82	24.35	1836.06	6.42		7.71	0.07	0.54	0.78	0.12	10.09	5.09	103.64	52.50	336.74	112.15	1409.34	231.00	14708.34	10.67	46.86	1290.03
CRMO11-05M_243	767.33	28.21	1338.76	9.73	0.11	13.42	0.01	0.52	0.90	0.28	7.33	4.93	78.91	39.72	238.15	78.00	1004.42	123.56	9332.05	10.54	50.47	768.16
CRMO11S-05_83	1177.38	18.81	3301.93	3.79		5.61	0.08	0.91	3.67	0.39	28.00	14.92	243.38	103.55	560.83	155.10	1593.82	249.26	16392.22	4.25	59.81	707.95
CRMO11-05L_219	632.59	20.16	1302.95	8.65	0.04	11.70	0.03	0.23	0.61	0.28	7.97	4.55	81.08	37.84	228.15	78.69	968.40	117.29	10165.32	9.68	47.79	976.48
CRMO11S-05_88	981.46	13.48	2615.00	3.19	0.10	3.23	0.06	0.73	2.28	0.24	24.31	11.84	204.73	82.75	434.62	118.74	1220.66	177.73	16007.71	3.46	25.64	602.80
CRMO11-05M_242	1763.24	66.37	4140.88	10.13	0.19	12.00	0.12	1.83	5.23	0.89	49.51	21.23	347.44	127.42	607.35	151.26	1608.76	182.60	13266.96	21.61	181.45	4906.99
Neoarchean																						
CRMO11-05S_273	923.32	11.28	2544.86	1.71	0.07	3.48	0.08	0.64	2.21	0.24	27.72	13.55	201.92	78.15	366.94	81.12	732.15	109.08	13898.06	1.58	31.64	269.94
CRMO11-05M_168	783.99	28.73	1388.99	7.19	1.63	16.52	0.63	4.04	2.41	0.21	10.13	5.21	88.46	40.81	243.06	81.56	938.09	123.43	11104.04	8.84	64.34	951.65

Table D2.4 CRMO11-05 Trace Element Concentrations con't
Concentrations (ppm)

Spot	P	Ti	Y	Nb	La	Ce	Pr	Nd	Sm	Eu	Gd	Tb	Dy	Ho	Er	Tm	Yb	Lu	Hf	Ta	Th	U
CRMO11-05M_173	826.16	9.07	1792.16	2.01		7.04	0.03	0.69	2.31	0.36	19.22	8.94	141.82	56.97	301.80	83.48	862.63	109.35	11455.75	0.61	36.18	96.21
CRMO11-05S_274	794.45	7.25	1941.76	1.91		4.76	0.07	0.86	2.33	0.18	19.64	9.55	147.38	60.56	310.24	79.15	760.65	119.73	13996.34	1.34	59.43	140.74
CRMO11S-05_93	834.23	29.41	2493.35	8.75	0.07	10.94	0.02	0.65	2.92	0.38	27.32	12.14	191.14	77.77	394.41	101.76	981.87	147.48	18450.67	13.05	140.21	753.25
CRMO11-05S_275	851.76	9.05	2034.89	2.46		5.86	0.07	0.90	2.37	0.35	25.81	10.71	161.26	65.36	322.42	76.40	744.70	117.87	14384.53	2.12	109.37	223.30
CRMO11-05S_268	687.90	13.33	1505.92	3.21	0.36	8.57	0.00	1.05	2.07	0.23	17.02	7.64	113.03	45.63	250.34	67.41	700.12	107.76	13145.00	1.38	118.96	217.26
CRMO11S-05_91	990.25	13.64	2997.41	4.97		9.99	0.04	0.91	2.81	0.37	30.99	14.32	232.68	96.54	490.04	125.37	1172.59	188.36	16238.47	3.35	110.92	227.37
CRMO11-05M_167	779.82	12.75	1708.62	6.50		8.17	0.06	0.61	2.25	0.33	16.50	8.06	137.55	53.05	285.80	86.07	931.84	118.59	11005.67	3.85	66.38	216.96
CRMO11-05L_217	739.64	14.20	1635.67	3.69	0.07	15.14	0.07	1.11	3.05	0.47	22.50	9.91	139.75	52.36	241.69	64.93	692.14	77.97	9881.44	1.99	105.50	170.55
CRMO11-05M_245B	889.89	7.56	1766.34	3.35		8.00		0.66	3.05	0.48	26.35	10.06	144.44	57.25	273.61	70.99	772.74	92.45	12082.40	2.12	124.27	181.77
CRMO11-05M_177	793.83	11.61	1820.94	2.63	0.07	6.67	0.05	1.24	3.49	0.34	23.28	10.94	159.11	58.67	282.85	75.21	749.66	91.06	11698.77	1.38	84.68	104.33
CRMO11-05M_244	843.69	10.57	1868.25	2.21	0.00	12.64		1.84	4.86	0.53	27.93	11.82	168.17	60.74	282.31	71.95	755.53	83.50	10607.98	1.00	105.10	113.54
CRMO11S-05_81	1254.26	10.52	3402.15	5.20	0.06	6.87	0.03	0.93	3.57	0.36	32.09	14.66	244.85	108.05	607.66	169.70	1741.39	273.65	16378.70	3.41	95.51	137.05
CRMO11S-05_92	772.01	10.96	2160.54	2.46	0.04	11.56	0.05	1.60	4.52	0.41	32.27	12.53	179.76	71.07	335.20	78.78	755.34	111.40	15572.64	1.08	117.73	95.96
CRMO11-05L_226	843.81	11.78	1800.95	2.65	0.10	11.53	0.05	1.77	4.22	0.32	25.38	10.93	164.29	58.41	274.89	73.54	770.02	86.80	10287.96	1.15	107.13	94.87
CRMO11-05M_245A	818.46	7.32	1703.25	3.88	0.00	7.64	0.10	1.24	2.75	0.42	25.03	9.32	142.34	53.99	266.76	70.59	781.16	83.74	10813.13	2.17	123.32	187.92
CRMO11S-05_84	823.48	15.76	2256.95	2.22	0.09	12.83	0.09	1.64	4.98	0.34	33.67	13.30	186.89	72.63	352.16	83.29	785.45	118.46	15448.94	0.87	137.26	74.54
CRMO11-05M_171	1174.36	13.03	2758.03	3.02	0.02	8.89	0.03	1.62	5.10	0.45	36.42	15.60	237.15	89.86	434.53	116.43	1170.79	143.10	11906.15	1.70	104.16	211.91
CRMO11-05M_174	877.71	12.04	2067.03	2.68	0.04	10.76	0.07	1.24	5.28	0.39	28.85	11.96	182.07	65.66	311.30	82.74	836.89	104.37	11892.68	1.23	99.34	138.95
CRMO11-05L_220	920.48	11.57	2375.09	3.67		21.54	0.08	2.46	5.54	0.69	40.50	15.89	219.48	78.44	355.20	91.08	906.61	100.78	9913.36	1.12	219.51	202.15
CRMO11S-05_86	1098.97	9.81	3144.28	3.23	0.17	8.21	0.09	1.60	5.12	0.41	37.59	17.22	253.75	102.27	491.09	123.54	1161.18	174.45	16139.72	1.47	131.09	189.30
CRMO11S-05_85	936.29	15.03	2830.40	3.76		13.45	0.11	1.62	5.46	0.34	42.05	16.34	234.63	92.01	452.29	110.91	1041.53	160.85	17211.76	1.99	172.23	187.81
CRMO11-05L_218	835.87	11.69	1659.72	2.97	0.05	11.93	0.15	1.65	5.18	0.51	31.02	10.96	154.51	54.27	253.44	64.73	679.21	74.19	9328.30	1.13	107.83	104.85
CRMO11-05L_229	1073.74	9.21	2190.77	4.17	0.07	9.27	0.09	1.43	3.95	0.43	27.64	12.05	184.19	70.78	362.50	107.16	1162.94	134.70	10818.96	2.19	100.40	258.60
CRMO11S-05_87	745.76	10.80	1950.66	2.32		13.36	0.09	1.91	4.93	0.46	33.01	11.63	169.22	64.23	306.66	75.92	732.66	107.93	15167.39	0.78	173.86	68.58
CRMO11-05L_223	822.88	7.06	1579.22	2.37	0.15	6.36	0.11	0.92	4.09	0.44	21.63	9.33	141.11	50.90	239.57	63.82	683.83	76.41	9449.61	1.20	113.26	95.81
CRMO11-05M_169	1798.29	14.11	4202.30	10.43	0.01	12.96	0.04	1.73	5.40	0.58	45.58	21.13	333.72	134.78	679.90	190.27	1953.52	245.29	11764.65	6.34	175.92	329.97
CRMO11-05L_227	911.15	9.44	1894.00	2.42		11.10	0.10	1.61	4.20	0.30	28.75	11.68	170.48	61.65	290.41	76.88	795.63	92.40	10554.76	0.88	112.94	118.87
CRMO11-05L_222	833.47	12.22	1574.07	2.00	0.02	10.33	0.07	1.41	4.66	0.45	26.98	10.12	145.94	51.66	238.13	65.25	691.96	76.04	9776.08	0.98	83.53	74.13
CRMO11-05M_170	1082.13	18.61	2482.64	4.33	0.05	10.78	0.06	1.92	5.87	0.52	37.96	14.45	218.82	81.04	385.53	99.84	984.90	122.55	11347.37	1.09	126.78	43.69
CRMO11-05M_175	805.18	12.69	1845.19	1.98	0.09	10.58	0.08	1.83	4.54	0.33	32.35	11.79	168.15	60.09	284.38	72.45	731.85	92.85	12152.92	0.63	95.94	115.50

Table D2.5 CRMO11-07 Trace Element Concentrations

Concentrations (ppm)

Spot	P	Ti	Y	Nb	La	Ce	Pr	Nd	Sm	Eu	Gd	Tb	Dy	Ho	Er	Tm	Yb	Lu	Hf	Ta	Th	U
Mesoarchean 2																						
CRMO11-07_M_127	45.20	0.20	7711.18	12.25		65.22	0.22	11.17	53.41	3.88	291.13	111.79	1220.67	462.55	1721.84	445.05	4788.19	473.93	94003.17	9.23	1437.12	2032.74
CRMO11-07_S_211	44.59	0.22	6515.37	11.18	0.33	44.89	0.18	11.21	34.46	4.77	253.18	95.33	1024.10	410.57	1527.61	418.88	4376.72	506.05	110578.63	12.11	1191.68	2454.60
CRMO11-07_S_206	68.47	0.23	9991.66	15.46	1.62	77.04	1.76	22.34	70.17	6.22	411.20	162.52	1665.10	633.92	2235.26	590.39	6122.80	622.48	99277.32	13.64	2228.02	3209.77
CRMO11-07_M_131	47.91	0.13	3446.18	10.43	0.10	46.17	0.56	2.88	31.43	3.22	140.89	47.11	532.31	216.18	798.88	235.29	2666.21	257.44	98384.40	9.95	668.38	1543.12
CRMO11-07_S_207	45.99	0.20	5040.23	10.81		47.73	0.76	5.66	24.39	2.74	165.03	63.50	743.27	300.37	1125.66	327.78	3519.23	377.53	101090.30	12.17	857.00	1769.97
CRMO11-07_M_140	26.69	0.29	1952.72	7.68		25.13		1.44	5.36	0.83	37.42	21.91	241.46	112.25	483.46	151.77	1893.16	232.59	122110.53	13.34	534.27	2962.63
CRMO11-07_M_133	65.79	0.15	7438.12	12.05		43.85	0.19	8.95	56.18	9.20	312.16	122.06	1243.97	449.53	1648.50	426.21	4606.07	467.93	86827.76	10.14	1250.90	1732.59
CRMO11-07_M_130	82.26	0.52	6877.11	43.29	5.85	34.56	1.80	12.69	20.85	0.69	158.72	73.26	904.61	392.37	1572.80	497.43	5815.93	615.04	115416.65	63.03	2912.38	12942.44
Neoarchean																						
CRMO11-07_M_128	61.55	0.25	5333.40	12.84		56.33	0.16	6.63	38.45	3.30	200.10	76.08	832.01	324.97	1227.33	326.67	3484.73	372.69	101143.51	13.59	1219.39	2423.68
CRMO11-07_M_129	69.43	0.22	6463.65	13.71		50.68	0.41	7.10	29.88	1.94	213.62	91.67	914.00	389.79	1501.25	391.25	4050.83	457.50	100182.84	13.04	1362.19	2537.95
CRMO11-07_M_141	184.82	0.92	15702.00	59.40	21.84	76.84	9.49	52.19	56.30	3.16	384.50	177.50	2149.05	959.65	3798.47	1071.17	11342.90	1214.25	127216.50	70.45	7235.59	22589.01
CRMO11-07_M_134	39.94	0.19	2939.22	11.50	0.24	46.38	0.23	5.80	16.79	1.63	105.62	42.51	444.04	180.35	670.92	190.96	2072.18	219.26	97542.37	11.47	613.49	1191.15
CRMO11-07_S_218	67.96	0.20	5061.47	12.65	13.25	59.63	5.47	29.92	40.22	4.89	208.00	83.72	796.37	316.22	1110.43	297.69	3264.76	341.43	105661.00	11.01	736.47	1318.72
CRMO11-07_S_216	48.65	0.21	3300.33	10.19	0.35	43.43	0.16	4.36	21.80	1.80	111.65	41.51	508.56	202.39	781.41	216.71	2371.65	277.75	108734.92	11.79	731.69	1681.87
CRMO11-07_S_212	59.99	0.23	5141.99	13.16	1.21	56.67	1.12	8.40	24.62	3.51	180.24	67.85	760.86	308.57	1177.47	324.85	3361.86	396.93	106408.79	12.90	1005.83	1836.43
CRMO11-07_M_138	125.17	0.56	11525.70	66.29	1.82	46.27	2.38	15.60	39.04	2.58	280.84	136.33	1675.92	694.79	2609.67	683.00	7181.72	752.58	123148.89	69.79	4476.21	17922.74
CRMO11-07_M_139	39.69	0.16	3177.26	11.09	0.64	50.02	0.31	5.46	18.96	2.92	103.22	43.48	449.35	174.66	739.08	201.51	2251.32	254.58	104278.20	10.18	701.71	1371.20
CRMO11-07_M_135	48.30	0.25	3765.86	10.50		41.66	0.44	6.97	27.75	2.56	139.41	55.82	602.83	230.14	848.12	225.97	2366.48	241.67	95910.32	8.61	390.30	893.26
CRMO11-07_S_217	64.84	0.19	3747.75	10.44	4.31	65.59	1.79	15.44	24.78	2.63	129.53	51.90	557.25	230.64	885.32	240.63	2610.24	285.55	112020.89	11.94	1238.77	2334.17
CRMO11-07_S_220	47.61	0.17	3301.27	12.63		44.85	0.46	8.29	13.94	2.08	121.95	44.67	488.70	197.26	765.33	220.59	2420.75	270.82	107842.64	14.48	508.82	1367.35
CRMO11-07_S_209	51.12	0.24	4202.45	13.69		51.55	0.52	6.85	27.05	3.16	167.80	61.32	655.89	253.64	962.26	249.06	2628.68	285.24	113657.09	16.20	1039.12	1364.58
CRMO11-07_S_21	344.79	0.24	4364.00	14.13		49.16	0.39	6.48	23.62	1.64	139.44	55.04	644.68	260.35	990.65	279.22	2972.90	360.68	119625.19	15.28	706.36	2280.85
CRMO11-07_M_136	27.56	0.22	1524.36	8.17	0.49	17.83		4.81	11.59	2.41	36.63	18.05	202.98	81.74	397.01	133.29	1752.33	202.99	111594.39	17.12	338.22	4716.24

Table D2.6 CRMO11-12 Trace Element Concentrations

Concentrations (ppm)

Spot	P	Ti	Y	Nb	La	Ce	Pr	Nd	Sm	Eu	Gd	Tb	Dy	Ho	Er	Tm	Yb	Lu	Hf	Ta	Th	U
Paleoarchean																						
CRMO11-12_S_184	45.46	0.72	7259.84	37.75	0.28	117.17	0.29	4.67	23.68	10.28	159.36	71.48	924.30	405.61	1756.84	552.15	6711.68	827.72	104982.31	42.95	2692.54	6802.33
CRMO11-12_L_17	116.24	5.07	946.17	2.31	0.07	28.66	0.05	1.01	3.28	0.84	15.50	5.68	93.80	40.81	153.58	37.08	477.59	82.47	15548.14	2.00	393.26	550.95
Mesoarchean 1																						
CRMO11-12_L_14	106.49	4.93	985.99	3.84	0.09	22.04	0.05	0.29	2.01	0.56	16.06	6.35	85.96	32.04	157.81	42.67	443.47	61.75	15506.15	3.03	386.86	588.42
CRMO11-12_S_179	129.12	0.51	10956.18	57.79	0.07	34.35	0.01	2.57	24.57	6.69	264.25	124.48	1525.37	677.20	2690.86	742.43	8350.68	836.20	78751.38	39.44	1728.63	2875.45
CRMO11-12_L_13	499.80	16.36	4036.97	16.59	0.06	63.26	0.05	1.26	6.72	1.71	66.62	28.39	364.80	141.11	639.05	158.56	1594.01	206.26	17285.83	13.01	2984.45	3148.27
CRMO11-12_L_7	145.54	5.35	928.99	4.20		19.22	0.00	0.26	1.97	0.40	13.08	5.59	76.96	31.81	147.77	44.19	533.43	72.09	14281.38	6.43	236.57	528.97
CRMO11-12_S_190	77.32	0.82	6131.82	83.63	0.18	52.44			7.56	2.58	90.55	49.59	705.48	357.47	1596.68	529.29	7222.31	1006.39	172782.05	193.25	1947.96	10278.25
CRMO11-12_L_36	267.36	7.40	1770.01	9.47	0.03	18.60	0.07	0.33	2.00	0.46	21.40	9.56	162.93	67.57	306.00	82.78	1050.91	163.48	16380.36	12.09	693.98	1481.40
Neoarchean																						
CRMO11-12_L_31	187.34	10.39	1114.48	10.11	0.01	5.90		0.37	1.86	0.07	10.72	6.09	88.47	37.06	185.06	56.36	670.58	92.18	20173.87	28.08	138.82	1349.38
CRMO11-12_L_16	1055.95	11.38	4467.90	5.87	15.80	29.47	3.30	23.65	11.41	0.72	48.50	26.57	480.50	187.25	810.53	219.69	2810.41	386.88	16081.57	4.45	552.44	2972.07
CRMO11-12_S_181	233.60	1.39	20987.77	84.86	0.73	160.98	1.37	15.22	74.73	10.66	606.12	277.66	3270.59	1278.84	4882.54	1271.63	13168.13	1334.64	121704.67	52.04	7466.81	20648.03
CRMO11-12_S_201	56.14	0.99	3193.50	35.57	2.49	21.02	0.26	4.99	16.28	1.61	64.78	31.68	403.65	171.15	772.93	257.10	3496.76	385.09	122458.06	155.52	1068.69	8285.87
CRMO11-12_L_26	171.78	5.53	887.56	4.81	0.03	10.39	0.02	0.96	3.01	0.20	19.74	6.96	78.81	29.77	134.95	34.49	358.21	49.14	17158.37	13.55	152.05	361.75
CRMO11-12_L_22	232.82	11.80	1188.63	7.35	1.08	7.11	0.16	1.53	1.37	0.14	8.99	4.88	80.58	37.87	212.30	72.87	908.49	127.32	18660.16	40.82	139.75	1260.91
CRMO11-12_S_178	55.82	0.74	2851.92	8.40	0.94	30.63	0.73	8.76	18.04	3.53	124.06	49.31	455.46	171.52	592.61	170.43	1898.92	206.66	120768.70	4.12	957.24	3498.16
CRMO11-12_L_29	248.63	7.79	1375.98	4.70	0.12	8.16	0.05	0.73	1.98	0.12	16.55	7.52	118.19	49.97	234.91	63.01	671.51	77.34	17275.86	7.42	139.84	1128.28
CRMO11-12_L_12B	340.24	6.46	2090.13	4.79	0.56	18.72	0.05	1.37	4.17	1.06	31.88	13.71	180.39	73.91	348.57	93.32	993.37	139.47	16890.71	11.79	614.75	1264.54
CRMO11-12_S_185	77.85	1.46	6578.95	44.95	0.68	28.68	0.35	2.94	12.56	1.11	133.14	68.34	861.28	370.90	1542.43	455.05	5108.54	570.73	153386.98	93.87	1084.27	19679.49
Paleoproterozoic																						
CRMO11-12_L_12A	251.04	4.80	1268.33	2.18	0.48	12.44	0.05	1.10	2.42	0.51	17.47	7.87	112.39	46.35	210.14	53.03	559.39	86.28	15598.12	4.61	404.43	937.00
CRMO11-12_S_189	140.59	2.11	13503.73	113.77	0.36	29.89	0.15	0.98	24.78	1.63	201.38	129.14	1694.54	759.17	3104.74	874.14	8713.04	929.59	168855.75	202.51	2024.44	29844.38
CRMO11-12_S_196	89.62	1.34	6780.58	96.42	1.26	24.91	0.22	3.07	17.78	1.64	135.65	64.13	845.59	356.88	1499.79	443.38	4966.35	604.73	159355.56	688.64	1291.71	17589.91
CRMO11-12_L_25	281.37	9.62	1985.88	8.38	0.08	17.54	0.15	2.09	6.66	0.23	39.82	17.29	211.97	70.18	273.11	57.65	502.69	57.82	19238.15	5.62	588.58	2248.65
CRMO11-12_S_203	76.82	1.02	5307.50	48.58	0.74	34.64	0.25	5.46	17.91	1.32	112.43	59.53	681.26	289.64	1179.13	404.52	5628.11	684.03	162265.05	257.49	1721.31	13230.30
CRMO11-12_S_200	73.69	0.57	5301.71	16.72		41.53	0.56	8.01	42.09	2.68	215.27	83.46	871.98	306.14	1113.62	281.07	2868.05	311.05	123148.30	10.38	2293.40	7127.04
CRMO11-12_S_197	98.70	1.23	8779.97	57.66	0.13	53.46	0.51	3.58	22.07	2.86	221.80	108.92	1253.26	515.54	1978.18	523.31	5292.80	592.34	149074.94	84.79	1824.92	15375.10

Table D2.6 CRMO11-12 Trace Element Concentrations con't
Concentrations (ppm)

Spot	P	Ti	Y	Nb	La	Ce	Pr	Nd	Sm	Eu	Gd	Tb	Dy	Ho	Er	Tm	Yb	Lu	Hf	Ta	Th	U
CRMO11-12_L_18	131.48	3.81	712.16	1.37		9.49	0.04	1.35	2.15	0.28	19.03	6.28	64.53	24.95	102.26	23.55	225.71	32.55	16368.03	0.85	120.72	66.10
CRMO11-12_L_34	191.41	6.88	1491.73	3.62	0.11	12.43	0.07	1.66	4.75	0.16	32.77	13.31	136.04	48.61	207.55	48.06	407.26	50.30	21687.17	2.92	477.80	2044.73
CRMO11-12_L_32	205.23	6.54	1221.11	5.83	0.04	14.26	0.08	1.26	4.41	0.22	34.83	13.64	146.56	44.16	141.17	26.35	200.47	21.17	20225.48	3.06	327.13	1140.02
CRMO11-12_L_8	92.21	2.66	406.42	0.93	0.01	8.08	0.04	0.85	3.10	0.28	11.47	3.63	44.88	15.89	60.94	14.48	154.87	19.64	13322.58	0.55	82.76	46.65
CRMO11-12_L_21	223.61	7.40	1396.63	5.38		14.39	0.05	1.36	6.06	0.26	28.77	12.14	150.16	49.65	194.35	41.83	375.93	42.23	17853.77	3.67	399.79	1718.51
CRMO11-12_L_9	190.33	6.10	1121.81	3.16	0.04	8.76	0.07	0.95	3.49	0.10	23.63	9.62	114.60	42.32	159.04	36.95	329.72	38.75	17524.12	2.83	395.20	1133.94
CRMO11-12_L_19	136.21	2.39	642.44	1.32		9.17	0.05	1.00	3.59	0.31	17.99	6.08	66.73	22.12	94.92	22.87	221.75	29.54	13930.27	0.73	103.01	51.63
CRMO11-12_S_191	77.92	1.02	6746.61	22.93	0.08	46.75	0.43	8.83	44.46	2.52	242.75	102.03	1050.22	399.05	1391.47	348.17	3662.28	364.93	146709.60	22.02	3259.72	17953.52
CRMO11-12_S_199	77.60	1.17	5843.08	19.85	1.05	35.97	0.68	8.26	36.38	1.62	185.23	86.56	895.98	332.97	1208.16	301.83	2907.74	328.28	152596.60	23.98	3491.26	23882.93
CRMO11-12_L_37A	205.67	6.94	1370.65	2.62	0.05	11.34	0.09	2.00	5.36	0.27	29.01	11.82	130.57	46.50	190.44	41.80	366.00	47.66	20058.54	2.22	408.69	914.83
CRMO11-12_S_202	100.73	1.37	8012.05	50.33	1.17	57.93	1.19	7.64	38.91	2.17	222.74	119.92	1281.51	467.10	1576.04	369.08	3191.68	276.42	142096.25	54.98	2152.61	30276.13
CRMO11-12_S_187	48.45	0.38	3152.92	11.69		37.62	0.07	8.23	25.56	1.09	124.06	46.82	502.96	185.63	696.10	174.72	1760.42	207.94	124809.14	9.28	1248.84	2557.11
CRMO11-12_L_23	270.69	10.08	1699.68	9.19		14.71	0.09	1.17	3.89	0.10	28.55	12.96	163.90	60.97	254.58	58.04	532.48	58.31	18342.32	6.13	273.93	2284.84
CRMO11-12_L_20	279.21	3.37	1763.96	1.76		19.34	0.21	5.69	16.29	1.02	76.79	21.54	217.10	68.76	243.27	52.75	482.32	57.77	13532.42	0.69	379.42	123.96
CRMO11-12_S_188	72.04	0.66	5591.29	14.09	0.51	48.43	0.54	7.58	35.74	3.50	229.36	91.85	891.47	321.64	1163.42	276.81	2704.37	310.33	124651.97	8.40	1711.96	3926.92
CRMO11-12_S_204	85.52	1.22	7134.87	37.46	0.11	50.70	0.35	7.45	30.60	1.92	211.84	103.30	1148.85	412.25	1346.05	314.82	2792.48	259.45	148882.57	26.67	1840.56	15582.14
CRMO11-12_L_35	143.28	2.80	720.85	1.45		13.17	0.08	1.60	4.01	0.17	20.71	6.04	74.86	29.04	106.14	22.25	228.95	36.88	17033.53	0.84	132.57	73.38
CRMO11-12_S_182	57.84	0.73	2462.87	9.01		17.41	0.46	8.92	30.47	1.88	133.27	43.62	441.26	143.24	505.99	132.24	1326.70	150.27	135283.80	4.10	1463.59	2003.46
CRMO11-12_S_194	56.80	0.38	3630.14	11.29	0.72	45.91	0.61	8.24	27.09	1.58	167.49	62.10	584.27	218.86	768.15	193.86	2030.75	226.44	115047.12	8.03	1067.83	1224.24
CRMO11-12_L_10	197.17	6.16	741.25	2.01	0.81	7.68	0.38	3.27	5.45	0.18	25.91	7.93	85.60	27.90	99.17	20.68	194.75	23.65	18684.16	1.00	608.31	318.73
CRMO11-12_S_180	64.78	0.54	2760.39	7.70	0.06	19.25	0.48	10.16	26.87	1.92	155.91	50.73	469.14	170.15	562.89	142.05	1582.98	165.15	124111.51	4.77	615.19	1154.40
CRMO11-12_L_24	190.55	7.69	846.39	2.27	0.50	6.88	0.20	2.34	4.27	0.10	21.87	7.60	92.91	29.52	121.70	27.09	268.02	35.47	18169.65	2.34	524.61	576.36
CRMO11-12_S_192	80.34	0.60	4720.88	14.89	2.47	28.05	1.53	17.71	54.28	3.14	244.32	92.85	864.50	290.55	955.44	215.52	2087.37	238.14	147237.67	9.80	4281.54	2377.31
CRMO11-12_L_33	157.31	3.92	668.56	1.21	0.15	5.41	0.09	2.10	3.53	0.19	20.79	6.52	72.89	23.65	91.67	21.62	202.23	27.23	17528.44	0.94	176.24	249.41
CRMO11-12_L_30	130.71	4.07	480.61	0.93	0.24	4.26	0.09	1.49	2.77	0.31	13.59	4.53	54.51	18.34	65.33	16.08	153.90	20.03	15534.66	0.36	115.85	184.57
CRMO11-12_L_11	202.79	5.29	916.45	2.05	1.10	8.38	0.50	4.35	7.22	0.19	31.94	10.54	110.61	33.78	122.85	25.94	240.68	29.21	18819.22	0.87	512.00	201.99
CRMO11-12_S_183	131.95	1.43	10147.99	42.21	11.12	55.32	2.82	15.31	31.60	1.98	221.09	118.85	1387.19	573.24	2171.27	549.09	5460.98	605.91	164560.27	98.16	2017.46	26998.32
CRMO11-12_L_15	125.88	5.84	640.69	1.97	0.00	5.96	0.04	0.93	3.23	0.11	17.96	6.32	73.48	22.21	88.63	19.96	174.75	22.25	18322.87	1.04	326.48	542.19
CRMO11-12_L_28	180.44	5.21	691.25	2.15	0.10	6.28	0.10	1.24	3.91	0.13	26.01	7.57	81.64	25.94	93.94	20.70	182.62	22.37	19001.78	1.14	585.51	366.83

Table D2.7 CRMO11-13 Trace Element Concentrations

Concentrations (ppm)

Spot	P	Ti	Y	Nb	La	Ce	Pr	Nd	Sm	Eu	Gd	Tb	Dy	Ho	Er	Tm	Yb	Lu	Hf	Ta	Th	U
Mesoarchean 2																						
CRMO11-13_S_177	69.40	0.42	7808.71	20.27	0.91	95.16	2.16	30.78	83.16	18.41	340.87	121.32	1268.16	473.25	1761.86	484.69	5219.78	585.87	82324.91	11.74	1180.33	1008.40
CRMO11-13_S_175	57.89	0.41	9985.43	17.45		140.17	1.96	35.27	101.63	15.00	424.29	168.53	1594.28	607.99	2199.57	581.43	6231.98	641.36	83107.40	12.88	2479.63	1866.55
CRMO11-13_L_5	84.71	2.15	595.43	1.88		20.58	0.04	0.75	1.73	0.25	11.51	4.37	55.45	21.30	95.91	25.65	262.21	34.92	13920.95	1.28	106.21	86.01
CRMO11-13_S_164	50.09	0.38	5761.11	19.32	0.28	85.24	1.11	14.21	40.27	7.98	220.94	82.71	881.17	342.92	1353.45	391.87	4243.36	502.27	95079.91	14.08	1341.39	1209.33
CRMO11-13_S_166	86.02	42.64	14667.17	67.99	1.25	150.39	2.69	36.80	108.42	16.38	559.96	216.09	2233.73	862.24	3379.11	905.52	9174.92	1087.89	107476.60	34.36	5776.57	5374.68
CRMO11-13_S_160	41.90	0.30	3594.04	21.96		94.80	0.30	4.23	20.17	2.91	108.36	43.75	531.13	213.77	856.19	238.00	2750.14	308.23	104261.18	13.74	1109.48	1407.67
CRMO11-13_S_144	38.75	0.31	2589.92	16.70		81.54	0.03	2.83	12.96	2.73	86.78	32.27	373.49	153.32	610.29	182.12	2096.93	228.69	91824.62	12.55	816.35	1132.81
CRMO11-13_S_157	100.25	0.35	7822.33	28.36	36.58	183.66	9.20	45.74	66.07	13.36	291.74	114.29	1300.36	489.50	1851.61	491.04	5390.88	551.81	93909.64	18.95	2243.77	1987.79
CRMO11-13_L_3B	333.28	2.91	891.00	2.21	10.69	37.18	2.40	16.21	7.40	0.86	22.32	8.01	92.49	31.24	135.39	34.21	342.41	42.53	12558.03	1.24	128.75	86.38
CRMO11-13_S_152	66.14	0.32	9856.37	17.87	0.20	139.56	1.12	15.94	73.13	13.21	409.55	154.55	1539.38	594.88	2214.44	577.84	5961.05	655.93	95350.05	13.96	2437.22	1861.99
CRMO11-13_S_161	30.59	0.28	2232.06	9.57	0.05	44.50	0.04	3.55	9.23	4.59	72.10	28.66	345.54	131.38	526.98	157.35	1786.07	197.70	97327.38	5.50	251.48	435.76
CRMO11-13_S_150	72.88	0.33	6965.33	15.48		89.06	1.43	20.63	62.99	14.66	298.44	107.72	1128.69	417.18	1565.89	408.83	4230.82	494.68	88773.84	7.95	1287.75	905.15
CRMO11-13_S_172	108.45	0.33	7295.75	29.35	24.87	172.11	8.68	34.62	53.03	9.12	273.45	107.78	1146.56	434.99	1685.90	463.16	5073.43	547.90	91553.34	21.74	2193.35	2041.18
CRMO11-13_S_176	53.47	0.38	5059.98	19.11	1.45	103.46	0.65	9.48	29.45	7.63	174.57	70.01	723.09	287.77	1121.78	315.52	3778.76	399.41	88140.37	13.18	1408.09	1901.63
CRMO11-13_S_151	34.69	0.38	2804.69	16.47	0.32	72.22		5.44	10.53	2.87	79.69	36.93	384.95	160.58	670.10	188.04	2144.14	247.91	104241.22	12.88	626.28	882.09
Neoarchean																						
CRMO11-13_S_159	43.08	0.30	4277.47	22.20	0.02	84.06	0.16	5.51	22.48	3.61	122.91	55.17	617.23	249.87	1004.49	275.69	2997.06	350.61	101987.75	16.49	1135.11	1428.10
CRMO11-13_L_6	155.67	0.35	10315.68	24.69	40.04	184.54	11.12	57.31	84.71	15.86	416.98	151.53	1554.03	625.71	2248.52	625.46	6904.66	706.89	81733.43	14.37	3794.04	2270.05
CRMO11-13_S_142	112.30	2.68	879.59	3.52		26.76	0.07	1.02	2.90	0.35	17.20	6.33	86.57	31.82	141.18	34.99	342.39	46.17	13397.05	1.72	195.90	149.89
CRMO11-13_S_165	33.86	0.34	2853.32	17.24	0.15	88.39	0.32	3.60	14.94	2.99	77.89	33.76	399.12	158.40	678.89	194.61	2265.06	261.43	111462.72	13.13	830.42	1032.36
CRMO11-13_S_147	83.59	0.38	7968.57	32.44	0.57	100.05	0.97	9.95	50.15	8.84	258.75	110.92	1248.25	471.08	1758.37	519.47	5754.43	578.40	94253.41	23.10	2638.77	4296.13
CRMO11-13_L_3A	191.37	2.23	560.67	1.19	1.25	13.03	0.38	3.33	2.46	0.58	14.62	4.39	54.66	19.75	86.41	22.27	224.94	31.40	11724.96	0.67	54.53	43.64
CRMO11-13_S_154	56.56	0.31	5184.84	26.04		110.94	0.09	6.40	30.46	4.52	181.22	69.28	786.07	306.36	1167.39	322.99	3521.84	382.91	98443.21	16.21	1755.67	1642.81
CRMO11-13_S_146	61.77	0.33	5349.71	25.89	2.11	75.32	0.91	8.99	24.49	6.21	194.28	78.55	846.33	316.24	1226.95	343.59	3808.92	391.89	96130.45	24.20	1805.98	2851.65
CRMO11-13_S_168	43.50	0.29	2815.18	14.43		80.75	0.29	0.11	21.69	3.71	65.45	38.11	394.25	163.66	672.00	205.06	2496.67	254.09	106973.48	10.77	856.32	1202.07
CRMO11-13_S_162	486.58	0.79	12625.43	89.06	238.73	339.40	62.72	224.70	101.56	11.21	353.70	148.80	1788.82	750.44	3151.41	882.84	9618.65	1087.56	118263.93	84.77	6040.60	13525.11
CRMO11-13_S_173	44.39	0.26	2772.73	12.64	0.24	60.23	0.42	3.04	11.27	3.09	87.82	33.69	396.64	162.55	648.19	188.18	2150.07	226.53	93047.96	10.60	493.21	766.80
CRMO11-13_L_2	220.78	2.35	693.58	1.53	1.53	14.46	0.41	2.51	2.53	0.59	12.72	5.78	65.60	24.92	110.99	27.73	296.12	39.19	12649.51	1.14	91.85	127.76
CRMO11-13_S_174	58.14	0.28	4472.70	20.72	0.51	80.58	0.24	4.73	26.39	4.87	153.43	58.47	659.59	270.24	1039.50	291.18	3412.78	374.49	91203.97	15.75	1308.24	2220.36

Table D2.7 CRMO11-13 Trace Element Concentrations con't

Spot	Concentrations (ppm)																					
	P	Ti	Y	Nb	La	Ce	Pr	Nd	Sm	Eu	Gd	Tb	Dy	Ho	Er	Tm	Yb	Lu	Hf	Ta	Th	U
CRMO11-13_S_148	72.84	0.30	6227.64	30.29		133.07	0.25	6.72	37.56	6.43	218.63	85.85	957.23	362.91	1418.65	397.64	4372.42	460.41	94967.98	23.50	2748.06	2917.13
CRMO11-13_L_1	68.27	1.92	383.15	0.80	0.00	5.42	0.05	0.71	0.97	0.32	7.95	2.68	34.16	13.28	59.26	16.62	171.44	23.47	11510.94	0.57	15.69	15.95
CRMO11-13_S_143	27.40	0.24	1547.24	4.56		24.10	0.25	3.84	7.58	2.73	52.96	19.62	236.39	92.88	345.76	108.57	1249.78	137.76	92477.94	5.12	88.18	713.94
CRMO11-13_S_153	51.87	0.40	3770.66	27.96	0.91	37.46	0.63	3.76	11.63	3.45	106.07	42.59	489.25	213.88	870.03	239.81	2709.94	317.53	105010.59	32.60	1221.20	3549.04
CRMO11-13_S_169	80.44	0.28	7006.77	18.87	0.84	123.77	0.09	9.46	58.56	8.20	267.67	108.14	1143.43	426.80	1594.79	438.76	4798.97	486.74	99640.22	12.94	1905.67	1733.38
CRMO11-13_S_149	34.97	0.41	2530.89	5.79		25.03	0.37	4.17	13.79	4.85	81.64	34.22	351.44	141.31	545.10	158.08	1822.71	204.39	95041.61	5.80	94.32	185.53
CRMO11-13_S_171	37.22	0.27	2247.61	7.70		23.94	0.40	5.51	15.50	4.12	59.57	32.13	344.54	134.16	517.38	158.26	1910.14	203.65	89681.51	5.78	103.74	211.55

Table D2.8 CRMO11-14 Trace Element Concentrations

Spot	Concentrations (ppm)																					
	P	Ti	Y	Nb	La	Ce	Pr	Nd	Sm	Eu	Gd	Tb	Dy	Ho	Er	Tm	Yb	Lu	Hf	Ta	Th	U
Paleoarchean																						
CRMO11-14S_98	343	15.22	962	1.78	0.356	14.98	0.0772	1.332	4.10	1.08	21.5	7.51	98.9	35.1	149	39.5	469	50.8	10904	0.73	177	297
CRMO11-14S_83	220	12.09	634	0.70		3.27	0.0272	0.851	2.51	0.44	14.1	5.02	64.0	23.0	95	23.6	249	27.3	8718	0.63	38	42
CRMO11-14S_86	296	32.04	1085	0.81		13.51	0.1467	3.565	8.58	2.84	36.8	11.02	120.4	39.2	157	39.1	439	47.8	10339	0.21	579	1062
CRMO11-14M_44	294	54.74	954	33.01	0.136	10.18	0.0461	0.554	1.59	0.09	11.6	5.33	78.2	33.1	150	40.1	487	64.2	11389	51.47	294	964
CRMO11-14S_89	362	35.43	987	5.38	0.025	5.77	0.0441	0.784	2.34	0.37	15.7	6.21	89.9	35.1	163	46.7	595	62.2	11439	14.82	106	817
CRMO11-14S_92	428	52.41	1695	1.32	0.048	26.80	0.3884	7.016	15.26	5.01	70.1	20.00	201.3	62.5	239	57.6	644	64.3	9209	0.43	1223	1856
CRMO11-14M_41	185	28.35	493	2.54	0.035	3.25	0.0214	0.296	0.74	0.19	6.0	3.04	42.7	18.3	85	28.1	387	40.4	13930	4.56	41	582
CRMO11-14M_40	271	18.86	792	1.31		5.28	0.0130	0.563	3.07	0.94	16.7	6.56	80.6	29.3	124	34.5	443	43.9	11933	0.49	95	456
CRMO11-14L_17B	283	15.11	909	1.38		10.46	0.0220	0.677	2.09	0.44	16.9	6.02	80.6	32.1	147	36.5	398	57.7	13814	0.85	215	256
CRMO11-14M_46	158	12.56	546	1.33		7.44	0.0321	0.757	1.94	0.53	12.1	4.17	53.4	19.3	87	22.9	257	27.7	9020	0.88	73	133
CRMO11-14M_45B	195	33.52	664	2.09		5.29		0.414	2.17	0.18	10.5	4.98	66.9	24.3	97	23.6	273	32.0	11956	3.56	112	997
CRMO11-14M_42	750	66.04	2077	8.33	3.815	23.15	1.0850	5.382	7.74	1.82	38.4	14.52	195.5	72.4	340	97.3	1207	125.4	15939	7.95	563	2327
CRMO11-14L_31B	213	39.55	880	5.15	0.014	17.74	0.0789	1.494	4.42	1.42	26.1	8.21	97.1	33.5	135	30.7	322	39.0	13732	1.74	670	889
CRMO11-14M_45A	201	13.24	676	1.93		8.17	0.0145	0.261	2.60	0.51	13.0	5.28	65.5	25.3	101	28.9	346	36.9	9287	1.24	67	165
Mesoarchean 2																						
CRMO11-14M_34	761	31.62	2732	12.88	0.061	18.30	0.0907	1.828	6.25	0.77	43.2	19.03	271.9	103.4	458	122.2	1455	149.9	9028	7.10	500	1411

Table D2.8 CRMO11-14 Trace Element Concentrations con't

Concentrations (ppm)

Spot	P	Ti	Y	Nb	La	Ce	Pr	Nd	Sm	Eu	Gd	Tb	Dy	Ho	Er	Tm	Yb	Lu	Hf	Ta	Th	U
CRMO11-14XL_25	463	23.29	1311	3.13	0.155	6.55	0.0164	0.740	3.08	1.04	18.2	8.00	114.8	47.0	220	61.3	721	82.3	9523	2.33	154	511
CRMO11-14L_13	933	24.62	3159	4.23	0.377	11.37	0.1044	2.059	6.82	0.89	48.8	20.69	295.0	116.1	523	126.0	1368	178.3	11765	2.33	432	769
CRMO11-14XL_33	757	11.70	1971	3.32	0.085	8.59	0.0834	1.383	4.02	0.74	33.6	13.37	187.2	71.9	328	86.2	984	110.7	9195	1.84	248	580
CRMO11-14M_65	539	19.80	1920	8.03		18.59	0.0767	1.616	5.39	0.71	36.8	14.48	195.9	72.5	312	80.6	912	93.1	9196	4.03	434	892
CRMO11-14L_17A	231	11.54	1016	1.79	0.020	8.82	0.0244	1.135	2.74	0.35	19.6	7.03	95.6	37.1	169	41.8	442	65.0	14538	1.09	84	118
CRMO11-14M_56	1026	16.06	2902	3.60	0.707	12.01	0.2599	2.396	6.50	0.91	46.0	19.26	277.7	110.2	489	117.9	1344	161.2	10063	2.03	388	828
CRMO11-14L_24	562	20.38	2081	2.97	0.053	16.39	0.0889	2.263	5.63	0.58	36.5	14.71	196.5	72.7	334	81.2	836	114.4	12768	1.53	324	460
CRMO11-14XL_31	523	21.20	2226	8.96	0.080	18.22	0.1150	1.476	5.46	0.62	38.9	16.63	223.2	83.6	362	92.2	991	109.0	9452	4.03	457	803
CRMO11-14XL_36	741	20.57	2695	9.46	0.002	19.11	0.1342	2.099	6.57	0.95	46.8	19.98	276.2	105.0	466	117.1	1254	139.1	10005	3.78	551	904
CRMO11-14L_1	459	23.37	2349	9.33		21.25	0.0530	1.634	6.64	0.72	42.7	17.55	231.9	86.7	380	95.6	1006	117.7	11227	4.64	576	863
CRMO11-14XL_27	143	14.35	379	1.53		3.58		0.222	0.65	0.09	5.7	2.27	32.5	13.3	66	18.0	220	26.5	10414	1.03	42	159
CRMO11-14M_39	425	22.95	1298	4.75	0.032	11.48	0.0427	1.089	2.95	1.16	23.3	9.39	130.4	49.7	217	57.8	691	66.8	9607	2.79	241	606
CRMO11-14L_22	826	20.85	3176	3.80	0.337	10.41	0.1452	2.298	6.57	0.85	50.8	20.79	282.7	113.1	513	125.0	1275	182.0	13699	2.37	382	658
CRMO11-14L_6	1040	33.05	4091	5.04	0.155	14.95	0.1396	3.315	8.97	1.31	68.5	29.31	396.4	150.7	664	166.0	1700	226.4	11549	2.78	676	1001
CRMO11-14M_38	630	25.93	2077	7.47	0.031	16.53	0.0818	1.728	5.41	0.69	38.2	15.69	217.8	79.1	338	90.8	1078	99.6	8961	3.58	396	861
CRMO11-14S_97	401	17.05	1501	5.49	0.005	15.08	0.0873	1.386	5.26	0.55	25.8	11.31	157.0	56.5	245	63.2	711	76.4	9645	2.70	298	592
CRMO11-14XL_20	547	20.54	2283	9.17	0.003	18.62	0.0948	1.489	5.84	0.77	40.1	16.85	223.3	83.7	365	92.8	1022	107.2	9087	4.07	491	846
CRMO11-14M_67	456	20.42	1930	4.54	0.032	11.25	0.0413	1.131	5.62	0.74	34.9	14.19	198.8	72.8	310	81.7	950	112.7	10280	2.64	288	589
CRMO11-14XL_24	371	13.90	1378	4.38		10.47	0.0469	1.307	3.58	0.56	24.7	10.50	137.7	53.0	231	59.7	673	74.7	9744	2.96	288	615
CRMO11-14S_91	527	19.95	2025	8.30	0.032	18.82	0.0533	1.945	4.65	0.73	37.5	16.05	209.7	77.1	332	84.3	945	100.3	9019	4.19	438	851
CRMO11-14L_23	708	19.59	2550	3.49	0.061	8.26	0.0824	1.237	5.04	0.64	37.1	16.35	222.5	91.7	418	102.9	1075	148.4	13444	2.03	295	573
CRMO11-14M_51	579	23.98	2822	11.31	0.038	23.01	0.0722	2.145	6.70	0.85	51.0	21.19	272.7	101.9	446	110.7	1162	132.0	10617	5.20	603	1016
CRMO11-14L_29	745	32.07	3729	13.56	0.080	30.22	0.1050	2.954	8.72	1.16	69.8	27.96	378.2	142.2	600	145.1	1478	187.7	12024	6.44	1222	1327
CRMO11-14XL_21	257	12.28	906	2.87		7.40		0.489	2.25	0.35	14.8	6.48	88.5	33.9	153	40.1	467	52.0	9675	2.10	140	366
CRMO11-14XL_37	350	16.58	1496	5.03	0.147	12.55	0.0901	0.916	4.00	0.65	27.0	10.68	145.2	55.8	244	62.7	697	80.7	10319	2.73	287	522
CRMO11-14XL_19	694	29.25	2420	8.57		17.56	0.0729	1.869	4.99	0.95	43.0	17.19	227.6	89.4	390	101.3	1114	121.8	9732	4.07	565	978
CRMO11-14L_14	574	21.13	1896	3.13	0.022	8.17	0.0365	0.871	3.91	0.49	27.8	12.13	178.7	67.8	310	78.7	824	111.6	12183	1.83	241	467
CRMO11-14L_7	335	20.94	1480	4.77	0.005	11.22	0.0587	0.860	3.20	0.56	24.0	9.99	138.8	55.2	247	62.3	642	83.4	12719	2.83	283	494
CRMO11-14L_16	458	19.03	2123	6.67	0.019	14.45	0.0599	1.506	4.58	0.59	36.8	15.12	207.7	79.2	347	84.1	893	115.9	12844	3.70	404	632
CRMO11-14XL_23	535	21.23	2033	6.95	0.187	14.62	0.0443	1.424	4.92	0.45	34.3	14.64	202.4	77.2	329	84.5	934	101.9	10021	4.15	443	862
CRMO11-14M_64	589	25.09	1652	4.89	0.004	10.53	0.0511	0.892	4.09	0.70	28.8	12.03	166.5	63.7	277	74.7	859	91.1	9110	2.07	240	578
CRMO11-14S_90	575	20.63	2110	8.75	0.068	21.23	0.1015	1.752	4.83	0.85	37.6	16.61	212.1	81.1	338	84.6	971	99.7	8285	3.96	494	881
CRMO11-14L_12	670	21.35	2720	5.36	0.415	13.76	0.1821	2.055	5.93	0.80	41.1	18.96	253.0	99.7	436	107.1	1114	151.4	12833	2.72	529	745

Table D2.8 CRMO11-14 Trace Element Concentrations con't
Concentrations (ppm)

Spot	P	Ti	Y	Nb	La	Ce	Pr	Nd	Sm	Eu	Gd	Tb	Dy	Ho	Er	Tm	Yb	Lu	Hf	Ta	Th	U
CRMO11-14M_35	227	11.48	672	3.05		5.21	0.0133	0.128	1.33	0.23	9.8	4.47	62.3	25.4	112	30.3	370	39.4	11455	2.02	86	248
CRMO11-14L_4	740	49.17	5713	8.57	0.021	24.00	0.3764	8.180	19.84	1.98	118.6	43.57	563.9	208.0	895	212.5	2128	269.4	11728	4.71	1217	1515
CRMO11-14M_61	600	19.34	1547	3.40	0.164	8.29	0.0849	1.069	3.12	0.51	25.8	10.95	147.7	57.5	258	69.0	789	85.1	9640	2.02	206	526
CRMO11-14L_8	564	29.94	2918	9.39	0.051	19.72	0.1358	2.399	7.20	0.75	47.2	19.98	279.1	108.0	475	115.1	1177	158.1	12931	4.98	814	1027
CRMO11-14L_11	126	11.92	491	1.34		4.06	0.0069	0.155	0.66	0.13	6.3	2.78	40.7	17.7	84	22.0	234	34.9	14023	1.17	62	148
CRMO11-14M_55	595	28.95	2335	9.72	0.034	19.27	0.0758	2.162	6.27	0.80	40.1	17.76	244.5	90.3	378	97.6	1085	120.1	9213	4.29	697	1168
CRMO11-14M_47	310	27.65	996	2.89	0.046	9.47	0.0416	1.147	3.67	0.33	19.8	8.04	101.2	37.6	167	41.8	489	56.1	10167	2.51	220	546
CRMO11-14S_100	333	19.57	1077	3.67		9.60	0.0236	0.911	2.29	0.43	19.2	8.30	105.2	42.0	183	48.0	549	59.9	10657	2.30	224	511
CRMO11-14L_10	1244	30.16	5661	10.29	0.048	22.51	0.1524	3.350	11.54	1.41	89.5	37.75	518.4	198.4	855	213.3	2118	301.3	12137	5.35	1183	1430
CRMO11-14M_66	375	19.12	825	2.56	2.219	9.44	0.5568	3.191	1.95	0.18	12.2	5.46	75.5	30.8	143	39.4	455	51.5	10212	2.11	90	333
CRMO11-14S_95	981	36.03	2856	7.73	0.036	19.12	0.0739	2.210	6.79	1.05	50.4	21.33	287.2	107.8	459	118.2	1355	141.7	9490	3.48	718	1231
CRMO11-14M_62	392	17.23	939	3.04		5.94	0.0128	0.457	1.95	0.27	14.6	6.29	88.1	35.4	162	43.7	516	55.9	10046	1.91	102	323
CRMO11-14L_30	847	43.51	4911	21.25	0.071	47.55	0.2318	4.610	11.61	1.53	89.5	37.42	492.1	182.4	777	181.7	1803	224.9	11990	8.77	2088	1924
CRMO11-14L_31A	176	21.78	520	1.95	0.003	21.39	0.0468	1.017	3.37	0.15	14.1	4.61	54.9	17.9	74	18.1	186	21.0	14012	1.06	210	210
CRMO11-14XL_29	245	13.77	721	2.58		7.26	0.0156	0.334	1.69	0.25	11.2	4.91	69.1	28.0	123	32.4	378	41.9	10064	1.65	120	298
CRMO11-14S_96	1008	35.53	3683	6.34	0.058	19.78	0.2147	5.330	12.81	1.86	78.0	30.01	384.5	139.8	590	151.6	1693	175.8	8847	2.87	800	1303
CRMO11-14XL_32	1003	29.81	2702	4.16	1.303	12.99	0.3288	2.346	6.55	0.97	46.3	19.45	271.5	101.9	453	118.5	1336	143.4	8922	2.32	363	785
CRMO11-14M_54	576	23.65	2731	11.70	0.045	22.37	0.1010	2.183	6.61	0.84	46.3	19.88	268.4	101.3	444	113.7	1213	129.7	9908	4.56	617	983
CRMO11-14S_82B	292	23.99	741	2.30	0.043	10.06	0.0253	1.534	3.66	0.11	15.1	7.08	87.9	31.2	120	30.1	303	33.2	10635	1.92	121	476
CRMO11-14L_5	1043	24.96	3400	3.25	1.867	12.60	0.4458	3.196	7.40	0.90	53.5	23.36	319.7	126.4	552	136.8	1453	191.6	11760	2.15	455	766
CRMO11-14M_58	513	63.49	1719	8.44	0.037	9.76	0.0368	0.643	2.58	0.18	20.5	10.04	152.8	63.0	289	87.7	1092	126.0	14557	10.59	310	2270
CRMO11-14XL_22	794	24.34	3136	6.37		16.77	0.1332	2.960	8.30	1.05	62.2	24.61	320.6	119.0	501	125.1	1378	144.8	9564	3.88	523	934
CRMO11-14XL_35	142	16.77	374	1.91	0.083	3.79	0.0110	0.123	0.44	0.17	4.9	1.94	31.6	12.9	65	18.8	233	29.1	13610	2.05	41	212
CRMO11-14S_94	546	19.70	1559	2.83		8.73	0.0190	1.009	3.60	0.49	25.9	11.78	154.6	58.9	257	66.7	781	84.5	9956	1.72	208	508
CRMO11-14XL_30	179	9.86	423	1.12		19.24	0.0403	0.732	2.28	0.12	15.1	4.56	51.6	16.8	62	14.2	139	13.8	9311	0.43	68	58
CRMO11-14L_3	349	13.93	1189	4.13	0.015	37.28	0.1361	2.438	6.79	0.27	34.8	12.38	143.2	46.7	177	36.9	328	36.2	12403	1.16	176	118
CRMO11-14L_21	337	13.95	1408	4.53	0.019	36.12	0.1123	2.399	6.13	0.34	38.2	14.28	162.8	54.6	204	41.2	350	43.2	13836	1.28	163	131
CRMO11-14L_25	26423	27.31	3892	7.90	468.294	1118.86	179.7527	925.006	233.00	9.69	257.1	48.84	451.1	142.9	577	132.0	1318	183.2	12105	3.87	846	1052
CRMO11-14L_32	227	33.95	810	3.73	0.025	37.65	0.1088	1.970	4.73	0.19	23.7	7.89	87.0	29.4	115	27.0	266	31.9	14275	1.95	607	809
CRMO11-14S_88	386	14.11	1173	3.88		7.31	0.0216	0.532	2.69	0.37	17.8	8.18	109.5	42.5	190	51.0	595	66.3	9357	2.87	149	392
CRMO11-14L_33	356	38.79	1656	6.13	0.062	51.36	0.4444	7.987	15.80	0.56	59.1	17.27	184.4	57.8	222	48.0	475	53.6	15826	3.33	1060	921
CRMO11-14L_18A	239	9.52	776	1.65		24.62	0.0677	1.624	5.56	0.29	23.3	7.71	87.6	28.2	112	22.8	204	26.3	12661	0.60	122	70
CRMO11-14L_27	243	11.30	975	1.85	0.023	29.23	0.1219	2.262	5.29	0.22	30.5	10.45	117.1	39.1	145	29.1	253	29.4	11452	0.49	150	55

Table D2.8 CRMO11-14 Trace Element Concentrations con't
Concentrations (ppm)

Spot	P	Ti	Y	Nb	La	Ce	Pr	Nd	Sm	Eu	Gd	Tb	Dy	Ho	Er	Tm	Yb	Lu	Hf	Ta	Th	U
CRMO11-14M_52	808	28.31	3159	13.01	0.008	27.06	0.0900	2.306	9.81	0.97	59.0	25.47	326.8	119.4	503	125.0	1383	156.3	10128	5.69	921	1276
CRMO11-14M_59	449	15.34	1319	5.16	0.034	10.71	0.0451	0.645	3.22	0.46	22.6	9.62	137.3	51.8	225	61.4	727	80.9	9469	2.83	188	471
CRMO11-14M_48	219	12.93	499	1.32	0.001	27.76	0.1356	2.152	4.36	0.24	18.6	5.47	59.7	19.9	74	16.7	181	19.3	10322	0.47	153	73
CRMO11-14L_18B	229	12.04	858	1.64		27.52	0.1066	2.198	5.23	0.31	25.2	8.80	97.0	32.7	127	25.7	228	29.1	14926	0.53	137	76
CRMO11-14M_37	1066	22.45	2274	2.97	15.387	26.36	2.7747	13.251	7.46	0.45	38.2	17.25	232.1	86.0	376	102.1	1192	116.2	10129	2.15	244	969
CRMO11-14L_26	248	8.51	1140	1.55	0.002	29.29	0.0991	2.645	5.91	0.42	36.6	12.28	139.9	44.5	172	33.5	290	33.6	11554	0.36	174	54
CRMO11-14M_49	932	27.28	2753	3.92	0.144	14.80	0.0596	2.150	7.66	0.82	50.0	19.42	270.4	103.2	446	111.5	1268	150.3	9486	2.53	442	825
CRMO11-14S_82A	377	11.60	1134	2.51		15.50	0.0585	2.779	6.03	0.27	32.8	12.10	136.4	45.0	167	37.7	357	33.6	9423	0.59	151	108
CRMO11-14M_57	652	38.52	1758	6.80	23.344	36.84	3.0038	12.955	4.15	0.29	21.5	10.32	149.6	64.7	337	102.6	1263	157.0	10762	8.81	307	1723
CRMO11-14M_53	203	11.88	475	1.79	0.024	22.50	0.0815	1.595	3.52	0.13	16.1	4.95	60.9	20.1	71	17.1	170	17.6	10690	0.66	90	74
CRMO11-14XL_28	767	24.60	2606	4.51	0.143	14.80	0.1051	1.611	7.10	1.15	42.9	18.13	246.3	95.3	427	112.3	1273	144.7	9560	3.01	502	987
CRMO11-14M_63	469	15.79	1482	3.63		8.83	0.0250	0.777	3.82	0.52	26.7	11.21	151.7	58.2	246	64.9	764	83.7	9936	2.76	209	482
CRMO11-14L_19	135	23.33	414	0.89	0.083	4.55	0.0131	0.086	1.05	0.07	5.7	2.35	31.9	14.3	71	20.5	228	35.5	17652	1.96	113	757
CRMO11-14M_36	803	27.53	2038	4.01	0.342	10.06	0.1159	1.034	4.03	0.42	29.1	13.85	197.7	75.9	336	93.6	1179	113.2	9434	3.16	163	891
CRMO11-14L_15A	904	26.40	2991	2.92	1.759	12.60	0.5989	2.779	6.29	0.69	44.3	19.16	284.2	111.6	506	122.7	1319	175.4	12949	2.02	362	686
CRMO11-14L_2	473	17.81	1654	3.04	0.054	9.96	0.0107	1.031	3.53	0.61	28.0	11.58	157.4	60.6	271	67.3	730	88.0	11550	2.35	259	492
CRMO11-14S_81	229	9.61	515	1.30		25.61	0.1164	1.970	4.69	0.17	15.9	5.80	61.5	20.1	78	18.6	202	21.6	10406	0.52	108	65
CRMO11-14L_15B	852	20.44	2664	2.51	1.227	11.33	0.4078	2.688	4.74	0.70	40.8	17.41	253.4	100.8	447	110.2	1159	158.9	12053	1.95	343	638
CRMO11-14S_93	228	18.71	534	0.92	0.019	15.77	0.0724	1.381	3.53	1.05	17.8	5.30	60.8	19.9	80	20.6	225	26.2	10687	0.27	376	616
CRMO11-14S_99	237	11.97	609	2.01		30.10	0.0834	2.138	4.77	0.28	22.1	7.08	75.9	24.1	91	19.9	197	20.4	10557	0.68	153	102
CRMO11-14S_87	551	17.44	1389	3.44	0.010	7.66	0.0176	0.429	2.75	0.36	20.8	8.87	128.6	49.1	227	61.7	716	76.4	10978	3.66	178	533
CRMO11-14L_20	199	6.37	687	1.22	0.001	27.34	0.1214	2.007	4.14	0.22	21.2	7.03	76.5	25.2	106	25.0	240	34.1	13064	0.57	131	63
CRMO11-14S_84	818	21.09	2223	3.36		11.10	0.0025	1.041	5.75	0.79	41.1	16.08	214.4	82.1	364	94.5	1073	115.6	9867	2.31	320	700
Neoproterozoic																						
CRMO11-14S_85	275	11.00	664	2.25	0.017	16.64	0.0158	0.940	3.19	0.19	14.8	6.04	73.2	25.4	103	25.0	276	29.4	10745	1.36	92	238
CRMO11-14M_43B	221	8.07	517	1.86	0.042	22.05	0.0974	1.473	4.01	0.22	15.7	5.40	56.6	18.4	79	19.0	211	22.8	11587	1.03	121	104
CRMO11-14M_43A	227	9.53	569	2.17	0.079	26.09	0.1253	1.753	5.10	0.41	18.5	6.08	68.9	21.7	90	21.6	248	22.4	10056	0.92	155	128
CRMO11-14XL_34	161	12.32	342	0.97	0.095	25.86	0.0996	1.706	4.14	0.21	15.6	4.47	46.2	13.5	50	11.4	121	13.5	9461	0.35	121	35
CRMO11-14L_28	177	11.77	589	1.59		30.78	0.0713	2.040	4.08	0.19	21.1	6.36	69.2	22.7	86	17.8	169	21.3	12032	0.55	221	78
CRMO11-14M_60	196	13.86	417	1.40		30.65	0.0932	2.203	4.78	0.17	19.0	5.28	54.9	16.5	60	13.5	143	14.3	9489	0.48	134	55
CRMO11-14M_50	175	13.94	380	1.30		25.88	0.0600	1.338	3.72	0.20	16.4	4.89	53.5	16.2	57	12.2	128	14.5	9894	0.38	116	48

Table D2.9 CRMO11-15 Trace Element Concentrations

Concentrations (ppm)

Spot	P	Ti	Y	Nb	La	Ce	Pr	Nd	Sm	Eu	Gd	Tb	Dy	Ho	Er	Tm	Yb	Lu	Hf	Ta	Th	U
Paleoarchean																						
CRMO11-15S_116	214	15.01	847	2.18	0.086	11.92	0.1845	5.308	5.94	1.68	17.2	6.53	78.6	29.8	137	39.4	532	58.4	10593	1.07	371	445
CRMO11-15S_117	193	8.36	547	1.98	0.016	3.11		0.216	0.70	0.15	6.3	3.05	49.0	20.0	98	30.0	407	47.0	11743	1.95	58	428
CRMO11-15S_108	2649	395.80	1739	40.06	21.552	41.74	5.4161	27.346	11.28	0.38	26.3	9.07	127.5	56.5	323	114.2	1661	221.4	21495	54.13	203	2543
CRMO11-15XL_41	289	14.62	765	9.41	0.129	6.18	0.0421	1.715	3.05	1.20	15.7	5.47	70.0	26.5	127	37.1	460	52.3	9297	9.62	129	566
CRMO11-15S_107	262	17.56	722	5.31	0.114	1.75	0.0455	0.240	0.64	0.10	6.2	3.34	56.4	24.8	133	42.5	606	74.6	14316	4.81	62	1498
Mesoarchean 1																						
CRMO11-15XL_42	516	28.07	1931	7.56	0.687	17.08	0.2117	2.621	7.61	1.67	46.8	17.07	213.7	73.7	304	75.4	822	79.8	10357	3.79	581	1875
CRMO11-15XL_50	460	32.34	2140	6.79	0.094	17.35	0.0997	1.673	8.16	1.93	54.4	21.03	249.7	82.4	308	73.0	761	68.6	11250	3.15	624	1877
CRMO11-15XL_51	262	9.90	633	0.58		8.70	0.2036	3.743	4.82	2.46	27.8	7.66	82.4	23.3	89	21.0	223	22.9	7234	0.26	102	118
CRMO11-15XL_46	525	41.34	878	1.62	3.354	10.46	0.7045	5.616	6.02	1.63	24.3	8.41	96.1	33.0	136	33.9	395	41.0	8704	0.84	165	536
CRMO11-15S_110	227	10.37	629	1.01		7.04	0.0678	1.437	3.30	1.44	16.1	5.18	67.5	23.5	96	25.7	287	30.8	7134	0.39	114	228
CRMO11-15XL_48	344	45.75	972	1.96		7.65	0.1226	1.953	4.38	1.81	24.0	8.53	102.4	35.5	153	39.2	452	48.2	7251	1.17	231	515
CRMO11-15XL_55	476	33.93	2634	8.15		18.40	0.0511	2.252	8.28	2.43	55.7	21.35	281.1	101.9	429	107.9	1203	116.4	8139	2.35	605	1666
CRMO11-15S_103	318	7.42	1159	3.37		6.38	0.0202	0.884	4.05	1.26	25.4	9.26	122.3	41.4	174	44.1	479	51.6	9567	1.35	149	505
CRMO11-15S_109	873	8.77	862	1.90	7.884	20.38	1.5853	9.687	7.13	1.49	23.4	8.01	93.5	33.5	134	32.8	363	39.0	7387	0.60	197	424
CRMO11-15XL_54	2153	7.91	593	0.89	14.503	39.93	5.1159	26.672	11.81	2.36	29.2	7.78	75.6	23.1	83	20.6	233	22.5	7025	0.53	116	189
CRMO11-15S_101	246	8.05	682	0.71	0.006	5.68	0.1087	2.128	4.35	1.78	23.5	7.20	76.8	26.1	103	25.8	290	32.5	7524	0.36	106	187
CRMO11-15XL_39	269	11.26	1167	2.38	0.175	7.03		1.051	4.42	1.23	24.6	9.30	121.2	44.9	198	50.2	558	60.5	7659	0.97	196	536
CRMO11-15XL_45	516	12.85	1381	1.71	3.986	19.49	1.1862	12.971	18.15	6.27	66.9	18.07	177.5	54.0	198	48.1	510	52.3	7473	0.67	375	526
CRMO11-15S_115	220	8.67	950	1.30		5.85	0.0521	1.371	2.65	1.19	17.4	7.13	93.4	36.4	160	44.0	534	55.7	7062	0.68	112	402
CRMO11-15S_118	269	13.09	1266	1.41	0.038	8.25	0.2275	3.903	8.74	2.63	38.0	12.30	145.8	49.5	200	50.6	583	60.9	7543	0.57	243	518
CRMO11-15S_104	305	18.17	1281	7.31		6.14	0.0031	0.634	2.64	0.71	23.6	9.95	130.3	49.4	202	51.8	560	60.2	10818	4.94	306	1491
CRMO11-15S_102	299	9.49	1386	2.23	0.032	11.16	0.1666	2.769	5.78	2.59	40.8	13.62	154.0	52.8	204	48.0	504	52.7	7805	0.86	278	443
CRMO11-15XL_40	232	95.76	680	2.53	0.073	9.41	0.0016	1.183	3.40	1.19	18.9	6.54	78.3	24.6	100	25.5	275	28.0	8642	1.12	310	594
CRMO11-15S_120	807	12.57	1758	3.24	2.380	17.29	0.7547	4.554	7.88	1.84	39.3	14.73	183.9	66.0	275	68.3	770	84.0	9102	1.15	369	845
CRMO11-15S_125	201	6.96	544	0.69	0.037	6.21	0.0858	2.149	4.19	1.56	17.9	5.23	63.1	20.1	85	20.4	233	25.4	8576	0.28	102	165
CRMO11-15S_122	478	7.58	1209	1.62		2.92	0.0606	0.376	1.91	0.06	16.8	7.78	112.2	42.7	188	50.2	574	59.0	12550	1.66	115	695
CRMO11-15XL_44	425	12.71	1052	2.46	0.093	4.50	0.1236	0.841	3.07	0.36	19.6	7.93	105.4	37.3	155	42.4	476	49.4	10916	3.13	201	820
CRMO11-15XL_39A	285	9.05	885	2.25	0.410	2.89		0.595	1.42	0.39	8.1	4.72	75.9	31.3	160	45.2	561	59.6	12719	3.73	65	786
CRMO11-15S_114	188	9.72	696	1.88	0.022	9.63	0.0832	1.429	3.01	1.15	16.9	5.79	71.2	25.1	107	27.8	322	33.1	9078	0.75	138	353
CRMO11-15S_124	1022	13.52	1508	2.84	24.194	40.91	4.3460	19.326	6.21	0.43	25.6	10.45	140.0	51.6	239	66.0	771	79.2	11911	4.15	177	1148
CRMO11-15S_113	250	8.95	760	1.04		7.97	0.0505	1.645	5.11	1.66	22.3	7.57	86.0	29.4	116	30.3	342	36.7	7912	0.50	197	395

Table D2.9 CRMO11-15 Trace Element Concentrations con't

Concentrations (ppm)																						
Spot	P	Ti	Y	Nb	La	Ce	Pr	Nd	Sm	Eu	Gd	Tb	Dy	Ho	Er	Tm	Yb	Lu	Hf	Ta	Th	U
CRMO11-15XL_49	358	174.95	856	2.48		3.38	0.0165	1.131	2.86	0.53	18.1	7.21	86.7	30.7	132	34.6	391	39.7	9991	1.78	128	497
CRMO11-15S_121	371	12.79	872	3.95	0.032	4.09	0.0141	0.416	1.62	0.29	9.2	4.61	73.0	31.0	156	50.0	768	82.9	13212	14.96	114	1083
CRMO11-15S_119	435	12.26	972	2.58	0.024	3.36		0.611	2.14	0.23	13.9	6.75	90.7	35.1	162	43.8	534	54.4	11413	4.21	179	1336
CRMO11-15S_105	406	14.94	961	3.97	0.103	1.89	0.0407	0.535	1.08	0.05	9.4	5.40	81.6	31.7	152	45.0	579	63.8	13555	13.94	71	1519
CRMO11-15S_123	976	25.97	968	20.71	6.881	13.20	1.5919	7.147	4.95	0.27	12.5	4.42	69.7	32.7	199	74.8	1159	162.2	12422	38.30	92	2137
CRMO11-15XL_52	389	9.35	811	1.50	0.243	1.78	0.0305	0.381	1.09		9.6	4.64	64.3	27.7	133	43.3	548	59.7	11293	4.99	74	877
CRMO11-15XL_43	746	58.92	3984	7.57	0.103	31.04	0.2667	5.592	19.64	4.12	117.1	41.94	488.6	155.2	571	127.6	1282	113.3	10389	3.11	1637	4080
CRMO11-15XL_53	740	63.16	3350	18.00	0.133	28.86	0.1501	2.501	12.20	2.02	77.8	29.72	371.3	129.2	512	123.6	1332	121.2	10913	7.32	2017	6000
Paleogene																						
CRMO11-15S_111	137	3.02	195	1.39		4.45	0.0187	0.770	2.55	0.27	12.9	4.14	32.1	7.1	17	3.2	25	2.5	12014	2.12	68	849
CRMO11-15S_112	254	3.41	796	4.01		7.27	0.0236	0.528	3.02	0.23	22.2	9.73	105.6	30.6	98	18.6	157	13.2	12448	7.22	88	3273
CRMO11-15S_106	303	7.14	716	1.98		6.28	0.0682	1.560	5.28	0.13	31.6	9.60	100.4	27.1	85	18.6	188	18.6	10176	0.47	155	119

Table D2.10 CRMO11-16 Trace Element Concentrations

Concentrations (ppm)																						
Spot	P	Ti	Y	Nb	La	Ce	Pr	Nd	Sm	Eu	Gd	Tb	Dy	Ho	Er	Tm	Yb	Lu	Hf	Ta	Th	U
Paleoarchean																						
CRMO11S-16_71	4629	36.67	4481	23.52	23.571	67.85	8.6623	45.734	14.08	0.97	49.3	22.43	320.5	135.6	679	174.9	1685	251.6	20122	22.05	629	2028
CRMO11S-16_73	674	22.79	1700	5.11	3.167	38.41	0.9606	7.635	5.60	0.94	27.1	9.74	129.2	50.1	246	63.4	618	99.1	16721	6.48	400	873
Mesoarchean 1																						
CRMO11S-16_69	499	23.96	2773	4.31	0.113	149.96	0.8414	15.003	19.64	6.57	76.1	21.29	237.1	81.0	369	93.3	892	141.0	10875	1.91	1698	865
CRMO11S-16_70	282	19.61	1619	4.13		62.05	0.1664	2.171	5.76	1.87	36.2	11.09	131.5	46.9	227	56.1	555	87.3	13669	2.20	1101	906
CRMO11S-16_72	580	5.17	1688	1.75		9.50	0.0202	0.847	4.31	0.27	26.8	10.01	141.4	52.5	250	58.5	556	83.4	17287	0.91	121	123
CRMO11S-16_77	339	17.55	1706	2.58	0.021	22.43	0.0546	1.381	5.45	1.60	33.7	11.86	144.2	54.8	252	61.5	573	86.0	14633	1.43	619	1002
CRMO11S-16_67	373	13.35	1776	4.27	0.235	66.84	0.2693	3.759	7.78	2.53	39.7	11.95	149.9	55.3	253	61.8	608	91.2	12643	2.28	732	756

Table D2.10 CRMO11-16 Trace Element Concentrations con't

Concentrations (ppm)																						
Spot	P	Ti	Y	Nb	La	Ce	Pr	Nd	Sm	Eu	Gd	Tb	Dy	Ho	Er	Tm	Yb	Lu	Hf	Ta	Th	U
CRMO11S-16_76	652	16.18	2066	3.63	0.831	39.94	0.3308	4.664	7.14	2.74	43.2	12.82	166.7	61.9	281	69.1	668	105.7	14442	2.33	490	865
CRMO11S-16_78	325	30.00	2465	4.66	0.255	114.52	0.4928	7.439	15.96	5.75	79.6	21.14	229.8	75.6	324	79.5	747	111.9	11555	2.03	2425	1385
CRMO11S-16_74a	270	25.07	1498	4.58		18.76	0.1036	0.559	2.62	0.80	25.6	7.80	115.9	44.3	219	56.6	563	93.7	21004	2.46	711	1887
CRMO11-16M_164	563	29.58	1883	9.36	2.677	24.20	0.8046	6.682	4.29	0.87	25.7	9.92	146.9	57.0	284	77.8	848	111.2	11837	5.00	791	1627
CRMO11S-16_74b	269	24.52	1396	2.98	0.092	16.81	0.0284	0.819	1.90	0.67	22.7	7.55	104.1	40.1	215	53.4	536	87.9	19308	2.27	571	1650
CRMO11S-16_68	485	11.79	1148	2.97	1.805	48.40	0.6337	6.357	5.38	1.08	25.1	7.54	91.9	34.8	162	42.0	414	64.3	13833	2.93	523	666
CRMO11S-16_75	269	21.70	1504	4.71	0.028	33.32	0.1006	1.295	4.11	1.07	25.8	8.86	116.1	44.2	220	56.6	579	90.0	17158	10.06	636	1463
CRMO11S-16_79	396	6.52	1099	1.38		14.23	0.0916	1.779	4.11	0.63	26.2	7.82	103.4	35.1	156	37.0	344	49.9	12346	0.58	92	53
CRMO11-16M_166	230	10.77	552	1.29		3.30	0.0231	0.256	0.70	0.25	5.8	2.56	40.6	15.7	86	27.0	325	43.0	12217	2.54	53	641
CRMO11-16M_165	79	12.98	317	1.01		6.70		0.278	0.52	0.23	3.9	1.37	22.1	9.0	49	15.3	204	37.3	18353	0.61	124	931

Table D2.11 CRMO11-17 Trace Element Concentrations

Concentrations (ppm)																						
Spot	P	Ti	Y	Nb	La	Ce	Pr	Nd	Sm	Eu	Gd	Tb	Dy	Ho	Er	Tm	Yb	Lu	Hf	Ta	Th	U
Paleoarchean																						
CRMO11-17M_75	201	14.84	822	8.31	0.058	3.59	0.0383	0.740	2.29	0.50	15.3	5.90	77.9	29.9	128	33.0	363	38.1	11013	11.22	56	405
CRMO11-17M_73	192	10.59	1317	3.81	0.005	7.98	0.0318	1.450	4.60	0.95	27.3	10.28	131.7	50.1	211	51.6	559	56.0	7448	1.77	150	216
CRMO11-17S_149	944	312.51	2175	27.69	1.134	18.31	0.4188	3.896	3.95	0.44	20.6	8.79	147.0	65.3	376	123.0	1667	195.4	9884	19.79	508	1511
CRMO11-17S_142	284	39.17	2501	8.32	16.784	28.72	3.0667	18.266	15.25	1.43	71.7	24.45	295.6	98.4	385	90.3	987	98.0	6590	4.35	274	423
CRMO11-17S_130	421	16.21	1220	8.72	1.604	18.55	0.6035	2.824	4.81	0.39	21.9	8.80	117.0	44.8	194	52.7	637	65.2	10578	5.34	307	728
CRMO11-17M_72	72	11.45	356	2.59		1.99		0.268	0.44	0.14	3.7	1.66	25.9	12.0	63	21.4	299	37.6	7735	3.89	69	633
CRMO11-17M_76	839	15.14	653	2.96	6.308	20.59	2.0236	11.506	4.74	0.79	17.5	5.30	63.7	23.3	103	26.4	317	37.6	10831	3.95	218	683
CRMO11-17S_134	265	27.95	687	26.68	0.030	5.32	0.0406	0.377	1.28	0.25	7.8	3.21	52.1	22.4	123	45.0	736	98.5	17009	111.35	189	1071
Mesoarchean 1																						
CRMO11-17S_138	255	17.33	1307	3.37		32.99	0.1634	2.582	6.22	2.06	35.4	11.02	131.2	46.6	196	52.7	623	58.7	9531	2.10	531	1124
CRMO11-17S_148	265	11.50	796	2.32	0.038	8.18	0.0580	0.479	1.87	0.59	13.5	5.50	73.4	27.5	124	34.0	399	41.8	10485	2.76	153	778

Table D2.11 CRMO11-17 Trace Element Concentrations

Concentrations (ppm)																						
Spot	P	Ti	Y	Nb	La	Ce	Pr	Nd	Sm	Eu	Gd	Tb	Dy	Ho	Er	Tm	Yb	Lu	Hf	Ta	Th	U
CRMO11-17S_128	10308	13.66	826	1.95	128.430	285.92	40.1162	204.070	51.80	2.66	61.5	11.19	99.0	30.5	120	30.2	332	36.4	10524	1.41	289	848
CRMO11-17S_147	1781	12.54	819	2.81	21.969	56.52	6.6071	32.679	10.68	0.95	23.5	7.39	83.1	29.5	121	33.2	375	39.6	9715	1.74	283	848
CRMO11-17S_145	372	22.73	529	1.10	3.765	21.52	1.1409	6.713	6.66	0.70	19.7	5.45	61.3	18.8	74	18.7	211	21.9	10844	0.80	277	355
CRMO11-17S_132	229	17.45	940	2.95	0.052	17.39	0.0750	1.614	3.37	0.97	21.1	7.27	92.3	35.0	148	42.0	506	46.4	8922	1.96	294	1060
CRMO11-17S_126	95	7.05	306	0.43		1.01	0.0110	0.156	1.13	0.20	5.6	2.17	28.1	10.7	47	13.2	159	18.1	9706	0.33	23	220
CRMO11-17S_144	107	8.19	368	1.03		5.62	0.0269	0.099	0.74	0.24	6.4	2.14	32.5	12.8	59	16.6	212	23.3	10024	1.04	116	432
CRMO11-17S_131	13563	14.61	875	1.98	171.738	378.99	51.7096	275.551	70.56	2.90	74.6	13.37	111.0	30.3	127	31.1	349	37.1	9713	1.25	164	517
CRMO11-17S_143	95	7.17	294	0.81	0.061	4.66		0.092	0.72	0.25	4.5	1.87	26.6	9.7	49	13.8	166	19.1	10049	1.25	71	365
CRMO11-17S_146	170	10.73	508	1.34	0.225	9.13	0.0641	0.586	1.55	0.31	10.5	3.76	46.0	17.0	79	21.1	248	26.7	9941	1.39	183	769
CRMO11-17S_135	637	371.27	1628	12.22	1.760	49.94	0.5025	5.457	6.34	1.71	26.5	9.76	126.8	53.0	259	72.2	893	91.7	7435	4.95	677	2732
CRMO11-17M_74	236	20.10	702	1.78	0.658	14.86	0.3217	2.173	2.57	0.55	14.4	5.36	67.1	24.7	107	28.9	326	35.2	11201	1.68	310	883
CRMO11-17S_139	742	13.18	672	2.28	5.350	34.06	2.1718	10.705	6.23	1.10	19.4	5.87	70.5	24.5	107	28.8	335	34.7	10085	1.50	569	906
CRMO11-17S_137	491	22.84	1648	3.84	0.123	14.40	0.0725	2.172	6.43	0.66	37.6	14.23	176.7	62.9	264	70.0	844	82.0	10956	2.20	527	1239
CRMO11-17S_140	330	16.08	809	5.96		11.42	0.0462	0.846	2.71	0.55	10.2	3.83	56.6	26.7	151	51.1	723	84.4	8155	2.79	286	1016
CRMO11-17S_133	288	5.68	545	0.67	0.061	2.85	0.0315	0.300	1.69	0.12	8.9	3.94	53.5	20.3	86	23.8	267	27.3	10137	0.73	48	265
CRMO11-17S_129	341	15.19	981	2.83	0.448	19.53	0.1978	1.755	4.07	0.91	20.4	7.85	96.8	33.9	146	39.2	445	45.4	9163	1.44	360	944
CRMO11-17S_127	159	8.83	477	1.51	0.016	2.38		0.022	0.98	0.23	8.0	3.79	46.1	16.6	70	18.3	205	21.0	10366	1.11	53	568
Neoarchean																						
CRMO11-17S_136	345	6.09	844	2.38	0.006	12.61	0.0203	0.809	2.96	0.26	20.2	6.89	86.6	31.0	125	33.1	371	35.5	9057	1.61	81	48
CRMO11-17S_150	261	4.64	524	1.40		7.90	0.0523	0.432	1.82	0.14	10.8	4.09	51.1	18.3	80	19.4	223	23.3	8252	0.88	39	43

Table D2.12 CRMO11-18 Trace Element Concentrations

Concentrations (ppm)																						
Spot	P	Ti	Y	Nb	La	Ce	Pr	Nd	Sm	Eu	Gd	Tb	Dy	Ho	Er	Tm	Yb	Lu	Hf	Ta	Th	U
Paleoarchean																						
CRMO11-18S_156	382	3.86	828	2.70		7.35	0.0195	0.470	1.47	0.27	12.2	5.42	78.3	31.8	139	39.1	468	48.0	9443	1.53	56	137

Table D2.12 CRMO11-18 Trace Element Concentrations con't

Concentrations (ppm)

Spot	P	Ti	Y	Nb	La	Ce	Pr	Nd	Sm	Eu	Gd	Tb	Dy	Ho	Er	Tm	Yb	Lu	Hf	Ta	Th	U
CRMO11-18S_155	962	7.84	2089	4.87	0.142	14.10	0.0682	1.547	4.89	1.10	34.9	14.65	201.3	79.7	350	94.6	1143	117.6	8372	2.39	201	434
Mesoarchean 1																						
CRMO11-18S_153	356	15.44	1013	1.50	0.029	13.17	0.1030	2.610	6.48	2.14	31.2	10.07	113.8	37.9	149	35.8	412	39.7	7921	0.67	304	640
CRMO11-18S_152	658	38.41	1635	12.83	0.053	6.15	0.0444	0.639	1.96	0.37	18.6	8.71	133.9	53.7	275	92.7	1372	149.1	17965	30.33	221	2217
CRMO11-18M_77	340	14.01	964	1.21		14.23	0.1768	2.808	5.83	2.53	28.3	9.12	105.0	36.0	150	37.6	407	44.5	7448	0.45	176	182
CRMO11-18XS_61	226	8.32	406	0.70	0.023	10.12	0.2285	2.931	5.99	2.26	20.4	5.84	56.1	15.2	50	11.3	107	9.9	6796	0.19	70	86
CRMO11-18XS_56	359	11.56	1398	3.26	0.030	18.57	0.1460	2.900	7.15	2.49	38.7	13.17	162.5	54.3	219	53.2	576	55.9	8206	0.86	319	454
CRMO11-18XS_72	440	40.40	2627	12.81	0.053	27.96	0.0983	2.446	13.97	4.00	80.5	28.06	311.2	96.7	354	80.3	803	81.9	12003	4.30	1249	2378
CRMO11-18XS_69	1413	10.77	1072	2.16	12.307	39.12	4.7423	31.023	25.43	6.24	71.2	18.30	157.7	39.9	125	25.8	242	21.5	9089	0.64	327	329
CRMO11-18XS_73	1467	16.28	1349	3.12	13.803	43.41	4.2396	23.254	20.78	4.69	66.9	18.76	184.4	49.7	163	33.8	306	30.3	9488	1.03	359	459
CRMO11-18S_151	520	10.28	623	0.85	2.180	18.96	0.7356	5.897	8.10	2.94	29.1	7.80	78.9	22.1	82	18.7	197	18.8	6742	0.47	165	195
CRMO11-18XS_70	277	12.09	984	1.70	0.040	21.28	0.6732	12.493	19.85	6.33	65.5	16.89	151.1	36.1	114	23.5	215	18.6	9042	0.66	330	292
CRMO11-18M_79	487	40.05	2789	10.44	0.133	20.37	0.0689	1.371	6.53	1.75	53.7	23.58	302.2	106.0	413	98.6	1018	93.9	13566	3.77	644	1981
CRMO11-18XS_71	385	25.27	1889	7.83	0.091	10.91	0.0767	0.974	5.78	2.01	42.4	18.02	209.4	67.9	272	69.2	756	78.9	14441	8.72	448	1380
CRMO11-18XS_62	516	8.12	1342	1.94	0.103	12.20	0.0328	1.616	4.42	0.17	26.7	9.93	137.4	50.4	220	56.8	664	69.8	9921	1.08	102	129
CRMO11-18XS_60	468	35.28	1257	5.19		6.75	0.0130	0.699	2.56	0.41	20.9	8.74	119.4	46.2	199	55.4	629	63.3	13714	6.55	428	1969
CRMO11-18XS_64	1166	27.54	1128	5.98	902.168	1080.53	137.6873	477.384	84.07	2.51	68.6	9.70	96.9	36.4	202	72.8	1108	131.3	18594	26.56	688	1480
CRMO11-18XS_68	374	32.33	1444	8.08		6.35		0.219	1.87	0.42	14.6	7.78	129.4	49.9	233	67.9	830	87.2	14651	9.94	190	2482
CRMO11-18S_154	469	17.03	1042	3.81		5.64	0.0010	0.376	1.73	0.18	11.8	5.70	85.2	34.8	175	54.1	741	77.5	12421	8.40	71	1075
CRMO11-18S_157	611	55.65	1219	8.18	0.173	3.63	0.1023	1.093	2.82	0.08	14.3	7.98	109.4	38.8	190	62.9	919	91.1	17704	23.14	89	2081
CRMO11-18XS_59	334	14.17	1169	1.86	0.022	12.38	0.4110	5.606	10.83	3.73	41.4	12.19	138.8	45.0	178	43.8	483	50.0	9583	1.96	228	490
CRMO11-18XS_65	364	7.35	884	1.45		9.41	0.0303	1.205	3.18	0.16	19.6	7.38	92.5	32.5	136	36.5	422	44.9	12190	4.50	69	313
CRMO11-18S_158	465	6.31	941	1.69	0.016	11.60	0.0635	0.712	3.04	0.18	20.6	7.51	97.1	35.4	151	38.6	462	45.0	8284	0.63	88	114
CRMO11-18XS_58	502	9.50	1274	2.17	0.168	5.40	0.1489	2.075	5.40	0.96	27.1	9.96	125.2	45.9	190	49.2	570	55.8	10824	1.77	144	421
CRMO11-18M_78	643	33.21	2983	8.62	0.048	17.79	0.0723	2.312	6.80	1.71	57.7	24.48	323.6	114.2	455	106.9	1051	100.8	13299	3.24	525	2236
CRMO11-18XS_57	553	9.74	1321	3.21	0.205	8.40	0.0175	0.786	2.91	0.09	18.4	8.83	124.9	47.7	225	63.5	758	80.7	10522	3.84	80	492
CRMO11-18XS_67	534	16.85	1476	2.79	0.438	10.82	0.0869	2.621	6.36	0.97	28.2	11.68	151.3	53.6	241	63.7	727	74.1	11255	2.56	290	796
CRMO11-18XS_74	454	19.93	1206	3.20	0.091	2.76		0.498	1.62	0.14	12.4	6.45	101.0	40.1	194	55.0	651	69.4	14584	7.57	88	967

Table D2.13 CRMO11-19 Trace Element Concentrations

Spot	Concentrations (ppm)																					
	P	Ti	Y	Nb	La	Ce	Pr	Nd	Sm	Eu	Gd	Tb	Dy	Ho	Er	Tm	Yb	Lu	Hf	Ta	Th	U
Paleogene																						
CRMO11-19XS_79	140	6.66	578	3.41		14.39	0.0146	0.570	2.84	0.90	12.5	4.91	54.7	21.0	94	26.8	336	34.6	7736	1.58	113	256
CRMO11-19XS_83	4927	9.87	2060	7.01	110.187	276.07	28.3849	134.744	45.81	10.78	88.5	23.52	243.4	79.7	321	80.9	879	94.9	7253	1.99	625	505
CRMO11-19XS_82	1085	12.01	1346	4.90	14.314	44.99	2.9116	16.108	10.75	2.93	39.1	12.29	139.7	49.7	213	58.0	697	75.4	7733	1.99	278	381
CRMO11-19XS_78	467	2.86	1511	18.31	4.843	47.13	1.5263	8.333	7.19	1.28	29.2	10.92	136.0	52.7	247	70.3	880	95.0	9656	7.53	667	1421
CRMO11-19XS_75	256	3.36	1682	6.71	0.133	26.07	0.1958	4.779	9.57	1.52	44.5	14.71	176.1	63.0	271	73.0	854	86.2	9323	3.89	629	1233
CRMO11-19XS_81	489	12.07	3425	20.38	1.631	119.91	1.0078	14.737	24.73	8.45	95.9	31.97	365.3	127.5	535	136.3	1540	162.9	8644	5.96	1406	1102
CRMO11-19XS_80	2669	4.84	1070	15.02	38.509	95.30	6.3308	28.066	6.94	1.72	20.1	7.20	89.7	35.9	172	52.1	679	81.5	9962	5.46	718	1180
CRMO11-19XS_85	197	10.47	1544	20.31	0.216	105.79	0.1974	4.364	9.46	3.40	41.6	13.03	158.4	55.0	237	66.2	795	88.7	8283	5.46	1690	868
CRMO11-19XS_76	163	3.67	1595	21.28	0.035	28.09	0.1004	1.745	5.26	0.68	28.5	11.63	154.9	57.8	263	74.7	905	98.5	10192	9.52	953	2345
CRMO11-19XS_84	214	2.32	1015	15.82	0.182	29.13	0.0688	1.233	1.94	0.51	11.6	5.61	76.6	33.1	168	52.3	716	92.6	11150	7.52	768	2076

Square Mountain trace element concentrations
Table D2.1 SM10-A3 Trace Element Concentrations
 Concentrations (ppm)

Spot	P	Ti	Y	Zr	Nb	La	Ce	Pr	Nd	Sm	Eu	Gd	Tb	Dy	Ho	Er	Tm	Yb	Lu	Hf	Ta	Th	U
Mesoarchean 1																							
SM10A3S_35B	1360.27	24.61	3231.86	520937.34	10.27	9.06	20.45	2.18	9.58	9.50	0.53	41.99	17.75	297.78	112.60	523.23	147.67	1639.59	194.94	12187.50	15.77	447.69	1484.89
SM10A3S_36B	1228.92	15.88	3672.87	515253.40	11.22	6.27	13.95	1.21	9.63	8.82	0.68	46.61	19.52	347.76	123.83	571.94	147.68	1495.84	170.01	10747.16	7.37	414.72	1041.31
SM10A3S_35A	1478.87	7.44	4442.99	656715.79	14.20	0.64	3.88	0.09	1.63	6.41	0.49	52.51	22.78	409.99	146.56	710.24	191.85	2139.57	217.27	13217.45	6.93	68.32	276.89
Neoarchean																							
SM10A3S_37	242.76	7.09	905.62	630285.67	4.78	0.04	7.33	0.06	0.95	2.38	0.41	14.12	5.57	84.20	30.04	141.39	36.11	402.48	45.83	10387.76	3.43	156.52	293.89
SM10A3S_36A	449.66	23.72	1499.19	654099.85	11.86	4.43	9.83	0.50	5.37	3.30	0.56	23.12	9.24	136.24	49.70	232.88	67.50	834.58	96.07	12132.68	25.58	726.10	2023.33
SM10A3S_32A	306.77	14.22	627.07	635093.57	10.74	3.99	7.01	0.77	5.02	0.96	0.46	5.78	2.46	41.45	17.28	113.13	45.43	720.04	96.90	8905.01	42.40	224.97	1362.98
SM10A3S_38A	119.84	54.81	373.77	660943.92	4.29	1.42	1.92	0.38	1.97	0.21	0.16	3.75	2.41	38.34	12.26	59.36	17.89	204.85	21.11	14909.35	4.39	67.85	711.31
SM10A3S_31	9274.76	12.35	614.47	611113.71	3.44	276.00	438.25	61.60	296.19	67.87	0.54	61.86	9.45	78.00	18.60	71.10	20.02	196.31	22.92	11789.46	5.26	158.33	689.82
SM10A3S_22A	396.77	158.96	1315.03	614281.22	8.12	3.22	14.16	0.74	4.40	5.72	1.90	35.59	10.04	140.56	44.01	176.95	47.38	559.61	52.50	9883.61	11.14	758.22	1421.94
SM10A3S_26A	800.33	13.03	1238.28	648623.97	3.92	2.18	11.76	0.70	7.05	6.69	2.24	31.40	9.45	125.59	40.30	175.82	42.01	487.57	46.05	10132.71	3.70	645.53	1125.63
SM10A3S_33B	113.21	15.56	405.26	526258.00	2.85	1.10	2.44	0.06	0.44	1.48	0.12	4.66	1.88	30.08	14.10	62.84	18.67	210.63	26.18	11702.86	4.52	143.85	877.36
SM10A3S_43	82.53	4.14	261.60	506104.53	4.32	0.14	0.82				0.06	1.82	0.57	15.57	6.11	54.06	25.60	426.24	69.18	12178.81	33.44	36.86	602.67
SM10A3S_39	311.51	56.23	918.93	541540.98	6.11	25.97	32.30	4.28	24.68	6.50	0.57	14.55	5.49	78.42	25.52	121.76	33.87	402.02	44.49	9414.98	21.43	207.01	1438.97
SM10A3S_32B	285.82	26.80	765.96	515193.50	15.20	2.51	5.36	0.45	3.09	0.25	0.32	5.49	1.92	42.06	21.04	149.16	51.21	680.72	95.67	8395.08	23.03	159.28	1135.13
SM10A3S_34	229.95	1154.05	568.32	554911.04	8.96	6.54	11.05	1.32	5.65	1.95	0.28	8.31	2.84	40.90	17.11	86.95	22.66	256.14	30.16	9800.67	6.18	888.50	1540.54
SM10A3S_23A	180.78	281.35	588.51	603798.16	9.56	0.59	2.89	0.18	0.94	1.12	0.31	6.62	2.79	49.24	18.16	82.95	26.28	321.38	39.29	11779.82	10.56	308.36	1256.74
SM10A3S_23B	107.30	13.85	319.51	533572.96	4.78	0.07	0.92		0.79		0.31	1.96	0.75	17.67	9.14	53.58	20.67	326.23	43.97	11717.38	20.63	119.54	902.84
SM10A3S_25	535.91	78.45	1062.88	565988.67	8.43	14.71	48.88	3.53	16.24	5.98	1.08	19.93	7.53	106.23	34.91	140.70	34.11	345.89	34.73	10815.09	6.17	537.77	1467.85
SM10A3S_42A	177.56	90.00	480.17	577810.27	6.66	13.84	21.45	2.90	10.91	3.06	0.23	6.91	2.21	36.59	13.91	71.71	19.37	248.36	28.79	11361.83	8.95	575.81	1584.38
SM10A3S_41A	1597.36	25.04	1090.62	652449.42	7.98	24.48	38.76	3.72	21.65	5.31	0.91	27.80	6.83	109.45	35.28	153.24	43.25	487.53	53.38	10448.38	11.67	575.21	1236.72
SM10A3S_33A	225.54	117.18	762.03	632151.08	10.41	3.83	8.40	0.98	2.59	1.40	0.33	10.13	3.53	68.70	25.44	110.22	30.14	357.99	39.64	12663.95	8.47	486.89	1625.85
SM10A3S_42B	215.16	18.34	547.02	500279.02	3.84	3.20	6.57	0.52	0.83	1.09	0.23	9.69	2.73	46.92	18.21	85.92	23.65	250.46	32.14	11307.09	5.89	317.76	1394.92
SM10A3S_40	1045.23	779.04	2589.98	558782.37	14.47	14.39	12.24	5.91	40.67	28.63	3.20	74.40	18.89	226.60	65.76	278.15	69.65	755.81	89.76	8540.37	19.07	259.44	1895.07
SM10A3S_27A	424.49	294.06	1140.38	591998.02	10.22	4.32	12.98	1.31	7.42	7.08	1.61	26.39	8.45	103.52	36.68	166.55	46.64	524.67	55.73	9557.36	7.67	731.31	1847.56
SM10A3S_24	784.77	63.21	1383.41	576997.35	10.26	17.80	42.47	3.77	23.72	10.86	1.83	36.50	10.72	144.84	45.26	185.94	48.68	508.11	56.21	8968.34	8.84	1426.32	2062.33
SM10A3S_28A	491.14	53.75	1878.08	641813.87	8.10	7.54	24.19	1.42	10.98	7.47	2.36	45.57	13.21	171.52	55.59	252.57	65.84	735.34	78.00	9406.10	9.05	1505.91	2273.99
SM10A3S_29B	461.31	52.56	1601.77	488780.38	10.43	4.90	18.82	0.94	6.43	9.52	1.29	30.99	11.41	147.95	53.14	215.60	56.60	582.33	63.22	7966.58	8.97	1242.17	2101.28
SM10A3S_30	387.48	31.66	1172.79	602151.46	14.14	4.68	13.00	1.23	7.94	4.56	0.04	14.54	5.79	87.91	31.39	167.56	46.41	532.39	56.22	9808.53	40.65	2510.57	3175.24

Table D2.1 SM10-A3 Trace Element Concentrations con't

Concentrations (ppm)

Spot	P	Ti	Y	Zr	Nb	La	Ce	Pr	Nd	Sm	Eu	Gd	Tb	Dy	Ho	Er	Tm	Yb	Lu	Hf	Ta	Th	U
SM10A3S_41B	590.14	50.54	1835.89	512551.79	12.68	6.91	21.17	2.10	7.30	6.90	1.31	25.87	12.22	156.81	56.73	245.54	63.84	649.39	73.29	9389.14	25.24	1223.43	2649.68
SM10A3S_29A	406.24	54.72	1714.55	587177.75	9.15	5.51	16.89	1.00	7.52	7.57	1.66	42.39	12.45	168.56	54.92	235.22	60.10	705.51	65.63	9035.91	8.89	1354.12	2311.76

Table D3.2 SM10-C2 Trace Element Concentrations

Concentrations (ppm)

Spot	P	Ti	Y	Zr	Nb	La	Ce	Pr	Nd	Sm	Eu	Gd	Tb	Dy	Ho	Er	Tm	Yb	Lu	Hf	Ta	Th	U
Mesoarchean 2																							
SM10C2M_17	443.65	49.57	834.07	451540.41	8.43	1.97	4.02	0.55	2.51	1.95	0.03	10.29	4.70	69.01	21.36	108.37	36.82	498.04	58.06	19006.93	24.56	56.78	1342.21
SM10C2M_20A	10638.03	10.50	1169.02	588281.10	4.46	230.41	373.58	51.29	311.56	93.44	2.29	104.49	23.97	189.89	39.32	133.20	24.92	250.70	23.99	8714.06	4.88	316.41	511.25
SM10C2M_20B	4004.31	5.81	668.37	557854.59	1.33	45.08	86.49	12.11	65.19	27.63	2.81	43.59	9.89	92.69	24.75	90.68	21.46	225.76	22.75	8130.45	1.24	330.01	321.27
SM10C2S_70A	751.61	16.10	1507.28	622522.00	7.81	0.06	1.59	0.31	1.93	2.09	0.05	13.12	7.21	135.57	43.99	230.51	69.63	858.71	77.01	21091.92	17.49	106.75	2251.39
Neoarchean																							
SM10C2S_80	778.79	23.28	2363.74	582742.28	4.37	9.32	11.07	5.28	43.42	35.75	4.41	97.00	24.74	259.23	70.80	276.94	72.07	717.81	75.60	10314.96	3.01	262.22	1144.20
SM10C2S_73	500.55	10.11	1786.32	639372.90	7.08		10.31	0.01	1.69	4.44	0.76	30.61	12.55	174.75	57.07	253.86	66.15	697.56	76.19	12276.02	6.49	272.41	1518.05
SM10C2S_78	672.21	9.81	2126.92	640086.59	3.40		12.98		0.77	7.08	1.84	46.51	16.44	223.17	67.96	302.67	78.25	883.90	86.18	11318.95	2.93	256.62	1799.92
SM10C2S_69	799.19	11.06	1572.63	610143.61	7.02	0.68	3.88	0.16	3.39	5.00	0.45	23.86	10.78	147.09	49.13	210.27	65.34	807.99	85.85	13455.32	37.44	127.46	2367.00
SM10C2S_74	538.66	17.11	1653.87	533330.97	10.62	0.46	17.12	0.30	2.36	6.86	0.90	35.24	13.30	155.62	55.85	243.87	66.23	711.68	84.06	11249.08	9.85	489.70	2938.11
SM10C2S_79	657.28	18.31	1926.54	592019.18	12.34	0.82	17.40	0.34	3.47	7.29	1.60	44.90	17.62	211.25	62.03	253.24	62.76	631.44	61.96	11782.26	18.64	569.50	4132.97
SM10C2S_71	403.53	19.68	671.03	613171.37	16.62	2.08	3.22	0.45	2.45	1.25	0.03	6.91	3.31	52.90	18.02	91.03	32.29	455.81	58.46	18677.99	100.05	58.66	1155.54
SM10C2M_18	1119.03	28.25	2056.73	539021.71	24.56	2.70	7.23	1.19	9.23	4.34	0.10	22.83	9.76	165.50	62.83	321.88	111.54	1486.11	163.10	21186.99	45.32	203.08	3515.23
SM10C2S_72B	559.69	6.33	1091.92	504244.72	28.05	2.58	6.80	0.95	7.92	2.42		10.46	5.78	95.46	31.52	132.85	39.86	473.75	61.60	17246.22	128.12	50.77	1925.85
SM10C2S_76	531.46	24.84	1028.70	520044.50	16.73	2.62	8.44	1.16	8.47	2.98	0.17	12.35	6.15	81.74	32.26	166.79	55.83	749.60	101.59	17828.38	78.97	71.26	1292.64
SM10C2S_68	616.86	7.65	1081.29	569309.19	12.28	1.32	3.16	0.48	4.12	2.07	0.04	10.18	7.00	95.37	31.37	154.38	51.01	668.89	73.97	14004.89	41.51	95.95	2519.59
SM10C2M_21B	687.25	25.15	1323.22	471604.87	40.30	2.03	4.94	0.52	3.66	4.58		22.51	8.46	115.30	39.84	183.24	64.89	858.22	110.83	23454.84	235.57	106.33	2434.76
SM10C2M_21A	386.65	7.94	784.72	585473.89	13.12	0.49	2.27	0.14	1.50	0.61		8.69	3.92	71.76	21.80	114.86	36.48	504.41	52.59	19033.31	65.38	59.63	1594.99
SM10C2S_77	823.07	13.48	1437.98	614114.02	13.22	7.22	17.55	3.71	22.06	14.90	0.34	25.43	10.26	129.99	43.46	190.12	57.01	647.09	71.65	15602.69	31.76	282.31	4414.49
SM10C2S_75	429.76	5.79	905.18	518092.97	19.23	0.59	2.50	0.13	2.36	3.44	0.11	12.36	4.78	81.80	27.27	117.18	42.74	520.77	64.78	16669.59	76.26	65.53	1692.64

Table D3.3 SM10-C3 Trace Element Concentrations

Concentrations (ppm)

Spot	P	Ti	Y	Zr	Nb	La	Ce	Pr	Nd	Sm	Eu	Gd	Tb	Dy	Ho	Er	Tm	Yb	Lu	Hf	Ta	Th	U
Paleoarchean																							
SM10C3S_61	344.01	18.15	1491.17	539435.51	12.60	1.57	6.90	0.76	4.23	4.47	0.28	23.99	8.45	132.57	48.12	208.65	62.27	642.21	68.56	12433.60	9.22	407.34	1199.46
SM10C3M_2B	343.35	5.34	1139.16	515919.45	4.37	0.14	8.63		0.99	3.86	0.35	28.53	8.82	120.36	40.41	175.42	49.77	489.61	58.43	10646.60	2.23	220.57	232.69
SM10C3M_2A	271.49	9.88	773.97	688629.85	2.60	0.18	7.74		1.28	3.71	0.05	17.47	5.81	79.40	24.31	106.04	27.33	335.52	32.82	13711.32	1.94	262.30	232.27
SM10C3M_1B	660.33	3.04	620.03	521507.42	2.32	1.03	9.58	0.65	4.15	4.13	0.12	14.66	4.56	62.77	20.37	84.32	21.48	232.69	27.97	11397.63	1.11	287.68	261.05
Neoarchean																							
SM10C3M_1A	373.39	21.62	1696.96	654441.53	7.24	1.53	16.34	0.63	6.20	7.41	1.48	42.72	14.18	182.33	57.99	230.63	58.24	636.73	54.15	12852.43	6.47	771.90	1639.44
SM10C3S_62	366.90	28.98	1603.71	582973.93	10.75	2.88	16.80	0.70	3.07	3.55	1.01	26.50	11.04	147.47	51.16	228.83	62.00	621.07	66.91	11300.98	8.93	533.28	2477.92
SM10C3M_16	486.93	29.62	2831.28	633048.68	14.30	0.13	10.80	0.05	0.80	6.99	1.56	47.22	19.54	270.49	89.51	391.96	98.31	1006.91	108.50	10789.34	8.28	452.01	3720.50
SM10C3S_64	1928.93	37.57	2000.32	587270.05	43.13	13.16	37.93	5.53	39.45	21.15	0.96	39.46	12.50	163.00	59.15	332.93	113.23	1506.23	186.70	11267.60	92.83	2406.18	5080.09
SM10C3M_6	606.06	40.48	3365.91	595938.56	16.51	0.18	18.13	0.05	1.89	9.38	2.65	73.61	26.47	354.97	112.27	454.97	112.97	1121.02	111.16	9901.16	9.62	997.47	5507.43
SM10C3M_5	200.75	24.73	1125.56	603712.05	7.86	1.82	27.44	0.93	6.97	5.93	0.72	15.64	5.28	74.26	28.06	149.74	44.37	607.09	83.77	12022.58	5.37	435.75	1567.82
SM10C3S_67	745.79	24.10	1797.13	605733.87	34.99	10.49	24.16	3.16	15.45	6.81	0.44	20.02	9.19	127.83	52.47	270.40	86.51	1018.59	121.95	13865.14	45.54	315.61	2922.56
SM10C3S_45	734.34	31.60	1825.39	619214.33	31.19	0.46	3.66	0.23	1.16	1.81	0.15	11.77	6.91	125.58	52.77	313.06	112.58	1542.31	186.04	12543.95	113.37	115.64	2866.37
SM10C3S_57	2182.10	51.37	2496.52	630824.19	53.79	27.73	65.28	9.16	59.15	17.12	0.27	29.82	9.71	161.65	71.11	421.14	133.55	1705.86	206.98	12022.49	62.29	864.47	4054.30
SM10C3S_65	5924.87	12.01	770.75	511918.02	2.39	83.24	200.68	29.27	191.69	55.19	1.06	56.57	11.72	76.68	24.40	94.59	30.03	355.73	48.75	11580.11	2.15	630.69	1377.42
SM10C3M_7	352.70	36.68	1794.13	582065.27	14.69		9.85		0.51	3.15	0.56	20.17	8.85	135.48	52.46	280.40	82.58	1025.54	120.12	11659.22	21.19	599.92	4408.27
SM10C3M_15	514.51	37.07	2544.04	643670.29	12.75	1.23	13.49	0.43	4.65	7.25	2.17	43.48	17.92	241.63	80.31	361.89	93.26	965.29	107.14	11171.78	11.53	472.62	2739.45
SM10C3M_4	152.91	10.95	579.17	598872.93	4.72	0.11	12.63	0.05	0.61	0.57	0.26	7.11	2.44	41.21	15.87	85.91	27.13	356.23	46.22	11960.43	4.45	167.27	849.93
SM10C3S_63	419.74	29.14	1608.95	597972.85	16.31	0.28	6.84	0.14	0.81	2.40	0.30	15.95	8.49	136.03	51.31	245.68	67.22	786.72	84.40	13961.42	20.73	525.05	3194.97
SM10C3S_49	613.15	15.78	1103.98	582966.07	24.85	9.35	14.31	1.93	11.46	3.40	0.13	10.27	3.92	75.02	33.13	200.71	78.47	1184.76	146.62	12876.62	195.29	92.83	1426.48
SM10C3S_60A	407.44	73.75	1006.99	646917.02	23.58	0.69	5.05	0.23	0.80		0.29	8.67	4.25	75.03	29.74	157.98	55.97	819.06	91.29	16824.65	99.23	107.58	1555.63
SM10C3M_13A	781.30	45.88	1834.17	647876.72	67.49	6.89	20.12	2.74	18.64	8.22	0.25	15.33	5.36	91.41	43.52	265.95	103.48	1587.55	182.86	14059.75	116.17	211.97	2686.82
SM10C3M_14A	450.83	24.05	1368.30	697163.09	46.48	0.26	4.50	0.18		1.36	0.06	9.39	4.91	83.53	36.75	190.60	72.59	1096.62	139.43	16268.64	183.71	135.42	1815.92
SM10C3S_58	578.61	32.82	1699.00	607783.72	31.09	2.84	10.36	0.71	3.49	2.85	0.18	14.98	7.41	118.18	50.92	281.69	87.62	1129.85	140.63	12816.85	34.05	507.90	2754.54
SM10C3S_53	600.82	28.80	1398.10	557822.55	24.18	3.01	7.72	0.84	5.01	3.02	0.18	13.77	5.74	100.39	38.81	221.76	77.90	1114.51	140.19	11420.28	78.39	118.71	1932.67
SM10C3M_12A	732.81	36.01	1358.66	648772.27	61.88	11.40	22.59	3.26	25.23	6.55	0.01	8.80	4.57	89.36	36.74	219.78	86.28	1324.81	160.19	13217.20	129.41	97.91	2333.03
SM10C3S_52	1273.91	40.62	3904.29	587097.44	22.43	49.13	82.24	18.28	108.06	59.62	2.80	121.98	34.67	385.29	109.72	455.28	111.87	1228.65	132.82	14770.11	36.48	529.82	3500.76
SM10C3S_48	899.93	34.11	2048.97	511095.42	30.48	10.12	20.43	3.74	24.84	15.89	0.50	43.61	13.50	172.43	67.30	328.85	122.01	1572.37	193.83	12495.06	108.21	253.92	2415.80
SM10C3M_3	422.15	8.33	1313.20	669117.27	22.21	0.07	6.02		0.61	1.21	0.16	9.99	4.76	86.86	36.63	212.56	69.20	887.78	107.19	15103.93	31.57	138.29	2156.38
SM10C3S_66A	915.44	46.13	2651.62	594047.06	47.53	18.35	40.08	4.73	27.17	18.52	1.39	46.99	16.06	233.63	80.92	411.79	123.13	1469.64	153.57	12692.06	40.55	3267.39	6690.59
SM10C3M_11	538.36	20.65	1548.46	557714.94	47.42	0.28	7.33	0.09	3.05	3.19	0.09	13.65	6.10	105.06	45.49	243.87	85.99	1115.32	135.97	12329.42	120.89	1468.95	3448.21

Table D3.3 SM10-C3 Trace Element Concentrations con't

Concentrations (ppm)																							
Spot	P	Ti	Y	Zr	Nb	La	Ce	Pr	Nd	Sm	Eu	Gd	Tb	Dy	Ho	Er	Tm	Yb	Lu	Hf	Ta	Th	U
SM10C3S_47B	1182.77	53.23	3184.40	484794.50	45.36	45.09	219.36	42.63	325.25	175.86	9.36	242.64	60.00	553.92	135.11	468.74	124.06	1268.65	146.55	11442.02	60.52	5916.79	26173.62
SM10C3S_55	696.46	42.74	3525.77	623377.15	19.34	0.13	36.37	0.13	3.02	11.53	3.24	74.50	28.00	369.17	112.54	464.26	113.88	1105.78	115.01	10645.17	14.71	1409.88	5330.76
SM10C3S_56	893.73	52.43	2928.71	582221.69	34.14	4.94	32.02	5.61	39.78	20.06	0.71	47.28	17.21	257.36	92.21	456.65	131.87	1534.25	181.96	15783.53	70.72	1583.45	7186.12
SM10C3S_66B	812.08	30.11	2551.86	491428.52	26.69	8.31	18.74	1.48	7.41	7.16	0.43	28.66	12.79	209.19	81.06	405.05	121.96	1271.41	167.35	12739.40	41.09	447.95	3548.09
SM10C3M_8A	489.26	43.26	2366.75	573435.32	30.96	15.39	89.98	18.29	121.50	58.85	0.90	84.76	21.13	229.88	72.52	351.43	108.28	1381.61	158.34	12983.54	20.45	1436.96	10844.47
SM10C3S_44	855.25	24.91	951.98	574193.42	27.01	3.33	9.02	1.09	7.62	2.69	0.17	7.28	3.71	67.80	27.09	153.16	61.67	882.30	117.52	12526.33	104.60	1440.15	1802.02
SM10C3S_46	327.56	5.21	818.66	596762.63	21.88	0.04	2.80		0.03			4.39	2.69	45.97	20.95	132.68	54.07	931.99	134.94	12764.57	126.30	24.11	580.05
SM10C3S_59	663.36	45.29	3319.07	598450.84	18.33	0.75	25.31	0.37	3.53	9.94	2.54	72.08	26.53	344.02	108.42	444.69	109.50	1080.58	109.80	10359.42	13.40	1073.72	5884.79
SM10C3M_8B	1088.79	42.75	3948.80	505512.03	23.26	56.44	312.94	64.42	466.99	220.37	5.76	314.90	80.63	697.61	165.57	581.59	124.54	1272.26	152.80	12383.67	17.12	8625.82	38223.79
SM10C3M_10	40750.69	18.01	2101.37	575662.73	27.83	557.15	1169.10	184.24	1038.61	238.68	3.92	238.17	34.64	253.71	55.30	224.29	65.27	864.47	133.92	13374.18	137.58	112.43	935.35
SM10C3S_50	1275.83	26.36	1674.80	500500.14	29.16	24.24	46.55	5.19	37.38	12.11	0.11	22.83	8.26	130.35	49.90	290.47	103.89	1366.66	168.16	12429.18	148.54	151.78	2221.57
SM10C3S_51	1052.06	58.92	2616.33	563850.27	50.43	28.75	117.14	22.72	167.84	78.31	1.28	96.42	26.55	273.60	82.42	383.52	110.01	1237.71	139.96	12296.58	29.24	3732.43	10170.70
SM10C3S_54	589.62	223.76	7455.57	563323.28	57.19	36.80	244.46	45.49	380.18	324.59	26.95	605.02	178.15	1689.65	356.83	1129.43	233.06	2023.74	194.29	12380.30	60.61	6807.57	64534.63

Table D3.4 SM10-C4 Trace Element Concentrations

Concentrations (ppm)																							
Spot	P	Ti	Y	Zr	Nb	La	Ce	Pr	Nd	Sm	Eu	Gd	Tb	Dy	Ho	Er	Tm	Yb	Lu	Hf	Ta	Th	U
Neoproterozoic																							
SM10C4M_32	256.53	190.34	1052.74	712261.35	7.14	0.06	19.95	0.19	3.57	4.46	0.27	18.67	7.67	86.74	35.05	160.55	41.58	432.44	49.33	9751.75	2.57	341.87	264.18
SM10C4M_14B	260.08	13.85	2020.33	770103.63	4.71	0.06	36.52	0.19	2.92	13.42	3.61	66.45	18.29	214.54	69.77	287.12	76.49	726.03	82.74	8335.62	1.67	1181.71	1154.28
SM10C4M_40	418.57	7.27	1273.12	739987.93	5.53	0.07	5.79	0.26	2.61	6.40	0.89	20.88	7.41	117.07	43.83	187.96	55.52	593.43	66.59	11200.81	2.40	228.82	668.88
SM10C4M_25B	301.69	13.76	2472.79	777740.26	4.55		24.95		0.46	7.69	2.65	55.38	17.45	228.99	79.13	375.09	102.38	1005.00	121.61	9585.78	1.90	395.22	974.46
SM10C4M_69	376.61	25.08	6205.19	760430.86	7.82		71.43	0.18	3.83	19.54	8.12	147.42	47.79	582.59	206.08	905.19	211.60	2100.60	217.26	9732.23	2.19	1638.08	2168.23
SM10C4M_15B	257.18	20.38	2204.76	763834.09	7.89		71.50	0.27	5.41	17.93	7.51	87.70	22.58	241.04	70.14	287.91	74.53	704.18	78.35	10604.35	3.26	2555.92	2122.72
SM10C4M_3	512.31	32.95	3120.14	694349.34	15.69	0.28	26.40	0.15	0.78	5.22	1.79	45.52	18.80	257.56	98.10	477.78	128.13	1482.89	148.01	11142.86	13.77	991.02	2920.05

Table D3.4 SM10-C4 Trace Element Concentrations con't
Concentrations (ppm)

Spot	P	Ti	Y	Zr	Nb	La	Ce	Pr	Nd	Sm	Eu	Gd	Tb	Dy	Ho	Er	Tm	Yb	Lu	Hf	Ta	Th	U
SM10C4M_30A	456.44	9.81	2390.30	587009.06	15.47		40.41	0.10	4.04	8.87	1.58	51.79	17.57	261.14	82.22	393.98	101.95	1243.28	114.65	10047.07	8.05	1194.00	2641.03
SM10C4L_87	455.61	18.92	3251.92	768065.33	12.02	0.11	8.80		0.80	3.55	1.08	36.79	16.59	274.57	105.64	519.63	134.68	1399.62	188.00	16368.79	5.49	525.04	1835.31
SM10C4M_26A	394.64	37.46	5897.84	648491.64	16.05	1.88	276.38	2.23	41.08	63.64	18.52	243.41	65.42	729.46	221.09	873.85	200.95	2152.38	195.81	9780.08	7.61	4073.53	2303.79
SM10C4L_90	500.20	27.06	3180.96	866877.28	17.24	0.06	23.30	0.07	2.73	6.38	1.71	56.65	19.29	273.11	102.43	495.95	128.54	1513.79	191.15	16232.54	12.52	1154.17	2069.34
SM10C4M_49	672.08	57.49	2675.91	699087.96	16.93	179.24	231.20	32.04	114.24	23.52	1.17	45.83	15.99	203.72	84.25	416.01	115.79	1320.08	140.31	9296.54	14.94	4366.54	4436.00
SM10C4M_44	122.79	6.27	471.85	724789.78	4.89		5.94			1.23	0.10	5.17	2.44	34.54	13.95	70.12	22.13	260.68	32.94	10001.25	5.31	109.10	782.95
SM10C4L_86	591.41	26.70	2988.00	765705.16	12.16	0.12	7.18	0.07	0.97	3.54	0.41	27.59	13.93	241.53	94.59	475.58	130.53	1364.23	186.92	18125.88	10.00	454.77	2152.83
SM10C4M_65	550.17	17.46	2080.62	777801.02	11.40	0.07	13.29		1.07	1.99	1.06	31.96	10.92	188.56	69.21	338.94	96.77	981.82	116.22	12026.73	5.90	763.43	1997.61
SM10C4L_81A	388.20	14.79	1817.38	809857.76	21.66		10.31			2.57	0.17	17.85	8.15	144.53	54.61	279.94	76.54	886.62	112.22	22472.07	28.68	221.01	1976.31
SM10C4M_68	304.94	27.81	2612.93	697085.04	7.79	0.69	27.16	0.28	1.96	7.41	3.25	55.20	18.74	234.94	84.64	392.12	98.36	1032.49	113.95	10278.12	3.65	624.02	1462.31
SM10C4M_17	570.62	45.58	5173.14	755254.33	18.70	0.45	81.61	0.25	4.59	19.98	6.88	125.29	39.21	493.34	174.58	740.59	172.33	1715.97	178.69	10300.74	4.85	3175.58	3471.00
SM10C4L_84A	165.27	13.41	1092.68	836409.30	9.65	0.12	10.84	0.06	0.80	1.68	0.11	14.20	5.68	92.98	34.06	161.35	47.67	527.35	67.87	20643.31	10.96	207.79	1160.40
SM10C4M_57	274.05	11.07	1005.86	717162.96	5.63		12.31		0.80	1.93	0.14	15.10	6.37	84.12	30.77	147.52	38.99	428.45	44.99	12569.91	6.34	227.47	1734.82
SM10C4M_55	306.85	9.65	735.41	640831.17	7.54	0.55	12.75	0.31	1.93	2.86	0.30	14.67	5.34	69.25	24.73	133.17	35.14	431.74	42.40	12743.06	9.06	197.03	879.37
SM10C4L_103	287.80	44.70	4222.90	753303.53	19.77	0.07	74.24	0.22	5.46	17.48	5.56	110.90	34.81	446.70	141.22	607.07	140.77	1363.90	169.21	14746.15	8.87	3763.33	3299.83
SM10C4M_21B	1232.13	13.26	1432.86	858270.25	11.82	5.32	37.01	1.68	11.37	12.34	1.30	35.46	10.60	125.67	48.64	210.05	54.67	572.00	69.28	11389.99	6.31	957.56	2056.73
SM10C4M_51	328.76	21.58	1194.23	712095.07	9.54		21.48		1.33	2.78	0.35	30.91	8.57	108.61	36.23	168.40	50.66	527.48	64.26	10158.92	7.78	423.48	2351.43
SM10C4M_6	320.71	4.54	1230.13	705374.82	5.99		24.57	0.11	1.16	3.87	1.09	27.29	9.13	113.74	39.40	182.42	49.52	581.14	59.26	9471.26	3.78	505.08	1325.57
SM10C4M_38B	328.78	14.98	1305.25	729928.78	5.86	0.07	21.29	0.21	1.05	8.10	0.97	32.47	9.57	130.07	40.04	172.36	49.75	476.69	49.89	9861.47	4.76	458.66	1743.75
SM10C4M_14A	504.61	10.47	1451.16	593850.66	9.93		11.39	0.07		2.82	0.59	23.54	9.78	134.97	46.72	247.41	64.75	801.11	71.10	13249.41	8.00	222.83	1830.16
SM10C4L_90B	434.85	10.81	1877.01	650717.96	16.38		20.91		1.01	4.28	0.54	26.62	11.48	160.99	60.45	265.25	74.24	759.90	102.24	17047.86	23.26	559.61	1554.09
SM10C4L_85	77.48	5.11	296.97	665612.80	0.79		0.67				0.17	1.76	0.71	16.86	8.66	53.55	17.67	243.65	46.49	13721.14	1.05	6.58	276.48
SM10C4M_61	1036.44	30.62	1657.25	693362.22	40.19	4.94	11.07	1.31	7.85	2.74	0.11	23.50	8.49	130.72	49.69	254.60	74.10	950.60	109.32	20732.49	98.82	188.27	2106.58
SM10C4M_59	300.27	1.89	935.05	715885.26	10.65		7.80			0.44		7.70	4.36	63.18	29.01	155.16	44.26	512.64	54.73	13311.10	6.60	98.29	888.21
SM10C4M_12	533.95	17.10	2140.92	742443.59	8.57	0.12	26.39	0.09	1.69	7.77	0.77	44.60	14.56	182.47	69.79	329.00	85.60	1013.08	120.39	10494.57	6.92	531.62	2703.62
SM10C4M_83	359.81	16.10	1482.23	713186.51	6.88	0.14	27.59	0.16	2.43	5.45	1.26	39.35	11.68	141.60	48.93	213.50	53.70	566.18	57.01	9843.15	4.84	806.89	2212.62
SM10C4L_88A	286.50	32.10	3335.51	819113.34	27.83	1.07	25.63	0.36	2.90	7.62	3.61	66.39	19.99	312.71	109.21	483.34	120.48	1249.94	154.37	16241.34	15.00	1997.06	2426.30
SM10C4M_77	240.53	18.21	1280.53	727064.77	8.86		25.10	0.07	0.87	4.05	0.38	24.18	8.72	115.07	41.83	189.05	48.14	553.55	59.70	10645.50	7.60	769.42	1846.81
SM10C4M_24A	273.63	6.85	1071.18	649557.35	10.03	0.21	5.88			2.06	0.73	14.93	5.58	92.44	36.52	173.77	55.24	744.19	74.26	20866.31	23.93	123.52	806.63
SM10C4M_72	387.44	27.54	2057.11	784148.56	11.10	0.12	23.24	0.11	2.08	6.34	2.40	39.82	13.41	189.78	71.84	313.03	78.40	891.72	93.32	10678.80	6.81	906.09	2336.95
SM10C4L_94	520.86	11.04	2063.00	753273.81	15.62	0.17	5.06	0.01	0.29	1.50	0.13	14.77	8.11	131.30	57.29	320.87	98.33	1153.38	159.92	17739.48	23.38	196.73	2014.97
SM10C4M_15A	302.89	2.87	1056.53	655344.53	14.18		4.18		0.42			7.32	4.83	76.77	33.11	189.23	56.20	779.39	75.50	17668.14	15.64	89.64	1593.31
SM10C4L_100	487.98	24.58	3611.52	777343.89	22.82	0.40	19.98		1.37	4.98	0.59	43.02	18.41	295.69	108.61	521.75	142.81	1530.16	208.42	24961.36	41.24	1268.84	3153.19
SM10C4M_38A	285.87	18.19	921.72	543543.82	5.75		13.84	0.18	0.33	3.73	0.71	21.46	8.15	99.56	31.54	154.60	35.17	453.01	39.61	10865.06	4.19	259.19	1210.21

Table D3.4 SM10-C4 Trace Element Concentrations con't
Concentrations (ppm)

Spot	P	Ti	Y	Zr	Nb	La	Ce	Pr	Nd	Sm	Eu	Gd	Tb	Dy	Ho	Er	Tm	Yb	Lu	Hf	Ta	Th	U
SM10C4M_29	298.51	4.07	1122.68	760952.41	11.82		6.62			0.51	0.25	10.37	4.81	70.29	33.69	175.89	54.32	610.57	77.30	12444.43	16.57	137.44	2237.87
SM10C4M_84	518.15	18.50	1254.90	686078.61	27.78	2.30	10.75	0.55	3.38	2.15	0.15	13.60	5.69	93.92	38.11	213.46	63.01	793.56	92.71	14714.81	34.21	194.13	2365.64
SM10C4M_27	184.97	0.70	926.13	740625.44	9.30		10.46		0.41	1.70	0.34	11.75	5.26	68.71	28.46	147.01	42.22	494.05	59.64	12452.35	13.88	254.47	1595.02
SM10C4M_2B	1029.00	17.37	2197.06	732384.19	19.23	1.14	9.66	0.35	3.07	3.10		34.95	11.90	171.30	65.15	319.06	107.31	1175.28	130.17	11485.00	10.92	378.29	2705.53
SM10C4M_71	333.22	23.11	1490.94	641216.22	12.84	0.38	12.51		0.40	2.15	0.87	21.86	8.72	136.87	48.43	240.85	63.72	786.59	74.87	17681.04	17.06	1013.43	1948.87
SM10C4M_31	506.47	5.33	1350.42	695010.92	14.87	4.81	4.59	2.34	17.13	7.87	1.79	25.42	9.05	103.91	36.24	176.40	50.68	639.46	72.71	16631.45	19.48	66.63	1474.89
SM10C4M_47	560.15	28.06	2848.48	698648.28	9.61		31.52	0.49	6.01	12.71	1.28	65.05	19.75	261.76	85.10	385.51	109.13	1132.67	123.80	9032.02	7.62	1031.93	3810.38
SM10C4L_84B	220.06	7.29	950.25	670683.71	8.99	0.26	10.23		0.70	2.10		12.27	4.67	75.37	31.05	141.26	43.55	463.86	68.74	17630.98	11.75	183.68	1528.62
SM10C4L_102	1519.50	75.37	1556.99	732595.32	9.39	109.41	137.62	19.46	94.09	18.68	0.39	22.09	7.51	117.46	46.66	271.27	87.10	1061.57	165.24	25236.33	16.20	1093.42	1978.97
SM10C4M_53	242.15	3.37	711.71	718096.26	7.55		7.35		0.36	2.40	0.19	15.63	3.76	60.07	22.08	95.71	29.55	315.42	35.89	10466.35	8.76	177.48	1857.26
SM10C4M_52	505.06	18.64	782.91	738369.60	9.48	3.11	10.09	0.93	6.73	0.95		7.94	3.38	52.49	22.35	118.31	43.87	513.46	71.39	9039.56	11.92	425.47	2091.60
SM10C4M_2A	399.42	10.70	1075.58	583887.65	9.93	0.39	4.40	0.08	0.49	1.52		13.94	6.29	93.45	35.04	202.97	61.12	874.41	89.78	14072.19	8.32	168.03	1529.54
SM10C4M_21A	210.04	4.60	743.68	655207.93	11.48	0.40	4.87		0.43	1.04	0.33	7.12	4.01	55.89	22.86	135.07	41.23	526.90	58.30	14843.11	11.37	213.00	1988.69
SM10C4M_33	369.97	7.14	1020.35	767078.75	13.24	0.32	4.32	0.16	0.59	2.62	0.21	11.18	4.29	72.21	28.60	157.55	54.17	604.64	74.24	12639.76	17.84	105.65	2259.48
SM10C4M_10	410.48	11.43	980.94	706203.09	25.10	5.04	11.39	1.25	6.07	3.38	0.10	8.02	3.33	57.65	24.71	152.11	57.96	785.45	108.56	19050.01	84.61	87.89	1828.64
SM10C4L_93	364.14	206.16	1585.30	738327.84	22.40	2.14	10.08	0.37	2.68	2.24	0.35	15.78	6.57	115.70	46.92	254.44	78.92	955.00	143.97	21162.53	31.88	293.01	2431.05
SM10C4L_97A	421.95	16.08	1661.57	798153.66	16.76	5.16	10.91	0.65	7.18	4.76		14.39	6.64	112.87	50.49	283.32	87.68	1123.83	151.79	21044.21	32.70	184.66	3045.57
Paleogene																							
SM10C4M_19	352.50	3.13	1285.42	730565.54	15.10		4.48	0.04		1.10	0.14	15.17	6.09	92.01	37.51	180.39	50.97	563.31	68.80	13750.57	24.74	137.60	3282.35
SM10C4M_18A	368.17	2.18	2524.83	647870.75	27.29		8.51			2.46	0.40	21.99	13.31	216.02	79.34	393.95	107.95	1274.62	122.27	15358.27	54.64	316.56	7772.01
SM10C4L_104	363.37	2.36	2130.23	774823.50	17.10		7.74		0.46	2.56	0.33	27.37	12.02	182.03	62.38	269.94	66.09	653.77	82.63	17988.87	29.35	379.97	5158.56
SM10C4M_54	391.04	6.57	1547.56	715676.13	18.67		6.73			1.69	0.38	18.29	9.08	127.43	44.56	203.65	61.87	613.20	64.17	11693.08	24.35	224.07	4862.64
SM10C4M_63B	751.00	4.44	2353.03	808708.24	29.16	0.25	6.24	0.12	1.15	2.54	0.20	16.27	8.91	142.68	66.27	371.14	124.67	1384.10	167.49	12743.53	38.69	317.58	5397.31
SM10C4M_82	276.70	1.91	1035.43	711158.12	12.38	0.06	8.28	0.05	0.33	1.45	0.13	13.25	6.02	80.61	29.82	139.66	36.62	465.65	52.47	11905.39	30.77	286.00	3476.86
SM10C4M_46	444.07	1.60	1958.32	672693.29	21.05		7.24		0.02	1.26	0.30	16.73	8.77	137.44	58.29	294.92	84.79	1007.10	103.16	11615.92	34.61	240.95	6068.88
SM10C4L_82A	310.30	4.45	1882.55	833553.41	14.80		8.28	0.06	0.23	3.35	0.49	24.94	10.50	161.61	53.45	238.13	61.57	633.79	76.45	19086.36	24.96	344.41	4142.49
SM10C4M_13B	455.42	4.71	2157.01	685520.82	21.96		7.68		0.86	1.92	0.28	24.93	10.87	168.55	63.34	296.48	76.49	847.94	89.34	12896.87	35.96	257.27	5665.73
SM10C4L_96	460.30	0.45	2794.84	743460.79	26.05		9.75		0.61	2.87	0.39	32.69	17.57	245.52	78.78	334.58	81.90	805.22	98.80	17133.06	39.74	494.33	7315.87
SM10C4M_23	523.55	1.99	2744.93	812627.91	25.24		8.42		0.49	2.56	0.26	29.30	13.20	208.82	80.47	383.24	99.27	1087.61	120.98	15036.46	49.63	383.58	7802.20
SM10C4L_101	505.10	4.88	3576.73	765831.72	31.15	0.15	9.07	0.06	0.48	3.15	0.41	32.10	17.32	291.41	104.32	494.89	122.28	1239.70	163.43	19342.53	57.02	514.67	8303.72
SM10C4M_11	606.99	6.96	2485.39	760653.19	25.04		8.24	0.06	0.80	3.17	0.57	25.98	12.99	193.27	74.72	327.65	91.32	899.13	99.23	11901.88	38.82	366.91	7894.91
SM10C4M_37	535.12		2379.29	669186.43	24.38		7.60	0.02	0.61	2.03	0.13	21.40	13.63	189.15	70.88	311.60	76.65	855.60	83.20	12807.18	39.73	323.37	7070.95
SM10C4M_76	567.08	2.25	2296.01	785029.26	35.64		11.40	0.06	0.21	4.35	0.40	36.73	13.06	203.46	71.44	301.32	82.12	805.90	90.77	12036.05	41.00	505.45	8407.52

Table D3.4 SM10-C4 Trace Element Concentrations con't
Concentrations (ppm)

Spot	P	Ti	Y	Zr	Nb	La	Ce	Pr	Nd	Sm	Eu	Gd	Tb	Dy	Ho	Er	Tm	Yb	Lu	Hf	Ta	Th	U
SM10C4M_48B	574.80	3.46	2239.99	749739.61	26.31		8.73		1.06	1.57	0.33	25.33	12.17	178.07	62.77	282.29	81.78	842.90	87.03	11453.35	38.27	262.11	6419.64
SM10C4M_70	456.75	2.93	2512.20	752915.96	27.76		8.47		0.43	1.35	0.51	22.93	11.86	192.76	73.79	357.67	95.49	1062.38	111.51	13384.04	48.72	298.45	6759.97
SM10C4M_79	428.55		1848.70	711179.02	16.92		8.21	0.01	0.50	3.39	0.30	25.96	11.26	155.70	53.25	232.22	58.09	615.47	61.67	12021.12	29.49	351.22	6176.81
SM10C4M_16	409.84	2.61	1966.76	756050.93	17.99		6.38		0.24	1.15	0.13	21.39	10.29	156.22	58.18	271.17	71.58	745.27	79.74	13933.07	28.71	248.07	5508.30
SM10C4M_22	363.44	3.86	1643.85	771146.40	18.88		6.01			0.87	0.25	11.83	6.41	106.88	48.34	266.58	76.63	924.59	110.09	14202.05	31.21	174.74	4220.02
SM10C4M_28B	430.43	2.15	1612.53	794908.89	17.10		6.83			2.44	0.37	19.20	9.04	140.50	45.52	198.88	54.69	528.18	59.44	13073.04	27.87	282.51	5774.69
SM10C4M_75	422.67	0.23	2103.30	718362.91	19.47		6.51		0.22	2.37	0.33	21.47	11.53	170.13	60.53	277.52	69.83	757.71	78.63	13223.48	33.34	303.67	6458.61
SM10C4M_7A	477.93	3.88	1883.03	542941.53	19.44		8.50			2.08	0.07	26.23	10.77	169.26	60.26	287.18	74.02	810.61	68.00	12114.29	33.24	295.20	6670.56
SM10C4M_60	355.96	2.41	1441.68	746292.49	15.74		5.60		0.32	1.81	0.27	14.99	7.17	108.29	42.22	201.91	55.99	632.91	66.95	13528.86	25.49	166.73	3886.67
SM10C4M_45	658.81	9.35	2723.97	710879.86	30.03	0.88	9.00	0.25	0.99	2.59	0.52	28.96	12.38	198.31	79.18	419.68	122.30	1465.19	154.17	12244.18	42.98	391.30	6442.19
SM10C4M_62	467.25		2469.61	729514.47	25.61		7.95			2.48	0.27	20.61	10.91	173.08	73.34	360.95	97.23	1131.66	120.02	13567.40	45.81	290.06	6708.77
SM10C4M_4A	473.57	8.75	3153.75	608961.93	30.74		14.39	0.12	1.44	7.39	0.74	49.46	21.14	305.31	111.32	527.98	138.24	1642.46	149.74	11805.50	25.51	605.61	6348.07
SM10C4L_83	340.49	3.19	2143.60	775830.77	11.17		13.27	0.04	0.27	4.40	0.67	32.85	13.08	195.67	64.87	278.91	70.69	698.54	91.94	15299.73	12.23	642.96	3999.08
SM10C4M_35	490.10		2379.28	709769.11	29.45		9.93			3.80	0.05	38.06	15.43	199.39	66.47	276.37	72.21	732.59	74.72	11366.01	39.65	470.17	8768.65
SM10C4M_4B	404.37	8.82	2109.83	744102.41	17.69		10.56		1.55	3.39	0.81	33.86	13.83	178.11	61.66	278.03	79.86	856.57	91.42	9426.68	14.72	311.02	3545.71
SM10C4M_67	485.43	4.36	2712.10	767269.66	28.67		7.95		0.51	1.78	0.45	26.77	12.42	196.37	76.52	376.09	102.70	1114.31	122.17	14188.42	51.46	315.43	6823.16
SM10C4L_91	467.43	5.17	2965.49	766523.04	29.24		9.46		0.53	3.99	0.37	34.37	17.54	261.08	86.16	361.48	87.12	863.54	103.98	18527.66	46.41	509.28	7812.14
SM10C4M_86	415.56	5.87	1717.14	698457.56	11.76		8.81	0.22	2.87	0.42	0.42	25.23	10.70	144.07	52.61	237.91	61.28	709.53	70.48	10112.64	11.65	286.06	3387.58
SM10C4M_50	385.86	0.80	1731.46	690072.60	20.23		6.54	0.15	1.60	0.26	17.17	8.42	132.07	51.72	239.04	64.88	730.52	73.33	12531.90	31.36	265.95	5604.63	
SM10C4M_58	531.70	5.48	2558.10	718280.60	25.38		8.30		0.15	2.67	0.39	26.42	14.61	204.18	74.34	334.79	84.93	916.73	91.27	12992.42	40.96	339.27	7394.58
SM10C4M_42	473.16	4.83	1949.14	704473.78	19.75		6.48		0.15	1.74	0.24	19.83	11.05	157.05	59.25	277.92	75.25	836.43	81.97	12944.49	37.87	254.94	6451.53
SM10C4M_43	505.72	7.29	2335.87	693005.09	25.39		8.06		0.33	1.45	0.08	24.71	12.74	179.78	68.88	316.55	85.47	951.07	92.81	12595.56	42.18	287.01	7177.74
SM10C4M_1	452.33	7.83	1836.67	660867.94	18.34		6.83	0.03		2.00	0.29	23.39	10.13	150.59	56.14	246.25	63.63	706.65	67.58	12138.41	30.38	268.19	6271.91
SM10C4M_64	462.05	2.44	2709.60	753885.60	28.43	0.02	8.72	0.39	3.09	3.09	0.39	30.46	14.36	214.24	80.61	370.66	92.19	996.61	102.47	13872.92	47.58	314.73	7024.35
SM10C4M_66	305.19	7.51	2012.48	674045.22	13.09		9.42	0.41	3.55	0.80	0.80	31.44	12.61	184.75	66.25	317.36	80.69	929.42	92.69	13609.65	18.31	309.78	3500.53
SM10C4M_28A	299.72	3.35	1644.61	661177.96	10.04		10.06	0.10	0.88	2.47	0.77	27.22	12.88	149.31	54.19	244.24	61.11	722.36	70.77	13323.94	14.63	304.28	3088.09
SM10C4L_82B	410.50	3.63	2809.79	627736.71	26.58		9.08	0.13	1.13	5.07	0.32	36.39	19.18	260.71	86.81	336.33	89.95	761.19	99.94	16325.78	39.20	602.31	7953.91
SM10C4M_81	473.71	3.50	2116.99	708580.48	29.39		9.27		0.09	2.56	0.49	30.07	13.58	184.49	64.64	279.78	70.23	765.43	77.18	12183.75	38.35	372.64	7073.34
SM10C4M_74	262.76	3.99	1161.82	593006.00	17.38	1.16	5.76	0.13	1.82	1.00	0.26	6.12	3.79	82.06	38.68	221.67	74.96	1013.90	99.06	13143.46	32.81	95.87	2758.44
SM10C4M_7B	541.16	2.74	2252.90	692460.11	24.43		8.64			1.74	0.26	24.33	12.36	185.88	69.43	285.13	83.47	770.55	81.29	11627.20	32.43	385.30	8138.44
SM10C4M_36	536.21	2.10	2008.60	713563.45	22.42		6.89			2.14	0.05	22.05	10.78	169.66	57.85	263.62	72.51	710.32	76.02	11588.65	33.44	258.54	6224.23
SM10C4M_20A	771.21	7.13	3669.43	643234.61	40.96	0.55	9.83	0.16	0.95	5.16	0.44	32.86	13.94	277.90	116.00	653.50	198.59	2480.06	259.08	16447.07	61.33	401.13	7430.55
SM10C4L_95	437.85	1.81	2842.87	736156.29	26.68		8.01		0.30	0.97	0.44	19.67	10.80	194.67	78.92	431.26	126.90	1422.45	190.73	17061.27	38.30	244.25	4851.14

Table D3.4 SM10-C4 Trace Element Concentrations con't

Concentrations (ppm)																							
Spot	P	Ti	Y	Zr	Nb	La	Ce	Pr	Nd	Sm	Eu	Gd	Tb	Dy	Ho	Er	Tm	Yb	Lu	Hf	Ta	Th	U
SM10C4M_73	556.25	12.63	2960.42	619006.97	29.20	0.39	17.33	0.17	2.45	7.51	1.00	53.43	22.32	295.05	101.85	466.51	118.87	1395.08	123.85	11435.06	26.32	860.36	7117.43
SM10C4M_41	399.76	3.44	1737.24	686337.63	18.39		8.57		0.45	2.29	0.26	23.82	10.81	153.44	51.09	225.50	55.36	605.95	60.31	11984.58	29.69	317.80	6002.39
SM10C4M_5	706.12	8.42	3700.08	688820.69	46.76		9.67		0.43	3.26	0.37	37.30	18.35	279.97	108.73	532.31	140.07	1604.00	153.58	12662.79	65.45	540.65	10173.31
SM10C4L_98	478.30	2.28	2962.28	744624.39	29.57	0.13	8.27	0.06	0.52	2.01	0.34	25.82	14.39	237.52	85.53	409.82	106.74	1090.69	139.23	18379.20	51.08	375.39	6519.46
SM10C4M_13A	531.35	2.59	2527.33	731997.78	31.00		8.74		0.49	4.24	0.36	27.39	12.56	200.31	76.63	345.66	90.15	1022.84	101.47	12956.38	35.99	292.82	6292.05
SM10C4L_89	621.04	2.28	3730.16	759334.75	36.48	0.04	8.55	0.06	0.41	2.07	0.23	24.82	14.06	268.26	107.73	586.03	169.49	1878.12	257.07	19562.57	56.36	413.36	6773.26
SM10C4M_56	294.86	2.51	1167.59	721528.74	8.33		7.40		0.35	1.30	0.24	17.39	7.21	98.51	35.74	160.60	40.22	464.94	48.58	11541.18	10.84	266.29	3206.25
SM10C4M_48A	548.21	9.50	3047.77	588156.05	32.75		11.20			3.83	0.48	38.00	19.53	302.83	100.14	468.84	114.78	1371.57	114.86	13235.64	58.94	407.06	9405.08
SM10C4L_92	209.44	3.33	1003.81	778253.07	6.18		6.62			1.70	0.12	13.36	6.28	89.29	31.89	140.70	35.41	364.42	44.80	16547.72	9.20	195.77	2055.05
SM10C4L_99	204.31	3.67	1240.94	826015.52	17.41		4.30	0.00		0.93	0.17	7.74	4.08	81.53	35.86	197.81	59.65	683.93	98.79	19743.87	29.36	104.35	2521.12
SM10C4M_78A	281.45	5.26	1175.46	607866.29	13.26		8.61			2.39	0.01	13.53	8.35	111.03	37.92	195.91	57.19	652.06	62.27	14146.64	22.94	207.38	3786.25
SM10C4M_63A	763.32	8.33	2728.21	652418.20	22.13	0.78	9.44	0.22	1.51	4.63	0.24	26.99	13.69	222.95	88.26	454.99	118.84	1543.99	149.12	14765.28	35.33	328.08	6130.70
SM10C4M_8	225.48	1.69	654.32	704822.50	6.10		3.03			0.66		7.17	2.93	50.72	19.17	90.66	26.41	316.15	32.30	13806.61	15.07	68.98	2211.19
SM10C4M_80A	1338.61	15.02	3407.62	579684.00	34.01	8.24	22.90	3.56	17.61	12.22	0.56	37.69	17.48	248.45	114.57	645.87	196.86	2688.55	267.11	14291.72	56.76	438.89	7858.37

Table D5.1 HM11-01 Trace Element Concentrations

Concentrations (ppm)																							
Spot	P	Ti	Y	Zr	Nb	La	Ce	Pr	Nd	Sm	Eu	Gd	Tb	Dy	Ho	Er	Tm	Yb	Lu	Hf	Ta	Th	U
Paleoarchean																							
HM11-01_M_43		67.33	16.71	845.34	8.02	0.30	22.76	0.12	1.13	2.11	1.01	14.17	5.44	82.88	32.99	156.37	40.48	442.51	52.07	8544.78	2.47	454.70	2040.98
HM11-01_M_42		97.24	14.69	816.83	8.26	0.46	19.14	0.13	1.10	1.82	1.22	10.48	5.12	77.13	32.06	150.11	40.59	443.49	49.57	9082.12	3.78	436.19	2189.26
Neoarchean																							
HM11-01_M_50		378.42	6.69	2086.04	15.03	2.35	43.99	1.07	12.54	16.91	1.88	65.40	20.48	232.68	78.33	298.75	68.76	709.99	71.53	8644.92	6.24	749.88	501.27
HM11-01_M_48		215.77	5.67	1321.74	14.16	0.36	11.24	0.20	1.83	3.31	1.24	20.42	8.91	122.75	46.15	216.80	63.31	742.57	78.06	9965.42	11.21	169.56	988.76
HM11-01_M_44		290.62	16.96	2826.77	12.50	0.33	26.91	0.30	5.30	10.07	3.23	59.80	21.89	277.43	102.27	429.28	113.90	1189.48	129.41	8409.32	4.00	570.50	1206.32
HM11-01_M_45		181.92	10.97	958.87	32.04	0.31	6.72	0.22	1.02	1.20	0.39	9.23	4.68	80.99	36.16	180.54	54.37	627.03	66.20	12340.69	19.04	108.78	1410.99
HM11-01_M_52		162.04	14.76	865.13	27.62	1.06	8.38	0.21	1.39	1.37	0.42	10.28	4.97	81.91	33.41	164.92	43.12	471.39	50.69	11348.72	13.44	144.55	1398.47
HM11-01_M_49		183.96	9.74	900.53	36.09	27.28	16.53	4.20	21.92	6.59	2.10	14.83	6.07	85.59	33.15	163.49	46.16	551.28	59.92	12212.20	29.12	191.09	1574.08
Paleoproterozoic																							
HM11-01_M_53		193.93	12.40	1339.68	34.97	15.14	16.05	2.41	9.56	3.98	1.45	14.31	7.25	112.81	47.94	234.90	68.88	780.80	88.86	12439.83	24.85	204.24	2052.02
HM11-01_M_46		198.03	9.55	1023.42	39.90	14.19	19.20	1.99	9.80	5.61	2.37	14.22	6.52	96.95	38.73	181.78	55.00	666.79	72.82	10923.03	30.35	163.68	1723.58
HM11-01_M_54		165.65	14.65	970.06	21.54	8.19	16.18	1.73	10.91	4.65	9.40	14.68	5.42	81.36	34.94	177.48	49.94	565.46	70.20	10448.56	10.17	169.68	1635.50

Table D5.2 HM11-06 Trace Element Concentrations

Concentrations (ppm)																							
Spot	P	Ti	Y	Zr	Nb	La	Ce	Pr	Nd	Sm	Eu	Gd	Tb	Dy	Ho	Er	Tm	Yb	Lu	Hf	Ta	Th	U
Neoarchean																							
HM11-06_S_149		266.32	1.42	1720.76	3.35	0.00	17.17	0.04	2.14	7.10	0.37	39.53	14.57	178.27	64.72	261.20	65.40	686.65	67.48	10025.50	2.08	372.17	530.42
HM11-06_S_150		260.99	0.73	2204.03	3.72	0.01	23.77	0.08	2.16	8.17	0.25	52.79	18.18	233.43	85.55	349.71	86.65	893.63	92.38	11399.06	1.96	404.40	295.69
HM11-06_S_155		174.06	0.93	1979.09	2.12		17.10	0.36	6.70	12.22	2.63	55.73	18.05	222.81	76.94	308.74	75.49	792.93	81.98	9480.55	0.87	168.38	118.70
HM11-06_S_152		149.76	1.31	1079.64	3.03	0.01	15.41	0.05	1.34	4.28	0.56	23.29	8.99	111.24	40.65	171.77	44.30	481.98	53.63	10419.39	1.28	118.57	113.09
HM11-06_M_165		215.87	1.35	1663.79	7.74	0.00	15.82	0.04	0.69	3.79	0.12	27.33	11.22	148.97	59.78	272.57	66.37	654.66	95.16	17582.70	4.87	284.08	368.58
HM11-06_S_147		179.51	1.40	975.46	4.39	0.02	11.93	0.04	1.11	4.12	0.13	19.32	7.63	99.72	36.34	151.47	40.55	437.67	45.74	10541.53	2.81	218.53	475.70
HM11-06_M_167		187.70	1.23	1523.16	6.49		16.42	0.02	0.89	3.31	0.12	26.92	10.48	141.40	54.66	243.08	59.66	580.86	85.04	17507.28	3.51	280.09	321.09

Table D5.2 HM11-06 Trace Element Concentrations con't

Spot	Concentrations (ppm)																						
	P	Ti	Y	Zr	Nb	La	Ce	Pr	Nd	Sm	Eu	Gd	Tb	Dy	Ho	Er	Tm	Yb	Lu	Hf	Ta	Th	U
HM11-06_M_166		180.81	1.14	1613.79	5.27	0.41	24.04	0.22	2.33	5.42	0.64	33.99	11.90	151.45	61.13	260.00	63.22	586.69	85.89	15866.66	2.20	289.80	206.35
HM11-06_S_151		345.42	0.80	808.64	2.43	1.92	14.66	0.72	3.71	3.71	0.75	18.17	6.31	79.60	29.74	130.20	34.05	380.23	41.87	10126.39	1.09	74.04	111.39
HM11-06_S_146A		201.20	2.44	814.57	2.25	0.11	4.49	0.07	0.59	2.90	0.15	13.75	6.08	76.32	28.46	129.15	33.70	380.89	38.93	11490.07	1.50	126.20	396.56
HM11-06_S_145		231.44	2.02	1012.31	3.75	0.06	6.18	0.02	0.61	2.34	0.12	16.05	7.20	97.14	35.90	148.17	38.34	409.02	41.58	11328.10	2.43	183.70	780.97
HM11-06_S_161B		295.48	1.07	1626.98	4.03	0.12	12.38	0.07	1.98	5.86	0.20	29.54	11.50	150.63	60.16	280.22	78.21	969.56	108.73	12680.95	3.21	235.23	727.56
HM11-06_S_154		301.23	3.68	1787.26	2.87		9.02	0.07	2.49	5.73	2.15	33.52	12.69	170.56	66.18	304.58	83.72	964.93	116.60	8649.59	0.95	97.43	147.89
HM11-06_S_159		154.20	1.09	784.32	4.14		22.61	0.03	0.79	2.01	0.44	13.78	4.65	68.07	27.65	128.67	36.78	429.43	51.96	10855.66	2.01	153.95	296.48
HM11-06_S_146B		236.84	6.81	1050.62	3.90	0.94	9.08	0.46	3.21	3.81	5.69	17.43	7.15	95.86	35.91	169.14	50.62	588.44	55.95	11129.68	3.70	161.31	1027.73
HM11-06_S_143		194.32	2.93	1209.97	3.63	0.39	37.76	0.24	2.05	3.69	0.95	23.46	8.56	111.95	44.11	195.75	54.71	686.49	75.09	12489.93	6.50	353.55	665.98
HM11-06_S_163		242.91	1.62	1253.35	4.93	0.07	8.42	0.08	1.02	2.87	0.13	20.09	8.74	120.18	44.99	195.56	54.43	614.96	65.67	11304.83	2.93	163.29	461.10
HM11-06_S_158		121.33	1.04	893.09	3.12	0.01	14.67	0.14	2.05	4.24	0.79	22.33	7.28	93.04	34.81	151.14	40.98	507.11	53.36	10831.36	2.62	104.47	331.92
HM11-06_S_161A		299.48	1.04	1927.93	2.00	0.23	7.17	0.10	1.23	3.69	0.28	24.21	10.64	150.40	68.12	369.76	100.08	1003.40	201.08	8715.17	0.58	93.44	523.99
HM11-06_S_162		203.34	16.55	1047.84	3.90	0.35	5.11	0.13	1.39	1.66	0.55	12.46	5.47	80.80	34.76	173.98	50.82	601.48	84.35	11979.86	5.61	121.79	781.70
HM11-06_S_144		87.86	0.76	499.08	3.03	0.03	19.99	0.07	0.68	1.55	0.29	9.48	3.50	42.64	17.37	78.83	23.89	312.82	34.88	11077.16	2.61	190.64	395.31
Paleoproterozoic																							
HM11-06_S_160		197.49	5.31	1250.39	6.37	0.92	9.11	0.43	2.69	3.48	4.68	15.01	6.87	99.49	41.00	221.50	61.09	694.61	112.17	11371.25	6.91	204.01	1354.15
HM11-06_S_153		51.12	1.09	394.01	2.62	0.16	1.60	0.05	0.07	0.20	0.13	1.87	1.30	21.48	11.54	70.51	23.09	296.32	50.25	11252.16	3.15	14.72	460.42
Paleogene																							
HM11-06_S_156		366.46	0.33	4394.64	179.54	1.11	24.34	0.61	4.72	8.95	0.24	65.57	28.85	394.89	151.92	694.32	196.15	2263.97	247.39	14014.82	115.66	2538.43	9941.42
HM11-06_S_157		304.29	0.68	6996.67	345.63	0.05	38.87	0.06	2.14	13.39	0.43	117.25	51.16	693.60	257.88	1115.03	309.30	3389.23	340.86	13683.92	147.03	4222.27	15106.20